The extinct genus *Hexaprotodon* Falconer & Cautley, 1836 (Mammalia, Artiodactyla, Hippopotamidae) in Asia: paleoecology and taxonomy

Het uitgestorven genus *Hexaprotodon* Falconer & Cautley, 1836 (Mammalia, Artiodatyla, Hippopotamidae) in Azië: paleoecologie en taxonomie

(met een samenvatting in het Nederlands)

Proefschrift

ter verkrijging van de graad van doctor
aan de Universiteit Utrecht
op gezag van de rector magnificus, prof.dr. J.C. Stoof,
ingevolge het besluit van het college voor promoties
in het openbaar te verdedigen op
donderdag 11 december 2008 des middags te 4.15 uur

door

Johanna Augusta de Visser

geboren op 18 april 1961
te 's-Hertogenbosch

Promotoren: Prof. dr. J.W.F. Reumer
Prof. dr. P.L. de Boer

Co-promotor: Dr. J. de Vos

SAMENVATTING

Paleontologie bestudeert de in fossielen neergelegde wisselwerking van taxonomie, biogeografie en ecologie, waarbij de verspreiding van soorten wordt bepaald door ecologische randvoorwaarden. Een opmerkelijk aspect, waarin de Aziatische *Hexaprotodon* (nijlpaard) verschilt van andere fossiele zoogdiertaxa, is dat hij in sommige vindplaatsen zeer talrijk is, terwijl in andere vindplaatsen die er verder, qua faunasamenstelling, erg op lijken, geheel ontbreekt of zeer zeldzaam is.

Gedurende geologisch-paleontologisch veldwerk in 1989 en 1990 in de buurt van New Mirpur (Azad Kashmir, Pakistan), bleek dat in het bovenste deel van de Plio-Pleistocene Samwal Formatie nijlpaardfossielen zeer zeldzaam zijn, terwijl in het onderste deel van de Samwal Formatie, dat ook een Plio-Pleistocene ouderdom heeft, in hetzelfde zoögeografische gebied ligt en ook bestaat uit rivierafzettingen, ze veelvuldig voorkomen (Hussain *et al.*, 1992). Behrensmeyer (1976, 1985) kwam tot de conclusie dat in bepaalde submilieu's van het riviersysteem van het Turkana Meer (voormalig Rudolf Meer, Kenia, Afrika), zoals in het overstromingsgebied, duidelijk minder fossiele nijlpaarden worden gevonden dan in andere submilieu's, zoals de rivierbedding.

In Hoofdstuk 2 wordt de biologie en ecologie van het recente nijlpaard *Hippopotamus amphibius* beschreven. Mazza (1995) concludeerde aan de hand van de kleine hoek, die de achterkant van de schedel maakt met de horizontale lijn tussen de occipitale condyles en de voorkant van de kop, dat de Pleistocene Hippopotamidae *H. gorgops* uit Afrika and *H. tiberinus* uit Europa zich meer voedden met aquatische planten dan met gras. Bij *Hippopotamus amphibius* (een graseter) is deze hoek groter, wat van invloed is op de aanhechting van spieren en de bijtkracht. Mazza (1995) concludeerde hieruit dat *H. amphibius* meer kracht nodig had om het meer taaie gras te verwerken. In de hier beschreven fossielen uit Indonesië en India komt deze hoek overeen met die van *H. amphibius*, zodat aannemelijk is dat deze Aziatische fossiele nijlpaarden ook hoofdzakelijk graseters waren en een vergelijkbare levenswijze hadden.

Om vast te stellen of de aan- of afwezigheid van fossiele nijlpaarden in Aziatische vindplaatsen verklaard kan worden op grond van paleo-ecologische factoren, zoals gesuggereerd door Behrensmeyer (1976, 1985) voor het Turkana Meer in Afrika, werden de sedimenten, de taphonomie en de fossiele fauna van de Onder- en Boven Samwal Formatie in hun samenhang bestudeerd (deel A, Hoofdstuk 3). De conclusie is dat de paleo-ecologie van de fauna's inderdaad verschilt en dat afzetting plaatsvond in verschillende sedimentaire milieu's.

Taxonomie is belangrijk om vast te stellen of de fossielen tot verschillende soorten behoren, want als het om meerdere soorten gaat, is het logisch om aan te nemen dat ook de ecologische omstandigheden verschillen. Coryndon (1976) beschreef verscheidene (sub)soorten van nijlpaarden in Afrika. Zij verklaarde het voorkomen van de diverse (sub)soorten in Afrika dan ook aan de hand van ecologische verschillen; elke (sub)soort in zijn eigen habitat.

Ook van nijlpaarden in Azië zijn veel (sub)soorten beschreven. Om vast te stellen of er werkelijk zoveel (sub)soorten in Azië onderscheiden moeten worden werd een studie verricht naar de taxonomie van de Aziatische nijlpaarden (taxonomisch deel, deel B). Dit deel B begint met een overzicht van het bestudeerde materiaal (schedels, kaken en gebitten) en van de vindplaatsen van de fossielen (Hoofdstuk 4 en Appendix III). De gebruikte nomenclatuur met betrekking tot de premolaren en molaren wordt beschreven in Appendix IV. De meetmethodes voor alle bestudeerde elementen worden beschreven in Appendix V. De metingen worden in tabellen en diagrammen weergegeven in Appendix VI en geïnterpreteerd in Hoofdstuk 5.

De basis voor taxonomie is de beschrijving van de fossielen. De morfologische en biometrische beschrijving van het materiaal staat in Appendix VII. Om vergelijking te vergemakkelijken zijn alle elementen afzonderlijk en in detail beschreven. Een samenvatting en een discussie hierover staan in Hoofdstuk 5 en Appendix VIII .

De variatie die binnen een soort voorkomt is van belang voor de taxonomie, maar bepaalde verschillen zouden veroorzaakt kunnen zijn door seksuele dimorfie. In Hoofdstuk 6 wordt de seksuele dimorfie en de variatie van het recente nijlpaard *Hippopotamus amphibius* (gebaseerd op Hooijer, 1950) besproken. De conclusie is dat de variatie in grootte en morfologie bij *Hippopotamus amphibius* groot is.

Daarnaast is een gedetailleerde vergelijking gemaakt van de morfologie en biometrie van de bestudeerde fossielen. Speciaal is daarbij aandacht besteed aan drie vindplaatsen op Java (Indonesië), te weten Kali Glagah, Kedung Brubus en Ngandong, omdat de bio- en chronostratigrafische posities van deze vindplaatsen goed bekend zijn. In het nijlpaardmateriaal van deze drie vindplaatsen werden bepaalde verschillen gevonden (Hoofdstuk 7, Appendices IX en X), maar deze zijn niet kenmerkend genoeg om een onderverdeling in (sub)soorten te rechtvaardigen. Wel kan een evolutionaire trend worden onderscheiden, waarbij het nijlpaard van Kali Glagah kleiner is dan dat van Kedung Brubus. Deze op zijn beurt is weer kleiner dan dat van Ngandong (Hoofdstuk 7, Appendices IX en X). these species and that the changes that occur are due to local evolution of *Hexaprotodon*. Biometrische vergelijking laat tevens zien dat het materiaal van Java duidelijk kleiner is dan dat van het continentale deel van Azië (Hoofdstuk 8, Appendix XI).

In Hoofdstuk 9 (Appendices XII en XIII) wordt een revisie van het genus *Hexaprotodon* van het continentale deel van Azië voorgesteld. Na bestudering van de literatuur en gebaseerd op de studies in de voorgaande hoofdstukken wordt de conclusie getrokken dat tijdens het Plio-Pleistoceen in continentaal Azië slechts één soort voorkwam, *Hexaprotodon sivalensis* Falconer & Cautley, 1836.

Hetzelfde geldt voor Java (Hoofdstuk 10 en Appendix XIV), waar ook slechts één soort wordt onderscheiden, *Hexaprotodon sivajavanicus* Dubois, 1908. Op Java en in het continentale deel van Azië komen dus lang niet zoveel (sub)soorten voor als is gesuggereerd door auteurs, zoals Falconer & Cautley (1836), Hooijer (1950), Dubois (1908) en Deraniyagala (1936). Het verwaarlozen van de grote intraspecifieke variatie die voorkomt bij recente en fossiele nijlpaarden speelt hierbij een rol.

The extinct genus *Hexaprotodon* Falconer & Cautley, 1836 (Mammalia, Artiodactyla, Hippopotamidae) in Asia: paleoecology and taxonomy

Johanna Augusta de Visser

Keywords: paleontology, paleoecology, taxonomy, Hippopotamidae, sedimentology, fluvial deposits, Asia, Java, Upper-Siwaliks, Plio-Pleistocene

SUMMARY

Paleontology studies the interaction between taxonomy, biogeography and ecology, incorporated in the fossils; the distribution of species is determined by ecological conditions. A remarkable aspect, in which the Asian *Hexaprotodon* (hippopotamus) differs from other fossil mammal taxa, is that in some localities they are abundant, while in other localities, which are fairly similar in faunal composition, their fossils are lacking completely or are very scarce. During geological-paleontological fieldwork in 1989 and 1990 in Pakistan near New Mirpur (Azad Kashmir), it turned out that in the upper part of the Plio-Pleistocene Samwal Formation fossils of hippopotamus are scarce, while in the lower part, also of Plio-Pleistocene age, in the same zoogeographical area and also in fluviatile sediments, they occur frequently (Hussain *et al.*, 1992).

In Chapter 2 the biology and ecology of the recent *Hippopotamus amphibius* is described. Mazza (1995) concluded from the small angle between the back of the skull and the horizontal line between the occipital condyles and the front of the muzzle, that the Pleistocene *Hippopotamus gorgops* from Africa and *Hippopotamus tiberinus* from Europe fed more on aquatic plants than on grasses. In *Hippopotamus amphibius*, which feed on grasses, this angle is larger, resulting in increased muscle attachment and biting force. Mazza (1995) thus concluded that *H. amphibius* needs more strength to cope with tough grasses. In the fossils from India and Indonesia described here, this angle resembles that of *H. amphibius*. Therefore it is likely that these fossil hippopotami also mainly fed on grasses and lived in a similar way.

Behrensmeyer (1976, 1985) studied fossil assemblages "...to determine whether paleoecologic factors are present in the faunas from different sedimentary environments". She concluded that in certain subenvironments of river systems (Lake Turkana Basin, former Lake Rudolf Basin, Kenya, Africa), like the floodplain, clearly less hippopotamus fossils are found, than in other subenvironments, like the river bed. To identify whether the presence or absence of hippopotamus in Asian localities can be explained on the basis of paleoecological factors, as suggested by Behrensmeyer (1976, 1985) for the Lake Turkana Basin in Africa, a comparison is made between the sediments, the taphonomy and the fossil assemblages of the Upper and Lower Samwal Formation (part A, Chapter 3). It is concluded that the paleoecological characteristics of the faunas are different because of deposition in different sedimentary environments.

Taxonomy is important to determine if fossils belong to different species, because if different species are involved, it is logical to assume that also different ecological conditions are involved. Coryndon (1976) described several (sub)species of hippopotamus in Africa. Indeed, she explained the occurrence of the different (sub)species by ecologische differences; each (sub)species in its own habitat.

Also from Asia many (sub)species have been described. To determine if really so many subspecies need to be distinguished in Asia, a taxonomical study was done (taxonomical part, part B). This part B starts with an overview of the studied material (skulls, mandibles and dentition) and the fossil localities (Chapter 4 and Appendix III). The nomenclature for the premolars and molars is explained in Appendix IV. The measuring

method for all elements is explained in Appendix V. The measurements are given in tables (Appendix VI) and diagrams, and are interpreted in Chapter 5.

The basis of taxonomy is the description of the fossils. The morphological and biometrical descriptions of the material are given in Appendix VII. In order to facilitate a comparison, all elements have been described separately and in detail. A summary and discussion of the descriptions are given in Chapter 5 and Appendix VIII.

The variation within a species is important for the taxonomy. Yet, certain differences might be related to sexual dimorphism. The sexual dimorphism and variation in the extant *Hippopotamus amphibius* (based on Hooijer, 1950) is discussed in Chapter 6.
It is concluded that the variation in size and morphology in *Hippopotamus amphibius* is large.
A detailed comparison is made of the morphology and biometric data of the studied fossils. Special attention was paid to the localities Kali Glagah, Kedung Brubus and Ngandong on Java (Indonesia), because the bio- and chronostratigraphical positions of these localities are well known. Differences in the hippopotamus material from these three localities are not significant enough to warrant a subdivision in (sub)species (Chapter 7 and Appendices IX and X). The general trend is that the Kali Glagah hippopotamus is smaller than the one from Kedung Brubus, which again is smaller than that from Ngandong (Chapter 7, Appendices IX and X).
Biometry shows that the material from Java is clearly smaller than that from continental Asia (Chapter 8, Appendix XI).

In Chapter 9 (Appendices XII and XIII) a revision of the genus *Hexaprotodon* of continental Asia is made. After reviewing the literature and based on the results in the previous chapters, it is concluded that during the Plio-Pleistocene, *Hexaprotodon sivalensis* Falconer & Cautley, 1836 was the only species in continental Asia.

The same holds for Java (Chapter 10, Appendix XIV), where also only one species, *Hexaprotodon sivajavanicus* Dubois, 1908, occured. Apparently, on Java and in continental Asia not as many (sub)species occur as was suggested by authors like Falconer & Cautley (1836), Dubois (1908), Deraniyagala (1936) and Hooijer (1950), who neglected the large intraspecific variation in the fossil and extant Hippopotamidae.

Contents

1. GENERAL INTRODUCTION

There are two genera of hippopotamus: *Hippopotamus* Linnaeus, 1758 and *Hexaprotodon* Falconer & Cautley, 1836. The main difference between these genera is found in the number of incisors: *Hexaprotodon* has six incisors, both in the upper and lower jaw, whereas *Hippopotamus* has four (tetraprotodont). Other differences in the morphology of the skull are given in Chapter 9.4.

Hexaprotodon originated in Africa where they first occurred some 8 Ma B.P. (Pickford, 1983). *Hippopotamus* first occurred in Africa during the Late-Pliocene (Kahlke, 1990) and evolved from Hexaprotodon (Van der Made, 1999). In Asia, the first occurrence of Hexaprotodon is recorded at 6.1 Ma B.P. (Dennell, 2004) or possibly as early as 7.2 Ma B.P. (Barry *et al.*, 2002). The last occurrence is dated at 1.7 Ma B.P. (Dennell *et al.* 2006). On Java (Indonesia), hippopotamus arrived some 2 Ma B.P. and vanished about 125 ka B.P. (Van den Bergh, 1996). The Asian hippopotamus all belong to the genus *Hexaprotodon.*

Hexaprotodon fossils are abundant in some localities on the Indian subcontinent, Indonesia and in Africa, while in other localities, similar in faunal composition with respect to other species, they are completely lacking or very scarce. Other fossil mammal taxa do not show such extreme differences. Fossil hippopotami are lacking in the Plio-Pleistocene deposits of the Karewa Basin in India (Kotlia, 1985). In the upper part of the Samwal Formation in the Upper Siwaliks (Pakistan) they are scarce, and in the lower part of the Samwal Formation of roughly the same age (Plio-Pleistocene), in the same zoogeographical area, and also in fluviatile sediments, they are abundant (Hussain *et al.*, 1992).

In Trinil (Java, Indonesia) fossils of hippopotamus are lacking, and in Kedung Brubus, only 30 km from Trinil they are present. Both sites represent fluviatile sediments (De Vos & Sondaar, 1982).

Behrensmeyer (1976, 1985) studied the Plio-Pleistocene fossil assemblages of the Lake Turkana Basin (former Lake Rudolf Basin, Kenya, Africa) to determine whether different sedimentary environments show different paleoecologic features. She found that in certain subenvironments of the river system, like in the floodplain, clearly less hippopotamus fossils occur than in other subenvironments like the river bed.

Coryndon (1976) stated that a complex hippopotamus fauna of Plio-Pleistocene age, with different species of hippopotamus, characterizes the Turkana Basin. She ascribed this to possible differences in biotope, like woods, rivers and lakes.

From Asia, many (sub)species of *Hexaprotodon* have been described. Fossils of hippopotamus in the Siwaliks, such as *Hippopotamus (Hexaprotodon) sivalensis*, were described by Falconer and Cautley (1836). These authors showed illustrations of specimens of three other species, without giving a description. They are: *Hippopotamus (Tetraprotodon) palaeindicus, Hippopotamus (Hexaprotodon) namadicus* and *Hippopotamus (Hexaprotodon) iravaticus*. Hooijer (1950), in a review of Asian hippopotamus material, distinguished many subspecies on the Indian subcontinent: *Hippopotamus sivalensis sivalensis* Falconer & Cautley, 1836; *H. s. namadicus* Falconer & Cautley, 1836; *H. s. palaeindicus* Falconer & Cautley, 1836; *H. s. sinhaleyus* Deraniyagala, 1936 and on Java *H .s. sivajavanicus* (Dubois, 1908); *H. s. koenigswaldi* (Hooijer, 1942), *H. s. soloensis* Hooijer, 1950 and *H.s. duboisi* Hooijer, 1950.

The aim of this study is twofold:

1. to determine if the local presence and absence of hippopotamus in the Plio-Pleistocene deposits in the Mirpur Area in Pakistan can be explained on the basis of paleoecological factors, as suggested by Behrensmeyer (1976, 1985) on the basis of her study of the Lake Turkana Basin in Africa (part A).
2. to determine if there are really so many subspecies in Asia as have been suggested by various authors (part B).

The revision of the taxonomy is based on a comparison of the extant species *Hippopotamus amphibius* with fossil material from various collections from Java and India (part B).

2. THE BIOLOGY AND ECOLOGY OF THE RECENT *HIPPOPOTAMUS AMPHIBIUS*

Hippopotamus amphibius is a megaherbivore living in Africa, south of the Sahara. A school of Hippopotamidae consists of 3 groups, territorial males, females with their offspring, and bachelors. The sexes live segregated and there are no social bonds between the adults of a group, although they like to be together. The females live within a territory to which they return each morning after feeding. Their choice of territory is partly based on the quality of the male, but more likely depends on topographical features such as water depth, the lack of a strong current and the presence of sand banks. The males only show territorial behaviour in the water (Eltringham, 1999).

Present-day Hippopotamidae do not eat aquatic vegetation to any extent (except in times of food shortage). They eat mainly grasses during the night, and may walk several kilometres away from the river in search for food. Feeding is individual. They select preferably short grasses. "They do not select for grass species as such but merely select the patches of sward in which to feed" (Eltringham, 1999, p. 81). Hippopotamus grazing ground consists of patches of short grasses, where the animals feed, interspersed with areas of long grass. "Such a habit encourages the growth of short, creeping grasses that hippopotamus favours" (Eltringham, 1999, p. 81). Lewison & Carter (2004) showed that hippopotami increase bite rate when foraging farther away from the river. Where the quality of food is low, there is an increase in bite rate and a decrease in the time spent searching. Lewison & Carter (2004, p. 135) suggested that the vegetation is evaluated based on available energy (quality) and search time defined as distance to the river. Increased intake of food when farther from the river is most effective in terms of net energy and search efficiency (Lewison & Carter, 2004, p. 128).

Hippopotami effect their environment by trampling the paths they visit during feeding. The consequence is that these paths are vulnerable to erosion. Rainwater cannot infiltrate into the ground and merely runs over the surface. Feeding on low grasses also adds to erosion.

Hippopotamidae form isolated groups which seldom meet. They tend not to migrate, even if there is a shortage of food. Little is known about the migration of Hippopotamidae, but it is plausible that males migrate and create new offspring elsewhere thus avoiding inbreeding (Eltringham, 1999).

They do not migrate over water as they are not very good swimmers, except in brackish and salty water, where floating is easier. In rivers and lakes they mainly walk on the bottom. They dislike deep water and strong currents. If they get into deep water by accident, they do not swim, but "they progress by a series of porpoise-like leaps off the bottom" (Eltringham, 1999, p. 3).

Another reason not to migrate is that migrating costs a lot of energy. Indeed hippopotami are very economical with their energy; they only eat 40 kg - 100 kg of food a night and they do not move about a lot in the water. They spend their entire day in the water (for temperature regulation) or sunbathing on a sandbank and they only graze during the night (Eltringham, 1999). Although they are protected from sunburn and infections by the red secretion of their skin (Saikawa *et al.*, 2004), they tend to stay close to the water during the day.

Babies hippopotamus are born in the water and they travel on the back of their mother when the water is too deep (Eltringham, 1999). A reason for not being good swimmers might be that hippopotamus cannot float, like elephants do. Elephants produce a lot of gas, which enables them to float. Indeed the amount of food they eat is much larger; an elephant spends its entire day searching for food and its digestion is not at all efficient. Their excrements consist for the larger part of undigested plant remains. *Hippopotamus* has a ruminant-like stomach, consisting of 3 or 4 chambers (depending on the definition of a chamber), two of which are blind sacs. There is no caecum. Non-ruminant plant eaters, like elephants and horses, have a very long caecum. In the caecum, mainly fermentation of cellulose takes place by means of bacteria, which produces a lot of gas. In hippopotamus the fermentation of cellulose presumably takes place in blind sacs and the food is retained in the gut for a longer time thus giving more time for fermentation. The weight of the food consumed is very low for an animal that big and indeed the weight of the gut contents is much higher than in ruminants leading to the suspicion that many hippopotami only feed every other night (Eltringham, 1999).

Mazza (1995) compared the forces applied to the lever system (nuchal crest - occipital condyles – muzzle) in the skull, represented by the angle between the nuchal crest and the occipital condyles (the back of the skull) and the horizontal line between the occipital condyles and the front of the muzzle of *H. amphibius* with the Pleistocene *Hippopotamus gorgops* from Africa and *Hippopotamus tiberinus* from Europe. This angle is nearly 90° in *H. amphibius* and much smaller in *H. gorgops and H. tiberinus.* This means that the grass-eating *H. amphibius* has more extensive jaw movements, which is possibly linked to the presence of particularly tough items in the diet. Thus he concluded that the fossil hippopotami *H. gorgops* and *H. tiberinus* probably fed more on aquatic plants than on grasses. In the fossils from India and Indonesia, described in this paper, this angle resembles that of *H. amphibius*, indicating that they were grass eaters.

Boisserie *et al.* (2005) compared stable carbon isotope composition and micro-wear of tooth enamel of late Miocene hippopotami from Chad with that of *Hippopotamus amphibius*, and concluded that diets of Miocene and recent hippopotami are comparable. There are no indications that the fossil Hippopotamidae from India and Indonesia described in this paper, lived in a very different way from their living relatives.

PART A

3. COMPARISON OF LOCALITIES WITH AND WITHOUT FOSSIL HIPPOPOTAMIDAE IN THE MANGLA-SAMWAL AREA (PAKISTAN)

3.1. INTRODUCTION

Geological-paleontological fieldwork was carried out by a combined team of Howard University (Washington), Geological Survey of Pakistan (Islamabad), National Museum of

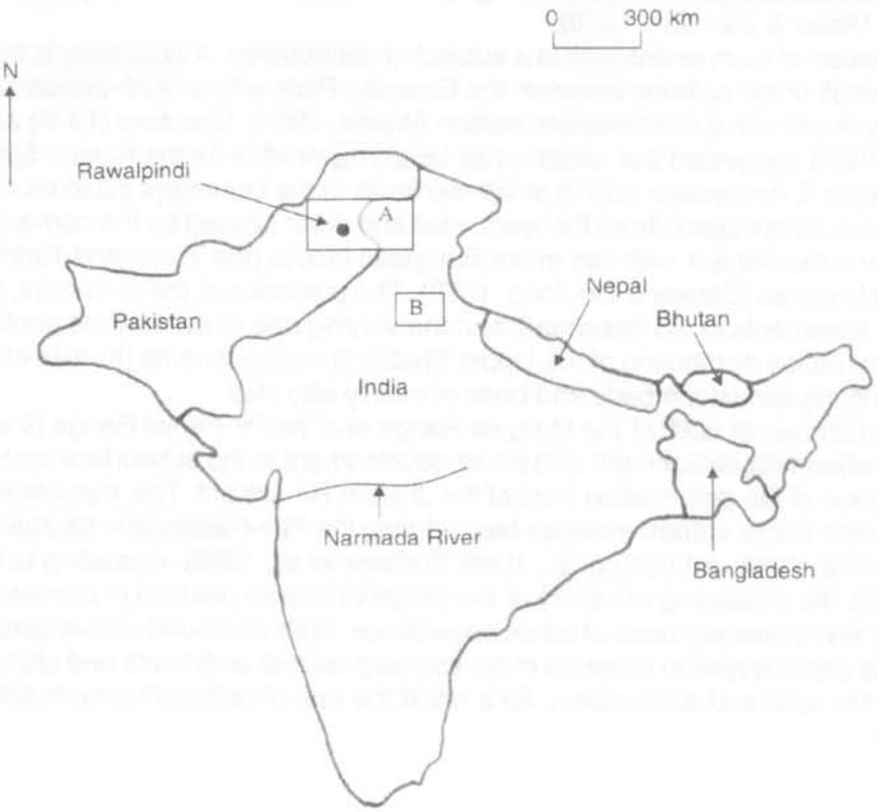

Fig. 1. The Mangla-Samwal area (A; see Fig. 2.) and localities in the Siwaliks where Dubois collected hippopotamus fossils (B; see Fig.13.).

Natural History at Leiden (Naturalis, The Netherlands) and Utrecht University (The Netherlands) in 1984 - 1990 in the Mangla-Samwal Anticline (Figs.1 and 2), about 5 km south of New Mirpur (Azad Kashmir, Pakistan).

The field area measures 19 x 7.5 km^2 (Fig. 3). In the Mangla-Samwal area some 50 fossil localities were discovered. Two extensive bentonite layers, dated 2.4 $\pm$ 0.20 Ma B.P. and 2.56 $\pm$ 0.21 Ma B.P. (Opdyke *et al.*, 1979), were used to correlate the profiles and localities. Five profiles were measured and described, the Jhelawala Kas, Jhel Kas, Samwal, Dok Dara en Rakh sections (Fig. 3 and Appendices I-A – I-E).

Fossil Hippopotamidae are abundant at some places and rare in others. All fossil localities in the Mangla-Samwal area represent fluvial sediments. Below the bentonite layers Hippopotamidae are abundant, in between them and above they are very rare. Behrensmeyer (1976, 1985) and Cutler *et al.* (1999) suggested that such phenomenon can be explained on the basis of paleoecological factors, like an aquatic or non-aquatic environment and vegetation cover (bush, open wood, dense wood, lake bed, plains and swamp), as reflected by sedimentary facies. To check and further elaborate this hypothesis, a comparison is made of localities with and without Hippopotamidae. Differences between sedimentary facies, fossil assemblages and taphonomy are analysed.

3.2 THE SEDIMENTS FROM THE LOWER AND THE UPPER SAMWAL FORMATION

3.2.1. GEOLOGICAL SETTING

The thrust belt of the Himalayan Foreland Basin (Fig. 2) is characterised by sinuous traces with alternating re-entrants and salients (Kumar *et al.*, 2004). A re-entrant is an indentation, a sharp inflexion in the strike of the orogenic belt. It forms a large hairpin-like structure bounded by thrust faults (cf. 1 in Fig 2). The Mangla-Samwal Anticline is located in the NW-SE oriented Jhelum Re-entrant Molasse Basin.

The Jhelum Re-entrant (2 in Fig. 2) is the southern extension of the North-West Syntaxis (1 in Fig. 2; Wadia, 1931), also known as the Hazara-Kashmir Syntaxis (Calkins *et al.*, 1975). It is situated between the Margala Range (4 in Fig. 2) in the west and the Pir Panjal Range in the east (5 in Fig.2.; Visser & Johnson, 1978).

The formation of such re-entrants is a subject of controversy. A possibility is that this structure is the result of the collision between the Eurasian Plate with a north-projecting spur of the Indian subcontinent with a northwestern motion (Wadia, 1931). Crawford (1974) and later Klootwijk *et al.* (1986) suggested that rotation has been responsible for the Kasmir Syntaxis. According to Seeber & Armbruster (1979) strike-slip faults in the basement could be responsible. Simultaneous compression from the west, east and north caused by the convergence of the Indo-Pakistan subcontinent with two minor European blocks (the Turan and Tarim Blocks) is another possible cause (Sarwar & De Jong, 1979). The presence of the re-entrant, the thrust movements, the lineaments in the basement, and the varying rate of subsidence controlled the lateral and vertical facies distribution of the Upper Siwalik fluvial sediments (Kumar *et al.*, 2004), resulting in alternating sandstone beds and beds of mainly silty clay.

Repeated phases of uplift of the Margala Range and the Pir Panjal Range (4 and 5 in Fig. 2) in combination with detachment and thrust development in the subsurface caused the southward migration of the deformation front of the Jhelum Re-entrant. This has influenced the sedimentation within the re-entrant molasse basin during the Plio-Pleistocene (Burbank, 1983; Burbank & Raynolds, 1984; Johnson *et al.*, 1986; Burbank *et al.*, 1986). According to Raynolds & Johnson (1985), the increasing proximity of the orogenic margin resulted in increased sediment supply and increased rates of basin subsidence. With continued convergence of the orogenic belt, the site in question received more source-proximal sediments and ultimately became involved in uplift and deformation. As a result the rate of sediment accumulation in this area diminished.

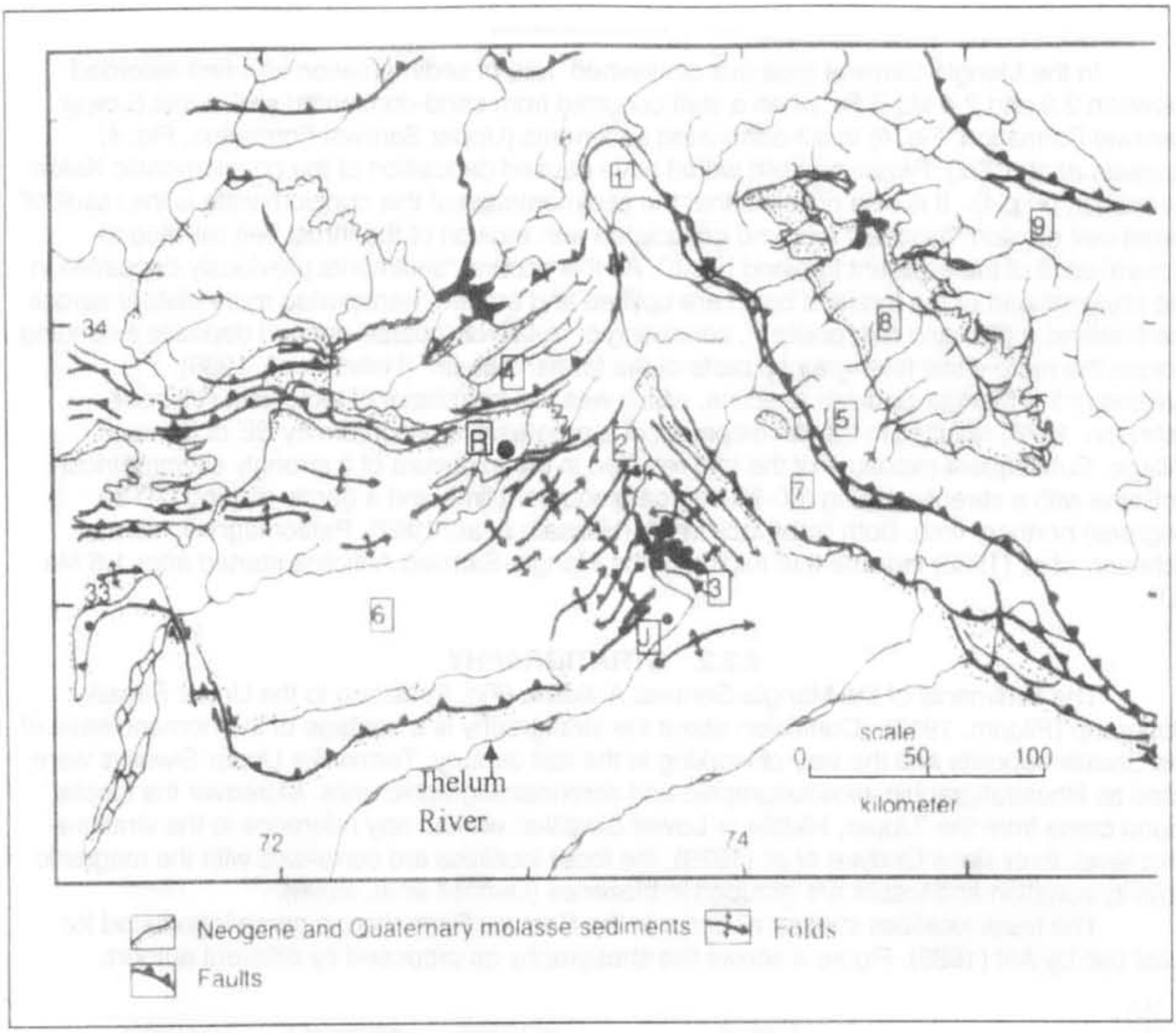

Fig. 2. The geological setting of the Mangla-Samwal area (A in Fig. 1). Modified after Burbank & Reynolds (1984). 1 = North-West Syntaxis; 2 = Jhelum Re-entrant; 3 = Mangla-Samwal area with the town of New Mirpur (see Fig. 3); 4 = Margala Range; 5 = Pir Panjal Range; 6 = Potwar Plateau; 7 = Main Boundary Thrust ; 8 = Kashmir Basin; 9 = Great Himalayan Range; J = Jhelum; R = Rawalpindi.

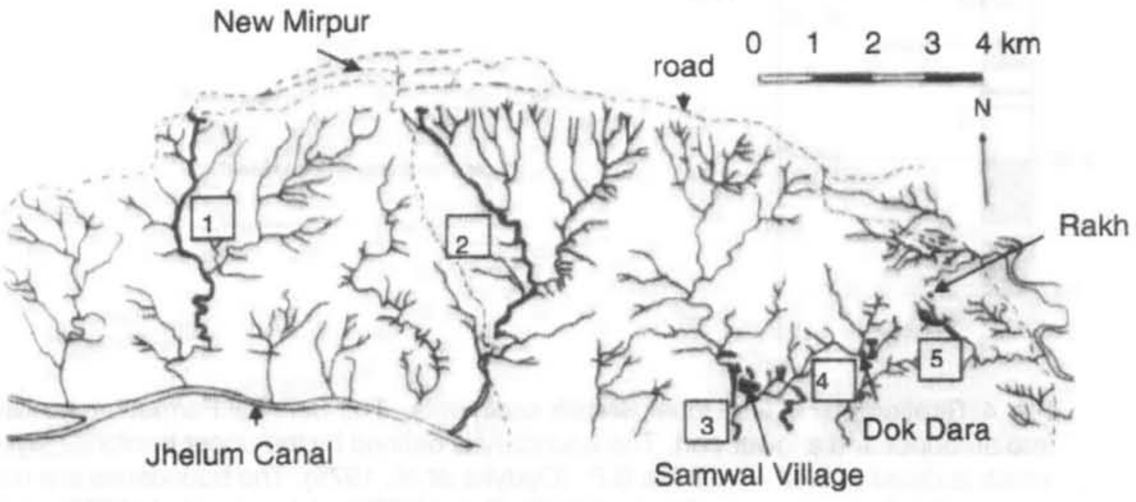

Fig. 3. The Mangla-Samwal area (Fig. 2, no. 3). Location of the Jhelawala Kas (1), Jhel Kas (2), Samwal (3), Dok Dara (4) en Rakh (5) sections.

In the Mangla-Samwal area this diminished rate of sedimentation was first recorded between 2.9 and 2.4 Ma B.P., when a shift occurred from sand-dominated sediments (Lower Samwal Formation, Fig. 4) to silt-dominated sediments (Upper Samwal Formation, Fig. 4; Hussain *et al.* 1992). Renewed uplift would have caused deposition of the conglomeratic Kakra Formation (Fig. 4). It is also possible that the sedimentation of this conglomerate is the result of thrust-belt erosion. "Isostatic rebound associated with erosion of the thrust belt will lead to flexural uplift of the adjacent foreland basin". As this occurs, "sediments previously deposited in the proximal part of the foreland basin are uplifted and eroded, transported more distally across the foreland region and redeposited", consisting of "relatively coarse-grained deposits extending across the more distal finer-grained parts of the foreland basin" (Heller *et al.*, 1988).
Folding of the Mangla-Samwal Anticline, which was the last phase of tectonism (Visser & Johnson, 1978) resulted in the development of a progressive unconformity SE of Samwal Village. Subsequent exposure of the fold resulted in the exposure of a strongly asymmetrical anticline with a steeply sloping (60-90 degrees) southern limb and a gently dipping (10-30 degrees) northern limb. Both limbs lack faults (Hussain *et al.*, 1992). Paleomagnetic data of Johnson *et al.* (1986) indicate that folding of the Mangla-Samwal Anticline started after 1.6 Ma B.P.

3.2.2. STRATIGRAPHY

The sediments of the Mangla-Samwal Anticline (Fig. 5) belong to the Upper Siwalik Subgroup (Pilgrim, 1913). Confusion about the stratigraphy is a heritage of the nomenclature of the Siwalik deposits and the way of working in the last century. Terms like Upper Siwaliks were used as lithostratigraphic, biostratigraphic and chronostratigraphic units. Moreover the fossils found came from the "Upper, Middle or Lower Siwaliks" without any reference to the stratigraphic level. Ever since Opdyke *et al.* (1979), the fossil localities are correlated with the magnetic polarity zonation and fossils are grouped in biozones (Dennell *et al.*, 2006).

The fossil localities studied all occur in the Samwal Formation, a name introduced for local use by Arif (1985). Figure 4 shows the stratigraphy as proposed by different authors.

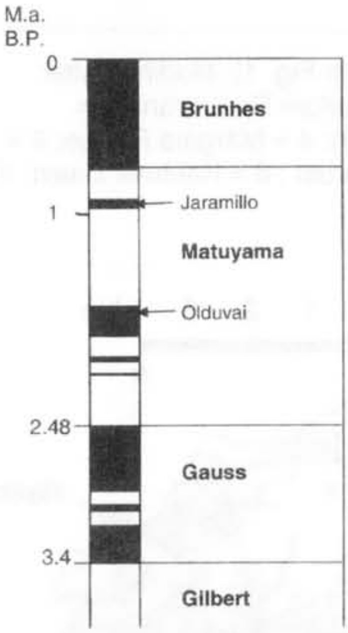

Classical nomenclature of the Siwaliks (Pilgrim, 1913)	Fatmi (1973)	Johnson et al. (1979)	Arif (1985)
"Boulder Conglomerate"	Lei Conglomerate	Mirpur gravels and silt	Mirpur Formation
			Kakra Formation
"Pinjor"			
	Soan Formation	Upper Siwalik	
"Tatrot"			Samwal Formation

Fig. 4. Stratigraphy of the Upper Siwalik sediments. The Samwal Formation is divided into an upper and a lower part. The boundary is defined by the upper bentonite layer, which is dated at 2.40 + 0.20 Ma B.P. (Opdyke *et al.*, 1979). The boundaries are not given in this figure because Pilgrim (1913), Fatmi (1973), Johnson *et al.* (1979) and Arif (1985) did not give exact boundaries, but they are shown is Fig. 5.

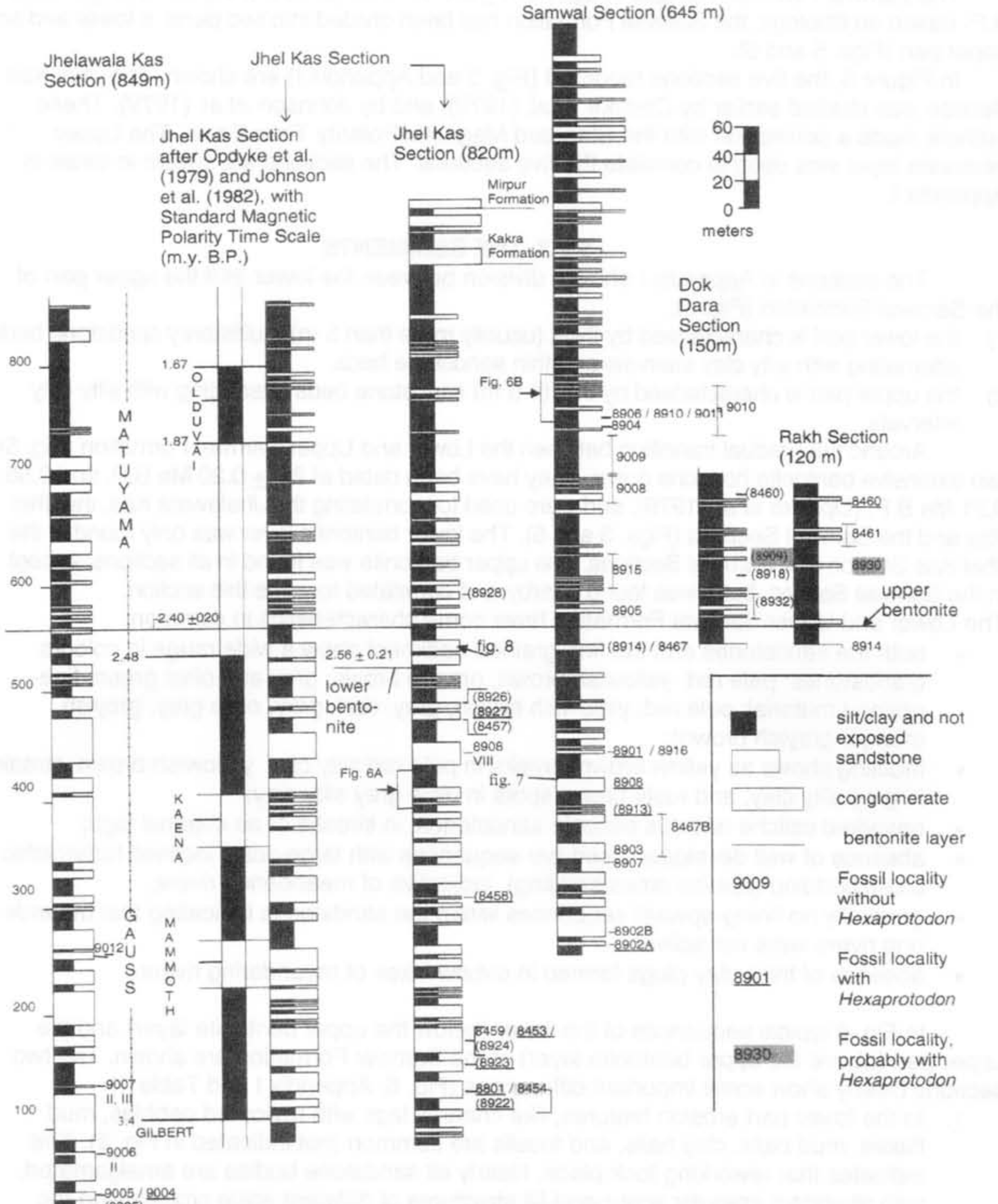

Fig. 5. Schematic representation of the five sections (Fig. 3) in the Mangla-Samwal Anticline. The sediments belong to the Samwal Formation, except at the top of the Jhel Kas Section where the Kakra and Mirpur Formations occur. Correlation of the sections was established by tracing the upper bentonite layer. The numbers indicate fossil localities in the section, numbers between brackets are localities that were traced towards the nearest section. All localities have the prefix HGSP (Howard Geological Survey of Pakistan).

The Samwal Formation ranges in age from $\pm$ 3.4 Ma B.P. (base not exposed) to $\pm$ 1.6 Ma B.P. Based on lithology, the Samwal Formation has been divided into two parts, a lower and an upper part (Figs. 5 and 6).

In Figure 5, the five sections recorded (Fig. 3 and Appendix I) are shown. The Jhel Kas Section was studied earlier by Opdyke *et al.* (1979), and by Johnson *et al.* (1979). These authors made a correlation with the Standard Magnetic Polarity Time Scale. The Upper bentonite layer was used to correlate the five sections. The sections are shown in detail in Appendix I.

3.2.3. THE SEDIMENTS

The sections in Appendix I show a division between the lower and the upper part of the Samwal Formation (Fig. 5):

1) the lower part is characterised by thick (usually more than 5 m) multistorey sandstone beds alternating with silty clay intervals and thin sandstone beds.
2) the upper part is characterised by thin (1-5 m) sandstone beds alternating with silty clay intervals.

Around the gradual transition between the Lower and Upper Samwal Formation (Fig. 5) two extensive bentonite horizons occur. They have been dated at 2.4 $\pm$ 0.20 Ma B.P. and 2.56 $\pm$ 0.21 Ma B.P. (Opdyke *et al.*, 1979), and were used for correlating the Jhelawala Kas, the Jhel Kas and the Samwal Sections (Figs. 3 and 5). The lower bentonite layer was only found in the Jhel Kas Section and Samwal Sections. The upper bentonite was found in all sections, except in the Samwal Section, but it was found nearby and correlated towards this section.
The Lower and Upper Samwal Formation have some characteristics in common:

- both the sandstones and the fine-grained sediment show a wide range in colours (sandstones: pale red, yellowish brown, orange brown, grey and olive green; fine-grained material: pale red, yellowish brown, grey, dark grey, olive grey, greyish orange, greyish brown);
- mottling shows as yellow brown streaks in pale red silty clay, yellowish brown streaks in grey silty clay, and rusty brown spots in olive grey silty clay;
- reworked caliche nodules occur in sandstones, in streaks or as channel lags;
- absence of well developed point-bar sequences with large-scale inclined heterolithic cross bedding (epsilon cross bedding), indicative of meandering rivers;
- generally no fining-upward sequences within the sandstones indicating that meandering rivers were not active
- absence of thick clay plugs formed in oxbow lakes of meandering rivers.

In Fig. 6 typical sequences of the lower (below the upper bentonite layer) and the upper part (above the upper bentonite layer) of the Samwal Formation are shown. The two sections clearly show some important differences (Fig. 6, Appendix I and Table 1).

1. In the lower part erosion features, like channel lags with reworked pebbles, mud flakes, mud balls, clay balls, and fossils are common (not indicated in Fig. 5). This indicates that reworking took place. Nearly all sandstone bodies are amalgamated, with abundant irregular scour-and-fill structures of different scale crosscutting the sandstones. At various places incisions within the sandstones are about 2-4 m deep indicating that these (minor) channels reached depths of at least that magnitude. These erosional features are related to the braided character of the river and the vertical stacking of the deposits (multistorey sandstones). In the upper part few erosion surfaces are present, especially at the bases of sandstones. Internal erosion surfaces are not common. Most sandstones in the upper part were deposited as sheets under high-velocity conditions, likely during (short) periods of high discharge.
2. The lower part shows a variety of sedimentary structures on different scales, such as channel fills, bars, parallel lamination, low-angle cross bedding, planar and trough cross bedding. Planar and trough cross bedded sets with preserved parts of the sets being up to 1.5 m high (Fig. 7) occur. In these sandstones fossils were found. They

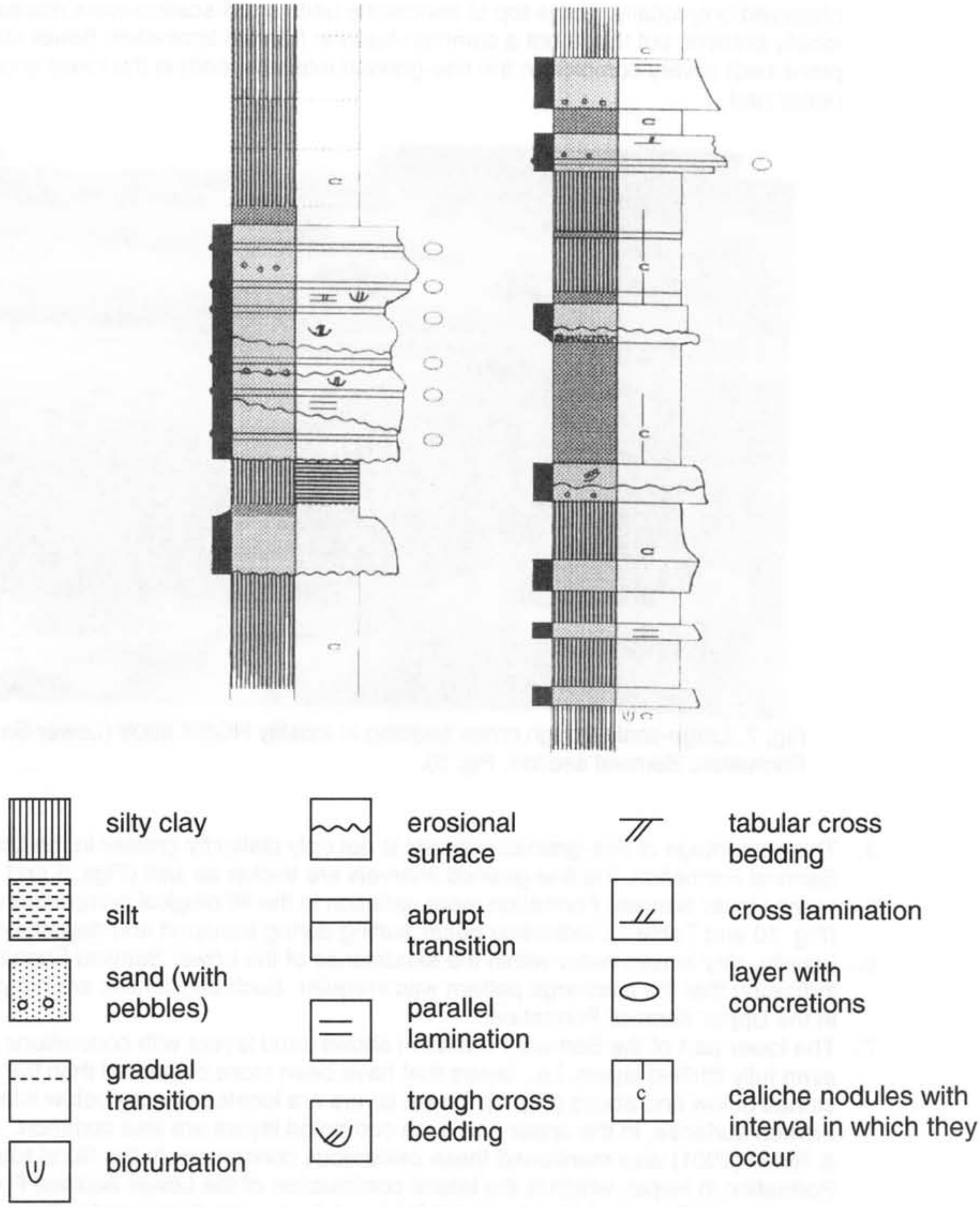

Fig. 6 A.: typical sequence in the Lower Samwal Formation; B.: typical sequence in the Upper Samwal Formation. The position of the sequences in the profiles is shown in Fig. 5.

also contain remains of tree trunks and wood. The high-angle dipping and steep slip faces of the planar cross bedding are related to the migration of high bars (cf. Coleman, 1969;.cf. Reineck & Singh, 1980).

3. In the upper part sedimentary structures are less common than in the lower part, parallel lamination being most common. Planar and trough cross bedding was observed only locally. At the top of sandstone units small-scale current ripples are locally present, but this is not a common feature. Parallel lamination (lower stage plane bed) is very common in the fine-grained intervals, both in the lower and the upper part.

Fig. 7. Large-scale trough cross bedding in locality HGSP 8908 (Lower Samwal Formation, Samwal section, Fig. 5).

4. The percentage of fine-grained material is not only distinctly greater in the Upper Samwal Formation, the fine-grained intervals are thicker as well (Figs. 5 and 10).
5. In the Upper Samwal Formation more variation in the lithological composition occurs (Fig. 10 and Table 1), indicating better sorting during transport and deposition.
6. Locally, clay lenses occur within the sandstones of the Lower Samwal Formation, indicating that the discharge pattern was irregular. Such clay lenses are not present in the Upper Samwal Formation.
7. The lower part of the Samwal Formation shows sand layers with concretions and even fully lithified layers, i.e., layers that have been more cemented than the sandstones below and above (Fig. 8). These layers are located directly below internal erosion surfaces. In the upper part such cemented layers are less common. Corvinus & Rimal (2001) also mentioned these calcareous concretions in the Surai Khola Formation in Nepal, which is the lateral continuation of the Lower Samwal Formation. According to Tandon & Varshney (1991) "such layers are developed in the subaerial vadose zone due to capillary action under alternating wet and dry climatic conditions". Kumar *et al.* (2004) suggest that "the occurrence of these cemented layers" in combination "with erosion surfaces may be due to channel avulsion at a relatively fixed point, which caused erosion of overbank facies" resulting in locally alternating wet and dry conditions. In the upper Samwal Formation such cemented layers are rare.
8. Current directions: the sandstones from the Lower Samwal Formation show a small variation in current directions, i.e., south-east to south (Hussain *et al.*, 1992: Fig. 4), in accordance with the braided character of the river. In the Upper Samwal Formation

few current directions were measurable; they mostly indicate transport to the south-east. Among the few measurable current directions, there was evidence for variable current directions in HGSP 8904 where moreover an east-west orientated channel fill was found on the other side of the hill (not in Appendix I). These deposits very much resemble the multistorey sandstones of the Dehra Dun subbasin, a Himalayan Foreland Basin in India, described by Kumar et al. (2004), which have a similar tectonical setting and were interpreted as alluvial fan deposits.

Fig. 8. Parallel lamination in sandstone of the Lower Samwal Formation, some laminae having been more cemented than others. The pole measures 1 m. See for position Figure 5.

9. North of Samwal a single channel sandstone layer of 11 m thick in the Lower Samwal Formation completely wedges out over a horizontal distance of 35 m, approximately perpendicular to the paleocurrent direction. Such was not seen in the sandstones of the Upper Samwal Formation.
10. In the lower part bioturbation, mottling and caliche nodules are less common than in the upper part (Fig. 6), indicating the (periodic) presence and evaporation of water during deposition of the upper part and/or a lower deposition rate in the upper part.

These observations lead to the conclusion that the sediments of the **Lower Samwal Formation** have been deposited by major trunk rivers, with a braided character and a catchment in the Himalayan Mountains. The course of these major trunk rivers was constrained by the Jhelum Re-entrant (Visser & Johnson, 1978), which explains the multistorey character of the sandstones and also the small variation in transport directions (S – SE). These deposits resemble the more proximal parts of the recent Kosi Fluvial Fan, which has a similar tectonical setting (Kumar *et al.*, 2004). The laterally discontinuous thin sandstones (1-3 m) are interpreted as crevasse deposits (cf. Jenkinson et al., 1989).
The horizontally bedded sandstones in the **Upper Samwal Formation** were deposited as sheet floods in the upper flow regime. The combination of the sedimentary structures in the upper part suggest that this part was deposited by a system of smaller-scaled streams on the fan as described for the Markanda terminal fan in India by Parkash *et al.* (1983). The commonly observed increase in the percentage of horizontally bedded sand facies from apex to toe of the fan (Parkash *et al.*, 1983) suggests that the upper part of the Samwal Formation

represents the more distal part of the fan system. Most of the sedimentary structures, like trough and planar cross bedded sand, cross laminated sand and flaser bedded sand, as described for the Markanda Fan (Parkash *et al.*, 1983), have been lost due to bioturbation. The presence of a grey mollusc-bearing silty layer in localities HSGP 8906 and HGSP 8910 (Samwal Section, Fig. 5) indicates that in depressions, perhaps between distinct lobes, lacustrine environments established, which is in accordance with fossils of crocodiles and turtles found in these localities.

In the lower part of the Samwal Formation, the fine-grained material was mainly deposited as overbank deposits. In the upper part of the Samwal Formation the fines were deposited as overbank deposits, crevasse splays and in the channels by settling from suspension during relatively low discharge.

3.2.4. LATERAL DIFFERENCES IN THE SAMWAL FORMATION

The three main sections (Fig. 3), from west to east, Jhelawala Kas (850 m), Jhel Kas (820 m) and Samwal Section (645 m), show the following differences (Table 2).

- From west to east there is a decrease in the percentage of sandstones in the lower part (Figs. 9-11 and Table 2);
- The average maximum thickness of the sandstones also decreases from west to east, both in the upper and lower part (Figs. 9-11 and Table 2).

The Jhelawala Kas Section lies closer to the north-south axis of the re-entrant basin (the depocentre) than the Jhel Kas and Samwal Sections (Fig. 3). This explains the decrease in the percentage of sandstone and in the thickness of sandstone beds from west to east, moving away from the re-entrant, caused by the more lateral position. By measuring the thickness of the sediments between two volcanic ash layers, Visser & Johnson (1978) indeed found that the sedimentation rate increased towards the apex of the re-entrant. A more rapid subsidence of the structural trough in the centre of the re-entrant as compared to the adjacent parts of the molasse basin (Visser & Johnson, 1978) led to increased accommodation space and sedimentation rate towards the apex of the Jhelum Re-entrant (Johnson *et al.*, 1979). Indeed, re-entrants are the major sources of sediment, as they are the preferential sites for the passage of major rivers into the molasse basin (Raynolds, 1980).

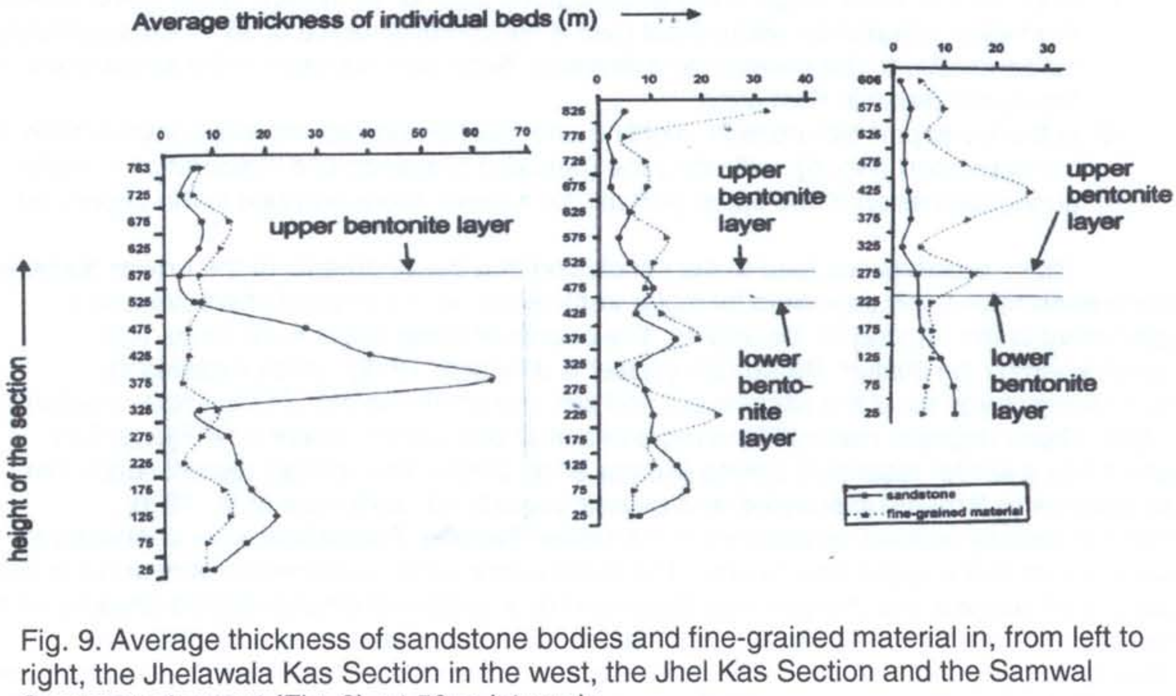

Fig. 9. Average thickness of sandstone bodies and fine-grained material in, from left to right, the Jhelawala Kas Section in the west, the Jhel Kas Section and the Samwal Section to the east (Fig. 3), at 50 m intervals.

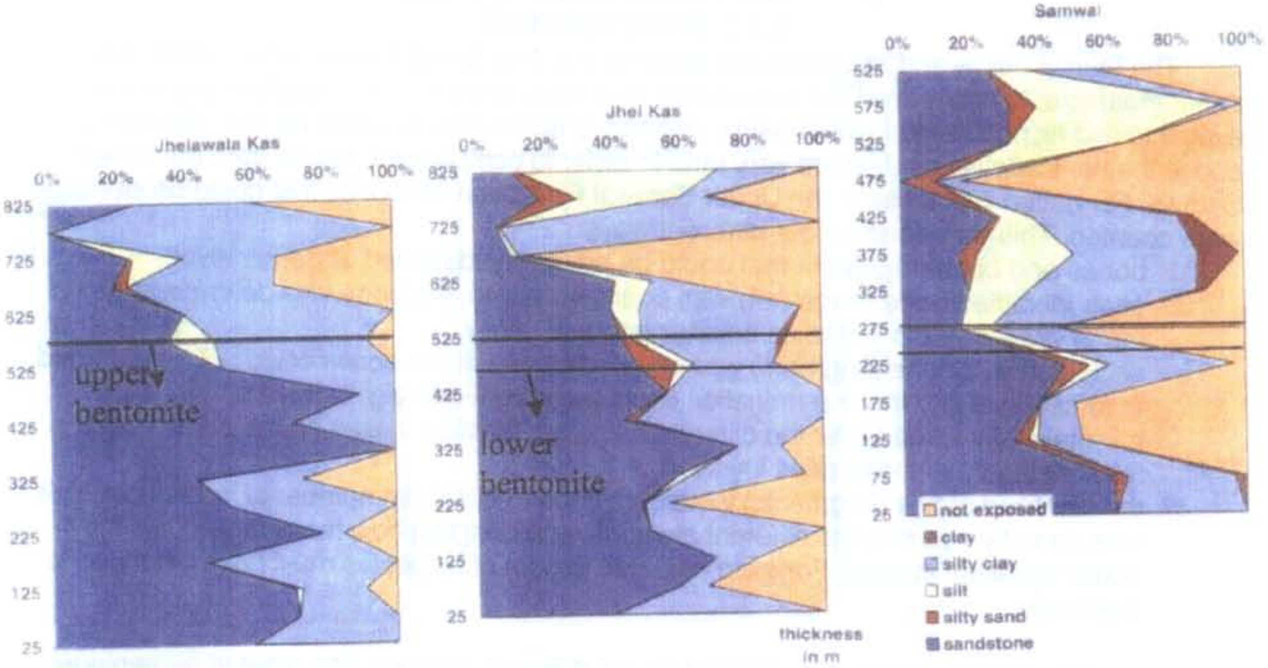

Fig. 10. The lithological composition in percentages for 50 m intervals shows the lateral differences in lithology and grain size between the three main sections (Fig. 3).

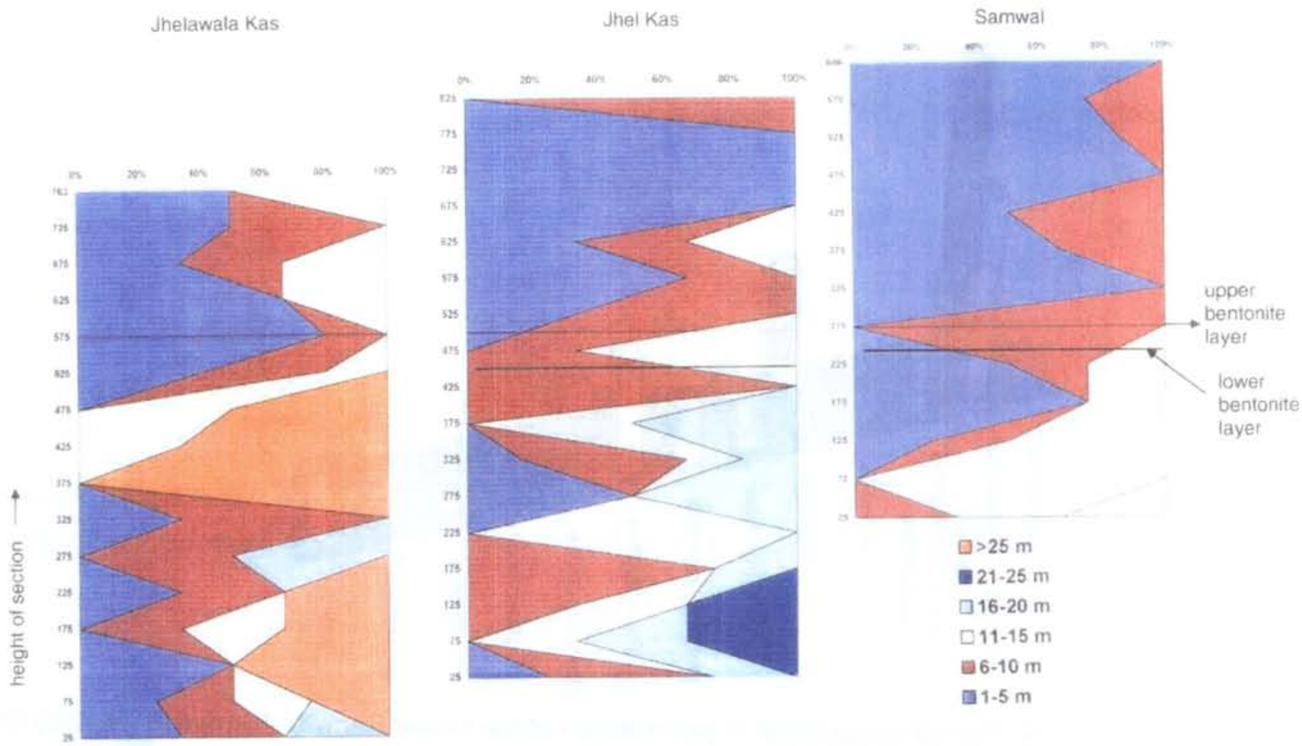

Fig. 11. The percentage of sandstone beds with different thickness for 50 m intervals From left to right the Jhelawala Kas, Jhel Kas and Samwal Sections.

3.3. THE FOSSIL ASSEMBLAGES

3.3.1. INTRODUCTION

The faunas below and above the bentonite layers (Fig. 5 and Tussain *et al.*, 1992: Fig. 5) are comparable; at family level the same kinds of animals were found. Therefore one would expect to find hippopotamus fossils below and above the bentonite layers as well. However, above the bentonite layers they are very rare. In order to compare the fossils from the Lower Samwal Formation with those in the Upper Samwal Formation, all bones that could be identified were counted. This was done in four different ways:

1. bones and bone fragments that could be positively identified at genus level;
2. each identified bone (fragment) was counted as one. If a bone was determined at family level, it was counted as belonging to that family.
3. each identified bone (fragment) was counted as one. If the bones could not be identified at family level and the determination could be assigned to e.g. carnivora, they were proportionally spread over the different carnivore families, based on the percentages from method 2 of the families involved.
4. the identified bones (fragments) were converted to minimum number of individuals. This was done by counting the different elements and deciding how many individuals they could represent at least. For example 5 left femora of a species must have belonged to 5 animals.

Although the percentages are different for the different methods, the order in percentages is quite comparable (Table 3). The results of method 3 are shown in Fig. 12. From this figure, it is apparent that there are significant differences, especially with respect to Hippopotamidae, crocodiles, turtles, Equidae and Proboscidae.

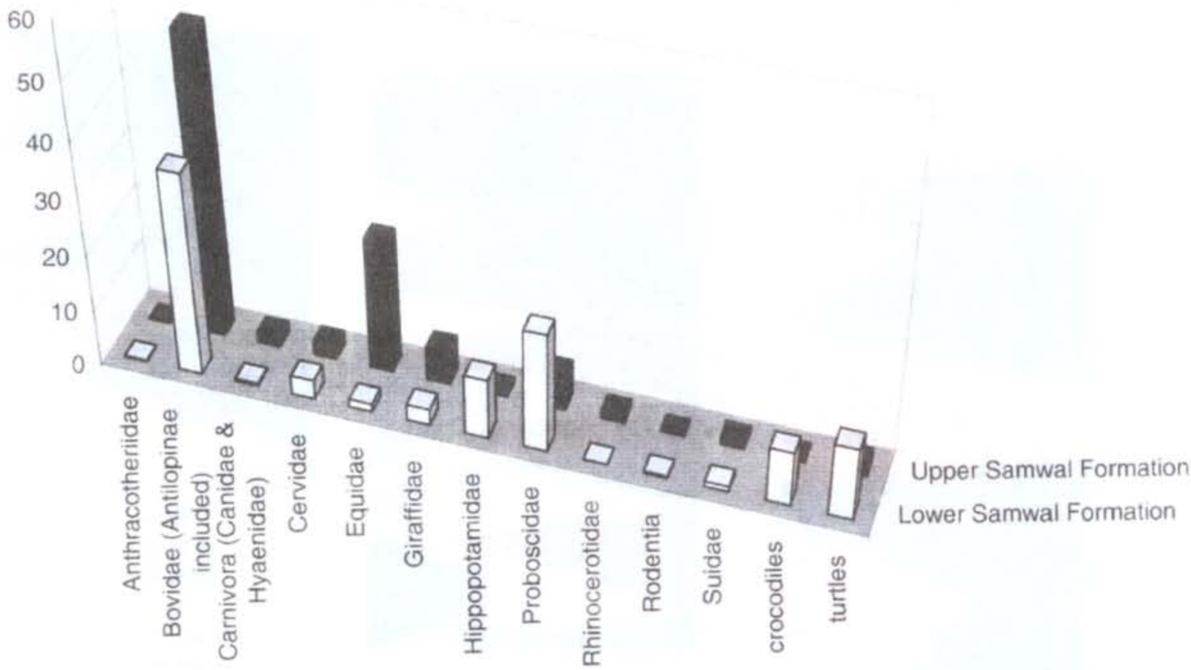

Fig. 12. Faunal composition in percentages of the Lower Samwal Formation (N=435) and the Upper Samwal Formation (N=762). Percentages from Table 3, method 3.

3.3.2. COMPARISON OF THE FOSSIL ASSEMBLAGES

To test if the differences in composition (π) between the fossil assemblages 1 and 2 (below and above the ash layers) are significant, a method of Wonnacott & Wonnacott (1977) was used. This method starts from the principle that there is a normal division (Gauss-division) of the differences compared. This method was especially designed for comparing small samples. In their formula 8.44, the 95% reliability of the difference is determined (Wonnacott & Wonnacott, 1977):

$$\pi_1 - \pi_2 = (P_1 - P_2) \pm 1.96 \sqrt{\frac{P_1\,(1-)}{N_1} + \frac{P_2\,(1-P_2)}{N_2}}$$

in which

$\pi_1 - \pi_2$ = the difference between the composition of the fossil assemblages. If there is a possibility that the difference is zero (no difference) then the difference is not significant;

P_1 = percentage divided by 100 of the fossils found at the Lower Samwal Formation, based on the numbers in Table 3;

P_2 = percentage divided by 100 of the fossils found at the Upper Samwal Formation, based on the numbers in Table 3;

N_1 = the total number of fossils found in the Lower Samwal Formation;

N_2 = the total number of fossils found in the Upper Samwal Formation.

In Table 4 the results are shown for all four methods of counting mentioned above in Chapter 3.3.1. using formula 8.44 of Wonnacott & Wonnacott (1977).

If the difference between π_1 and π_2 could be 0 (so if one is negative and the other positive), then the difference is considered not significant, because 0 falls within the reliability interval of 95%. The results in Table 4 show that there is a significant difference between the sites below and above the bentonite layers for *Hexaprotodon*, crocodiles, turtles, Proboscidae and Equidae. The first four are less abundant above the bentonite layers, the latter is more abundant. For the equids and *Hexaprotodon* all four methods give a significant difference. For proboscids, crocodiles and turtles method 4 does not give a significant difference. This is ascribed to the way in which the tusk fragments, dermal plate fragments and fragments of the carapax were counted. Where a lot of those fragments were present at a site, they were still counted as one individual, because there was no proof that more individuals had been present. Indeed, in this way the differences between the sites below and above the bentonite layers were smothered.

3.4. TAPHONOMY

3.4.1. COMPARISON

Voorhies (1969) made a division in groups, based on the transportability of fossil vertebrates, which explains the bones found in a certain environment. The fossils in Voorhies Group I are easily transportable elements, Voorhies Group II represents fossils that are variably transportable and fossils of Voorhies Group III are hard to transport and are commonly found to have been deposited as part of channel lags.

In the Samwal Formation three types of taphonomy (not identical to Voorhies Groups) occur (Table 5). The position of the localities is shown in Fig. 5. The three types of taphonomy are:

1. scattered occurrences of isolated bones in multistorey sandstone beds, ranging in thickness from 6 to 24 m (average 10.5 m). The fossils (N=334) occur as part of channel

lags at the base of sandstone beds in a matrix of coarse sand, in association with mud balls, reworked caliche nodules and/or pebbles. They are also present in the middle of sandstone layers, in cross bedded sandstone facies. In these sandstones no caliche nodules were found. The trough and planar cross bedding in these sandstones show well preserved foresets of up to 1.5 m high. The sandstones also contain remains of tree trunks and wood. Some of the bones (N=159) have been well preserved, like a complete *Hemibos* skull, while others have suffered from transport (fragments N=175). The representation of the bones is shown in Table 5. Most elements are molars (37.5%). Long bones, like femur, tibia, radius and ulna are present, although most are broken (Table 5). Fragile bones like scapula, costa and vertebra are present, although not frequent (14). Small bones like carpalia and tarsalia are present (12).

2. low fossil concentrations or isolated fossils found in relatively thin sandstone beds (1-7 m, average 3 m thick). These beds can be traced over distances of 1 km at maximum. The sandstone beds consist of very coarse to fine sand and show fining-upward. Two channels were recognized. Trough cross bedding is locally present in the sandstone beds and also parallel lamination occasionally occurs. This type includes localities with proboscidean remains of a single individual and localities with crocodile, turtle and bovid material. Most fossils are molars (39%). The long bones are damaged quite often, but not as often as in the first type (7 out of 10; 70%). Fragile bones are less represented compared to the first type (only 2 fragments), indicating more intense weathering and/or transport, compared with taphonomy type 1. Only one carpal bone was found (Table 5).
3 taphonomy type 3 occurs only in the Upper Samwal Formation. The sediments in which the fossils are embedded consist of (sandy) silt, overlying medium to coarse sandstone beds. The fossiliferous layers are generally overlain by a fine-grained, bioturbated interval with abundant pedogenic calcium carbonate nodules (caliche). Parallel lamination is the only sedimentological structure encountered in these layers. Fossils have often been partly dissolved, presumably during soil formation.

The fossils of **taphonomy type 1** are consistent with Voorhies Group III, in which most bones are hard to transport, like skulls, mandibles and teeth (Table 5) and are found as part of channel lags or in trough and planar cross bedded sands. In this taphonomy group, they make up 53.6% of the bones. The long bones are almost all fragmented (29 out of 33; 88%). Other fossils show signs of rounding which indicates that they were reworked or suffered from weathering before they were buried.

The sedimentological features of Voorhies Group III indicate high-energy conditions in channels. Bones of mammals that perished close to the river were transported during some time over some distance before a thick sand cover covered them. In this environment, the fossils found are of water-bound animals like Hippopotamidae, crocodiles and turtles, i.e., animals living and dying in or near the river. The percentage of these animals is quite large (33.2%) compared to their percentage in taphonomy group 3 (3.3%). This taphonomy is primarily found in the Lower Samwal Formation (19 out of 21 localities) and mostly in the Jhel Kas Section (11 out of 21 localities; Appendix II).

The fossils found in **taphonomy type 2** representing bones that are hard to transport, mostly belong to Voorhies Group III (58.5%), as well. It resembles taphonomy type 1, but the sandstones in which the bones are found are much thinner and the bones were mostly not deposited as part of channel lags, like in taphonomy type 1; the sandstones generally do not have any mud balls, reworked caliche nodules or pebbles. This type of taphonomy occurs mostly in the Lower Samwal Formation (10 out of 15 localities) in the Jhel Kas and Samwal Sections (Table 5 and Appendix II).

The fossils of **taphonomy type 3** represent all three Voorhies Groups, indicating that hardly any transport took place. Of the long bones 75% is fragmented, which indicates weathering and/or trampling. Fragile bones (4.7%) and all small bones like carpalia and tarsalia are present (8.5%). The bones were not transported (over long distances) and accumulated in a fairly complete (some bones are still articulated) and fresh state and were rapidly covered with sediment. All bones are represented, including very small ones like sesamoids and fragile ones, like fibulae. The fossils were found in crevasse deposits, in abandoned channels and behind the levees on the floodplain. Water-bound animals are far less abundant than in the other two taphonomy types, which is an indication that water was possibly not present throughout the year.

Among the localities belonging to this taphonomy type are HGSP 8460 and HGSP 8904, both with a very high concentration of fossil remains, of which some are still articulated. Long bones are usually complete but fractured, and fragmented bones are found as well. A number of long bones shows a preferred orientation. In locality HGSP 8460, 25% of the long bones (N=71) have a north-south orientation, consistent with the general N-S current direction. In locality HGSP 8904, 22.5% (N=80) have an east-west orientation. This matches the channel direction in the sandstone layer about 0.65 m below the fossil layer. In both localities fragile and small bones are abundant. This indicates that the water current was strong enough to orientate the long bones consistent with the general current direction, but not strong enough to transport and carry away the small bones. The bones only sporadically show tooth marks, indicating only incidental scavenging of bones by carnivores.

This type of taphonomy is most likely the result of mass starvation. At locality HGSP 8460, the high percentage of isolated teeth can be explained by their high density and compact structure, causing them to have a high burial potential and not easily to be transported. More or less the same applies for the metapodials and large tarsal bones, which are also compactly built and have subrounded surfaces (Behrensmeyer, 1975, 1976). The lack or low frequency of fragile and light elements is due to low burial potential and fluvial sorting (cf. Voorhies, 1969; Behrensmeyer, 1991). A possible explanation is that the elements have been derived from a nearby death assemblage, which could have been caused by animals dying from drought at a place where water used to be (cf. Shipman, 1981). Water flow later removed the lighter elements from the site and orientated the long bones. The tooth marks, which were sporadically found and the presence of coprolites point to carnivore activity. The completeness of the major part of the material indicates rapid sediment coverage, although the fracturing seen on the long bones suggest that especially these bones suffered from weathering before burial (De Visser, 1996). This locality gives a good representation of the fossil fauna at that particular moment of (mass) mortality, because the fossils represent many different taxa.

At locality HGSP 8904, the presence of very light and small bones and the of articulated elements show that they were probably transported as (parts of) complete skeletons. Once they had been laid down, no or not much transport took place anymore. Some fractured bones were dissected by (now clay-filled) cracks, with the pieces still in the correct relative position, indicating that no vertical post-depositional soil movement occurred. Therefore, the presence of bone fragments, vertical standing bones and broken elements was most likely caused by trampling. Sporadical tooth marks, coprolites and remains of Hyaenidae and Canidae indicate the presence and activity of carnivores. The faunal composition of this locality is dominated by (young) bovids. An explanation for this is that HGSP 8904 represents drowned animals, e.g. a large herd of migrating bovids crossing a river, like still happens in the Serengeti, Africa (Sinclair & Norton-Griffiths, 1995). There many animals drown, especially young ones (De Visser, 1996). Their carcasses accumulate in large quantities downstream (Behrensmeyer & Hill, 1980).

3.4.2. DISCUSSION

As described above, fossils are found in or near fossil fluvial channel fills in the **Lower Samwal Formation**. Hippopotamus finds are abundant (taphonomy types 1 and 2, Chapter 3.4.1.). The difference between taphonomy types 1 and 2 is related to the lateral differences described in Chapter 3.2.3. Type 1 occurs mainly in the Jhelawala Kas Section in the west, close to the depocentre of the Jhelum Re-entrant, and type 2 occurs mainly in the Jhel Kas and Samwal Sections, further away from the depocentre, where the sandstones are thinner.

In the **Upper Samwal Formation**, on the other hand, hippopotamus fossils are rare and fossils are found in crevasse deposits, abandoned channel fills and in the floodplain (taphonomy type 3). This is in accordance with the results of Behrensmeyer (1976 and 1985), who found abundant *Hippopotamus* fossils (6 - 21% of all fossils found in the Lake Turkana region in Africa) in the more aquatic environments (channels and delta margins) and low amounts (2% of all fossils found in that area) of *Hippopotamus* in floodplain assemblages (Behrensmeyer, 1976: Table 2). There is no reason not to conclude that also in Asia the presence or absence of Hippopotamidae can be explained by paleoecological factors as Behrensmeyer (1976 and 1985) demonstrated for the Lake Turkana region in Africa.

According to Badgley (1986) bone assemblages in the Siwalik system that experienced fluvial transport are a good representation of the original community composition.

Basu (2004) concluded that the ecosystem of the Siwaliks in India primarily existed of wooded grassland and grassland, and that after 2.5 Ma the ecosystem became increasingly dry and in favour of the grassland. This is consistent with the results of analyses of soil carbonates ($\delta^{13}C$), that show a clear increase of grassland environment in the nearby Pabbi Hills after 1.7 Ma (Dennell *et al.*, 2006). After 1.7 Ma, aquatic habitats were far less abundant than before (Basu, 2004). This change of ecosystem, consistent with the sedimentological data, was caused by a change in climate, triggered by the tectonic activity described in Chapter 3.2.1. (Burbank & Raynolds, 1984; Burbank *et al.*, 1986) or by a global change towards a cooler, drier and more variable climate associated with the start of glaciations (Patnaik, 2003). This climate change also triggered the migration of *Equus* into Asia (Hussain *et al.*, 1992).

Basu (2004) recognized two distinct faunal zones below and above a tuff layer (of volcanic origin, comparable with the bentonite layers) in the Jammu area (India), which was dated at 2.5 Ma. Patnaik (2003) recorded a significant change in the faunal composition of the rodents in India, also around 2.5 Ma, with a great diversification of murid species. He explained this as the result of an intensification of monsoons, "which is supported by the occurrence of a diverse palynological assemblage, reflecting alternately wet and dry conditions". This is also found by Jablonski (2004) who concludes that the disappearance of *Hexaprotodon sivalensis* was due to a "dramatic increase in seasonal patterns of rainfall and river flow, which would have resulted in many river systems being dry for months of the year". This seasonality of rainfall was the result of an "intensification of the winter and summer monsoons", related to the uplift of the Tibetan Plateau (Jablonski, 2004). Dennell (2004) reacted to this by stating that *Hexaprotodon sivalensis* persisted in the Pabbi Hills area until at least 1.7 Ma, so longer than in the Samwal area (2 Ma). According to Dennell *et al.* (2006), *Hexaprotodon* became extinct during or shortly after the Olduvai subchron in the Pabbi Hills area. Therefore the disappearance of the hippopotami from the Samwal Area is probably the result of a local change in the river system, rather than only extinction due to the climate change.

3.4.3. CONCLUSION

The difference between the Lower and the Upper Samwal Formation is the result of a climate change, caused by tectonic activity, in combination with global climate change. The channels became smaller and the many pedogenic features like mottling and the presence of caliche nodules suggest that the streams did not carry water the year round. This is confirmed by other studies and it is concluded that an intensification of monsoons caused seasonality in rainfall.

The difference in faunal composition and the taphonomy of the fossils between the Upper and Lower Samwal Formation and the rarity of hippopotamus in the Upper Samwal Formation is also due to this change in climate and the consequent change in the river system.

PART B: PALEONTOLOGY

INTRODUCTION

In the previous chapter, it was demonstrated that the presence or absence of hippopotamus fossils in continental Asia is related to paleoecological factors as previously suggested by Behrensmeyer (1976,1985) for the Lake Turkana Basin.
In the Lake Turkana Basin, Coryndon (1976) distinguished a lot of different fossil hippopotamus species. One of her explanations was that these species lived in different biotopes. Also from Asia many (sub)species are mentioned in the literature. In order to decide if the explanation of Coryndon (1976) is applicable for the Siwaliks, it first must be decided if all (sub)species distinguished in the Siwaliks are indeed valid (sub)species. For this purpose, the fossil hippopotamus material from continental Asia and Java was studied in detail.

4. MATERIAL

In Naturalis, the National Museum of Natural History in Leiden (The Netherlands) the Dubois collection (Coll. Dub.) was studied. This material was collected by Dubois in 1894-1895 in the Siwaliks (India) and between 1890 and 1899 on Java. In Fig. 13, the localities in the Siwaliks are shown. For this figure the diary and the map of Dubois (1894-1895) were used to relocate the sites. The location of Bharon is not sure; on the map of Dubois (1894-1895) it is called Baro. Considering the multiple way in which names have been written, it is likely that Bharon and Kodawala are located as indicated in Fig. 13. The fourth locality, Naliwala (=Nuliwala) was not found on Dubois' map.

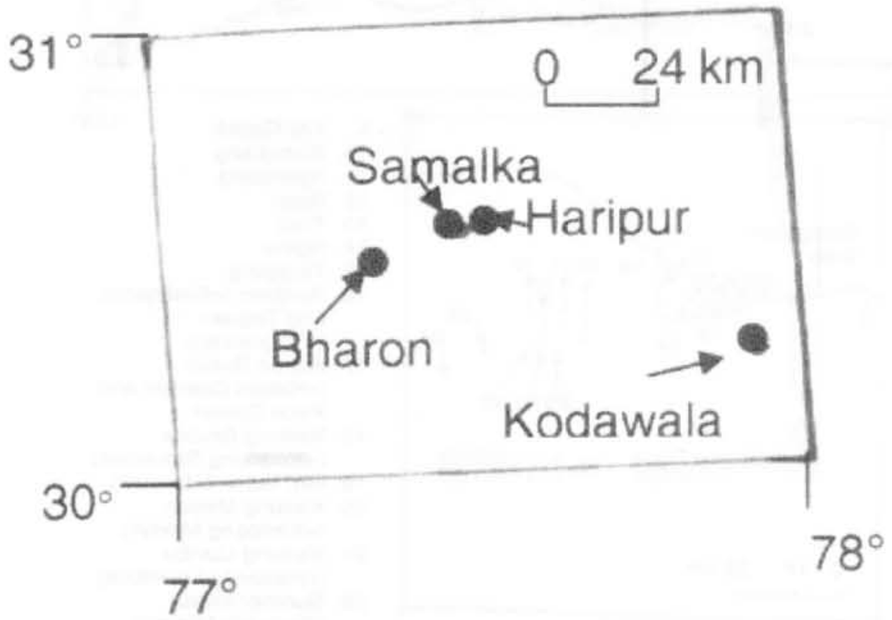

Fig. 13. The localities in the Siwaliks (see also Fig. 2B). Samalka is situated just west of Haripur (=Haripoor). For Kodawala several spellings were used. On the map of Dubois is it difficult to read, but it looks like Kohawala. This name is also used in the diary. Also Kalawala is used. On a map of Falconer & Cautley (1836) this same locality is called Kalowala.

Hexaprotodon fossils from Java (Indonesia) were studied at the Geological Museum in Bandung, the Museum of Sangiran and the laboratory Bioanthropologi and Paleoanthropologi in Yogyakarta.

At the Geological Research and Development Centre, Quarternary Geology Laboratory, in Bandung, several collections were studied, among which the fossils collected under the direction of Von Koenigswald in the 1930's (numbers beginning with K), the fossils collected by the Geological Survey and studied by Van der Maarel in 1932 (numbers beginning with M) and the fossils collected by the joint research project of the University of Tokyo and the Geological Survey of Indonesia in the 1970's (numbers beginning with SA). All the studied material is listed in Appendix III.

The localities on Java are shown in Figs. 14-16. In Fig. 14, most of the localities of Dubois are shown, based on his own map, the coordinates given in the catalogue of Naturalis, Leiden (The Netherlands) and the map of Theunissen *et al.*, (1990, p. 40). The localities Kali Bringin, Kedung Kuduh, Medalem, Rahang Bawah, Rahang Atas and Tjipanarabun could not be relocated.

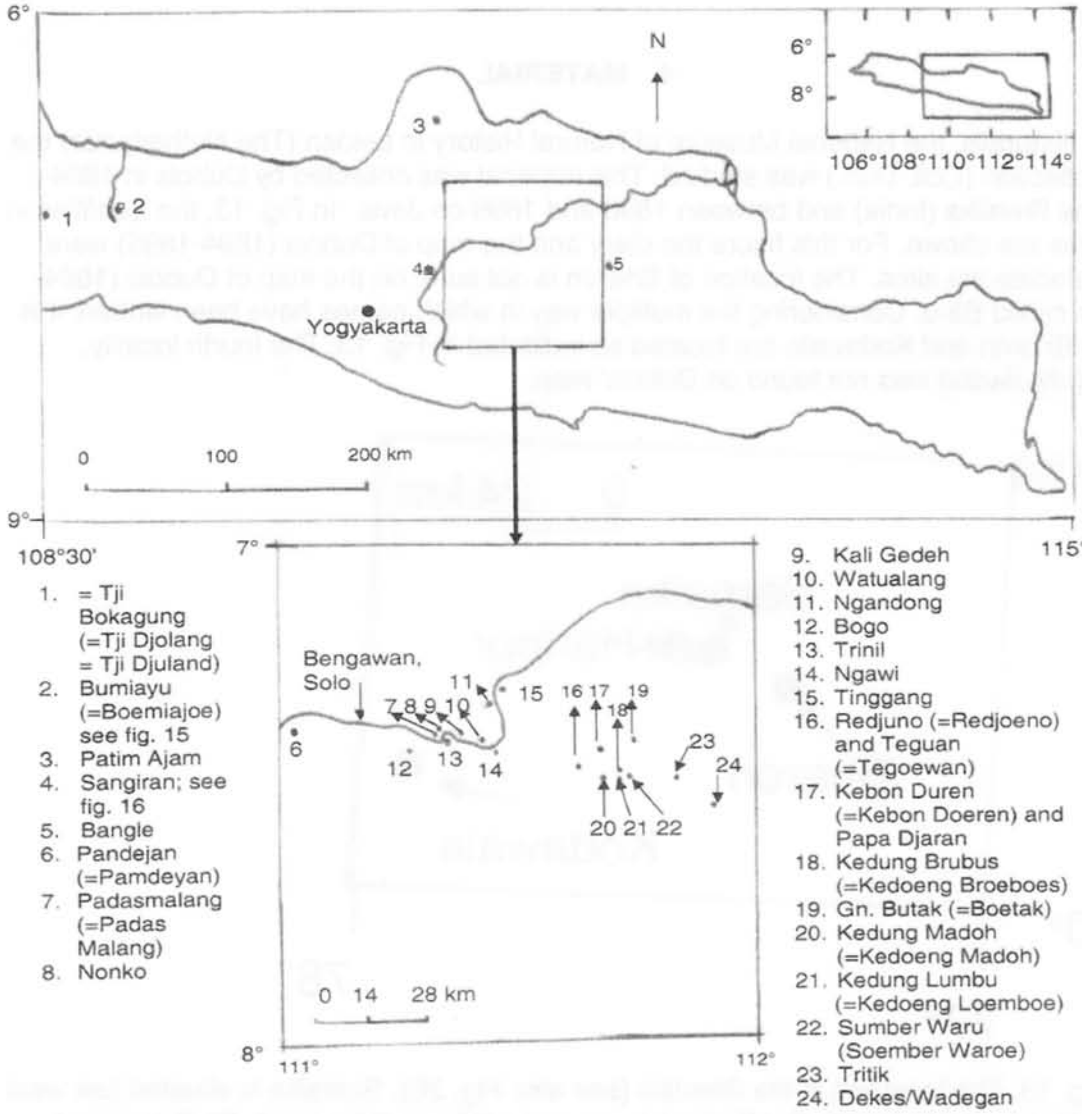

Fig. 14. The localities on Java, that were reconstructed on the basis of the map of Dubois and the coordinates in the catalogue of Naturalis. The upper map is based on Theunissen *et al.* (1990).

Fig. 15 shows the Bumiayu area. Fig. 16 shows the localities in the Sangiran Dome area (4 in Fig. 14). These localities are discussed in Watanabe *et al.* (1985). The Pd site III-14, Grenzbank, is situated in the Brankal site (Watanabe *et al.*, 1985: profile S 39 and page 14 and pages 158-160).

The Triangulation Point near Ngebung (Fig. 16) is shown in profile S 36 of Watanabe *et al.* (1985, page 20 and 164). The Cemoro Dam site is shown in the profile on page 18

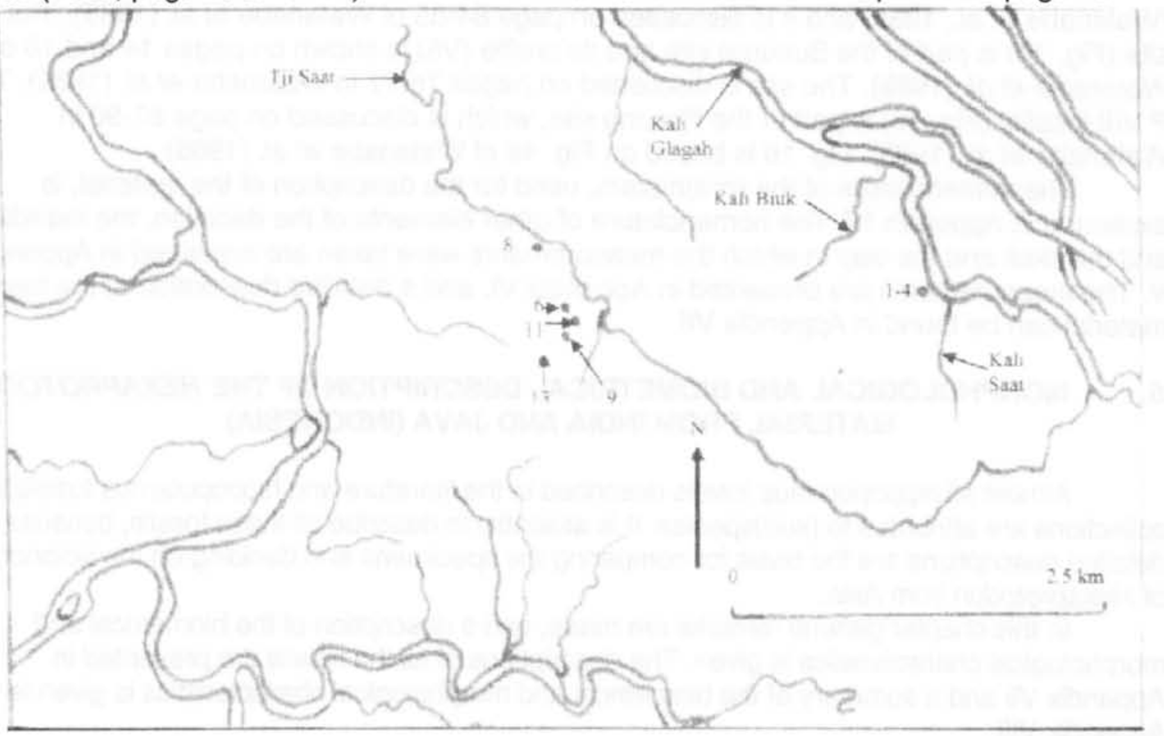

Fig. 15. The localities of the Bumiayu area (2 in Fig. 14), based on Van der Maarel (1932, map 1). The numbers indicate the localities of Van der Maarel (1932).

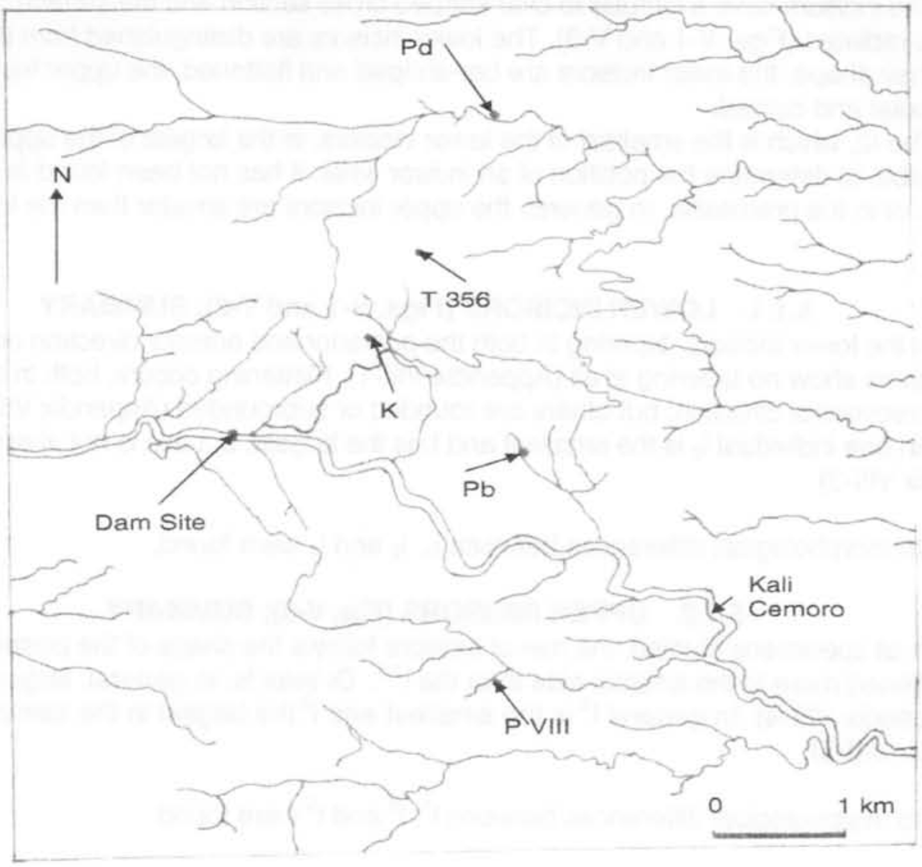

Fig. 16. The localities in the Sangiran Dome area (4 in Fig. 14). Pd = Pd III-14, Grenzbank; T356 = Triangulation Point (Ngebung); K = Krikilan; Dam Site = Cemoro

Dam Site; PB = New Pb site (Pb stream) and PVIII = P VIII digging site. After Fig. 48. In Watanabe *et al.* (1985).

(Watanabe *et al.*, 1985) and it is discussed on page 84-85 of Watanabe *et al.* (1985). The Pb site (Fig. 16) is part of the Bukuran site and its profile (V5) is shown on pages 14 and 18 of Watanabe *et al.* (1985). The site is discussed on pages 75-77 in Watanabe *et al.* (1985). The P VIII locality (Fig. 16) is part of the Pucung site, which is discussed on page 87-90 in Watanabe *et al.* (1985). Fig. 16 is based on Fig. 48 of Watanabe *et al.* (1985).

The nomenclature of the (pre)molars, used for the description of the material, is explained in Appendix IV. The nomenclature of other elements of the dentition, the mandible and the skull and the way in which the measurements were taken are explained in Appendix V. The measurements are presented in Appendix VI, and a detailed description of the fossil material can be found in Appendix VII.

5. MORPHOLOGICAL AND BIOMETRICAL DESCRIPTION OF THE *HEXAPROTODON* MATERIAL FROM INDIA AND JAVA (INDONESIA)

Almost all hippopotamus fossils described in the literature and hippopotamus fossils in collections are attributed to (sub)species. It is essential to describe all these fossils, because detailed descriptions are the basis for comparing the specimens and deciding on the taxonomy of *Hexaprotodon* from Asia.

In this chapter general remarks are made, and a description of the biometrical and morphological characteristics is given. The descriptions of all the fossils are presented in Appendix VII and a summary of the biometrical and morphological characteristics is given is Appendix VIII.

5.1. INCISORS

The incisors have a circular to oval-shaped cross section and the surface of the cross section is radiated (Figs. V-1 and V-3). The lower incisors are distinguished from the upper incisors by their shape: the lower incisors are bar-shaped and flattened, the upper incisors are more circular and curved.

The I2, which is the smallest of the lower incisors, is the largest of the upper incisors. It is impossible to determine the position of an incisor when it has not been found *in situ* in the mandible or in the premaxilla. In general, the upper incisors are smaller than the lower incisors.

5.1.1. LOWER INCISORS (Figs. V-1 and V-2); SUMMARY

In the lower incisors, tapering in both the posterior and anterior direction occurs, but other incisors show no tapering at all (Appendix VIII-1). Flattening occurs, both in linguobuccal and in dorsoventral direction, but others are rounded or subrounded (Appendix VIII-2). In general, in one individual I_2 is the smallest and I_1 is the largest, but this is not always the case (Appendix VIII-3)

No morphological differences between I_1, I_2 and I_3 were found.

5.1.2. UPPER INCISORS (Fig. V-3); SUMMARY

In all specimens studied, the row of incisors follows the shape of the premaxilla and the I^2 is positioned more to the anterior side than the $I^{1,3}$. Dt max is, in general, larger than the dt min (Appendix VIII-4). In general I^3 is the smallest and I^2 the largest in the same individual (Appendix VIII-5).

No morphological differences between I^1, I^2 and I^3 were found.

5.2. CANINES

The lower canines are distinguished from the upper canines by their cross section. The lower canines have a pear-shaped cross section (Fig. V-4). The upper canines have a heart-shaped to reniform cross section with a deep posterior groove (Fig. V-5). They are both bent in buccal direction and they have longitudinal striations.

5.2.1. LOWER CANINES (Figs. V-2 and V-4); SUMMARY

All lower canines where the root is not damaged show a cavity, suggesting that the canines grew throughout life. This can be seen in K 720, Coll. Dub. 100/1 and Coll. Dub. 308d/1.

The anterior part is smaller than the posterior part, but more posteriorly, in the alveolus, the lower canine becomes smaller again as it disappears into the jaw. The width is in general less than the height (Appendix VIII-6).

The striations on the canines may be fine or coarse. It is not clear if this has anything to do with the age of the animal. Most lower canines have a shallow groove on the buccal side (Appendix VIII-7). The lingual side may be grooved or smooth (Appendix VIII-8).

5.2.2. UPPER CANINES (Fig. V-5); SUMMARY

In the only upper canine, where this part has not been damaged (Coll. Dub. 308/3), the root shows a cavity, suggesting that also the upper canines grew throughout life.

The width is greater than the height on the lingual side in all specimens, and the width is in general greater than the height on the buccal side (Appendix VIII-9). The height on the buccal side is in general greater than the height on the lingual side (Appendix VIII-10).

Most upper canines have a buccal groove (Appendix VIII-11). Some have a lingual groove (Appendix VIII-12).

5.3. PREMOLARS

The lower premolars are distinguished from the upper premolars by their lesser width. The upper premolars have some sort of posterolingual platform; the lower premolars do not have such a platform. The (D)P^4 is molariform, P_4 is pointed and DP_4 is oblong.

5.3.1. LOWER PREMOLARS (Figs. IV-1 and V-6); SUMMARY

The DP_2 and DP_3 are smaller than the P_2 and P_3 (Appendix VI-9, VI-10 and VI-12). In general, the P_2 is the smallest and P_4 the largest of the three (Appendix VIII-13). The length is greater than the width (Appendix VIII-14). The width on the anterior side is larger than the width on the posterior side in all P_2's, in some P_3's and not in any P_4 (Appendix VIII-14). The crown height on the anterior side is smaller than on the posterior side in all unworn premolars (Appendix VIII-15).

The length is greater than the width in most alveoli of premolars (Appendix VIII-16). The width on the anterior side is greater than the width on the posterior side in most P_2's and some P_3's, but in P_4's it is smaller (Appendix VIII-17).

The width of the anterior root is smaller than that of the posterior root in most P_2's and P_3's, and in all P_4's.

There is a great variability in morphology and size of the premolars. All lower premolars have a protoconid (main cusp). The wear of the lower premolars seems to have started initially on the anterior side and continues in posterior direction with continuing wear. This is indicated by hardly worn premolars with tiny wear facets on the anterior side. In very worn premolars, the wear facet is present both on the anterior and posterior sides.

The number of lower premolars varies from 3 to 4. There are no P_1's preserved in the mandible, but in the first described two mandibles (without number), described in Appendix VII.9, circular alveoli of the P_1 occur. This is also the case in Coll. Dub. 2904. These alveoli indicate that the P_1 is one-rooted. In four other mandibles (Coll. Dub. 99, Coll. Dub. 2929 and 3147 and in the skeleton from Kali Glagah) there is a rugosity in the jaw, which might indicate the rudimental alveolus of a P_1. Other mandibles do not show any indication of the presence of a P_1. One single P_1 is described (K 675/1; Appendix VII.5).

The P_2 is one- or two-rooted, the roots being circular to oval-shaped. Where there are two roots, the anterior root tends to be more oval-shaped, the posterior root more circular.

The P_3 is more complex than the P_2 and the P_4. The P_3 has two roots, an anterior oval-shaped root and a posterior root, which is circular or oval-shaped. The P_4 has two roots, oval-shaped to circular. It cannot be excluded that some isolated premolars described as P_3's are in fact P_2 or P_4, which would explain the majority of P_3's. The P_4 is distinguished by its greater width.

The morphology of the DP_2 differs from that of the P_2. The DP_2 is simpler than the P_2; it has no anterior or posterior lobes and no cingula. The protoconid is a sharp cusp and there is no metaconid.

The DP_3 in the material studied is only represented by an alveolus. The DP_4 is totally different from the other premolars. It is oblong, has six cusps and it is molariform. The length of the DP_4 is greater than that of the P_4.

The anterior lobe may be tiny, normal or very robust. It may be crenulated or not. The anterior lobe in the P_2's is not robust. In the P_1 (K 675/1), there is no anterior lobe. The P_2's and P_3's show an increasing presence of the anterior lobe and the P_4's all have an anterior lobe (Appendix VIII-19).

The paraconid (Appendix VIII-20), the paraconulid (Appendix VIII-21), the metaconid (Appendix VIII-22) and the protoprecristid (Appendix VIII-23) are present in some and absent in others.

The protoprecristid, the protopostcristid and the protoendocristid are either knobby, crenulated or smooth. The protopostcristid and the protoendocristid are sometimes both present, in some specimens only the first one is present, in others only the second one, or they are both absent (Appendix VIII-24).

The posterior cusps also show a great variety. In some specimens only the hypoconid is present, in others both the hypoconid and the entoconid are present, or both the hypoconid and the hypoconulid, or they are all three present, or they are all three absent, or there are a lot of little cusplets, among which are probably (some of) the posterior cusps (Appendix VIII-25). There is an increase in posterior cusps from P_1 to P_4 (Appendix VIII-25).

The cingulum on the lingual side is often clearer and more pronounced than on the buccal side. The cingulum is crenulated or not, it may occupy just a part of the lingual or buccal side, or it may surround the entire premolar. The premolars either have no cingulum, or a cingulum on the lingual side only or both on the lingual and buccal sides (Appendix VIII-26).

The posterior lobe shows an increase in presence from P_1 to P_4 (Appendix VIII-27).

5.3.2. UPPER PREMOLARS (Figs. IV-2 and V-7); SUMMARY

In general the P^1 is the smallest and P^3 the largest in the same individual (Appendix VIII-28). The length is greater than the width on the posterior side in all alveoli and in most of the upper premolars, but there is a decrease in the percentage "length greater than width" from 100% in P^1 to 29.4% in P^4 (Appendix VIII-29). In all specimens in which this is visible, there is hardly a diastema between the canine and the P^1. In crania in which more premolars are present, there are several alveoli of P^1's, or the P^1 is broken, but there is no morphology of P^1's preserved in the jaws. However, some isolated P^1's have been preserved.

The upper P^{1-3} are characterised by the presence of one main cusp, the paracone, which bends in lingual direction. In most P^{2-3}, a posterior platform is present, which is often covered by crenulated ridges or cusplets. The P^3 is more complex than the P^2; it has more cusps and ridges. The P^4 is molariform: the wear facet is plus-shaped. This could be result of the wear of a four-lobate paracone, or it could be the result of the wear of more than one cusp. The lingual side often shows grooves. The P^4's that are present in maxillae are very worn. Molars present in these maxillae are also very worn. Hooijer (1950) claims that the P^4 is rotated over 90°, with its posterior surface facing inward.

Of the milk dentition, only specimens of DP^4 were encountered. In maxilla with a DP^4, the P^4 is not developed. This can be concluded from the fact that the P^{2-3} are not very worn or that the M^3 is not yet fully erupted. This is the case in Coll. Dub. 96, Coll. Dub. 1702, Coll. Dub.

2188, Coll. Dub. 2920. In Coll. Dub. 2907/1, a diastema is present between the P^3 and the M^1, indicating that the P^4 did not develop. In Coll. Dub. 1702, the maxilla is damaged and it is clear that below the DP^4, no P^4 is present. This phenomenon was also described by Boekschoten & Sondaar (1972, p. 328) and by Sondaar (1977) for the hippopotami from Cyprus.

It seems that the wear begins on the anterior side and continues on the posterior side with progressing wear.

The anterior lobe, the paraprecrista, the parapostcrista and the posterior lobe may be smooth, knobby or crenulated. Most upper premolars have an anterior lobe (Appendix VIII-30).

P^1 and P^2 do not have a paraprecrista, but most P^3's have (Appendix VIII-31). Some upper premolars have a primocone, others have not (Appendix VIII-32).

The wear facet is situated both on the anterior and posterior sides. In other upper premolars it is present only on the anterior side or only on the posterior side or it is quite straight (Appendix VIII-33).

There is a cingulum only on the lingual side, or on both the lingual and buccal sides or there is no cingulum at all (Appendix VIII-34).

P^1's do not have a metacone, the P^2's sometimes have a metacone and the presence of the metacone increases with the P^3's (Appendix VIII-35).

The P^1's do not have a parapostcrista, but the P^2's and P^3's do (Appendix VIII-36). The paraendocrista shows an increase in presence from P^1 to P^3 (Appendix VIII-37). Besides the parapost- and the paraendocrista, additional ridges occur only in the P^3's (Appendix VIII-38).

Some premolars do not have a posterior platform. The presence of this platform increases from P^1 to P^3 (Appendix VIII-39). Most upper premolars have a posterior lobe, but not always (Appendix VIII-40).

The roots of P^1 and P^2 may consist of one circular to oval-shaped root, or of two 8-shaped roots, or two roots fused into one, or two separate roots. P^1 and P^2 may even have three roots. The P^3's show two morphologies: 1) two anterior roots fused to one, and two posterior roots fused to one, which results in two half-moon-shaped roots or 2) two anterior roots fused to one, and two posterior roots fused to one with an extra root on the lingual side (Appendix VIII-41).

5.4. MOLARS

The lower molars are distinguished from the upper molars by their relatively small size; the upper molars have a greater width. The wear in lower molars is lower on the buccal side than on the lingual side. In upper molars it is the other way round.

5.4.1. LOWER MOLARS (Figs. IV-3 and V-8); SUMMARY

In general, the length is least in M_1, greater in M_2 and in M_3 it is greatest (Appendix VIII-42). This applies also to the width on the anterior side and on the posterior side (Appendix VIII-42). The length is greater than the width in nearly all lower molars (Appendix VIII-42). The width on the anterior side is less than on the posterior side in all M_1's (100%), but this percentage decreases for M_2 and M_3 (Appendix VIII-42).

In 50% of the lower molars, the protoconid is larger than the metaconid. In the other 50% the protoconid is either smaller or of the same size as the metaconid. This occurs more in the M_3's than in the M_2's. This was not actually measured but visually established. In general the protoconid is situated more anteriorly than the metaconid (Appendix VIII-43).

The anterior lobe is present in most lower molars. In many molars the anterior lobe is connected with the protoconid. In one molar it is connected with the metaconid, but also no connection of the anterior lobe with the protoconid or metaconid occurs (Appendix VIII-44).

A metapoststylid is present in most molars, but there are also molars with only the protopoststylid, or with both the metapoststylid and the protopoststylid, or with none of these ridges (Appendix VIII-45).

A hypoprestylid is present in most molars, but there are also molars with only the entoprestylid developed, or with both a hypo- and entoprestylid, or without these ridges (Appendix VIII-46).

The metapoststylid is situated lingually from the hypoprestylid (or entoprestylid, in the case of the M_1 of Coll. Dub. 2008) in most molars. In other molars the metapoststylid and the hypoprestylid are lying opposite each other, or the metapoststylid is situated buccally from the hypoprestylid (Appendix VIII-47).

The hypoconid is larger than the entoconid in most molars. In other molars, the hypoconid and the entoconid are about the same size, or the hypoconid is smaller than the entoconid, or the hypoconid and the entoconid form one ridge (Appendix VIII-48).

The posterior lobe is present in about 50% of the molars. In most of these molars the posterior lobe is not connected with the hypoconid (Appendix VIII-49).

Most molars have a heptaconid, a pentaconid and a hexaconid (posterior cusps). They mostly occur in the M_2's. In all molars, the heptaconid is larger than the pentaconid, which is always a separate cusp. In most molars the hexaconid is larger than the pentaconid. The heptaconid and the hexaconid are often attached, touching or forming one ridge. In molars with a posterior lobe, this lobe is mostly connected with the posterior cusps (Appendix VIII-50). In the M_3's the posterior cusps are in 11% (N=47) of the cases replaced by a crenulated ridge which goes from the heptaconid towards the lingual and buccal sides and in which the penta- and hexaconid are less obviously present or even not distinguishable anymore. This is the case in Coll. Dub. 314b, Coll. Dub. 323a/2, Coll. Dub.323b, Coll. Dub. 2076/10 and Coll. Dub. 2917.

The M_3 is the only molar in which in 47% (N=34) of the specimens a hypopostconulid is regularly present, i.e., in the specimens without no. (locality Sangiran), K 657, K 723/1, K 723/2, K 723/3, K 727, K 731, K 740, K 743, K 745, K 746, Coll. Dub. 99 sin and dex, Coll. Dub. 2318b and Coll. Dub. 11464.

Most M_1's have an accessory buccal cusp. The presence of this cusp decreases in M_2 and M_3. Some molars have an accessory lingual cusp and some have both (Appendix VIII-51).

The majority of the molars does not have a cingulum. Few molars have a cingulum on the lingual side, others have a cingulum on the buccal side or on both sides (Appendix VIII-52).

The roots are bent in posterior direction. The talonid shows an indentation on the lingual side. The buccal side is more or less in a row with the rest of the molars. The M_1 and the M_2 have four roots, the M_3 has five roots.

5.4.2. UPPER MOLARS (Figs. IV-4 and V-9); SUMMARY

In general M^1 is smaller than M^2 and M^3, which are of about the same size (Appendix VIII-53). In most molars the length is greater than the width on the anterior side. The percentage "length greater than width" decreases a little from M^1 (91%) to M^3 (82%). In the rest of the molars, the length is less than the width on the anterior side or they are about the same size (Appendix VIII-53).

In most upper molars the length is greater than the width on the posterior side. The percentage "length greater than width" increases a bit from M^1 (67%) to M^3 (96%). In the rest of the molars the length is less than the width on the posterior side or they are about the same size (Appendix VIII-53).

The width on the anterior side is less than on the posterior side in all M^1's (100%). This percentage decreases for the M^2's, and the M^3's are mostly broader on the anterior side (Appendix VIII-53).

Most upper molars have an anterior lobe. It is connected with the protocone, or with the paracone, or both with the proto- and paracone, or it is not connected with any cusp. The anterior lobe is connected mostly with the protocone. The fact that from M^1 to M^3 the percentage of the anterior lobe connected with the protocone increases (0% - 22% - 57% respectively in M^1, M^2 and M^3), and the percentage fused molars decreases (89% - 66% - 37% in M^1, M^2 and M^3 respectively) suggests that the anterior lobe was connected with the protocone in the molars with now fused cusps, but this is not sure, although the middle-aged, old and very old molars show increasingly more fused cusps (Appendix VIII-54). Among the M^1's there are no molars with a crenulated anterior lobe. In the M^2's 12.5% of the anterior lobes is crenulated, and in 16%

of the M^{3}'s the anterior lobe is crenulated or knobby. The anterior lobe continues into a cingulum on the lingual side only, or in a cingulum on the buccal side only, or into a cingulum on both sides, or it does not continue in a cingulum on either side (Appendix VIII-54)

The paracone is mostly of about the same size as the protocone, but it may also be smaller or larger than the protocone (Appendix VIII-55).

In the M^{1}'s, the metacone is of about the same size as the tetracone. In the M^{2}'s the metacone is mostly larger than the tetracone and in the M^{3}'s the metacone is larger, smaller or of about the same size as the tetracone (Appendix VIII-56).

The parapoststyle is situated buccally from the metaprestyle ("*palaeindicus*-type"; Hooijer, 1950) in most upper molars. But they are also situated opposite each other ("*sivalensis*-type"; Hooijer, 1950), or the parapoststyle is situated lingually from the metaprestyle (Appendix VIII-57). It seems as though the parapoststyle and the metaprestyle have a tendency to be situated more opposite each other from M^1 to M^3.

The protopoststyle and the tetraprestyle are situated opposite each other in most molars. In the other molars the protopoststyle is situated lingually or buccally from the tetraprestyle (Appendix VIII-58).

The metacone (including the metaprestyle) is extending more to the anterior side than the tetracone (including the tetraprestyle) in most molars (Appendix VIII-59).

The protocone mostly has a trilobate shape, but it may also be star-shaped, circular or oval-shaped (Appendix VIII-60). The paracone mostly has a trilobate shape, but it may be also star-shaped or oval-shaped (Appendix VIII-61). The metacone mostly has a trilobate shape, but it may also be star-shaped, oval-shaped, half-moon-shaped or triangular (Appendix VIII-62). The tetracone mostly has a trilobate shape, but may also be star-shaped, oval-shaped, half-moon-shaped or circular (Appendix VIII-63).

The paracone (including the parapoststyle) is extending more to the posterior side than the protocone (including the protopoststyle) in most molars. In other molars the protocone (including the protopoststyle) extends more to the posterior side than the paracone (including the parapoststyle), or they extend both to the same degree in posterior direction (Appendix VIII-64).

Most upper molars have a posterior lobe, but not all (Appendix VIII-65). Where a posterior lobe is present, it may be fused with the cusps due to wear or it forms an isolated ridge, or it is connected with the tetracone, or it is connected with the metacone, or it is connected with both the meta- and tetracone, or it is connected with the meta- and/or the tetrapostconules (Appendix VIII-66). The posterior lobe may either not continue into a cingulum or it continues into a cingulum on the lingual side, or on the buccal side, or on both sides. (Appendix VIII-66).

Some molars do not have a cingulum, but the majority has a cingulum on both the lingual and buccal sides, or only on the lingual side or only on the buccal side (Appendix VIII-67). Of the molars with a cingulum, this cingulum is crenulated in 41% (N=74). It is crenulated in 25% of the M^{1}'s, 38% of the M^{2}'s and 42% of the M^{3}'s.

Some molars do not have extra cusps. Others have an accessory buccal cusp. This occurs mostly in the M^{1}'s. Two accessory buccal cusps occur only in M^{1}'s. An accessory lingual cusp is mainly present in some M^{2}'s. Both an accessory lingual and buccal cusp occur more in M^{1}'s than in the other molars. M^{1}'s do not have any other extra cusps. A meta- or tetrapostconule may be present in some M^{2}'s and M^{3}'s, some have both. Occasionally there is an accessory buccal cusp and a meta- or tetrapostconule. An accessory lingual cusp and the tetraconule, accessory buccal and lingual cusps and a metapostconule, and extra cusps in other places only occur in some M^{3}'s (Appendix VIII-68).

5.5. MANDIBLE (Figs. V-2, V-10 and V-11); SUMMARY

Some mandibles have alveoli of the P_1, like the three specimens without number (skeleton, Geological Museum, Bandung; Locality Rahang Bawah (Museum Sangiran) and Locality Medalem), Coll. Dub. 2904 and Coll. Dub. 2910. Other mandibles have a rugosity between the P_2 and the canine, which might indicate a rudiment of a P_1. This occurs in Coll.

Dub. 99, Coll. Dub. 2929 and Coll. Dub. 3147. There are also mandibles without any trace of a P_1, like the specimens without number (locality: Ngandong, Geological Museum, Bandung) and SA 270378.

Some mandibles show a divergence of the row of molars both in anterior and posterior direction, like 22 G, the specimen without number (locality: Medalem) and Coll. Dub. 99. Other mandibles only show divergence in anterior direction; the posterior part of the row of molars is quite parallel. This occurs in the specimen without number (skeleton, Geological Museum, Bandung), in 4-4A and in Coll. Dub. 2916.

The length of the symphysis varies from about 120 mm to 140 mm (Appendix VI-24). From the 15 measurements, the two measurements of 150 mm were estimated and 8 measurements were minimum measurements, due to damage. One measurement was of a juvenile. So, not many conclusions can be drawn.

The height of the symphysis varies from 57 mm to 110 mm (Appendix VI-24), with an average of 71.2 mm (N=12). It can roughly be divided into two categories: a small one with heights from 57–80 mm and a large one with heights from 90-110 mm. This is not likely to be the result of sexual dimorphism, because the sizes of the lower canines suggest the mandibles to be male, whereas the values of the height of the symphysis contradicts this. It might indicate an evolutionary trend.

In all specimens in which this is visible, the length of the row P_2-P_4 is less than the length of the row M_1-M_3; the ratio varies from 0.57 to 0.68, with an average of 0.66 (N=6). Only in the specimen from the Siwaliks (Coll. Dub. 3147), the row P_2-P_4 is very long; the ratio P_2-P_4 / M_1-M_3 is 0.92 (Appendix VI-25).

A summary of the biometrical characteristics is given in Appendix VIII-26.

5.6. CRANIUM (FIGS. V-12 – V-17); SUMMARY

From the descriptions it is concluded that the variation in cranial characteristics in fully grown specimens is quite great. The premaxilla has different shapes (Fig. V-12). The molar row is parallel or divergent in posterior direction. In two specimens from Kedung Lumbu one has a parallel row of molars (Coll. Dub. 2188), and the other has a molar row which is divergent in posterior direction (Coll. Dub. 1702). The obliquity of the M_3 with regard to the rest of the row of molars also differs in specimens from the same locality. In Coll. Dub. 2203 (Kedung Brubus) the M_3 is situated obliquely, in Coll. Dub. 2908 (also from Kedung Brubus) it is not. The smallest part of the muzzle is situated below the P_4, between the P_4 and M_1 or between the P_3 and P_4.

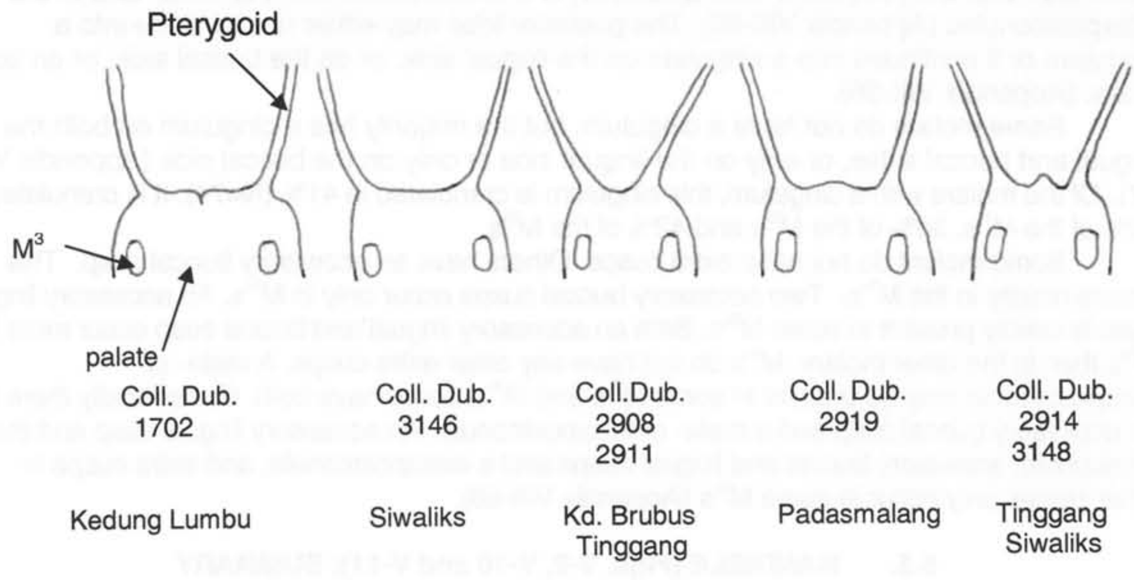

Fig. 17. Ventral view of the posterior side of the palate and the pterygoids. See also Fig. V-17B, measurements 12, 15, 21 and 22 and Appendix VI-31. The shape is quit variable. The drawings are not to scale.

The palate is flat or hollow, the posterior side of the palate has different shapes (Fig. 17); Coll. Dub. 2914 and Coll. Dub. 2919, both from locality Tinggang, have a different shape. Also the specimens Coll. Dub. 3146 and Coll. Dub. 3148 (both from the Siwaliks) have different shapes. This is also the case for the shape of the bulla: in Coll. Dub. 2914 (from Tinggang) it is circular with an extension in anterior direction, in Coll. Dub. 2919 (also from locality Tinggang) it is small and oval-shaped. The bulla from the Siwalik specimens are different; they are wing-like (see Fig. 18).

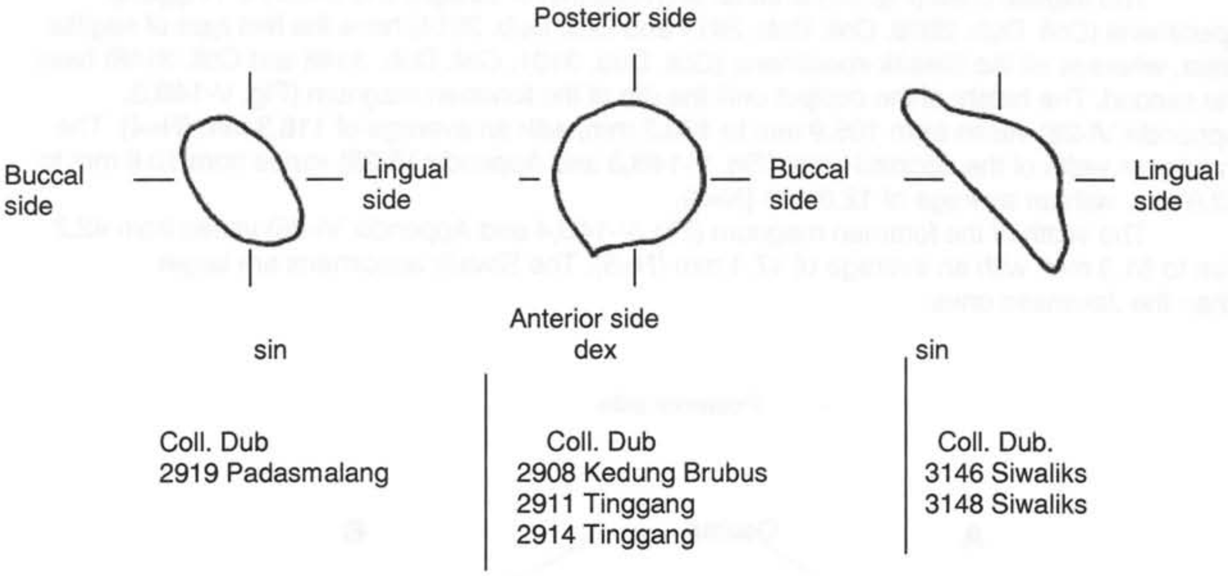

Fig. 18. Ventral view of differently shaped bullae. The drawings are not to scale. Sin is a left one; dex is a right one.

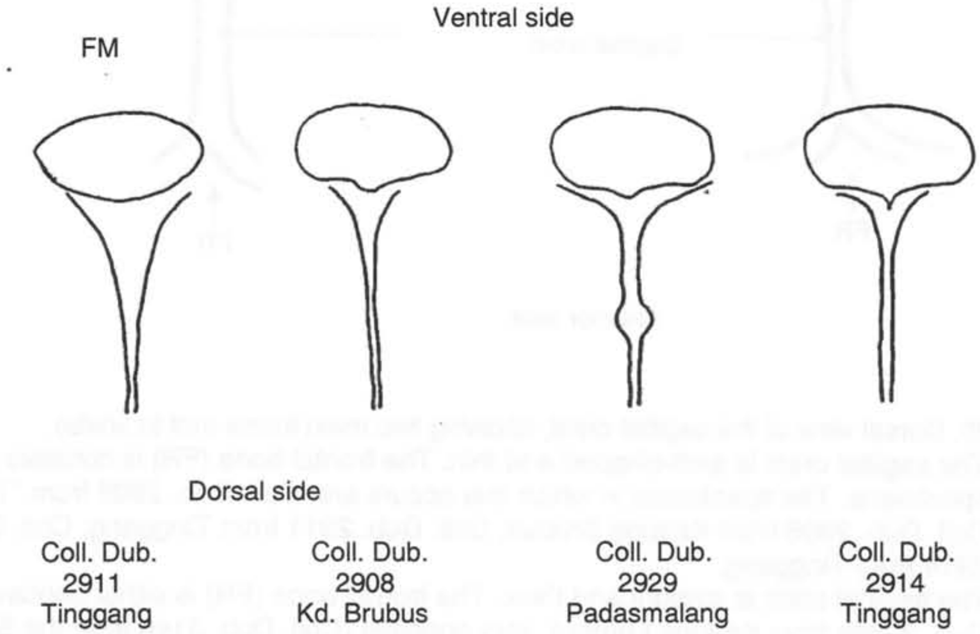

Fig. 19. Posterior view of the differently shaped foramen magnum (FM) and the occipital crest (OC). Drawing is not to scale.

The measurements of the squamosal (Figs. V-16 and V-17) are given in Appendix VI-30. The transition between the jugal bone and the squamosal in Coll. Dub. 2914 is situated at the posterior rim of the pterygoid; in another specimen from Tinggang (Coll. Dub. 2911) it is situated more anteriorly. The foramen magnum is different in all the Tinggang specimens (Fig. 19). It is round and broad in Coll. Dub. 2911, very prominent in Coll. Dub. 2914 and small in Coll. Dub. 2919. The frontal bone is straight, slightly concave or very concave. These varieties are all present in the Tinggang specimens: it is straight in Coll. Dub. 2919, slightly concave in Coll. Dub. 2911 and very concave in Coll. Dub. 2914.

The sagittal crest (Fig. 20) is either arch-like/thin or straight and thick. All Tinggang specimens (Coll. Dub. 2909, Coll. Dub. 2911 and Coll. Dub. 2914) have the first type of sagittal crest, whereas all the Siwalik specimens (Coll. Dub. 3101, Coll. Dub. 3146 and Coll. 3148) have the second. The height of the occiput until the rim of the foramen magnum (Fig. V-14B,2, Appendix VI-28) varies from 105.9 mm to 130.2 mm, with an average of 118.8 mm (N=4). The maximum width of the occipital crest (Fig. V-14B,3 and Appendix VI-28) varies from 10.6 mm to 13.6 mm, with an average of 12.6 mm (N=3).

The width of the foramen magnum (Fig. V-14B,4 and Appendix VI-28) varies from 42.2 mm to 51.3 mm, with an average of 47.4 mm (N=5). The Siwalik specimens are larger than the Javanese ones.

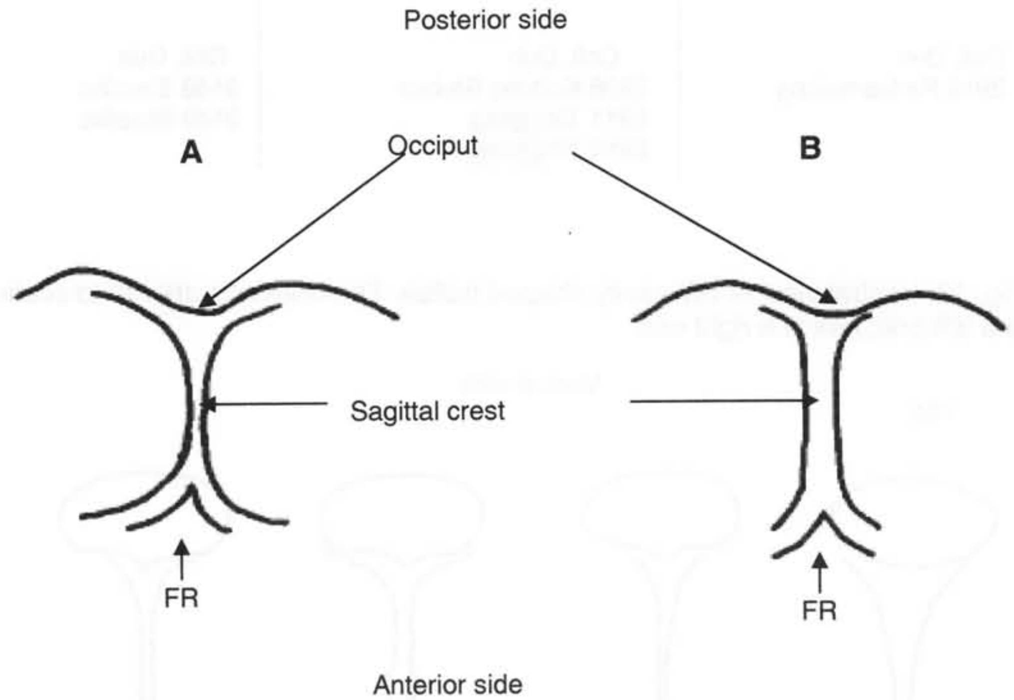

Fig. 20. Dorsal view of the sagittal crest, showing two main forms (not to scale).

A. The sagittal crest is arch-shaped and thin. The frontal bone (FR) is concave in all specimens. The specimens in which this occurs are: Coll. Dub. 2902 from "Trinil"; Coll. Dub. 2908 from Kedung Brubus; Coll. Dub. 2911 from Tinggang; Coll. Dub. 2914 from Tinggang.

B. The sagittal crest is straight and thick. The frontal bone (FR) is either concave (Coll. Dub. 2084a from Kedung Lumbu), very concave (Coll. Dub. 3146 from the Siwaliks and Coll. Dub. 5006 from Kedung Lumbu) or straight (the Kali Glagah skeleton, Coll. Dub. 2919 from Padasmalang, Coll. Dub. 3101 and 3148, both from the Siwaliks).

The variety in crania is great; two extremes are Coll. Dub. 3101 and Coll. Dub. 3146 (both from the Siwaliks). The first has a flat, broad and long skull, the other a high and short one. Coll. Dub. 3101 has a low occiput (Fig. V-13B,5 and Appendix VI-27), whereas Coll. Dub 3146 has a very high occiput. The orbits in Coll. Dub. 3101 are low, in Coll. Dub. 3146 they are high (Fig. V-13B,12 and Appendix VI-27). The length of the cranium is high in Coll. Dub. 3101 and less in Coll. Dub. 3146 (Fig. V-15B,8 and Appendix VI-29). The same can be seen in Fig. V-17B,16 (Appendix VI-32) and also in Fig. V-15B,10 (Appendix VI-29), although the length of Coll. Dub. 3146 is still quite greater than those from Java. The broadness of Coll. Dub. 3101 and Coll. Dub. 3146 is demonstrated in Fig. V-17B,26 (Appendix VI-32), although Coll. Dub. 3148 is comparable in width with the Javanese specimens.
Because the sagittal crest has a function in the attachment of muscles, it seems obvious that animals with type B had more neck muscles than those with type A, but the meaning of this is not clear.

A summary of the biometrical characteristics is given in the Appendix VI-33.

5.7. CONCLUSION

There is a great variability in the morphology and biometry of the studied specimens. The lower incisors taper mostly in anterior direction and most are flattened in linguobuccal direction. The complexity of the premolars and molars increases from P_2 to P_4, from P^1 to P^3 and from M1 to M3 (both lower and upper molars). In the premolars this is caused by more cusps and ridges in several places, in the molars is it caused by increased crenulation of ridges. The mandibles and crania also show a great variety. Not only is there a great variety of isolated characteristics, but also the combination of all features varies greatly; all combinations of characteristics seem possible. Therefore, there is not a single combination of characteristics that can be used to distinguish (sub)species.

6. SEXUAL DIMORPHISM AND VARIATION IN SIZE IN *HIPPOPOTAMUS AMPHIBIUS*

Before comparing the biometrics and morphology of the hippopotami from the Siwaliks and Java, it is useful to get an idea about the sexual dimorphism and variation in the extant *Hippopotamus amphibius.*

Hooijer (1950) measured skulls of *Hippopotamus amphibius* from isolated, recent material from different places in Africa (Congo, Zanzibar*, Zambezi River (Mozambique) the Nile (Egypt), South Africa, Kenya, Uganda) and from individuals from zoos. The sex of most animals was known, so that sexual dimorphism in Hippopotamidae, if present, should become clear.

** (Although Van der Maarel (1932) stated that he had strong doubts about the correctness of the statement, for it seemed to him "highly improbable [...] that in this relatively small island near Africa's E. coast hippopotami should occur, these being surely bound to large rivers.")*

6.1. SEXUAL DIMORPHISM IN *HIPPOPOTAMUS AMPHIBIUS*

Fig. 21 shows the measurements of the circumference and the greater diameter (maximum) of the lower canines (measurements 8 and 9 from Table 1A of Hooijer, 1950). There is clearly sexual dimorphism in the lower canines; the lower canines of the males are much bigger than those of the females. Both the minimum diameter and the maximum diameter of the lower canines are less for females than for males. The minimum diameter ranges from 34-51 cm in males and from 25-34 cm in females (Hooijer, 1950, Table 1A, no 10; Hooijer names this: the smaller diameter).

As far as can be determined by the measurements of Hooijer (1950, Tables IA en IB), 92% of 49 different parameters (excluding the measurements of angles and ratio's) shows that the maximum value of these parameters is larger for the males than for the females (total number of measurements = 1205). Only 39% of the minimum values for the males is larger than the minimum values for the females. Of all measurements, 84% shows a smaller average for the females than for the males, but a real gap between the values for the males and the females, indicating sexual dimorphism in *Hippopotamus amphibius,* only occurs in the lower canines.

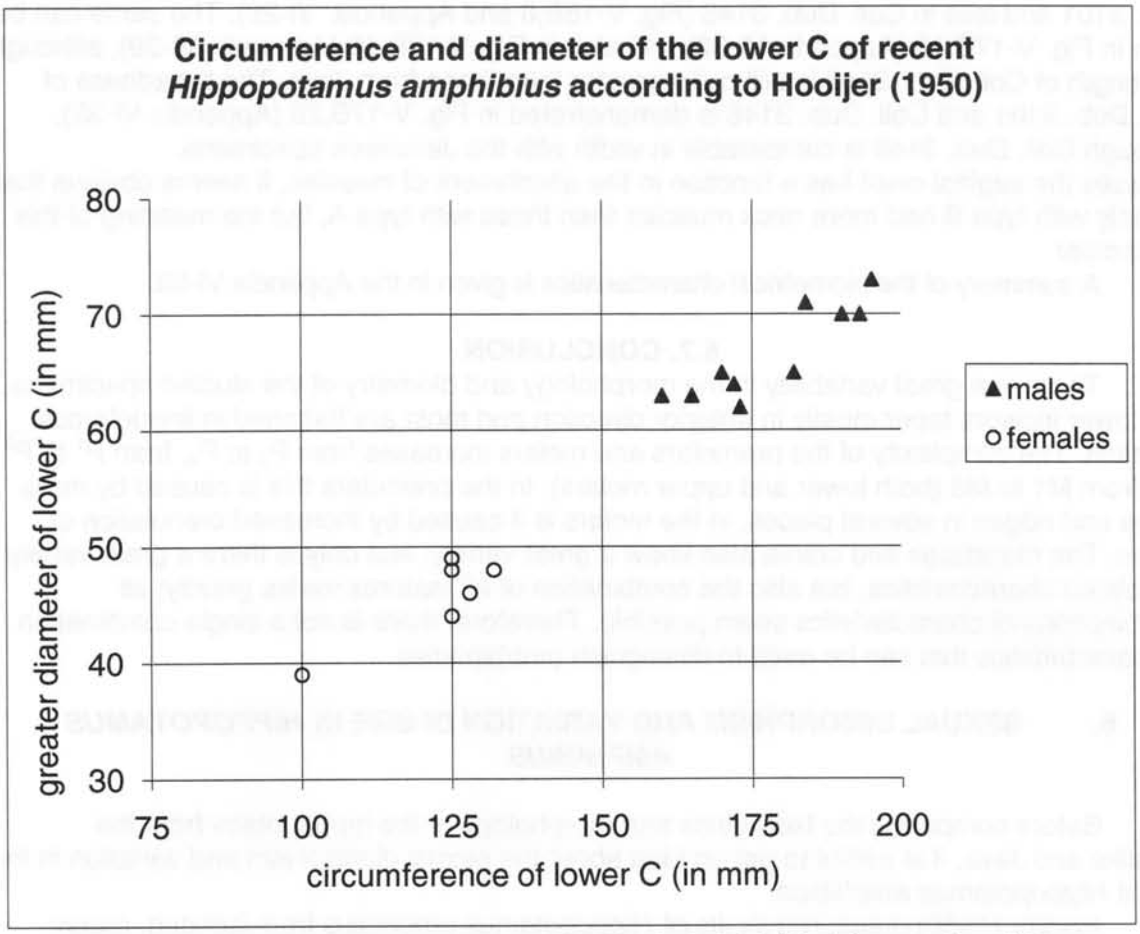

Fig. 21. Measurements taken from Hooijer (1950, Table 1A, nos. 8 and 9).

6.2. VARIATION IN *HIPPOPOTAMUS AMPHIBIUS*

Hooijer (1950) reviewed the different subspecies of *Hippopotamus amphibius*, that were distinguished in the past, like *Hippopotamus amphibius amphibius* L. from the Nile, *H. a. capensis* Desmoulins (1825) from the Cape, *H. a. constrictus* Miller (1910) from Angola, *H. a. kiboko* Heller (1914) from Kenya and *H. a. tschadensis* Schwarz (1914) from Nigeria. Hooijer (1950) concluded that "the supposed differential characters", between the different subspecies as defined by the above mentioned authors, "do not occur constantly in skulls from a special region in Africa. These characteristics are found in every combination, without preference to a special locality."

However, the measurements of Hooijer (1950) do indicate some differences as can be seen in Fig. 22.

Three specimens of *H. amphibius* with unknown sex from west Africa are definitely smaller than the other specimens and also smaller than the dimensions from males from west Africa. These three specimens are therefore likely to represent females. Between the measurements from east and south Africa there is no clear difference, although the values for the female skulls from east Africa are slightly larger than those from south Africa. In the male skulls the one from south Africa is largest, although this concerns only one measurement. Other measurements give similar pictures.

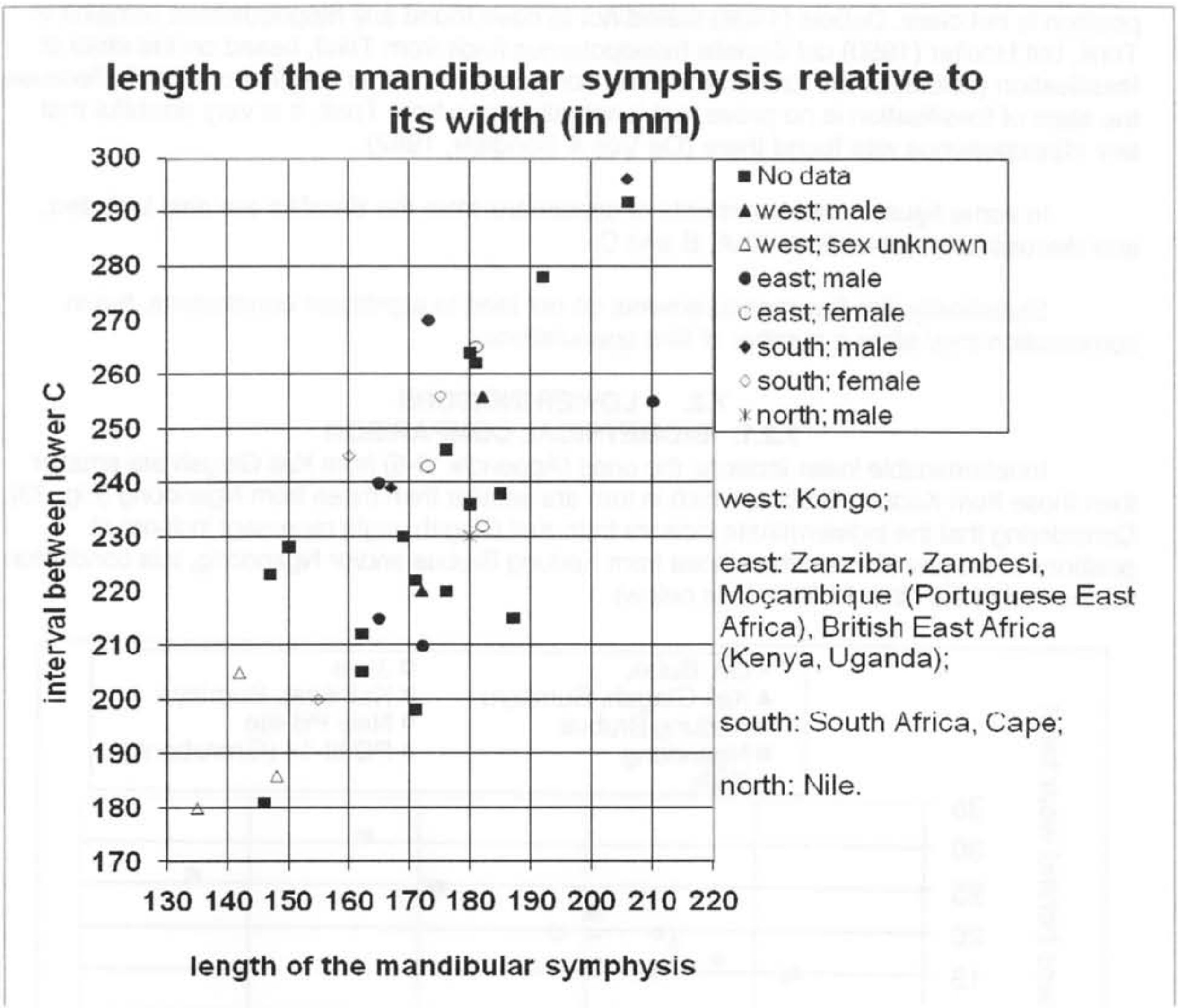

Fig. 22. Measurements from Hooijer (1950, Table 1A, nos. 36 and 40 and Table III, of material from different parts of Africa.

From this, the conclusion is drawn that there is sexual dimorphism, but only very clear in the lower canines. In post-cranial material sexual dimorphism might be present, but this was not studied, due to lack of material.

There are differences in size in *Hippopotamus amphibius* from different parts of Africa, but not clear enough to warrant a subdivision in (sub)species.

7. BIOMETRICAL AND MORPHOLOGICAL COMPARISONS OF *HEXAPROTODON* FROM SEVERAL JAVANESE SITES

7.1. THE LOCALITIES AND THEIR STRATIGRAPHIC POSITION

As mentioned in Chapter 5, several (sub)species of Asian and the Javanese hippopotami have been described. Here comparisons are made between the hippopotami from several Javanese sites to decide if such a division in (sub)species is justified. On Java (Indonesia) several hippopotamus finds have been recorded from the "Satir" (2.0-1.5 Ma) and "Ci Saat " (1.2 Ma) Faunas in the Bumiayu area, from Kedung Brubus (0.8 Ma) and Ngandong (Late Pleistocene). Stratigraphical positions were determined by Van den Bergh *et al.* (1996). As only the stratigraphical position of the localities Kali Glagah ("Satir"-fauna) in the Bumiayu area, Kedung Brubus and Ngandong are known, the fossils from these localities are discussed. Hippopotami from other localities on Java are included in the figures in order to get a more complete picture, but are not further discussed, because their stratigraphic position is not clear. Dubois (1908) stated not to have found any hippopotamus remains in Trinil, but Hooijer (1950) did declare hippopotamus finds from Trinil, based on the state of fossilisation (colour) of the fossils, which he compared with other fossils from Trinil. Because the state of fossilisation is no prove that it actually came from Trinil, it is very doubtful that any *Hippopotamus* was found there (De Vos & Sondaar, 1982).

In some figures, measurements of specimens from the Siwaliks are also included, and discussed in Appendices XI-A, B and C.

Statistically, the few measurements do not lead to significant conclusions, but in combination they allow a number of firm speculations.

7.2. LOWER INCISORS

7.2.1. BIOMETRICAL COMPARISON

Indeterminable lower incisors: the ones (Appendix VI-5) from Kali Glagah are smaller than those from Kedung Brubus, which in turn are smaller than those from Ngandong (Fig. 23). Considering that the indeterminate incisors from Kali Glagah might represent incisors at positions in the jaw different than those from Kedung Brubus and/or Ngandong, this conclusion fits the that of the other incisors (see below).

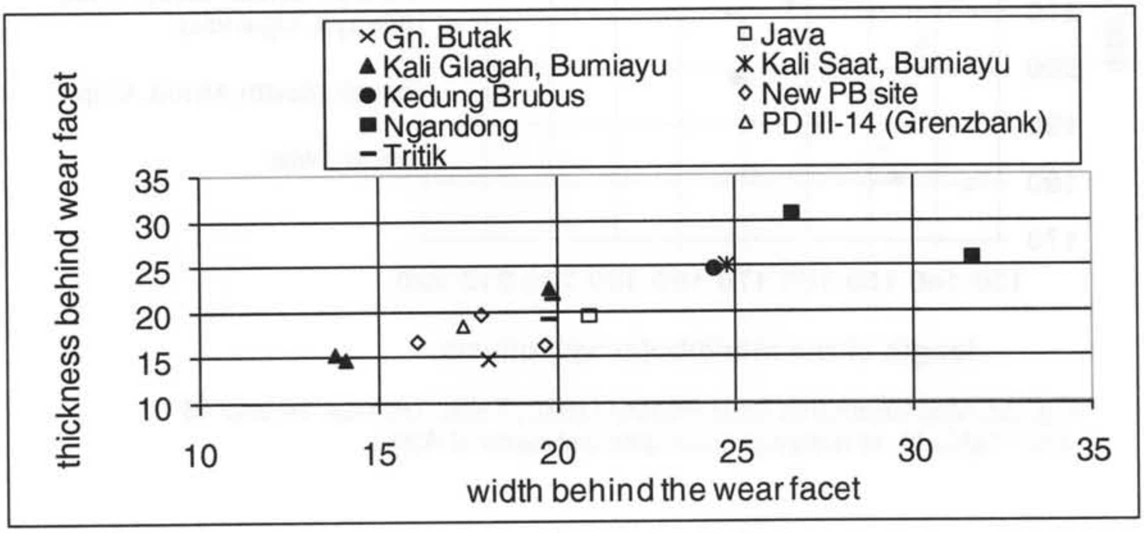

Fig. 23. Thickness and width of indeterminable lower incisors, measured behind the wear facet (Appendix VI-5) of hippopotami from a number of localities on Java.

The same pattern (smallest in Kali Glagah and largest in Ngandong) is seen with respect to the ratio between the width of the indeterminable incisors both behind the wear facet and at the posterior end the length of the incisor and with respect to the ratio between the thickness both behind the wear facet and at the posterior end and the length of the incisor (Appendix VI-5). The lengths of the incisors from Kali Glagah and Kedung Brubus are comparable, those of Ngandong are greater.

Determinable lower incisors: these are shown in Fig. 24 (Appendix VI-1 – VI-3). In the Kali Glagah specimens, the I_1 is slightly (2%) larger than the I_2. In the Kedung Brubus specimens, the difference between the size of I_1 and I_2 is greater; I_2 is 71% - 85% of the size of I_1.The Ngandong specimens show even greater differences with I_2 being 59% - 73% of the size of I_1.

In the Kedung Brubus specimens, the diameter of I_1 is mostly larger than of the I_3 (I_3 is 70% - 113% of the size of the I_1; average 84%). In the Ngandong specimens, the difference between I_1 and I_3 is less; the I_3 is 80% - 98% of the size of the I_1 (Appendix VI-1 – VI-3).

In the Kedung Brubus specimens, the size of I_2 is 90% - 106% of I_3. In the Ngandong specimens, the I_2 is 70% - 74% of that of the I_3. It seems that in the Ngandong specimens the I_2 is less important. The I_3 in the Kali Glagah specimen was not measurable due to damage (Appendix VI-1 – VI-3) .

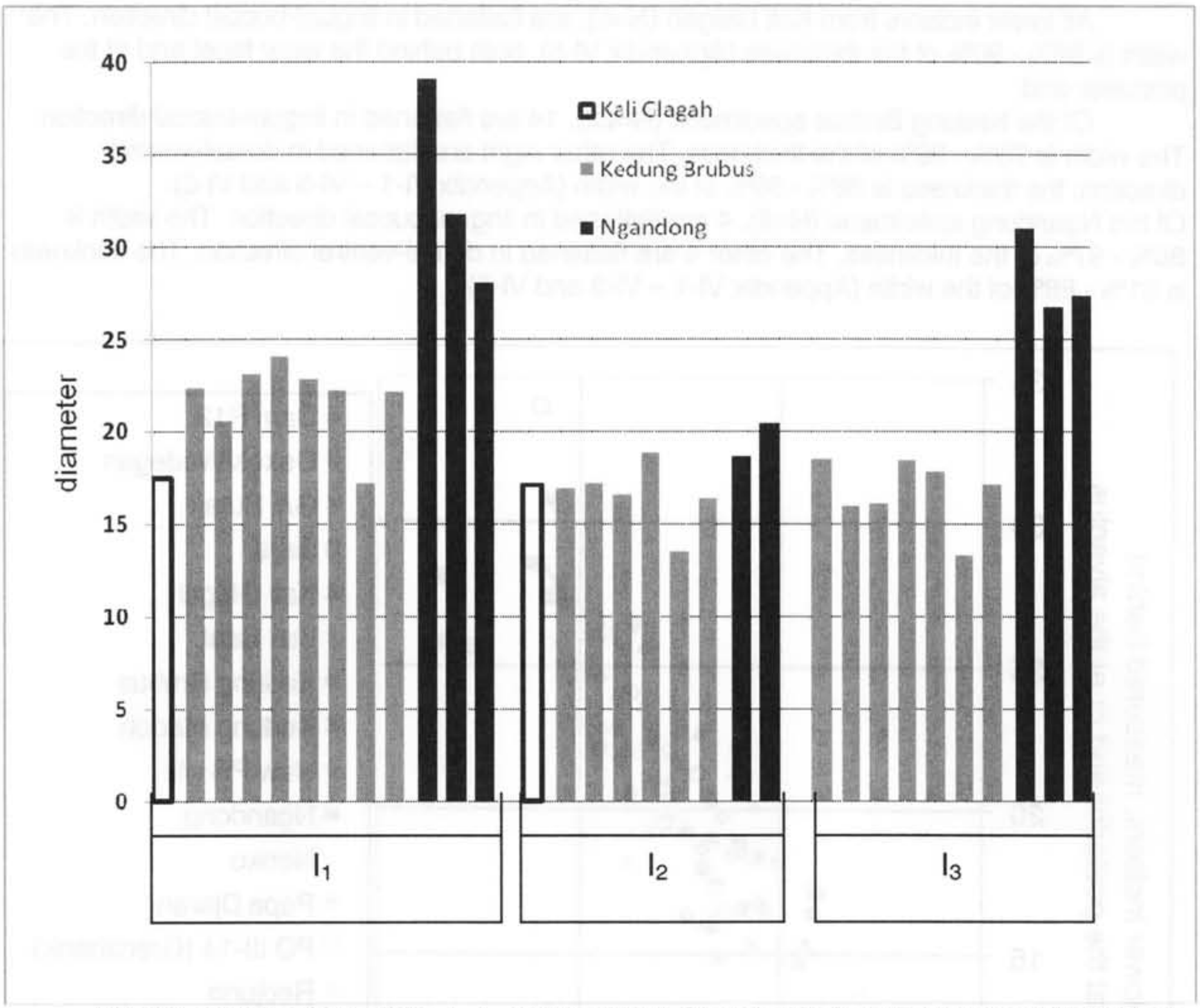

Fig. 24. Comparison of the I_1, I_2 and I_3 of Kali Glagah, Kedung Brubus and Ngandong. The measurements (Appendix VI-1 – VI-3) used are: the width of the alveolus, the width behind the wear facet, the width at the posterior end, the thickness of the alveolus, the thickness behind the wear facet and the thickness at the posterior end.

Comparing the width behind the wear facet and the thickness behind the wear facet of I_3, (measurements from Appendix VI-3), the value from Ngandong is again larger than that from Kedung Brubus.

Figure 25 shows the measurements of the width and thickness of all lower incisors (I_1, I_2, I_3 and indeterminable incisors, measured at the alveolus, behind the wear facet or at the posterior end (measurements in Appendix VI-1 – VI-3 and VI-5)). The smallest incisors are those from Kali Glagah, where the variation is quite large (minimum width 10.1 mm, maximum 21.8 mm; minimum thickness 11.2 mm, maximum 25.7 mm). The lower incisors from Kedung Brubus also show a great variation in diameter (width: minimum 13.3 mm maximum 25.8 mm; thickness: minimum 16.0 mm, maximum 27.3 mm). The lower incisors from Ngandong are larger than most other incisors (width: minimum 18.6 mm, maximum 39.0 mm; thickness: minimum 20.4 mm, maximum 30.8 mm).

Considering all lower incisors from Appendix VI-1 – VI-3 and VI-5, it is clear that the lower incisors from Kedung Brubus and Ngandong show little tapering (i.e., narrowing); the thickness behind the wear facet is similar to the thickness at the posterior end. In some specimens the thickness is greater at the posterior end, in other specimens it is greater behind the wear facet, but the differences are very small. The lower incisors of Kali Glagah, however, all taper in posterior direction and the thickness on the posterior side is 72% – 79% of the thickness behind the wear facet.

All lower incisors from Kali Glagah (N=6), are flattened in lingual-buccal direction. The width is 84% - 90% of the thickness (Appendix VI-5), both behind the wear facet and at the posterior end.

Of the Kedung Brubus specimens (N=22), 14 are flattened in lingual-buccal direction. The width is 78% - 98% of the thickness. The other eight are flattened in dorsal-ventral direction; the thickness is 86% - 99% of the width (Appendix VI-1 – VI-3 and VI-5).
Of the Ngandong specimens (N=8), 4 are flattened in lingual-buccal direction The width is 86% - 97% of the thickness. The other 4 are flattened in dorsal-ventral direction. The thickness is 81% - 88% of the width (Appendix VI-1 – VI-3 and VI-5).

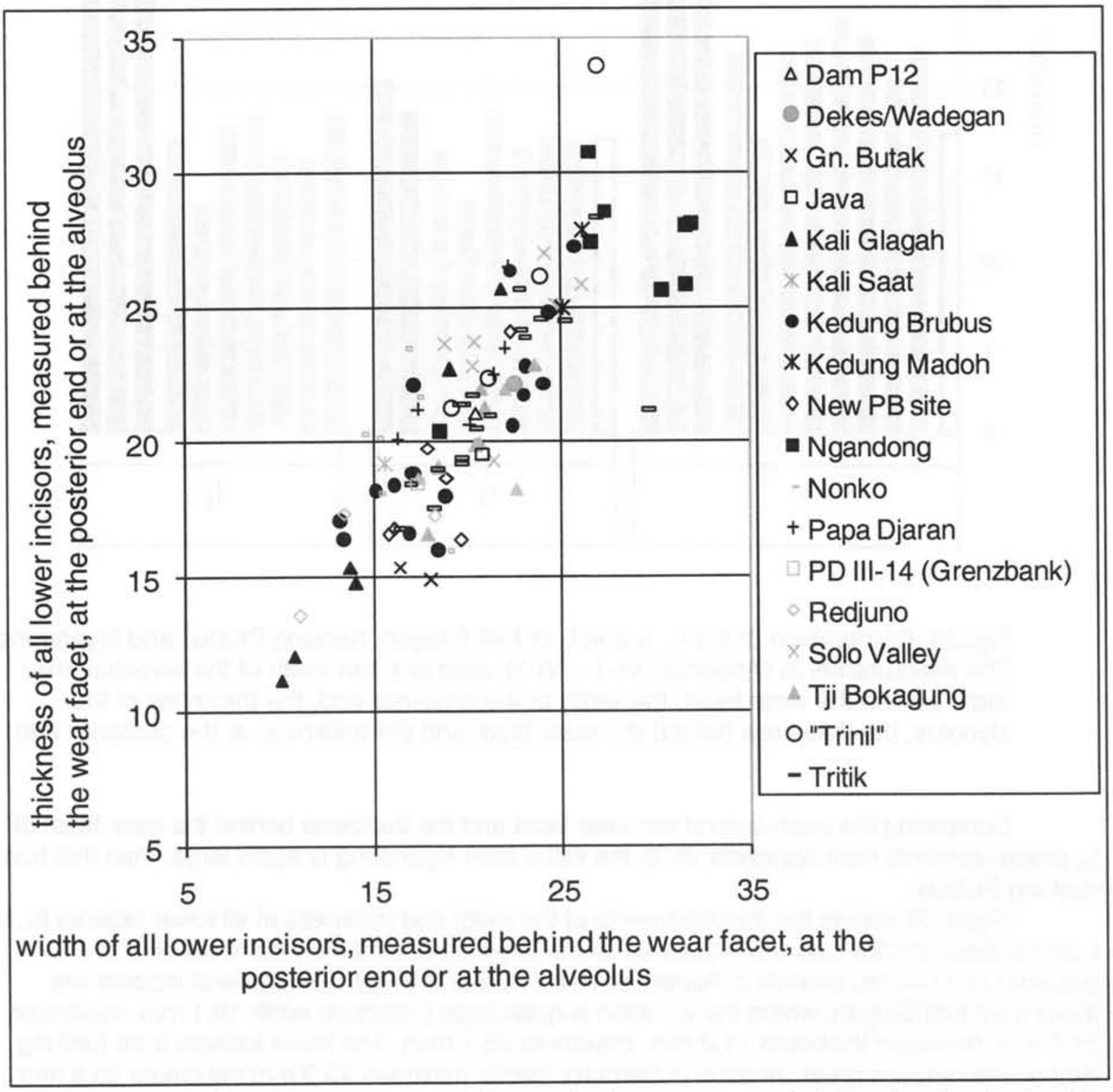

Fig. 25. Width and thickness of all lower incisors measured at the alveolus, behind the wear facet and at the posterior end (Appendix VI-1 – VI-3 and VI-5).

7.2.2. MORPHOLOGICAL COMPARISON

Apart from size, there are hardly any differences between the lower incisors from the different localities. The only characteristic worth mentioning is that two lower incisors from Kedung Brubus show one or more grooves on the dorsal, buccal and lingual sides. Such grooves are not present in the specimens from Ngandong (N=6); there are no morphological descriptions of lower incisors from Kali Glagah.

7.2.3. CONCLUSIONS WITH REGARD TO THE LOWER INCISORS

The lower incisors from Kali Glagah are smaller than those from Kedung Brubus and show little variation. They all taper in posterior direction and they are all flattened in lingual-buccal direction.

The lower incisors from Kedung Brubus are smaller than those from Ngandong. They show more variation than those of Kali Glagah and show tapering in anterior as well as posterior direction and flattening both in lingual-buccal and dorsal-ventral direction. Moreover, several lower incisors from Kedung Brubus show one or more grooves. Those grooves are not present in the lower incisors from Ngandong. The I_2 of the Ngandong specimens is much smaller than the $I_{1,3}$. This is not the case in the Kedung Brubus specimens. There is a decrease from stratigraphically old to young specimens in the flattening in lingual-buccal direction from 100% in the Kali Glagah specimens and 64% in the Kedung Brubus specimens to 50% in the Ngandong specimens. It is not clear what the function of this flattening and presence of grooves is.

7.3. UPPER INCISORS

In the material studied, there are no upper incisors from Ngandong. In Fig. 26 the minimum and maximum diameters of all upper incisors are shown. Measurements are given in Appendix VI-6. The Kali Glagah specimen is smaller than those from Kedung Brubus. No morphological differences could be distinguished between I^1, I^2 and I^3.

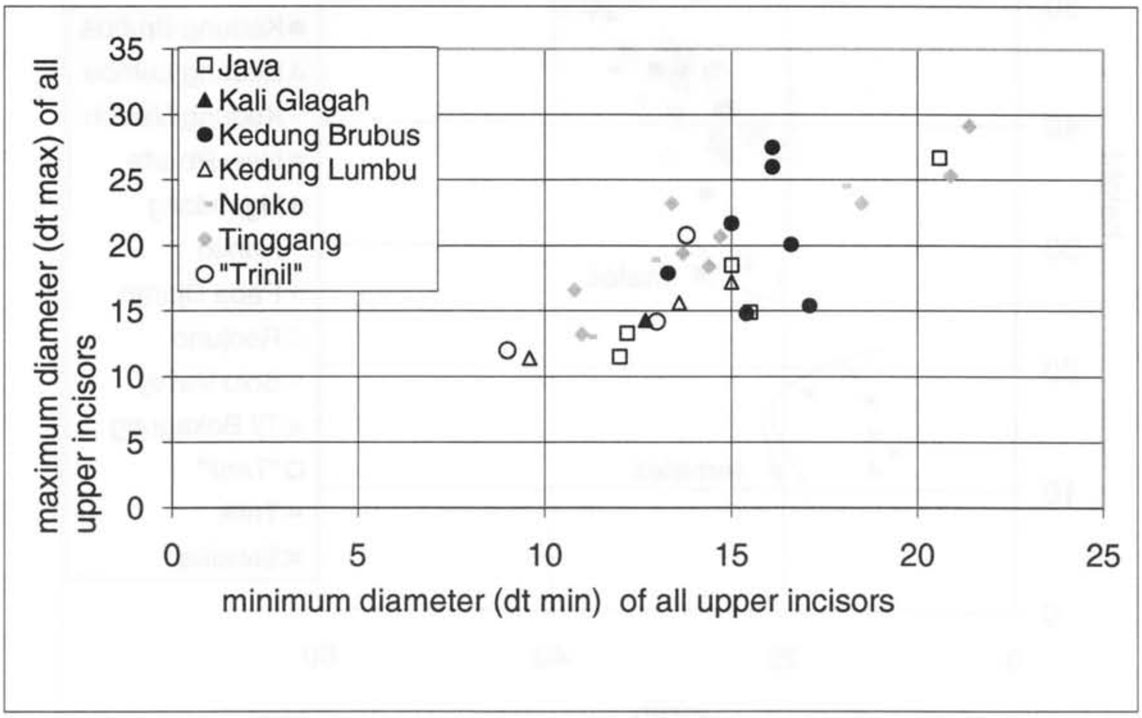

Fig. 26. Minimum and maximum diameter of the upper incisors (Appendix VI-6).

7.4. LOWER CANINES

In Fig. 27 the width and height are shown (Appendix VI-7). As there is a clear sexual dimorphism in *Hippopotamus amphibius* (Hooijer 1950; see also Fig. 21), the smaller canines should represent females. The measurements from Kali Glagah show the canine of a small individual (female and/or juvenile) and that of a very large male, larger than most other canines.

The Kedung Brubus specimens show a great variation; the width ranges from 25.0 mm to 37.2 mm, the height ranges from 37.4 mm to 60.3 mm. The Ngandong specimen is of average size (Fig. 27).

In Fig. 28 the same sexual dimorphism is seen, indicated by the dotted line. There are more measurements from females in Fig. 28 that are missing in Fig. 27 because of damage.

The length of the canine is related to the length of the curvature (Appendix VI-7), except for one specimen without number from Bumiayu excavation 8 (Kali Saat). In this specimen the canine is very curved relative to its length. No differences can be distinguished in this figure between the specimens from Kali Glagah, Kedung Brubus and Ngandong.

No morphological differences between the specimens of the different localities can be distinguished.

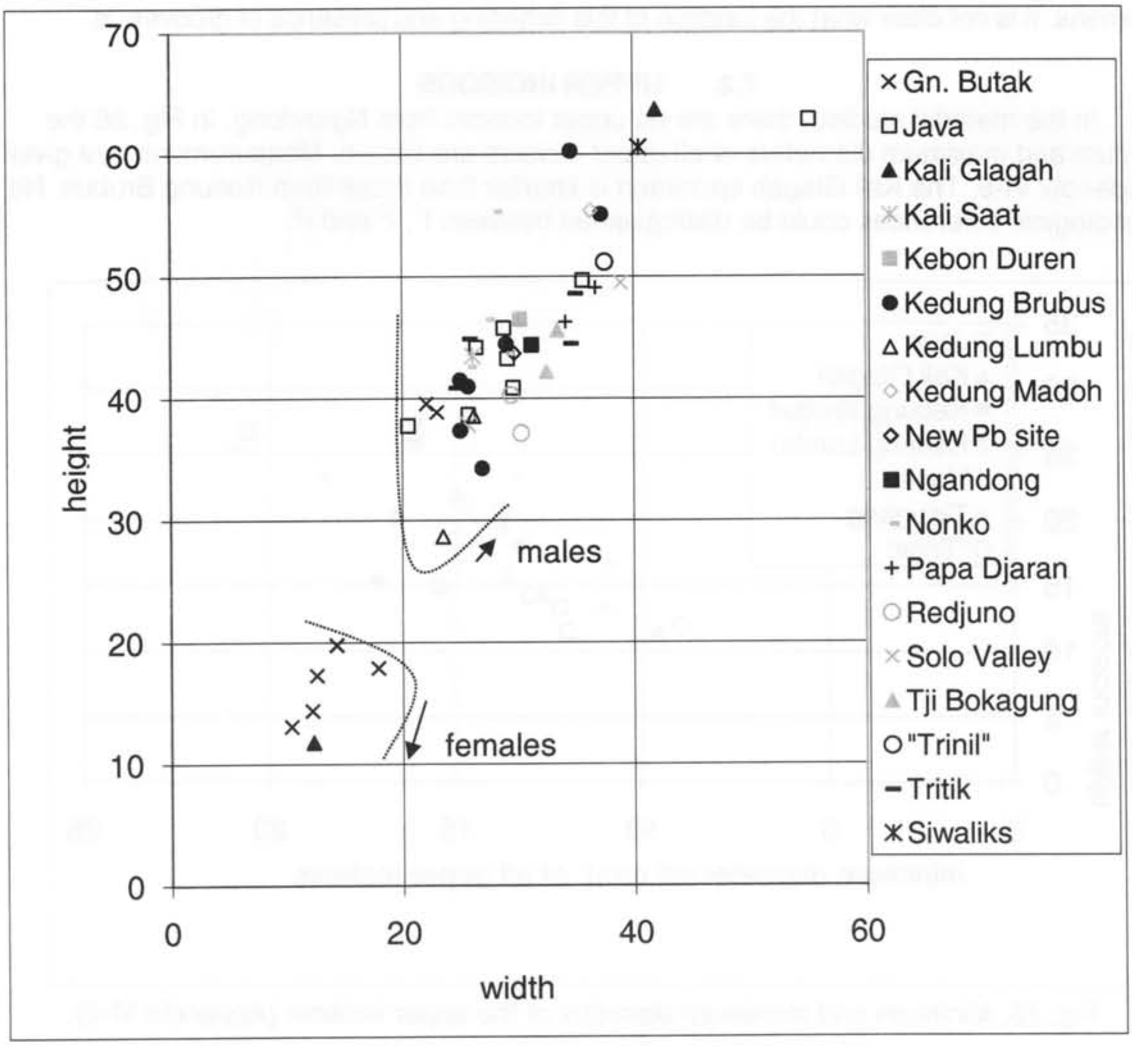

Fig. 27. Diameter of the lower canines (Appendix VI-7).

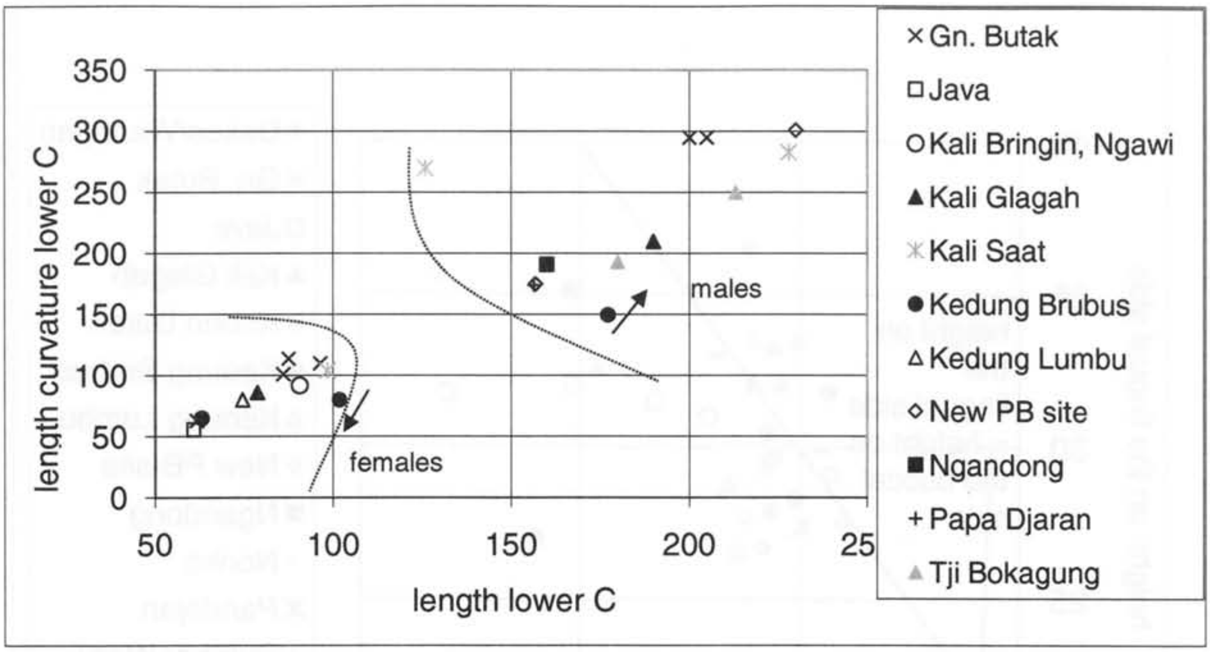

Fig. 28. Length of the lower canines (Appendix VI-7).

7.5. UPPER CANINES

7.5.1. BIOMETRICAL COMPARISON

In Fig. 29 the height, both on the buccal and on the lingual sides is shown (Appendix VI-8). In both Kali Glagah specimens (K 716/2 and K 732), the height on the buccal side is less than on the lingual side (ratio 0.94 and 0.96); the Kali Glagah canines are quite symmetrical (both on the left side of the solid line in Fig. 29). In the Kedung Brubus specimens, the ratio between the two measurements varies from 0.88 to 1.55, so the variation is quite large; there are symmetrical canines and asymmetrical ones. In the Ngandong specimen the ratio is 1.15 and that upper canine thus is asymmetrical.

Both width and length (Appendix VI-8) of the Kali Glagah specimens are greater than the Kedung Brubus specimens. In Fig. 30, the height on the buccal side and the length shows the same pattern (Appendix VI-8); the Kali Glagah specimens are higher than those from Kedung Brubus and also higher than that from Ngandong. The height on the buccal side for the Ngandong specimen is larger than for the Kali Glagah and Kedung Brubus specimens.

Comparing the width and the length of the curvature (Appendix VI-8), the Kali Glagah specimen is more curved than the Kedung Brubus specimens. Fig. 31, in which the height on the buccal side is shown vs. the length of the curvature, shows the same pattern (Appendix VI-8). The Kali Glagah specimen is more curved than the others. The height on the buccal side of the Ngandong specimen is larger than that of the others.

7.5.2. MORPHOLOGICAL COMPARISON

There are no major differences in morphology between the material of the different localities. The only thing worth mentioning is that the buccal groove in the Kali Glagah specimens is not or only slightly present. The variation in the Kedung Brubus specimens is greater; the buccal groove is either not present in some specimens, in others it is small, and also specimens occur in which it is robust. In the Ngandong specimen it is very robust.

7.5.3. CONCLUSIONS WITH REGARD TO THE UPPER CANINES

There is a trend in the symmetry of the upper canines; The Kali Glagah specimens are quite symmetrical, there is more variation in the Kedung Brubus specimens and the Ngandong specimen is quite asymmetrical.

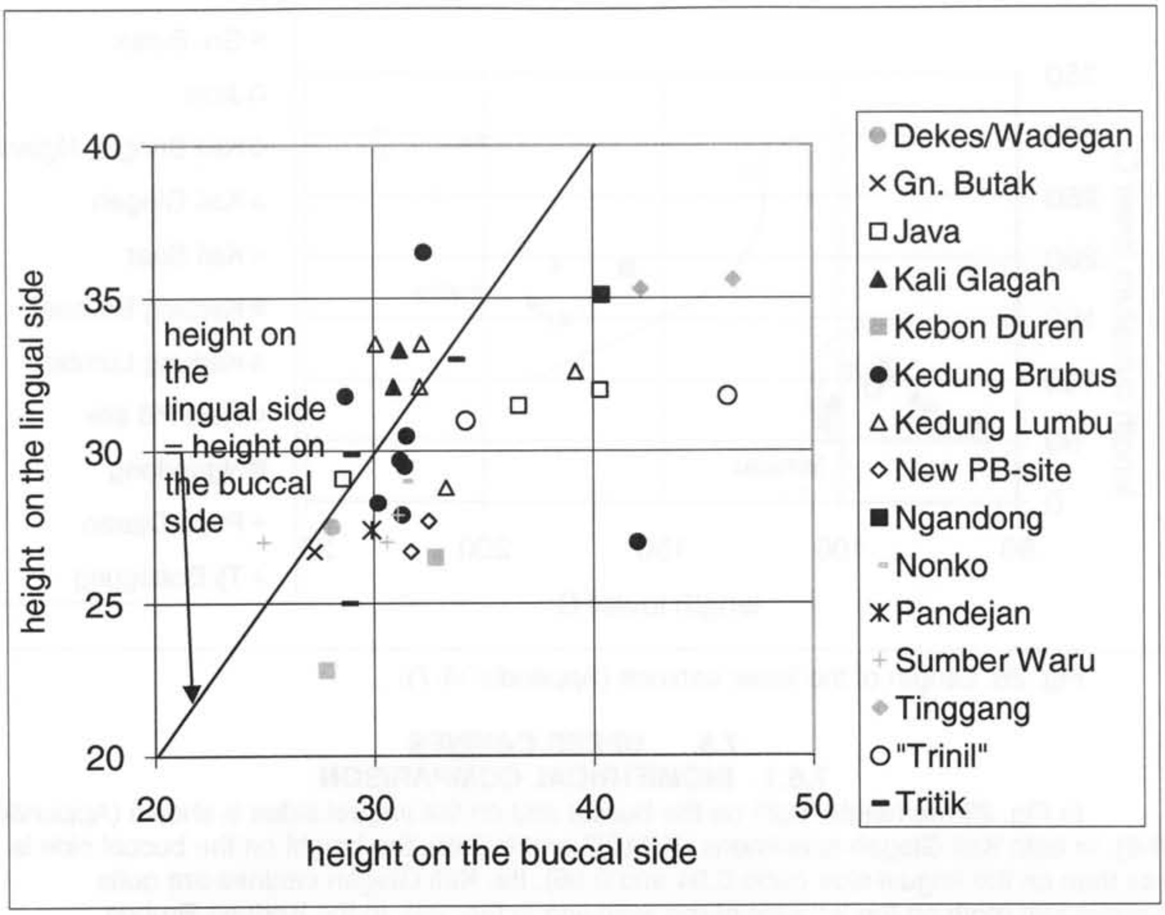

Fig. 29. Height of the upper canines (Appendix VI-8).

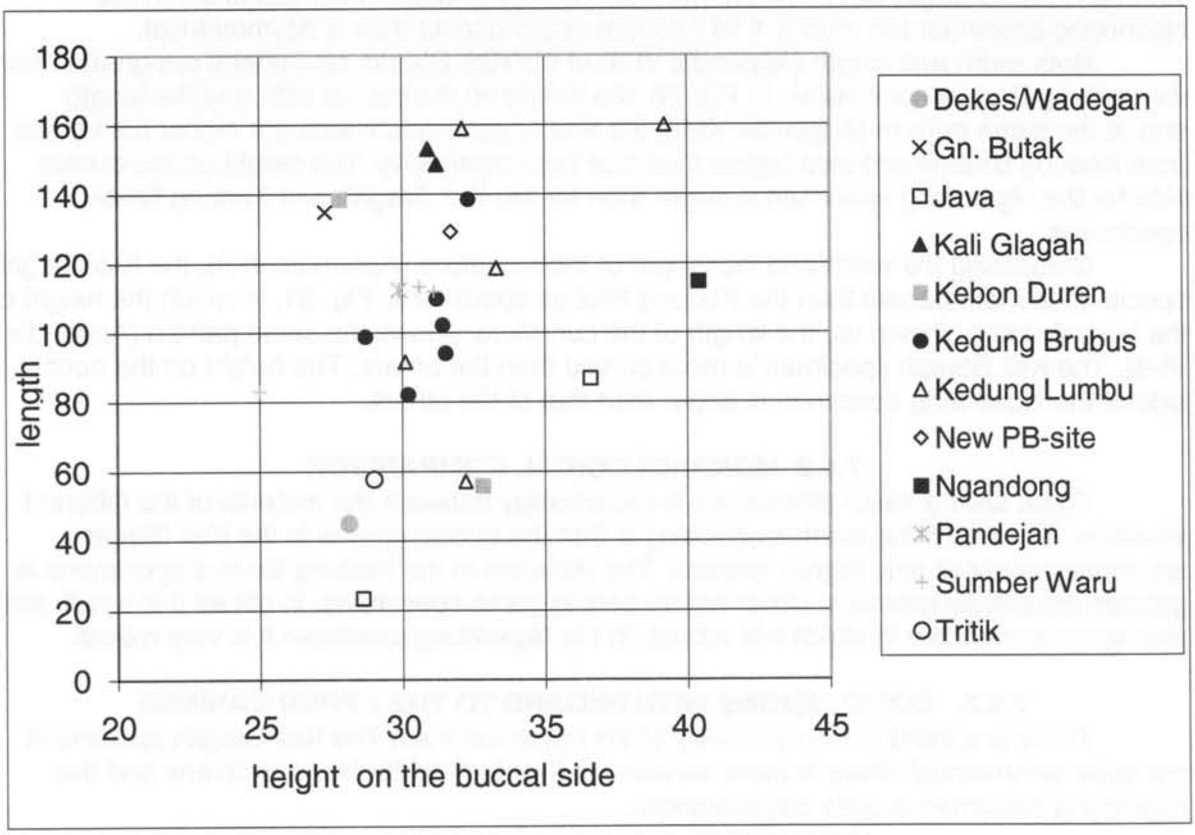

Fig. 30. Height and length of upper C (Appendix VI-8).

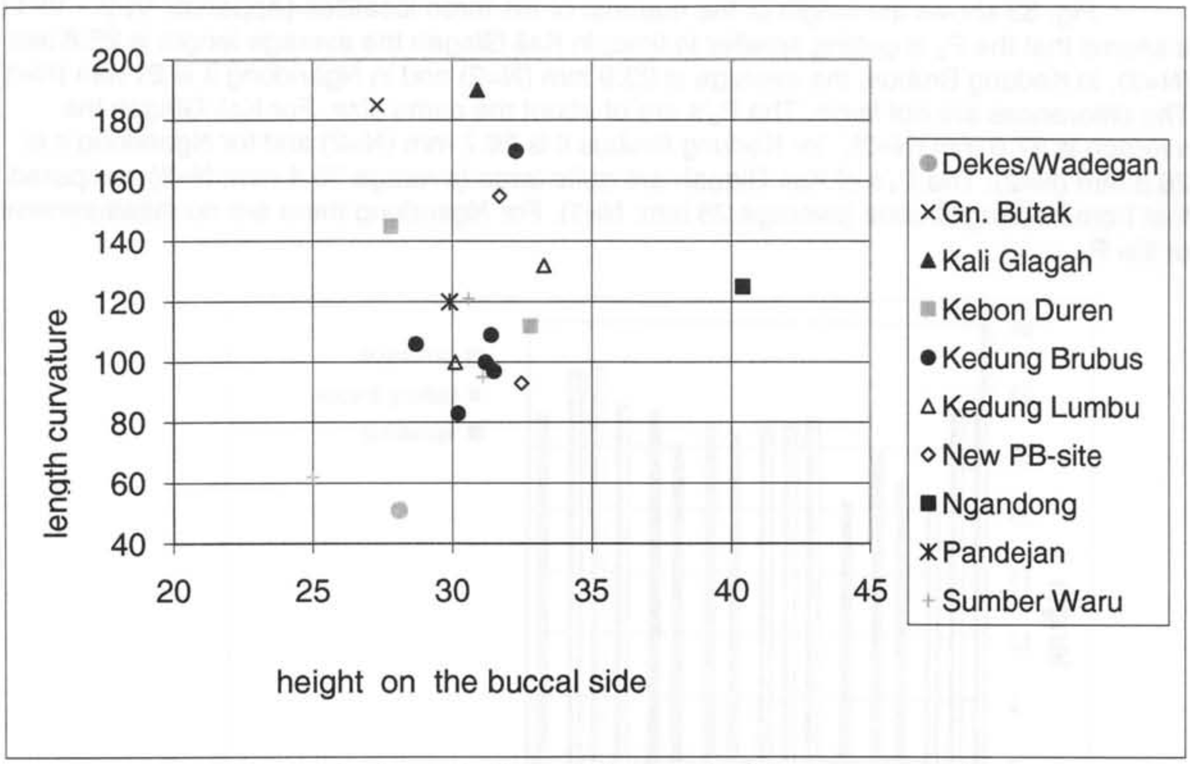

Fig. 31. Height on the buccal side and the length of the curvature of the upper canines (Appendix VI-8).

7.6. LOWER PREMOLARS

7.6.1. BIOMETRICAL COMPARISON

Regarding the width of the anterior and the posterior root (Appendix VI-9 and VI-10), the Kali Glagah specimen is smaller than that of the Ngandong specimen. The same pattern is seen in Fig. 32, in which the crown height of unworn P_3's is shown (Appendix VI-10). The crown height of the Ngandong specimens is greater than that from Kali Glagah.

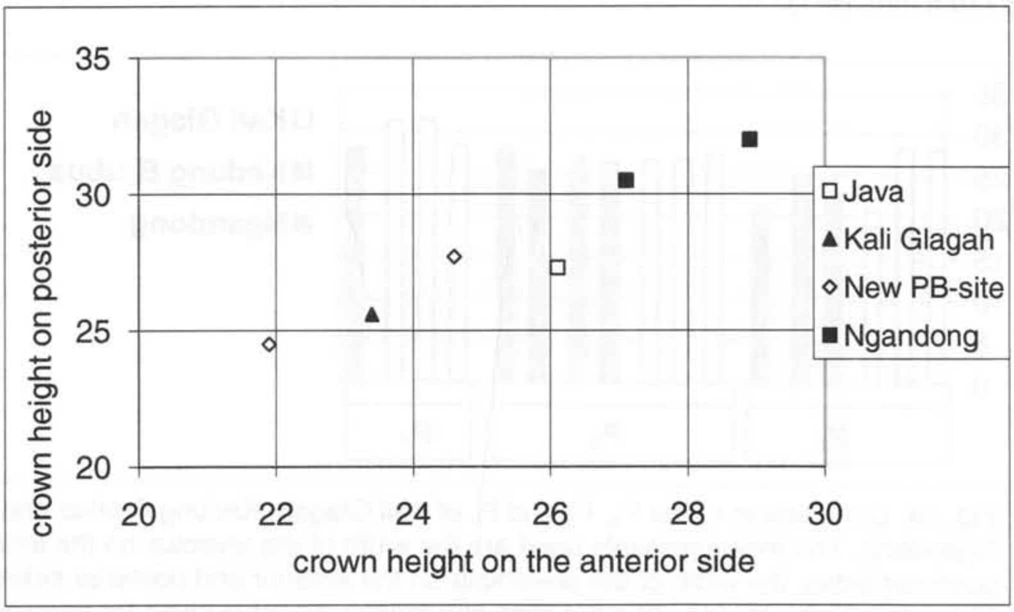

Fig. 32. Crown height of unworn P_3's (Appendix VI-10).

Fig. 33 shows the length of the material of the three localities (Appendix VI-9 – VI-11). It seems that the P_2 is getting smaller in time; in Kali Glagah the average length is 25.8 mm (N=3), in Kedung Brubus, the average is 23.9 mm (N=2) and in Ngandong it is 21 mm (N=1). The differences are not large. The P_3's are of about the same size. For Kali Glagah the average is 27.0 mm (N=3), for Kedung Brubus it is 26.7 mm (N=2) and for Ngandong it is 26.8 mm (N=2). The P_4's of Kali Glagah are quite large (average 30.4 mm; N=3) compared to that from Kedung Brubus (average 28 mm; N=1). For Ngandong there are no measurements of the P_4.

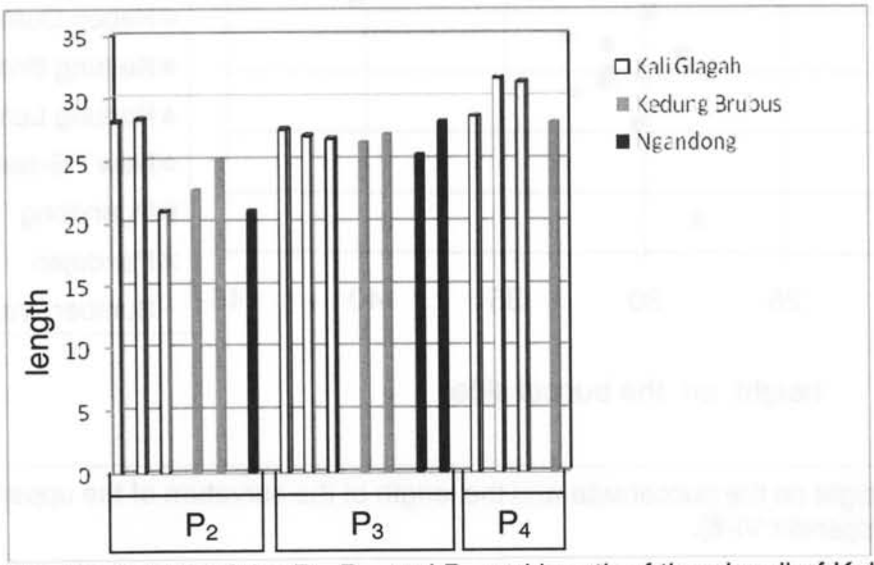

Fig. 33. Length of the P_2, P_3, and P_4 and length of the alveoli of Kali Glagah, Kedung Brubus and Ngandong (Appendix VI-9 – VI-11).

In Fig. 34 the width for all three localities is shown (Appendix VI-9 – VI-11). It seems that the P_2 from Kali Glagah is smaller than the others. For Kali Glagah the average is 14.8 mm (N=3), for Kedung Brubus it is 16.2 mm (N=2) and for Ngandong it is 17.2 mm (N=1). In the P_3, there are not many differences. The average width for the Kali Glagah specimens is 15.5 mm (N=3), for Kedung Brubus it is 14.7 mm (N=2) and for Ngandong it is 17.6 mm (N=2). The P_4 of Kali Glagah is larger (average 21.9 mm; N=3) than that from Kedung Brubus (19.5 mm; N=1).

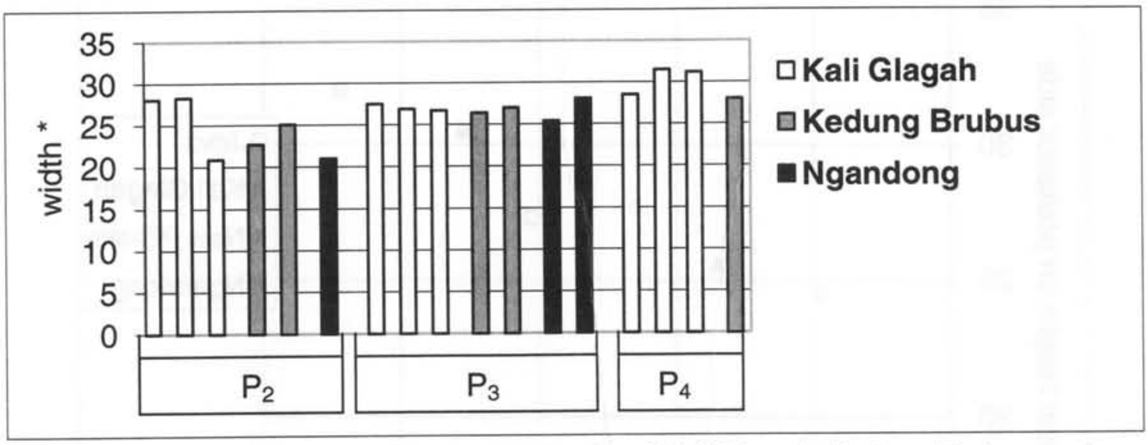

Fig. 34. Comparison of the P_2, P_3 and P_4 of Kali Glagah, Kedung Brubus and Ngandong. The measurements used are the width of the alveolus on the anterior and posterior sides, the width of the premolars on the anterior and posterior sides (Appendix VI-9 – VI-11). *If more than one measurement is given for one specimen, than the largest measurement is used.

7.6.2. MORPHOLOGICAL COMPARISON

P_2: there is one P_2 from Kali Glagah (K 693), two from Kedung Brubus (Coll. Dub. 2318c/3 and Coll. Dub. 2318c/4) and one from Ngandong (K 689). The P_2 of Kali Glagah is very simple, with no anterior or posterior lobes, no cingula, no additional cusps and no additional ridges. The P_2's from Kedung Brubus are less crenulated than that from Ngandong. The Kedung Brubus specimens have an anterior lobe and so does the Ngandong specimen, but in this last one, it is crenulated. The Kedung Brubus specimens do not have a metaconid, the Ngandong specimen does. The protoprecristid is not present or it is smooth in the Kedung Brubus specimens, in the Ngandong specimen it is knobby. The Kedung Brubus specimens have a hypoconid, the Ngandong specimen does not. In the Kedung Brubus specimens the protopostcristid and the protoendocristid are present, in the Ngandong specimen they are not clear. In one Kedung Brubus premolar (P_2 of Coll. Dub. 2318c/3), the posterior root is larger than the anterior one. This is also the case in the Ngandong specimen K 689.

P_3: there are two P_3's from Kali Glagah (without number: skeleton Geological Museum, Bandung and K 698), one from Kedung Brubus (Coll. Dub. 2318c/1) and two from Ngandong (K 685 and K 699). Anterior and posterior lobes are present in all P_3's, but in the Ngandong specimens the posterior lobe is crenulated and the anterior lobe is more robust than in the P_3's both from Kali Glagah and Kedung Brubus. The same holds for the cingula, both on the lingual and buccal sides; in the Ngandong specimens they are very crenulated, in the other specimens they are not crenulated. The paraconid and the paraconulid are very small in the Kali Glagah specimens, in the Ngandong specimens they are not present at all. In all specimens the metaconid and the hypoconid are present. The protoprecristid (not crenulated) is present in the Kali Glagah specimen (K 698), in the Ngandong specimens it is crenulated. The Kali Glagah specimen does not have a hypoconulid, the Kedung Brubus specimen does have this cusplet, in the Ngandong specimens it is either present or not. The entoconid is not present in the Kali Glagah specimen, but it is present in the Kedung Brubus and Ngandong specimens. The specimens from Kali Glagah and Kedung Brubus do not have a protopost- or a protoendocristid. In the Ngandong specimens these ridges are present and crenulated. In the Kali Glagah and Kedung Brubus specimens there are no traces of a metapostcristid, in one Ngandong specimen is it crenulated (K 699). In the Ngandong specimen (K 699) the anterior root is larger than the posterior root. In the Kali Glagah specimen (K 698) they are of about the same size (Appendix VI-10).

P_4: there are three P_4's from Kali Glagah (without number: skeleton in Geological Museum, Bandung and K 675/2, K 675/3) and one from Kedung Brubus (Coll. Dub. 2318c/2). In the P_4's, the specimen of Kedung Brubus is very worn and there are no morphologies preserved in the specimens from Ngandong, so there is nothing to compare.
K 675/1 is probably a P_1, in the Kedung Brubus and Ngandong specimens no P_1's could be distinguished.

7.6.3. CONCLUSIONS WITH REGARD TO THE LOWER PREMOLARS

The differences in the lower premolars are very small. The trends observed need to be confirmed by more fossil material to prove if they are indeed true trends.

From the morphology, the conclusion is drawn that the Kali Glagah specimens, the oldest, are simple, the Kedung Brubus specimens show more variation and the young Ngandong specimens are very crenulated. According to Kahlke (1999), increasingly complicated folding of enamel ridges is an adaptation to harder and tougher food. This is confirmed by the crown height in the P_3's form Ngandong, which are higher than other P_3's and certainly higher than the specimen from Kali Glagah (Appendix VI-10 and Fig. 32).

7.7. UPPER PREMOLARS

From the three localities, upper premolars were only found in Kedung Brubus.

7.8. LOWER MOLARS

7.8.1. BIOMETRICAL COMPARISON

From the measurements given in Appendix VI-18 – VI-20 and the scatter diagrams of these measurements, some conclusions are drawn.

M_1: there are two M_1's from Kali Glagah (M_1 sin and dex in the skeleton from Geological Museum, Bandung), three from Kedung Brubus (Coll. Dub. 2076/6, Coll. Dub. 2916 sin and dex) and one from Ngandong (K 727).

Fig. 35 shows that length of the M_1's measured on the lingual side (Appendix VI-18) is least in the specimen from Kedung Brubus and greatest in that of Ngandong.

The length on the lingual side of the Kali Glagah specimens (Fig. 35) is somewhat less than that of Ngandong. The ratio of the lingual length and width, measured both on the anterior side (not in Fig. 35) and on the posterior side (Fig. 35) is closest to one (the solid line) in the specimens from Kedung Brubus. The ratio between the width on the anterior side and the width on the posterior side in the Kedung Brubus and Ngandong specimens is not very different (Appendix VI-18).

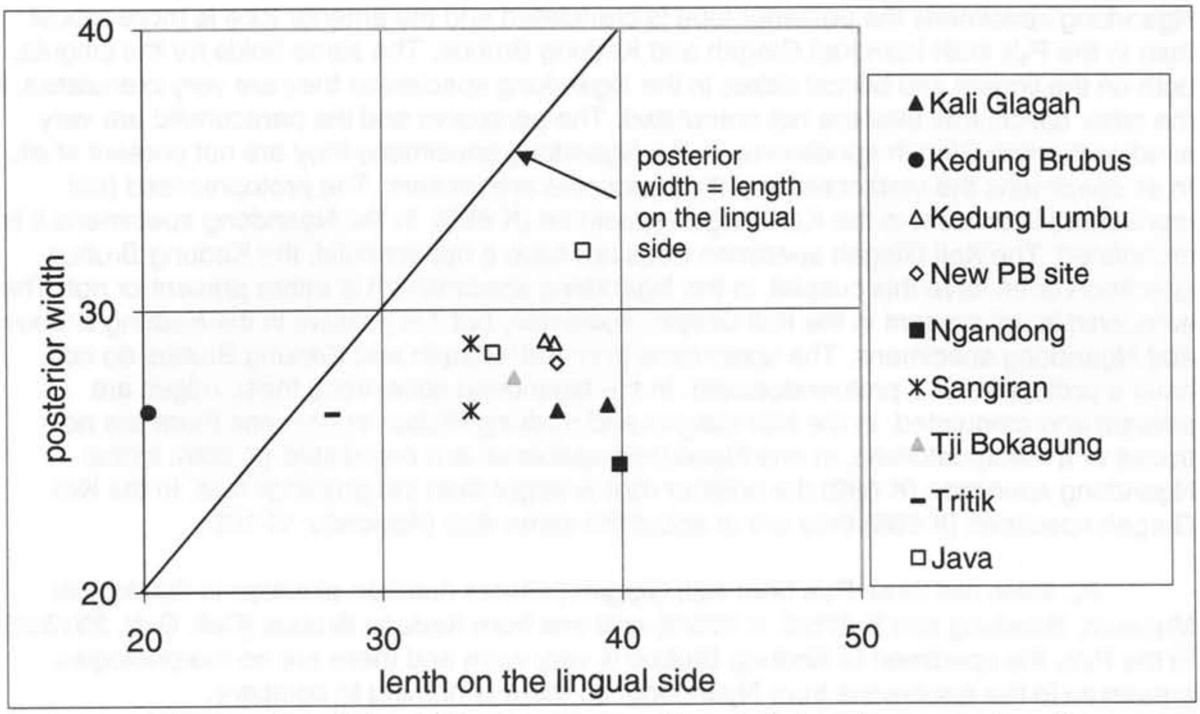

Fig. 35. The size of M_1: width, measured on the posterior side versus length, measured on the lingual side.

M_2: there are two M_2's from Kali Glagah (M_2 sin and dex in the skeleton from Geological Museum, Bandung), five from Kedung Brubus (Coll. Dub. 323a/1, Coll. Dub. 2013, Coll. Dub. 2076a/7, Coll. Dub. 2916 sin and dex) and five from Ngandong (M_2 sin and dex in skull in Geological Museum (Bandung) K 150, K 657 and K 727).

In the M_2's, both the length and the width on the anterior side (Appendix VI-19) are again greater in the Ngandong specimens. The Kedung Brubus specimens are much smaller. The same is shown in Fig.36, in which the widths measured both on the anterior and posterior sides are shown (Appendix VI-19).

Fig. 37 shows that the length is least in the Kedung Brubus specimens. The width on the posterior side (Appendix VI-19) is smallest in the Kedung Brubus specimens, greater for the Kali Glagah specimens and greatest for the Ngandong specimens.

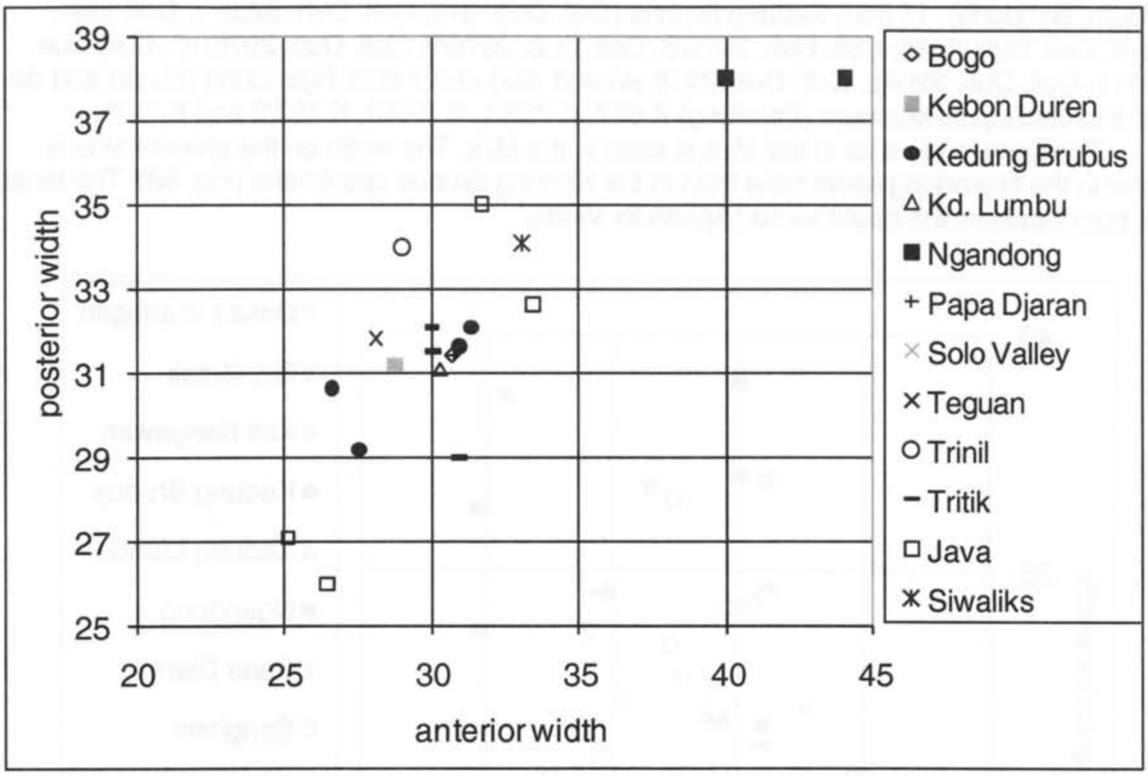

Fig. 36. Width of the M_2's measured on the anterior and posterior sides.

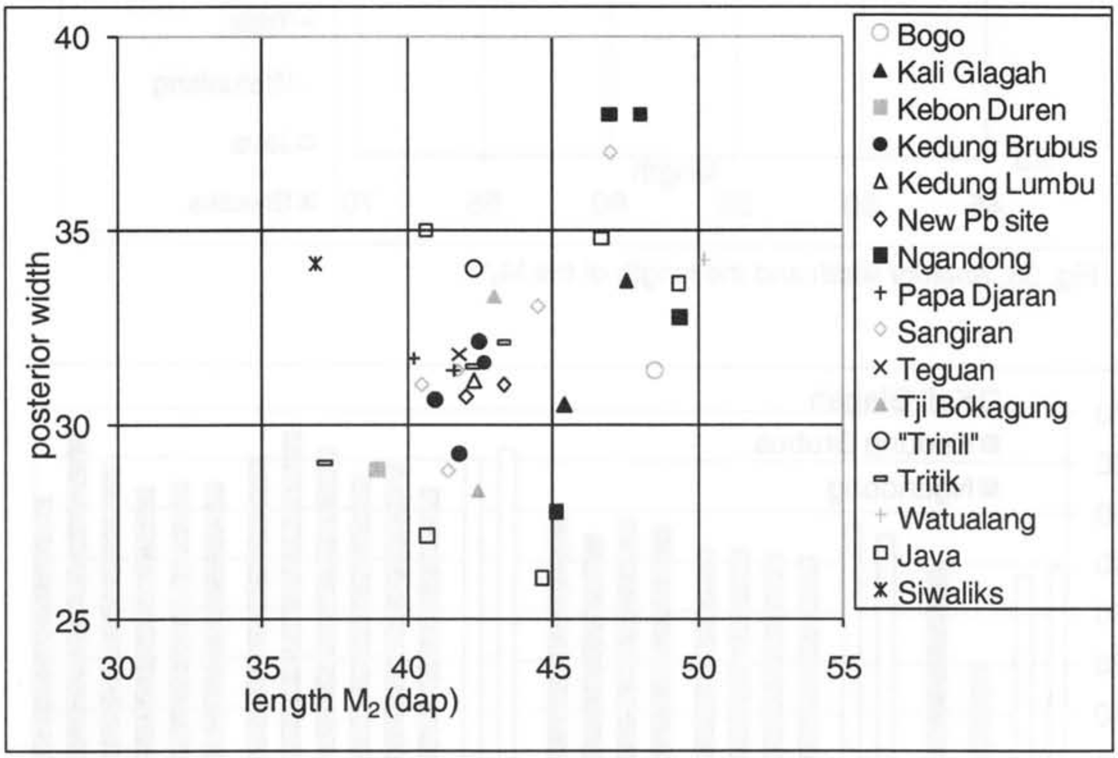

Fig. 37. Posterior width and the length of the M_2's.

M_3: there are two M_3's from Kali Glagah (M_3 sin and dex in the skeleton from Geological Museum, Bandung), 11 from Kedung Brubus (Coll. Dub. 310, Coll. Dub. 323a/1, Coll. Dub. 323a/2, Coll. Dub. 323b, Coll. Dub. 2076/8, Coll. Dub. 2076/9, Coll. Dub. 2076/10, Coll. Dub 2076/11, Coll. Dub. 2204b, Coll. Dub. 2916 sin and dex) and 7 from Ngandong (M_3 sin and dex in skull in Geological Museum (Bandung) K 657, K 723/1, K 723/2, K 723/3 and K 727).

The same picture as in the M_2's is seen in the M_3's. The width on the anterior side is greater in the Ngandong specimens than in the Kedung Brubus specimens (Fig. 38). The length is for both localities the about same (Appendix VI-20).

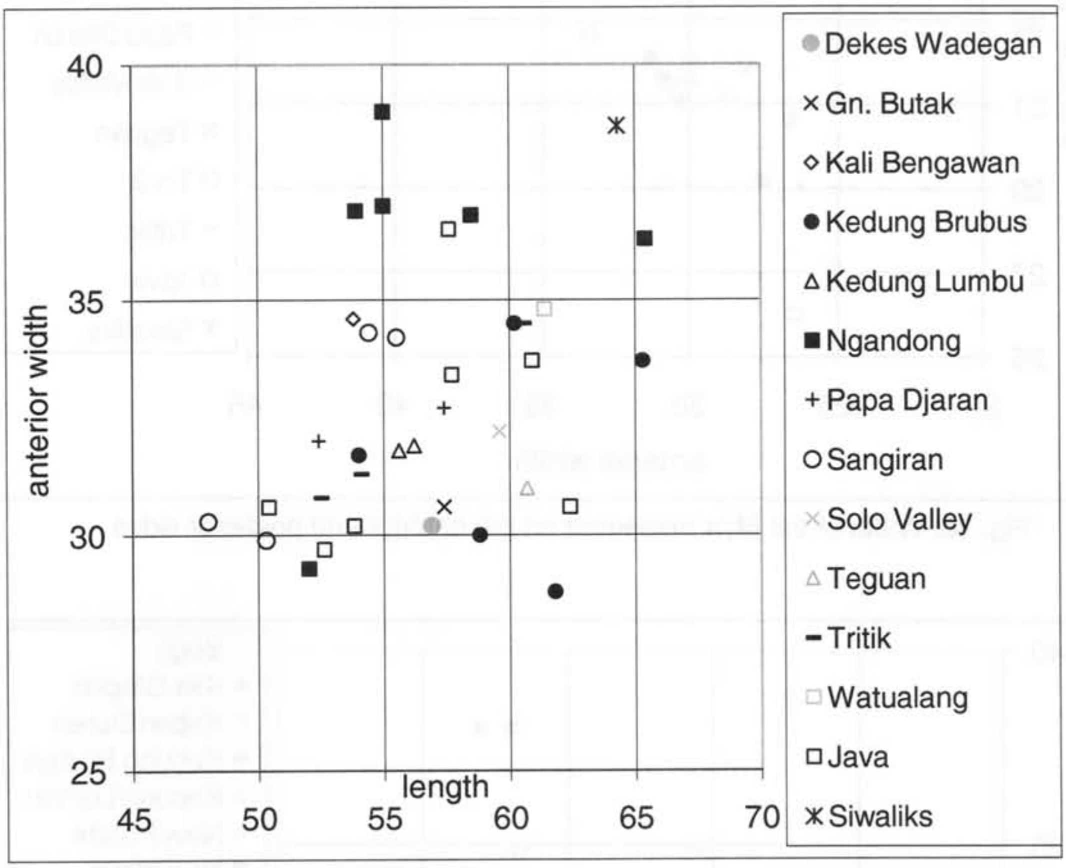

Fig. 38. Anterior width and the length of the M_3's.

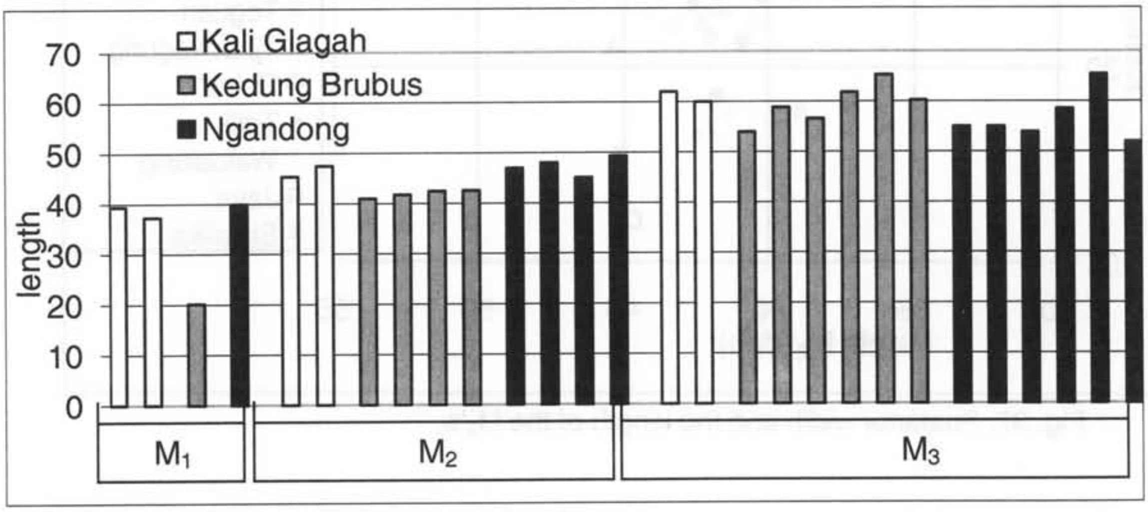

ig.

Fig. 39. Comparison of the length of the M_1, M_2 and M_3 of Kali Glagah, Kedung Brubus and Ngandong.

No differences are found in the ratio between the length and the posterior width between the specimens from Kali Glagah and Kedung Brubus (Appendix VI-20).

In the Figs. 39, 40 and 41 the length and the width, measured both on the anterior and posterior sides of the M_1, M_2 and M_3 are shown for all three localities. The length of the M_1 (Fig 39; Appendix VI-18 – VI-20) is less than that of the M_2 and that of the M_2 is smaller than the M_3. This is very clear in the Kedung Brubus and the Ngandong specimens. In the Kali Glagah specimens this difference is not very clear.

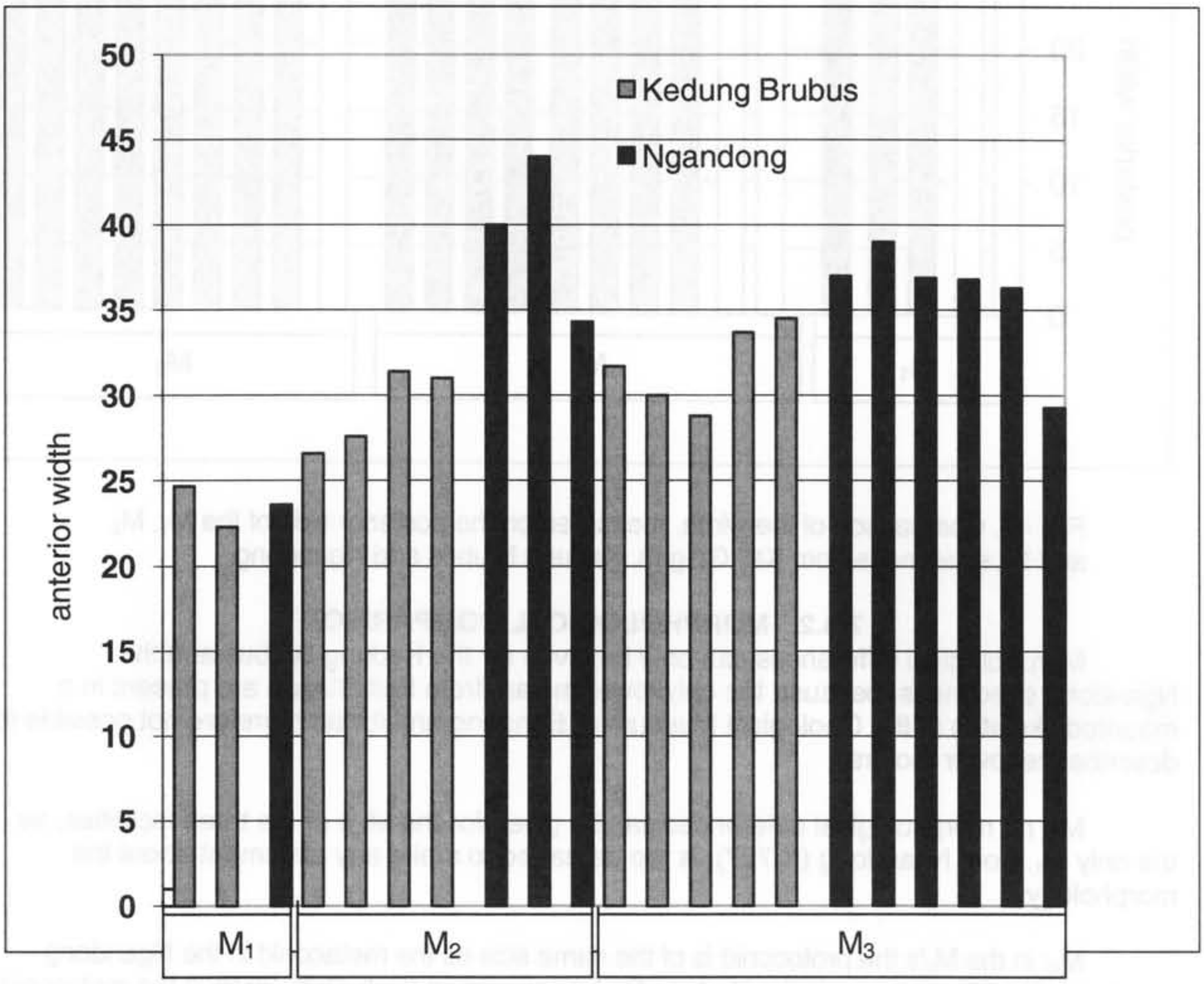

Fig. 40. Comparison of the width, measured on the anterior side of the M_1, M_2 and M_3 from Kedung Brubus and Ngandong (there are no measurements for the Kali Glagah specimens).

In the Kedung Brubus specimens, the anterior width increases from M_1 to M_3 (Fig. 40; Appendix VI-18 – VI-20). Especially, the M_2 and M_3 of Kedung Brubus are smaller than the M_2 and M_3 of Ngandong.

In the Kali Glagah specimens, the posterior width (Fig. 41; Appendix VI-18 – VI-20), of the M_1 is less than that of the $M_{2\text{-}3}$, which are of about the same size. In the Kedung Brubus specimens, this width shows an increase from M_1 to M_3. In the Ngandong specimens, the M_2 is quite a bit larger than the M_1. It seems that the M_2 in the Ngandong specimens becomes more important. Unfortunately, no measurements of M_3's from Ngandong were available.

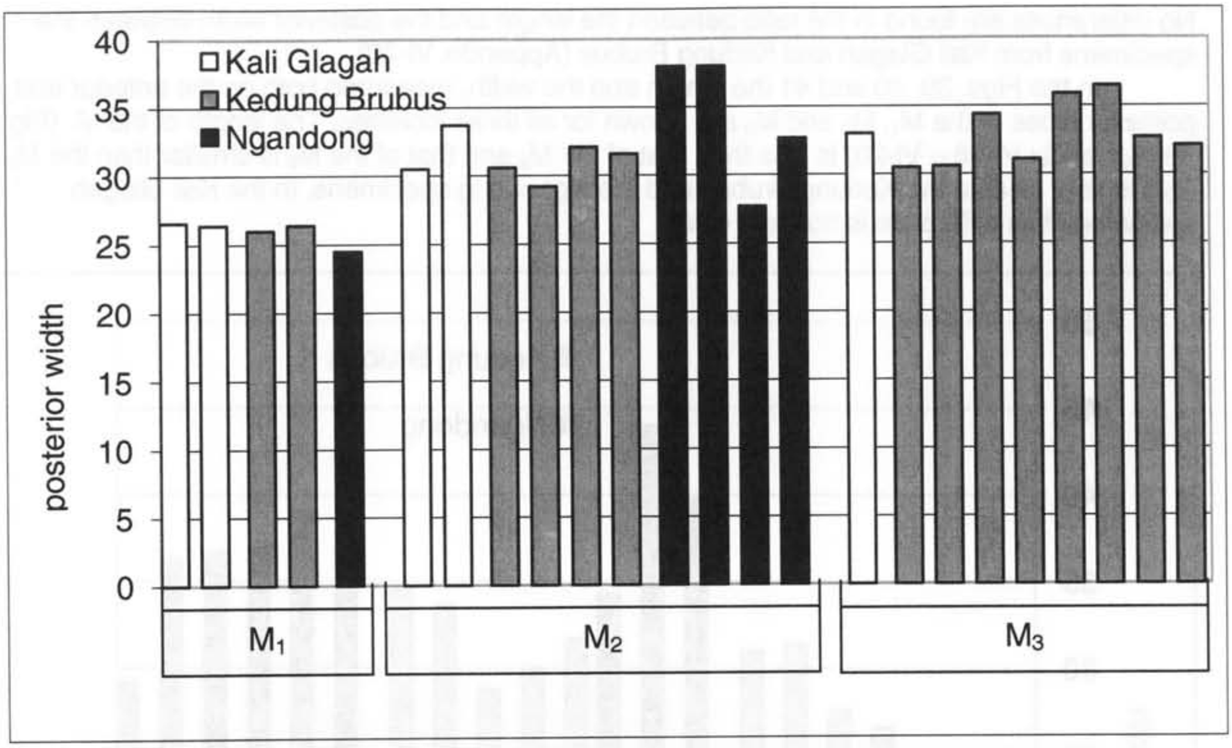

Fig. 41. Comparison of the width, measured on the posterior side of the M_1, M_2 and M_3 specimens from Kali Glagah, Kedung Brubus and Ngandong.

7.8.2. MORPHOLOGICAL COMPARISON

Morphological differences can only be given for the Kedung Brubus and the Ngandong specimens, because the only lower molars from Kali Glagah are present in a mounted skeleton in the Geological Museum of Bandung and it was therefore not possible to describe the lower molars.

M_1: no morphological differences can be given for the M_1's of the three localities, as the only M_1, from Ngandong (K 727), is too damaged to make any statement about the morphology.

M_2: in the M_2's the protoconid is of the same size as the metaconid in the Ngandong specimen (K 150), whereas in the Kedung Brubus specimen (Coll. Dub. 2076/7) the metaconid is larger than the protoconid. In the other Kedung Brubus specimen (Coll. Dub. 2013) these cusps are fused to wear and it cannot be verified if the same is the case in this molar.

Another difference is that in the Ngandong specimen (K 150) the anterior lobe is connected with the protoconid, in the Kedung Brubus specimen (Coll. Dub. 2076/7) the anterior lobe is neither connected with the protoconid nor with the metaconid. The other Kedung Brubus molar (Coll. Dub. 2013) is too worn to verify such difference. In the Ngandong specimen, the metapoststylid is positioned lingually from the hypoprestylid, whereas in the Kedung Brubus specimen (Coll. Dub. 2076/7) they are positioned opposite each other. The other Kedung Brubus M_2 (Coll. Dub. 2013) is too worn to verify such difference. The Ngandong specimen does not have an accessory buccal cusp, the Kedung Brubus specimens do. The Ngandong specimen does not have any cingulum. The Kedung Brubus specimens do have cingula; in Coll. Dub. 2013 there is one on the lingual side, in Coll. Dub. 2076/7 there is one on the buccal side.

M_3: comparing the morphology of the five M_3's from Ngandong (K 657, K 723/1, K 723/2, K 723/3 and K 727) with the nine M_3's from Kedung Brubus (Coll. Dub. 310, Coll. Dub. 323a/1, Coll. Dub. 323a/2, Coll. Dub. 323b, Coll. Dub. 2916 sin and dex, Coll. Dub. 2204b, Coll. Dub. 2076/10 and Coll. Dub. 2076/11) leads to the conclusion that there is one difference. In all five

Ngandong specimens, a hypopostconulid is present, which is not the case in the three Kedung Brubus specimens (Coll. Dub. 323a/2, Coll. Dub. 2204b and Coll. Dub. 2076/10), in which the cusps are not fused due to wear.

7.8.3. CONCLUSIONS WITH REGARD TO THE LOWER MOLARS

The Ngandong specimens are larger than those from Kali Glagah and Kedung Brubus. The number of molars involved is too small, to draw any conclusions about the morphological differences.

7.9. UPPER MOLARS

7.9.1. BIOMETRICAL COMPARISON

From the measurements given in Appendix VI-21 – VI-23 and the scatter diagrams of these data, some conclusions are drawn.

M^1: there are four M^1's from Kali Glagah (M^1 sin and dex in the skeleton from Geological Museum, Bandung, K 674/1 and K 674/2), three from Kedung Brubus (K 749, Coll. Dub. 2908 sin and dex), and one from Ngandong (K 734/1).

Fig. 42 shows that the length of the M^1's (Appendix VI-21) from Kali Glagah is less than that of the specimens from Kedung Brubus, which in turn are smaller than the Ngandong specimen. Also the anterior width of the Kali Glagah specimens (Fig. 42) is less than in those of Kedung Brubus, which in turn is slightly smaller than that of Ngandong. The posterior width is about the same for all three localities.

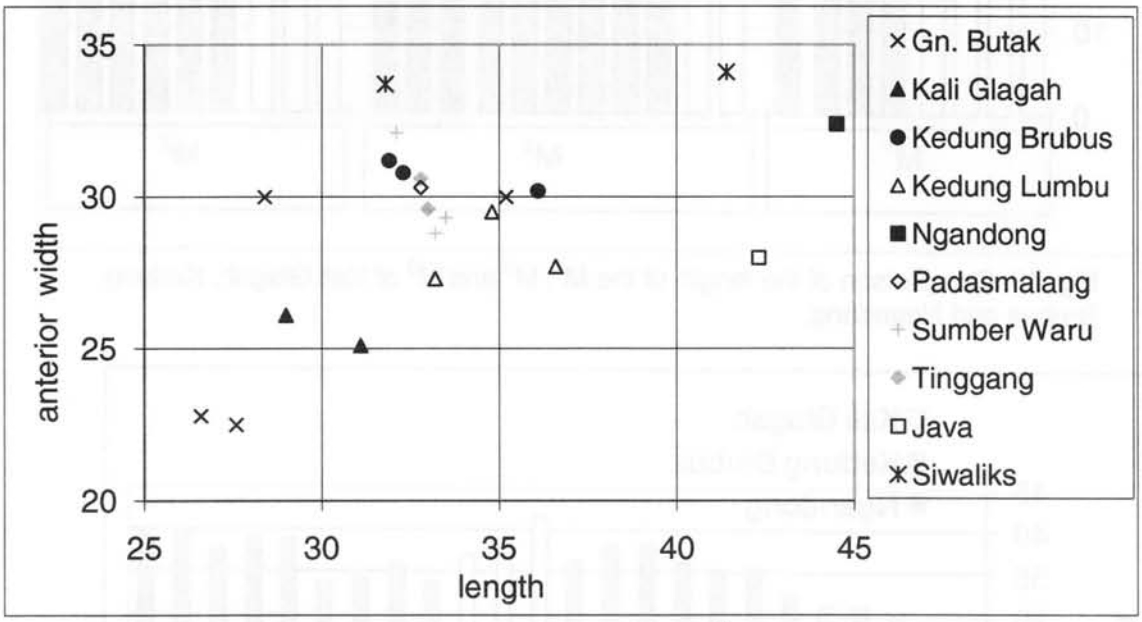

Fig. 42. The anterior width and the length of the M^1's.

M^2: there are three M^2's from Kali Glagah (M^2 sin and dex in the skeleton from Geological Museum, Bandung and K 672), seven from Kedung Brubus (K 749, Coll. Dub. 2008b/1, Coll. Dub. 2008b/2, Coll. Dub. 2203, Coll. Dub. 2908 sin and dex and Coll. Dub. 11466) and three from Ngandong (K 676, K 723/4 and K 734/2).

In the M^2's, both the length and the posterior width (Appendix VI-22) are again larger in the Ngandong specimens. The Kedung Brubus and the Kali Glagah specimens are of about the same size.

M^3: there are three M^3's from Kali Glagah (M^3 sin and dex in skeleton from Geological Museum, Bandung and K 694), 11 from Kedung Brubus (K 749, Coll. Dub. 2076/12, Coll. Dub.

2076/13, Coll. Dub. 2076/14, Coll. Dub. 2076/15, Coll. Dub. 2203, Coll. Dub. 2205/1, Coll. Dub. 2205/2, Coll. Dub. 2318d, Coll. Dub. 2908 sin and dex) and none from Ngandong.
The width, both on the anterior and posterior sides (Appendix VI-23) shows not much difference between the Kali Glagah and the Kedung Brubus specimens.

In Figs. 43, 44 and 45, the length and anterior and posterior widths of the M^1, M^2 and M^3 are shown for all three localities. The length of the M^1 is less than that of the M^2 for all three localities (Fig. 43). The length of the M^1's from Kali Glagah ranges from 29.0 mm to 35.3 mm with an average of 32.5 mm (N=4); in the M^2 the range is 46.1 mm to 47 mm with an average of 46.6 mm (N=2). In the Kedung Brubus specimens the length ranges from 31.9 mm to 36.1 mm

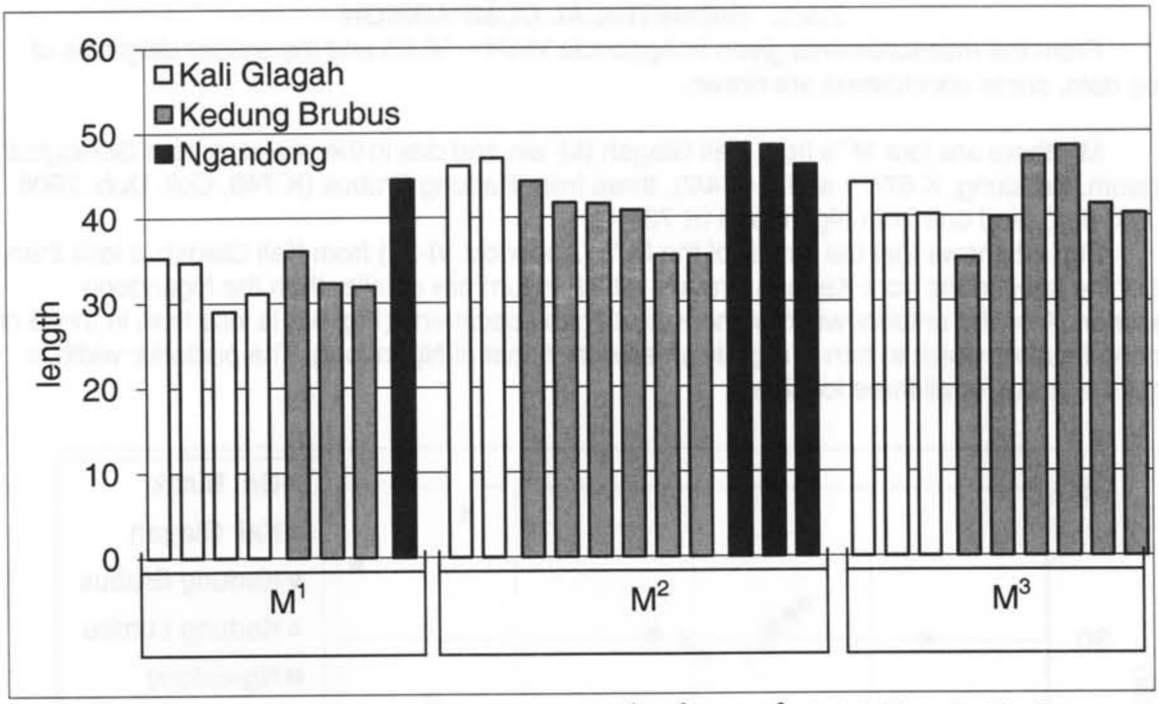

Fig. 43. Comparison of the length of the M^1, M^2 and M^3 of Kali Glagah, Kedung Brubus and Ngandong.

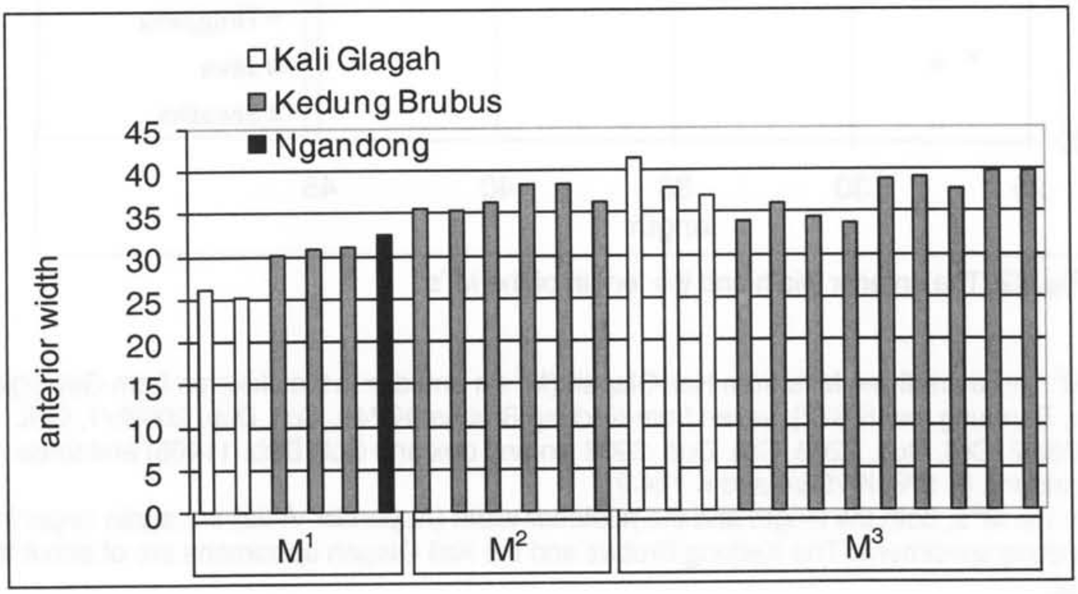

Fig. 44. Comparison of the anterior width of M^1, M^2 and M^3 of Kali Glagah, Kedung Brubus and Ngandong.

in the M^1, with an average of 33.4 mm (N=3), and in the M^2 from 35.5 mm to 44.3 mm with an average of 39.9 mm (N=6). In the Ngandong specimens there is only one measurement for the M^1 (44.5 mm), and the length in the M^2 ranges from 46.1 mm to 48.6 mm with an average of 47.7 mm (N=3).

The length of the M^2 is greater than of the M^3 in the Kali Glagah specimens (Fig. 43; Appendix VI-21 – VI-23). In the M^2, the length ranges from 46.1 mm to 47 mm with an average of 46.6 mm (N=2), in the M^3 it ranges from 40 mm to 44 mm with an average of 41.4 mm. In the Kedung Brubus specimens, the M^2 is slightly smaller than the M^3; The M^2 ranges from 35.5 mm to 44.3 mm, with an average of 39.9 mm (N=6), and in the M^3 it ranges from 35.1 mm to 48.3 mm, with an average of 42.0 mm (N=6).

In the Kedung Brubus specimens, the anterior width (Fig. 44; Appendix VI-21 – VI-23) becomes greater from M^1 to M^3. In M^1 the values range from 30.2 mm to 31.2 mm, with an average of 30.7 mm (N=3), in the M^2 they range from 35.3 mm to 38.5 mm with an average of 36.7 mm (N=6) and in the M^3 they range from 33.7 mm to 39.8 mm, with an average of 37.0 mm (N=9). In the Kali Glagah specimens the M^1 is much smaller than the M^3. The M^1 ranges from 25.1 mm to 26.1 mm, with an average of 25.6 mm (N=2), in the M^3 the anterior width ranges from 36.9 mm to 41.4 mm, with an average of 38.8 mm (N=3). From Ngandong, there is only one M^1 in which this measurement could be taken; it is larger than the M^1 of Kali Glagah and Kedung Brubus.

In the Kali Glagah specimens, the posterior width (Fig. 45; Appendix VI-21 – VI-23) of the M^1 is less than that of the M^2. In the M^1 it ranges from 28.4 mm to 35 mm, with an average of 31.3 mm (N=4) and in the M^2 it ranges from 37 mm to 42.7 mm with an average of 39.6 mm (N=3). In the Kedung Brubus specimens, this width is smallest in the M^1's and largest in the M^2.

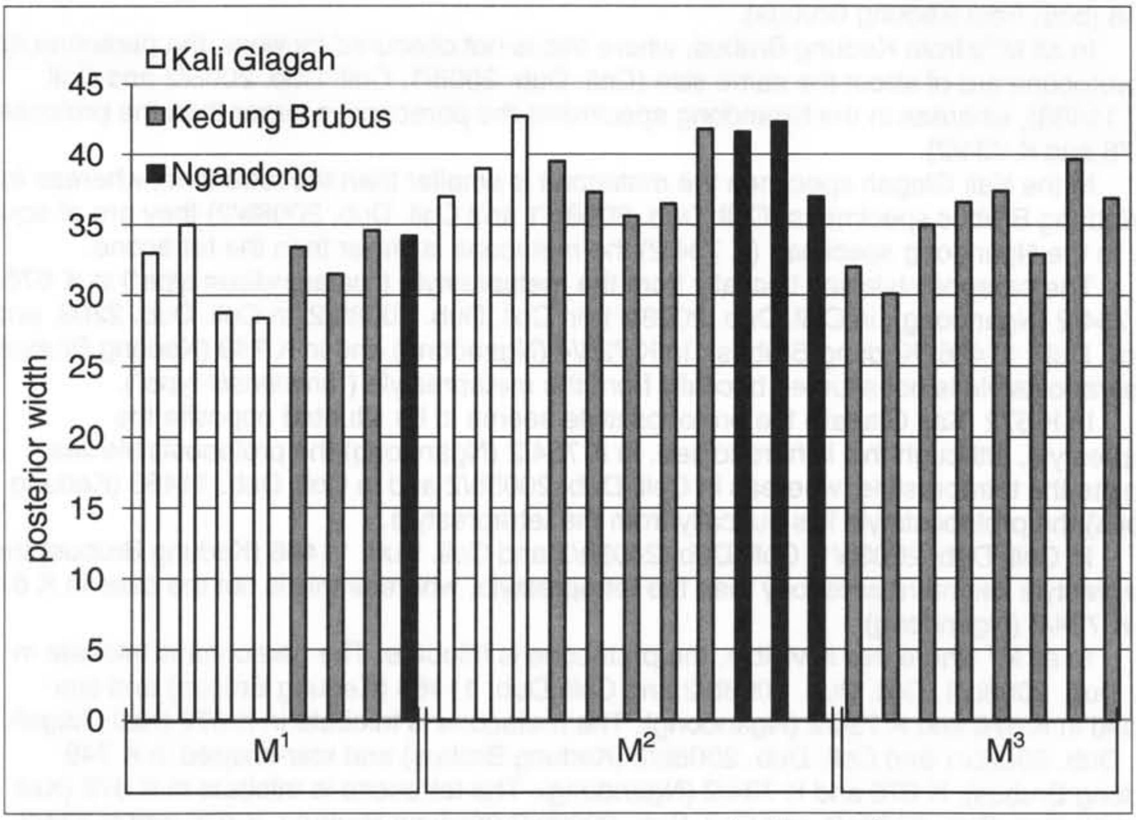

Fig. 45. Comparison of the posterior width of the M^1, M^2 and M^3 of Kali Glagah, Kedung Brubus and Ngandong.

The M^3 is larger than the M^1, but smaller than the M^2. In the M^1 this size ranges from 33.4 mm to 34.6 mm with an average of 33.2 mm (N=3), in the M^2 it ranges from 35.6 mm to 41.8 mm, with an average of 38.1 mm (N=5), and in the M^3 it ranges from 30.1 mm to 39.7 mm, with an average of 35.1 mm (N=8). In the Ngandong specimens the M^2 is quite a bit larger than the M^1. The M^1 measures 34.2 mm (N=1), the M^2 ranges from 37 mm to 42.3 mm, with an average of 40.3 mm (N=3). Unfortunately no M^3's from Ngandong were found.

7.9.2. MORPHOLOGICAL COMPARISON

M^1: there are only two M^1's which can be compared morphologically, i.e., K 749 from Kedung Brubus and K 734/1 from Ngandong. In the Kedung Brubus specimen, the anterior lobe continues into a cingulum only on the buccal side, in the Ngandong specimen, it continues into a cingulum only on the lingual side. The Kedung Brubus specimen has only a cingulum on the buccal side, the Ngandong specimen has a cingulum both on the lingual and buccal sides. The Kedung Brubus specimen has two accessory buccal cusps, the Ngandong specimen does not have any accessory cusps. Other differences cannot be seen, because of wear.

M^2: the M^2's from Kali Glagah (K 672), Kedung Brubus (K 749, Coll. Dub. 2008b/1, Coll. Dub. 2008b/2, Coll. Dub. 2203, Coll. Dub. 2908 sin and dex and Coll. Dub. 11466) and Ngandong (K 676, K 723/4 and K 734/2) all have an anterior lobe. The anterior lobe is connected with the protocone, in those molars where this can be distinguished (in the Kali Glagah specimen K 672, in the Kedung Brubus specimens Coll. Dub. 2008b/1, Coll. Dub. 2008b/2 and in the Ngandong specimens K 676 and K 734/2). Only in the Kedung Brubus specimen Coll. Dub. 11466 the anterior lobe is connected with the paracone.
The anterior lobe does not continue into a cingulum, nor on the lingual side, nor on the buccal side in K 676, K 734/2 (Ngandong), Coll. Dub. 2008b/1 (Kedung Brubus). It continues into a cingulum only on the lingual side in Coll. Dub. 2008b/2 and on both sides in Coll. Dub. 11466 (both from Kedung Brubus).

In all M^2's from Kedung Brubus, where this is not obscured by wear, the paracone and the protocone are of about the same size (Coll. Dub. 2008/1, Coll. Dub. 2008/2 and Coll. Dub. 11466), whereas in the Ngandong specimens the paracone is larger than the protocone (K 676 and K 734/2).

In the Kali Glagah specimen the metacone is smaller than the tetracone, whereas in the Kedung Brubus specimens (Coll. Dub. 2008b/1 and Coll. Dub. 2008b/2) they are of equal size. In the Ngandong specimen (K 734/2) the metacone is larger than the tetracone.

The parapoststyle lies buccally from the metaprestyle ("*palaeindicus*-type") in K 676, in K 734/2 (Ngandong), in Coll. Dub. 2008b/1, in Coll. Dub. 2008b/2, in Coll. Dub. 2203, and in Coll. Dub. 11466 (Kedung Brubus). In K 723/4 (Ngandong) and in K 749 (Kedung Brubus) the parapoststyle is not situated buccally from the metaprestyle ("*sivalensis*-type").

In K 672 (Kali Glagah) the protopoststyle seems to be situated opposite the tetraprestyle, although this is hard to see. In K 734/2 (Ngandong) the protopoststyle lies opposite the tetraprestyle, whereas in Coll. Dub. 2008b/2 and in Coll. Dub. 11466 (Kedung Brubus) the protopoststyle lies buccally from the tetraprestyle.

In Coll. Dub. 2008b/1, Coll. Dub. 2008b/2 and Coll. Dub. 11466 (Kedung Brubus) the metaprestyle lies more anteriorly than the tetraprestyle, whereas this is not the case in K 676 and K 734/2 (Ngandong).

In all M^2 where this is visible, the protocone is trilobate. The paracone is trilobate in Coll. Dub. 2008b/1, Coll. Dub. 2008b/2 and Coll. Dub. 11466 (Kedung Brubus) and star-shaped in K 676 and K 734/2 (Ngandong). The metacone is trilobate in K 672 (Kali Glagah, Coll. Dub. 2008b/1 and Coll. Dub. 2008b/2 (Kedung Brubus) and star-shaped in K 749 (Kedung Brubus), K 676 and K 734/2 (Ngandong). The tetracone is trilobate in K 672 (Kali Glagah), Coll. Dub. 2008b/1 and Coll. Dub. 2008b/2 (Kedung Brubus), K 676 and K 734/2 (Ngandong) and star-shaped in K 749 (Kedung Brubus).

In all upper molars where this could be distinguished, the paracone is situated more to the posterior side than the protocone. They also nearly all have a posterior lobe, except

Coll. Dub. 2908 dex (the left one is broken) from Kedung Brubus. In all molars where this could be distinguished, the posterior lobe is connected with the tetracone.

K 672 (Kali Glagah), Coll. Dub. 2008b/2, Coll. Dub. 2908 dex (Kedung Brubus), K 676, K 723/4 and K 734/2 (Ngandong) have a cingulum on the lingual side. Coll. Dub. 2203 (Kedung Brubus) only has a cingulum on the buccal side (the lingual side is worn). K 749, Coll. Dub. 2008b/1 and coll. 11466 (Kedung Brubus) have a cingulum both on the lingual and the buccal side. Coll. Dub. 2908 sin (Kedung Brubus) has no cingulum on the buccal side (the lingual side is worn).

K 672 (Kali Glagah), K 749, Coll. Dub. 2203, Coll. Dub. 11466 (Kedung Brubus), K 676 and K 734/2 (Ngandong) do not have any additional cusps. K 723/4 (Ngandong) has an accessory lingual cusp. Coll. Dub. 2008b/2 (Kedung Brubus) has both a tetrapostconule and an accessory buccal cusp. Coll. Dub. 2908 sin and dex have an accessory buccal cusp.

M^3: in the M^3's from Kali Glagah the paracone is smaller than the protocone, whereas in the Kedung Brubus specimens these cusps are of equal size.

In the Kali Glagah specimen the parapoststyle lies opposite the metaprestyle (the so-called "*sivalensis*-type", Hooijer, 1950), whereas in the Kedung Brubus specimens the parapoststyle lies buccally from the metaprestyle (the so-called "*palaeindicus*-type", Hooijer, 1950) (Coll. Dub. 2203, Coll. Dub. 2205/1, Coll. Dub. 2205/2, Coll. Dub. 2908 sin and dex). K 749 does not have a metaprestyle. The same is the case for the protopoststyle and the tetraprestyle. In the Kali Glagah specimen these styles lies opposite each other, in the Kedung Brubus specimens there is either no tetraprestyle present (K 749, Coll. Dub. 2205/1 and Coll. Dub. 2205/2 or the protopoststyle lies buccally from the tetraprestyle (Coll. Dub. 2318d and Coll. Dub. 2908).

All four cusps (proto-, para-, meta- and tetracone) have a trilobate shape in the Kali Glagah specimen, whereas in the Kedung Brubus specimens there is more variation in the shape of these cusps. In K 749, the protocone is round, the paracone is trilobate and the meta- and tetracone are half-moon-shaped. In Coll. Dub. 2076/13, the protocone is star-shaped, in coll. Dub. 2076/14, the tetracone is star-shaped, in Coll. Dub. 2076/15, the metacone is oval-shaped and the tetracone is round. In Coll. Dub. 2205/1, the proto- and paracone are star-shaped and the tetracone is oval-shaped. In Coll. Dub. 2205/2, the metacone is triangular and the tetracone is oval-shaped. In Coll. Dub. 2318d the meta- and tetracone are half-moon-shaped.

The Kali Glagah specimen does not have any additional cusps. Most Kedung Brubus specimens where this could be distinguished do have additional cusps. K 749 has an additional cusp anterior of the paracone, Coll. Dub. 2076/14 has a metapostconule, Coll. Dub. 2203 has an accessory buccal cusp, Coll. Dub. 2205/2 has a meta- and tetrapostconule, Coll. Dub. 2318d has accessory lingual and buccal cusps and a metapostconule, Coll. Dub. 2908 has an accessory lingual cusp. Only Coll. Dub. 2205/1 has no additional cusps.

7.9.3. CONCLUSIONS WITH REGARD TO THE UPPER MOLARS

M^1: the M^1's from Kali Glagah are smaller than those from Kedung Brubus, which in turn are smaller than the one from Ngandong, but the differences are not very large.

M^2: in the M^2's, the length of the specimens from Kali Glagah is greater than those from Kedung Brubus, but smaller than those from Ngandong. Regarding the posterior width, the specimens from Kali Glagah are smaller than those from Kedung Brubus, which in turn are smaller than those from Ngandong.

M^3: the length of the M^3's from Kali Glagah is slightly smaller than those from Kedung Brubus. In general, the specimens from Kali Glagah are slightly smaller than those from Kedung Brubus and the Ngandong specimens are the largest.

Regarding the morphology, there is a difference in relative size of the para- and protocone. In the Kali Glagah specimen (K 694),the paracone is smaller than the protocone (M^3), in the Kedung Brubus specimens they are of equal size (M^2 and M^3) and in the Ngandong specimens the paracone is larger than the protocone (M^2). The same can be said about the meta- and tetracone: in the Kali Glagah specimen (K 672), the metacone is smaller than the tetracone, in the Kedung Brubus specimens they are of similar size and in the Ngandong specimens the metacone is larger than the tetracone (M^2). The Kali Glagah specimens do not have any additional cusps (M^2 and M^3), the Ngandong specimen has an accessory lingual cusp, whereas the Kedung Brubus specimens have a lot of variation in additional cusps on several places (M^2 and M^3). The Kedung Brubus specimens show a lot of variation. For example, all three localities have upper molars with a cingulum on the lingual side, but some Kedung Brubus specimens have molars with no cingulum, or only on the lingual side, or only on the buccal side, or on both sides. This might be due to the fact that the Kedung Brubus specimens are more numerous than the others are.

7.10. MANDIBLE

7.10.1. BIOMETRICAL COMPARISON

Differences in the length of the symphysis (Appendix VI-24) between the specimens from Kali Glagah (skeleton without number, Geological Museum, Bandung), Kedung Brubus (Coll. Dub. 2916 and Coll. Dub. 2931) and Ngandong (without number, Geological Museum, Bandung) could not be established, because all measurements are minimum measurements; the symphyses are not complete due to damage.

The height of the symphysis is smallest in the Kali Glagah specimen, greater in the Kedung Brubus specimens and greatest in the Ngandong specimen (Appendix VI-24).

Fig. 46 shows the width and the thickness of the ramus. The ramus of the Kali Glagah specimens (without number sin and dex; Geological Museum, Bandung) is smaller than in the Kedung Brubus specimens (Coll. Dub. 2174, Coll. Dub. 2916 sin and dex). Unfortunately there is no measurement of the width of the ramus from the Ngandong specimen (without number, Geological Museum, Bandung) but the thickness of the ramus is very much greater than those from Kali Glagah and Kedung Brubus (Appendix VI-24); in fact it is thicker than all other rami.

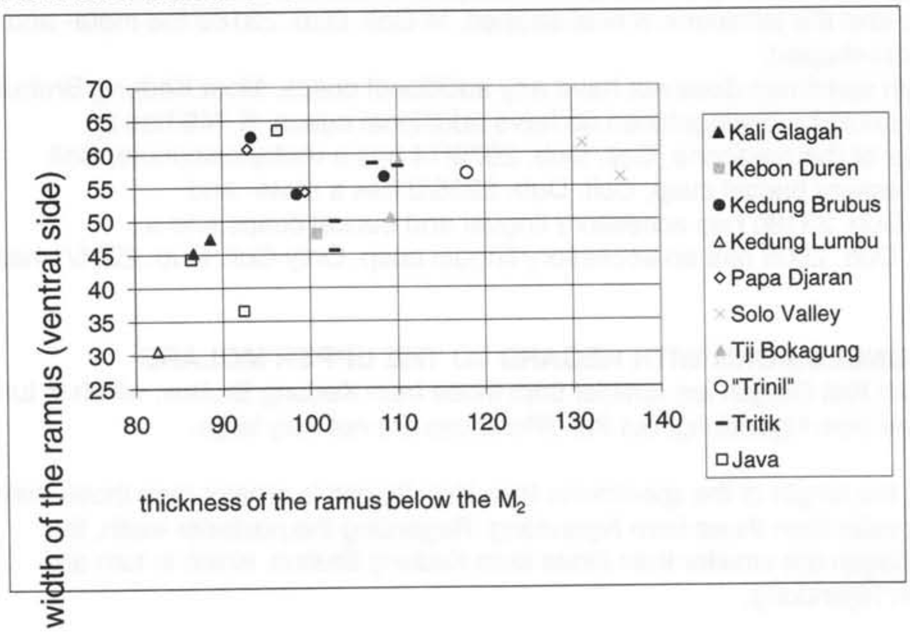

Fig. 46. The thickness and width of the ramus.

The distance between the left and right canine is less in the Ngandong specimen (without number, Geological Museum, Bandung) than in the Kali Glagah specimen (without number, Geological Museum, Bandung; Appendix VI-25).

The diastema between the canine and P_2 from Kedung Brubus (Coll. Dub. 2916 and Coll. Dub. 4908) is comparable in size with that from Ngandong (without number, Geological Museum, Bandung; Appendix VI-25).

In Fig. 47, the length of the row P_2-P_4 is compared with the length of the row M_1-M_3. The length of the row of molars in the Ngandong specimen (without number, Geological Museum, Bandung) is very much greater than in the Kedung Brubus specimens (Coll. Dub. 2916 sin and dex). The length P_2-P_4 is comparable; that from Ngandong is slightly shorter than those from Kedung Brubus.
A summary of the minimum and maximum measurements of the mandible is given is Appendix VI-26

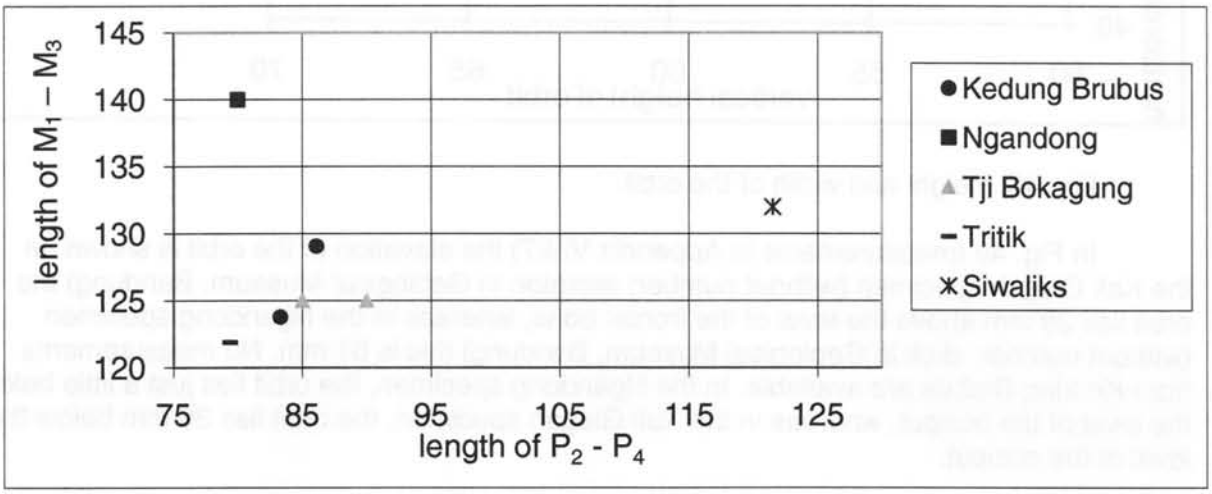

Fig. 47. Length of the rows of molars and premolars.

7.10.2. MORPHOLOGICAL COMPARISON

Morphologically not many differences were found. The Kali Glagah specimen (without number, Geological Museum, Bandung) has an alveolus of a (D)P_1 both on the left and right side; in the Kedung Brubus and Ngandong specimens there was no indication for the presence of a (D)P_1. There are, however, too few specimens from these localities to prove that this is characteristic.

7.10.3. CONCLUSIONS WITH REGARD TO THE MANDIBLE

Again, the Ngandong specimen is larger than the one from Kali Glagah and those from Kedung Brubus. Regarding the height of the symphysis and the thickness of the ramus (Appendix VI-24) the Kali Glagah specimen is smaller than the Kedung Brubus specimen (Coll. Dub. 2916). The length of the M_1-M_3 is greater in the Kali Glagah specimen than in the Kedung Brubus specimen (Appendix VI-25).

7.11. CRANIUM

7.11.1. BIOMETRICAL COMPARISON

In Fig. 48 (measurements in Appendix VI-27) the height and width of the orbit is shown. The height of the orbit is largest for the Kali Glagah specimen (without number; skeleton in Geological Museum, Bandung), a bit less high in the Kedung Brubus specimen (Coll. Dub. 2908) and smallest in the Ngandong specimen (without number; skull in Geological Museum, Bandung). The width of the orbit is comparable in size for the Kali Glagah and Kedung Brubus specimens, but the Ngandong specimen is smaller.

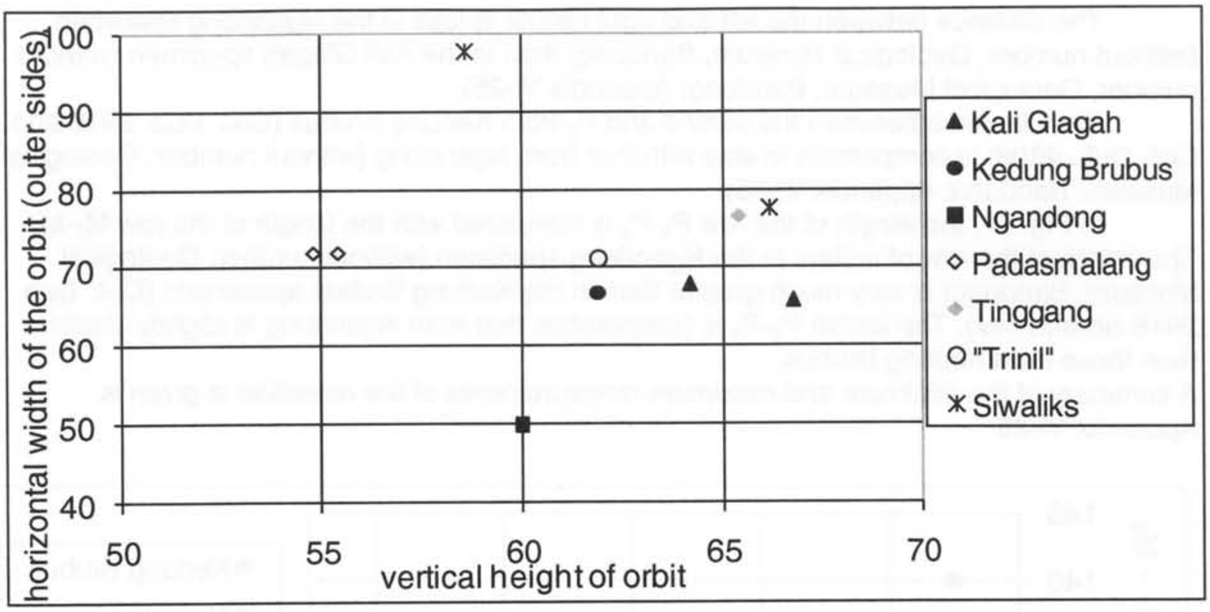

Fig. 48. Height and width of the orbit.

In Fig. 49 (measurements in Appendix VI-27) the elevation of the orbit is shown. In the Kali Glagah specimen (without number; skeleton in Geological Museum, Bandung) the orbit lies 28 mm above the level of the frontal bone, whereas in the Ngandong specimen (without number; skull in Geological Museum, Bandung) this is 61 mm. No measurements from Kedung Brubus are available. In the Ngandong specimen, the orbit lies just a little below the level of the occiput, whereas in the Kali Glagah specimen, the orbit lies 30 mm below the level of the occiput.

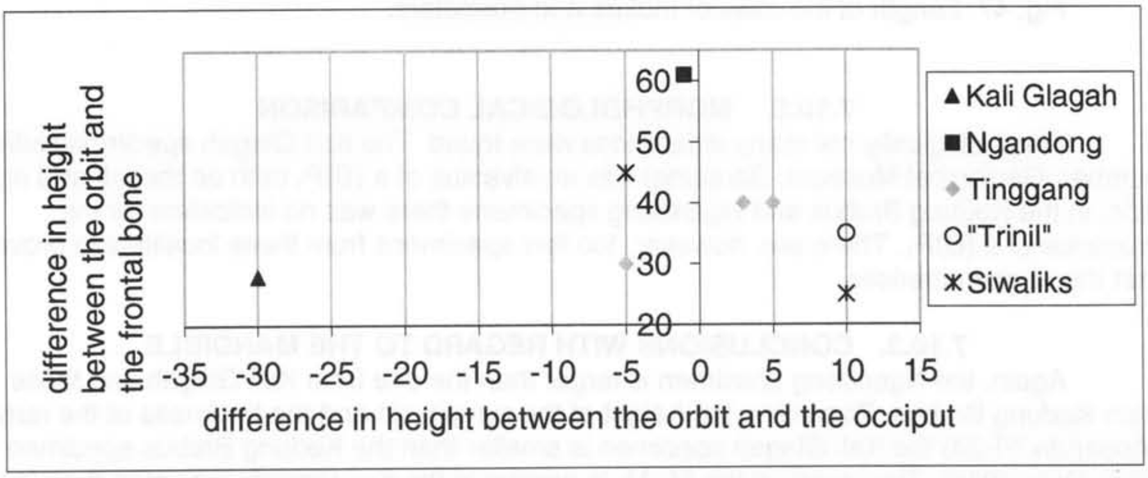

Fig. 49. Height of the orbit and the occiput. On the horizontal scale, a positive number indicates that he orbit lies above the level of the occiput, a negative number indicates that the orbit lies below the level of the occiput.

The height of the orbit to the base of the M^3 (Appendix VI-27) is smaller in the Kali Glagah specimen than in that from Kedung Brubus and Ngandong, although the measurements from Kedung Brubus are approximate measurements.

The distance of the nasal bone to the level of the occipital crest (Appendix VI-27) in the Ngandong specimen is larger than in all other measurements.

The maximum height of the occiput (Appendix VI-28) in the Kali Glagah and Kedung Brubus specimens are comparable in size, whereas that of the Ngandong specimen is greater.

There is not much difference in the distance between the occiput and the posterior end of the nasal bone in the material from the three localities (Appendix VI-29).

The maximum width of the nasal bone (Appendix VI-29) is least in the specimen from Kali Glagah, greater in the Ngandong specimen and greatest in the Kedung Brubus specimen (same specimens as mentioned above).

The distance between the occiput and the posterior rim of the orbit is the same for the three localities (Appendix VI-29).

The minimum width of the brain-case is comparable for the Kali Glagah and Kedung Brubus specimens, but the width in the Ngandong specimens is larger (Appendix VI-29).

The length of the sagittal crest (Appendix VI-29) is greater in the Kali Glagah specimen than in the Ngandong specimen. From Kedung Brubus no measurements were available.

The maximum distance between the zygomatic arch and the brain-case is larger in the Ngandong specimen than in the Kali Glagah specimen. The Kedung Brubus specimen is, in this respect, the smallest of the material from the three localities, but this is an approximate measurement (Appendix VI-29).

In Fig. 50 it is seen that the length of the molar row M^{1-3} (Appendix VI-31) is comparable for the Kali Glagah and Kedung Brubus specimens; the Ngandong specimen has the longest row of molars.

The width of the palate between the left and right M^1's is largest in the Kali Glagah specimen, a bit smaller in the Kedung Brubus specimen and smallest in the Ngandong specimen (Appendix VI-31).

The diastema between the P^2 and P^3 and the length P^2-M^3 (Appendix VI-31) is larger in the Ngandong specimen, than in the Kedung Brubus specimen. For these characters no data from Kali Glagah were available.

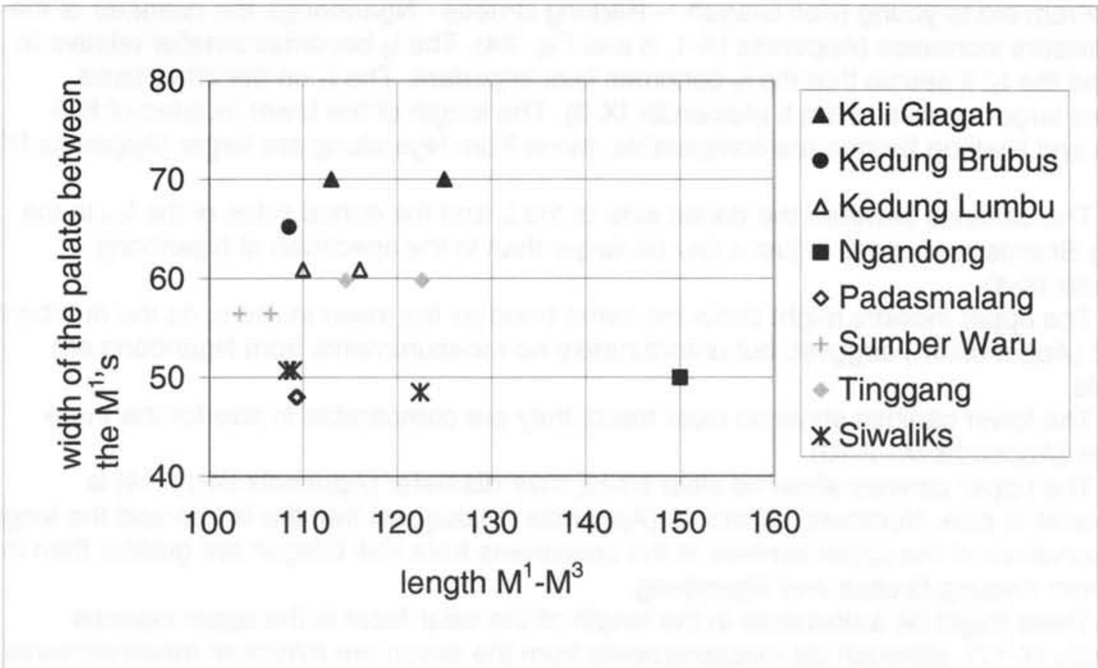

Fig. 50. Length M^1- M^3 and the width of the palate between the M^1's.

7.11.2. MORPHOLOGICAL COMPARISON

The variety in morphological features is great. In material from the same localities different morphologies are distinguished, as is already described in Chapter 5.6. No distinct differences in morphological features between the specimens from Kali Glagah, Kedung Brubus and Ngandong could be distinguished.

7.11.3. CONCLUSIONS WITH REGARD TO THE CRANIUM

The morphological variety is very large. The biometrical differences in the skull are small, but again some trends can be distinguished. The orbit becomes higher relative to the rest of the skull, but the orbit itself becomes smaller. The length of the sagittal crest could become shorter because, with the higher eyes, the hippopotamus did not need so much muscle attachment anymore to raise its head above the water. This may be an adaptation to an aquatic way of life. It must be kept in mind, though, that there is only one skull from Ngandong, so more material is needed to conform this possible trend.

7.12. GENERAL CONCLUSIONS AND DISCUSSION

A summary of the biometrics of the material of Kali Glagah, Kedung Brubus and Ngandong is given in Appendix IX, a summary of the morphological features in Appendix X. The numbers mentioned below refer to these Appendices.

7.12.1. BIOMETRICAL COMPARISON

Although the number of specimens is not adequate for statistical purposes, some conclusions are drawn. In general, from old to young, the material from Kali Glagah is smaller than the material from Kedung Brubus, which in turn is smaller than material from Ngandong (Appendix IX).

From old to young (Kali Glagah – Kedung Brubus - Ngandong), the diameter of the lower incisors increases (Appendix IX-1, 3 and Fig. 24). The I_2 becomes smaller relative to the I_1 and the I_3; it seems that the I_2 becomes less important. The I_3 on the other hand becomes larger relative to the I_1 (Appendix IX-3). The length of the lower incisors of Kali Glagah and Kedung Brubus are comparable, those from Ngandong are larger (Appendix IX-2).

The distance between the dorsal side of the I_2 and the dorsal sides of the $I_{1,3}$ in the Kedung Brubus specimens is just a tiny bit larger than in the specimen of Ngandong (Appendix IX-4).

The upper incisors might show the same trend as the lower incisors, as the numbers 5 and 6 (Appendix IX) suggest, but unfortunately no measurements from Ngandong are available.

The lower canines show no clear trend; they are comparable in size for the three localities (Appendix IX- 7-10).

The upper canines show no clear trend; their diameter (Appendix IX-11-14) is comparable in size. Numbers 15 and 16 (Appendix IX) suggest that the length and the length of the curvature of the upper canines in the specimens from Kali Glagah are greater than in those from Kedung Brubus and Ngandong.

There might be a decrease in the length of the wear facet in the upper canines (Appendix IX-17), although six measurements from the seven are minimum measurements due to damage. Number 18 (Appendix IX) might indicate that the upper canine from Kali Glagah is more curved than the ones from Kedung Brubus and Ngandong.

In the lower premolars there is no clear trend in size (Appendix IX-19-24). The length $P_2 – P_4$ (Appendix IX-48) in the Ngandong specimen is less than in the Kedung Brubus specimens.

No upper premolars from Kali Glagah and Ngandong were available, so no comparison could be made.

The lower molars from Kedung Brubus tend to be a bit smaller than the lower molars from Kali Glagah (Appendix IX, nos. 25, 28, 30, 31 and 49). The lower molars from Ngandong are of the same size (Appendix IX-26, 27, 30 and 31) as the molars from Kedung Brubus or slightly larger (Appendix IX-25, 28, 29, 32, 49 and 50). The posterior width of the M_3 does not show any trend (Appendix IX-33)

In the upper molars there is an increase in size of the M^1 (Appendix IX-34, 35 and in the average of 36). The M^2 of Kedung Brubus is smaller than the M^2 of Kali Glagah, and the M^2 of Ngandong is larger than those from Kali Glagah and Kedung Brubus (Appendix IX-37 and 39). The M^3 shows the same feature: the M^3 of Kedung Brubus is smaller than the M^3 of Kali Glagah (Appendix IX-40 and 41). Unfortunately no measurement of the M^3 of Ngandong is available. No conclusions can be drawn for the numbers 38 and 42 (Appendix IX).

In the mandible there is an increase (going from Kali Glagah to Kedung Brubus) in the height of the symphysis (Appendix IX-43), and the thickness of the ramus (Appendix IX- 44). Number 45 (Appendix IX) might also indicate an increase in size, but no measurements from Ngandong are available. The diastema between the C and the P_2 shows no clear trend (Appendix IX-47).

In the cranium there is an increase in the height of the orbit (Appendix IX-51 and 54), although the orbit itself becomes smaller (Appendix IX-52 and 53). The length of the sagittal crest becomes shorter because, with the higher eyes, the hippopotamus did not need so much muscle attachment anymore to raise its head above the water.

There is an overall increase in the height of the cranium and the mandible (Appendix IX-43, 44, 45, 51, 54, 55 and 60). The width of the cranium and mandible seems to decrease (Appendix IX-46, 56, 57 and 58). An exception is number 61 (Appendix IX), which shows an increase in the distance between the zygomatic arch and the brain-case, but this is undoubtedly related to the increase in the width of the brain-case (Appendix IX-63). The length of the cranium shows the same trend as the lower molars; first a decrease in size between the material from Kali Glagah and Kedung Brubus (Appendix IX-62 and 64), then an increase in size between the material from Kedung Brubus and Ngandong.
No clear trends can be distinguished for the numbers 59 and 65 (Appendix IX).

7.12.2. MORPHOLOGICAL COMPARISON

In Appendix X, the morphological features are summarised. In general, the specimens from Kali Glagah are more simple than those from Kedung Brubus and Ngandong. The material from Kedung Brubus show more variation in a number of features like grooves, cusps and cingula, compared with the specimens from Ngandong, which is turn show more crenulations in its ridges and more robust cusps than those from Kedung Brubus. This might be an adaptation to tougher food, which is also suggested by the greater crown height (Fig. 32).

Numbers 1-3 show that the lower incisors from Kali Glagah are simpler and with less variation than those from Kedung Brubus and Ngandong. This is also the case for the upper canines (Appendix X-5), for the lower premolars (Appendix X-6-25) and for the upper molars (Appendix X-32-51). The (pre)molars from Kali Glagah do not have many ridges or additional cusps (Appendix X).

Comparing the morphological features between the material from Kedung Brubus and Ngandong, the conclusion is drawn that the Kedung Brubus material shows most variation. The Ngandong specimens are simpler compared to the Kedung Brubus specimens in a number of features, like grooves, cusps and cingulum. This is obvious in the specimens with the numbers 3, 11, 20, 29, 30, 34, 42 (Appendix X).

From old to young (Kali Glagah - Kedung Brubus - Ngandong), the upper canines become less symmetrical (Appendix X-4) and the buccal groove in the upper canine becomes more dominant (Appendix X-5). In the (pre)molars there is an increase in the amount of ridges and cusps, which in the Ngandong specimens tend to be crenulated or more robust (Appendix X-6, 7, 8, 9, 10, 12, 14, 15, 16, 19, 21, 22, 23, 24, 31, 36, 39, 40). It seems that the alveolus of P_1, present in the Kali Glagah specimens disappears, but the number of mandibles involved is small (Appendix X-52).

In the P_3 there are two cusps (paraconid and paraconulid) which are present in the Kali Glagah specimens not in the Ngandong specimens (Appendix X-17 and 18). These cusps seem to have disappeared.

Another trend is present in the metacone and tetracone of the M^2. In the Kali Glagah specimen the metacone is smaller than the tetracone. In the Kedung Brubus specimens they are of about the same size and in the Ngandong specimen the metacone is larger than the tetracone (Appendix X-36).

Nothing can be said about the features of the numbers 26-28 (Appendix X), because the number of lower molars involved is much too small.

The sagittal crest (Appendix X-53) is straight and thick in the Kali Glagah specimen, whereas it is arch-shaped and thin in the Kedung Brubus and Ngandong specimens. There seems to be a shift in the place of attachment of the muscles. The ridge for attachment becomes thinner but is, on the other hand, increased in size by the arch-shape. It is not clear what the advantage of this change might implicate.

The frontal bone (Appendix X-54) in the Kali Glagah specimen is straight, whereas it is concave in the Kedung Brubus and Ngandong specimens. By becoming concave, the distance between the frontal bone and the orbits increases, which result in the eyes being higher than the rest of the muzzle. This might be an adaptation to a more amphibical way of living.

Do the differences in the measurements and the morphology of the material of Kali Glagah, Kedung Brubus and Ngandong warrant a subdivision of this material into different (sub)species? This question will be dealt with in Chapter 10, which is about the taxonomy of hippopotami from Java (Indonesia).

8. BIOMETRICAL AND MORPHOLOGICAL COMPARISON OF *HEXAPROTODON* BETWEEN THE JAVANESE AND SIWALIK SPECIMENS

8.1. BIOMETRICAL COMPARISON

From the measurements by Hooijer (1950, Table IA, II and III) it is obvious that the size of dental elements in Javanese *Hexaprotodon* is smaller than in *Hexaprotodon* from the Siwaliks (Pakistan, India). The dental elements of *Hexaprotodon* from Myanmar (former Burma) are smallest. This is shown in Figs. 51 and 52.

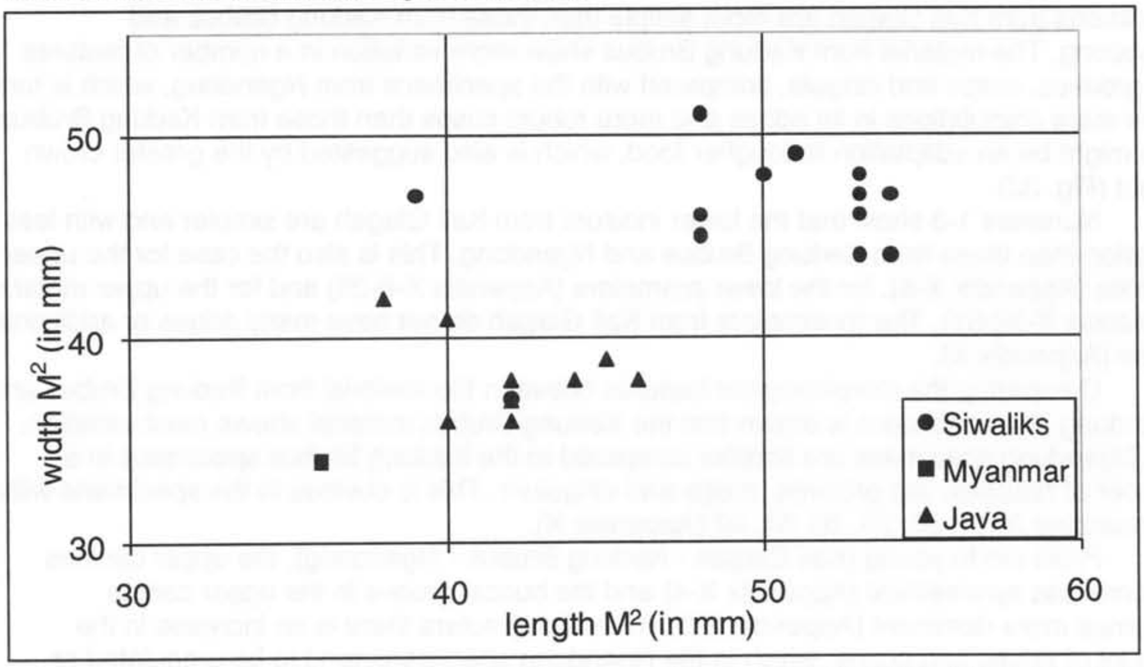

Fig. 51. Comparison of the M^2 between *Hexaprotodon* from the Siwaliks, Myanmar and Java.

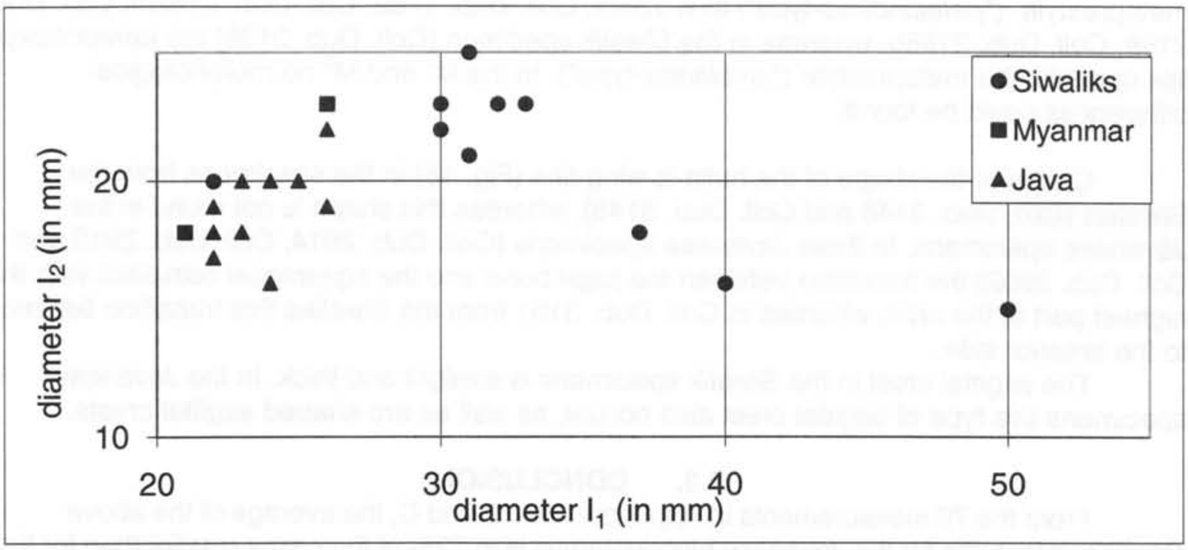

Fig. 52. Comparison of the I_1 en I_2 between *Hexaprotodon* from the Siwaliks, Myanmar and Java.

This general pattern is confirmed by the 19 measurements from Java and the Siwaliks, shown in Appendix XI-A. The Javanese values are smaller than those from the Siwaliks; the maximum values from Java are less than the minimum ones from the Siwaliks.

In Appendix XI-B the measurements from Java and the Siwaliks are shown to have an overlap. From these 54 measurements, 36 from Java have an average, which is less than the average from the Siwaliks (67%).

The average for the Javanese specimens is larger in 12 measurements (out of the 54 measurements; 22%) than those from the Siwaliks (Appendix XI-B, nos. 8, 17, 26, 27, 31, 32, 36, 37, 40, 48, 49, 50).

There are six measurements (out of the 54 measurements; 11%) with only one measurement from the Siwaliks, which falls within the range for the Javanese ones, so no distinction can be made between Java and the Siwaliks (Appendix XI-B, nos. 9, 10, 23, 39, 44, 52).

In Appendix XI-C three measurements are shown in which the minimum value for the Siwalik specimens is less than the maximum value for the Javanese specimens.

8.2. MORPHOLOGICAL COMPARISON (APPENDIX VIII)

P^4: in the P^4's from Java, 8 out of 9 have a cingulum on the lingual side only; only 1 out of 9 (Coll. Dub. 2023?/1) has a cingulum both on the lingual and the buccal sides. In the Siwalik specimens, all four P^4's have a cingulum on both sides. Both P^4's from Coll. Dub. 3101 have of two platforms, on the anterolingual and the posterobuccal sides, which is different from the cusps in the P^4 from Java, but this might be due to wear. The five maxilla's, that show that there is no P^4 to replace the DP^4, are all from Java (see Chapter 5.3.2.). This was not found in the Siwalik specimens.

Lower molars: the only difference found in the morphology of the lower molars is that the specimens from Java have no cingulum, or a cingulum on the lingual side or on the buccal side only. The Siwalik M_3 (Coll. Dub. 3147) has a cingulum both on the lingual and on the buccal side. Regarding all lower molars (N=85), The presence of a cingulum on both sides occurs only in 1.2% of the Siwalik specimens and in just some specimens (7%) from Java (M_1 from Coll. Dub. 2917 and 2922, M_2 of Coll. Dub. 2202, M_3 of Coll. Dub. 2006, Coll. Dub. 325d/2 and Coll. Dub. 2194).

Upper molars: the parapoststyle of the Javanese M^1's is situated buccally from the metaprestyle ("*palaeindicus*-type") in K 734/1, Coll. Dub. 1702, Coll. Dub. 2182/4, Coll. Dub. 2188, Coll. Dub. 2195b, whereas in the Siwalik specimen (Coll. Dub. 3138) the parapoststyle lies opposite the metaprestyle ("*sivalensis*-type"). In the M^2 and M^3 no morphological differences could be found.

Cranium: the shape of the bulla is wing-like (Fig. 18) in the specimens from the Siwaliks (Coll. Dub. 3146 and Coll. Dub. 3148), whereas this shape is not found in the Javanese specimens. In three Javanese specimens (Coll. Dub. 2914, Coll. Dub. 2919 and Coll. Dub. 2902) the transition between the jugal bone and the squamosal coincides with the highest part of the orbit, whereas in Coll. Dub. 3101 from the Siwaliks this transition lies more to the anterior side.

The sagittal crest in the Siwalik specimens is straight and thick. In the Javanese specimens this type of sagittal crest also occurs, as well as arc-shaped sagittal crests.

8.3. CONCLUSION

From the 76 measurements in Appendix XI-A, B and C, the average of the above mentioned features for the Javanese hippopotamus is in 72% of the cases smaller than for the ones from the Siwaliks. Although each individual measurement does not have a statistical value, the conclusion that the Javanese hippopotamus is smaller than the Siwalik one seems justified. The morphological differences are small and the number of specimens involved is too small to allow any conclusion regarding the morphology.

9. TAXONOMY OF THE GENUS *HEXAPROTODON* FROM THE ASIAN CONTINENT

9.1. INTRODUCTION

The hippopotami from Asia all belong to the genus *Hexaprotodon* Falconer & Cautley, 1836; Order Artiodactyla Owen, 1848; Family Hippopotamidae Gray, 1821.

In the 19th and the beginning of the 20th century, an attempt was made to distinguish several subspecies based on skull shape and proportions (Hooijer, 1950). Hooijer (1950) shows that the "distinguishing characters mentioned [...] are invalid even for racial distinction". According to Eltringham (1999) "it is not certain that these represent anything more than a classification of museum specimens. There may well be geographic variations in skull features but they are not obvious in the field as most of the alleged differences are relative". Boisserie (2005) in a review of the phylogeny and taxonomy based on cladistics, was able to distinguish Asiatic *Hexaprotodon* from other genera, but he could not distinguish the alleged subspecies, whereas he had no difficulty to do so in the African hippopotami.

A review of the literature about the (sub)species of *Hexaprotodon* (Hooijer, 1950 named them *Hippopotamus*) in continental Asia will be given, and especially of the (sub)species distinguished by Hooijer (1950). The species *Hexaprotodon dhokwazirensis* Akhtar & Bakr, 1995 will be discussed too. Based on the comparison given in Chapter 8 and the review of the literature, a revised taxonomy of the (sub)species is proposed.

9.2. SPECIES: REVIEW OF THE LITERATURE

9.2.1. *HIPPOPOTAMUS SIVALENSIS* FALCONER & CAUTLEY, 1836

- lectotype: British Museum M 2269, a skull, designated by Colbert (1935).
- cotype: a calvarium referred to by Falconer & Cautley (1836) in the original description, but these authors did not designate any particular specimen on which the description was based.
- horizon: according to Pilgrim (1913) some fossils of *Hippopotamus sivalensis* were found in the Dhok Pathan level, part of the Middle Siwalik deposits. The range for *H. sivalensis* is therefore "Lower Pliocene - Lower Pleistocene" (Pilgrim, 1913). Hooijer (1950) stated that "the species ranges from the Lower Pleistocene to the Upper Pleistocene." Barry *et al.* (2002) dated the first occurrences on the Indian subcontinent at 6.1 Ma B.P., or possibly even as early as 7.2. B.P. According to Corvinus & Nanda (1994) *H. sivalensis* is found in

the Dobatta and Surai Khola Formations in Nepal (skulls and parts of skulls, mandible fragments and some isolated teeth). They claim that these formations are equivalent to respectively the "Upper Siwaliks" and the "Middle-Upper Siwaliks".

- geographic range: Siwalik Hills and Nepal. Kahlke (1990) wrote that Chow (1961) claimed to have found *H. sivalensis* in south China (a molar fragment of Late Pliocene age). Also finds in Thailand (Von Koenigswald, 1959 and Ginsburg *et al.* 1982) and Malaysia (shaft of an immature radius; Hooijer 1962) have been reported.

Falconer & Cautley (1836) divided the genus *Hippopotamus* into two subgenera, *Hexaprotodon* and *Tetraprotodon*. According to Lydekker (1884), Owen (1845) had adopted *Hexaprotodon* and *Tetraprotodon* as generic names, but Lydekker (1884) did not see any reason to agree with this, because he stated to have seen other specimens with some sort of transition between hexa- and tetraprotodonty He stated that only the name *Hippopotamus* is a valid generic name. As the description of *H. sivalensis* by Falconer & Cautley (1836) is not very detailed, Lydekker (1884) came up with other characteristics to distinguish *H. sivalensis* from the living hippopotami. He stated that *H. sivalensis* has a longer mandibular symphysis, a small prominence of the orbits and an elongated astragalus as compared to *H. amphibius*. Matthew (1929) did not agree with Lydekker (1884) about these characteristics, because, according to him, they are too variable to be reliable. Although Matthew (1929) wrote: "I cannot see any very strong reason for according full generic rank to *Hexaprotodon*", he did use this name as such. Colbert (1935) finished this dispute by making a list with characteristics to distinguish the genus *Hexaprotodon* from the genus *Hippopotamus*. Furthermore he added a lot of characteristics to the diagnosis of *Hexaprotodon sivalensis*, amongst others that the first premolar is large (in *Hippopotamus amphibius* this tooth is reduced or absent), the C-P diastema is very short, the anterior molars diverge from each other (in *Hippopotamus amphibius* the tooth rows are approximately parallel), and the occiput is narrower and higher than in *Hippopotamus amphibius*. Hooijer (1950, p. 41) preferred to use the genus *Hippopotamus* and gave as diagnosis for *Hippopotamus sivalensis sivalensis*: "Size moderate to large, orbit low to moderate, occiput high to moderate, postdental part of calvarium long to moderate. Upper molars large with the lobes of the anterior cusps in the transverse valley opposed to those of the posterior cusps, and the posterior lobe of paracone never markedly extending labially beyond the anterior lobe of metacone" (= "*sivalensis*-type"), "cingulum variable in development. Mandibular symphysis very long to long relative to its width, and very low relative to its length. Ramus horizontalis low to moderately low at M_2 relative to its length, and height at M_2 equal to or less than length M_1-M_3. I_2 two-thirds to about equal in size to I_1, and I_3 slightly smaller than I_1."

9.2.2. *HIPPOPOTAMUS IRAVATICUS* FALCONER & CAUTLEY, 1836

- lectotype: British Museum 14771, a mandibular symphysis, Fauna Antiqua Sivalensis, plate LVII, Fig. 10.
- cotype: a mandibular symphysis figured in the Fauna Antiqua Sivalensis (Falconer & Cautley, 1836), Plate LVII, Fig. 11.
- horizon: according to Hooijer (1950) *Hippopotamus iravaticus* is found in the Upper Irrawaddy Beds (Siwaliks) of Lower Pleistocene age. Pilgrim (1913) stated that *H. iravaticus* was among the fossils found in the neighbourhood of Dhok Pathan and Hasnot (both in India), which are Middle Siwalik deposits. Colbert (1935) wrote "the Irrawaddy series of Burma would seem to be approximately correlative with the Middle and part of the Upper Siwalik beds of India." Later, Colbert (1943) correlated the Upper Irrawaddy fauna with the Pinjor fauna of the Siwaliks, which he thought to be of Lower Pleistocene age. Also Wadia (1953) agreed that *H. iravaticus* was found in the Middle Siwalik deposits and therefore contemporaneous with *H*ippopotamus *sivalensis*. Akhtar and Khurshid (1997) stated that it is proven that they were even present in the Lower Siwaliks.
- geographic range: Irrawaddy River Valley, Myanmar (former Burma). Pilgrim (1913, p. 300) wrote: "the [..] species seems to have been found in the Hasnot Beds" (India). So he claims that this species is also found outside Burma. It is not at all clear on what this assumption is based, as he does not give any references for these finds. After Pilgrim (1913), a lot of

authors just copy this assumption, without any reference or proof. According to Colbert (1943), *H. iravaticus* is confined to Burma. But recently Akhtar and Khurshid (1997) described a specimen of *H. Iravaticus* from the Upper Siwaliks of Pakistan.

Although Falconer & Cautley (1836) did not give a description of this species, some remarks were made, however, e.g. that *Hippopotamus (Hexaprotodon) iravaticus* is "supposed to have come from Ava", Myanmar (based on the matrix which was attached to the fossil) and that it is decidedly smaller than *Hippopotamus (Hexaprotodon) sivalensis*. Lydekker (1884, 1885) concluded that "this species is imperfectly known", but he agreed with Falconer & Cautley (1836) about the size of *Hippopotamus iravaticus*. Unfortunately at that time no cranium of this species had been found, but according to Lydekker (1884, 1885) "the mandible can be distinguished from *H. sivalensis* by the smaller size of the mandible, its proportionally longer symphysis (compared to its width), the alveoli of P_2 and P_3, which are more separated than in *H. sivalensis*". The fossil on which this species is founded, however, belongs to a subadult with the P_2 not yet fully erupted. Van der Maarel (1932) also noticed this and added: "the second specimen of the symphysis [the cotype] is in my opinion entirely worthless, being too fragmentary and figured on too small a scale". Also Boisserie (2005) rejected the lectotype because of its juvenile state.

An incomplete cranium was found and described by Colbert (1938). The molars on both sides are present, "the last premolar and the last molar erupting and unworn" (Colbert, 1938). So again this is not an adult. Colbert (1938) also observed differences in the molar pattern, but he concluded: "[...] the differences between the molars of *Hexaprotodon iravaticus* and *Hexaprotodon sivalensis* may be assigned, for the most part, to the greater size and robustness of the Indian species". Colbert (1938) also stated that the I_3 is laterally compressed.
In 1943, Colbert referred to several new specimens of *H. iravaticus*, i.e., two fragments of a mandible and a molar. He wrote: "The well-preserved single tooth is perhaps somewhat larger than average for this species, but it is definitely smaller than typical *H. sivalensis* molars".
Hooijer (1950) gave the diagnosis: "The smallest of the Asiatic species, closely comparable to *Hippopotamus lemerlei* Grandidier from Madagascar as to size. Six incisors in the lower jaw; I_2 slightly above, and I_3 below the level of I_1, and both not much smaller than I_1. Mandibular symphysis very long relative to its width. Upper molars of a simple structure, differing from those of *Hippopotamus sivalensis* F. & C. in the lesser expansion of the lobes of the cusps, and in the lesser development of the cingula. Orbit apparently hardly elevated, and rather central in position".

Hooijer (1950) admitted that he had not seen any specimen of this species but he stated that *H. iravaticus* should be treated as a species because it seems to differ in certain cranial and dental characters from the other Asiatic hippopotami. The orbits are rather central in position and they are hardly elevated, but he did not give any measurements to prove this.
There seems to be some disagreement on the position of the lower incisors. Lydekker (1884) stated that the I_2 is situated above the level of I_1 and I_3 is situated below the level of $I_{1/2}$. Colbert (1935), on the other hand, wrote that the I_2 lies dorsally from both $I_{1/3}$. Hooijer (1950) agreed with Lydekker (1884). The specimen described by Akhtar and Khurshid (1997) has an "I_2 slightly above and I_3 below the level of I_1".

Also about the size of the lower incisors some discussion went on. According to Colbert (1935) I_2 is much smaller than both I_1 and I_3, but according to Hooijer (1950) I_2 and I_3 are smaller than I_1. In fact I_2 is about 0.8-0.9 the size of I_1 and 0.9 to equal in size compared to I_3. So there is not much difference in size between $I_{2/3}$. I_1 is just a bit larger. Akhtar and Khurshid (1997) agreed: "the I_2 and I_3 are both not much smaller than I_1".

Colbert (1938) referred to another hippopotamus find from the Irrawaddy Beds, which might be *H. sivalensis*: "The probabilities are that this Burma specimen is referable to *Hexaprotodon sivalensis*, not only because of its size and general form, but also because of its contemporaneousness with and its contiguity to the Siwalik species" (Colbert, 1938). He was not sure though, because incisors were not found.

Besides *Hippopotamus iravaticus*, Hooijer (1950) claimed that in Myanmar (Burma) another subspecies is present, the larger *Hippopotamus sivalensis* cf. *palaeindicus*, which is said to originate from lower Pleistocene deposits.

9.2.3. *HEXAPROTODON DHOKWAZIRENSIS* AKHTAR & BAKR, 1995

- holotype: P.M.N.H. 87/114, a slightly damaged skull.
- horizon: Upper Siwaliks.
- geographic range: Dhokwazira, district Jhelum, Panjab (=Punjab), Pakistan.
- diagnosis: a *Hexaprotodon*, smaller than *Hexaprotodon sivalensis* and with relatively small P^1.

Besides the characteristics referred to in the diagnosis, Akhtar and Bakr (1995) described the diastema between the I^3 and the canine being relatively short in this species (40 mm), compared with *H. sivalensis* described by Colbert in 1935 (68 mm) and with *H. sivalensis soloensis* (52 mm) described by Hooijer (1950). Also the diastema between P^1 and the canine was said to be very short (12 mm), whereas in *H. sivalensis* it varies between 22 mm and 40 mm (Hooijer, 1950).

9.2.4. DISCUSSION ABOUT NAMES OF THE SPECIES

Although all hippopotamus material in Asia belong to the genus *Hexaprotodon*, it is often referred to in the text as *Hippopotamus*, because authors in the past named it *Hippopotamus*.

Falconer & Cautley (1836) were the first to distinguish *Hippopotamus iravaticus*. They did not give any description but they stated that *H. iravaticus* can be distinguished from *Hippopotamus sivalensis* (apart from the overall smaller size) by the smaller size of the mandible, its proportionally longer symphysis (compared to its width), and the alveoli of P_2 and P_3, which are more separated than in *H. sivalensis*.

Also Hooijer (1950) distinguished two species in Asia, *Hippopotamus sivalensis* and *Hippopotamus iravaticus*. The diagnoses of these two species are summarised in Appendix XII. According to Hooijer (1950) *H. iravaticus* was only found in Myanmar (former Burma), but Pilgrim (1913) wrote that it was also found near Hasnot (Siwalik Hills, former India, now Pakistan), although it is not clear on which this assumption is based.

From the data in Appendix XII the conclusion is drawn that the only feature which is clear enough to separate *H. iravaticus* and *H. sivalensis* is the size. *H. iravaticus* is said to be much smaller than all other Asian (sub)species. This is clear from Fig. 51 and from the measurements given by Hooijer (1950) in his Table II. But if the variation in *H. amphibius* is compared with this variation, the small value can be explained by variation. For example the difference between the smallest (37 mm) and the greatest length (54 mm) of the M^1 in *H. amphibius* is 17 mm (Hooijer, 1950: Table 1A), whereas the difference, comparing the smallest length (28 mm) of *Hippopotamus iravaticus* with the greatest length (46 mm) for *Hippopotamus sivalensis* is 18 mm (Hooijer, 1950: Table II).

Also the small size of the lower molars in *H. iravaticus* mentioned by Colbert (1935) cannot be confirmed, because if the measurements of Colbert (1935) are compared with the measurements given by Hooijer (1950, Table III) we see that the length of the M_2 in *Hippopotamus sivalensis* ranges from 43 mm to 52 mm, so the 47 mm for the length of the M_2 of *Hippopotamus iravaticus* is within the range of *Hippopotamus sivalensis*. The width of the M_2 of *H. sivalensis* ranges from 31 mm to 40 mm, so also the width of the M_2 of *H. iravaticus* (31 mm) falls within the range of *H. sivalensis*.

The sizes of the mandibles in Table III (Hooijer, 1950) are not at all convincing, because one mandible belongs to a subadult, and the other one is not really much smaller than *H. sivalensis*.

The dimensions of the lower incisors of *H. iravaticus* are within the range of those of *H. sivalensis* (Fig. 53), except for the one value of Akhtar & Khurshid (1997), which is very small (12 mm x 9 mm). The values of the lectotype BM 14771 are a bit small but the specimen is subadult, so this is not surprising.

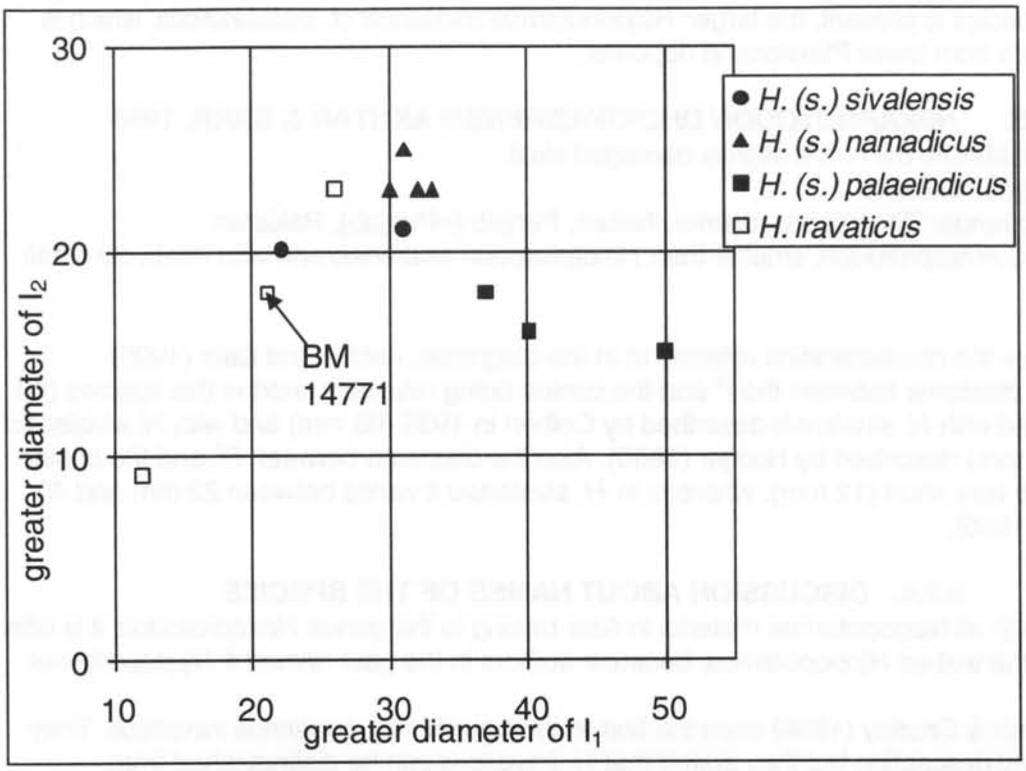

Fig. 53. The greater diameter of I_1 and I_2 of several subspecies of *Hexaprotodon sivalensis* and *Hexaprotodon iravaticus*. Measurements in mm from Hooijer (1950, Table III) and Akhtar & Khurshid (1997). BM 14771 is the lectotype of *H. iravaticus*.

The other characteristics distinguished by Falconer & Cautley (1836) cannot be proven by measurements. Of the diagnoses given by Hooijer (1950) only the numbers 3,5,7,8 and 10 (Appendix XII) need to be considered. From these, 3, 8 and 10 are characteristics of the genus *Hexaprotodon* and they do not differ from each other. The height of the orbits (Appendix XII, number 7) does not seem to differ either (no measurements for *H. iravaticus*). The relative length of the mandibular symphysis of *H. iravaticus* is indeed greater than that of *H. sivalensis* (Appendix XII, number 5), but Hooijer (1950: Table III) only gives one measurement of *H. iravaticus* and four of *H. sivalensis*. In the one specimen of *H. iravaticus* the length of the mandibular symphysis is greater (130 mm) than the interval between the canines (113 mm), whereas in *H. sivalensis* the length of the mandibular symphysis is less (172 mm, 166 mm, 172 mm and 163 mm) than the interval between the canines (184 mm, 173 mm, 203 mm and 194 mm). Akhtar & Khurshid (1997) give the length of the mandibular symphysis (150 mm), but no width. Therefore the relative length is not known. Also the interval between the canines is not given. So the relative length of the mandibular symphysis might be the only biometrical difference between these inferred species, although it is realized that the number of measurements is small. On the other hand, this difference might also be explained by the fact that in mammals the proportions of the skull and mandible in a subadult are very different from those in an adult, as can be seen in e.g. cows (De Vos, pers. com.) and woolly mammoths (Maschenko, 2002).

The reported differences between *H. iravaticus* and *H. sivalensis* are not at all convincing. Van der Maarel (1932) mentioned the "lateral compressed outer incisor" as being an important characteristic for taxonomy, but the specimen described later by Colbert (1943) does not show this feature, so again this is no good criterion.

Akhtar & Khurshid (1997) gave the dimensions of the P_1, P_2 and P_3. Hooijer did not give these, but the measurements that were taken by the author from Coll. Dub. 3147 from the

Siwaliks are comparable: the P_2 of Coll. Dub. 3147 is 31.2 mm x 17.7 mm (length x width), the one Akhtar and Khurshid (1997) measured is 30 mm x 19 mm. For the P_3, these values are 31.3 mm x 19.2 mm (Coll. Dub. 3147) and 31 mm x 20 mm (Akhtar & Khurshid, 1997).

Akhtar & Bakr (1995) stated about *Hexaprotodon dhokwazirensis*: "The most distinguishing feature is the size of the P^1, which is much smaller as compared to that of *H. sivalensis*." The length x width is 25 mm x 21 mm and according to them this is 44 mm x 28 mm in *H. sivalensis* (after Colbert, (1935), measured from his diagram). It is too premature to define a new species only based on one P^1, and only one measurement to compare with.
The preorbital length, the postorbital length and the width of the occiput are less than in *H. sivalensis*. The other measurements (height and length of orbit, width of zygomatic arches, width of palate at P^1 and height of occiput) are comparable with those of *H. sivalensis* (Akhtar & Bakr, 1995).

The conclusion is that there is only one species in continental Asia for which the name *Hexaprotodon sivalensis* is proposed.

9.3. SUBSPECIES: REVIEW OF THE LITERATURE

9.3.1. *HIPPOPOTAMUS SIVALENSIS SIVALENSIS* FALCONER & CAUTLEY,1836

- holotype: a calvarium from the Siwaliks described by Falconer & Cautley (1936).
- horizon: Upper Siwaliks, Lower Pleistocene according to Hooijer (1950).
- geographic range: Siwalik Hills, N. India and Pakistan.
- diagnosis according to Hooijer (1950): "Size variable, larger in the continental than in the Javan subspecies. Six incisors both in the upper and in the lower jaw. The upper C has a deep longitudinal groove on its posterior surface. The anterior premolars diverge from each other on the opposite sides of the calvarium and the mandible. The premaxillaries are in contact with each other along their entire length. The constricted part of the calvarium is less elongated and the maxillaries expand anteriorly more rapidly than in *H. amphibius* L. The nasals are hardly expanded posteriorly, and the lacrimal is separated from the nasal by an anteriorly prolongation of the frontal. The angular process of the mandible is not pointed forwards."

9.3.2. *HIPPOPOTAMUS SIVALENSIS NAMADICUS* FALCONER & CAUTLEY, 1836 AND *HIPPOPOTAMUS SIVALENSIS PALAEINDICUS* FALCONER & CAUTLEY, 1836

H. s. namadicus

- lectotype: mandible BM 36838, figured in Fauna Antiqua Sivalensis, plate LVIII, Fig. 3.
- cotypes: BM 36839 en 36840, figured in Fauna Antiqua Sivalensis resp. plate LVIII, Fig. 1 and 2.
- horizon: Middle or Upper Pleistocene, according to Hooijer (1950).
- geographic range: Narmada Valley (Central India).

H. s. palaeindicus

- lectotype: mandibular symphysis figured in Fauna Antiqua Sivalensis, plate LVII, Fig. 5.
- horizon: Middle or Upper Pleistocene according to Hooijer (1950), Late Pleistocene to Early Holocene according to Biswas (1987).
- geographic range: Narmada Valley (Central India).

Although Falconer & Cautley (1836) did not give a description of their species, some remarks were made, e.g. that *Hippopotamus (Tetraprotodon) palaeindicus* and *Hippopotamus (Hexaprotodon) namadicus* were found in the Narbada (=Nerbudda = Narmada) Beds in India. *H. (T.) palaeindicus* is characterised by the presence of four incisors, a different molar pattern (the so-called "*palaeindicus*-type", as opposed to the "*sivalensis*-type" of *Hippopotamus (Hexaprotodon) sivalensis*, remarkable occipital and sagittal crests and the orbits are higher above the level of the frontals than in *H.(H.) sivalensis*. The presence of four incisors in *H. (T.) palaeindicus* was the reason to designate the subgenera *Hexaprotodon* and *Tetraprotodon*.

While *H.(T.) palaeindicus* is only represented by crania, *H.(H.) namadicus* is only represented by mandibles. No remarks were made about *H.(H.) namadicus* except that it is "with other well-marked characteristics", larger than *Hippopotamus (Tetraprotodon) amphibius and H.(H.) sivalensis*.

Lydekker (1882 A and B, 1883, 1884) remarked that there were no descriptions of these species and filled the gap by making the descriptions himself. Regarding the so-called tetraprotodonty of *H.(T.) palaeindicus*, he came to the conclusion that the skull shown by Falconer & Cautley (1836) was damaged to such a degree, that it was not possible to tell if it was tetra- or hexaprotodont and that the reconstruction as tetraprotodont was probably wrong. He claimed to have seen other specimens in which some sort of transition between hexa- and tetraprotodonty was seen (in which the second incisor is definitely smaller than the other incisors) and on this ground he rejected the existence of *Hexaprotodon* and *Tetraprotodon* as subgenera, and only used the genus *Hippopotamus*.

In 1882 and 1883 Lydekker could not find indications to separate *Hippopotamus palaeindicus* and *Hippopotamus namadicus*. Moreover, because from *H. palaeindicus* only a cranium, and from *H. namadicus* only a mandible was depicted, he concluded that it could in fact be one species. In 1884, however, Lydekker changed his opinion and he gave several characteristics of the mandible to separate the species: "*H. namadicus* differs from the older *H. sivalensis* by I_2 being smaller than either of the others; the alveolus of I_2 is placed slightly above the level of those of the other incisors, although this does not seem to be always the case." The mandible is distinguished from *H. sivalensis* by "the more abrupt angle at the inferior border of the anterior extremity" (although this is not recognisable in his plates), relatively shorter symphysis (relative to its height), and a relatively shorter horizontal ramus (relative to its height).

Lydekker (1884) found that "*H. palaeindicus* differs from *H. sivalensis* by the I_2 which is much smaller than the other incisors; the descending process of the ramus is smaller and the horizontal ramus is much shorter". Comparing these descriptions, it does not seem too convincing, but Lydekker (1884) added: "In species in which the depth of the mandible is the same, the symphysis is shorter in *H. palaeindicus* than *H. namadicus*" and *H. namadicus* can be distinguished by having three small and subequal mandibular incisors (which is contradictory to what he stated above). "This, coupled with the larger size of the first and third pairs of incisors, and the smaller size of the second pair" [in *H. palaeindicus*], "indicates the specific distinctness of the two forms. This is confirmed by the difference in the position of the canines, which are placed more nearly on a level with the incisors in *H. namadicus* than in *H. palaeindicus*." (Lydekker, 1884) .

With respect to the crania, Lydekker (1884) did not know to which species they belonged, as from *H. namadicus* no crania were known, but he did give some characteristics which distinguish *H. namadicus/palaeindicus* from other species: "It is somewhat larger than *H. amphibius*; it is characterised by their prominent orbits; general shortness: small interval between posterior border of the palate and anterior zygomatic root, as well as by the extreme shortness of the pre-orbital constriction, and the backward position of the maxillary expansion; last molar has its posterior border placed slightly behind the free border of the palatines; which at once distinguishes these crania from those of all other species "except" [!] "one variety of *H. sivalensis*"; [M^3 does not extend in advance of the posterior border of the anterior zygomatic root] "whereas this is largely the case in the Narbada skulls; the Siwalik skulls are considerably longer, have a longer pre-orbital constriction, narrower molars; the shortness of the Narbada skulls is a character which accords equally well with both" [*H. namadicus* and *H. palaeindicus*] "the forms of lower jaws from that formation."

Considering the limb bones and vertebrae, Lydekker (1884) could not distinguish between *H. namadicus* and *H. palaeindicus*.

Van der Maarel (1932) could not agree with the assumption by Lydekker (1884) that the mandibular symphysis of *H. namadicus* is slightly longer than that of *H. palaeindicus*. Van der Maarel (1932) stated that on this basis they certainly cannot be distinguished, but he claimed that "there is no doubt that both forms are specifically distinct, as the incisors afford ample reason to separate the two." This was based on the I_2 being smaller than the other incisors in *H. namadicus* and the I_2 being very much smaller in *H. palaeindicus*.

Hooijer (1950) thought them to be two subspecies of *Hippopotamus sivalensis*. He was able to distinguish them and made two diagnoses. *Hippopotamus sivalensis namadicus*: "size large, mandibular symphysis very short relative to its width, and very high relative to its length. I_2 two-thirds to four-fifths the size of I_1, I_3 equal to or larger than I_1 in size" and *Hippopotamus sivalensis palaeindicus*: "Size large, orbit moderately elevated, occiput moderate to low, postdental part of calvarium short. Upper molars large, the posterior lobe of the paracone extends labially beyond the anterior lobe of the metacone. The upper molars extend more backward than the posterior border of the palate. Mandibular symphysis short to very short relative to its width, and high to very high relative to its length. Ramus horizontalis very high at M_2 relative to its length. I_1 and I_3 much enlarged; I_2 one-third to one-half the diameter of I_1, and I_3 equal to or larger than I_1 in size" (Hooijer, 1950).

According to Gentry (1997) the most distinguishing character of *H. namadicus* is that the "I_2 is more reduced and sometimes absent". With the last remark he seemed to refer to the (wrongly) reconstructed mandible figured in Fauna Antiqua Sivalensis (Falconer & Cautley, 1836), which seems to be tetraprotodont. Gentry (1997) admitted that the Narmada specimens in London all have six incisors, with reduced I_2's.

Biswas & Dassarma (1984) gave another distinguishing character, the posterior nasal choanae, which in *Hippopotamus namadicus* are narrow and V-shaped, whereas in *Hippopotamus palaeindicus* they are rounded. Unfortunately the choanae are not often preserved.

Biswas & Dassarma (1984) and Biswas (1987) stated that *H. namadicus* is found in the Narbada Middle and Lower deposit (Middle-Upper Pleistocene) and *H. palaeindicus* in the Narbada Upper deposit, which is of Upper Pleistocene - Lower Holocene age. From their data, it can be concluded that they did not occur contemporaneously.

9.3.3. HIPPOPOTAMUS SIVALENSIS DUBOISI HOOIJER, 1950

- holotype: a partial calvarium in the Dubois Collection (Dub. Coll. 3146) described and figured by Hooijer (1950, plate V, Fig. 3).
- horizon: Pleistocene, according to Hooijer (1950).
- geographic range according to Hooijer (1950): Naliwala on the Somb Nuddy opposite Haripur (=Haripoor), Sirmur State, Panjab (=Punjab) .
- diagnosis according to Hooijer (1950): "Size moderate, orbit very high, occiput moderate. Upper molars small and of the *palaeindicus* type."

9.3.4. *HIPPOPOTAMUS SIVALENSIS SINHALEYUS* DERANIYAGALA,1936

- holotype: the unworn left M_3 figured by Deraniyagala (1936, Figs. 1-3).
- horizon: Ratnapura. There seems to be some doubt about the age, because Hooijer (1950) writes: "Since the Ratnapura Beds, besides Upper Siwalik forms, contain *Elephas maximus* L. subsp., Deraniyagala (l.c., p. 53) supposes that there was redeposition in the Ratnapura Beds during late Pleistocene times."
- geographic range: Ratnapura district, Sri Lanka (Ceylon).
- diagnosis according to Hooijer (1950): "Size large, upper molars large and of the *palaeindicus* type. Lower incisors (I_1 and I_3 ?) much enlarged".

Hooijer (1950) did not give any measurements for this subspecies nor any stratigraphical context. The diagnosis by Hooijer (1950) resembles the diagnosis for *H. sivalensis palaeindicus* a lot. Unfortunately no remains of the calvarium and the mandible have been recovered so far, the species is based on dental remains only.

9.3.5. DISCUSSION ABOUT NAMES OF THE SUBSPECIES

Regarding *Hippopotamus sivalensis*, Hooijer (1950) distinguished four subspecies, *H. sivalensis namadicus* (Falconer & Cautley, 1836), *H. sivalensis palaeindicus* (Falconer & Cautley, 1836) *H. sivalensis sinhaleyus* Deraniyagala, 1936 and *H. sivalensis duboisi* Hooijer, 1950.

The diagnoses of the several species of *Hippopotamus* distinguished by Falconer & Cautley (1836), Lydekker (1984), Van der Maarel (1932) and Biswas & Dassarma (1984) and the subspecies of *Hippopotamus sivalensis* distinguished by Hooijer (1950) are summarised in Appendix XIII.

The size (Appendix XIII-1) is not a very valuable feature because it does not explain which size is meant exactly. Moreover, the fossils are hardly ever complete.

The crania (Appendix XIII-2) were described by Lydekker in 1884, but he gave no measurements. Also Hooijer (1950) did not give any measurements to prove the general shortness of the crania.

H. (s.) namadicus and *H.(s.) palaeindicus* are characterised by their prominent orbits (Appendix XIII-3) according to Lydekker (1884), although Hooijer (1950) stated that the orbits of *H. (s.) palaeindicus* are moderately elevated. In Fig. 54 the elevation of the orbits above the level of the frontals is compared with the height from the palatine (Hooijer's orbito-cephalic index) of *Hippopotamus sivalensis, H. (s.) duboisi* and *H. (s.) palaeindicus*. These measurements are compared to those *of Hippopotamus amphibius*. From Fig. 54 it is obvious that the variation in *Hippopotamus amphibius* is very large and the elevation of the orbits of the fossil hippopotami is comparable with the variation in *Hippopotamus amphibius*. The only measurement that does not fit is the one for *H. (s.) duboisi* that according to Hooijer (1950) has a very high orbit. The value for the elevation of the orbit above the level of the frontals, however, falls within the variation of *Hippopotamus amphibius*. But the height of the calvarium measured from the palatine is very low. As Hooijer (1950) did not describe how the measurement was taken, it cannot be explained why this height is so small. It even looks as though the measurement is wrong, because another, comparable measurement (the height of the orbit until the base of the M^3 in Appendix VI-27) is 140 mm for the same specimen and this value is in the same range as the other specimens.

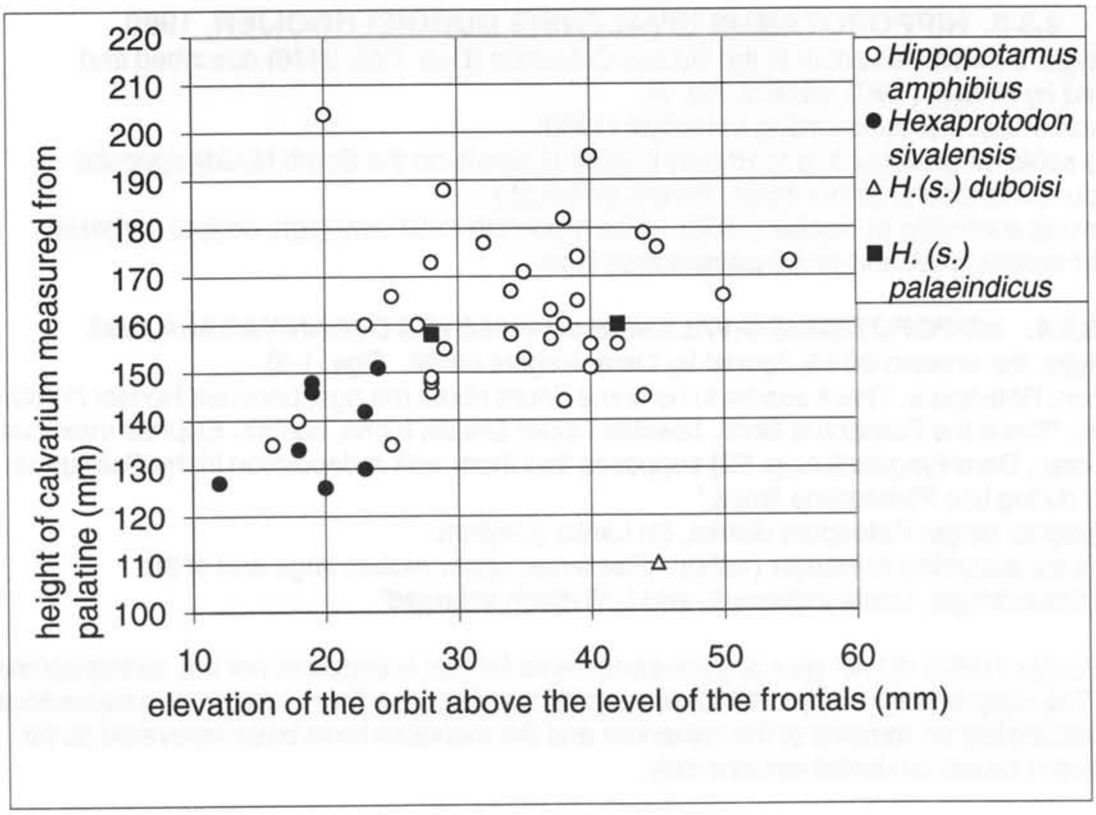

Fig. 54. Elevation of the orbits of several subspecies of hippopotami. Measurements from Hooijer (1950, Table I B, nos. 64 and 65 and Table II).

Another distinguishing feature according to Hooijer (1950) is the height of the occiput (Appendix XIII-4). The height and width of the occiput are shown in Fig. 55. Again, the variation of this feature is very large and the differences between *H. sivalensis*, *H. (s.) duboisi* (1 measurement) and *H. (s.) palaeindicus* (1 measurement) fall within the variation in the height and width of the occiput of *Hippopotamus amphibius*. So again this is not a convincing difference.

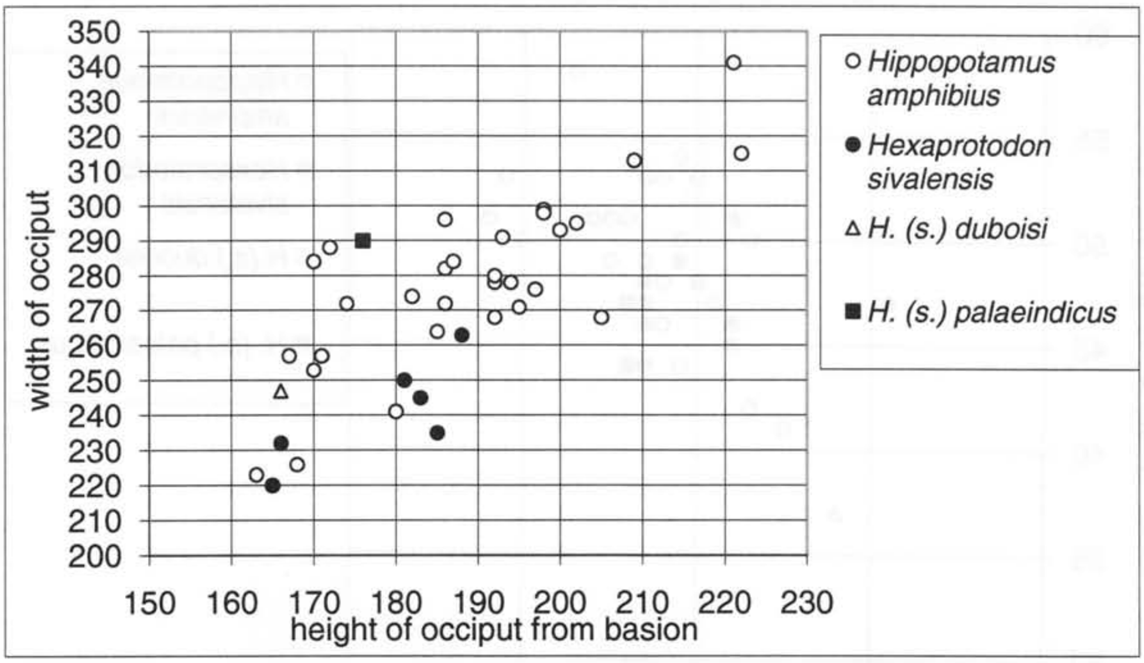

Fig. 55. Height and width of the occiput of several hippopotami. Measurements from Hooijer (1950, Table 1A, nos. 69 and 71 and Table II).

Data in Appendix XIII-5, show that the postdental part of *H. sivalensis* is long to moderate, in *H. (s.) palaeindicus* it is short. Hooijer (1950) does not give any measurements for *Hippopotamus amphibius*, but in the text he states that the variation in the P^4-M^3 index (which is a measure of the postdental part) varies from 74 to 96. (Hooijer, 1950: page 38).
In *Hippopotamus sivalensis* it varies between 63 and 77 (average 68.4; N=5) and in *H. (s.) palaeindicus* between 82 and 84 (N=2). Compared with the variation in *Hippopotamus amphibius*, again this is not a convincing difference between the presumed subspecies.

The sagittal crest does not occur in the diagnoses of the (sub)species, except the one for *H. (s.) palaeindicus* (Appendix XIII-6). According to Falconer and Cautley (1836) the subdivision of the genus is determined by, amongst others, the length of the sagittal crest. But Hooijer (1950) did not give any measurements of the length of the sagittal crest.

Biswas & Dassarma (1984) distinguished *H. namadicus* from *H. palaeindicus* on the basis of their nasal choanae (Appendix XIII-7), but this feature is hardly ever preserved.

The width of the upper molars varies in the different (sub)species as shown by the data in Appendix XIII-8. This can be seen in Fig. 56. Compared with the variation in *Hippopotamus amphibius*, the upper molars of *H. (s.) palaeindicus* are not significantly broader than those of *H. sivalensis*. Only the M^2 of *H. (s.) duboisi* is somewhat smaller, but this concerns only one measurement.

Regarding the structure of the upper molars, two types have been distinguished: the "*sivalensis*-type" and the "*palaeindicus*-type" (Hooijer, 1950), depending on the position of the parapoststyle and the metaprestyle. In the "*sivalensis*-type" the parapoststyle never extends labially beyond the metaprestyle whereas this does occur in the "*palaeindicus*-type" (Appendix XIII-9). However, these types may co-occur in the same individual, as is the case in the maxillary fragment (M^{2-3}) 2084b of the Dubois Collection. The M^2 is of the so-called "*palaeindicus*-type", and the M^3 is of the "*sivalensis*-type". So this is no feature to distinguish (sub)species. Hooijer (1950) also noticed this, but he explained it away (p. 83): "It is evident that the mutual position of the lobes of the cusps in the transverse valley of the upper molars does not always furnish a clue to the subspecific position of the specimen but [...] I would not like to ignore this point even though it is not a hard and fast rule; it is still the best character I could find for discrimination between the upper molars of the primitive and those of the progressive races of *H. sivalensis*."

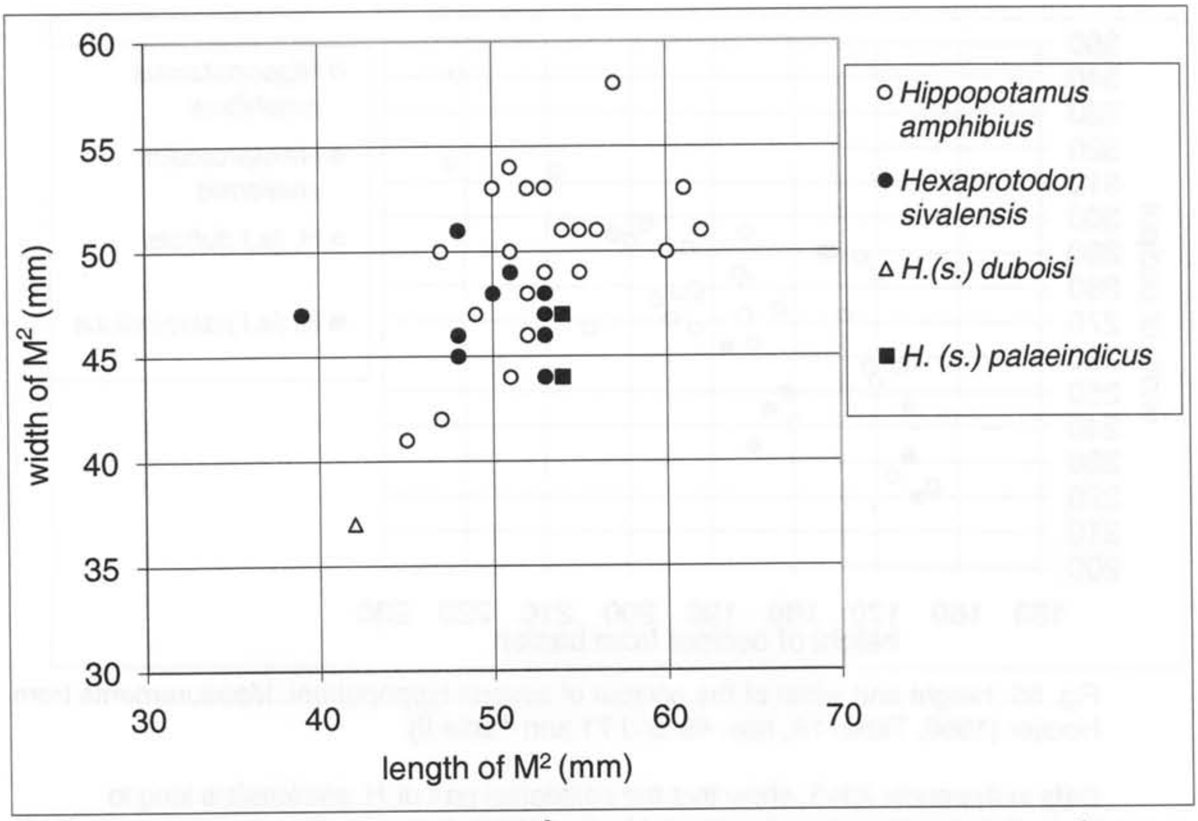

Fig. 56. Length and width of the M^2 of several hippopotami. Measurements from Hooijer (1950, Table I A, nos. 15 and 16 and Table III).

The development of the cingulum is variable in *H. sivalensis* and distinctly developed in *H (s.)* cf. *palaeindicus* (Appendix XIII-10) and for the other (sub)species no remarks about the cingulum were given, so this is also no good criterion.

The position of the M^3 with regard to the posterior border of the anterior zygomatic root and with regard to the posterior border of the palate is shown in Appendix XIII-11. Lydekker (1884) did not give any measurements for this feature and Hooijer (1950) only studied two crania of *H. (s.) palaeindicus*.

In the mandible, the angle at the inferior border of the anterior extremity (Appendix XIII-12) of *H. (s.). sivalensis* and *H. (s.) namadicus* seems to differ, but this is not proven by measurements and cannot be seen in the figures.

The best way to distinguish *H. (s.) namadicus* and *H. (s.) palaeindicus* from *H. sivalensis* according to the various authors is by the dimensions of the mandibular symphysis (Appendix XIII-13 and 14). In *H. (s.) sivalensis* the mandibular symphysis is very long to long relative to its width and very low relative to its length, whereas both in *H. (s.) namadicus* and *H. (s.) palaeindicus* it is short to very short and high to very high. This is shown in Figs. 57 and 58. In these figures, again, it is seen that the variation in the mandible is so great in *Hippopotamus amphibius* that the differences mentioned could be explained by variation.

Another important feature is said to be the ramus horizontalis (Appendix XIII-15), which in *H. (s.) namadicus* and *H. (s.) palaeindicus* is shorter than in *H. (s.) sivalensis*. A measure for this is the so-called ramus length-height index, of which Hooijer (1950) gave only five

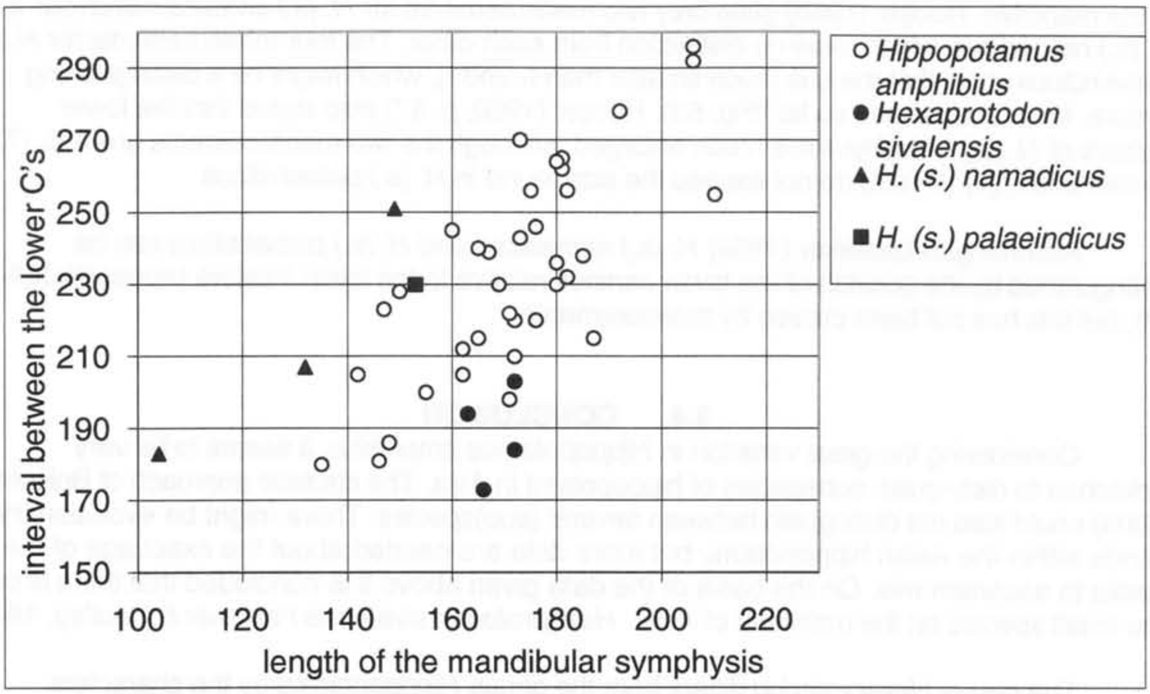

Fig. 57 Length of the mandibular symphysis relative to its width (determined by the interval between the left and right canine) for several hippopotamus species. Measurements in mm from Hooijer (1950, Table 1A, nos. 36 and 40 and Table III).

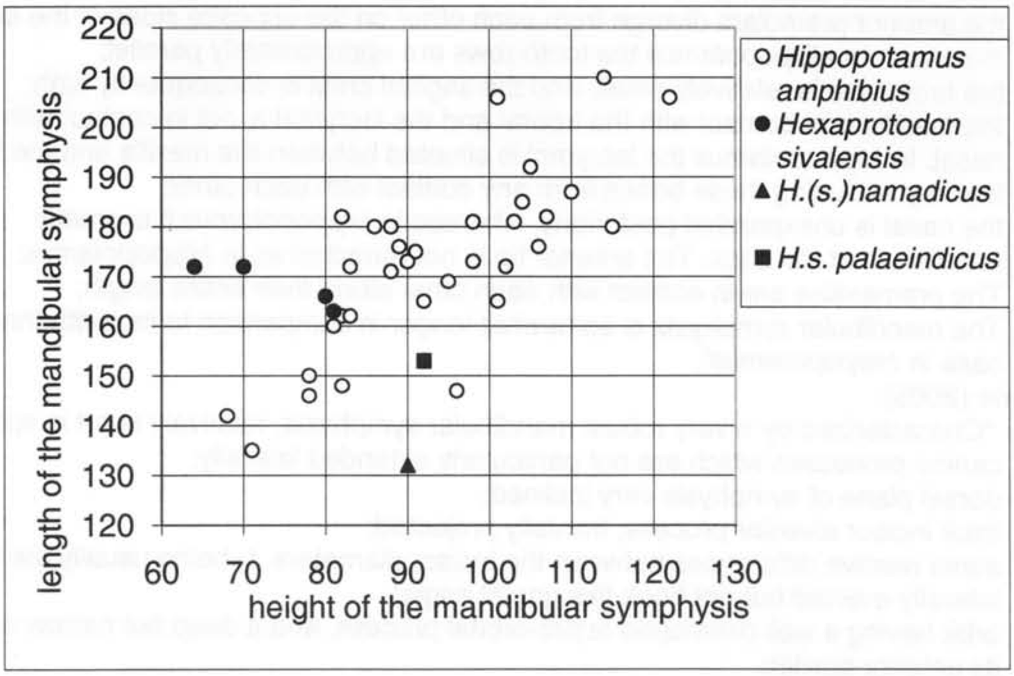

Fig. 58. Height of the mandibular symphysis relative to its length. Measurements from Hooijer (1950, Table 1A no. 36, Table 1B no. 42 and Table III)

measurements; four from *H. (s.) sivalensis* and only one from *H. (s.) palaeindicus*. This last one is indeed smaller than the other four, but as there are no measurements given for *H. amphibius*, nothing can be said about the variation in the ramus horizontalis.

The remarks made by Hooijer (1950) about the lower incisors (Appendix XIII-16 and 17) are correct, but the dimensions of the three incisors cannot be compared with the variation that occurs in *H. amphibius*, because the latter is tetraprotodont and has only 2 incisors on each side of the mandible. Hooijer (1950) gave only two measurements for *H. (s.) sivalensis* and four *for H. (s.) namadicus*, which allow no distinction from each other. The four measurements for *H. (s.) palaeindicus* show that the I_2 is much smaller than I_1 and I_3, which might be a distinguishing feature, the first clear one so far (Fig. 53). Hooijer (1950, p. 57) also stated that the lower incisors of *H. (s.) sinhaleyus* are much enlarged, although the two measurements given (I_1 (?) 49 mm and I_3 (?) 37 mm) do not exceed the size found in *H. (s.) palaeindicus*.

According to Lydekker (1884) *H. (s.) namadicus and H. (s.) palaeindicus* can be distinguished by the position of the lower canines relative to the lower incisors (Appendix XIII-18), but this has not been proven by measurements.

9.4. CONCLUSION

Considering the great variation in *Hippopotamus amphibius*, it seems to be very farfetched to distinguish subspecies of hippopotami in Asia. The cladistic approach of Boisserie (2005) could also not distinguish between several (sub)species. There might be evolutionary trends within the Asian hippopotami, but more data are needed about the exact age of the fossils to ascertain this. On the basis of the data given above it is concluded that there is only one fossil species on the mainland of Asia: *Hexaprotodon sivalensis* Falconer & Cautley, 1836.

The genus *Hexaprotodon* differs from the genus *Hippopotamus* by the characters defined by Colbert (1935) and by Boisserie (2005).

Colbert (1935):

- "There are six subequal incisors, as compared to four in *Hippopotamus*. The central incisors are not enlarged;
- the anterior premolars diverge from each other on the opposite sides of the skull and mandible. In *Hippopotamus* the tooth rows are approximately parallel;
- the braincase is relatively small, and the sagittal crest is consequently high;
- the maxilla is in contact with the frontal and the lacrymal is not in contact with the nasal. In *Hippopotamus* the lacrymal is situated between the maxilla and the frontal, thereby excluding these bones from any contact with each other;
- the nasal is unexpanded posteriorly, whereas in *Hippopotamus* it is greatly broadened at the back. The anterior tip is not retracted as in *Hippopotamus*;
- The premaxillae are in contact with each other along their entire length;
- The mandibular symphysis is somewhat longer in comparison to its width than is the case in *Hippopotamus*".

Boisserie (2005):

- "Characterized by a very robust mandibular symphysis, relatively short in spite of its canine processes which are not particularly extended laterally;
- dorsal plane of symphysis very inclined;
- thick incisor alveolar process, frontally projected;
  some relative differences between the incisor diameters, I_2 being usually the smallest;
- laterally everted but not hook-like gonial angle;
- orbit having a well developed supra-orbital process, and a deep but narrow notch at its anterior border;
- thick zygomatic arches;
- elevated sagittal crest on a transversally compressed braincase."

***Hexaprotodon sivalensis* Falconer & Cautley, 1836.**

- lectotype: British Museum M 2269 (skull).
- cotype: a calvarium referred to by Falconer & Cautley in the original description, but they did not designate any particular specimen on which the description was based.
- synonyms: the hippopotami from Asia described by Hooijer (1950), i.e.,
  - *Hippopotamus sivalensis sivalensis* (Falconer & Cautley, 1836);
  - *Hippopotamus sivalensis namadicus* (Falconer & Cautley, 1836);

- *Hippopotamus sivalensis palaeindicus* (Falconer & Cautley, 1836);
- *Hippopotamus sivalensis sinhaleyus* Deraniyagala, 1936;
- *Hippopotamus sivalensis duboisi* Hooijer, 1950;
- In the same book, Hooijer (1950) gives lists of synonyms for these subspecies;
- *Hexaprotodon dhokwazirensis* Akhtar & Bakr, 1995.

- revised diagnosis: Asian *Hexaprotodon* with the I_2 smaller and dorsally from the I_{1-3}, the bullae have a wing-like shape.
- type locality: Siwalik Hills (India).
- geographic range: Narmada Valley (India), Pakistan, Myanmar (former Burma), Nepal, Thailand, Malaysia, China(?), Sri Lanka.
- horizon: Upper Siwaliks.
- age: late Miocene-Pleistocene.

10. TAXONOMY OF THE GENUS *HEXAPROTODON* FROM JAVA (INDONESIA)

10.1. INTRODUCTION

Also in Java (Indonesia), *Hexaprotodon* is present and many authors, like Dubois (1908), Van der Maarel (1932), Von Koenigswald (1933, 1934) and Hooijer (1950) came to the conclusion that more than one (sub)species of *Hexaprotodon* occur on Java.

10.2. SUBSPECIES: REVIEW OF THE LITERATURE

A review is given of the three subspecies of *Hippopotamus sivalensis* distinguished by Hooijer (1950) in Java, i.e., *Hippopotamus sivalensis sivajavanicus* (Dubois, 1908), *Hippopotamus sivalensis koenigswaldi* (Hooijer, 1942) and *Hippopotamus sivalensis soloensis* Hooijer, 1950.

10.2.1. *HIPPOPOTAMUS SIVALENSIS SIVAJAVANICUS* (DUBOIS, 1908)

- holotype: a calvarium in the Dubois Collection (Coll. Dub. 2908) described and figured in Hooijer (1950, Pl. II, Fig. 4, Pl. III Fig. 2).
- horizon according to Hooijer (1950): Lower Pleistocene.
- geographic range, according to Hooijer (1950): western and central Java.

Dubois (1908) considered *Hexaprotodon sivajavanicus* as a species and in his diagnosis he wrote that *H. sivajavanicus* differs from *Hexaprotodon namadicus* and *Hexaprotodon palaeindicus* by the length of the mandibular symphysis and the relative size of the incisors. Regarding these characteristics and also regarding the shape of the skull, it resembles more *Hexaprotodon sivalensis*, but (besides its slightly smaller size) it differs from *Hexaprotodon sivalensis* by the greater difference in height between the nasal bone and the palate (relative to its length), by the relatively broader upper maxilla and especially by the not straight position of the lower incisors (Dubois, 1908).

According to Hooijer (1950) *Hippopotamus simplex* founded by Von Koenigswald (1933) would be a synonym for the subspecies *Hippopotamus sivalensis sivajavanicus*. Von Koenigswald (1933) founded his *Hippopotamus (Hexaprotodon) simplex* ("the least specialised Javan form, because the six subequal incisors were placed in a row") on the material from Kali Glagah described by Van der Maarel (1932), who referred it to *Hippopotamus sp.*, after comparison with *Hexaprotodon sivajavanicus* Dubois 1908, *Hippopotamus palaeindicus* Falconer & Cautley (F & C), 1836, *Hippopotamus namadicus* F & C, 1836, *Hippopotamus iravaticus* F & C, 1836 and *Hippopotamus sivalensis* F & C, 1836). Van der Maarel (1932) concluded that "comparisons of measurements and descriptions of the Javan specimens show that there is not the slightest reason for accepting the presence of more than one species."

In the diagnosis, Hooijer (1950) stated that the subspecies *Hippopotamus sivalensis sivajavanicus* is characterised by its "small size, moderately elevated orbit, long postdental part of the calvarium. The upper molars are small and of the "*sivalensis*"-type. The mandibular symphysis is short to very short relative to its width. I_2 is about equal in size to I_1 and I_3 is decidedly smaller than I_1".

10.2.2. *HIPPOPOTAMUS SIVALENSIS KOENIGSWALDI* (HOOIJER, 1942)

According to Hooijer (1950):

- cotypes: an unfigured mandible from Gunung Butak referred to by Von Koenigswald (1934, p. 192), and a lower molar figured by Von Koenigswald (l.c., Pl. IV Fig. 4), originating from the Jetis (= Djetis) deposits of Sangiran.
- horizon: Lower Pleistocene.
- geographic range: Java.

Von Koenigswald (1934) considered the cotypes as the cotypes of the species *Hippopotamus (Hexaprotodon) antiquus*: "the middle incisor in the lower jaw was moved up a little, compared to the other incisors. Smaller than *Hippopotamus (Hexaprotodon) simplex*".

According to Hooijer (1942) *H. antiquus* is a homonym and he proposed the name *H. koenigswaldi* instead. In 1950 however, Hooijer came to the conclusion that it would be better to designate this species to the subspecies *H. sivalensis koenigswaldi*. The diagnosis of the subspecies (Hooijer, 1950): "size small, orbit high, occiput moderate, postdental part of calvarium moderate. Upper molars small and either of the "*sivalensis*"- type or transitional between the latter and the "*palaeindicus*"- type. Mandibular symphysis moderate to short relative to its width, and low relative to its length. Ramus horizontalis moderately low at M_2 relative to its length, and height at M_2 less than length M_1-M_3. I_2 two-thirds to about equal in size to I_1, and I_3 three-fourths to about equal in size to I_1".

10.2.3. *HIPPOPOTAMUS SIVALENSIS SOLOENSIS* HOOIJER, 1950

According to Hooijer (1950):

- holotype: a calvarium in the Dubois Collection (Coll. Dub. 2914) described and figured in Hooijer (1950, Pl. II Fig. 1, Pl. III Fig. 1, Pl. VI Fig. 1).
- horizon: Middle and Upper Pleistocene.
- geographic range: Central and Eastern Java.

Von Koenigswald (1934) named this species *Hippopotamus namadicus*: "the incisors were reduced in size. About the size of *H. amphibius*, so larger than *H. simplex* and *H. antiquus*". Von Koenigswald (1934) thought *H. namadicus* from the Narbada Beds in Central India and the Javanese form to be identical.

Hooijer (1950) did not agree with Von Koenigswald (1934): "this is *H. sivalensis soloensis* with the diagnosis: "Size moderate, orbit very high, occiput moderate to low, postdental part of calvarium moderate. Upper molars small and of the "*palaeindicus*"-type. Mandibular symphysis short relative to its width, and very high relative to its length. Ramus horizontalis very high at M_2 relative to its length, and height at M_2 exceeding length M_1-M_3. I_2 three-fourths to about equal in size to I_1, and I_3 slightly smaller, or even larger than I_1. "It differs from *Hippopotamus sivalensis namadicus* in the mandibular symphysis being longer relative to its width, and in its smaller incisors of which I_3 is not usually larger than I_1." It differs from *H. s. palaeindicus* "in their higher orbits, longer postdental part, smaller molars, and in the molar series not extending behind the posterior border of the palate" (Hooijer, 1950).

10.3. DISCUSSION

The diagnoses of the different subspecies are summarised in Appendix XIV. From this appendix it can be seen that the differences are not really very clear. Hooijer (1950) admits this by writing: "There are upper molars from Java that cannot be referred with certainty to either of the two types ["*sivalensis*-type" and *palaeindicus*-type"], but this could be expected since there is intergradation in all of the characters serving to distinguish between the subspecies" [!!].

If we consider the different features mentioned in Appendix XIV, some conclusions can be drawn about the liability of the diagnoses. The size (Appendix XIV-1) is not a very valuable feature because it is not explained which size is meant exactly. Moreover, the fossils are hardly ever complete. From Table II and III (Hooijer, 1950) and Fig. 51 and 52, the conclusion is drawn that the Javanese *Hexaprotodon* is smaller than *Hexaprotodon* from the Siwaliks.

Hooijer (1950) claims that the orbit (Appendix XIV-2) is very diagnostic: moderately elevated in *H. s. sivajavanicus*, high in *H. s. koenigswaldi* and very high in *H. s. soloensis*. This is true, as can be seen in Fig. 59, but compared with the very great variation that occurs, both in *Hippopotamus amphibius* and in *Hexaprotodon sivalensis*, it is not diagnostic.

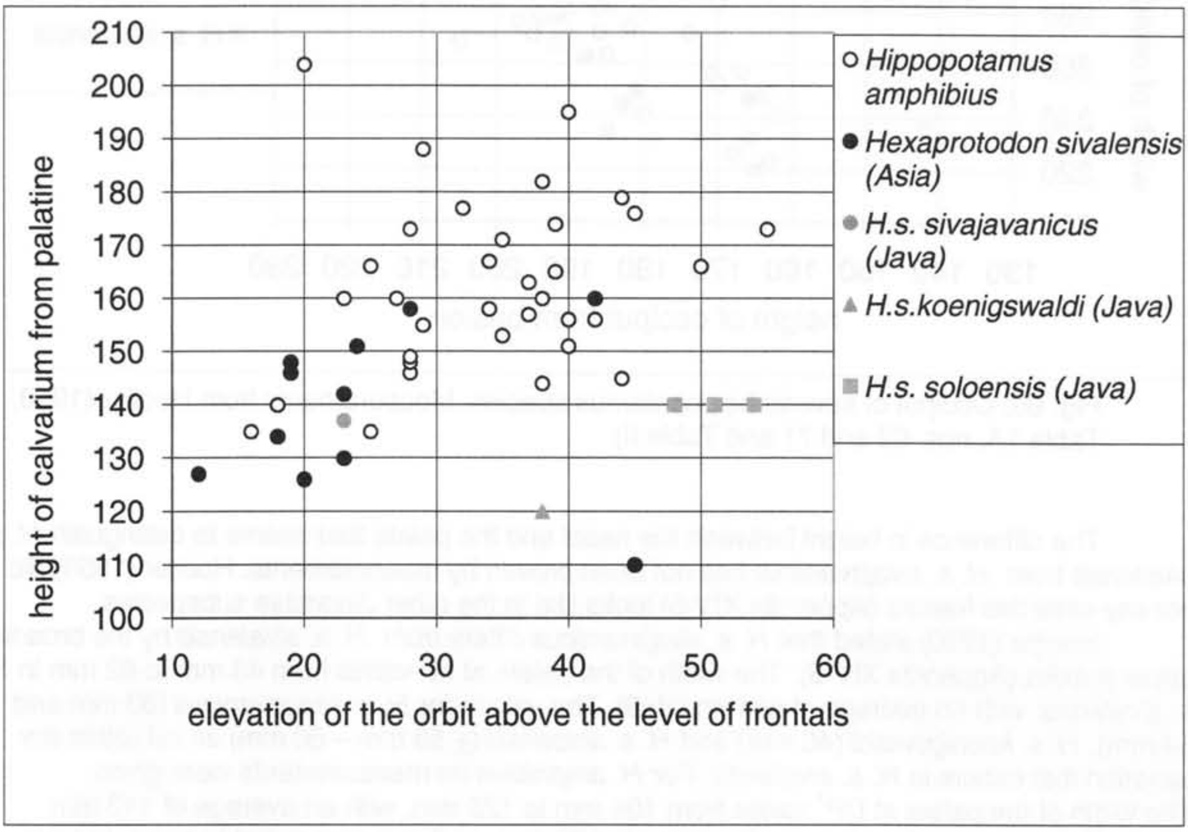

Fig. 59. Elevation of the orbits of several hippotamid species. Measurements from Hooijer (1950, Table I B, nos. 64 and 65 and Table II).

According to Appendix XIV-3 the occiput is moderate in *H. s. koenigswaldi* en moderate to low in *H. s. soloensis*,. For *H. s. sivajavanicus* no data are available. Regarding the variation that occurs in *H. amphibius*, the Javanese subspecies cannot be distinguished on this feature. The Javanese values of the height of the occiput are somewhat less than those from the Asian mainland, as is shown in Fig. 60.

According to Appendix XIV-4, the postdental part of *H. sivalensis* is long to moderate, in *H. s. sivajavanicus* it is long, in *H. s. koenigswaldi* it is moderate and in *H. s. soloensis* it is moderate and longer than in *H. s. palaeindicus*. Hooijer (1950) does not give any measurements for *Hippopotamus amphibius*, but in the text he stated that the variation in the P^4-M^3 index (which is a measure of the postdental part) varies from 74 to 96 (Hooijer, 1950: p. 38). In *Hexaprotodon sivalensis* the P^4-M^3 index varies between 63 and 77 (average 68.4; N=5) and in *H. s. palaeindicus* between 82 and 84 (N=2). In *H. s. sivajavanicus* it is 66 (N=1), in *H. s. koenigswaldi* 79 (N=1) and in *H. s. soloensis* 74 (N=2). Compared with the variation in *Hippopotamus amphibius*, again this is not convincing. The P^4-M^3 index again is somewhat smaller in the Javanese hippopotamus than in *H. sivalensis*.

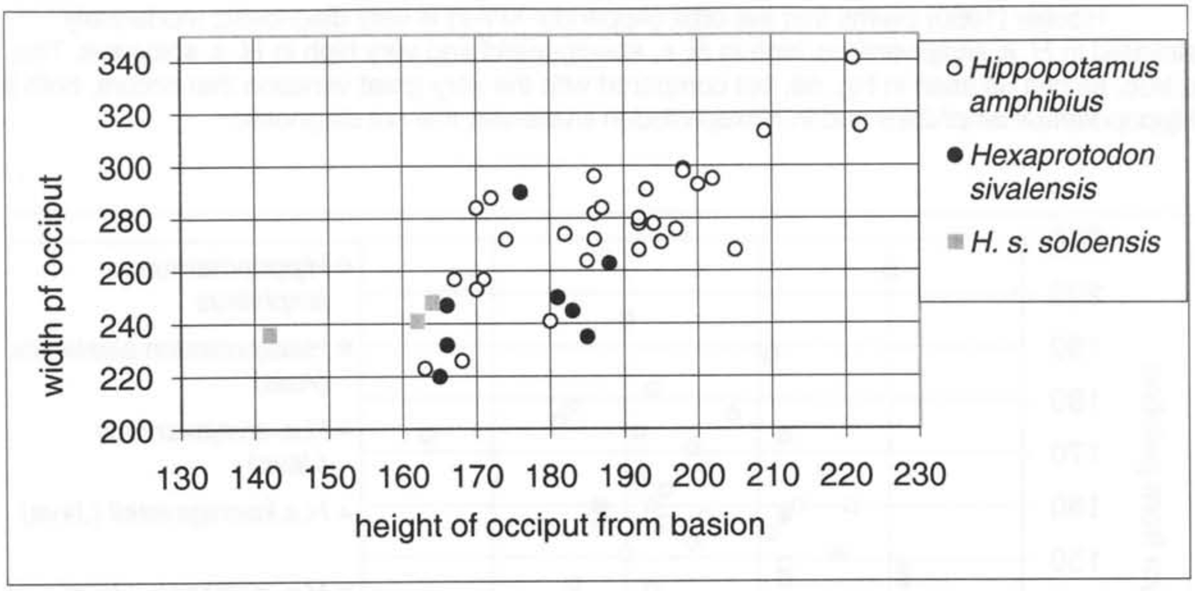

Fig. 60. Occiput of several hippopotamus species. Measurements from Hooijer (1950, Table 1A, nos. 69 and 71 and Table II).

The difference in height between the nasal and the palate that seems to distinguish *H. s. sivalensis* from *H. s. sivajavanicus* has not been proven by measurements. Hooijer (1950) did not say what this feature (Appendix XIV-5) looks like in the other Javanese subspecies.

Hooijer (1950) stated that *H. s. sivajavanicus* differs from *H. s. sivalensis* by the broader upper maxilla (Appendix XIV-6). The width of the palate at M^1 varies from 43 mm to 62 mm in *H. s. sivalensis*, with an average of 53 mm (N=9). The values for *H. s. sivajavanicus* (63 mm and 54 mm), *H. s. koenigswaldi* (46 mm) and *H. s. soloensis* ($\pm$ 58 mm – 60 mm) all fall within the variation that occurs in *H. s. sivalensis*. For *H. amphibius* no measurements were given. The width of the palate at DP^1 varies from 104 mm to 125 mm, with an average of 113 mm (N=6). The one value for *H. s. sivajavanicus* is 132 mm, so this is somewhat broader, but it is only one measurement. For *H. s. soloensis* only two approximate sizes were given ($\pm$ 116 mm and $\pm$ 123 mm) and this falls within the variation of *H. s. sivalensis*.

According to Appendix XIV-7, the upper molars of *H. s. sivajavanicus* are broader than those of *H. s. sivalensis*. The upper molars of *H. s. koenigswaldi* are small, and those of *H. s. soloensis* are smaller than those of *H. s. palaeindicus*. In Fig. 61 is shown that the upper molars of *H. s. sivajavanicus* are not at all broader than those of *H. sivalensis*; on the contrary, the upper molars of the Javanese hippopotami are smaller, both in length and width compared with those from the Indian mainland. Compared with the variation that occurs in the M^2 of *Hippopotamus amphibius*, the differences between the Javanese subspecies again are not convincing.

Regarding the pattern of the upper molars (Appendix XIV-8), in Appendix VII and in Chapter 9.3.5. it was already explained why this is not a good feature, as the two different types ("*sivalensis*"-type and "*palaeindicus*"-type) may co-occur in the same individual (like in Coll. Dub. 2084b).

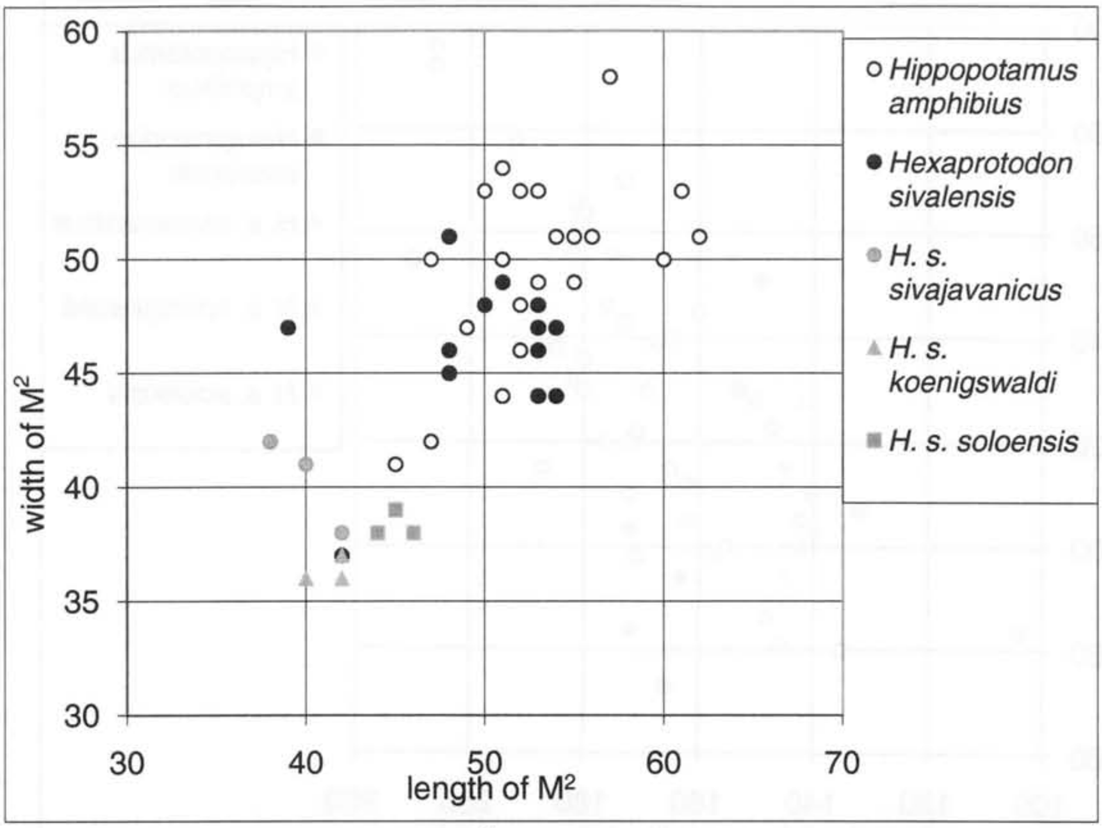

Fig. 61. Length and width of M^2 of several hippopotamus species. Measurements from Hooijer (1950, Table I A, nos. 15 and 16 and Table III).

The mandibular symphysis (Appendix XIV-9 and 10) is said to be short to very short relative to its width in *H. s. sivajavanicus*. In *H. s. koenigswaldi* the mandibular symphysis is moderate to short relative to its width and low relative to its length. In *H. s. soloensis* it is short relative to its width and very high relative to its length. This is shown in Figs. 62 and 63. In these figures, the approximate measurements are included, otherwise there were too few measurements available. Nevertheless, we see that the variation of the feature is so great in *Hippopotamus amphibius* that the differences in the other subspecies can be explained by variation.

The next feature is the ramus horizontalis (Appendix XIV-11), which in *H. s. koenigswaldi* is moderately low at M_2 relative to its length. In *H. s. soloensis* it is very high at M_2 relative to its length. A measure for this is the so-called ramus length-height index. This is the length of the ramus from front to M_3 as a percentage of its height at M_2. In *H. sivalensis* this index varies from 250 to 298 with an average of 268.5 (N=4).

For *H. s. sivajavanicus* there are no measurements. For *H. s. koenigswaldi* the ramus length-height index varies from 272 to 277 with an average of 274 (N=3) and in *H. s. soloensis* it varies from 214 to 232, with an average of 223 (N=2). As there are no measurements given for *H. amphibius*, nothing can be said about the variation that occurs in this feature, although the variation that occurs in *H. s. sivalensis* is quite great, as mentioned above.

The height of the ramus horizontalis at M_2 is less than the length M_1-M_3 in *H. s. koenigswaldi*, whereas in *H. s. soloensis* this height exceeds the length M_1-M_3 (Appendix XIV-12). The height of the ramus horizontalis at M_2 is smaller in all measurements from *H. amphibius*, *H. sivalensis* and *H. s. koenigswaldi*. Hooijer (1950) based the statement given in Appendix XIV on only one measurement, in which the height of the ramus exceeds the length M_1-M_3. From Fig. 64 the conclusion is drawn that the variation in this feature is again great. The length of M_1-M_3 of the Javanese hippopotamus is somewhat less than that from the Siwaliks.

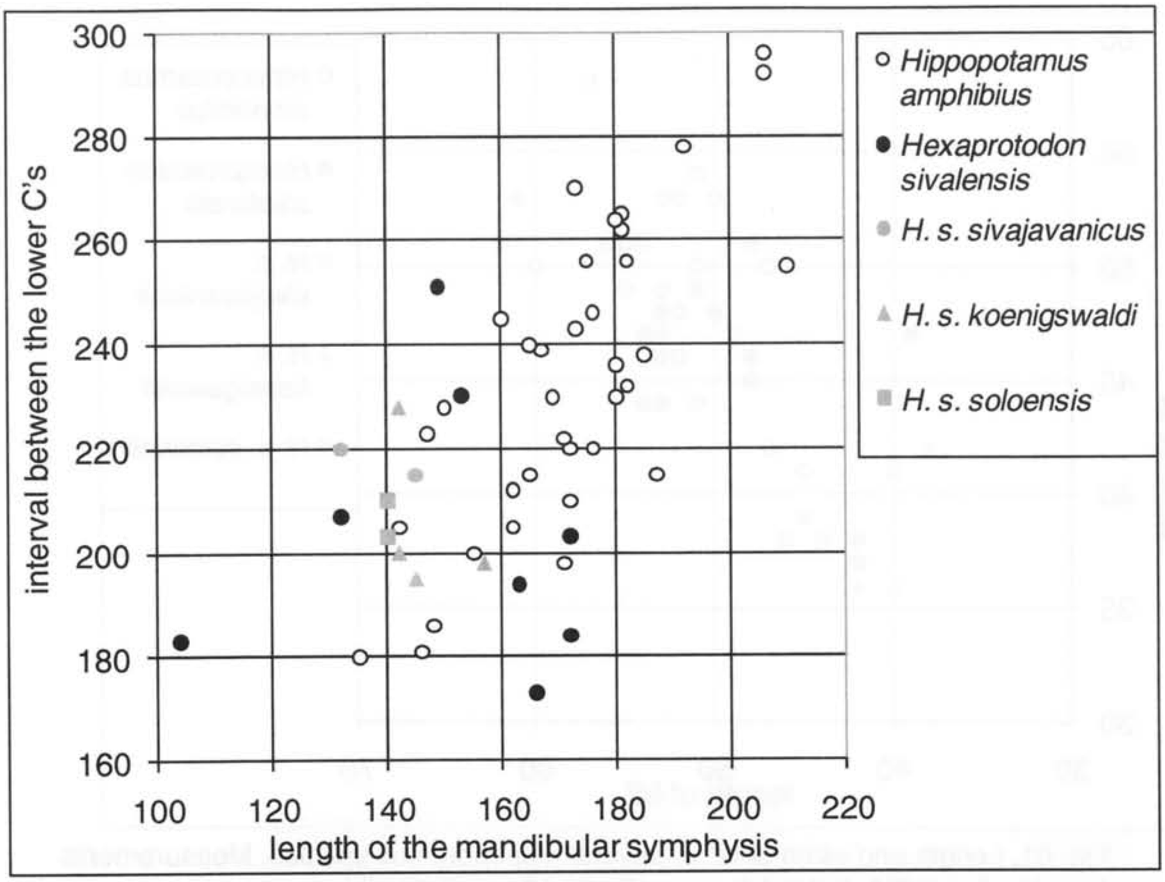

Fig. 62. Length of the mandibular symphysis relative to its width. Measurements from Hooijer (1950, Table 1A, nos. 36 and 40 and Table III).

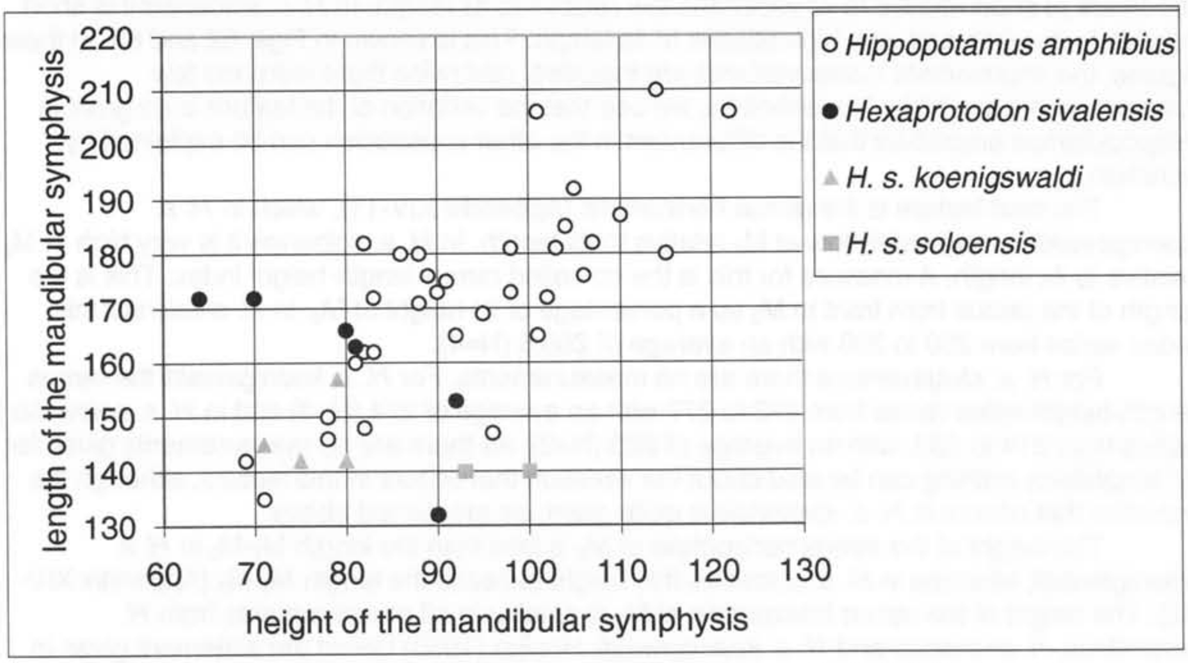

Fig. 63. Height of the mandibular symphysis relative to its length in several hippopotamus species. Measurements from Hooijer (1950, Table 1A no. 36, Table 1B no. 42 and Table III).

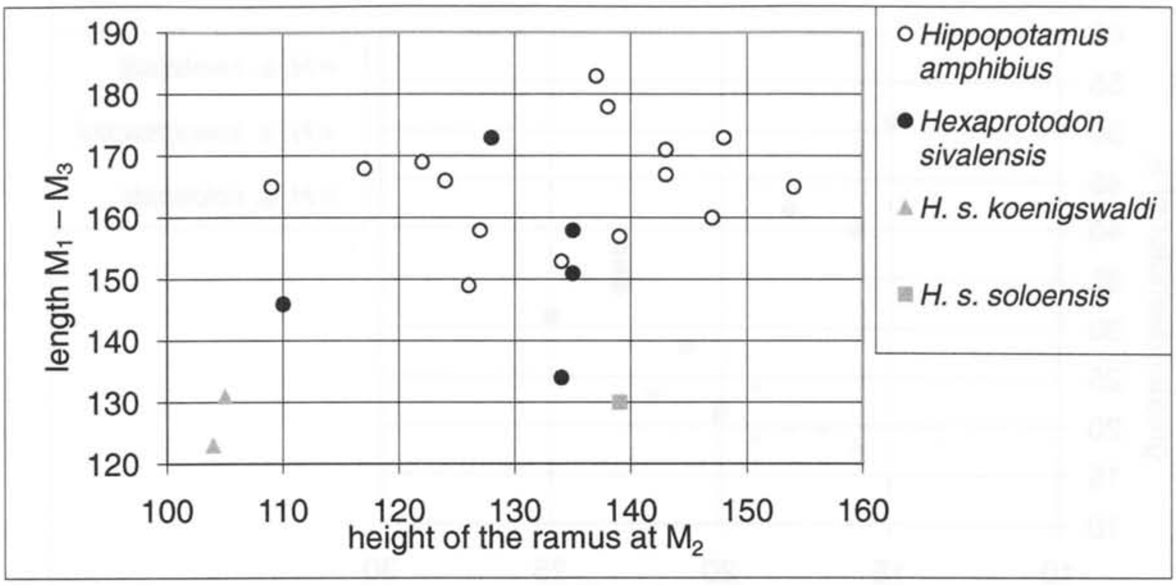

Fig. 64. Height of the ramus horizontalis compared to the length of $M_1 - M_3$. Measurements from Hooijer (1950, Table 1A, nos. 29 and 30 and Table III).

The remarks made by the various authors about the lower incisors (Appendix XIV-13) do not seem to mean anything. The values cannot be compared with the variation in *H. amphibius*, because the latter is tetraprotodont. From Figs. 65 and 66 only one conclusion can be drawn: the incisors of the Javanese hippopotamus are smaller than those of the Asian mainland. As to the not straight position of the lower incisors in the Javanese specimens, this also does not occur in the Siwalik ones, as was also mentioned by Hooijer (1950, p. 48): "This interesting specimen [coll. Dub. 3147 from the Siwaliks] clearly shows that the alveoli of three incisors do not run parallel to each other; that of the I_2, the smaller of the three, becomes higher relative to that of I_3 when passing from front to back." So this also cannot be a distinguishing feature.

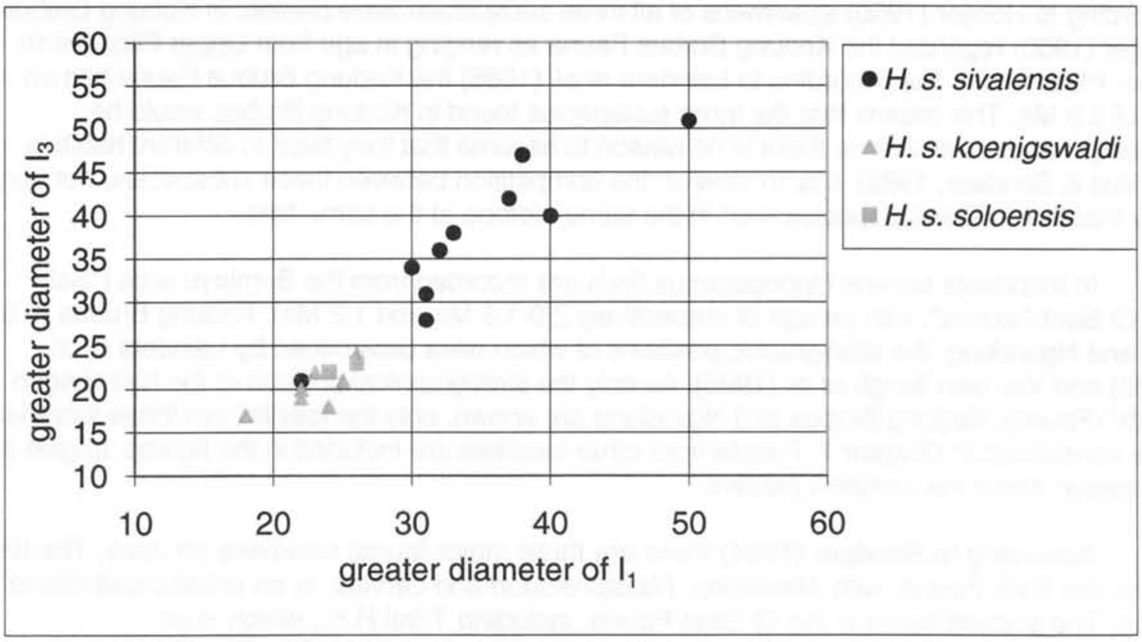

Fig. 65. The greater diameter of I_1 and I_3 of several hippopotamus species. Measurements from Hooijer (1950, Table III.

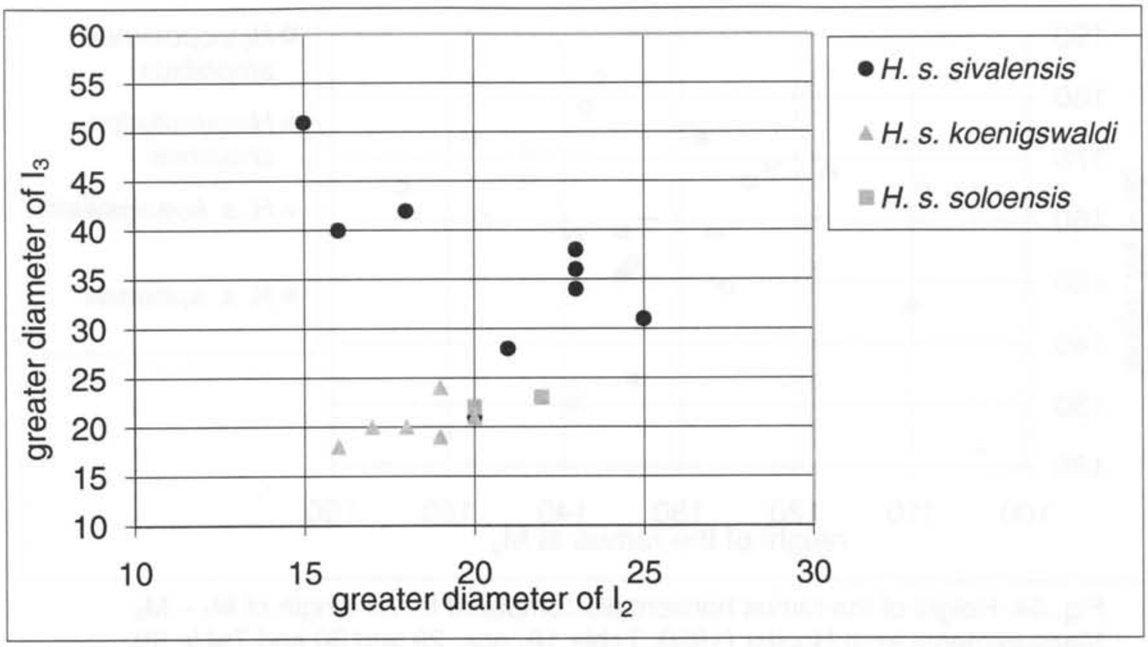

Fig. 66. The greater diameter of I_2 and I_3 of several hippopotamus species. Measurements from Hooijer (1950, Table III).

10.4. CONCLUSION

The definitions of the subspecies *H. s. sivajavanicus* (Dubois, 1908), *H. s. koenigswaldi* (Hooijer, 1942) and *H. s. soloensis* Hooijer, 1950 are based on 4 fossils and 7 Figs., 16 fossils and 11 Figs. respectively. At his page 109, however, Hooijer (1950) gives a list of more than a hundred fossils that he cannot designate to any of these subspecies. So he also faced the problem that it is rather impossible to designate an individual fossil to one of the subspecies, because the diagnoses are not clear enough and there is a lot of variation.

Hooijer (1950) distinguished these subspecies of *Hippopotamus* purely on morphology. According to Hooijer (1950) specimens of all three subspecies were present in Kedung Brubus. Hooijer (1950) regarded the Kedung Brubus Fauna as ranging in age from Upper Pliocene to Upper Pleistocene. But according to Leinders *et al.* (1985) the Kedung Brubus Fauna has an age of 0.8 Ma. This means that the three subspecies found in Kedung Brubus would be contemporaneous and since there is no reason to assume that they lived in different habitats (De Vos & Sondaar, 1982), it is, in view of the competition between these subspecies, not very likely that three different species lived in the same biotope at the same time.

In Indonesia several hippopotamus finds are recorded from the Bumiayu area ("Satir and Ci Saat Faunas", with an age of respectively 2.0-1.5 Ma and 1.2 Ma), Kedung Brubus (0.8 Ma) and Ngandong, the stratigraphic positions of which were determined by Leinders *et al.* (1985) and Van den Bergh *et al.* (1996). As only the stratigraphical position of the Kali Glagah ("Satir"-Fauna), Kedung Brubus and Ngandong are known, only the fossils from these localities were considered in Chapter 7. Fossils from other localities are included in the figures, to give an impression about the variation present.

According to Sondaar (1984) there are three major faunal turnovers on Java. The first fauna, the Satir Fauna, with *Mastodon*, *Hexaprotodon* and cervids, is an unbalanced island fauna. The second fauna is the Ci Saat Fauna, including Trinil H.K., which is an impoverished mainland fauna, with new arrivals of *Stegodon* and felids. The third is a mainland fauna found in Kedung Brubus, Ngandong and perhaps Punung and Wajak, characterised by a lot of new arrivals (Sondaar, 1984).

The first occurrence of *Hexaprotodon* was found in the Satir Fauna, the last occurrence in the Ngandong Fauna; it is not found anymore in the Punung Fauna. The *Hexaprotodon* in the Satir Fauna was named *Hippopotamus simplex* Von Koenigswald, 1933. The *Hexaprotodon* from Ci Saat, Kedung Brubus and Ngandong was named *Hexaprotodon sivalensis* (Sondaar, 1984; Table 2), suggesting that this *Hexaprotodon* was more advanced than *Hippopotamus simplex*. The conclusion drawn in this thesis is that there is no way to distinguish between these species and that the changes that occur are due to local evolution of *Hexaprotodon*. This implicates that there are no indications of new arrivals of *Hexaprotodon*.

The conclusion of Chapter 7 was that indeed there are differences between the *Hexaprotodon* from the localities Kali Glagah (Satir Fauna), Kedung Brubus and Ngandong but that these differences are not clear enough to warrant a division into different (sub)species. With respect to the material from Kali Glagah, Kedung Brubus and Ngandong the same problem arises as in Hooijers' subspecies. In general, the Kali Glagah material is smaller than the Kedung Brubus material and the Kedung Brubus material is smaller than the Ngandong material (Appendix IX), a trend also seen in Stegodon by Van den Bergh (1996, p. 63-64): "The *Stegodon* molar material from Ngandong, Grenjengan and Watualang appears to be uniform and can be clearly distinguished from analogue elements from Trinil H.K. and Kedung Brubus" and indeed, the hippopotamus material from Watualang is consistent with the Ngandong material (Figs. 37 and 38).

Also some morphological differences between the fossils from these three localities occur (Appendix X) but it is rather impossible to designate even the material from the other localities in Java to one of the types from Kali Glagah, Kedung Brubus or Ngandong. Therefore, the definition of (sub)species has no value at all and all hippopotamus fossils from Java are considered to represent one species. The fossil *Hexaprotodon* material from Java is definitely smaller than that from the Asian mainland (see also Chapter 8 and the Figs. 51, 52, 61, 64, 65, 66) and the species *Hexaprotodon sivajavanicus* Dubois, 1908 is proposed for the hippopotamus from Java:

***Hexaprotodon sivajavanicus* Dubois, 1908**

- holotype: a calvarium in the Dubois Collection (Coll. Dub 2908), described and figured in Hooijer (1950).
- synonyms: the hippopotami from Java described by Hooijer (1950), i.e.,
  - *Hippopotamus sivalensis sivajavanicus* (Dubois, 1908);
  - *Hippopotamus sivalensis koenigswaldi* (Hooijer, 1942)
  - *Hippopotamus sivalensis soloensis* Hooijer 1950.
  - In the same book, Hooijer (1950) gives lists of synonyms for these subspecies
- revised diagnosis: a *Hexaprotodon* in which I_2 is smaller and lies dorsally from the $I_{1-3.}$ It is smaller than *Hexaprotodon sivalensis* from continental Asia.
- type locality: Kedung Brubus (Java).
- geographic range: Java.
- age: Pliocene-Pleistocene.

Table 1.
Summary of the characteristic differences between the Lower and Upper Samwal Formation. The boundary between the two parts is defined at the upper bentonite layer.

	Lower Samwal Formation	Upper Samwal Formation
SANDSTONES	Average of the three main sections	Average of the three main sections
Average thickness of sandstones	9.30 m	3.0 m
% sandstone of total section length	54%	23%
% sandstones with thickness < 1 m	1%	2%
% sandstones with thickness 1-5 m	23%	75%
% sandstones with thickness 6-10 m	37%	16%
% sandstones with thickness 11-15 m	20%	7%
% sandstones with thickness > 15 m	19%	0%
prevailing grain size	medium - coarse	very fine - fine
sorting	moderately sorted	well sorted
FINER MATERIAL (% of all fine-grained material)		
clay	1%	2%
silty clay and clayey silt	90%	66%
silt	5%	28%
sandy silt	4%	4%
mottling	not common	common
calcrete / caliche nodules	not common	common

Table 2.
Lateral differences between the three main sections (Fig. 3) of the Samwal Formation.

UPPER SAMWAL FORMATION	Jhelawala Kas (849 m)	Jhel Kas (820 m)	Samwal (645 m)
Average thickness of sandstone beds	4.7 m	2.8 m	1.4 m
% sandstone of total section	23.2%	24%	21.9%
% sandy silt of total section	1.0%	2.3%	3.5%
% silt of total section	4.8%	16.3%	22.0%
% silty clay / clayey silt of total section	51.2%	31.7%	23.2%
% clay of total section	----	0.7%	2.7%
% not exposed of total section	19.8%	25.0%	26.7%
total number of sandstones (thicker than 1 m)	13	17	20
maximum thickness of sandstone beds	14.3 m	11.0 m	7.6 m
thickness distribution of sandstones:			
1 - 5 m	70%	65%	98%
5 - 10 m	15%	30%	2%
11 - 15 m	15%	5%	----
LOWER SAMWAL FORMATION			
Average thickness of sandstone beds	13.9 m	7.7 m	6.3 m
% sandstone of total section	65.8%	54.0%	43.0%
% sandy silt of total section	------	1.5%	2.6%
% silt of total section	1.0%	1.0%	2.9%
% silty clay / clayey silt of total section	28.5%	30.6%	24.9%
% clay of total section	----	------	0.6%
% not exposed of total section	4.7%	12.9%	26.0%
total number of sandstones (thicker than 1 m)	26	16	15
maximum thickness of sandstone beds	64.5 m	20 m	20 m
thickness distribution of sandstones:			
1 - 5 m	23%	12%	33%
6 - 10 m	35%	50%	27%
11 - 15 m	15%	19%	27%
16 - 20 m	8%	19%	13%
21 - 25 m	4%	----	----
more than 25 m	15%	----	----

Table 3.
The composition of the fossil assemblages in the Lower and Upper Samwal Formation.
Method 1: only the bones and bone fragments that were positively identified on genus level, were counted; method 2: every identified bone(fragment) was counted as one. If a bone was determined to family level, it was counted as belonging to that family; method 3: every identified bone (fragment) was counted as one. If the bones could not be identified to family level and the determination was assigned to e.g. carnivora, they were proportionally spread over the different canivora families, based on the percentages of the families involved; method 4: the bones or bone fragments were converted to minimum number of individuals (MNI). This was done by counting the different elements and deciding how many individuals they could represent at least. For example 5 left femora of a species must have belonged to 5 animals.

	Lower Samwal Formation Method 1		Upper Samwal Formation Method 1		Lower Samwal Formation Method 2		Upper Samwal Formation Method 2		Lower Samwal Formation Method 3		Upper Samwal Formation Method 3		Lower Samwal Formation Method 4		Upper Samwal Formation Method 4	
Family	No.	%	No.	%	No.	%	No.	%	No.	%	No.	%	No.	%	No.	%
Anthracotheriidae	1	0.2	0	0	1	0.1	0	0	1	0.2	0	0	1	0.7	0	0
Bovidae (Antilopinae included)	177	36.6	446	50.7	408	50.9	573	48.9	158	36.3	408	53.5	44	29.5	40	38.5
Carnivora (Canidae & Hyaenidae)	3	0.6	19	2.2	6	0.8	83	7.1	2	0.5	15	2.0	4	2.7	4	3.8
Cervidae	17	3.5	27	3.1	38	4.8	34	2.9	15	3.4	19	2.5	5	3.3	5	4.8
Equidae	6	1.2	198	22.5	7	0.9	244	20.8	6	1.4	180	23.6	5	3.3	21	20.2
Giraffidae	17	3.5	59	6.7	38	4.8	75	6.4	12	2.8	47	6.2	7	4.7	5	4.8
Hippopotamidae	54	11.2	12	1.4	59	7.4	15	1.3	46	10.6	5	0.7	19	12.8	2	1.9
Proboscidae	101	20.9	64	7.3	110	13.7	78	6.7	92	21.1	48	6.3	32	21.5	12	11.5
Rhinocerotidae	0	0	18	2.0	0	0	22	1.9	0	0	10	1.3	0	0	3	2.9
Rodentia	1	0.2	0	0	1	0.1	0	0	1	0.2	0	0	1	0.7	0	0
Suidae	7	1.4	14	1.6	8	1.0	19	1.6	4	0.9	10	1.3	4	2.7	2	1.9
crocodiles	44	9.1	6	0.7	55	6.8	7	0.6	42	9.7	4	0.5	14	9.4	4	3.8
turtles	56	11.6	16	1.8	70	8.7	21	1.8	56	12.9	16	2.1	13	8.7	6	5.9
total	484	100.0	879	100.0	801	100.0	1171	100.0	435	100.0	762	100.0	149	100.0	104	0

Table 4.
Significance of the differences between the fossil assemblages from the Lower and Upper Samwal Formation of all four methods. If the difference between π_1 and π_2 could be zero (so if one is negative and the other positive), than the difference is considered not to be significant, because zero falls within the reliability interval of 95%.

Family or Order	Formula 8.44 of Wonnacott & Wonnacott (1977)	The difference between π_1 and π_2 is significant
Bovidae (Antilopinae included)	method 1: $-0.087 < \pi_1 - \pi_2 < 0.195$	no
	method 2: $-0.025 < \pi_1 - \pi_2 < 0.065$	no
	method 3: $-0.115 < \pi_1 - \pi_2 < -0.229$	yes
	method 4: $-0.208 < \pi_1 - \pi_2 < 0.030$	no
Cervidae	method 1: $-0.016 < \pi_1 - \pi_2 < 0.024$	no
	method 2: $0.001 < \pi_1 - \pi_2 < 0.037$	yes
	method 3: $-0.011 < \pi_1 - \pi_2 < 0.029$	no
	method 4: $-0.065 < \pi_1 - \pi_2 < 0.035$	no
Giraffidae	method 1: $-0.055 < \pi_1 - \pi_2 < -0.009$	yes
	method 2: $-0.036 < \pi_1 - \pi_2 < 0.004$	no
	method 3: $-0.057 < \pi_1 - \pi_2 < -0.011$	yes
	method 4: $-0.054 < \pi_1 - \pi_2 < 0.052$	no
Equidae	method 1: $-0.242 < \pi_1 - \pi_2 < -0.184$	yes
	method 2: $-0.232 < \pi_1 - \pi_2 < -0.166$	yes
	method 3: $-0.254 < \pi_1 - \pi_2 < -0.190$	yes
	method 4: $-0.251 < \pi_1 - \pi_2 < -0.087$	yes
Proboscidae	method 1: $0.096 < \pi_1 - \pi_2 < 0.176$	yes
	method 2: $0.042 < \pi_1 - \pi_2 < 0.098$	yes
	method 3: $0.106 < \pi_1 - \pi_2 < 0.019$	yes
	method 4: $0.010 < \pi_1 - \pi_2 < 0.019$	yes
Rhinocerotidae	method 1: $-0.005 < \pi_1 - \pi_2 < 0.001$	no
	method 2: $-0.027 < \pi_1 - \pi_2 < -0.011$	yes
	method 3: $-0.020 < \pi_1 - \pi_2 < -0.005$	yes
	method 4: $-0.060 < \pi_1 - \pi_2 < 0.003$	no
Suidae	method 1: $-0.013 < \pi_1 - \pi_2 < 0.011$	no
	method 2: $-0.016 < \pi_1 - \pi_2 < 0.004$	no
	method 3: $-0.016 < \pi_1 - \pi_2 < 0.008$	no
	method 4: $-0.029 < \pi_1 - \pi_2 < 0.045$	no
Anthracotheriidae	method 1: $0.001 < \pi_1 - \pi_2 < -0.005$	no
	method 2: $-0.001 < \pi_1 - \pi_2 < 0.003$	no
	method 3: $-0.002 < \pi_1 - \pi_2 < 0.006$	no
	method 4: $-0.006 < \pi_1 - \pi_2 < 0.020$	no
Hippopotamidae	method 1: $0.067 < \pi_1 - \pi_2 < 0.129$	yes
	method 2: $0.042 < \pi_1 - \pi_2 < 0.080$	yes
	method 3: $0.069 < \pi_1 - \pi_2 < 0.129$	yes
	method 4: $0.049 < \pi_1 - \pi_2 < 0.169$	yes
Carnivora (Hyaenidae & Canidae)	method 1: $-0.028 < \pi_1 - \pi_2 < 0.004$	no
	method 2: $-0.126 < \pi_1 - \pi_2 < 0.000$	yes
	method 3: $-0.003 < \pi_1 - \pi_2 < -0.027$	yes
	method 4: $-0.056 < \pi_1 - \pi_2 < 0.034$	no
Rodentia	method 1: $0.001 < \pi_1 - \pi_2 < -0.005$	no
	method 2: $-0.001 < \pi_1 - \pi_2 < 0.003$	no
	method 3: $-0.002 < \pi_1 - \pi_2 < 0.006$	no
	method 4: $-0.006 < \pi_1 - \pi_2 < 0.020$	no
Crocodiles	method 1: $0.058 < \pi_1 - \pi_2 < 0.110$	yes
	method 2: $0.044 < \pi_1 - \pi_2 < 0.080$	yes
	method 3: $0.064 < \pi_1 - \pi_2 < 0.120$	yes
	method 4: $-0.005 < \pi_1 - \pi_2 < 0.115$	no
Turtles	method 1: $0.068 < \pi_1 - \pi_2 < 0.128$	yes
	method 2: $0.049 < \pi_1 - \pi_2 < 0.091$	yes
	method 3: $0.075 < \pi_1 - \pi_2 < 0.141$	yes
	method 4: $-0.036 < \pi_1 - \pi_2 < 0.092$	no

Table 5.
Representations of bones and bone fragments of the three taphonomic groups in the Voorhies (1969) / Behrensmeyer (1975) Transport Groups (Boaz, 1994). Group I consists of easily transported elements, Group I/II and II are variably transportable and Group III is deposited as part of a channel lag.
The position of the localities in the sections is shown in Fig. 5 and Appendix II. The localities are grouped based on the type of bones and the sedimentology.

Voorhies Group	Element	Taphonomy type 1 N=334			Taphonomy type 2 N = 118			Taphonomy type 3 N = 2307		
		bones	fragments	%	bones	fragments	%	bones	fragments	%
Group I	Costa	1	0	0.3	0	1	0.8	9	14	1.0
	Vertebra	5	2	2.1	0	1	0.8	31	36	2.9
	Sesamoid	0	0	0	0	0	0	18	0	0.8
	Patella	0	0	0	0	0	0	2	0	0.1
Group I/II	Scapula	0	6	1.8	0	0	0	2	17	0.8
	Phalange	4	3	2.1	3	1	3.4	155	83	10.3
	Ulna	0	2	0.6	1	0	0.8	15	11	1.1
	Astragalus	11	0	3.3	4	0	3.4	166	2	7.3
	Calcaneum	10	2	3.6	1	1	1.7	94	5	4.3
	Navicuboid	5	0	1.5	0	0	0	59	0	2.6
	Cuneiform	0	0	0	0	0	0	13	0	0.6
	Carpalia	4	0	1.2	1	0	0.8	60	1	2.6
	Magnum	0	0	0	0	0	0	12	0	0.5
	Unciform	0	0	0	0	0	0	3	0	0.1
	Scaphoid	1	0	0.3	0	0	0	6	0	0.3
	Lunare	0	0	0	0	0	0	4	0	0.2
Group II	Femur	0	5	1.5	0	2	1.7	9	19	1.2
	Tibia	0	9	2.7	1	2	2.5	22	61	3.6
	Radius	1	8	2.7	0	2	1.7	25	48	3.2
	Humerus	3	5	2.4	1	1	1.7	12	54	2.9
	Metapode	8	11	5.7	0	4	3.4	110	192	13.1
Group III	Skull	5	9	4.2	2	4	5.1	6	17	1.0
	Horncore/antler	4	14	5.4	0	3	2.5	2	59	2.6
	Mandible	15	7	6.6	5	9	11.9	63	81	6.2
	Tooth*	55	70	37.4	14	32	39.0	343	93	18.9
Rest	Pelvis	0	2	0.6	0	1	0.8	6	6	0.5
	Maxilla	2	1	0.9	0	1	0.8	30	59	3.9
	Tuskfragments	0	12	3.6	0	1	0.8	0	5	0.2
	Tarsalia	2	0	0.6	0	0	0.0	17	0	0.7
	Metapode condyle	0	0	0.0	0	0	0.0	1	60	2.6
	Fibula	0	0	0.0	0	0	0.0	9	0	0.4
	Carapax fragm	6	5	3.3	0	2	1.7	0	3	0.1
	Dermal plate of crocodile	13	1	4.2	7	0	5.9	2	0	0.1
	Coprolite	3	0	0.9	2	0	1.7	12	0	0.5
	Os indet	1	1	0.6	1	7	6.8	8	55	2.7
Totaal		159	175	100.0	43	75	100.0	1326	981	100.0

* molar, premolar, canine, incisor or milk dentition

Acknowledgements

In June of 1988, I finished my study of Geology at Utrecht University. Just a few months later, in September, the course of my life was going to be heavily influenced. It all started in Sardinia in 1988, during the International Conference "Early Man in Island Environments". University. Prof. Dr. Tasseer Hussain and Dr. Paul Sondaar asked me if I had any interest in going to Pakistan to do some fieldwork. As a result I went there in 1989 and 1990 for a total of four months, and I would like to thank those people who made it possible for me to go there: Prof. Dr. Tasseer Hussain of Howard University, Mr. A.H. Kazmi, Director General, Dr. Ibrahim Shah and Gr. Mahmood Raza of the Geological Survey of Pakistan. The fieldwork was supported by grants from the Smithsonian Institution (7087120000-13), the Geological Survey of Pakistan and the Netherlands Foundation for the Advancement of Tropical Research (WOTRO).

During the fieldwork we were surprised to see that in some places we didn't find any hippopotamus fossils at all, although you would expect them to find. I am grateful to Dr. Paul Sondaar, who put me on the track of the hippos ("isn't that something to do your thesis about?"). I would like to thank my colleagues in the field, Dr. Mohammad Arif, Dr. Paul Y. Sondaar, Dr. John de Vos, Dr. Karel Steensma, Dr. Gert van den Bergh, Dr. Jan van Dam and S.B. Malik for their friendship, discussions and support. We couldn't have done this fieldwork without the good care of the drivers Munsif Khan, Riaz Hussain and Ghulam Raza, the cook Ahmad Dad and the servant Rukan Saman.

In the Rest House where we were staying, we were joined by Dr. Hans de Bruyn, doing fieldwork in another area and Dr. Peter Friend with his student M. Assif Jah, who unfortunately was never able to finish his PhD-thesis; he died too young. I would like to thank them for their company and discussions. I would also thank the British team of Robin Dennell, who was working in the Pabbi Hills, with whom we spent some lovely afternoons.

I would also like the Pakistani people for their great hospitality, bringing tea to the site that we were excavating or inviting us to their homes for a meal. I was also greatly impressed by the hospitality of Mohammad Sharif Ch, his wife and their children Samra, Saima and Ahmed, who invited me nearly every evening for tea and Urdu lessons. Samra and I kept in contact sending each other e-mails, but since the devastating earthquake in Muzafarabad, where she had moved to, I have not heard from her...

Later, back in The Netherlands I have been exploring a lot of side roads. What we saw in Pakistan, also occurs in Africa; hippos in Olduvai, no hippos in Laetolil. That would also be interesting to study, as are hippos from islands. Therefore I would like to thank those people who helped or supported me, although their help didn't result in any tangible contribution to this thesis, because I later decided to restrict myself to the Asian hippos, instead of all the hippos in the world:

Prof. Dr. Laura Bonfiglio from the Universitá degli Studi di Messina, Instituto di Scienze della Terra in Messina (Sicilia, Italy) for kindly receiving me in the summer of 1990 and taking the time to tell me a lot about the hippos they find in Sicily.

From the Museum d'Histoire Naturelle in Paris, I would like Dr. Vera Eisenmann and Dr. Germaine Petter, who helped me to find literature while I was there in 1993 with Drs. Andries Spaan, who was also studying hippos, but a different subject.

In Cyprus there were a lot of people, in the summer of 1995, who made it possible to study the hippo from Akrotiri Aetokremnos, in alphabetical order: Dr. Demos Christou (director of the Department of Antiquities in Nikosia) Dr. Pavlos Flourentzos, (curator of Museums of the Department of Antiquities, Cyprus Museum, Nikosia), Dr. G. Petrides (director of the Cypriotic Geological Survey, Nikosia), Dr. Eleni Prokopiou (Archaeological Officer of the Archaeological Museum in Limassol), Dr. Sokrates Sawa (director of the Kourion Museum in Episkopi), Dr. Nancy Serwint (director of CAARI, the Cyprus American Archaeological Research Institute in Nikosia), Dr. Alan Simmons (University of Nevada, Dept. of Anthropology, Las Vegas, USA) and Dr. Stuart Swiny (former director of CAARI, the Cyprus American Archaeological Research Institute in Nikosia).

In 2001, I was invited to go to Crete to help with the excavation and studying the sedimentology of the locality "Digenis' Hand". I thank Dr. M. Dermitzakis from the National and Kapodistrian University of Athens for making this trip possible. I thank Dr. Alexandra van der Geer and Dr. George Lyras for their company and friendship; we laughed a lot! Later we were accompanied by Maria Mertzani (Technological Education Institute (TEI), Faculty of Graphic Arts & Design, Department of Conservation of Antiquities and Works of Art in Athens) and Dora Dourou (National and Kapodistrian University of Athens), whom I also thank for being there.

Meanwhile my thesis took more and more shape en I would like those people who helped me doing this: Prof. Dr. Poppe the Boer who initially helped me with the sedimentological part of the thesis and Dr. John de Vos of the Natural Museum Naturalis in Leiden, the Netherlands, for the opportunity to study the hippos from the Dubois Collection, for his everlasting patience, fruitful discussions, valuable indications to write the thesis and the many laughs we had. My regular visits to Naturalis to discuss yet another part of my thesis were very stimulating to me and drove me to go on. Without you, I wouldn't have been able to finish it. Thank you, John!

While I was studying the hippos in Leiden, the coffee breaks were always brightened by the presence of Reinier van Zelst en Cor Strang. I would also thank them for their fine sense of humour and the laughs we had.

During this time in Leiden, I stayed three days a week with Alexandra van der Geer, Paul Heystee and their children Carmen and Anna, who made me feel very at home. It took much longer than the several weeks I had planned; it lasted for months. I was always welcome and they made me feel even more at home, by putting a cuddly hippo on my bed and a hippo plate to eat from. Thanks you so much for your hospitality!

By the way, my first cuddly hippo was a gift from Gert van den Bergh. Many more would follow. The collection now exists of about 400 hippos in all sorts of shape, material and shape. Thanks everyone who ran into a hippo and bought it for me!

In 1996 I went to Java (Indonesia) with Dr. John de Vos en Dr. Paul Storm. I thank them for their company, friendship and patience. I would also like to thank Dr. Fachroel Aziz en Sudijono of the Quaternary Geology Laboratory (Geological Research and Development Centre) in Bandung for their help in Bandung and guidance in the field. I am also very grateful to Mr. Dik Dik of the Museum Geologi in Bandung to allow me to study the hippo skeleton that is mounted in the museum. I drew a lot of attention being busy with describing and measuring the hippo; I even made it to a photograph in the local newspaper.
During our fieldtrip I met Prof. Dr. Teuke Jacob of the Laboratory Bioanthropologi and Paleoanthropologi in Yogyakarta (Java, Indonesia). He showed his precious human skulls to Dr. Paul Storm, while I was studying the hippo fossils there.

At the end of writing this thesis (at least that is what I thought at the time) Dr. Alexandra van der Geer very seriously read it and gave me valuable indications to improve it. Thank you for your support during all these years.

Also Dr. Paul Sondaar read it and gave comments, until that day when his wife Mariëtte called to cancel the appointment I was going to have with Paul; he was ill. He died a few months later, on March 25th, 2003. I still think a lot about him and I miss him very much. He was a very inspiring man and we spent, together with fellow students, lovely times in Sardinië, Pakistan and in his old cottage Les Granges in France. Amongst many other things, he shared his love for food with us. Especially in Sardinia, he would come to my tent in the morning to spoil me with a cup of tea and something nice to eat, because he know I had a hard time getting up in the morning. Amazing what he could do with leftovers! Thanks Paul, I will never forget you.

Then finally, Prof. dr. Poppe de Boer and Prof. dr. Jelle Reumer reviewed this thesis. Especially Poppe was very serious in doing so and many corrections were made. By that time, I was really fed up with the whole thing. Thanks, Poppe and Jelle for your improvements (although you heard my teeth grinding…).

Finally I would like to thank all those people in my surroundings for their interest. First my parents, who made it possible to study geology. They and tante Riet van Zwieten supported me a great deal and were always interested in what I was doing and even read my publications.

I would like to thank all those people who, sometimes hesitatingly, asked me how my thesis was getting along: my family, fellow students, friends and colleagues from the NSPH. I am not going to name you all, in case I am forgetting someone, with one exception: my colleague for 12 years Yvonne Busink who always made it possible for me to go away if I wanted to, by working extra on my working days. Thanks, Yvonne!

At home, where I worked mostly on my thesis, I would like to thank the cats Paddy, Mitzi, Maro and Robbie for "helping" me, by sitting or lying on my papers, while I was busy. Especially the late Mitzi was very good at that.

Last but certainly not least, I would very, very much like to thank my friend Huub Glas. Huub, you gave me the opportunity, stimulation and space to do the things I like to do most. You're wonderful!

Curriculum Vitae

Johanna Augusta de Visser was born on April 18th, 1961 in 's-Hertogenbosch, The Netherlands. She attended secondary school in 's-Hertogenbosch (St. Jans Lyceum) in 1974 and in Vught (Maurick College) from 1975 to 1979 and graduated there with a diploma for Gymnasium α. But studying geology, a major interest ever since early childhood, required exact sciences. Therefore, from September 1979 to June 1980, she followed supplementary courses in chemistry and physics at Utrecht University, to start geology in September 1980. She obtained a M.Sc. degree in geology at Utrecht University, in the department of sedimentology in 1988. But her heart going out for fossil mammals, the Ph-D research on the fossil hippopotamids of Asia started in 1989, supported by a paid job in the library of the Netherlands School of Public Health (NSPH) in Utrecht during 12 years. After the NSPH, now NSPOH, had moved to Amsterdam and the library had been closed, she worked for about three years at a local building and demolition firm, where she coordinated the quality requirements. At the moment she is not working, but is enjoying her life at het wonderful house and large garden, which she shares with her friend Huub, her father, the cat Robbie and some chicken and goats.

REFERENCES

Akhtar, M. & Bakr, A., 1995. A new species of the genus *Hexaprotodon* from the Dhokwazira, district Jhelum, Punjab, Pakistan. – *Punjab University Journal of Zoology*, **vol. 10**: 49-53

Akhtar, M. & Khurshid, K., 1997. *Hexaprotodon iravaticus* Falconer and Cautley (Mammalia, Artiodactyla, Hippopotamidae) from Upper Siwaliks of Bhimber, Azad Kashmir, Pakistan. – *Punjab University Journal of Zoology*, **vol. 12**: 91-95

Arif, M., 1985. Stratigraphy and chronology of vertebrate fossil localities in the Mirpur area, Azad Kashmir. - *Geological Survey of Pakistan Information Release*, **vol. 264**: 1-13

Badgley, C., 1986. Taphonomy of mammalian fossil remains from Siwalik rocks of Pakistan. – *Paleobiology* **vol. 12(2)**: 119-142

Barry, J.C., Morgan, M.L.E., Flynn, L.J., Pilbeam, D., Behrensmeyer, A.K., Raza, S.M., Khan, I.A., Badgley, C., Hicks, J. & Kelly, J., 2002. Faunal and environmental change in the late Miocene Siwaliks of northern Pakistan. – *Palaeobiology*, **vol. 28 (2)**: 1-71

Basu, P.K., 2004. Siwalik mammals of the Jammu Sub-Himalaya, India: an appraisal of their diversity and habitats. – *Quaternary International*, **vol. 117 (1)**: 105-118

Behrensmeyer, A.K., 1975. The taphonomy and paleoecology of Plio-Pleistocene vertebrate assemblages east of Lake Rudolph, Kenya. – *Bulletin of the Museum Comparative Zoology*, **vol. 146**: 473-578

Behrensmeyer, A.K., 1976. Fossil essemblages in relation to sedimentary environments in the East Rudolf succession. In: Coppens, Y., Howell, F.C. & Isaac, G.Ll. & Leakey, R.E.F. (eds.). *Earliest Man and Environments in the Lake Rudolf Basin.* - University of Chicago Press: 383-401

Behrensmeyer, A.K., 1985. Taphonomy and the paleoecology reconstruction of hominid habitats in the Koobi Fora Formation. In: Beden, M., Behrensmeyer, A.K., Boaz, N.T. *et al.* (eds). *L'environment des hominidés au Plio-Pléistocène.* - Colloque International (Juin 1981) organisé par la Fondation Singer-Polignac Fondation Singer-Polignac et Masson, Paris: 309-324

Behrensmeyer, A.K., 1991. Terrestrial vertebrate accumulations. In: *Topics in Geobiology*, **vol. 9.** - Allison, A. & Briggs, E.G. (eds.): Releasing the data locked in the fossil record: 291-335

Behrensmeyer, A.K. & Hill, A.P., 1980. *Fossils in the making: vertebrate taphonomy and paleoecology*, University of Chicago Press: 1-338

Biswas, S., 1987. Quaternary mammalian record in peninsular and extrapeninsular India. – *Indian Journal of Earth Sciences*, **vol. 14 (3-4)**: 296-306

Biswas, S. & Dassarma, D.C., 1984. Fossil *hippopotamus* from Quaternary alluvial deposits of Narmada Valley in Madhya Pradesh. – *Records of the Geological Survey of India*, **vol.114 (2)**: 19-24

Boaz, D.D., 1994.Taphonomy and the fluvial environment, examples from Pliocene deposits of the Shungura Formation, Omo Basin, Ethiopia. – In: Corruccini, R.S. & Ciochon, R.L. (eds.). - *Integrative paths to the past; paleoanthropological advances to the past* in honor of F. Clark Howell. - Englewood Cliffs, New York, Prentice-Hall: 377-414

Boekschoten, G.J. & Sondaar, P.Y., 1972. On the fossil mammalia of Cyprus I. - *Koninklijke Nederlandse Akademie van Wetenschappen Proceedings series B*, **vol. 75 (4)**: 306-325

Boisserie, J-R., 2005. The phylogeny and taxonomy of Hippopotamidae (Mammalia: Artiodactyla): a review based on morphology and cladistic analysis. – *Zoological Journal of the Linnean Society*, **vol. 143**: 1-26

Boisserie, J-R., Zazzo, A., Merceron, G., Blondel, C., Vignaud, P., Likius, A., Mackaye, H.T. & Brunet, M., 2005. Diets of modern and late Miocene hippopotamids: Evidence from carbon isotope composition and micro-wear of tooth enamel. - *Palaeogeography, Palaeoclimatology, Palaeoecology*, **vol. 221 (1-2)**: 153-174

Burbank, D.W., 1983. The chronology of intermontane-basin development in the northwestern

Himalaya and the evolution of the Northwest Syntaxis. - *Earth and Planetary Science Letters*, **vol. 64, (1)**: 77-92
Burbank, D.W. & Raynolds, R.G.H., 1984. Sequential Late Cenozoic structural disruption of the northern Himalayan Foredeep. - *Nature*, **vol. 311**: 114-118
Burbank, D.W., Raynolds, R.G.H. & Johnson, G.D., 1986. Late Cenozoic tectonics and sedimentation in the north-western Himalayen foredeep: II. Eastern limb of the North-west Syntaxis and regional syntheses. In: Allen, P.A. & Homewood, P. (eds.). *Foreland Basins. - Special Publication 8 of the International Association of Sedimentologists*: 293-306
Calkins, J.A., Offield, T.W., Abdullah, S.K.M., Ali, S.T., 1975. Geology of the Southern Himalaya in Hazara, Pakistan, and adjacent Areas. - *U.S. Geological Survey Professional Paper* **vol. 716c**: 1-29
Chow, M-C., 1961. The first occurrence of fossil *Hippopotamus* in China. – *Vertebrata Palasiatica*, Peking, **vol. 5 (1)**: 39-40
Colbert, E.H., 1935. Siwalik mammals in the American Museum of Natural History. – *Transactions of the American philosophical society held at Philadelphia for promoting useful knowledge, new series* – **Vol. XXVI**: 1-401
Colbert, E.H., 1938. Fossil mammals from Burma in the American Museum of Natural History. – *Bulletin of the American Museum of National History*, **vol.74**: 419-424
Colbert, E.H., 1943. Pleistocene vertebrates collected in Burma by the American Southeast Asiatic Expedition. - *American Philosophical Society Transactions, new series*, **vol. 32**: 395-429
Coleman, J.M., 1969. Brahmaputra River: Channel process and sedimentation. – *Sedimentary Geology* **vol. 3, no. 2-3**: 129-239
Corvinus, G. & Nanda, A.C., 1994. Stratigraphy and palaeontology of the Siwalik Group of Surai Khola and Rota Khola in Nepal. – *Neues Jahrbuch für Geologie und Paläontologie Abhandlungen* **vol. 191 (1)**: 25-68
Corvinus, G., Rimal, L.N., 2001. Biostratigraphy and geology of the neogene Siwalik group of the Surai Khola and Rato Khola areas in Nepal. – *Palaeogeography, Palaeoclimatology, Palaeoecology*, **vol. 165 (3-4)**: 251-2790
Coryndon, S.C., 1976. Fossil Hippopotamidae from Plio-Pleistocene successions of the Rudolf Basin. In: Coppens, Y., Howell, F.C., Isaac, G.Ll. & Leakey, R.E.F. (eds.),. *Earliest Man and Environments in the Lake Rudolf Basin*. - University of Chicago Press: 238-250
Crawford, A.R., 1974. The Salt Range, the Kashmir Syntaxis and the Pamir Arc. – *Earth and Planetary Science Letters*, **vol. 22, issue 4**: 371-379
Cutler, A.H., Behrensmeyer, A.K., & Chapman, R.E. 1999. Environmental information in a recent bone assemblage: roles of taphonomic processes and ecological change. – *Palaeogeography, Palaeoclimatology, Palaeoecology*, **vol. 149 (1-4)**: 359-372
Dennell, R.W., 2004. Early Pleistocene hippopotamid extinctions, monsoonal climates, and river system histories in South and South West Asia: comment on Jablonski (2004) "The hippo's tale: how the anatomy and physiology of Late Neogene *Hexaprotodon* shed light on Late Neogene environmental change". - *Quaternary International* **vol. 117**: 119-123
Dennell, R., Coard, R. & Turner, A., 2006. The biostratigraphy and magnetic polarity zonation of the Pabbi Hills, northern Pakistan: An Upper Siwalik (Pinjor Stage) Upper Pliocene – Lower Pleistocene fluvial sequence. – *Palaeogeography, Palaeoclimatology, Palaeoecology*, **vol. 234**, **(2-4)**: 168 - 185
Deraniyagala, P.E.P., 1936. Some vertebrate fossils from Ceylon. – *Geological Magazine*, **vol. 73**: 316-318
Desmoulins, A., 1825. Hippopotame. – *Dictionnaire Classique d'Histoire Naturelle*, **vol. 8**, Paris: 215–225.
De Visser, J.A., 1996. The taphonomy of two fossil localities from the Plio-Pleistocene of Pakistan. In: Meléndez Hevia, G., Blasco Sancho, F. & Pérez Urresti, I. (eds.). - *II Reunión de tafonomía y fosilización*. - Zaragoza, Institución "Fernando el Católico": 407-412
De Vos, J. de & Sondaar, P.Y., 1982. The importance of the 'Dubois Collection' reconsidered.

In: Bartstra, G-J., Casparie, W.A. (eds.). - *Modern Quaternary Research in Southeast Asia*, **vol. 7**: 35-63
Dubois, E., 1894-1895. *Diary and map British India.* Unpublished, in possession of the Naturalis, The Netherlands
Dubois, E., 1908. Das geologische Alter der Kendeng oder Trinil-Fauna. – *Tijdschrift van het Koninklijk Nederlands Aardrijkskundig Genootschap*, series 2, **vol. XXV (6)**: 1235-70
Eltringham, S.K., 1999. *The hippos; natural history and conservation.* - Poyser Natural History. - Academic Press, London: 1-184
Falconer, H. & Cautley, P.T., 1836. On the fossil *hippopotamus* of the Sewalik Hills. – *Asiatic Researches* **vol. XIX**: 39-53
Gentry, A.W., 1997. The London collection of Narmada fossil mammals. - *Geological survey of India GSI., Special Publication* **no. 46**: 105-115
Gèze, R., 1980. *Les Hippopotamidae (Mammalia, Artiodactyla) du Plio-Pléistocène de l'Ethiopie (Afique Orientale).* - Paris, L'Université Pierre et Marie Curie : 1-116. Thesis
Ginsburg, L., Ingavat, R. & Sen, S., 1982. Découverte d'une fauna d'âge pléistocène moyen terminal (Loangien) dans le nord de la Thailande. – *Les Comptes Rendu de l'Académie des Sciences Paris*, série. 2, **vol. 294 (4)**: 295-297
Heller, E., 1914. Four new subspecies of large Mammals from equatorial Africa. – *Smithsonian Miscellaneous Collections*, **vol. 61** (22): 1-7
Heller, P.L., Angevine, Ch. L. & Winslow, N.S., 1988. Two-phase stratographic model of foreland-basin sequence. – *Geology*, **vol. 16**: 501-504
Hooijer, D.A., 1942. On the nomenclature of some fossil hippopotami. - Leiden, *Extrait des Archives Neérlandaises de Zoologie*, **tome VI, 2e et 3e livraison**: 279-282
Hooijer, D.A., 1950. The fossil Hippopotamidae of Asia, with notes on the recent species. – *Zoölogische Verhandelingen*, **no. 8**: 1-124
Hooijer, D.A., 1962. Report upon a collection of Pleistocene mammals from tin-bearing deposits in a limestone cave near Ipoh, Kinta Valley, Perak. – *Federated Museum Journal*, Kuala Lumpur **vol. 7**: 1-5
Hussain, S.T., Van den Bergh, G.D., Steensma, K.J., De Visser, J.A., De Vos, J., Arif, M., Van Dam, J., Sondaar, P.Y.& Malik, S.B., 1992. Biostratigraphy of the Plio-Pleistocene continental sediments (Upper Siwaliks) of the Mangla-Samwal Anticline, Azad Kashmir, Pakistan. – *Proceedings van de Koninklijke Nederlandse Akademie van Wetenschappen* **vol. 95 (1)**: 65-80.
Jablonski, N.G., 2004. The hippo's tale: how the anatomy and physiology of Late Neogene *Hexaprotodon* shed light on Late Neogene environmental change. - *Quaternary International*, **vol. 117 (1)**: 119-123
Jenkinson, R.D.S., Rendell, H.M., Dennell, R.W., Jah, M.A. & Sutherland, S.A., 1989. Upper Siwalik palaeoenvironments and palaeoecology in the Pabbi Hills, Northern Pakistan. – *Zeitschrift für Geomorphologie, - Neue Folge* **33 (4)**: 417-428
Johnson, G.D., Johnson, N.M., Opdyke, N.D. and Tahirkheli, R.A.K., 1979. Magnetic reversal stratigraphy and sedimentary tectonic history of the Upper Siwalik group, eastern Salt Range and southwestern Kashmir. In: Farah, A. & de Jong, K.A. (eds.). Geodynamics of Pakistan. - *Memoires of the Geological Survey of Pakistan*, **vol. 11**: 149-165
Johnson, G.D., Raynolds, R.G.H. & Burbank, D.W., 1986. Late Cenozoic tectonics and sedimentation in the north-western Himalayan foredeep: I. Trust ramping and associated deformation in the Potwar region. In: Allen, P.A. and Homewood, P. (eds.). *Foreland Basins. - Special Publication 8 of the International Association of Sedimentologists*: 273-292
Kahlke, R.-D., 1990. Zum Stand der Erforschung fossiler Hippopotamiden (Mammalia, Artiodactyla); Eine Übersicht. - *Quartärpaläontologie*, Berlin **vol. 8**: 107-118
Kahlke, R-D., 1999. *The history of the origin, evolution and dispersal of the Late Pleistocene Mammuthus-Coelodonta faunal complex in Eurasia (lage mammals)*: 5-219

Klootwijk, C.T., Nazirullah, R. & De Jong, K.A., 1986. Paleomagnetic constraints on formation of the Mianwali reentrant, Trans-Indus and western Salt Range, Pakistan. – *Earth and Planetary Science Letters*, **vol. 80 (3-4)**: 394-414

Kotlia, B.S., 1985. Vertebrate fossils and paleoenvironment of the Karewa Intermontane Basin, Kashmir, Northwestern India. - *Current Science*, **vol. 54 (24)**: 1275-1277

Kumar, R., Sangode, S.J. & Ghosh, S.K., 2004. A multistorey sandstone complex in the Himalayan Foreland Basin, NW Himalaya, India. - *Journal of Asian Earth Sciences*, **vol. 23 (3)**: 407-426

Leinders, J.J.M.M., Azz, F., Sondaar, P.Y. & de Vos, J., 1985. The age of the hominid-bearing deposits of Java: state of the art. - *Geologie & Mijnbouw* **vol. 64**: 167-173

Lewison, R.L. & Carter, J., 2004. Exploring behavior of an unusual megaherbivore: a spatially explicit foraging model of the hippopotamus. – *Ecological Modelling* **vol. 71**: 127-138

Lydekker, R., 1882 A. Note on some Siwalik and Jamna mammals. – *Records of the Geological Survey of India*, **vol. 15**: 28-33

Lydekker, R., 1882 B. Note on some Siwalik and Narbada fossils: The Narbada *Hippopotamus*. – *Records of the Geological Survey of India*, **vol.15**: 102-107

Lydekker, R., 1883. Synopsis of the fossil vertebrata of India.- *Records of the Geological Survey of India*, **vol. 16**: 61-93

Lydekker, R., 1884. *On Siwalik fossils in the Science and Art Museum Dublin*: 69-86

Lydekker, R., 1885. *Catalogue of the fossil mammalia in the British Museum (Natural History) Cromwell Road, S.W. Part II containing the Order Ungulata, Suborder* Artiodactyla: 1-324

Maschenko, E.N., 2002. Individual development, biology and evolution of the woolly mammoth. – *Cranium*, **vol. 19**, no. 1: 1-120

Matthew, W.D., 1929. Critical observations upon Siwalik mammals (exclusive of Proboscidae). – *Bulletin of the American Museum of Natioanl History*, **vol. 56**, art. VII: 437-560

Mazza, P., 1995. New evidence on the Plesitocene hippopotamuses of western Europe. – *Geologica Romana*, **vol. 31**: 61-120

Miller, G.S. Jr., 1910. Description of a new species of *Hippopotamus*. – *Smithsonian Miscellaneous Collections*, **vol. 54 (7)**: 1-3

Opdyke, N.D., Lindsay, E., Johnson, G.D, Johnson, N., Tahirkheli, R.A.K. & Mirza, M.A., 1979. Magnetic polarity stratigraphy and vertebrate paleontology of the Upper Siwalik Subgroup of northern Pakistan. - *Palaeogeography, Palaeoclimatology, Palaeoecology*, **vol. 27**: 1-34

Osborn, H.F., 1907. *Evolution of the mammalian molar teeth to and from the triangular type, including collected and revised researches on trituberculy and new sections on the forms and homologies of the molar teeth in the different orders of mammals.* - W.K. Gregory, New York: 1-250

Owen, R., 1845. *Descriptive and illustrated catalogue of the fossil organic remains of Mammalia and Aves contained in the Museum of the Royal College of Surgeons of England.* – London, Taylor: 1-391

Parkash, B., Awasthi, A.K. & Gohain, K.,1983. – Lithofacies of the Markanda terminal fan, Kurukshetra district, Haryana, India. – In: *Modern and ancient fluvial systems, Special Publication No. 6 of the International Association of Sedimentologists*: 337-344

Patnaik, R., 2003. Reconstruction of Upper Siwalik palaeoecology and palaeoclimatology using microfossil palaeocommunities. – *Palaeogeography, Palaeoclimatology, Palaeoecology* **vol. 197**: 133-150

Pickford, M., 1983. On the origins of Hippopotamidae together with descriptions of two new species, a new genus and a new subfamiliy form the Miocene of Kenya. – *Geobios* **vol 16**:193-217

Pilgrim, G.E., 1913. Correlation of the Siwaliks with mammal horizons of Europe. – *Records of the Geological Survey of India*, **vol. XLIII**: 264-326

Raynolds, R.G.H., 1980. *The Plio-Pleistocene structural and stratigraphic evolution of the eastern Potwar Plateau, Pakistan.* - Ph.D. dissertation, Dartmouth College, Hannover, New Hampshire: 1-264

Raynolds, R.G.H. & Johnson, G.D., 1985. Rates of Neogene depositional and deformational

processes, north-west Himalayan foredeep margin, Pakistan. – in: *The chronoly of the geological record*, N.J. Snelling (ed.). – Geological Society London, Special Publication, **vol.10**: 297-311
Reineck, H.-E. & Singh, I.B., 1980. *Depositional sedimentary environments with reverence to terrigenous clastics*. - Springer Verlag: 1-549
Saikawa, Y., Hashimoto, K., Nakata, M., Yoshihara, M., Nagai, K., Ida, M. & Komiya, T., 2004 Pigment chemistry: the red sweat of the hippopotamus. – *Nature* **vol. 429**: 363
Sarwar, G. and De Jong, K.A., 1979. Arcs, Oroclines, Syntaxes: the curvatures of mountain belts in Pakistan. In: Farah, A. & de Jong, K.A. (eds.). - *Geodynamics of Pakistan*. - Geological Survey of Pakistan, Quetta: 341-349
Schipman, P., 1981. *Life history of a fossil*. - Harvard University Press: 1-222
Schwarz, E., 1914. Diagnoses of new races of African ungulates. – *Annals and Magazine of Natural History*, **ser. 8, vol. 13**: 31-45
Seeber, L. & Armbruster, J., 1979. Seismicity of the Hazara Arc in Northern Pakistan; Decollement vs. basement faulting. In: Farah, A. & de Jong, K.A. (eds.). - *Geodynamics of Pakistan*. - Geological Survey of Pakistan, Quetta: 131-142
Sinclair, A.R.E. & Norton-Griffiths, M. (eds.), 1995. *Serengeti Dynamics of an ecosystem*. – University of Chicago Press: 389 pp
Sondaar, P.Y., 1977. Insularity and its effect on mammal evolution. In: Hecht, M.K., Goody, P.C. & Hecht, B.M. (eds.). – *Major patterns in vertebrate evolution*. – Plenum, New York: 671-707
Sondaar, P.Y., 1984. Faunal evolution and the mammalian biostratigraphy of Java.In: Andrews, P. & Franzen, J.-L. (eds.). – The early evolution of man with special emphasis on Southeast Asia and Africa. – *Courier Forschungs Institut Senckenberg*, **vol. 69**: 219-235
Tandon, S.K. & Varshney, S.K., 1991. Origin of selective carbonate cemented (concretionary) layers within mulitiestoried sandstone bodies of the Neogene Middle Siwalik Subgroup, NW Himalaya, India. – *Abstract, Birbal Sahni Birth Centenary Symposium on the Siwalik Basin, WIHG, Dehra Dun, India*: 45
Theunissen, B., De Vos, J., Sondaar, P.Y. & Aziz, F., 1990. The establishment of a chronological framework for the hominid-bearing deposits of Java; a historical survey. - *Geological Society of America, Special Paper* **vol. 242**: 1-40
Van Dam, J.A., 1989. *Veldwerkverslag 1989, verslag doctoraalveldwerk Mirpur Gebied, Azad Kashmir, Pakistan*. Unpublished report: 5-56
Van den Bergh, G.D., 1996. The Late Neogene elephantoid-bearing faunas of Indonesia and their palaeozoogeographic implications. A study of the terrestrial faunal succession of Sulawesi, Flores and Java, including evidence for early hominid dispersal east of Wallace's line. – *Scripta Geologica*, **no. 117**: 1-419
Van den Bergh, G.D., de Vos, J., Sondaar, P.Y. & Aziz, F., 1996. Pleistocene zoogeographic evolution of Java (Indonesia) and glacio-eustatic sea level fluctuations: a background for the presence of *Homo*. - *Indo-Pacific Prehistory Association Bulletin 14; Chiang May Papers*, **vol.1**: 7-21
Van der Made, J., 1995. Listriodontinae (Suidae, Mammalia), their evolution, systematics and distribution in time and space and the relevance for stratigraphy and paleobiogeography. - *Contributions to Tertiary and Quaternary Geology*, **vol. 33 (1-4)**: 3-254. Thesis
Van der Made, J., 1999. Superfamily Hippopotamoidea. – In: *The Miocene land mammals of Europe*. – Rössner, G.E. & Heissig, K. (eds.). – Verlag Dr. Friedrich Pfeil, München: 203-208
Van der Maarel, F.H., 1932. Contribution to the knowledge of the fossil Mammalian fauna of Java. – *Wetenschappelijke Mededeelingen van den Dienst van den Mijnbouw in Nederlands-Indië*, **no.15**: 1-208. Thesis
Visser, C.F. & Johnson, G.D., 1978. Tectonic control of Late Pliocene molasse sedimentation in a portion of the Jhelum Re-entrant, Pakistan. - *Geologische Rundschau*, **vol. 67 (1)**: 15-37
Von Koenigswald, G.H.R., 1933. Beitrag zur Kenntnis der fossielen Wirbeltiere Javas. – I. Teil. –

Wetenschappelijke Mededeelingen van den Dienst van den Mijnbouw in Nederlands-Indië, **no. 23**: 1-127
Von Koenigswald, G.H.R., 1934. Zur Stratigraphie des javanischen Pleistocän. - *De Ingenieur in Nederlands Indië*, **vol. 1, part 2, sect. 4**: 185-201
Von Koenigswald, G.H.R., 1935. Bemerkungen zur fossilen Säugetierfaunen Javas II. – *De Ingenieur in Nederlands Indië*, **vol. 2, part 10, sect. 4**: 85-88
Von Koenigswald, G.H.R., 1959. A *mastodon* and other fossil mammals from Thailand. - *Report of Investigation, Royal Department of Mines*, Bangkok **2**: 25-28
Voorhies, M. 1969. Taphonomy and population dynamics of an early Pliocene vertebrate fauna, Knox County, Nebraska. – *Contributions to Geology, Special Paper*, **no. 1**: 1-69
Wadia, D.N., 1931. The Syntaxis of the Northwestern Himalayas, its rock, tectonics and orogeny. – *Records of the Indian Geological Survey*, **vol. 65**: 189-220
Wadia, D.N., 1953 (third edition). *Geology of India*. – London
Watanabe, N. & Kadar, D. (eds.), 1985. Quaternary geology of the hominid fossilbearing formations in Java. - *Geological Research and Development Centre, Special Publication*, **no. 4**: 1-378
Wonnacott, T.H. & Wonnacott, R.J., 1977. *Introductory statistics*. - Wiley 3rd edition: 223-227

KEY TO SYMBOLS FOR APPENDIX I

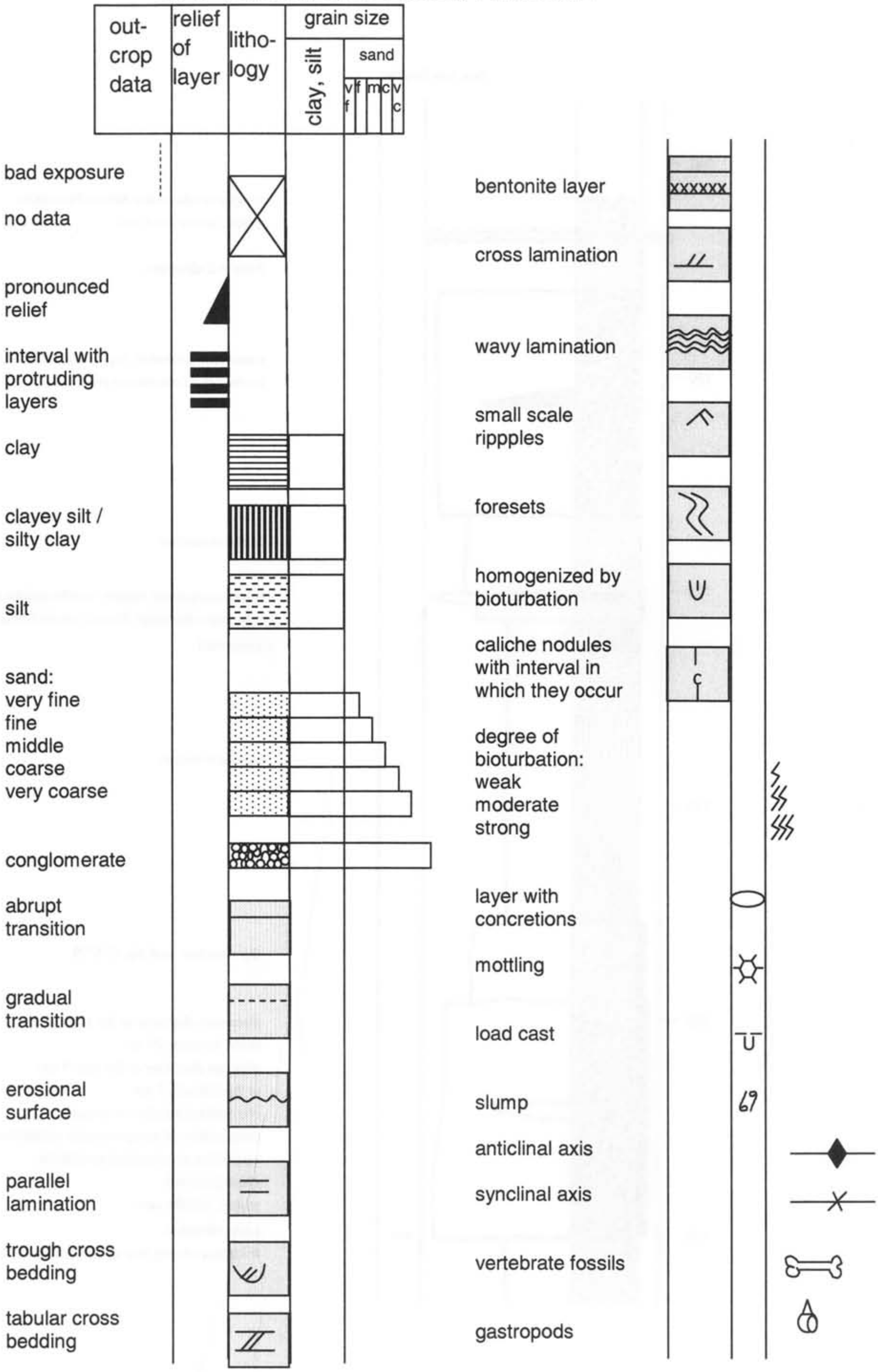

APPENDIX I-A JHEL KAS SECTION

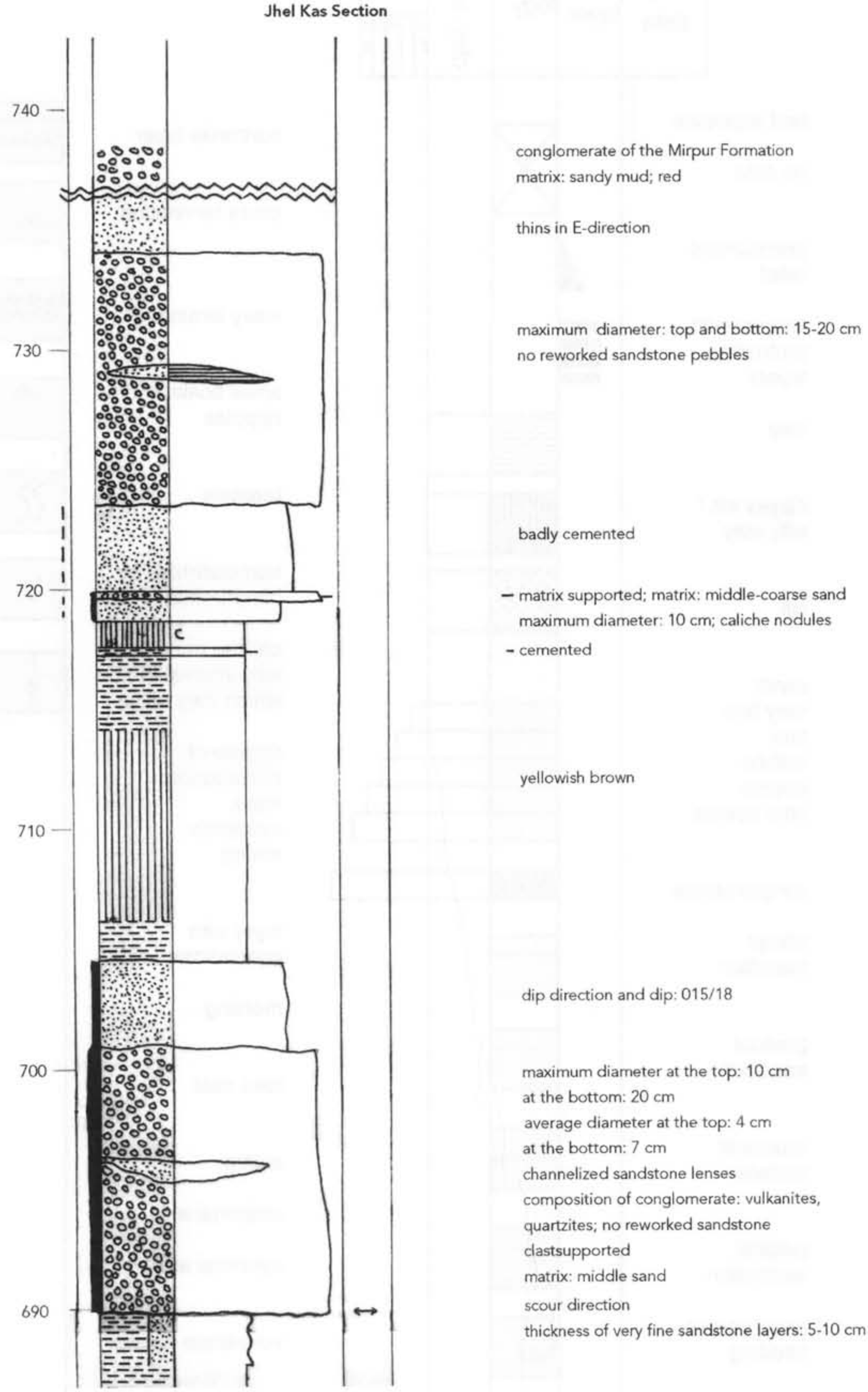

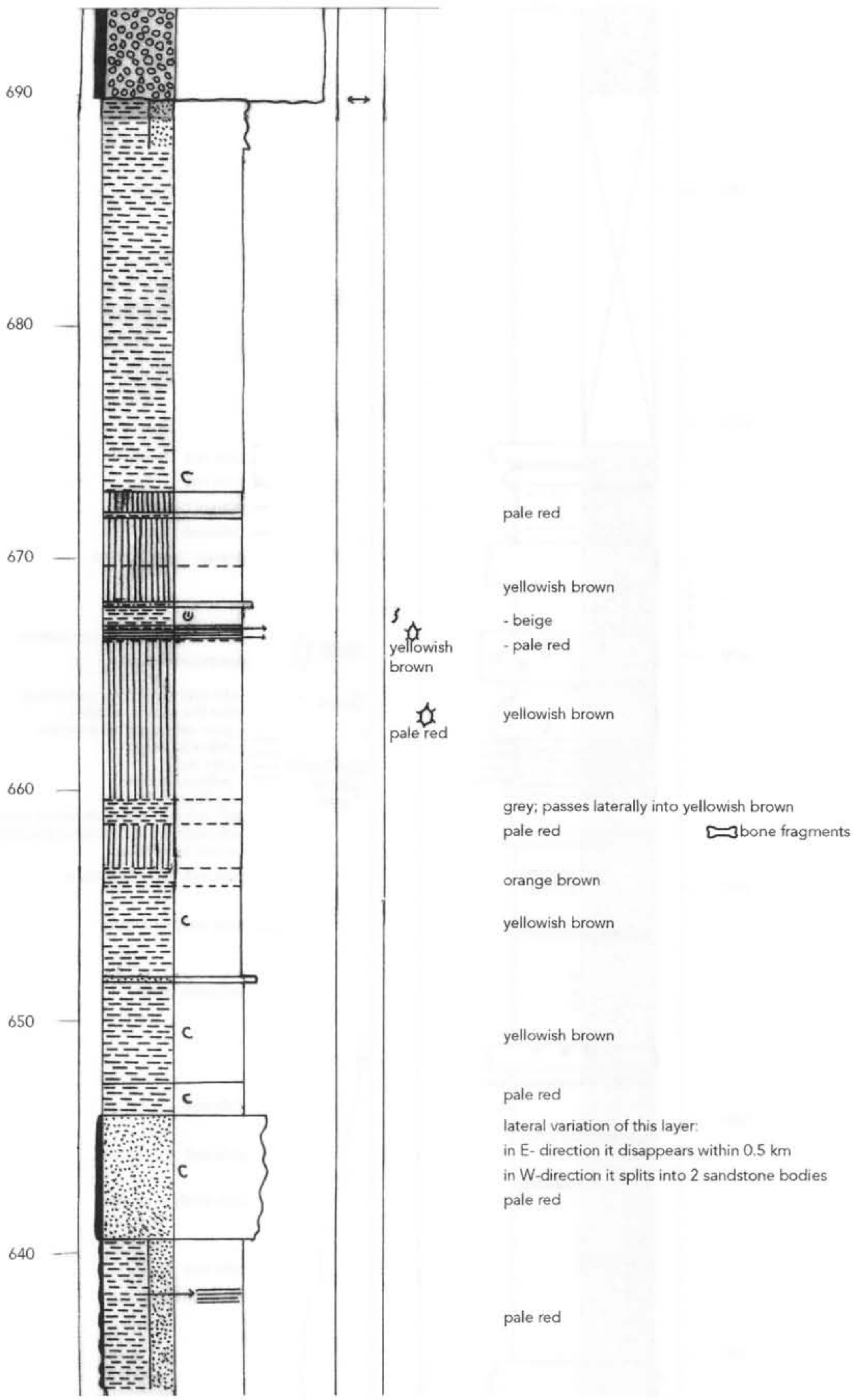
690
680
670
660
650
640
yellowish brown
pale red
pale red
yellowish brown
- beige
- pale red
yellowish brown
grey; passes laterally into yellowish brown
pale red
bone fragments
orange brown
yellowish brown
yellowish brown
pale red
lateral variation of this layer:
in E- direction it disappears within 0.5 km
in W-direction it splits into 2 sandstone bodies
pale red
pale red

App. 3

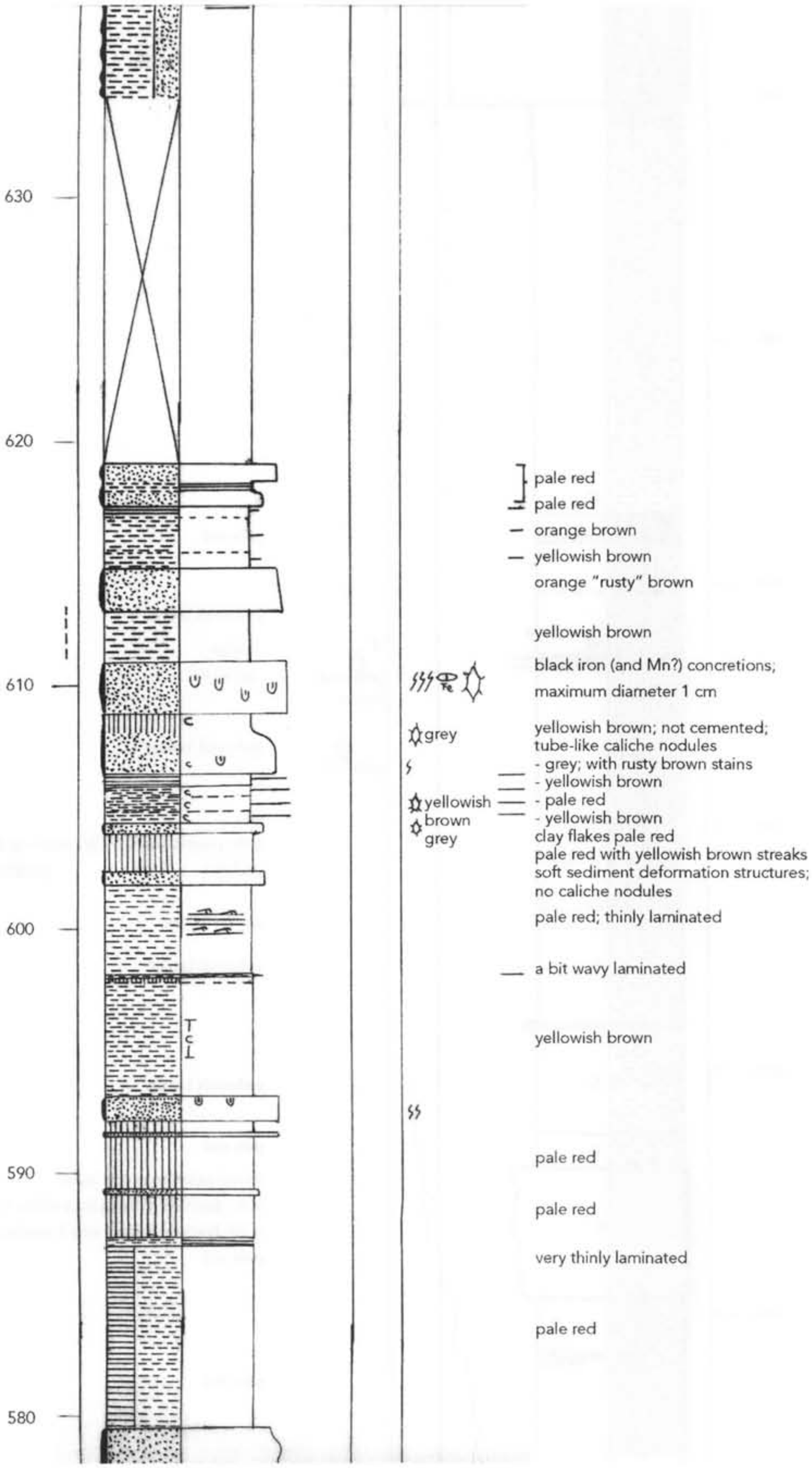
630
620
610
600
590
580
pale red
pale red
orange brown
yellowish brown
orange "rusty" brown
yellowish brown
black iron (and Mn?) concretions;
maximum diameter 1 cm
Fe
grey
yellowish brown; not cemented;
tube-like caliche nodules
- grey; with rusty brown stains
- yellowish brown
- pale red
- yellowish brown
yellowish
brown
grey
clay flakes pale red
pale red with yellowish brown streaks
soft sediment deformation structures;
no caliche nodules
pale red; thinly laminated
a bit wavy laminated
yellowish brown
pale red
pale red
very thinly laminated
pale red

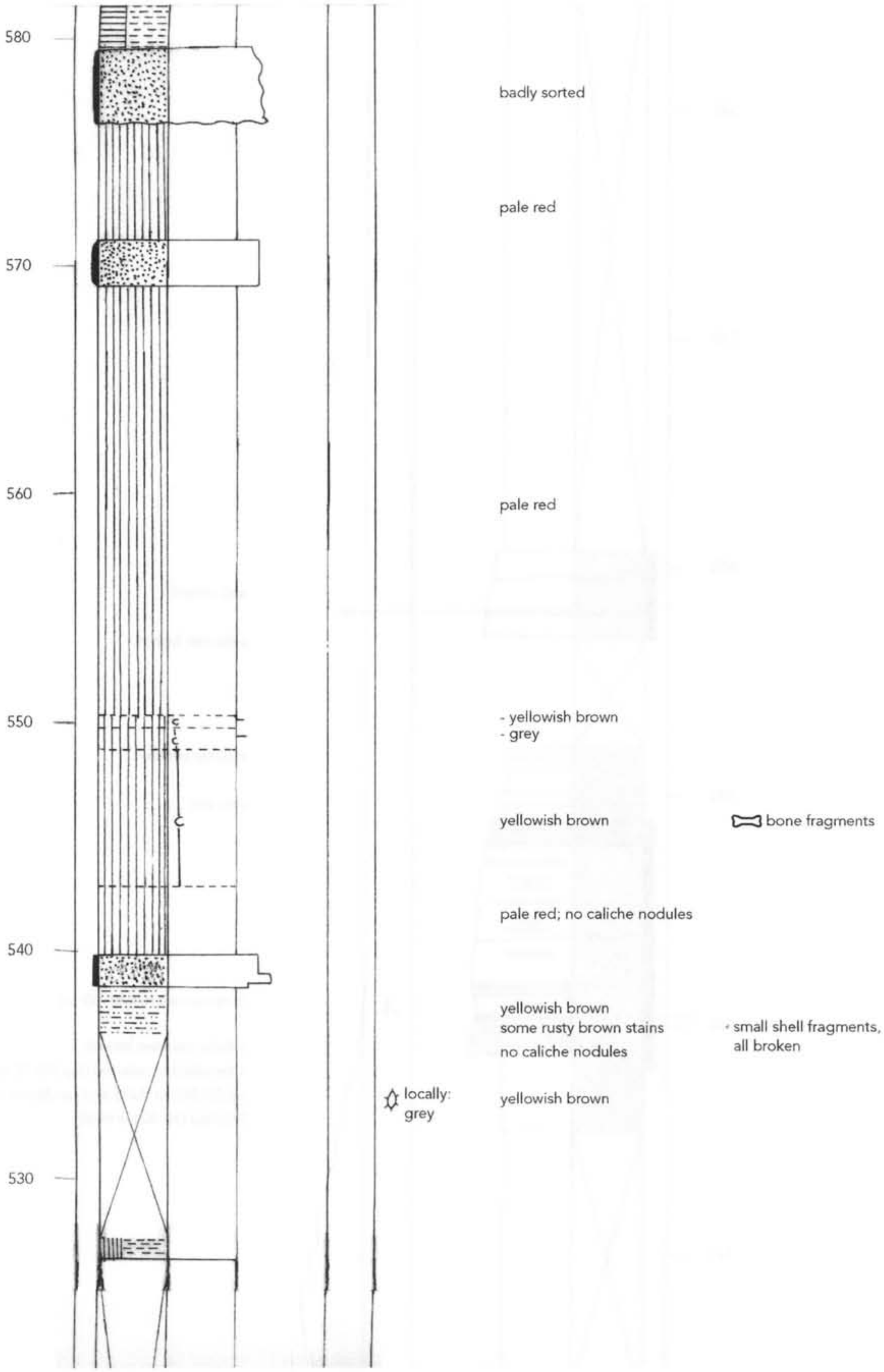
580
badly sorted
pale red
570
560
pale red
550
- yellowish brown
- grey
yellowish brown
bone fragments
pale red; no caliche nodules
540
yellowish brown
some rusty brown stains
no caliche nodules
small shell fragments,
all broken
locally:
grey
yellowish brown
530

App. 5

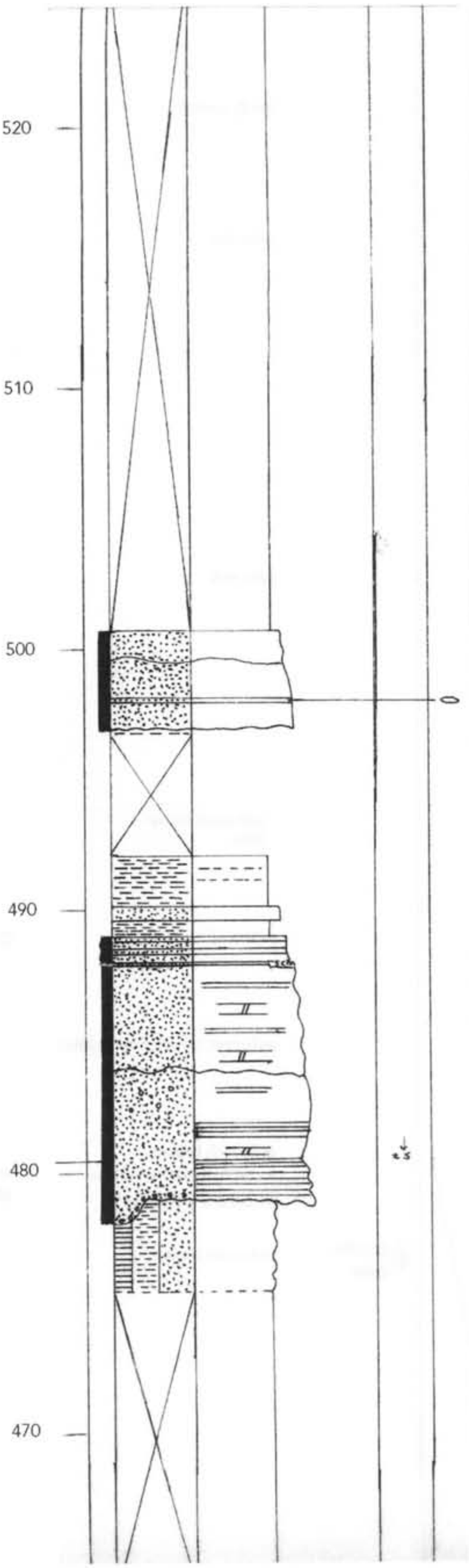

well sorted

yellowish brown

vaguely bedded

pale red

minimum set height: 30 cm

caliche nodules; streaks
alternation of pale red clay (10-15 cm thick), silt (30-50 cm thick) and sandstone, very fine-fine (10-40 cm thick)

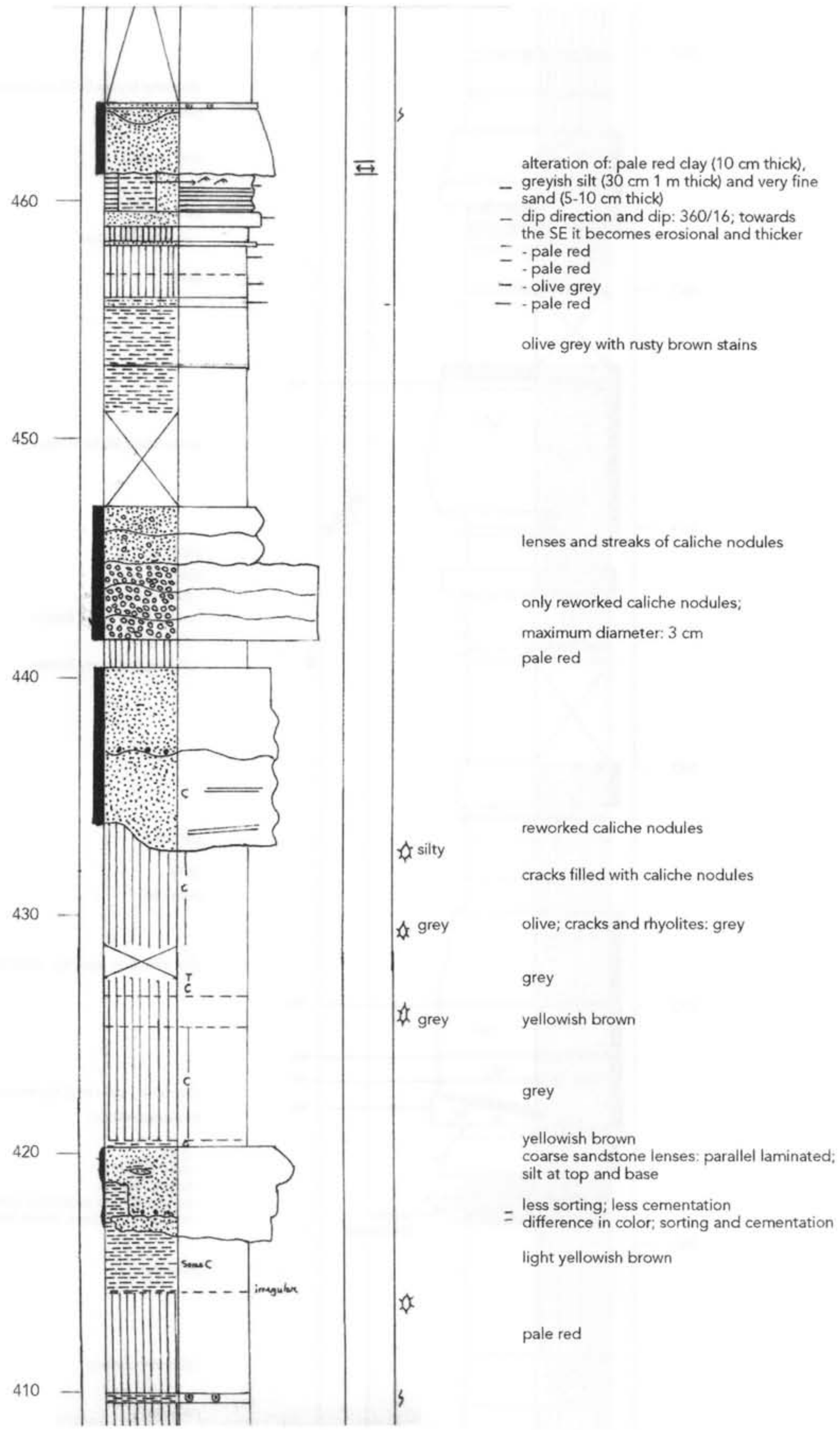
460
450
440
430
420
410
alteration of: pale red clay (10 cm thick), greyish silt (30 cm 1 m thick) and very fine sand (5-10 cm thick)
dip direction and dip: 360/16; towards the SE it becomes erosional and thicker
- pale red
- pale red
- olive grey
- pale red
olive grey with rusty brown stains
lenses and streaks of caliche nodules
only reworked caliche nodules;
maximum diameter: 3 cm
pale red
reworked caliche nodules
silty
cracks filled with caliche nodules
grey
olive; cracks and rhyolites: grey
grey
grey
yellowish brown
grey
yellowish brown
coarse sandstone lenses: parallel laminated; silt at top and base
less sorting; less cementation
difference in color; sorting and cementation
light yellowish brown
irregular
pale red

App. 7

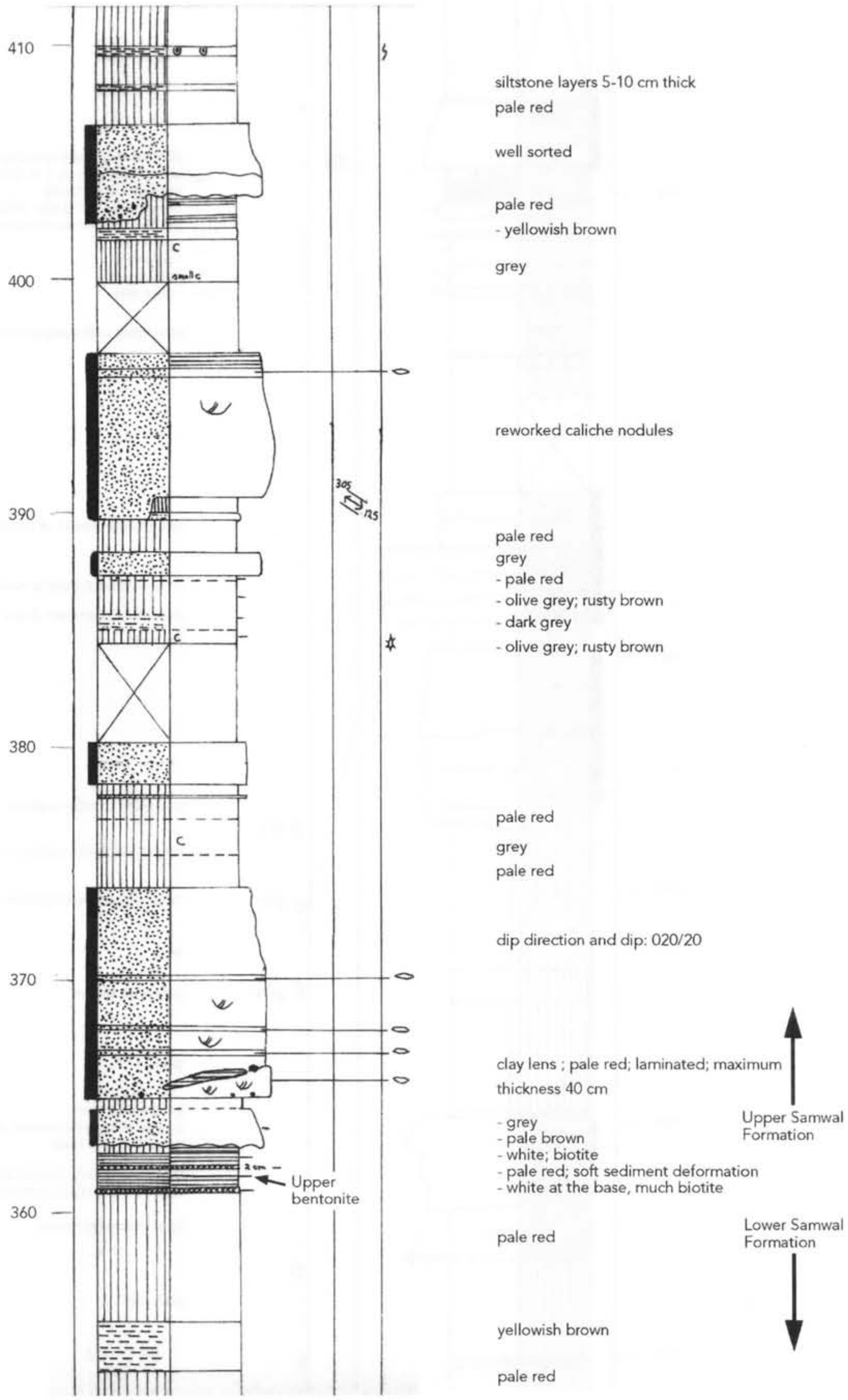
410
siltstone layers 5-10 cm thick
pale red
well sorted
pale red
- yellowish brown
c
small c
400
grey
reworked caliche nodules
305
125
390
pale red
grey
- pale red
- olive grey; rusty brown
- dark grey
c
- olive grey; rusty brown
380
pale red
c
grey
pale red
dip direction and dip: 020/20
370
clay lens ; pale red; laminated; maximum thickness 40 cm
- grey
- pale brown
- white; biotite
- pale red; soft sediment deformation
- white at the base, much biotite
2 cm
Upper bentonite
Upper Samwal Formation
360
pale red
Lower Samwal Formation
yellowish brown
pale red

App. 8

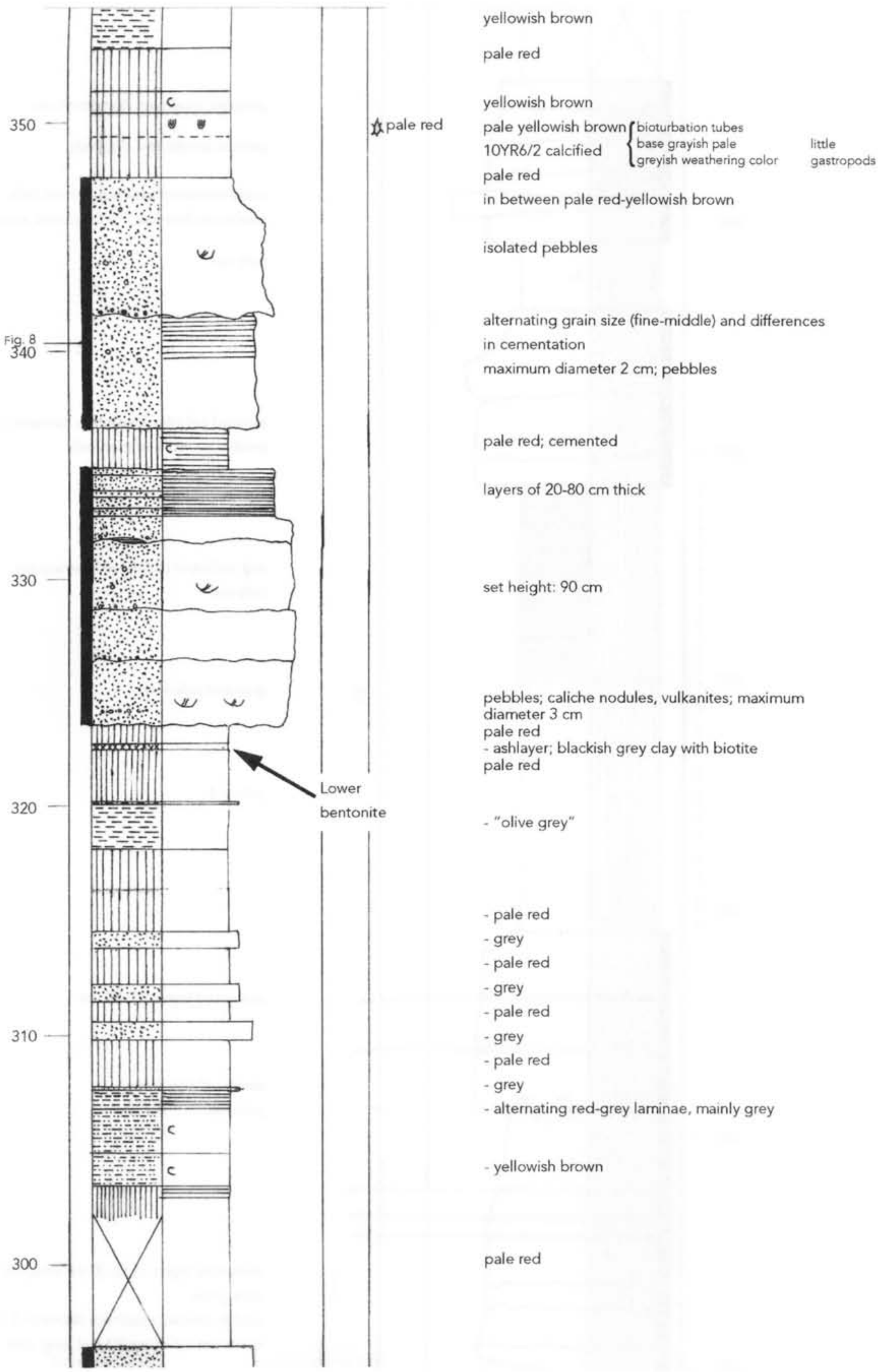
yellowish brown
pale red
yellowish brown
350
pale red
pale yellowish brown
10YR6/2 calcified
bioturbation tubes
base grayish pale
greyish weathering color
little
gastropods
pale red
in between pale red-yellowish brown
isolated pebbles
alternating grain size (fine-middle) and differences
in cementation
Fig. 8
340
maximum diameter 2 cm; pebbles
pale red; cemented
layers of 20-80 cm thick
330
set height: 90 cm
pebbles; caliche nodules, vulkanites; maximum
diameter 3 cm
pale red
- ashlayer; blackish grey clay with biotite
pale red
Lower
bentonite
320
- "olive grey"
- pale red
- grey
- pale red
- grey
- pale red
310
- grey
- pale red
- grey
- alternating red-grey laminae, mainly grey
- yellowish brown
300
pale red

App. 9

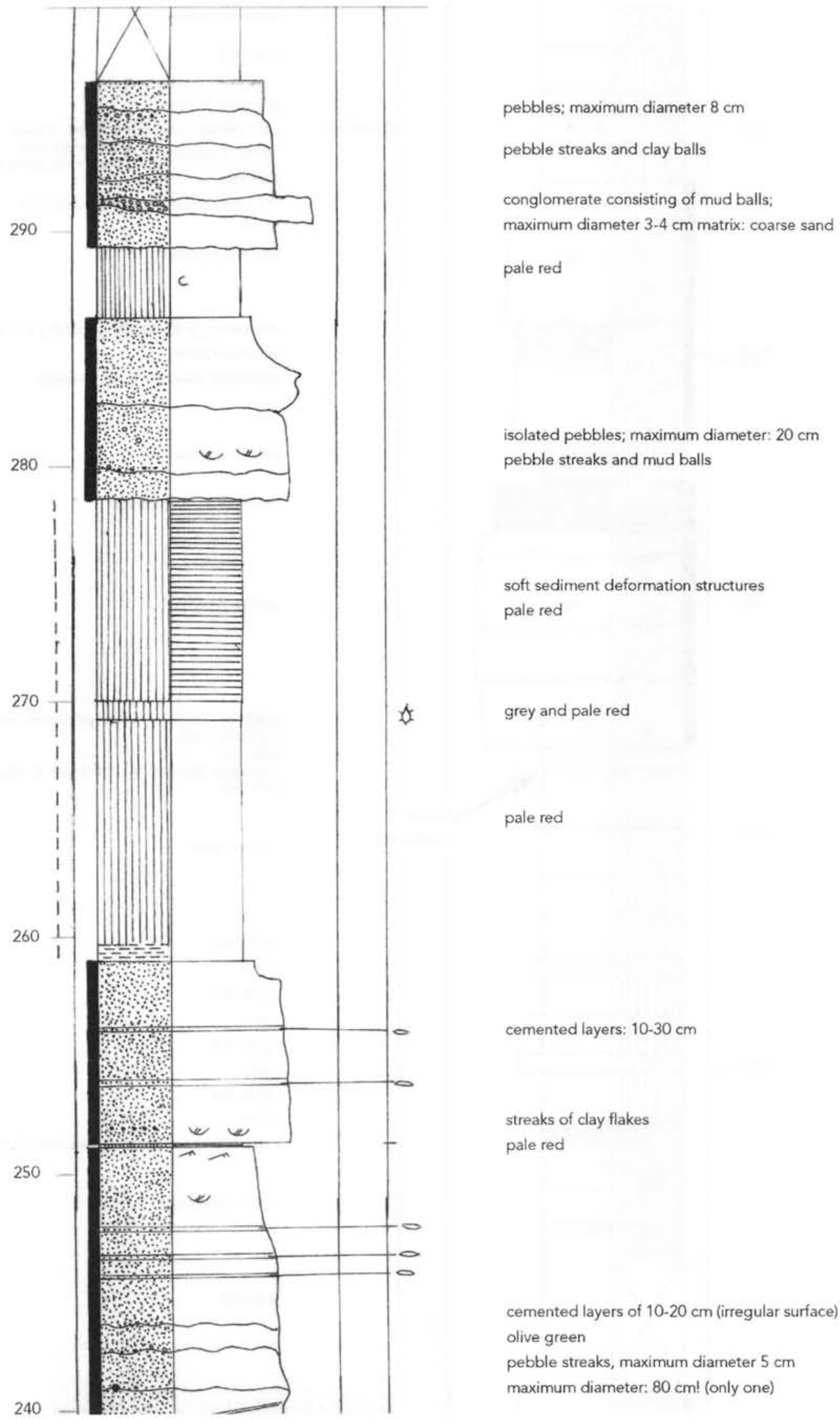
pebbles; maximum diameter 8 cm
pebble streaks and clay balls
conglomerate consisting of mud balls;
maximum diameter 3-4 cm matrix: coarse sand
290
pale red
c
isolated pebbles; maximum diameter: 20 cm
pebble streaks and mud balls
280
soft sediment deformation structures
pale red
270
grey and pale red
pale red
260
cemented layers: 10-30 cm
streaks of clay flakes
pale red
250
cemented layers of 10-20 cm (irregular surface)
olive green
pebble streaks, maximum diameter 5 cm
maximum diameter: 80 cm! (only one)
240

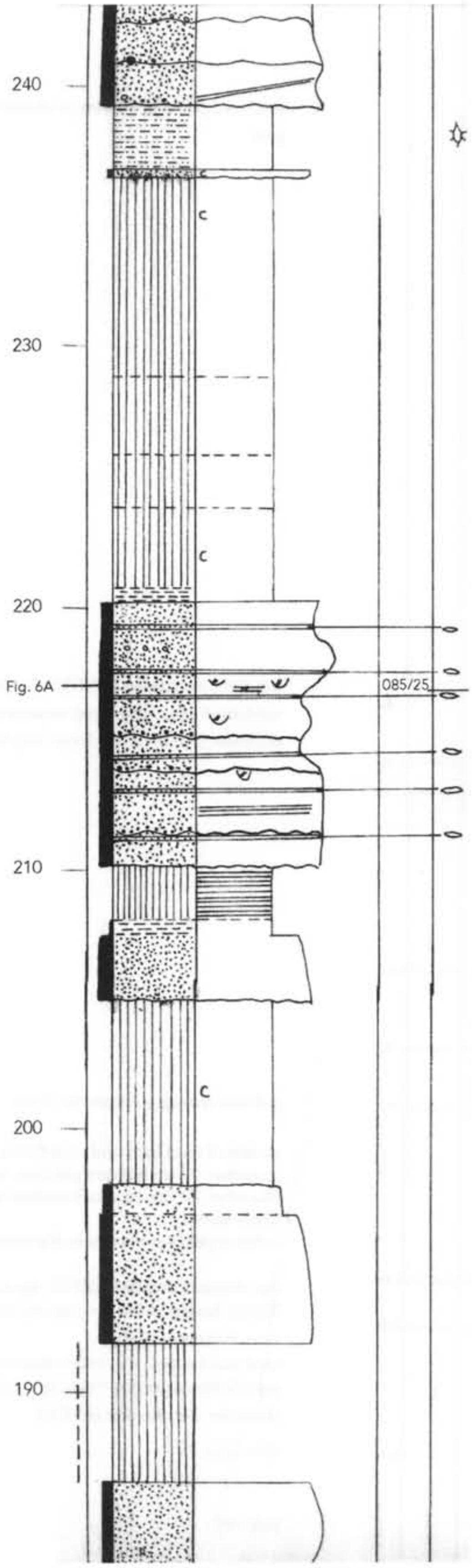

olive green
pebble streaks, maximum diameter: 5 cm
maximum diameter: 80 cm! (only one)
maximum diameter: 5 cm
pale red

yellowish brown

pale red

yellowish brown

pale red
variable grain size throughout layer
scattered pebbles; maximum diameter: 4 cm
small scale trough cross bedding (toesets); height 30 cm
tabular sets; sinuous form; height: 1.5 m
set height trough cross bedding: 40 cm
clay balls up to 8 cm

streaks of clay flakes

pale red

yellowish brown

pale red

pale red

yellowish brown

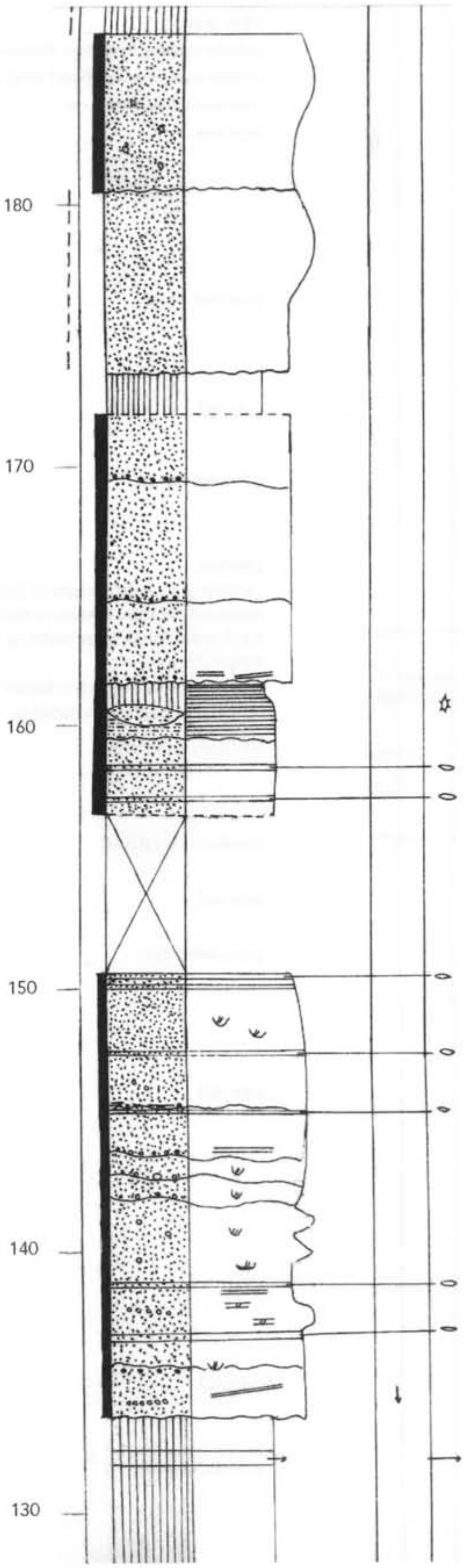

scattered pebbles; maximum diameter: 3 cm
grey

clay lens; disappears in NNW direction
sandstone lens in clay lens: maximum
thickness 80 cm; length 8 cm; very fine sand

pebbles maximum diameter: 5 cm

streaks of mud balls and mud flakes; maximum
diameter: 30 cm isolated pebbles; maximum
diameter: 20 cm; mud ball cavities up to 5 cm
badly sorted
isolated pebbles maximum diameter: 2 cm

dip direction and dip: 030/13. dip of foresets:
080/26 height of foresets: 60 cm; height trough
cross bedding: 70 cm
mud ball cavities; maximum diameter 12 cm
pebble streaks of clay flakes and pebbles; maximum
diameter: 2-3 cm, one of 18 cm

olive grey

pale red

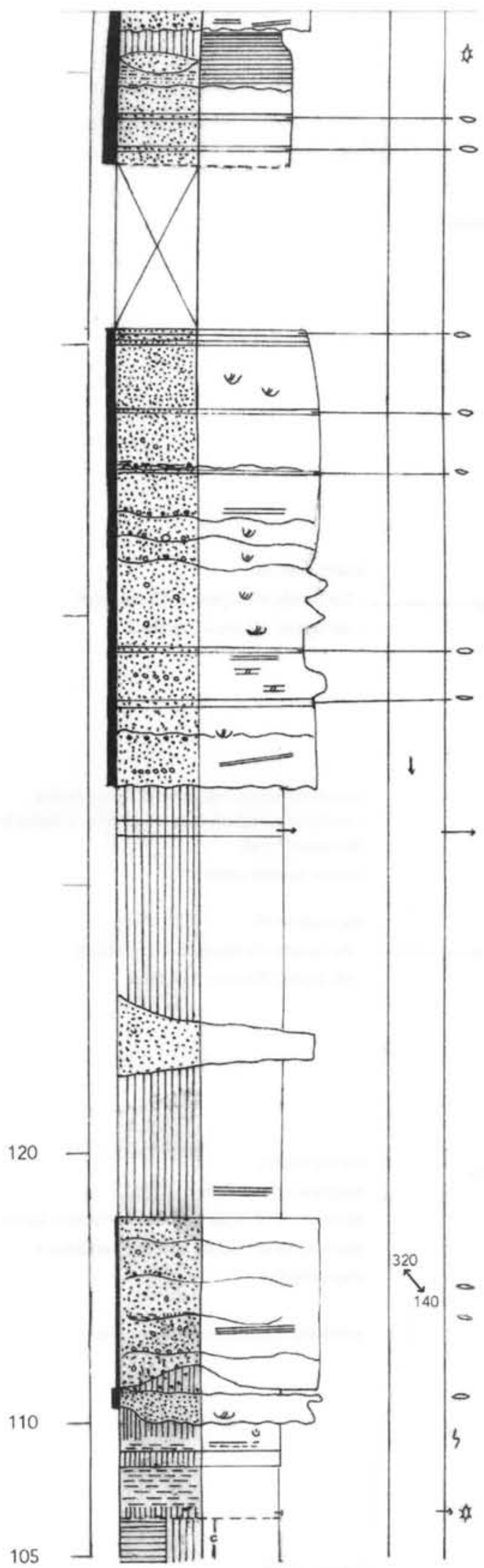

disappears within 10 m in N direction

pale red

estimated scour direction

isolated pebbles, maximum diameter 10 cm

mud balls in muddy lens
cross bedded with clay flakes; grey
vaguely laminated; visible by variation in color
pale red
olive grey, more evenly colored; with rusty brown
spots, mottled pale red – grey with rusty brown
spots
pale red

APPENDIX I-B SAMWAL SECTION

Samwal Section

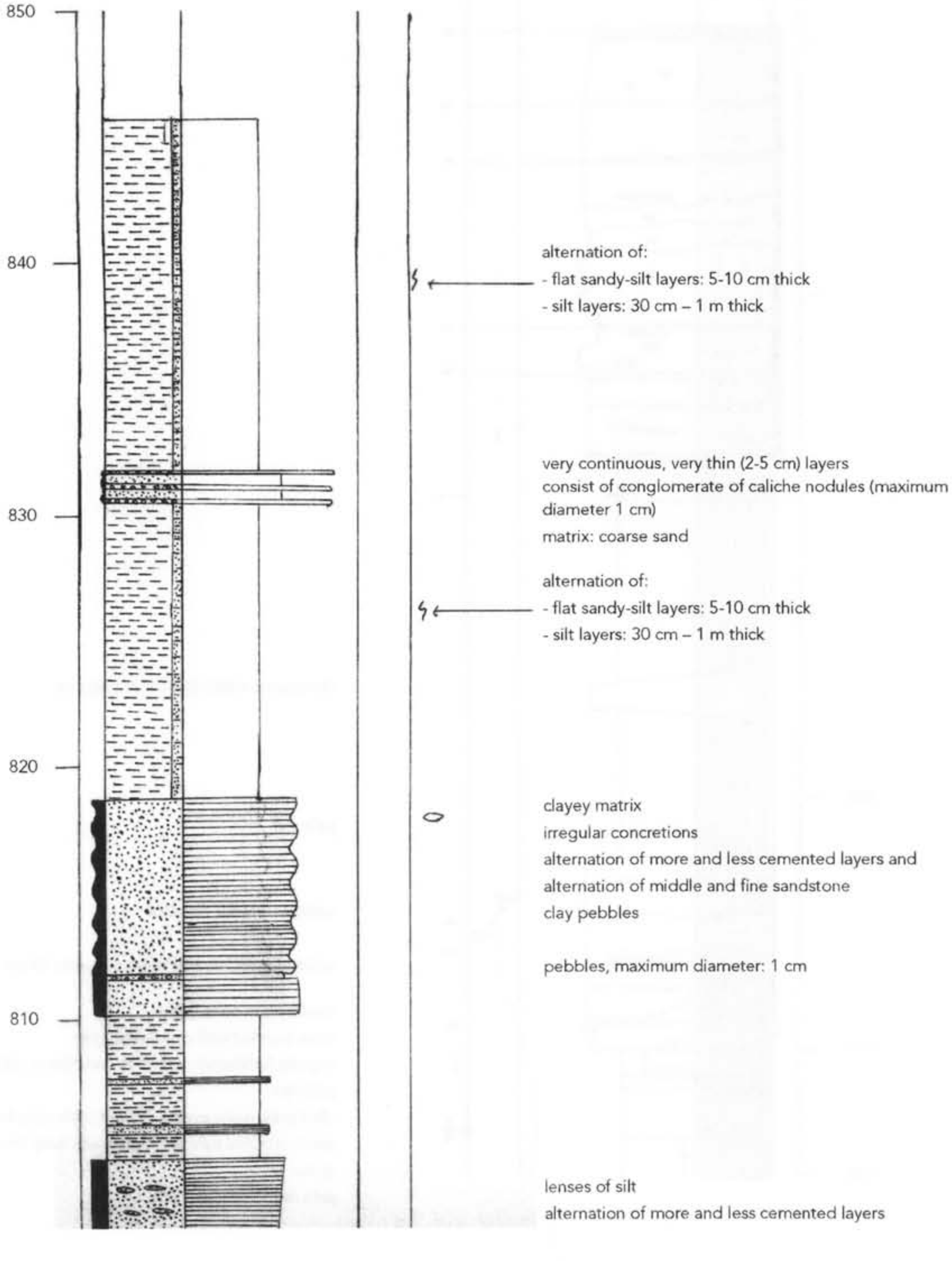

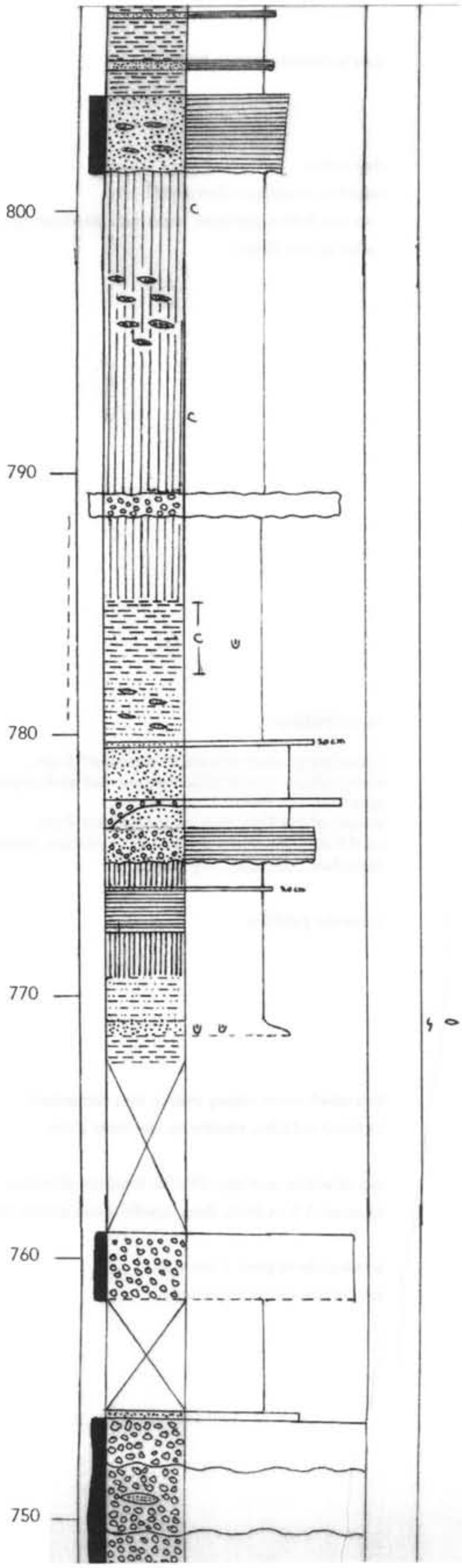

lenses of silt
alternation of more and less cemented layers

lenses of conglomerate: width 30 cm – 1 m, consists of caliche nodules

pebbles: maximum diameter 3 cm; consists mainly of caliche nodules

cemented caliche-like burrows

sandstone lenses (middle sand); width 1 cm; thickness 10-20- cm
wavy lenses

pebbles, maximum diameter 10 cm, mainly reworked sandstone, sandstone lens sandy at the top; more eastward conglomerate
pebbles, maximum diameter: 20 cm

pebbles, maximum diameter 20 cm
variable matrix– and clast supported
largest pebbles are reworked sandstone pebbles (less than 50%)

pebbles, maximum diameter: 30 cm;
subrounded – rounded mainly clast supported; variable matrix- and clast supported, fine sandy lens one reworked sandstone boulder with a diameter of 70 cm more than 50% of the pebbles are reworked sandstone,
but also quartzite (red, purple) present

App. 15

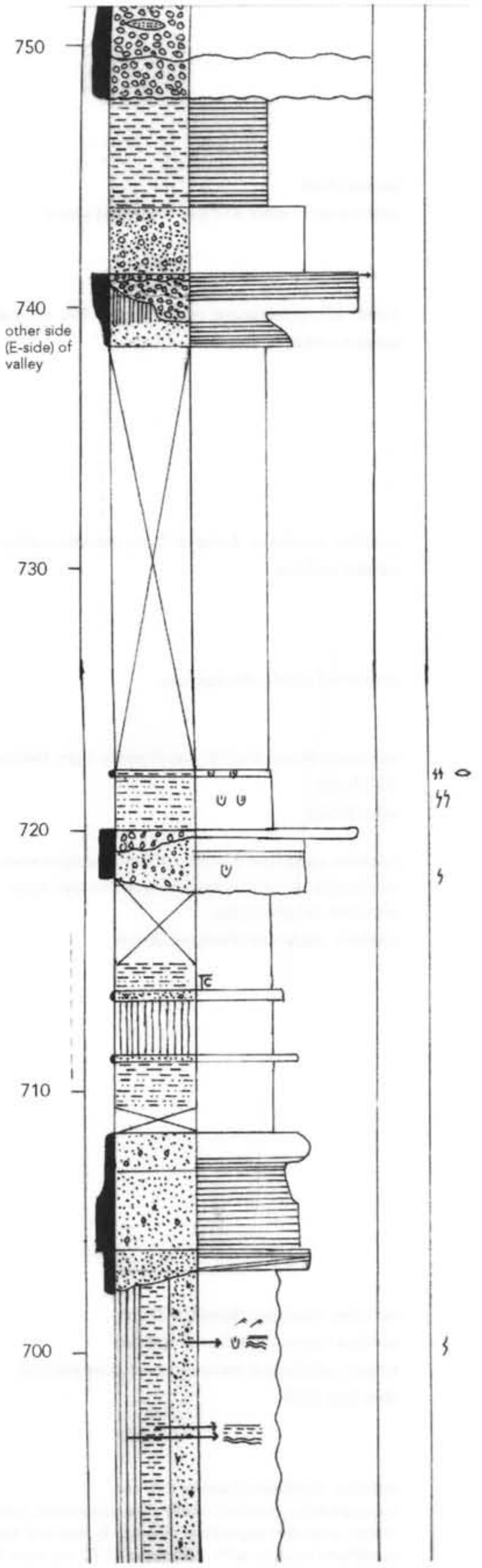

dark yellowish orange 10YR6/6

clay matrix

pebbles, maximum diameter: 5 cm

- no clay flakes; pebbles, maximum diameter: 20 cm
- a lot of clay flakes

cemented layer

matrix supported; maximum diameter 15 cm; composition: reworked sandstone, red and purple quartzite, clay flakes, black chert

streaks of pebbles, maximum diameter 2 cm

mud flakes, reworked sandstone: immature, biotite (intraclast), angular, very fine sand

vulcanite pebbles

less relief: more clayey matrix, less cemented

isolated pebbles, maximum diameter 2 cm

dip direction and dip: 195/58; loadcast direction 110-290

channel: 1.5 m thick, thins rapidly, gone within 10 m

small-scale ripples: 2 cm high

sandstone: much clay matrix

App. 16

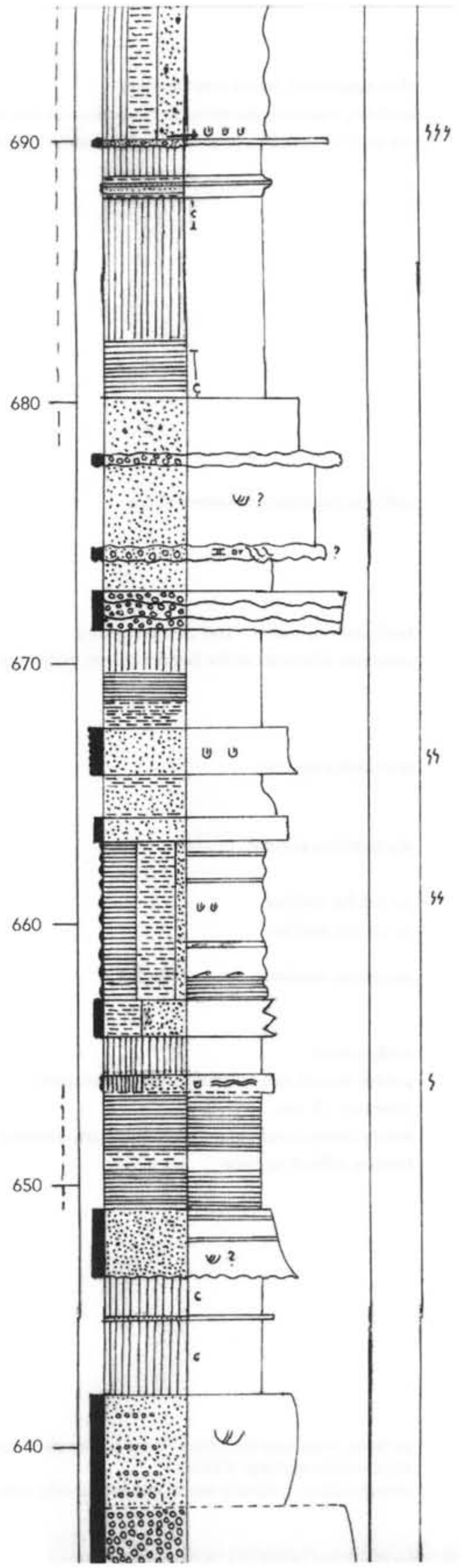

maximum diameter: 2 cm
moderate yellowish brown 10YR5/4
sandstone layers 10 cm thick

yellowish brown

some isolated pebbles; maximum diameter: 8 cm
matrix of the sand is clay
matrix- to clast supported; maximum diameter 8 cm

cross bedding: 60 cm high, or is it a channel fill?

dip direction and dip: 186/60; foreset: 194/80; angle between these two planes is 20°; very badly sorted; accretion? moderately well sorted; at the top more matrix supported clast supported; maximum diameter at the base: 5 cm, at the top: 6-8 cm
scour at base 110/70; slightly erosive

massif; differences in relief suggests that several layers are present

laminated very fine sandstone
sandstone layers, maximum thickness: 10 cm

small-scale ripples in very fine sandstone
silt and clay parallel laminated

alternation of maximum 6 cm very fine sandstone and 2-6 cm thick silty clay layers
yellowish brown
some caliche nodules on the surface

pale yellowish orange 10YR8/6

dip direction and dip: 180/52
set height: 10 cm
pebbly streaks parallel to bedding plane

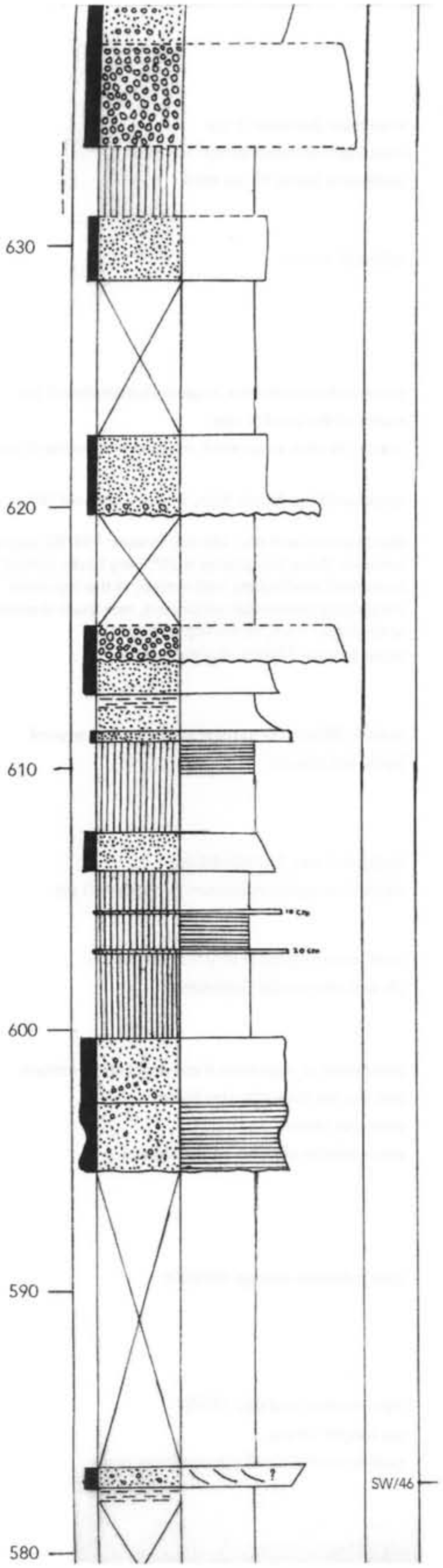

clast supported; matrix very fine sand
pebbles; maximum diameter: at the bottom 25 cm, at the top 15 cm composition a.o.: red and white quartzite

pebbles; maximum diameter: 18 cm

badly sorted; matrix – and clast supported
maximum diameter: at the bottom 10 cm, at the top: 5 cm

few caliche nodules

dip direction and dip: 180/60

no caliche nodules
no caliche nodules

no caliche nodules

badly sorted
pebble streaks and isolated pebbles; maximum diameter: 13 cm
locally concentration of pebbles; maximum diameter: 10 cm
laterally difficult to trace

pebbles, maximum diameter: 10 cm, locally clast supported
dip direction and dip: 180/60
cross bedding, probably lateral accretion (badly sorted)

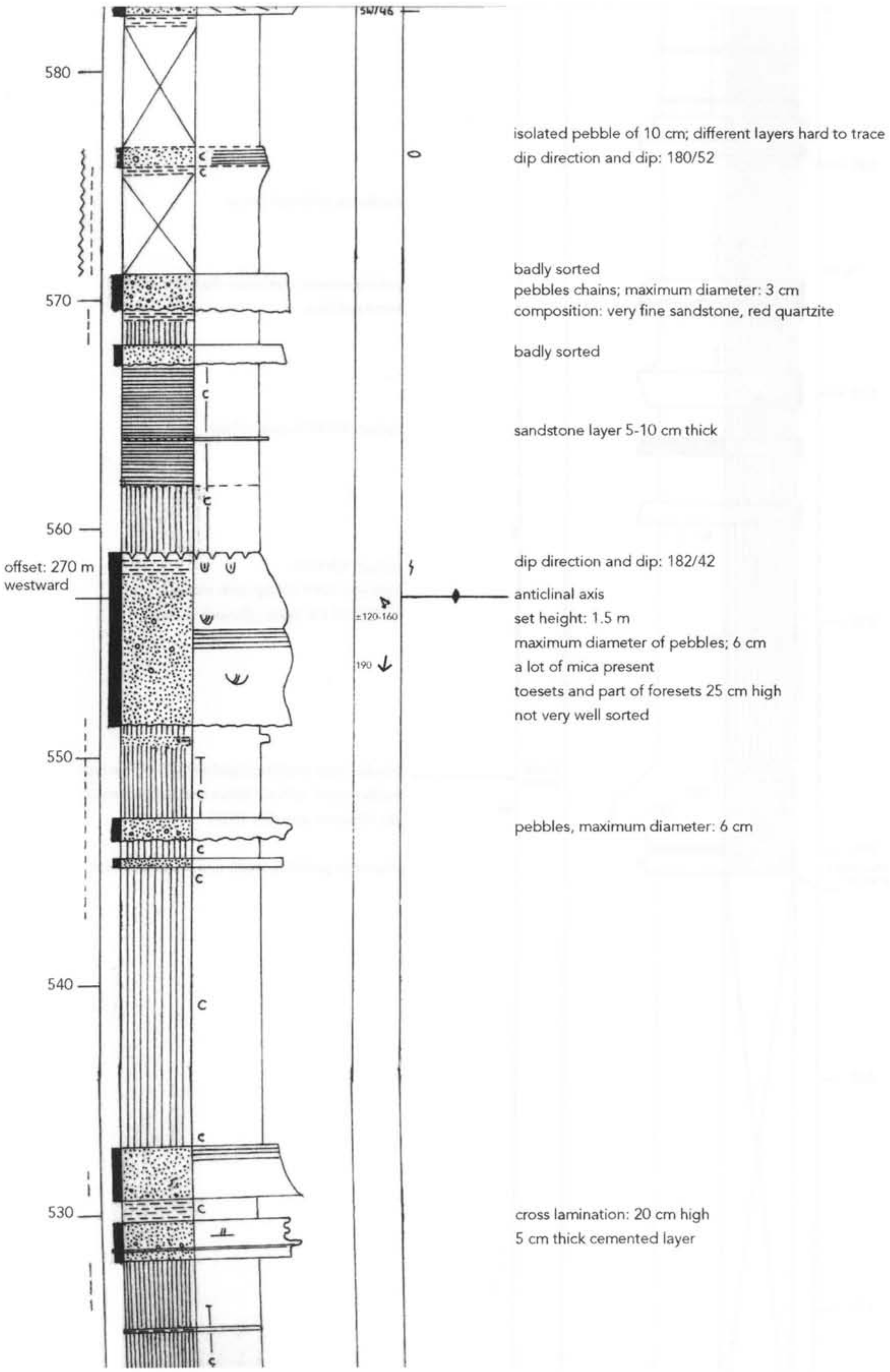
580
570
560
550
540
530
offset: 270 m
westward
SW/46
±120-160
190
isolated pebble of 10 cm; different layers hard to trace
dip direction and dip: 180/52
badly sorted
pebbles chains; maximum diameter: 3 cm
composition: very fine sandstone, red quartzite
badly sorted
sandstone layer 5-10 cm thick
dip direction and dip: 182/42
anticlinal axis
set height: 1.5 m
maximum diameter of pebbles; 6 cm
a lot of mica present
toesets and part of foresets 25 cm high
not very well sorted
pebbles, maximum diameter: 6 cm
cross lamination: 20 cm high
5 cm thick cemented layer

App. 19

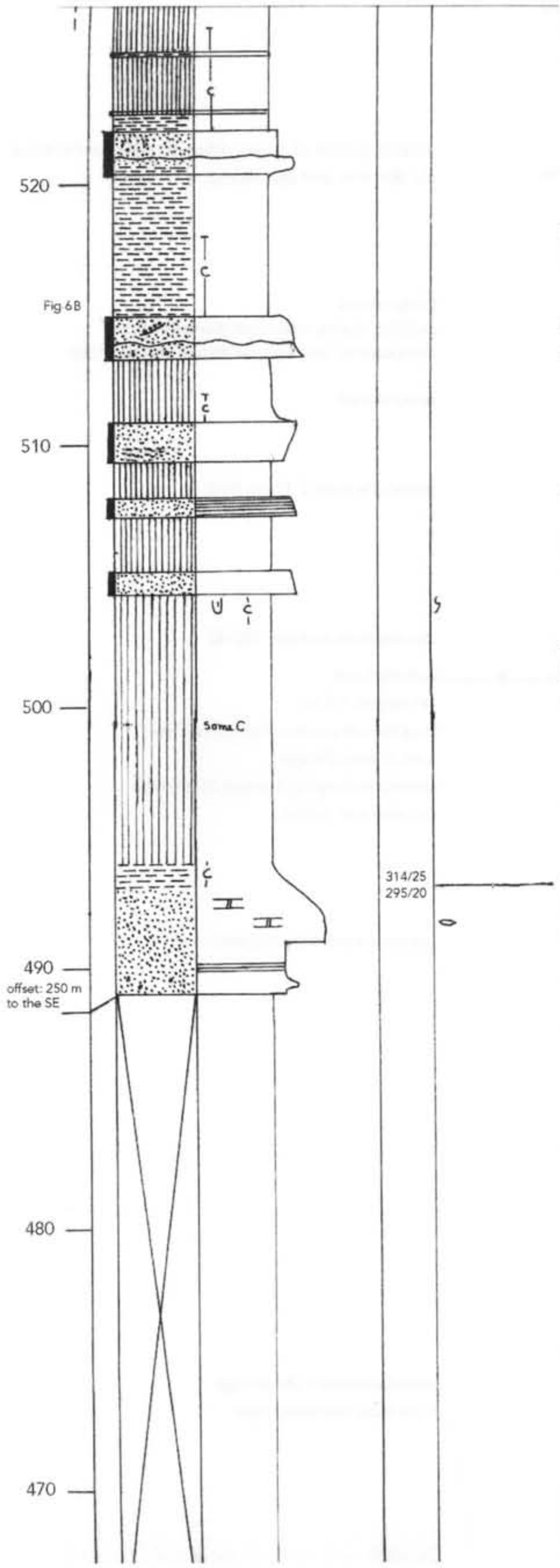

moderate yellowish brown

pebbly streaks, maximum diameter: 3 cm
some pebbles

colour: 10YR7/6 (see below)

colour: 10YR7/6
between 10YR 7/4 (greyish orange)
and 10 YR 6/6 (dark yellowish orange)

tabular cross bedding (epsilon?): 45-50 cm high
badly sorted; with silt flakes and pebbly streaks
dip direction and dip: 180/5

dispersed pebbles, maximum diameter: 1 cm

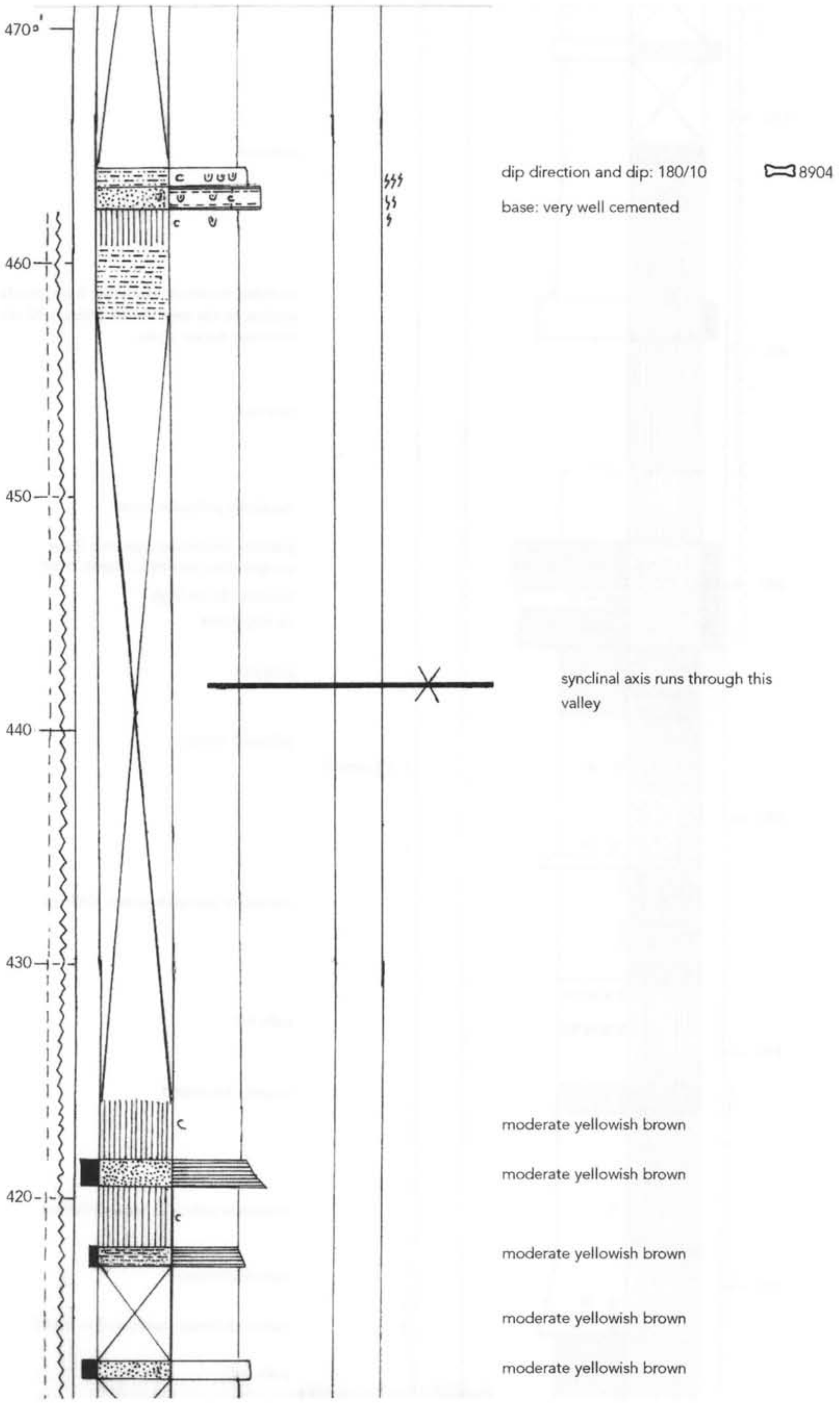

470
460
450
440
430
420
dip direction and dip: 180/10
8904
base: very well cemented
synclinal axis runs through this valley
moderate yellowish brown
moderate yellowish brown
moderate yellowish brown
moderate yellowish brown
moderate yellowish brown

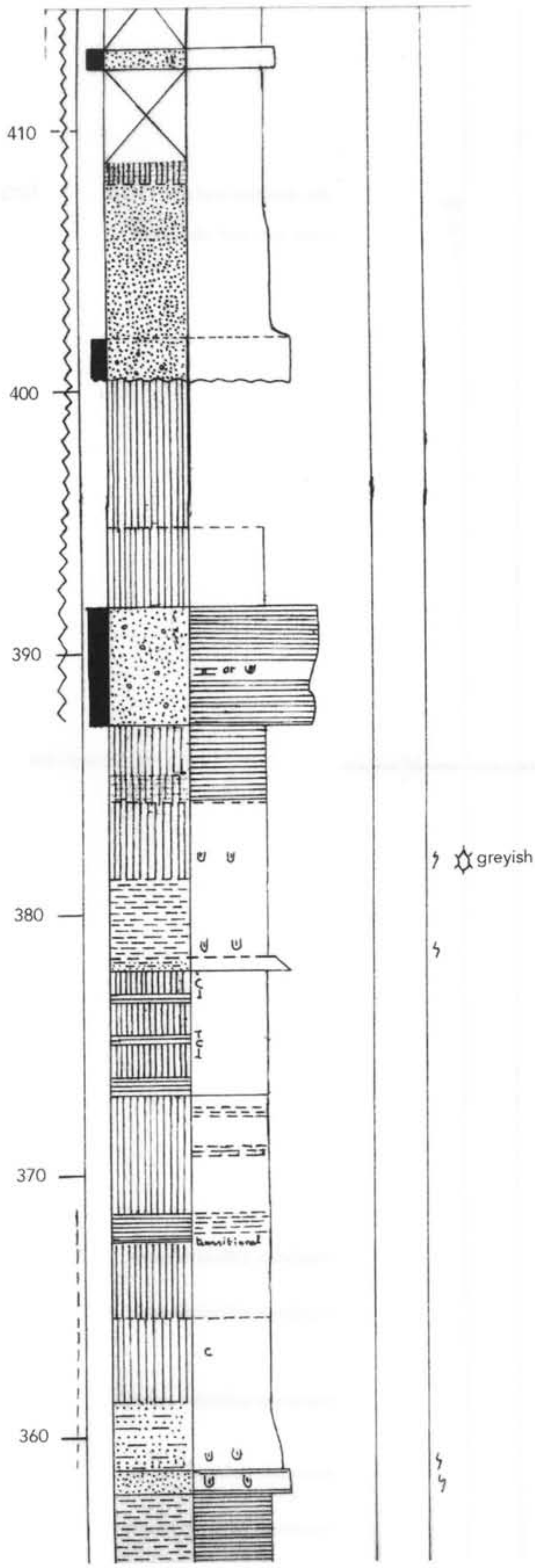

pale red

pebbles, maximum diameter: 5 cm; quartz, quartzite
erosive, to the west the thickness is 60 cm, then becomes thicker again

pale red

moderate yellowish brown

pebbles, maximum diameter: 2 cm;
composition: quartzite, quartz, chert

foresets: 20 cm high

no clay flakes

pale red

yellowish brown

moderate yellowish brown 10YR5/4

pale red

vaguely laminated

moderate yellowish brown 10YR5/4

yellowish brown

yellowish brown; laminated to massif

pale red

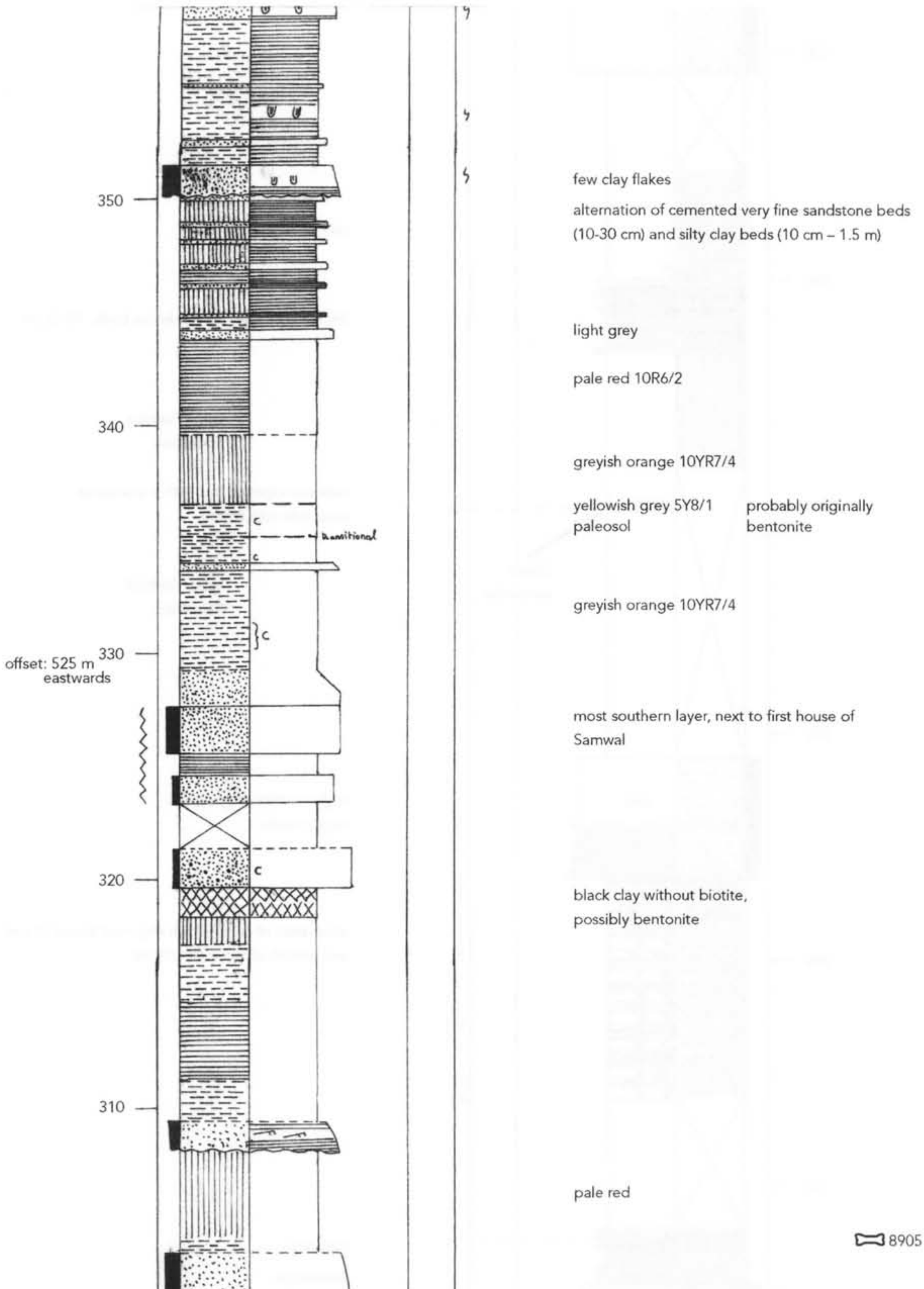
350
340
330
320
310
300
offset: 525 m eastwards
c
transitional
c
c
c
few clay flakes
alternation of cemented very fine sandstone beds (10-30 cm) and silty clay beds (10 cm – 1.5 m)
light grey
pale red 10R6/2
greyish orange 10YR7/4
yellowish grey 5Y8/1
paleosol
probably originally bentonite
greyish orange 10YR7/4
most southern layer, next to first house of Samwal
black clay without biotite, possibly bentonite
pale red
8905
greyish orange 10YR7/4
clayey matrix

App. 23

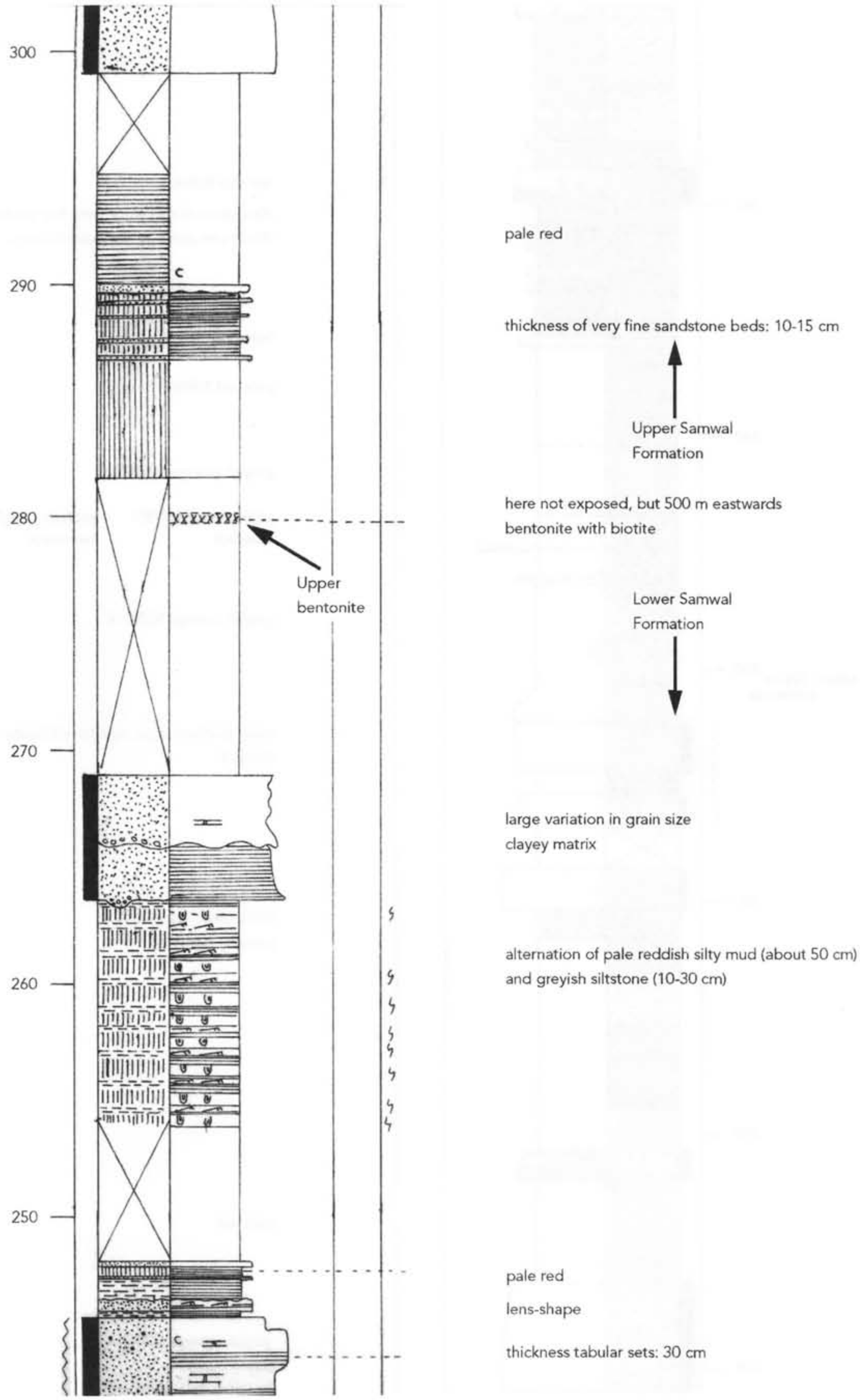
300
290
280
270
260
250
Upper
bentonite
pale red
thickness of very fine sandstone beds: 10-15 cm
Upper Samwal
Formation
here not exposed, but 500 m eastwards
bentonite with biotite
Lower Samwal
Formation
large variation in grain size
clayey matrix
alternation of pale reddish silty mud (about 50 cm)
and greyish siltstone (10-30 cm)
pale red
lens-shape
thickness tabular sets: 30 cm

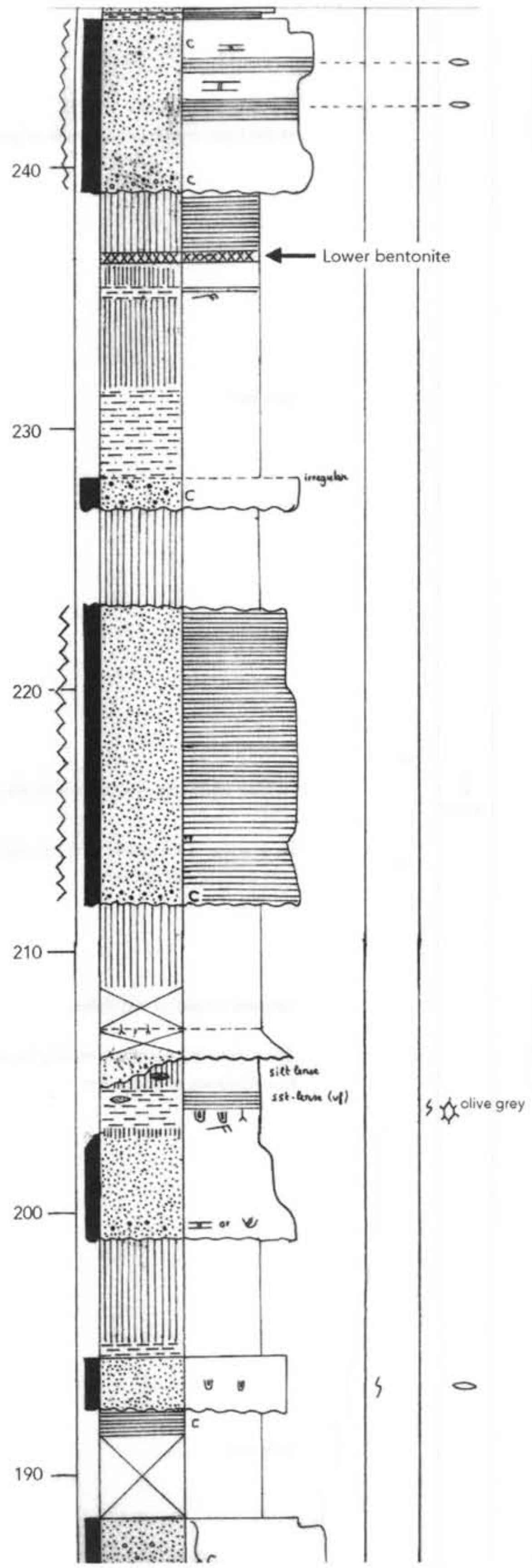

bentonite: black clay with biotite! colour: olive grey SY3/2

greyish silt

pale red

dip direction and dip: 170/75

greyish orange 10YR7/4

clay matrix

pale red

dip direction and dip: 175/80

pale red

irregular

bioturbation tubes: more grey – reddish gray; halo: olive

mica

forest height: 57 cm (toe and foresets)

pale red

100 m towards the east, the thickness increases to 10 m

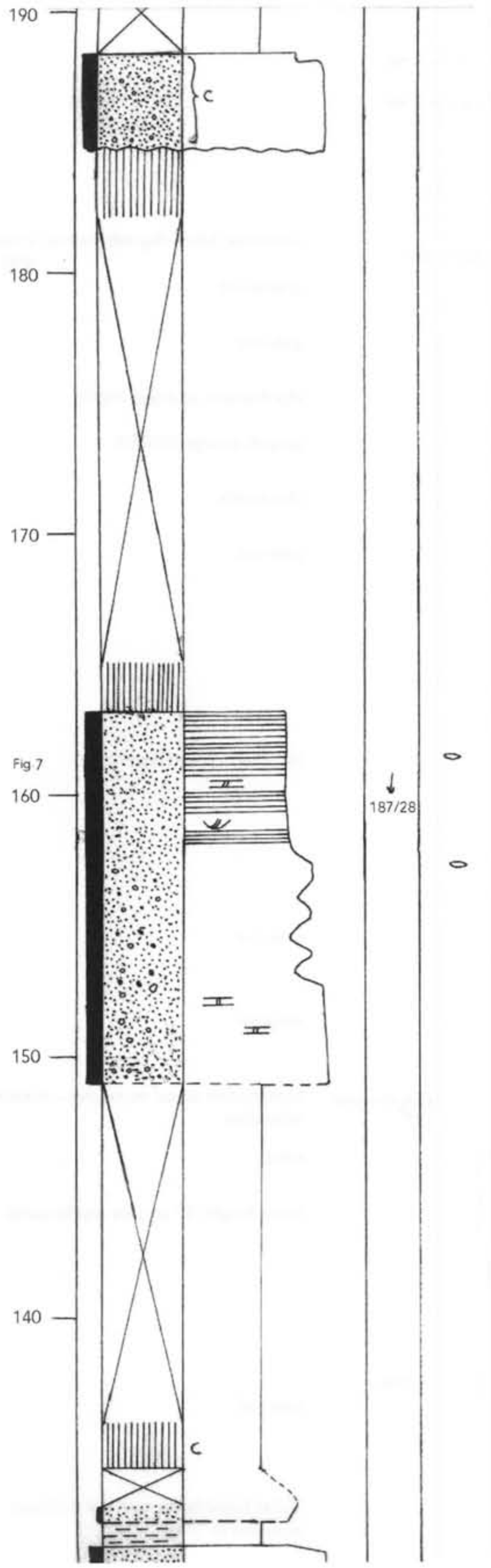

dip direction and dip: 180/60
at the base, maximum diameter of pebbles: 1 cm

pale red

tabular, sigmoidal sets, thickness: 40 cm — about 500 m East of sectionline

thickness of the foresets of the trough with cross bedding: 10 cm — correlated sandstone platform 8908

foresets consist of clay flakes

200 m laterally eastward: rapidly thinning to a thickness of about 2 m

pale red

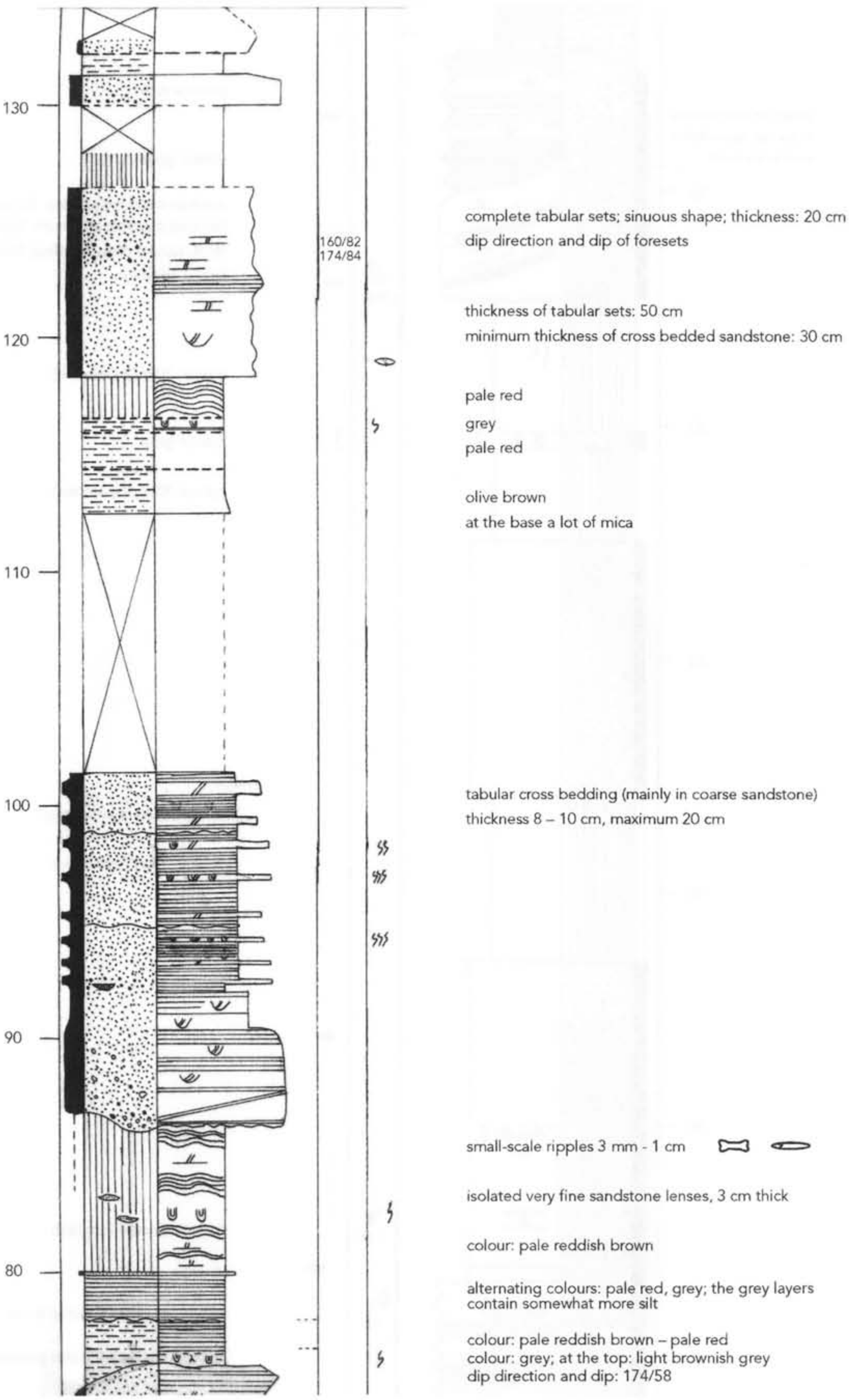
130
120
110
100
90
80
160/82
174/84
complete tabular sets; sinuous shape; thickness: 20 cm
dip direction and dip of foresets
thickness of tabular sets: 50 cm
minimum thickness of cross bedded sandstone: 30 cm
pale red
grey
pale red
olive brown
at the base a lot of mica
tabular cross bedding (mainly in coarse sandstone)
thickness 8 – 10 cm, maximum 20 cm
small-scale ripples 3 mm - 1 cm
isolated very fine sandstone lenses, 3 cm thick
colour: pale reddish brown
alternating colours: pale red, grey; the grey layers contain somewhat more silt
colour: pale reddish brown – pale red
colour: grey; at the top: light brownish grey
dip direction and dip: 174/58

offset: just after bending of the fold; about 500 m more to the south

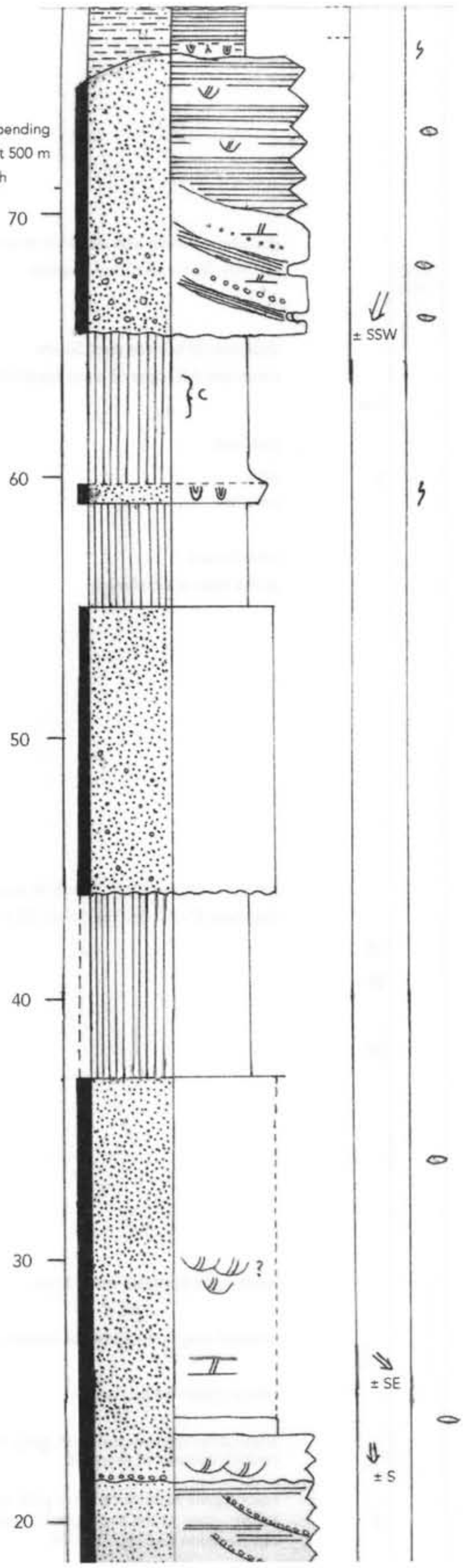

positive relief

colour: grey

medium sandstone layers: 10 cm thick; parallel laminated coarse sandstone layer, up to 1 m thick, tabular cross bedding; foresets 80 cm high lateral accretion

colour: 10R6/2 (pale red)

colour: grey

colour: 10R6/2 (pale red)

washed over near the top

colour: 10R6/2 (pale red)

foreset about 1.5 m high

maximum clast diameter: 6 cm

mainly quartz clasts; also present mica, Fe

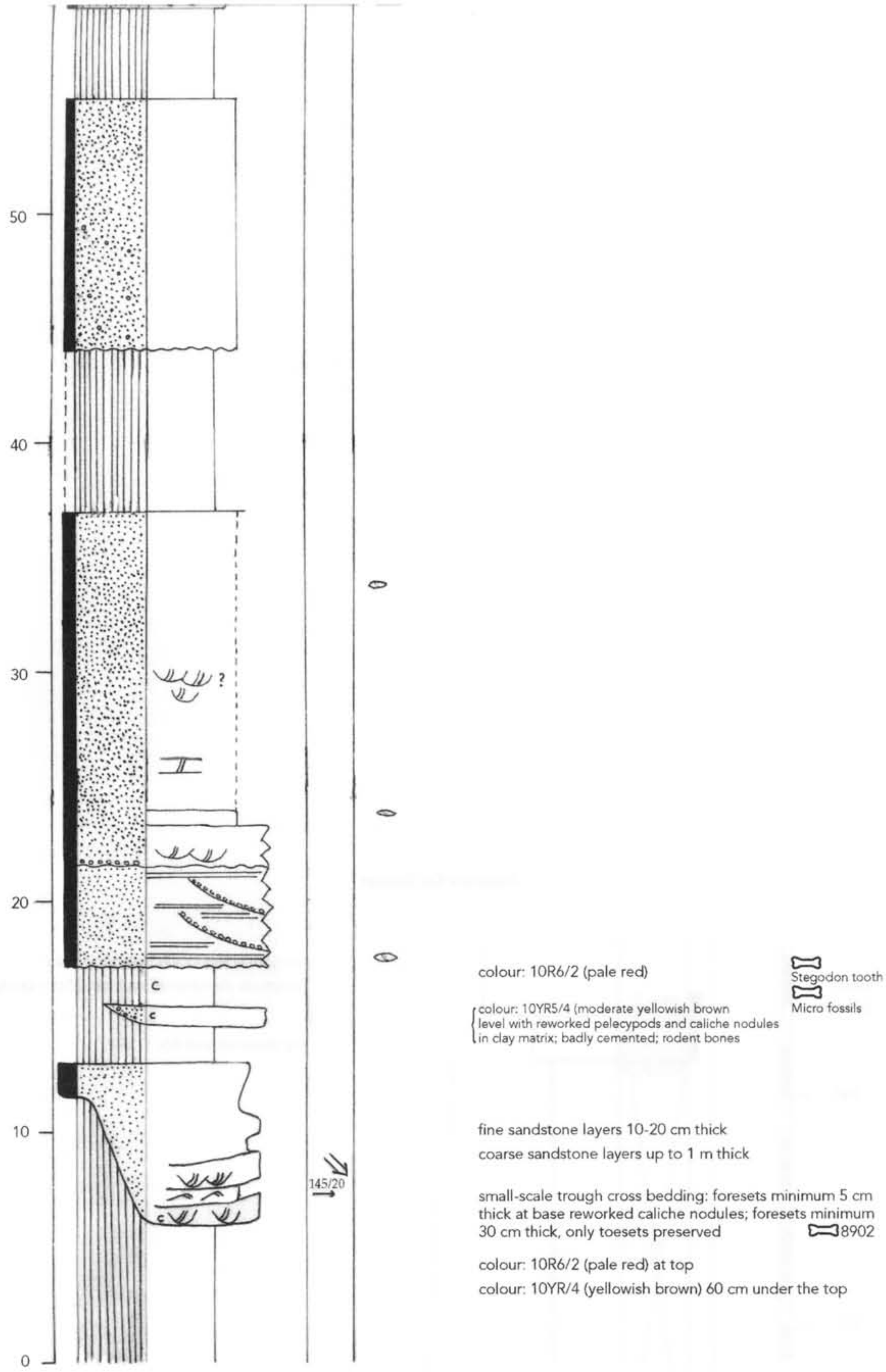

0
10
20
30
40
50
145/20
c
?
colour: 10R6/2 (pale red)
Stegodon tooth
Micro fossils
colour: 10YR5/4 (moderate yellowish brown
level with reworked pelecypods and caliche nodules
in clay matrix; badly cemented; rodent bones
fine sandstone layers 10-20 cm thick
coarse sandstone layers up to 1 m thick
small-scale trough cross bedding: foresets minimum 5 cm
thick at base reworked caliche nodules; foresets minimum
30 cm thick, only toesets preserved
8902
colour: 10R6/2 (pale red) at top
colour: 10YR/4 (yellowish brown) 60 cm under the top

APPENDIX I-C JHELAWALA KAS SECTION

Jhelawala Kas Section

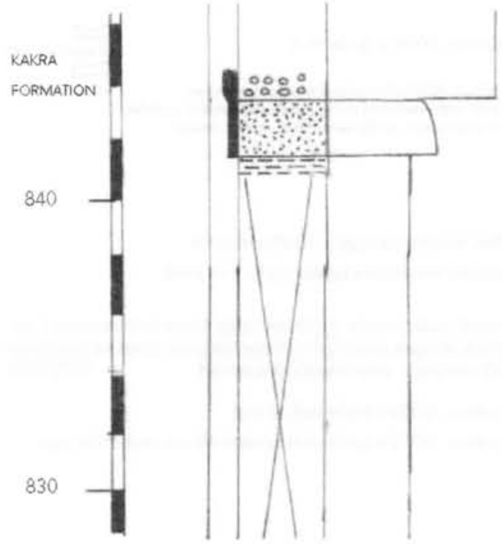

conglomerate; locally clast supported
maximum diameter of pebbles: 20 cm; sandy matrix

dip direction and dip: + 360/7

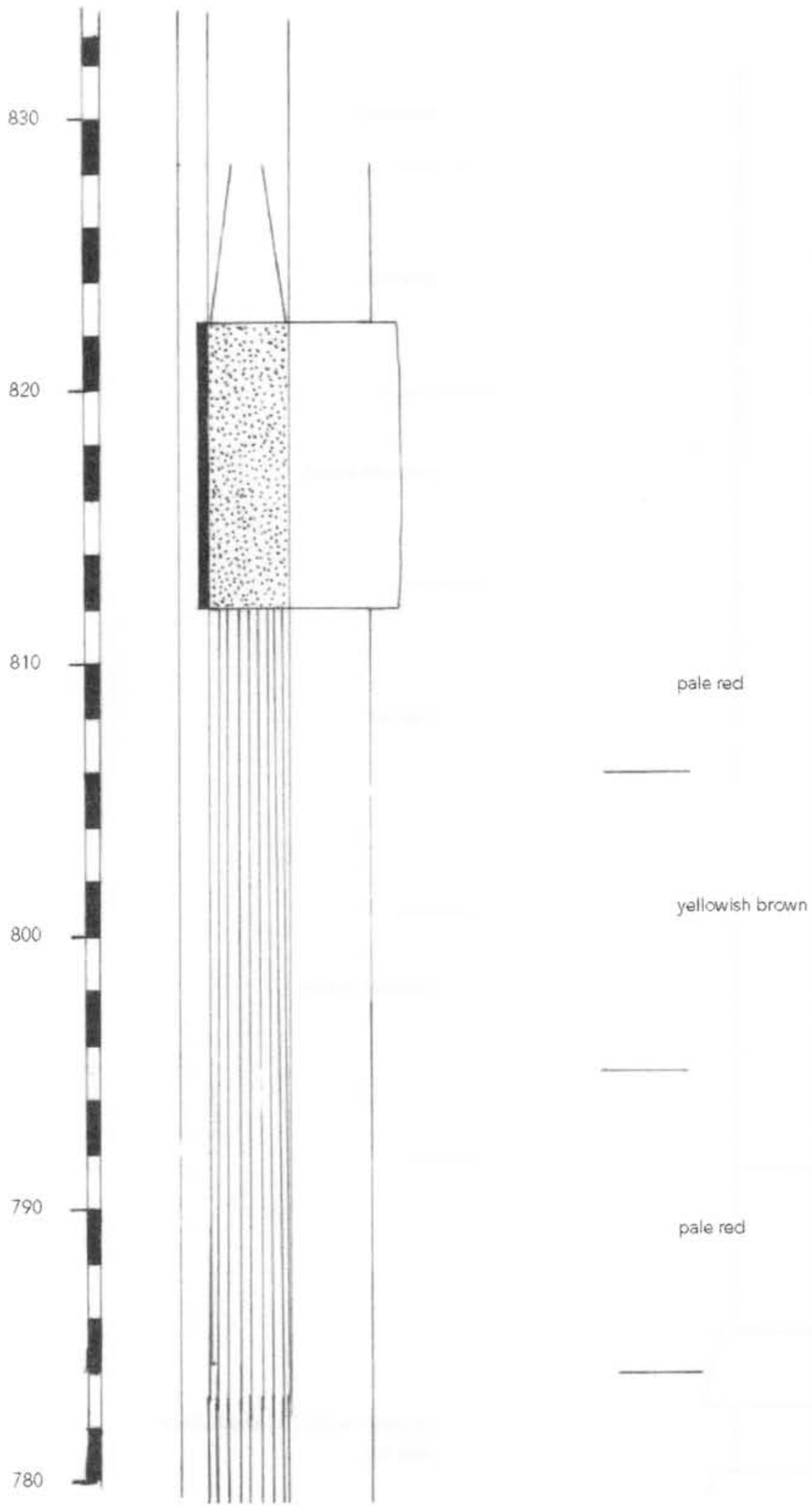

App. 31

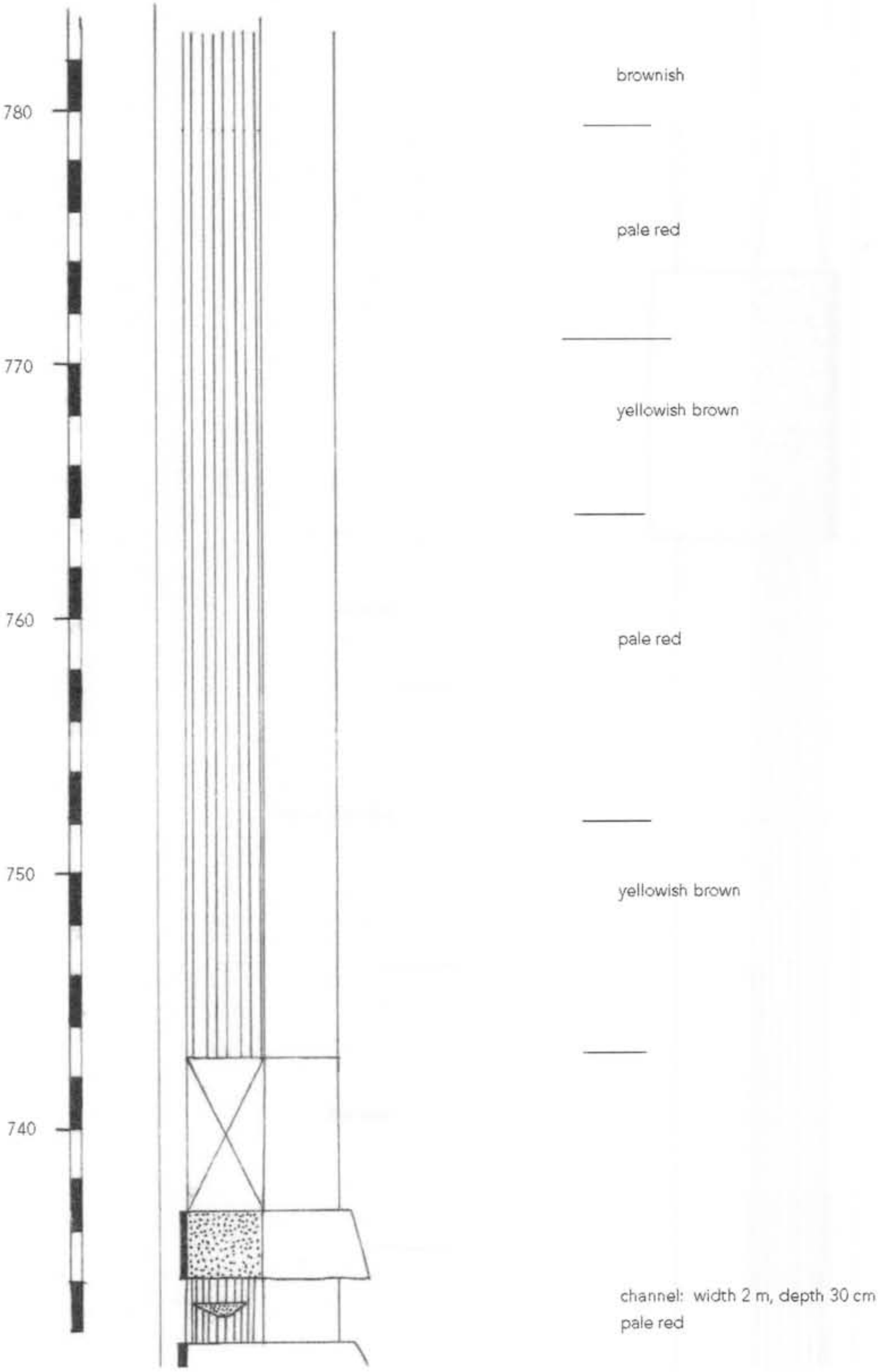
780
770
760
750
740
brownish
pale red
yellowish brown
pale red
yellowish brown
channel: width 2 m, depth 30 cm
pale red

App. 32

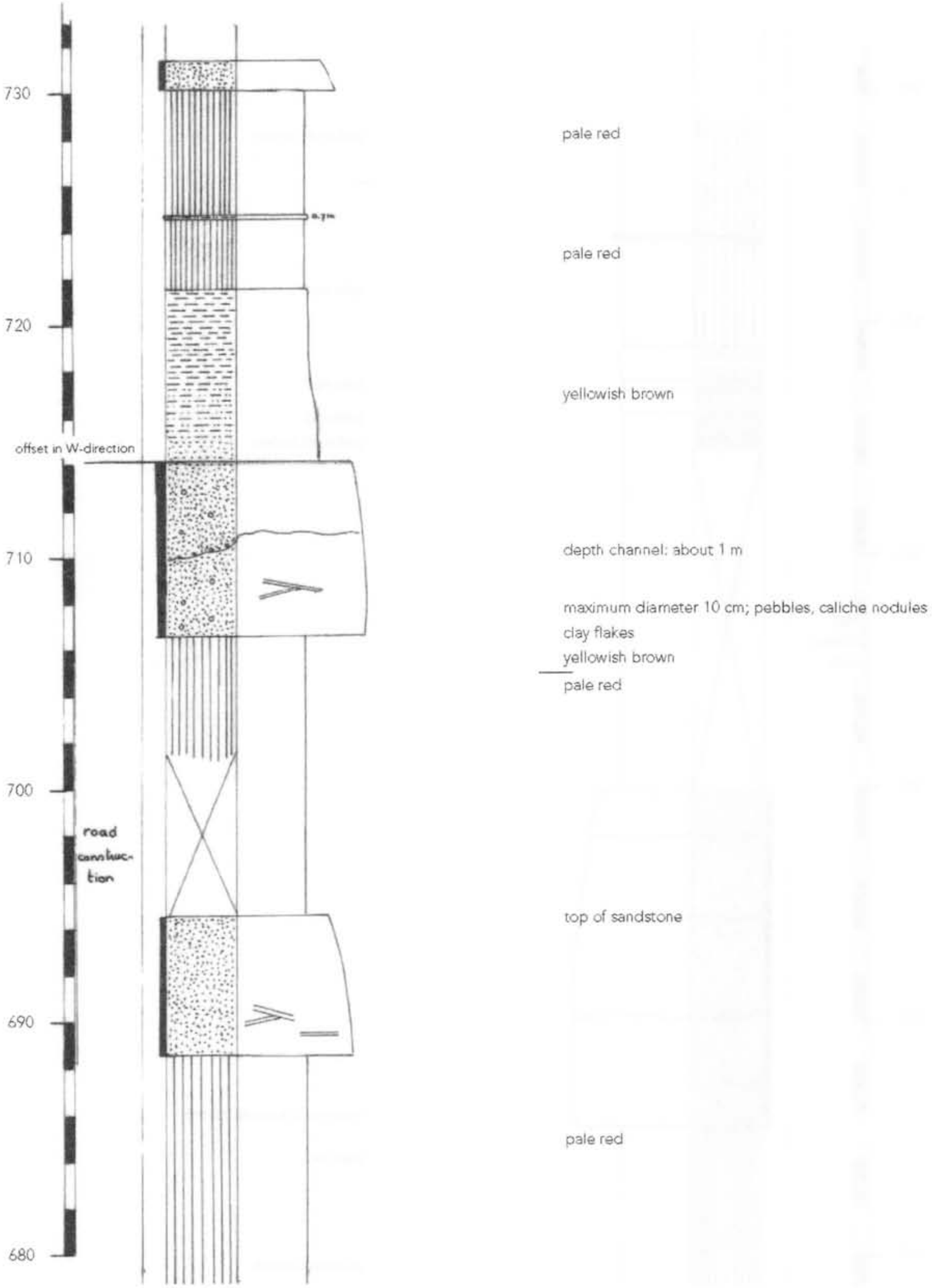
730
720
710
700
690
680
offset in W-direction
road
construc-
tion
pale red
pale red
yellowish brown
depth channel: about 1 m
maximum diameter 10 cm; pebbles, caliche nodules
clay flakes
yellowish brown
pale red
top of sandstone
pale red

App. 33

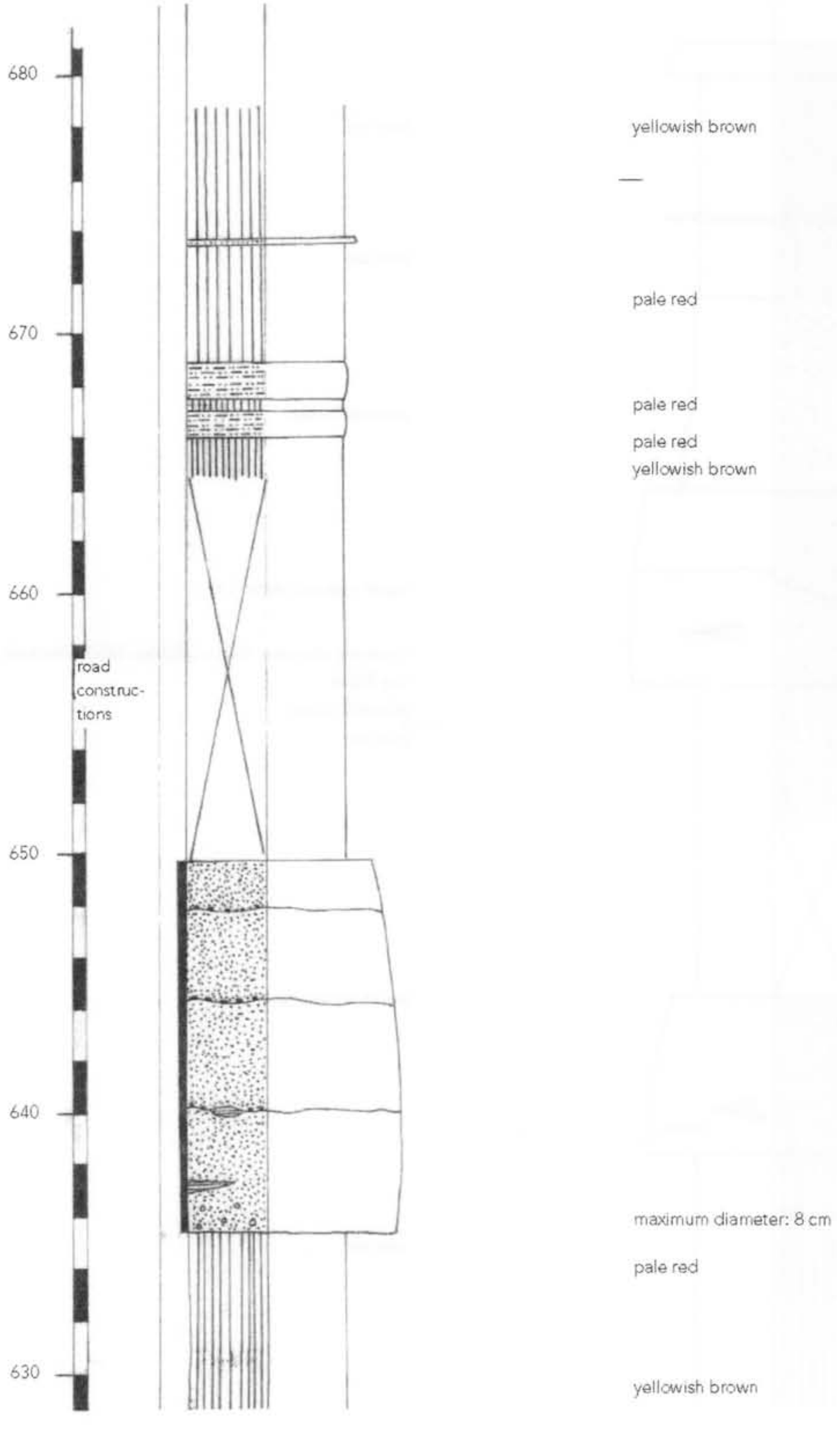
680
670
660
650
640
630
road constructions
yellowish brown
pale red
pale red
pale red
yellowish brown
maximum diameter: 8 cm
pale red
yellowish brown

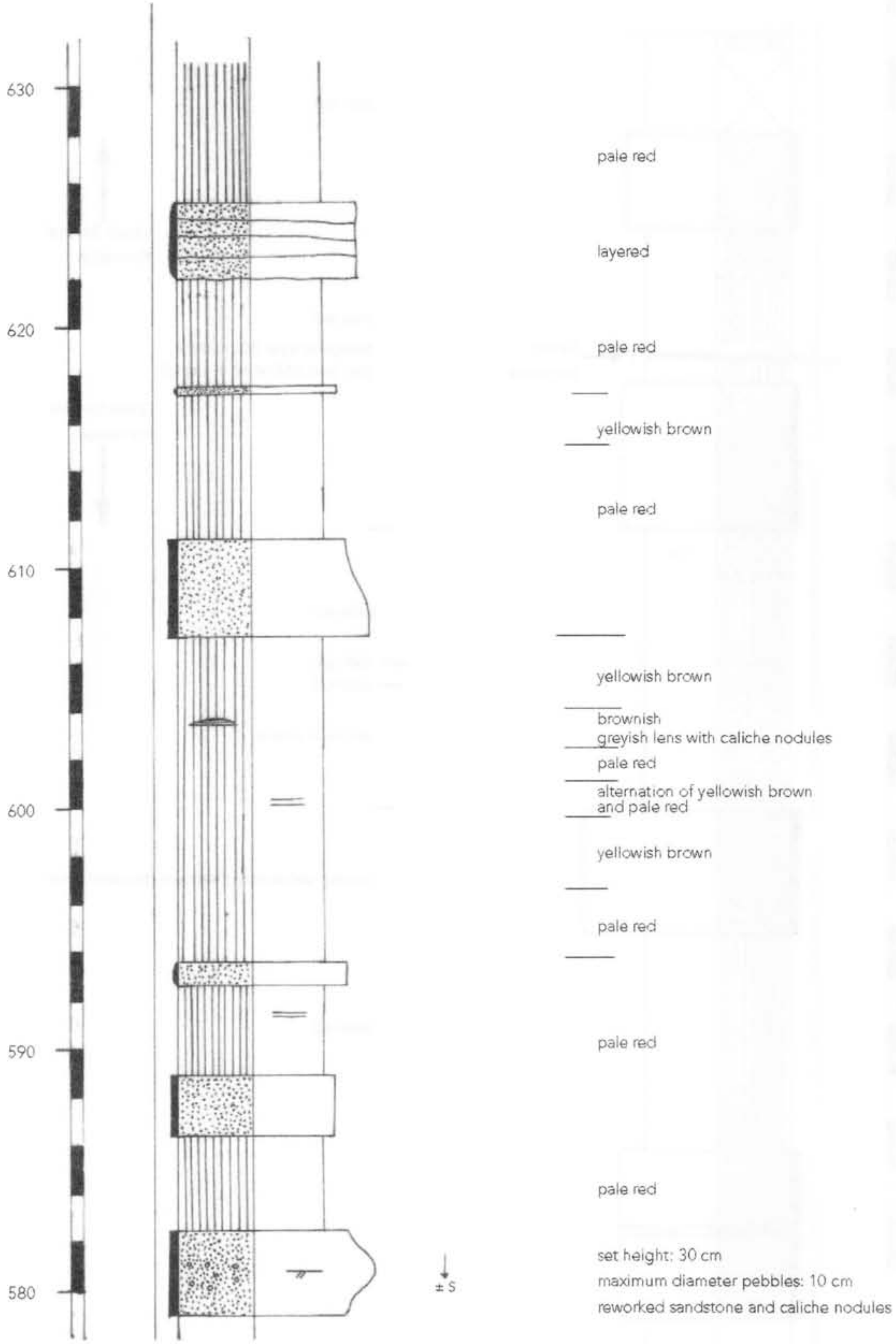

630
620
610
600
590
580
± S
pale red
layered
pale red
yellowish brown
pale red
yellowish brown
brownish
greyish lens with caliche nodules
pale red
alternation of yellowish brown
and pale red
yellowish brown
pale red
pale red
pale red
set height: 30 cm
maximum diameter pebbles: 10 cm
reworked sandstone and caliche nodules

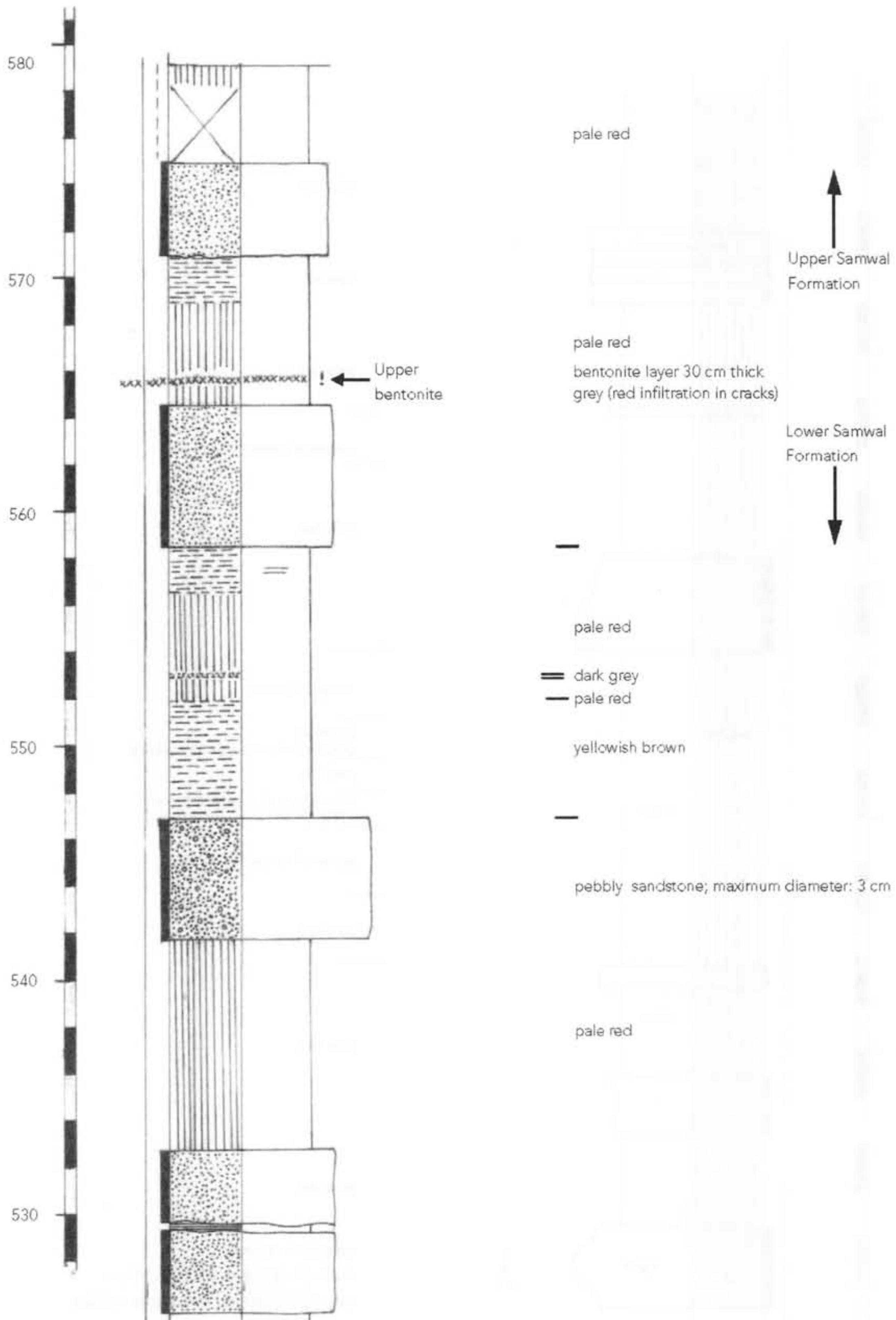
580
570
560
550
540
530
Upper
bentonite
pale red
Upper Samwal
Formation
pale red
bentonite layer 30 cm thick
grey (red infiltration in cracks)
Lower Samwal
Formation
pale red
dark grey
pale red
yellowish brown
pebbly sandstone; maximum diameter: 3 cm
pale red

App. 36

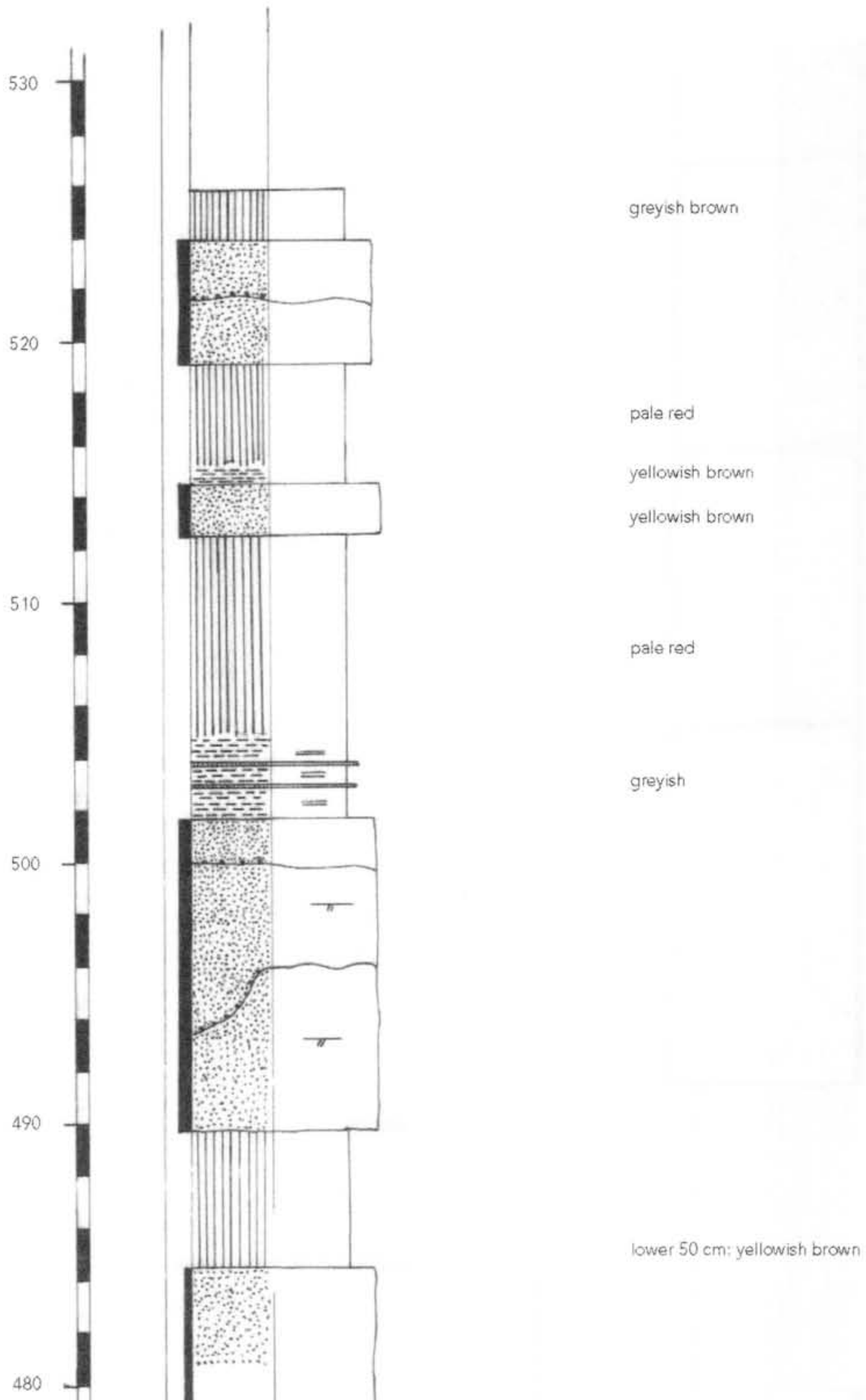
530
520
510
500
490
480
greyish brown
pale red
yellowish brown
yellowish brown
pale red
greyish
lower 50 cm: yellowish brown

App. 37

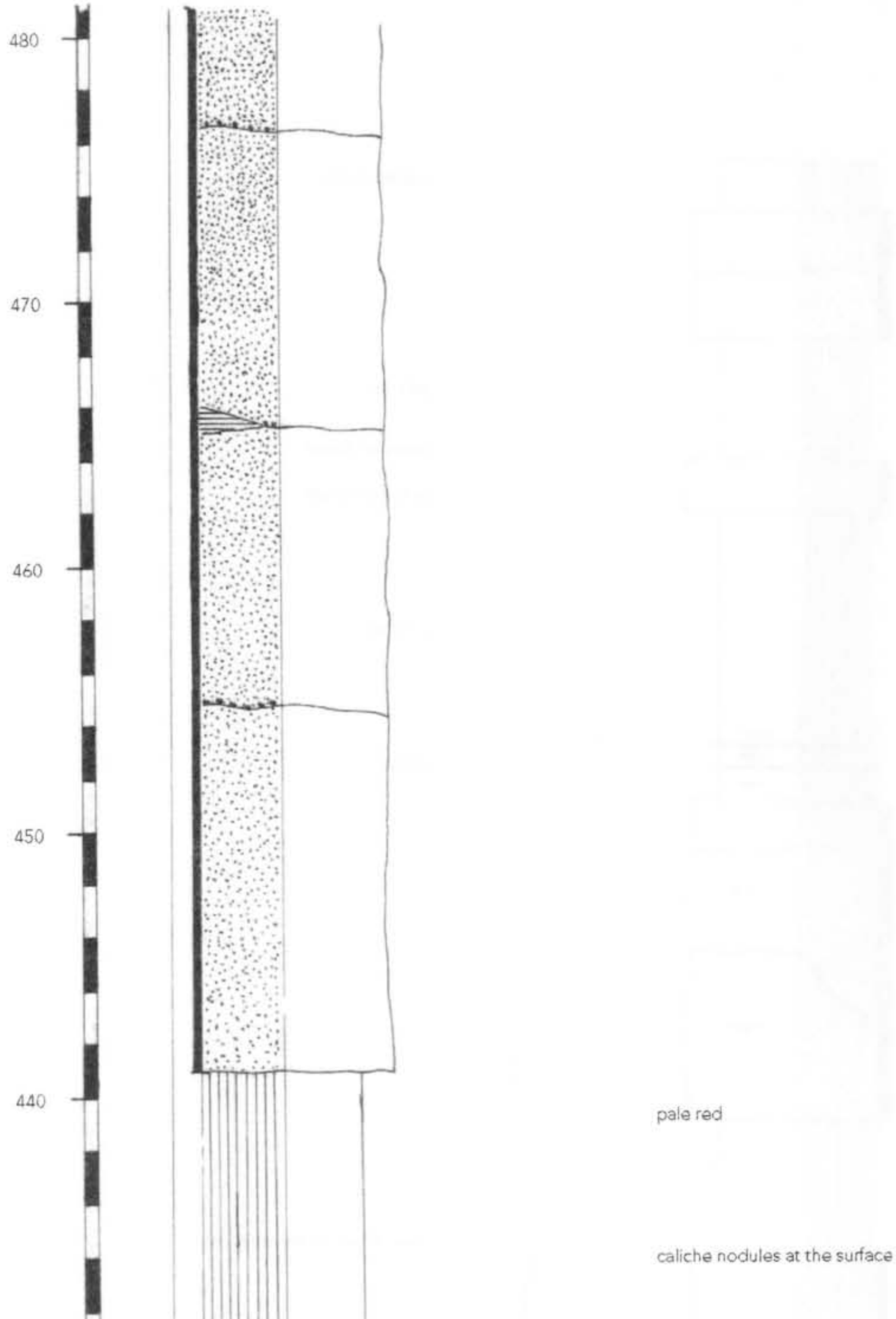
480
470
460
450
440
430
pale red
caliche nodules at the surface

App. 38

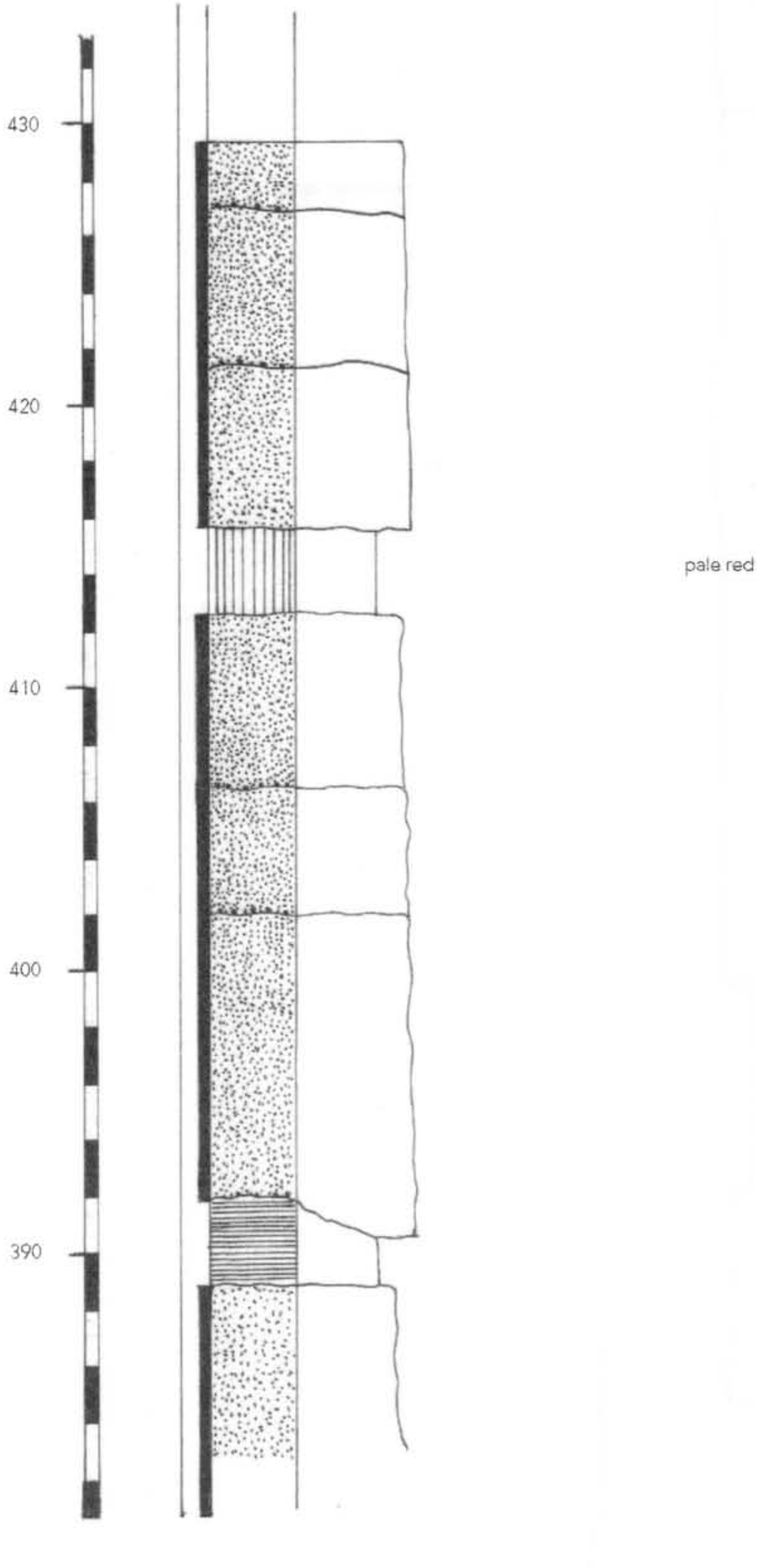
430
420
410
400
390
pale red

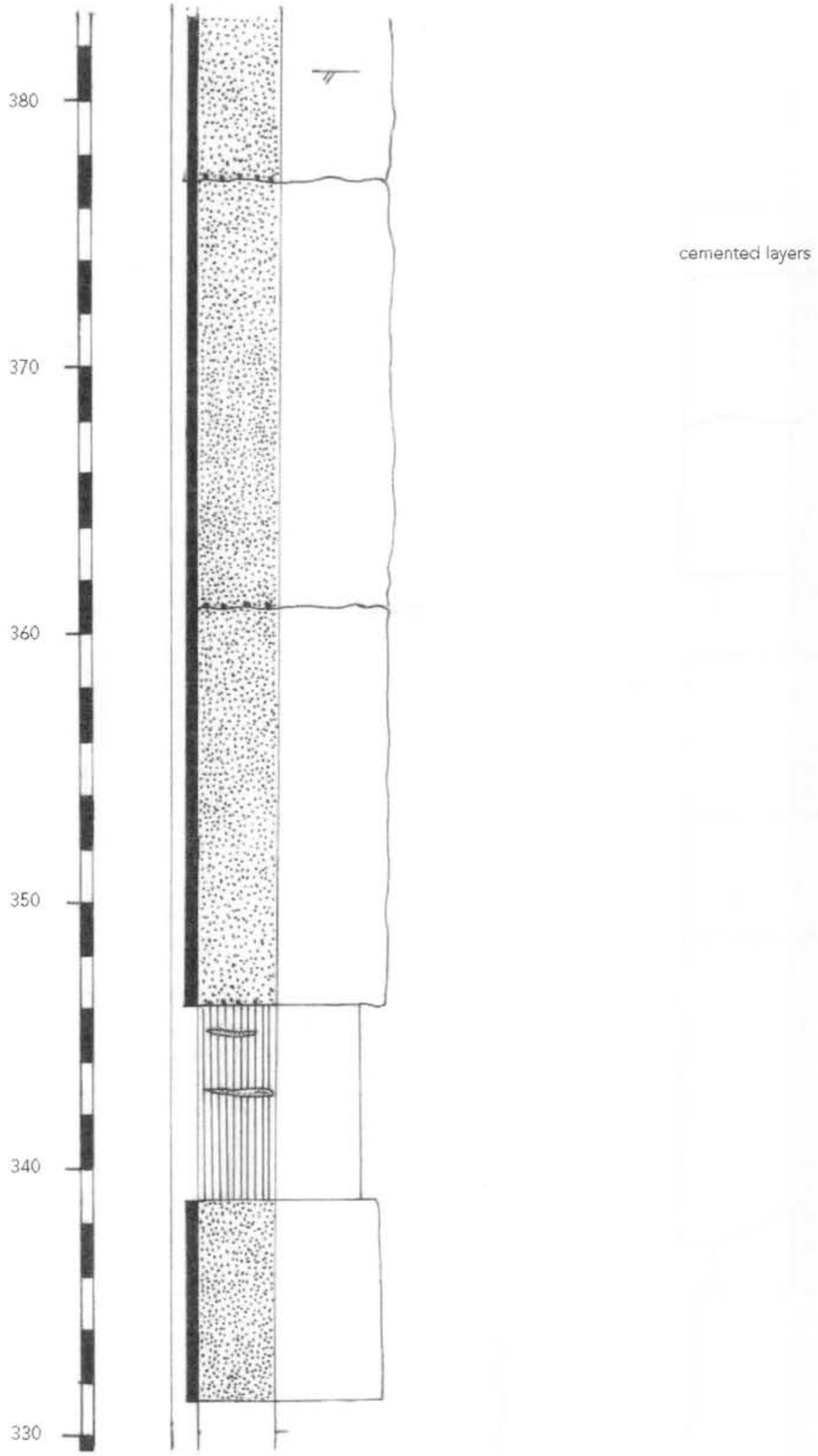
380
370
360
350
340
330
cemented layers

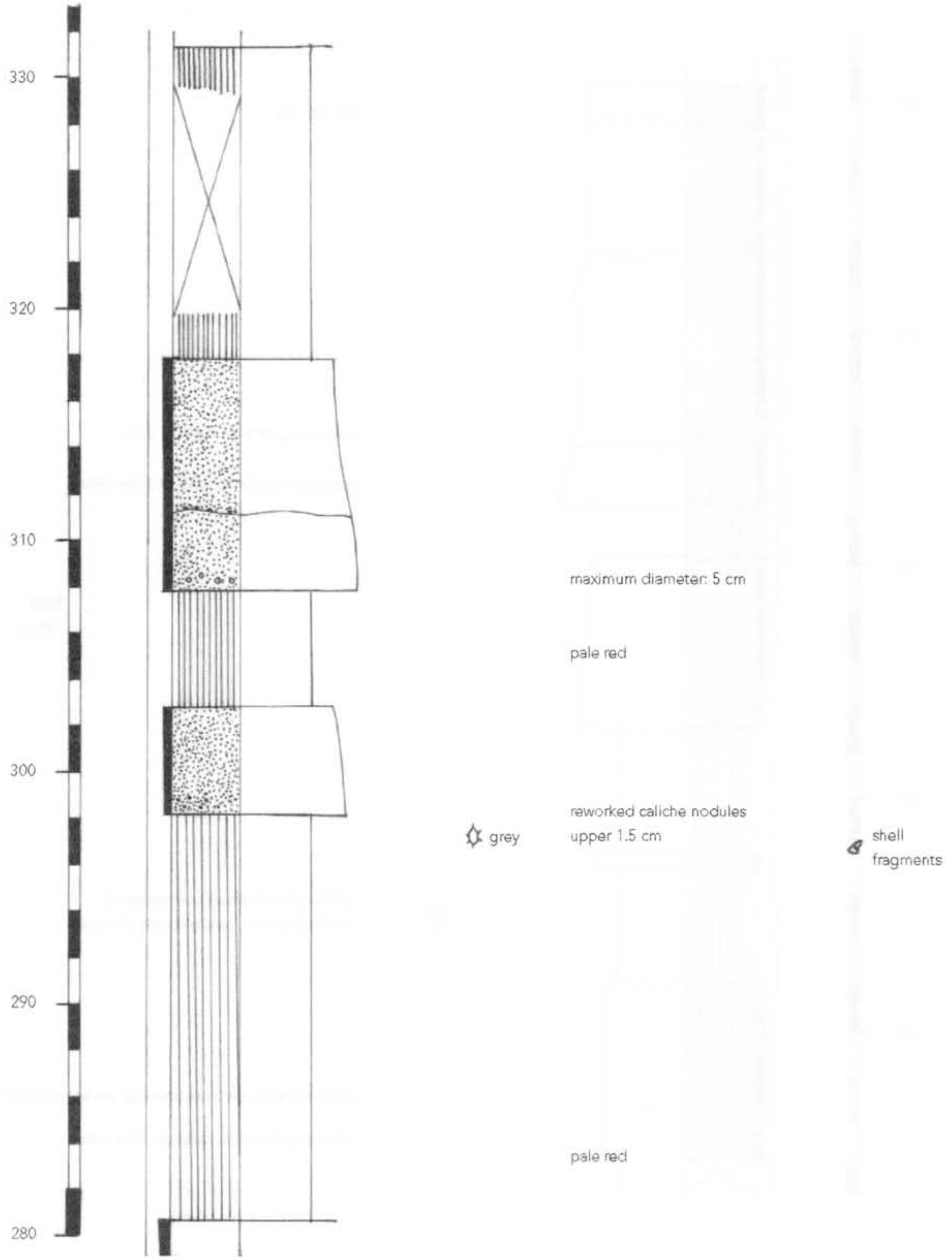

330
320
310
300
290
280
maximum diameter: 5 cm
pale red
reworked caliche nodules
upper 1.5 cm
grey
shell
fragments
pale red

App. 41

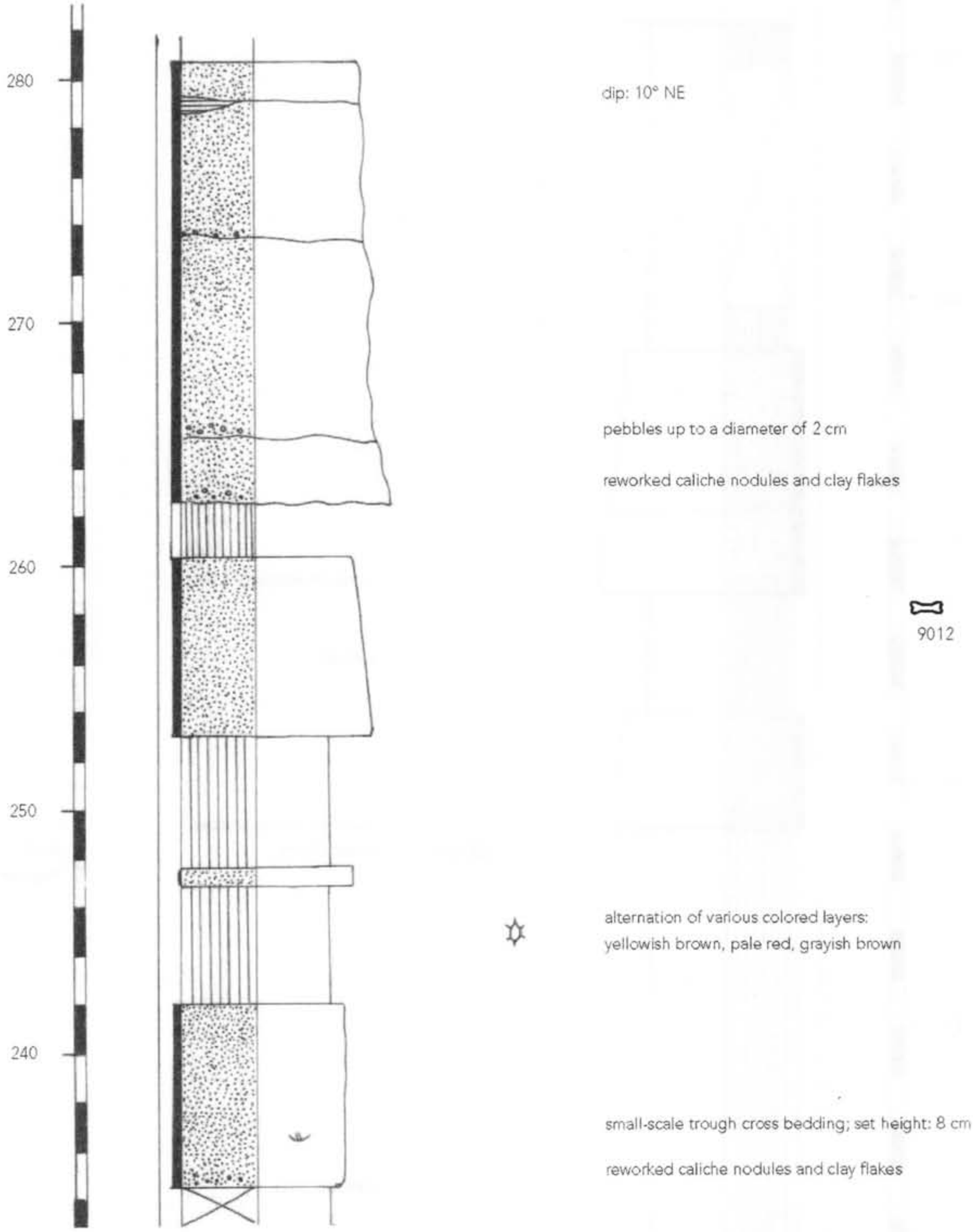
280
270
260
250
240
dip: 10° NE
pebbles up to a diameter of 2 cm
reworked caliche nodules and clay flakes
9012
alternation of various colored layers:
yellowish brown, pale red, grayish brown
small-scale trough cross bedding; set height: 8 cm
reworked caliche nodules and clay flakes

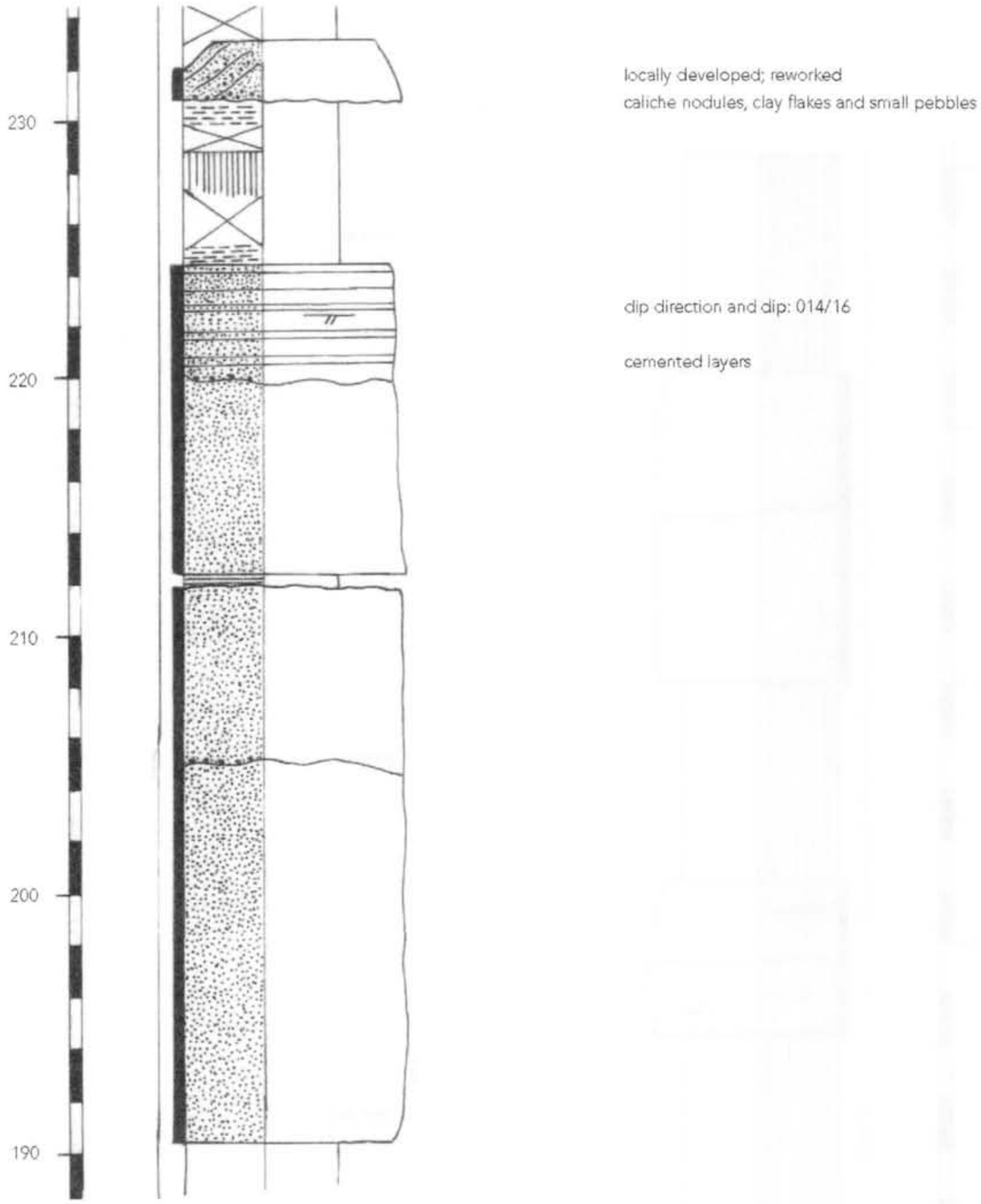
locally developed; reworked
caliche nodules, clay flakes and small pebbles
dip direction and dip: 014/16
cemented layers
230
220
210
200
190

App. 43

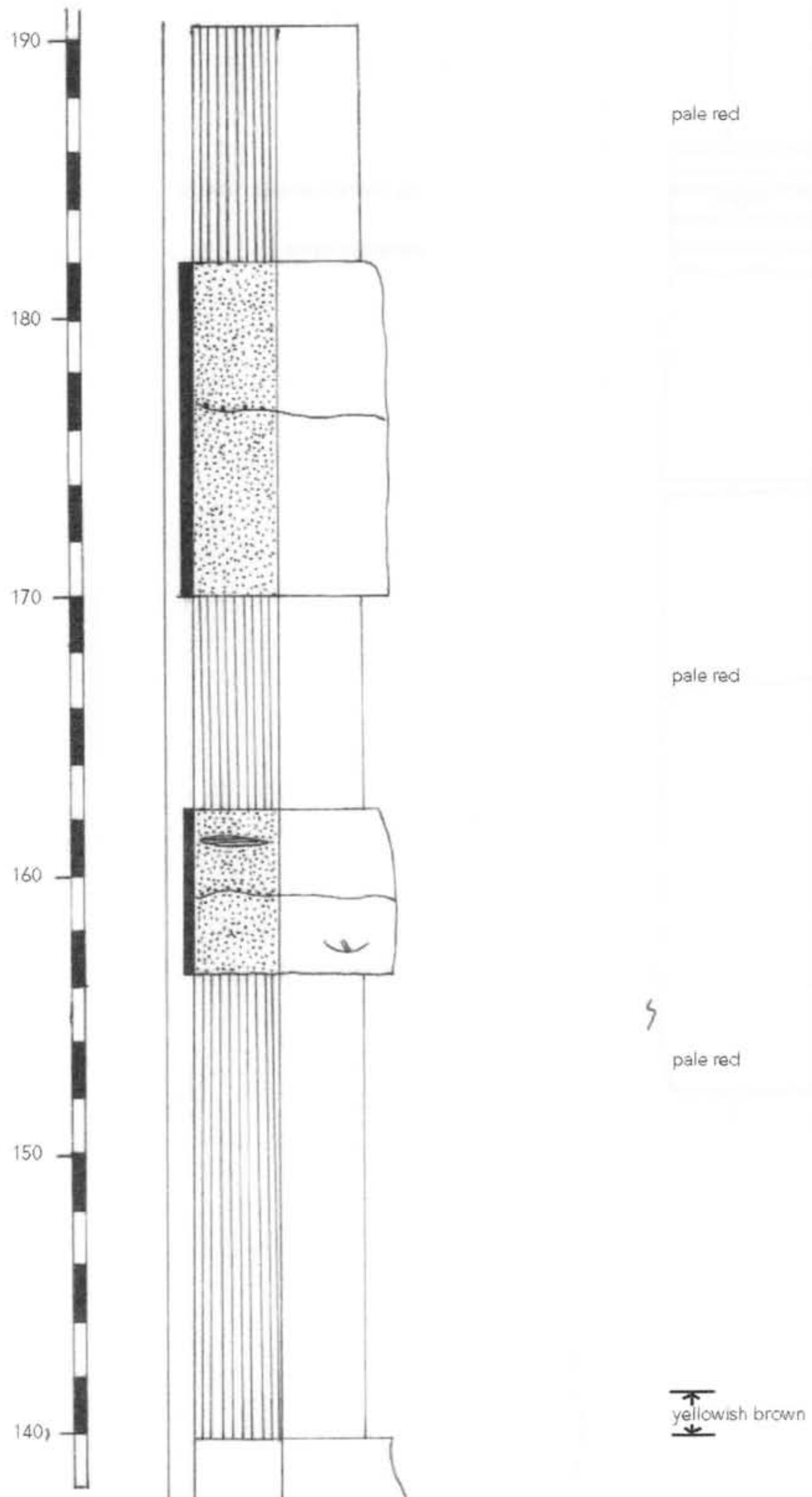
190
180
170
160
150
140
pale red
pale red
pale red
yellowish brown

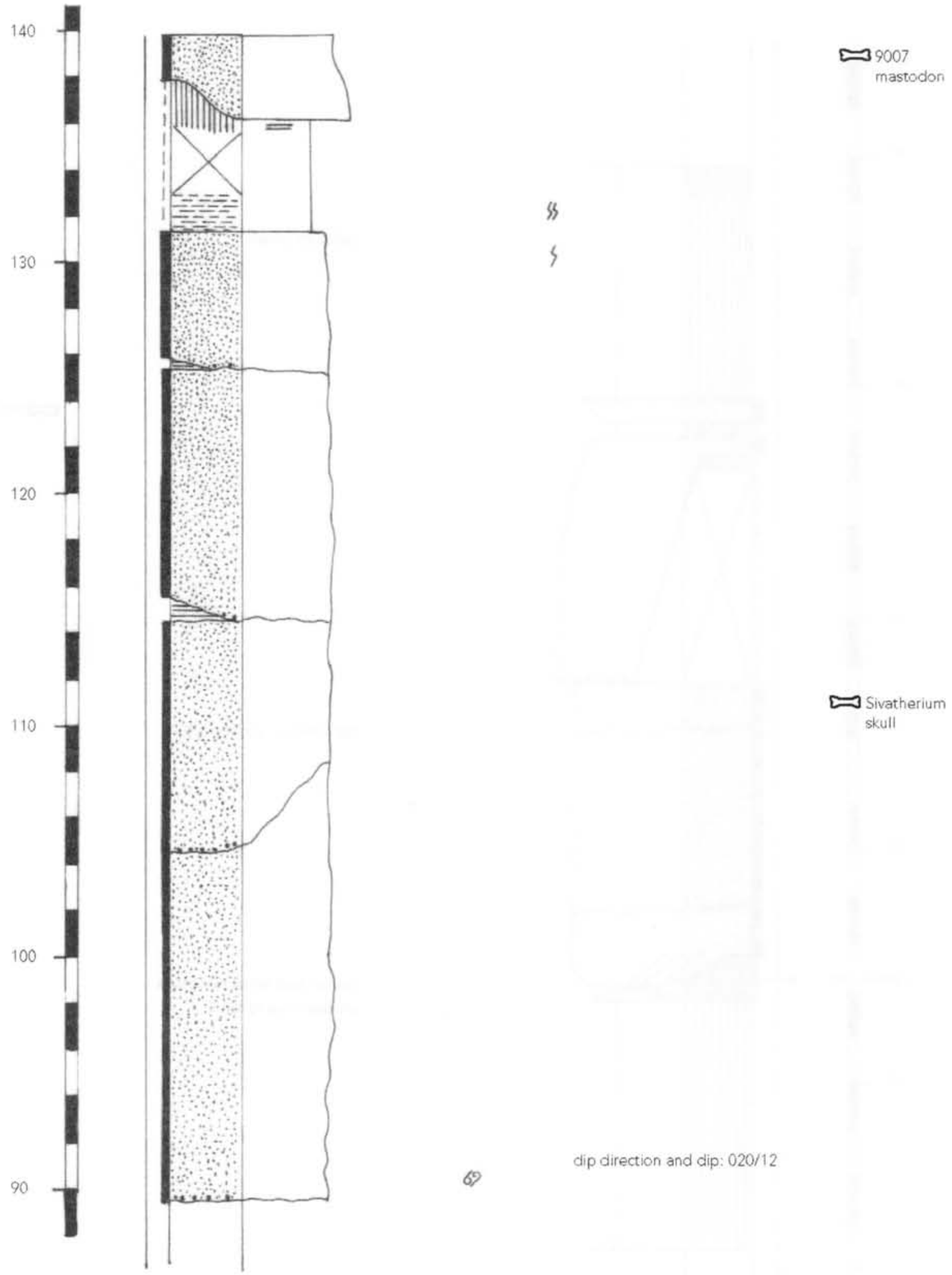

140
130
120
110
100
90
9007
mastodon
Sivatherium
skull
dip direction and dip: 020/12

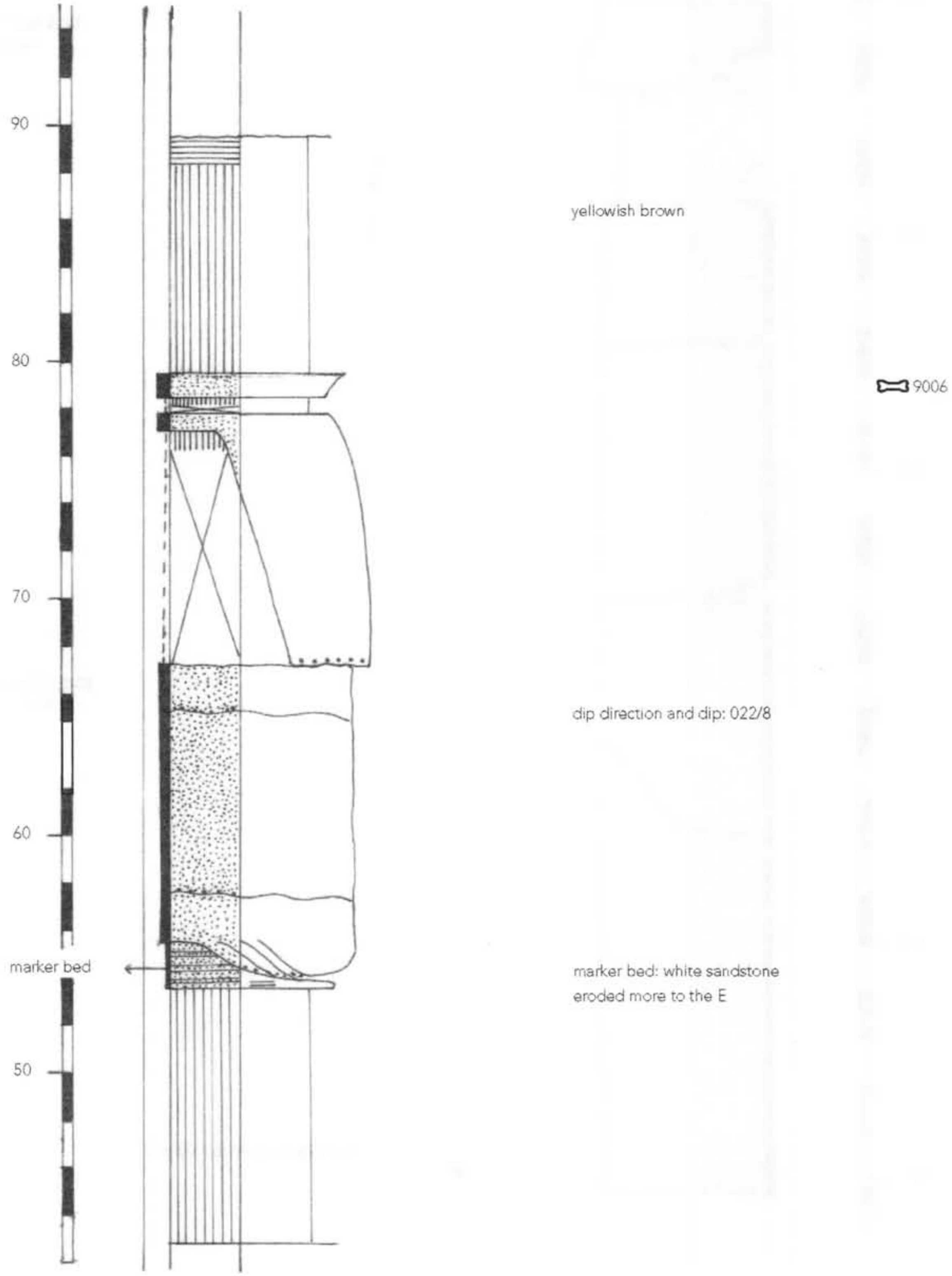
90
80
70
60
marker bed
50
yellowish brown
9006
dip direction and dip: 022/8
marker bed: white sandstone
eroded more to the E

App. 46

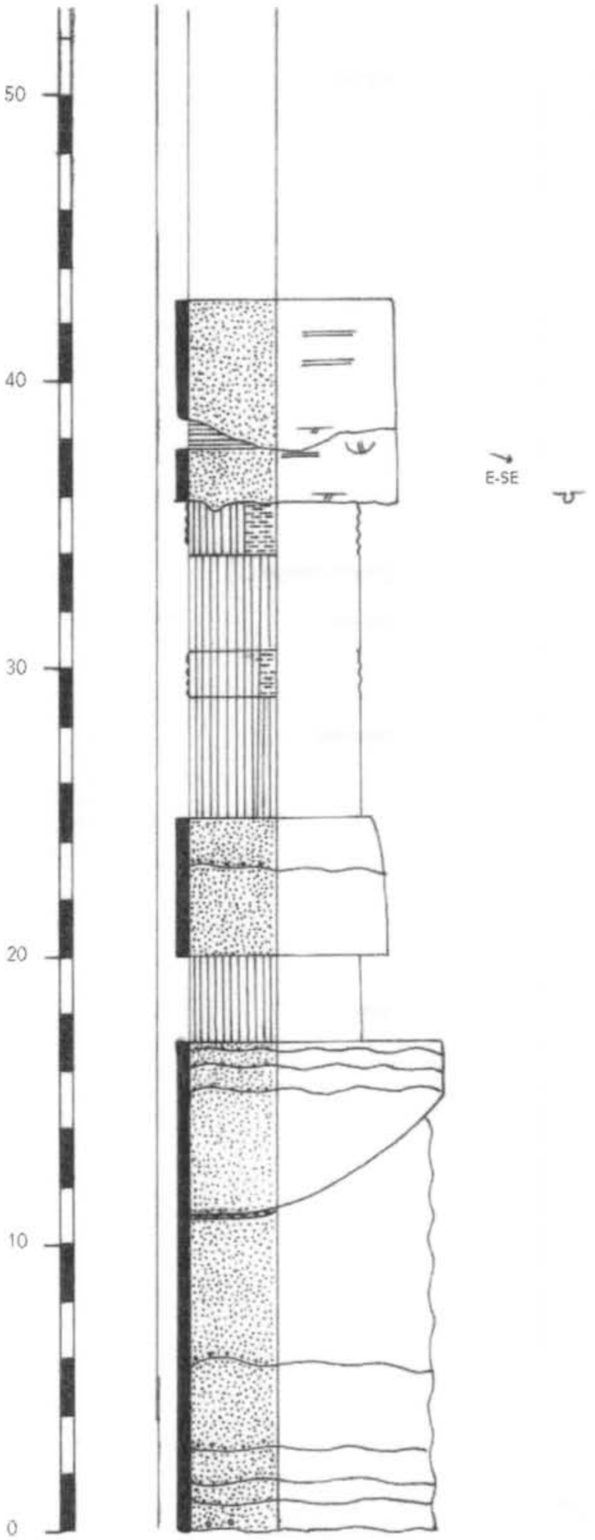

wedges out to the S

9005

tabular cross bedding; set height: 20 cm trough cross bedding; caliche nodules, clay plugs and pebbles (smaller than 1 cm) tabular cross bedding; minimum set height: 60 cm

4 silty layers 20-40 cm thick

4 silty layers 15-30 cm thick

core of anticline

dip direction and dip S-flank: 220/40; more to the south, the layers are overturned

dip direction and dip N-flank: 020/5

Dok Dara Section

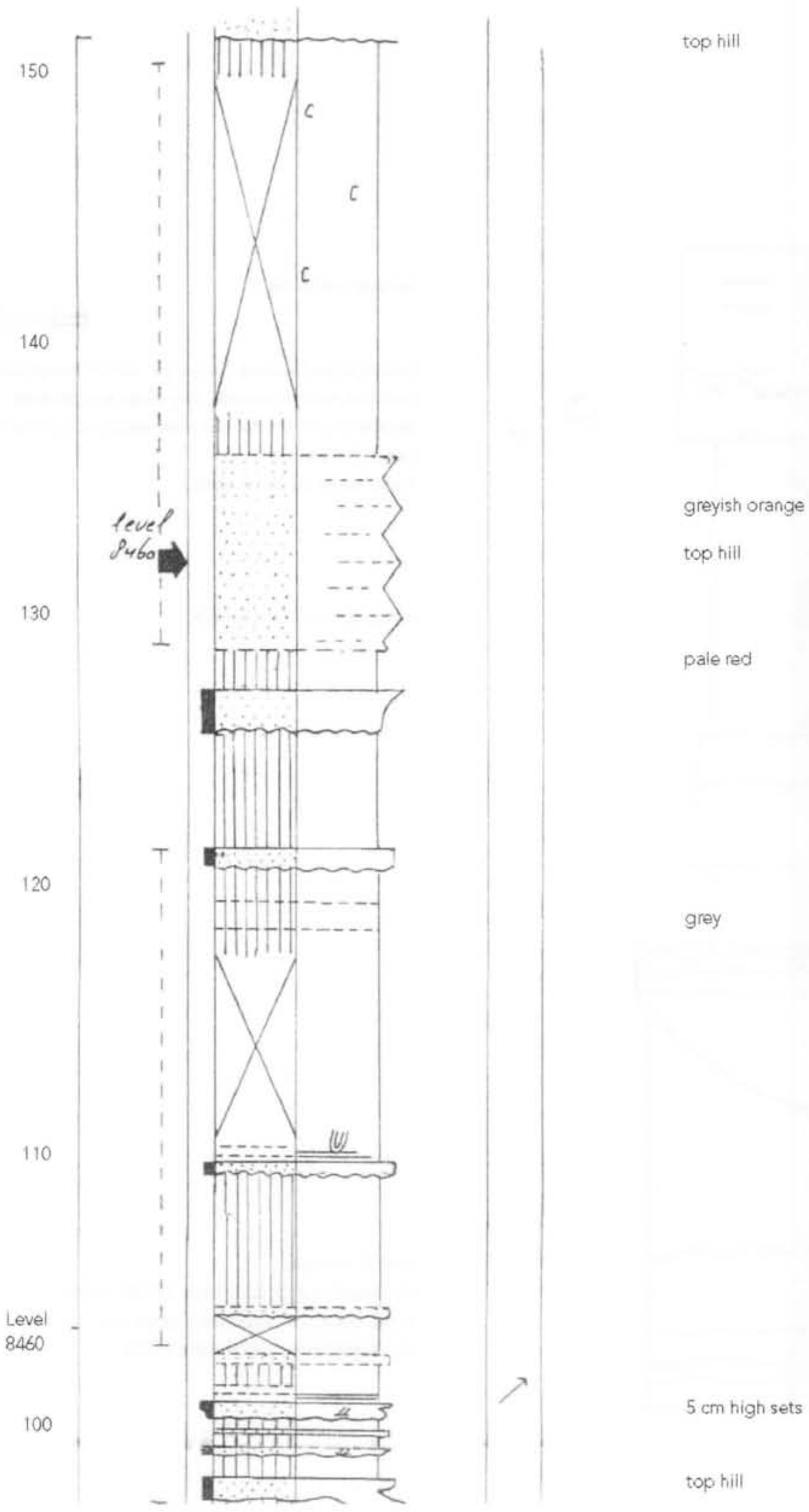

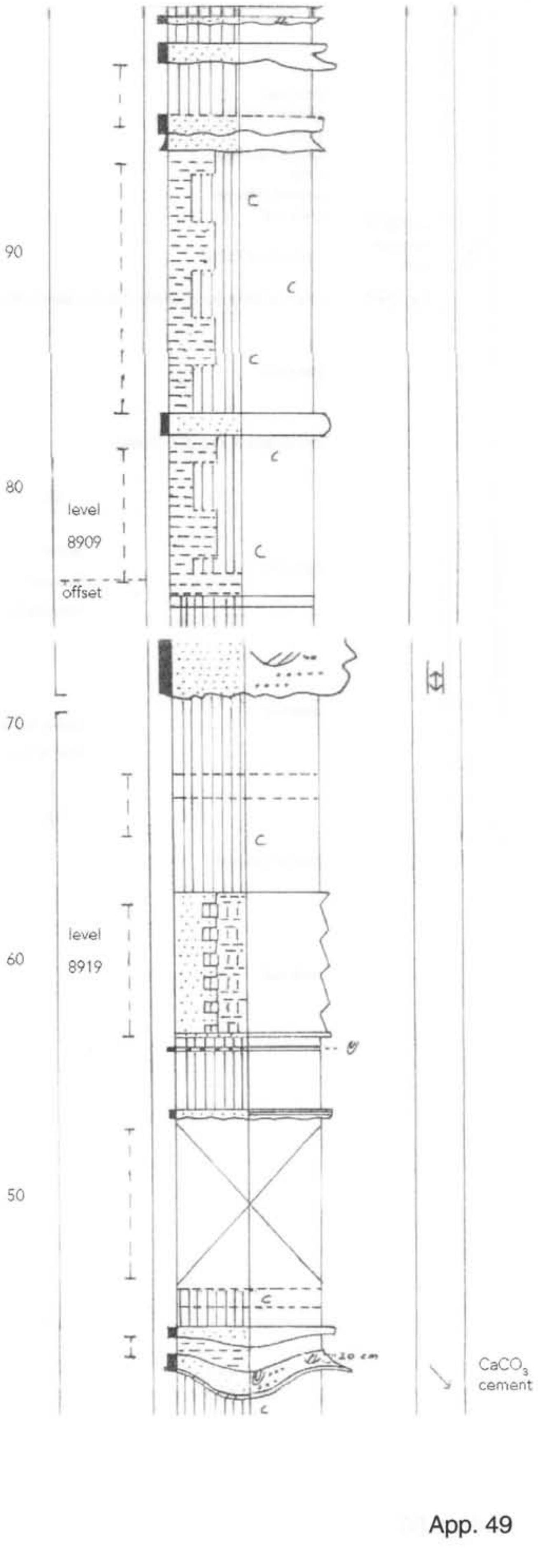

top hill

greyish orange

silty clay: alternating

greyish, orange and grey

silt: greyish orange

silty clay: alternating greyish,

orange and grey

grey

top large hill

streaks of mud flakes and caliche

nocules (diameter smaller than 1 cm)

channel dimension width: 130 cm, depth 40 cm

dip direction and dip: 185/60

grey

pale red

thickness beds 5-30 cm

alternation of silty clay, silt

and very fine sand

greyish green

greyish orange

dip direction and dip: 185/52

streaks with reworked caliche

nodulesand mud flakes

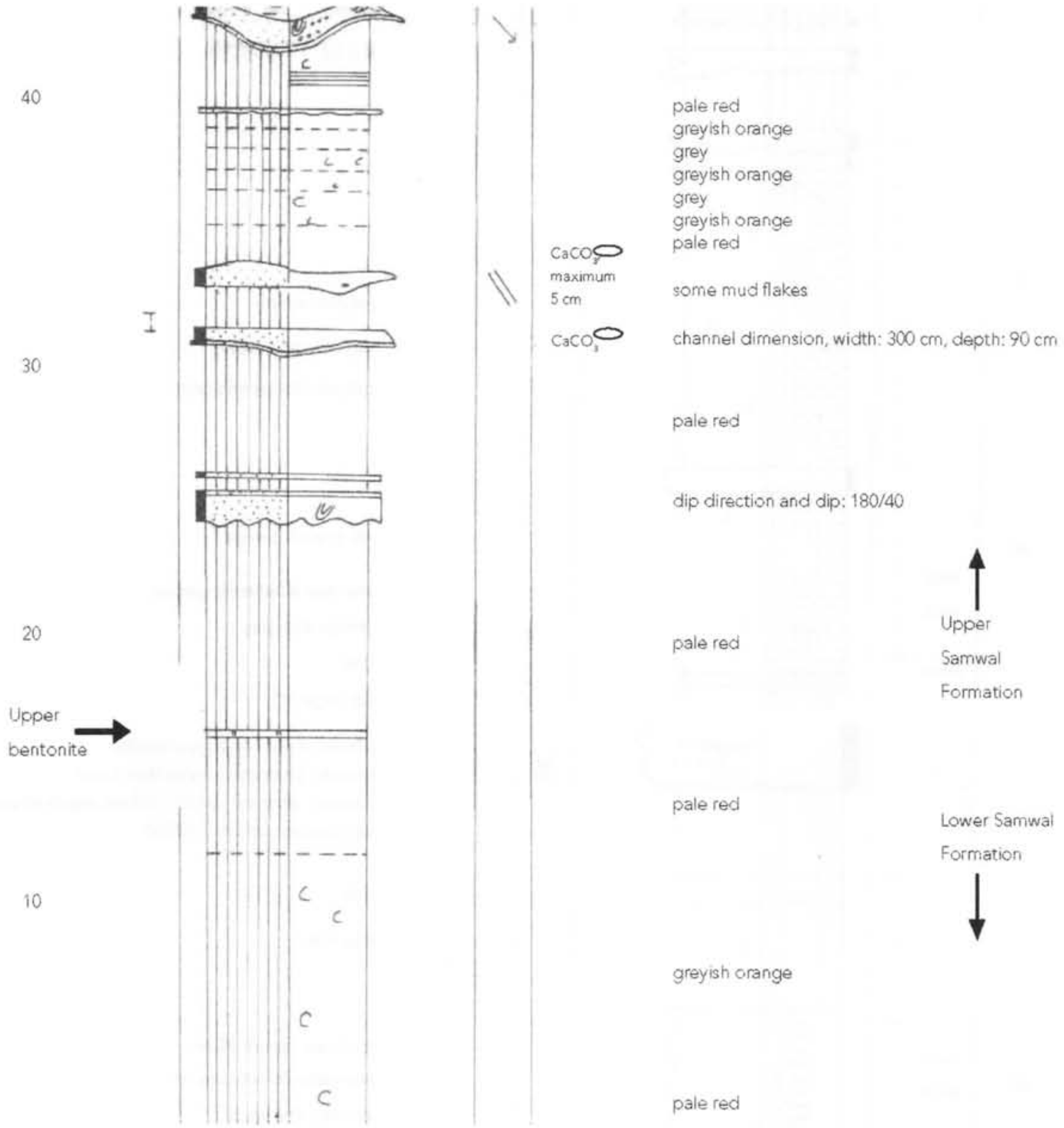

Section by J.A. van Dam (1989)

APPENDIX I-E RAKH SECTION

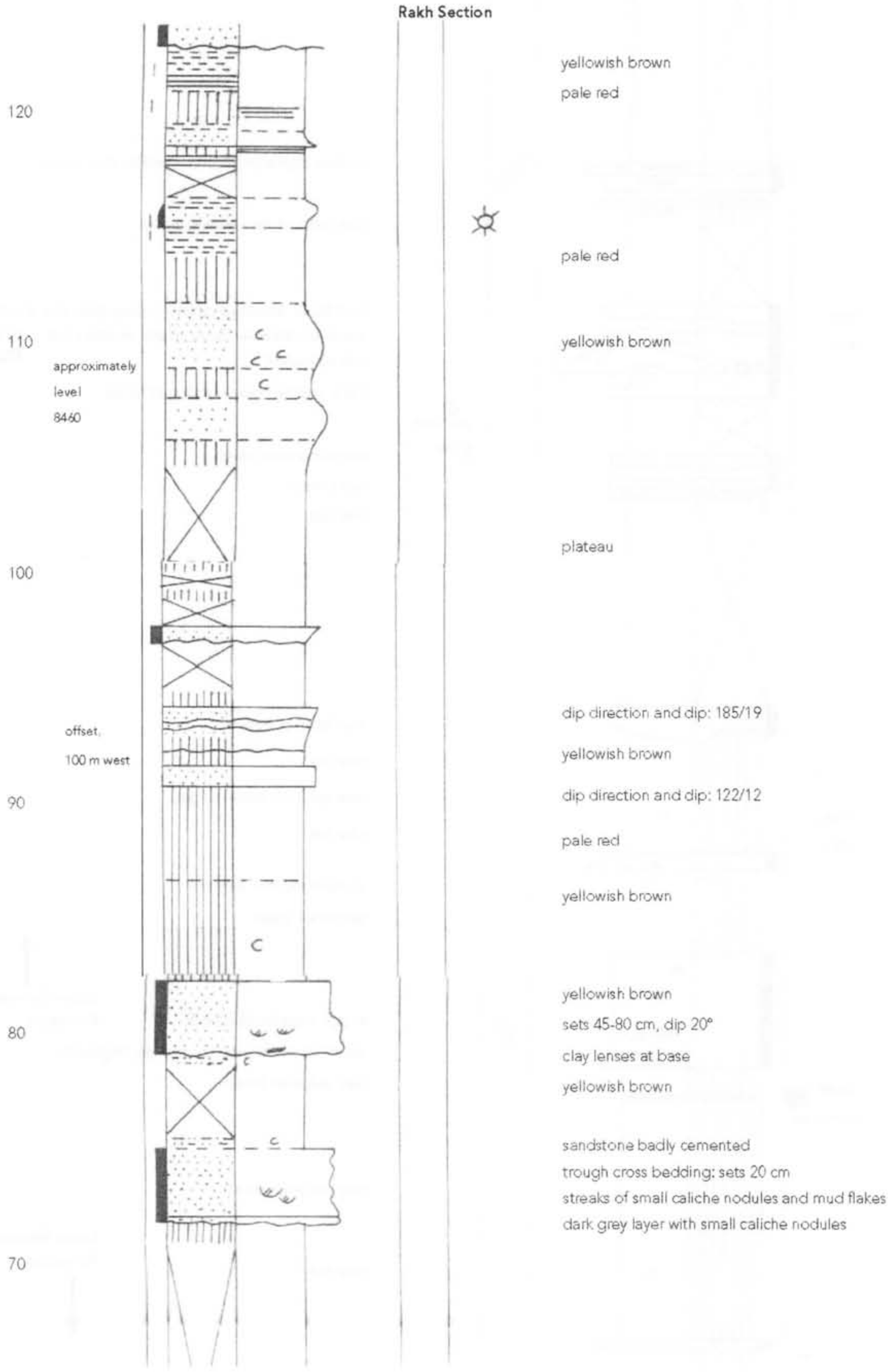

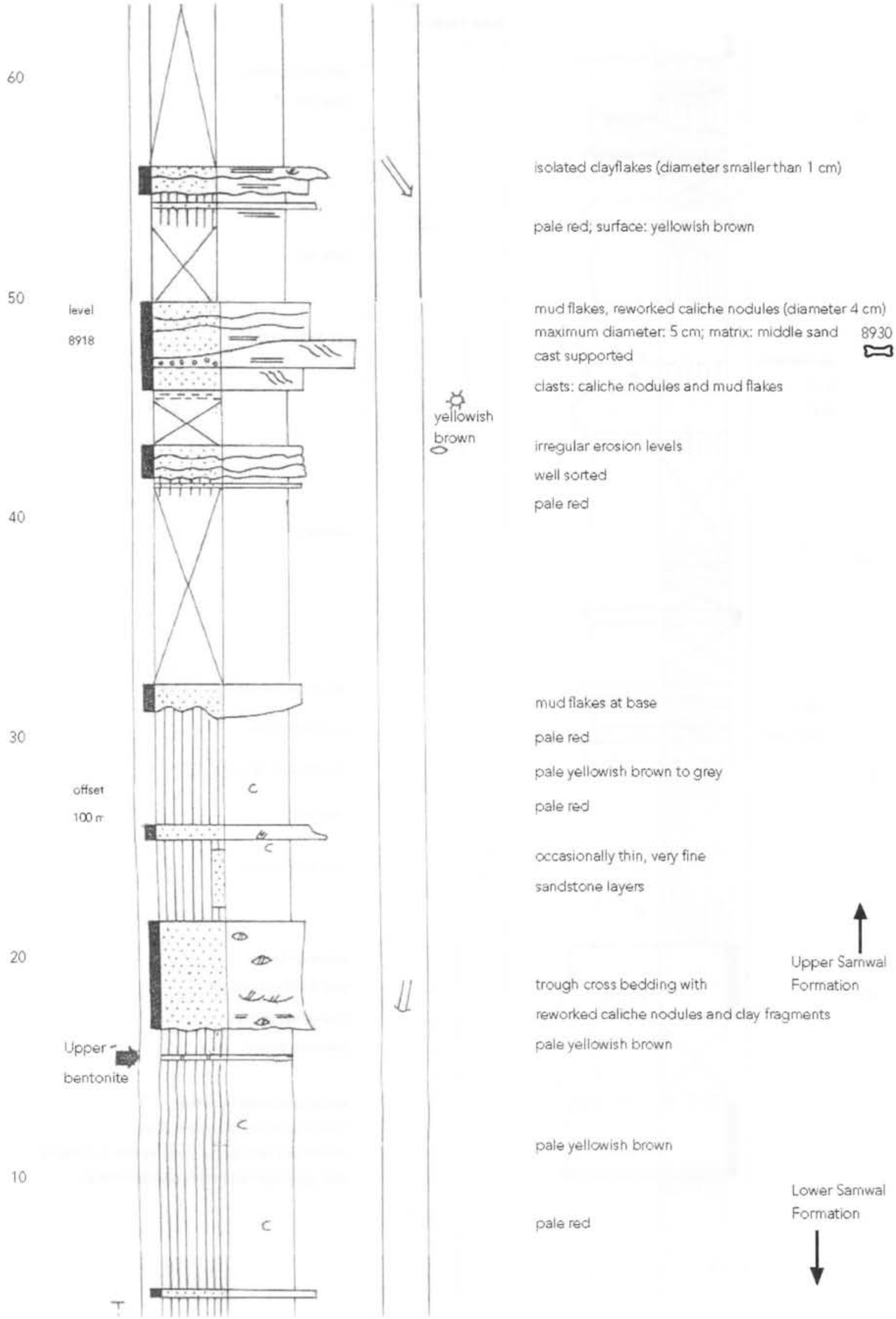
60
50
40
30
20
10
level
8918
offset
100 m
Upper
bentonite
yellowish
brown
isolated clayflakes (diameter smaller than 1 cm)
pale red; surface: yellowish brown
mud flakes, reworked caliche nodules (diameter 4 cm)
maximum diameter: 5 cm; matrix: middle sand
cast supported
clasts: caliche nodules and mud flakes
8930
irregular erosion levels
well sorted
pale red
mud flakes at base
pale red
pale yellowish brown to grey
pale red
occasionally thin, very fine
sandstone layers
Upper Samwal
Formation
trough cross bedding with
reworked caliche nodules and clay fragments
pale yellowish brown
pale yellowish brown
Lower Samwal
Formation
pale red

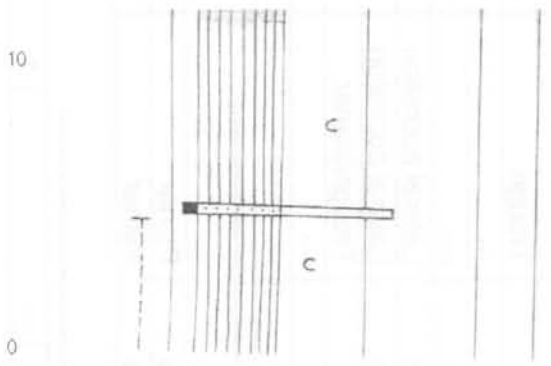

Section by J.A. van Dam (1989)

APPENDIX II SUMMARY OF THE CHARACTERISTICS OF THE FOSSIL LOCALITIES, ARRANGED IN CHRONOLOGICAL ORDER (9010 IS THE YOUNGEST, 8911 IS THE OLDEST LOCALITY.

Note the differences between the localities below (Lower Samwal Formation) and above (Upper Samwal Formation) the bentonite layers.
conglo = conglomerate; sst = sandstone; vf = very fine; f = fine; m = medium; c = coarse; vc = very coarse; parallel = parallel lamination; trough = trough cross bedding; planar = planar cross bedding; --- = no data available

Number of locality	Name of section	Located at section	Lithology	Grain size sand-stone	Caliche nodules present	Clay balls, pebbles present	Biotur-bation present	Internal erosion present	Sedimentary structures	Tapho-nomy type
9010	Samwal	Yes	Silt/sst	f	Yes	No	Yes	No	Parallel	3
8906	Samwal	Yes	Silt	---	Yes	At base	Yes	No	----	3
8910	Samwal	Yes	Silt	---	Yes	At base	Yes	No	---	3
9011	Samwal	Yes	Silt	---	Yes	At base	Yes	No	---	3
8904	Samwal	Yes	Sandy silt	---	Yes	No	Yes	No	---	3
9009	Samwal	Yes	Sandy silt	---	Yes	No	Yes	No	---	2
9008	Samwal	Yes	Sst	vf-f	Yes	No	No	No	Parallel	2
8460	Rakh	Yes	Sandy silt	---	Yes	No	Yes	No	---	3
8461	Rakh	Yes	Silt/sst	f-m	Yes	At base	No	No	Trough	2
8909	Dok Dara	No	Silt/clay	---	Yes	No	No	No	---	3
8915	Samwal	Yes	Silt	---	Yes	No	No	No	---	3
8930	Rakh	Yes	Conglo	vc	No	Yes	No	Yes	Lateral accretion	1
8918	Dok Dara	No	Sst	f-vc	No	Yes	No	Yes	Lateral accretion	2
8928	Jhel Kas	No	Sst	f-m	Reworked	No	No	No	Trough/planar	1
8932	Dok Dara	No	---	---	----	---	---	---	---	3
8905	Samwal	Yes	Sst	f-m	No	No	No	No	---	2

-------------**UPPER BENTONITE**-------------

8467	Samwal	Yes	Sst	m-c	No	Yes	No	Yes	Planar	1
8914	Rakh	Yes	Sst	m-c	No	Yes	No	Yes	Planar	1

-------------**LOWER BENTONITE**-------------

8926	Jhel Kas	No	Sst	f-c	No	Yes	No	Yes	---	1

Number of locality	Name of section	Located at section	Lithology	Grain size sand-stone	Caliche nodules present	Clay balls, pebbles present	Biotur-bation present	Internal erosion present	Sedimentary structures	Tapho-nomy type
8927	Jhel Kas	No	Sst	f-c	No	Yes	No	Yes	---	1
8457	Jhel Kas	No	Sst	vf-vc	No	Yes	No	Yes	Trough	2
8901	Samwal	Yes	Sst	m-vc	Reworked	Yes	No	No	---	2
8916	Samwal	Yes	Sst	m-vc	Reworked	Yes	No	No	---	2
8908	Jhel Kas	Yes	Sst	vf-c	No	Yes	No	Yes	Trough/planar/ parallel	1
8908	Samwal	Yes	Sst	vf-c	No	Yes	No	Yes	Lateral accretion	1
8913	Samwal	No	Sst	f-vc	No	Yes	No	No	---	2
8467 B	Samwal	Yes	Sst	vf-c	No	Yes	Yes	Yes	Trough/planar	1
8903	Samwal	Yes	Sst	vf-vc	No	Yes	Yes	Yes	Trough/planar	1
8907	Samwal	Yes	Sst	vf-vc	No	Yes	Yes	Yes	Trough/planar	1
8458	Jhel Kas	No	Sst	m	No	No	No	No	---	2
8902 B	Samwal	Yes	Sst	c-vc	No	Yes	No	Yes	Trough/planar	1
8902 A	Samwal	Yes	Sst	f-c	Reworked	No	No	Yes	Trough/channel	1
9012	Jhelawala Kas	Yes	Sst	f-m	No	No	No	No	---	2
8924	Jhel Kas	No	Sst	m-vc	No	Yes	No	Yes	Planar/channel	1
8453	Jhel Kas	Yes	Sst	m-vc	No	Yes	No	Yes	Planar/channel	1
8459	Jhel Kas	Yes	Sst	m-vc	No	Yes	No	Yes	Planar/channel	1
9007	Jhelawala Kas	Yes	Sst	f-c	No	No	No	No	Channel	2
8923	Jhel Kas	No	Sst	vc	No	Yes	No	Yes	Parallel	1
8922	Jhel Kas	No	Sst	m-vc	No	Yes	No	Yes	Trough	1
8801	Jhel Kas	Yes	Sst	m-vc	No	Yes	No	Yes	Trough	1
8454	Jhel Kas	Yes	Sst	m-vc	No	Yes	No	Yes	Trough	1
(8922)	Jhel Kas	No	Sst	m-c	No	Yes	No	Yes	Parallel	1
9006	Jhelawala Kas	Yes	Sst	f-vc	No	Yes	No	---	Channel	2
9004	Jhelawala Kas	Yes	Sst	m	Reworked	Yes	No	Yes	Trough/planar	1

Number of locality	Name of section	Located at section	Lithology	Grain size sand-stone	Caliche nodules present	Clay balls, pebbles present	Biotur-bation present	Internal erosion present	Sedimentary structures	Tapho-nomy type
9005	Jhelawala Kas	Yes	Sst	m	Reworked	Yes	No	Yes	Trough/planar	1
8925 C	Jhelawala Kas	No	Sst	vf-m	No	No	No	Yes	---	2
8925 B	Jhelawala Kas	No	Sst	vc	No	Yes	No	Yes	Channel	1
8925 A	Jhelawala Kas	No	Sst	vc	No	Yes	No	Yes	Channel	1
8911	Jhelawala Kas	No	---	---	---	---	---	---	---	2

APPENDIX III MATERIAL

From Java the following specimens were studied:

From the Geological Museum in Bandung, Indonesia:

Number	Locality	Description of element
without number	Kali Glagah	mounted skeleton (difficult to measure and describe): **mandible** with I (alveolus of left I_1 and I_2, rest broken, alveoli of C, alveoli of P_1, P_2 dex and P_3 dex; P_2 sin (broken), P_3 sin and P_4 dex, M_{1-3} sin and dex; **cranium** with M^{1-3} sin and dex
without number	Ngandong	skull and mandible with alveolus of left I_1, left I_2 and alveolus of left I_3, all P, except P_1 (all too damaged to describe or measure), M_{2-3} (no morphology described)
without number	Tjipanaruban	separate lower left C. See also Von Koenigswald (1935, Fig. 3)
without number	unknown (Java)	separate upper left C
K 15-947	unknown (Java)	part of a left maxilla with M^1 (completely worn), M^{2-3}
M 18	Bumiayu, excavation 8	part of a right maxilla with M^{1-3} see also Van der Maarel (1932, p. 87 and Plate VI, Figs. 3-4)
4-4A	unknown (Java)	mandible fragment with the alveolus of M_1, M_{2-3} (worn)
22 G	Tji Bokagung (Tji Djolang)	complete mandible with all I, both C, P_{2-4} sin and dex, M_{1-3} sin and dex (M_1 sin very damaged)
203	unknown (Java); label unreadable	separate lower left C
528?	Gn. Butak	separate upper right C
1746	Ngandong layer III	separate lower right C

From the Museum of Sangiran, Indonesia:

Number	Locality	Description of element
without number	Rahang Bawah	mandible with on the left side the alveoli of P_{1-4} and on the right side the alveolus of P_1. The right P_{2-4} are too worn to describe. No measurements were taken.
366	Rahang Atas	cranium with M^1 sin and dex (broken), M^{2-3}
341	locality unknown (Java)	cranium with left C
466	locality unknown (Java)	right mandible fragment with M_{2-3}

From the Laboratory Bioanthropologi and Paleoanthropologi in Yogyakarta, Indonesia:

Number	Locality	Description of element
without number	Medalem	mandible with on the left side the alveolus of P_1, P_2, P_3 (broken), the alveolus of P_4 and on the right side the alveoli of P_1, P_2 , P_3 and P_4 this fossil was in a showcase, therefore the values of the measurements are approximate
without number	Sangiran	left mandible fragment with $M_{1\text{-}3}$. Measurements taken with a measuring tape

From the Geological Research and Development Centre, Quaternary Geology Laboratory in Bandung, Indonesia:

Number	Locality	Description of element
SA 030979-14	New Pb site?	three pieces of a lower I; the pieces fit
SA 040979-16	New Pb site	three pieces of a lower I; the pieces fit
SA 040979-20N	New Pb site	1) separate left M1 (fits to 2) 2) mandible fragment with left M2 (fits to 1) 3) separate right M2 (fits to the M3 of SA 110979 see also Watanabe et al. (1985, Plate XXIII, Fig. 2)
SA 040979-24	New Pb site	separate upper left C
SA 040979-30D	New Pb site	1) separate upper right C 2) separate right P3 3) separate right P3
SA 040979-30L	New Pb site	separate lower left C
SA 040979-30M	New Pb site	separate lower right C
SA 110979	New Pb site	right M_3, fits to SA 040979-20N (3 see also Watanabe *et al.* (1985, Plate XXIII, Fig. 5)
SA 140979-7	New Pb site	six pieces of lower I, from which partly one incisor can be reconstructed
SA 160878-180	(Cemoro) Dam site, P12	little part of lower I (length 50.5 mm)
SA 230178	Pd III-14, grenzbank	part of right lower I
SA 230779	P VIII digging site	four pieces of lower right C
SA 270378	Triangulation Point, Ngebung	left mandible of a juvenile with the alveoli of all the incisors, the alveolus of dC, DP_2, the roots of DP_3 and Dp_4. The mandible is broken along the symphysis see also Watanabe *et al.* (1985, Plate XXIII, Fig. 1)
M 16	Bumiayu, excavation 9; Kali Biuk	separate lower right C see also Van der Maarel (1932, p. 88, spec. A, Plate V, Fig. 5)

Number	Locality	Description of element
Bumiayu exc. 8	Bumiayu excavation 8	separate lower left C. See also Van der Maarel (1932, p. 88, spec. B)
K 149	Kedung Kuduh, Sangiran	right mandible fragment with M_1 (broken and worn; no measurements could be taken), M_{2-3}. See Von Koenigswald (1934, Plate IV, Fig. 4)
K 150	Ngandong	separate right M_2. See Von Koenigswald (1934, Table IV, Figs. 5 and 6)
K 158	Tjipanarabun	separate lower left C in matrix. See also Von Koenigswald (1935, Plate IV, Fig. 4)
K 522	Kali Glagah	separate lower left C
K 525	Kali Glagah	1) separate left DP_4. On the other side of the premolar, under the hypoconid and the entoconid is a ticket on which is written: C/XVIII 16. 2) separate left DP_4 On the posterior side of this premolar is a ticket with the remark: C/XVIII 16.
K 6.. The number is not readable any more. K. Gl.. could refer to Kali Glagah, but it can also be read as K. 61.	Kali Glagah?	separate left P_3
K 653	Gn. Butak	1) separate left P_2 2) probably separate left P_3 3) separate left P_3 4) separate right P_3
K 654	Gn. Butak	separate lower left C
K 655	Gn. Butak	1) separate, worn right M^1 2) separate, worn left M^1 3) separate, worn left M^1
K 657	Ngandong	left mandible fragment with M_2 (very damaged) and M_3
K 672	Kali Glagah	separate, very damaged left M^2
K 674	Kali Glagah	1) separate left M^1 2) separate right M^1
K 675	Kali Glagah	1) separate probably right P_1 2) separate right P_4 3) separate left P_4
K 676	Ngandong	separate left M^2
K 685	Ngandong	separate left P_3
K 689	Ngandong	separate right P_2
K 693	Kali Glagah	separate right P_2

Number	Locality	Description of element
K 694	Kali Glagah	separate left M^3
K 698	Kali Glagah	separate left P_3
K 699	Ngandong	separate right P_3
K 705	Gn. Butak	(left maxilla fragment) with M^1 (totally worn), M^{2-3}
K 707	Gn. Butak	separate left M_3
K 710	Ngandong	1) separate lower right C 2) separate upper left C
K 713	Gn. Butak	1) no. 526 separate lower right C 2) no. 527 separate lower right C 3) without additional number, separate lower right C 4) no. 523 part of a separate lower C
K 714	unknown (Java)	(part of a right maxilla) with all I
K 715	Gn. Butak	1) separate lower right C 2) separate upper right C
K 716	Kali Glagah	1) separate lower right C 2) separate upper right C
K 716?	Kali Glagah	separate part of an upper I. the number was hardly readable; it possibly is 716, because it is the only number beginning with 71 that might be considered, although it is stated in the catalogue that K 716 is a lower canine.
K 717	Ngandong	1) Label on fossil: 7706 Ingraving I^c Ngandong laag II 23-3-32; catalogue of Von Koenigswald: 7705, Ingraving 1^c, Ngandong laag II, 23-3-32 (Pendek): left I 2) label on fossil: 1146^b Ingr: IB. blok F Ngandong laag IV; catalogue of Von Koenigswald: 1146^b Ingr.I^B blok F, laag II, 28-10-32 (Panjan): left I
K 718	Kali Glagah	three separate lower I, two left ones (1 and 2), one right one (3)
K 719	Kali Saat	separate left lower I
K 720	Kali Saat	1) piece of lower left C 2) piece of lower C
K 723	Ngandong	1) on the label is written: label 20 ... Ingraving... Ngandong ...g III.....8-31 (.... means not readable); separate left M_3 2) on the label is written: label 425, Ingraving IB, Ngandong laag II 1931; separate left M_3 3) on the label is written: 7481, Ingr. IV blok A ..... (.... means not readable); posterior part of a left M_3 4) separate left M^2

Number	Locality	Description of element
K 727	Ngandong (Rahang Bawah)	(left mandible) with M_1 (very damaged), $M_{2\text{-}3}$
K 731	Sangiran	(left mandible fragment) with $M_{1\text{-}3}$
K 732	Kali Glagah	(maxilla fragment) with left C
K 733	Kali Bringin, Ngawi	separate lower right C
K 734	Ngandong	1) separate, very ramshackle right M^1 2) separate, very ramshackle right M^2
K 740	Kali Bengawan, Solo	(left mandible fragment with) M_3
K 741	unknown (Java)	(right mandible fragment with) M_2 and M_3 (damaged)
K 742	Sangiran	1) separate left M_1, which fits to 2) (very worn) 2) separate left M_2, which fits to 1) 3) separate right M_3 these molars were together in a showcase, which seem to fit, but the M_3 is a right one
K 743	Sangiran	(right mandible fragment with) $M_{2\text{-}3}$
K 745	unknown (Java)	(right mandible fragment with) $M_{2\text{-}3}$
K 746	Watualang	(right mandible fragment with) $M_{2\text{-}3}$
K 747	Gn. Butak	separate right lower I
K 748	Pandeyan/Pandejan	separate upper left C
K 749	Kedung Brubus	(right maxilla fragment with) $M^{1\text{-}3}$
K 790	Ngandong	mandible, rather strange-looking and heavily restored, with left and right I_1, left I_2 and left I_3
K 1567	Gn. Butak	separate lower right C

From the Collection Dubois in Naturalis, the Nationaal Natuurhistorisch Museum (National Museum of Natural History) in Leiden, The Netherlands:

Number	Locality	Description of element
Coll. Dub. without no.	unknown (Java)	(piece of premaxilla with) an incisor
Coll. Dub. without no.	unknown (Java)	separate right DP^4
Coll. Dub. without no.	Java	left mandible fragment with C, the alveoli of $P_{2\text{-}4}$ it seems to belong to Coll. Dub. 4857, but it does not fit
Coll. Dub. 87	Kali Gedeh	1) separate left P_2 2) posterior part of a separate right M_3
Coll. Dub. 94	Pati Ajam	separate left P^3

Number	Locality	Description of element
Coll. Dub. 95	Tritik	two separate lower I, a left and a right one
Coll. Dub. 96	Kedung Brubus	(left maxilla fragment with) P^{2-3} and a small part of DP^4 (totally worn). In the box, where this premolar is stored, was a note: same colour as Coll.Dub.2203 and 284; belongs to Coll. Dub. 313
Coll. Dub. 97	Redjuno	left mandible fragment with M_1 (broken and not measurable, M_2 (broken) and M_3
Coll. Dub. 98	Java	right mandible fragment with C, M_{2-3} (the M_2 was only approximately measurable and is not in Appendix VI.19
Coll. Dub. 99	Tritik	mandible fragment, restored with plaster with all I, both C's, on the left side a rugosity which indicate P_1, P_{2-4} (broken) and on the right side the alveolus of P_2, P_3 (broken), P_4, M_{1-3} sin and dex (right M_1 broken and not measurable) see also Hooijer (1950, p. 73-74 and Plate X, Figs 1 and 3)
Coll. Dub. 100	Java	1) fragment of a lower left C 2) fragment of a lower C 3) part of a lower C 4) part of a lower C 5) posterior part of a separate right M^3
Coll. Dub. 105	Teguan	1) separate right P_4 2) separate probably left M_1 3) separate probably right M_2
Coll. Dub. 163a	Pati Ajam	separate right M^3. See also Hooijer (1950, p. 83 and Plate VIII, Fig. 8)
Coll. Dub. 272a	Bogo	separate right M_2
Coll. Dub. 272b	Bangle	separate right P_3
Coll. Dub. 285	Dekes/Wadegan	1) separate damaged left lower I 2) fragment of upper C 3) fragment of upper right C 4) separate left P_3 5) talonid of a separate right M_3 6) posterior or anterior part of M^2 or M^3 7) posterior or anterior part of M^2 or M^3 8) posterior or anterior part of M^2 or M^3

Number	Locality	Description of element
Coll. Dub. 308a	Sumber Waru	According to the catalogue of the Dubois Collection in Naturalis, the Nationaal Natuurhistorisch Museum (Leiden, The Netherlands), this is a mandible fragment. But it is a maxillary fragment as part of the palate is present and the molar is too broad for a lower molar. The molar (probably a M^2) is very worn and broken.
Coll. Dub. 308c	Kedung Brubus	separate upper left C
Coll. Dub. 308d	Java	1) fragment of lower right C 2) separate upper C 3) separate upper right C
Coll. Dub. 310	Kedung Brubus	left mandible fragment with $M_{2\text{-}3}$ (M_2 broken and not measurable)
Coll. Dub. 311	Kebon Duren	1) separate upper left C without a wear facet 2) separate upper right C
Coll. Dub. 313	Kedung Brubus	1) separate right P^3 2) separate right P^3
Coll. Dub. 314? without number; in the box with number Coll. Dub. 314	Kedung Lumbu?	fragment of lower right C (length 74.6 mm)
Coll. Dub. 314a	Kedung Lumbu	1) separate left M^3 2) separate right M^3 see also Hooijer (1950, p. 69 and Plate VIII, Figs. 13-14)
Coll. Dub. 314b	Kedung Lumbu	separate left M_3
Coll. Dub. 323a	Kedung Brubus	1) right mandible fragment with $M_{2\text{-}3}$ 2) separate left M_3
Coll. Dub. 323b	Kedung Brubus	separate right M_3
Coll. Dub. 323c	Java	small piece of mandible with probably a left DP_4
Coll. Dub. 324	Java	separate, totally worn M_1
Coll. Dub. 324a	Java	separate right P_2
Coll. Dub. 325d	Java	1) separate left P^4 2) separate right M_3 3) posterior part of a separate left M_3

Number	Locality	Description of element
Coll. Dub. 325f	"Trinil"*	1) fragment of an upper C 2) separate right P^4 3) separate, damaged right M^2 According to Hooijer (1950, p. 109) the exact locality is not known
Coll. Dub. 425a	Java	1) posterior part of a separate left P_3 2) separate left P^1 3) fragment of a separate, probably right P^3
Coll. Dub. 513	Nonko, NW of Trinil	mandible fragment with left I_1, left I_2 and left I_3 (all broken), posterior end of left C, part of the right C, probably right P_3 (broken). See also Hooijer (1950, p. 75)
Coll. Dub. 548	Kedung Lumbu	separate upper left C According to Hooijer (1950, p. 109) the exact locality is not known
Coll. Dub. 1483	Ngawi	separate left P_2
Coll. Dub. 1702	Kedung Lumbu	cranium fragment with alveolus of left P^1, P^2 sin and dex, P^3 dex, DP^4 dex, M^1 dex, $M^{2\text{-}3}$ sin and dex. See also Hooijer (1950, p. 81-82 and Plate VII, Fig. 2).
Coll. Dub. 1718	Bangle	part of a right mandible with the broken root of the P_3 and P_4
Coll. Dub. 1804	Redjuno near Teguan	right mandible fragment with I_1 and I_2, C, P_3 and P_4 (both broken), M_1 (not measurable), $M_{2\text{-}3}$
Coll. Dub. 1818	Redjuno	left mandible fragment with I_3, C, alveoli of $P_{2\text{-}4}$
Coll. Dub. 2000	Kedung Lumbu	1) separate upper left C 2) separate upper right C 3) separate right P_3
Coll. Dub. 2003a	Bogo	1) separate right M_2 2) separate right M_3
Coll. Dub. 2003b	Teg (=Teguan)	1) separate left P_3 2) separate right P_3 3) separate left P^3
Coll. Dub. 2004	Java	left maxilla fragment with $M^{2\text{-}3}$. According to the catalogue of the Dubois Collection (Naturalis, the National Museum of Natural History in Leiden, The Netherlands) it is a mandible fragment, but the morphology of the molars and, moreover, the remnants of the palate show that it is a maxillary fragment.
Coll. Dub. 2006	Java	separate left M_3
Coll. Dub. 2008	Java	separate left M_1
Coll. Dub. 2008a	Java	separate right M_2

Number	Locality	Description of element
Coll. Dub. 2008b	Kedung Brubus	1) separate right M^2. See also Hooijer (1950, p. 69 and Plate VIII, Figs. 11-12) 2) separate left M^2
Coll. Dub. 2013	Kedung Brubus	left mandible fragment with M_2
Coll. Dub. 2017	Java	1) fragment of a lower left or right C (length 26.6 mm); it is not clear which side is anterior or posterior 2) fragment of a right M_3 3) posterior part of a separate right M^2
Coll. Dub. 2019a	Kedung Brubus	separate lower left C, fits to a little part of a canine without a number.
Coll. Dub. 2019b	Papa Djaran, N of Kebon Duren	separate lower left C
Coll. Dub. 2019c	Kedung Brubus	separate upper right C
Coll. Dub. 2023	Java	1) fragment of P^4 2) fragment of a left P^3
Coll. Dub. 2023?	Sumber Waru?	In the box with these premolars was a note: "2023? colour like 2078 Sumber Waru". So it is not certain if these specimens have the number Coll. Dub. 2023 and the locality is assigned according to the similarity in colour with specimen from Coll. Dub. 2078 (which comes from Sumber Waru). 1) separate right P^4 2) separate right P^1 3) separate left P^1
Coll. Dub. 2023c	Sumber Waru	separate left M^1 (fits to Coll. Dub. 2195a) see also Hooijer (1950, p. 83 and Plate X, Fig. 4)
Coll. Dub. 2076	Kedung Brubus	There are six boxes with this number, with a total of 13 separate fragments of canines, ten of which are not measurable and the conclusion that they are upper canines is the only thing that can be said about it. 1) fragment of upper C 2) fragment of upper left? C 3) fragment of upper C 4) root of a P^1 5) lingual part of a probably left P^4 6) separate left M_1 7) left mandible fragment with M_1 (broken), M_2 (damaged) and the alveolus of M_3 8) separate right M_3 fragment 9) posterior part of a right M_3

Number	Locality	Description of element
Coll. Dub. 2076 (continued)	Kedung Brubus	10) posterior part of a right M_3 11) posterior part of a right M_3 12) anterior part of a separate right M^3 13) anterior part of a separate left M^3 14) posterior part of a separate (left?) M^3 15) posterior part of a separate left M^3 According to Hooijer (1950, p. 109) the exact locality is not known
Coll. Dub. 2076a	Kedung Brubus	1) separate upper I 2) separate upper I 3) separate lower right C 4) fragment of a separate lower C 5) fragment of a separate lower C according to Hooijer (1950, p. 109) the exact locality is not known
Coll. Dub. 2077a	Kedung Lumbu	1) separate lower I 2) separate right M^2 (see also Hooijer (1950, p. 83 and Plate VIII, Figs. 3-4)
Coll. Dub. 2077b	Kedung Lumbu	separate left M^3. See also Hooijer (1950, p. 83 and Plate VIII, Figs. 1-2)
Coll. Dub. 2077c	Java	1) separate right M^2 2) anterior part of a separate right M^2 or M^3
Coll. Dub. 2078	Sumber Waru	1) separate upper right C (between brackets no. 2080) 2) separate upper left C
Coll. Dub. 2079	Sumber Waru	maxilla with P^4 sin and dex, M^1 sin and dex (very worn and damaged), M^{2-3} sin and dex. See also Hooijer (1950, p. 62-63 and Plate V, Fig. 4)
Coll. Dub. 2080a	Sumber Waru	separate right M^3 (fits to Coll. Dub. 2195b) see also Hooijer (1950, p. 83 and Plate II, Fig. 2)
Coll. Dub. 2080b	Sumber Waru	separate upper right C According to Hooijer (1950, p. 109) the exact locality is not known
Coll. Dub. 2082	Teguan	right mandible fragment with M_{2-3}
Coll. Dub. 2084a	Kedung Lumbu	maxilla fragment
Coll. Dub. 2084b	Bogo	right maxilla fragment with M^{2-3} see also Hooijer (1950, p. 82-83 and Plate VIII, Fig. 5)
Coll. Dub. 2084c	Kedung Brubus	separate upper right C without a wear facet
Coll. Dub. 2084d	Kedung Brubus	separate lower left C

Number	Locality	Description of element
Coll. Dub. 2174	Kedung Brubus	left mandible fragment with C (front part is broken off), part of the root of P_2 and the alveoli of P_3 and P_4
Coll. Dub. 2182	Kedung Lumbu	according to Hooijer (1950, p. 109), the exact locality is not known 1) part of a right premaxilla with one I^2 and the alveolus of I^3 2) part of a (left?) premaxilla with two damaged alveoli of I 3) Part of a left maxilla with P^{1-2} (broken) 4) separate right M^1 5) separate bulla
Coll. Dub. 2188	Kedung Lumbu	left cranium fragment with DP^1 (broken), P^{2-3}, DP^4, M^1, M^2 (broken), M^3 see also Hooijer (1950, p. 69 and Plate VIII, Fig. 10)
Coll. Dub. 2189	Kedung Lumbu	part of a separate upper I^2
Coll. Dub. 2190a	Kedung Brubus	1) very big, separate lower right C 2) separate upper right C, restorated with plaster 3) separate, very ramshackle right C
Coll. Dub. 2191	Java	anterior part of a separate right M_2 or M_3
Coll. Dub. 2191a	Kedung Lumbu	separate upper right C. According to Hooijer (1950, p. 109) the exact locality is not known
Coll. Dub. 2191b	Java	1) separate upper I 2) fragment of lower C 3) fragment of lower C
Coll. Dub. 2192	Java	left mandible fragment with M_3
Coll. Dub. 2192b	Java	1) part of a separate right M_3 2) posterior part of a separate left M_3
Coll. Dub. 2193	Bangle	According to the catalogue this is a part of a mandible, but it is definitely part of a right maxilla. Part of the palate is preserved and moreover, the damaged alveolus of the canine shows that the canine had a posterior groove, which is only present in the upper canine. Alveolus of the right P^2, the roots of P^{3-4}
Coll. Dub. 2194	Java	(right mandible fragment with) M_3
Coll. Dub. 2195a	Sumber Waru	left maxilla fragment with M^{2-3} (fits to Coll. Dub. 2023c; M^1)
Coll. Dub. 2195b	Sumber Waru	right maxilla fragment with M^{1-2} (fits to Coll. Dub. 2080a; M^3) M^2: see also Hooijer (1950, Plate II, Fig. 2 and Plate X, Fig. 4)
Coll. Dub. 2196a	Kedung Lumbu	separate upper left C
Coll. Dub. 2201	Kebon Duren	(left mandible fragment with) a very worn M_2 and part of the root of M_3
Coll. Dub. 2202	Java	right mandible fragment with M_{2-3}

Number	Locality	Description of element
Coll. Dub. 2203	Kedung Brubus	right maxilla fragment with M^{2-3}. See also Hooijer (1950, p. 83)
Coll. Dub. 2204a	Kedung Brubus	damaged separate upper left C
Coll. Dub. 2204b	Kedung Brubus	right mandible fragment with M_3
Coll. Dub. 2205	Kedung Brubus	1) separate left M^3 (see also Hooijer (1950, p. 82 and Plate VIII, Figs. 6-7) 2) separate right M^3
Coll. Dub. 2206	Kedung Lumbu	separate occipital condyle According to Hooijer (1950, p. 109) the exact locality is not known
Coll. Dub. 2207a	Kedung Brubus	separate left lower I
Coll. Dub. 2207b	Kebon Duren	left mandible fragment with the alveolus of the P_4, alveolus of M_1 (damaged)
Coll. Dub. 2314	Papa Djaran, N of Kebon Duren	right mandible fragment with C (the crust of the canine is still in the jaw, but the centre of the canine is missing), M_{2-3}
Coll. Dub. 2318a	Bangle	separate left M^2 According to the catalogue of the Dubois Collection (Naturalis, the National Museum of Natural History in Leiden, The Netherlands) this should be a right maxilla from Bogo. On the fossil itself the locality "Bangle" has been painted. See also Hooijer (1950, p. 82 and Plate VIII, Fig. 9)
Coll. Dub. 2318b	Dekes/Wadegan	separate right M_3
Coll. Dub. 2318c	Kedung Brubus	1) separate left P_3 2) separate left P_4 3) separate right P_2 4) separate left P_2
Coll. Dub. 2318d	Kedung Brubus	separate left M^3 According to the catalogue of Naturalis, the National Natuurhistorisch Museum (Leiden, The Netherlands) and according to Hooijer (1950, p. 64 and Plate VIII, Fig. 15), this is an upper left M^2 but it is more likely that it is a left M^3, because it shows no indentation which indicates the presence of another molar on the posterior side.
Coll. Dub. 2318e	Dekes/Wadegan	separate right M^3 Locality: On the label on the fossil is written: Dekes/Wadegan. According to the catalogue of Naturalis, the National Natuurhistorisch Museum (Leiden, The Netherlands), it is a right upper M^1, with locality Kedung Brubus. According to Hooijer (1950, p. 64 and Plate VIII, Fig. 16) it is a right M^1 from Dekes/Wadegan. In my opinion it is a separate right M^3, because on the posterior side there is no sign of the presence of another molar.

Number	Locality	Description of element
Coll. Dub. 2319	Java	(left mandible fragment with) M_2 (broken) and M_3
Coll. Dub. 2460a	Java	separate left P^4
Coll. Dub. 2592	Teguan	separate left P^4
Coll. Dub. 2902	"Trinil"*	part of a right premaxilla with the alveoli of all I, broken right C, M^{2-3} see also Hooijer (1950, p. 81)
Coll. Dub. 2903	"Trinil"*	left (anterior part) and right mandible fragments with the alveolus of the right I_1, the left I_1 and the right I_2 and I_3, right C (broken), right M_{1-3} (broken) see also Hooijer (1950, p. 85)
Coll. Dub. 2904	Kebon Duren	left mandible fragment with broken C, the alveoli of P_{1-4}, M_1 (broken)
Coll. Dub. 2905	Papa Djaran, N of Kebon Duren	left mandible fragment with a damaged alveolus of the C, M_{2-3}
Coll. Dub. 2906	Java	left mandible fragment with part of the angular process, with the damaged alveolus of C, alveolus of M_2, M_3 (broken)
Coll. Dub. 2907	Nonko, NW of Trinil	1) cranium fragment with the alveoli of I^2 dex and I^3 dex and the alveolus of I^1 dex (broken), C dex, P^2 and P^3 dex (broken), M^1 dex (broken), M^2 dex, M^3 sin and dex (see also Hooijer, 1950, p. 68) 2) a separate (probably) I^2, which does not fit to any of the alveoli of 1)
Coll. Dub. 2908	Kedung Brubus	cranium with three alveoli of all I, except the I^1 dex, broken left C, right P^1 (broken), the alveolus of P^1 sin, P^2 sin (broken), P^2 dex, P^3 sin and dex, P^4 sin and dex (entirely worn), M^1 sin and dex (totally worn), M^2 sin and dex, M^3 sin (broken), M^3 dex. See also Hooijer (1950, p. 58, 61-62 and Plate II, Fig. 4 and Plate III, Fig. 2)
Coll. Dub. 2909	Tinggang	right part of a cranium with the alveoli of I^1 and I^2, alveoli of P^{1-3} (not measurable), P^4, M^{1-2}, M^3 (broken). See also Hooijer (1950, p. 80 and Plate VI, Fig. 2)
Coll. Dub. 2910	Tritik	mandible with I_1 sin and dex, I_2 sin, I_3 dex and the alveolus of I_3 sin (all incisors are broken; (the separate I_1 sin and dex and I_2 sin are also present), C (both broken), M_{2-3} (broken). See also Hooijer (1950 p. 73)
Coll. Dub. 2911	Tinggang	cranium with alveoli of I^1 sin and dex, and I^2 dex, left P^1 (not measurable), P^2 sin and dex (all broken), the alveoli of P^3 sin and dex, P^4 sin, P^4 dex (broken), M^1 sin (worn and broken), M^1 dex (worn), M^2 sin and dex, M^3 sin, M^3 dex (broken) See also Hooijer (1950, p. 79-80 and Plate VII, Fig. 1)
Coll. Dub. 2912	Java	separate lower I (length 50 mm)

Number	Locality	Description of element
Coll. Dub. 2914	Tinggang	cranium with all alveoli of I (except I^1 dex), both C (broken), alveoli of P^1 sin, P^2 sin and dex, P^3 sin and dex, P^4 sin and dex (broken), M^1 sin and dex (broken), M^2 sin (broken), M^2 dex (damaged), M^3 dex. See also Hooijer (1950, p. 77-80 and Plate II, 1 and Plate III, Fig. 1)
Coll. Dub. 2915	Solo Valley	left and right mandible fragment with all I (broken), C (alveoli of both C, right C broken), the alveolus of the left P_2 and the P_3 broken, M_1 sin and dex (broken) M_2 sin and dex (broken), M_3 sin (broken), M_3 dex. See also Hooijer (1950 p. 84 and Plate IV, Fig. 3, Plate VI, Fig. 3 and Plate IX, Fig. 2)
Coll. Dub. 2916	Kedung Brubus	left and right mandible with I_1 sin and dex, the alveolus of I_2 sin and I_3 sin, alveolus of left C, broken right C, alveolus of the left P_2, left P_3 and P_4 (both broken), the alveoli of the right $P_{2\text{-}4}$, M_1 sin (worn and broken), M_1 dex (worn and damaged), $M_{2\text{-}3}$ sin and dex. See also Hooijer (1950, p. 72 and Plate V, Fig. 2)
Coll. Dub. 2917	Kedung Lumbu	right mandible with C, alveoli of P_2 and P_3 (vaguely visible), P_4, $M_{1\text{-}3}$
Coll. Dub. 2918	Papa Djaran, N of Kebon Duren	mandible fragment with broken I_1 sin and dex, the alveolus of I_2 dex, I_2 sin and both I_3's, both C's broken, alveoli of $P_{2\text{-}4}$ sin and dex. See also Hooijer (1950, p. 74 and Plate IX, Fig. 3)
Coll. Dub. 2919	Padasmalang	cranium fragment with P^2 dex and P^4 sin (both broken), M^1 sin (very worn), M^1 dex (broken), M^2 sin (broken and very worn), M^2 dex (broken), M^3 sin (worn and damaged), M^3 dex (broken). See also Hooijer (1950, p. 67-68 and Plate II, Fig. 3 and Plate IV, Fig. 1)
Coll. Dub. 2920	Java	(left maxilla fragment with) a totally worn DP^4, $M^{1\text{-}3}$
Coll. Dub. 2921	Tritik	1) separate upper right C 2) part of a right maxilla with the alveoli of $P^{1\text{-}2}$
Coll. Dub. 2922	Kedung Lumbu	left mandible fragment with part of a broken C, the alveoli of $P_{2\text{-}3}$ (vaguely visible), P_2 (M_3 glued to Coll. Dub. 2917?). Restored with plaster
Coll. Dub. 2924	Java	1) fragment of a lower C 2) fragment of a lower C 3) half of a left lower C with part of the wear facet, the anterior part of the wear facet is missing. 4) posterior part of a separate left P^3
Coll. Dub. 2926	Java	(maxilla fragment with) left, broken C without a wear facet, P^3

Number	Locality	Description of element
Coll. Dub. 2929	Kedung Madoh	anterior mandible fragment with alveoli of I_1 sin and dex, I_2 dex and both I_3's, both alveoli of C (the alveolus of the left C is broken in longitudinal direction), rugosity indicating the position of P_1, P_2 dex and P_3 dex (both broken), part of the P_4 dex (broken). See also Hooijer (1950, p. 85 and Plate IX, Fig. 1)
Coll. Dub. 2931	Kedung Brubus	mandible with all I (broken), broken left C
Coll. Dub. 2932	Nonko, NW of Trinil	broken and damaged mandible fragment restored with plaster with broken I_1 sin, I_2 sin and dex, and I_3 sin and dex (all broken), left C, right C (broken)
Coll. Dub. 2933	Kebon Duren	maxilla fragment with the alveolus of P^2 sin, the root of P^2 dex, the alveolus of P^3 sin, P^3 dex, the alveoli of P^4 sin and dex
Coll. Dub. 2934	Kedung Brubus	mandible fragment with all I, half of the left C
Coll. Dub. 4234	Java	separate, very damaged upper C, especially on the dorsolingual side. The wear facet is present, but also damaged
Coll. Dub. 4474	Tritik	separate upper left C, the dorsal side is damaged
Coll. Dub, 4606	Java	piece of lower left C (length 48.7 mm)
Coll. Dub. 4857	Padasmalang	left mandible fragment with M_3 (broken, not measurable)
Coll. Dub. 4908	Kedung Brubus	right mandible fragment and a part of the left side with alveoli of I_2 and I_3, longitudinally broken alveolus of the C, the alveoli of $P_{2\text{-}4}$. See also Hooijer (1950, p. 85-86)
Coll. Dub. 5006	Kedung Lumbu	cranium fragment
Coll. Dub. 5527	Kedung Brubus	part (length 35.0 mm) of a separate left C, although it is not really very clear what the anterior or posterior side is
Coll. Dub. 5760	Java	anterior part of a separate left M^2
Coll. Dub. 5803	Java	part of lower C, with the dorsal part missing
Coll. Dub. 6490	Java	separate upper left C
Coll. Dub. 6491	Java	separate part of a lower right C
Coll. Dub. 6654	Java	very damaged, separate right M^2
Coll. Dub. 6927	Tritik	1) anterior part of a separate left M_2 2) posterior fragment of a separate M^3 3) anterior part of a separate left M^3

Number	Locality	Description of element
Coll. Dub. 6954	Tritik	1) fragment of lower C 2) fragment of lower C 3) fragment of upper C 4) fragment of upper left C 5) separate left P_4 6) separate left P_3 7) separate right M_2 8) separate left M^3 9) posterior part of a separate (right?) M^2
Coll. Dub. 8243	Kedung Brubus	part of a lower left C, behind the wear facet, the dorsal part is missing
Coll. Dub. 8473	Java	part of a lower C, the dorsal part is missing
Coll. Dub. 11092	"Trinil"*	1) separate right P_2 2) separate left P_2
Coll. Dub. 11463	Java	separate, damaged M_1
Coll. Dub. 11464	Bangle	posterior part of a left M_3
Coll. Dub. 11466	Kedung Brubus	separate M^2 or M^3
Coll. Dub. 13601	Java	separate right P^3

---

* Hooijer (1950) mentioned hippopotamus finds in Trinil, but this was based on the state of fossilisation (colour and texture) of the fossils (De Vos & Sondaar, 1982), so this is very doubtful, especially because Dubois (1908) stated not to have found any hippopotamus in Trinil. Therefore the locality name of Trinil is put between quotation marks.

Private collection of the author:

Number	Locality	Description of element
JA no. 67	unknown, bought in Sangiran (Java)	separate right P_3
JA no. 68	unknown, bought in Sangiran (Java)	separate left M_2

From the Siwaliks (India) the following specimens were studied:

From the Collection Dubois in Naturalis, the Nationaal Natuurhistorisch Museum (National Museum of Natural History) in Leiden, The Netherlands:

Number	Locality	Description of element
Coll. Dub. 3101	Samalka	cranium with P^3 sin (broken), P^3 dex (glued and covered with sediment; no morphology can be distinguished), P^4 sin and dex, M^1 sin and dex (totally worn), M^2 sin (broken), M^2 dex (damaged and worn), M^3 sin (broken), M^3 dex (totally worn). see also Hooijer (1950, p. 45-46)
Coll. Dub. 3137	Samalka 9	right maxilla fragment with M^1 (totally worn), M^2 (broken), M^3 (worn and broken) see also Hooijer (1950, p. 48)
Coll. Dub. 3138	Samalka 3	maxilla fragment with $M^{1\text{-}3}$ dex. see also Hooijer (1950, p. 46-48 and Plate IV, Fig. 2)
Coll. Dub. 3146	Naliwala, Punjab	cranium fragment with M^1 sin (broken), M^2 sin and dex, M^3 sin and dex (both broken). see also Hooijer (1950, p. 54-55 and Plate V, Fig. 3)
Coll. Dub. 3147	Bharon, Punjab	two fragments of right mandible, which fit together with the immeasurable alveoli of I, part of I_3, alveolus of the C with the buccal part of the canine in it (there is sediment attached to the broken part of the canine), rugosity indicating the position of (D)P_1, $P_{2\text{-}4}$ (broken), the alveolus of M_1, $M_{2\text{-}3}$ see also Hooijer (1950, p. 48 and Plate X, Fig. 2)
Coll. Dub. 3148	Kodawala	maxilla fragment with P^4 sin (broken), P^4 dex, $M^{1\text{-}3}$ (worn and/or broken) see also Hooijer (1950, p. 44-45 and Plate V, Fig. 5)

APPENDIX IV NOMENCLATURE OF THE PREMOLARS AND THE MOLARS

IV A INTRODUCTION

There is no standard nomenclature for the molars and premolars of hippopotamids. In only a few publications detailed descriptions of hippopotamid molars were given, each with its own nomenclature (Osborn, 1907; Hooijer, 1950; Gèze, 1980). Hooijer (1950) adopted Osborn's (1907) nomenclature to describe the lower molars. He designated the four main cusps as protoconid, metaconid, hypoconid and entoconid. He further used the term hypoconulid for the talonid and posterior lobe for the posterior extension of the metaconid. Gèze (1980) did not use a name for the posterior extension of the metaconid. With the term cingulum, Hooijer (1950) meant a cingulum on the lingual or buccal side, but Gèze (1980) mentioned the "cingulum mésial et distal", meaning the lobes on the anterior and posterior sides.
In this thesis, the nomenclature for the (pre)molars of suids of Van der Made (1995) is used. The names are merely descriptive and they do not say anything about the homology of the cusps.

Cusps that have been worn down can no longer be distinguished individually; they fuse. Three phases are distinguished:

- Adult	not or hardly worn;
- Middle-aged	(pre)molars are worn, but morphological features can still be seen;
- Old	(pre)molars are worn down to the extent that morphological features can no longer be distinguished.

IV B LOWER PREMOLARS

The characters are given in alphabetic order.

• accessory buccal cusp	accessory cusp in the valley between the hypoconid and the pentaconid in DP_4 (not drawn in Fig. IV-1);
• accessory lingual cusp	accessory cusp in the valley between the entoconid and the hexaconid in DP_4 (not drawn in Fig. IV-1);
• anterior lobe	lobe on the anterior side (Fig. IV-1 A,B,C,E);
• cingulum	ridge surrounding the premolar on the buccal and/or lingual side, mostly connected with the anterior or posterior lobe (Fig. IV-1 A-C);
• entoconid	cusp on the posterolingual side (Fig. IV-1 A,B,D,E);
• entopostconulid	accessory cusp on the posterior side of the entoconid (not drawn in Fig. IV-1);
• heptaconid	cusp on the posterobuccal side, posterior of the pentaconid in the DP_4 (Fig. IV-1 E);
• hexaconid	cusp on the posterolingual side of the talonid of the DP_4 (Fig. IV-1 E);
• hexaconulid	accessory cusp on the posterobuccal side of the hexaconid in the DP_4 (Fig. IV-1 E);
• hypoconid	cusp on the posterobuccal side (Fig. IV-1 A-E);
• hypoconulid	accessory cusp near the hypoconid (not drawn in Fig. IV-1);
• hypopostcristid	ridge that starts from the hypoconid in posterior direction (not drawn in Fig. IV-1);

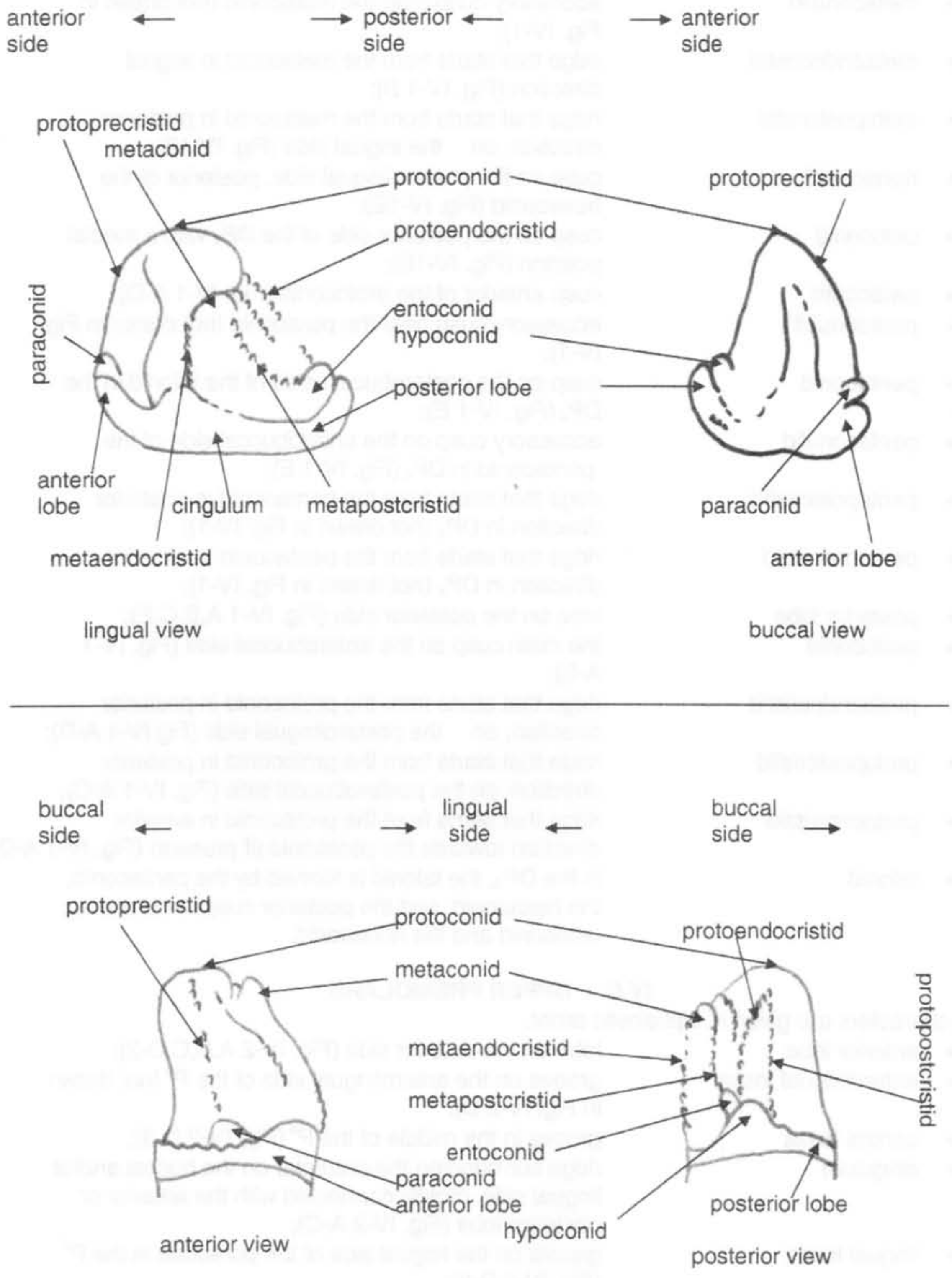

Fig. IV-1 A. Nomenclature of a left P_2 (schematic).

- hypopreconulid — accessory cusp on the anterior side of the hypoconid (not drawn in Fig. IV-1);
- hypoprecristid — ridge that starts from the hypoconid in anterior direction (not drawn in Fig. IV-1);
- metaconid — cusp on the anterolingual side (Fig. IV-1 B,C,E);

- metaconulid — accessory cusp near the metaconid (not drawn in Fig. IV-1);
- metaendocristid — ridge that starts from the metaconid in lingual direction (Fig. IV-1 B);
- metapostcristid — ridge that starts from the metaconid in posterior direction, on the lingual side (Fig. IV-1B);
- nonaconid — cusp on the posterolingual side, posterior of the hexaconid (Fig. IV-1E);
- octoconid — cusp on the posterior side of the DP_4 with a medial position (Fig. IV-1E);
- paraconid — cusp anterior of the protoconid (Fig. IV-1 A-D);
- paraconulid — accessory cusp near the paraconid (not drawn in Fig. IV-1);
- pentaconid — cusp on the posterobuccal side of the talonid in the DP_4 (Fig. IV-1 E);
- pentaconulid — accessory cusp on the anterobuccal side of the pentaconid in DP_4 (Fig. IV-1 E);
- pentapostcristid — ridge that starts from the pentaconid in posterior direction in DP_4 (not drawn in Fig. IV-1);
- pentaprecristid — ridge that starts from the pentaconid in anterior direction in DP_4 (not drawn in Fig. IV-1);
- posterior lobe — lobe on the posterior side (Fig. IV-1 A,B,C,E);
- protoconid — the main cusp on the anterobuccal side (Fig. IV-1 A-E);
- protoendocristid — ridge that starts from the protoconid in posterior direction, on the posterolingual side (Fig.IV-1 A-D);
- protopostcristid — ridge that starts from the protoconid in posterior direction, on the posterobuccal side (Fig. IV-1 A-C);
- protoprecristid — ridge that starts from the protoconid in anterior direction towards the paraconid (if present) (Fig. IV-1 A-D);
- talonid — in the DP_4, the talonid is formed by the pentaconid, the hexaconid, and the posterior cusps heptaconid, octoconid and the nonaconid.

IV C UPPER PREMOLARS

The characters are given in alphabetic order.

- anterior lobe — lobe on the anterior side (Fig. IV-2 A,B,C,D-2);
- anterolingual fossa — groove on the anterolingual side of the P^4 (not drawn in Fig. IV-2 D);
- central fossa — groove in the middle of the P^4 (Fig. IV-2 D-3);
- cingulum — ridge surrounding the premolar on the buccal and/or lingual side, mostly connected with the anterior or posterior lobe (Fig. IV-2 A-C);
- lingual fossa — groove on the lingual side of the paracone in the P^4 (Fig. IV-2 D-2);
- metacone — cusp posterior of the paracone (posterobuccal cusp, Fig. IV-2 C,D-3,E);
- metaprestyle — extension of the metacone in anterior direction in the DP^4 (Fig. IV-2E);
- paracone — cusp on the anterobuccal side (main cusp, Fig. IV-2 A-E);
- paraendocrista — ridge that starts from the paracone in posterior direction on the posterolingual side (Fig. IV-2 C);

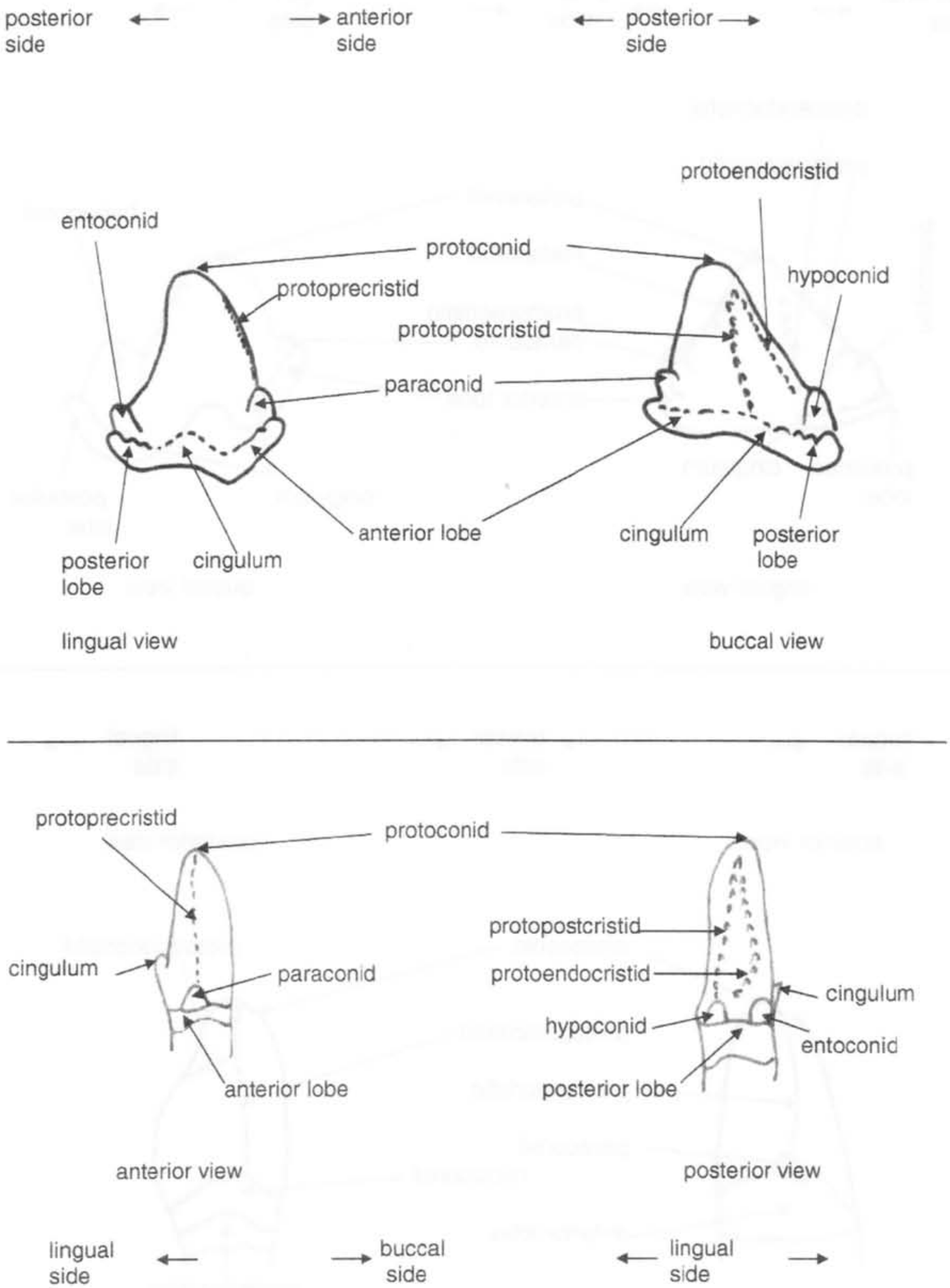

Fig. IV-1 B. Nomenclature of a right P_3 (Coll. Dub. 2003/3).

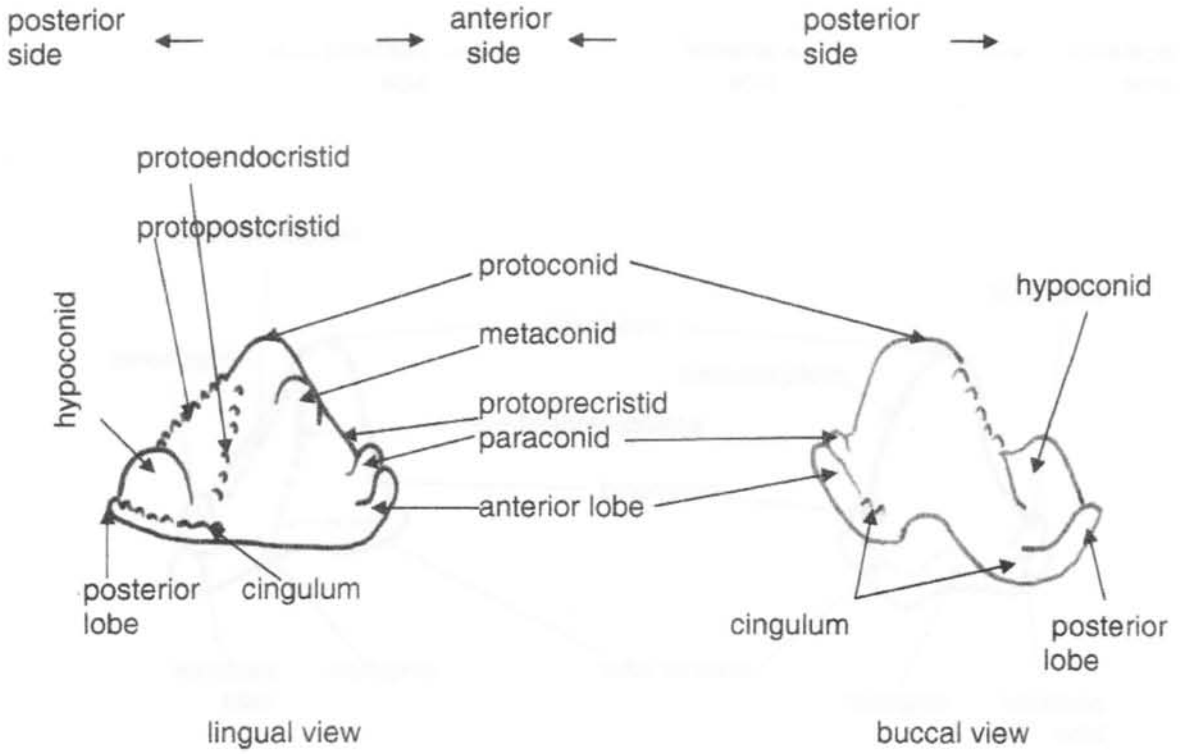

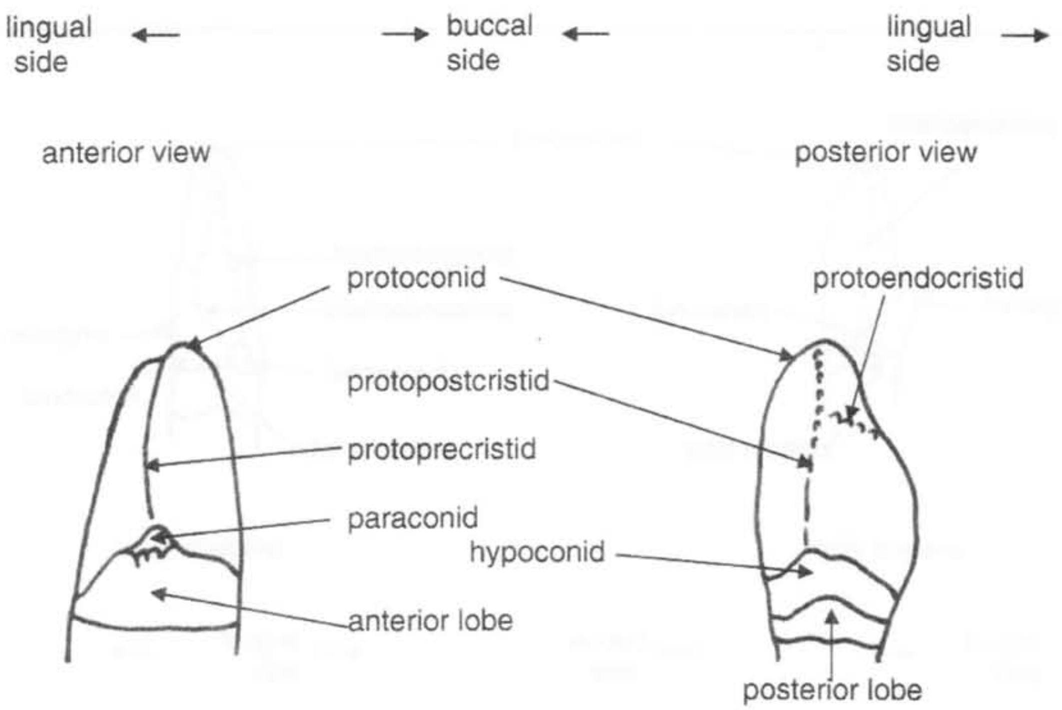

Fig. IV-1 C. Nomenclature of a left P_4 (Coll. Dub. 2922).

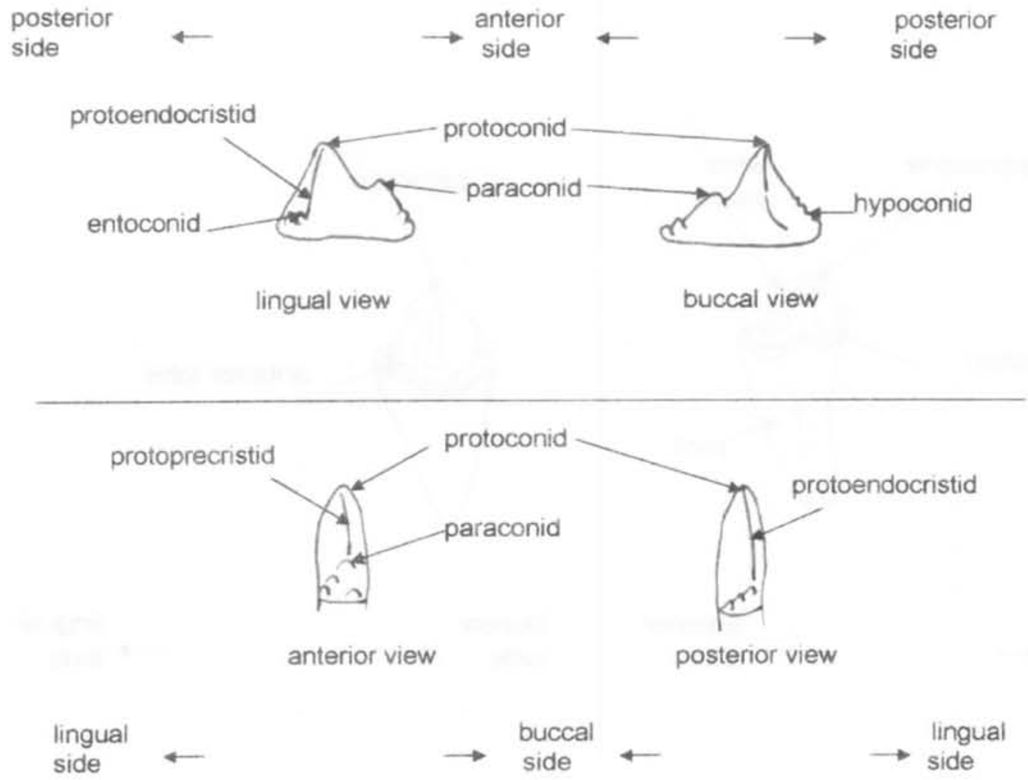

Fig. IV-1 D. Nomenclature of a left DP_2 (SA 270378).

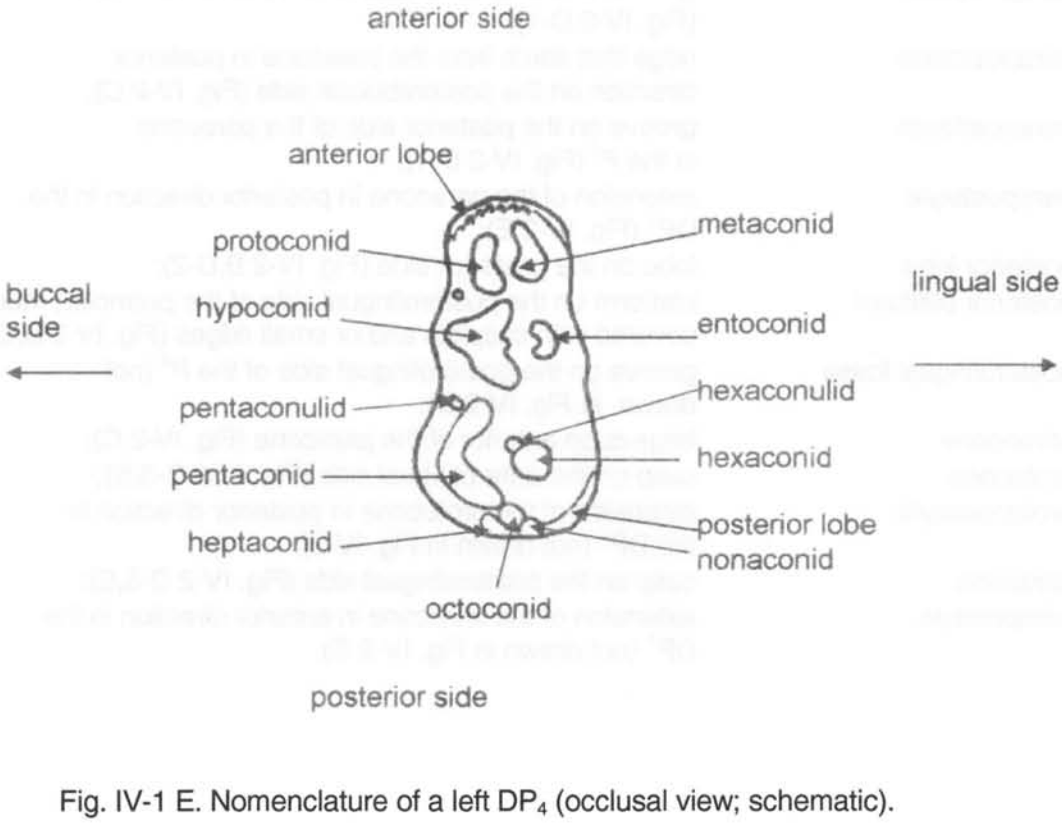

Fig. IV-1 E. Nomenclature of a left DP_4 (occlusal view; schematic).

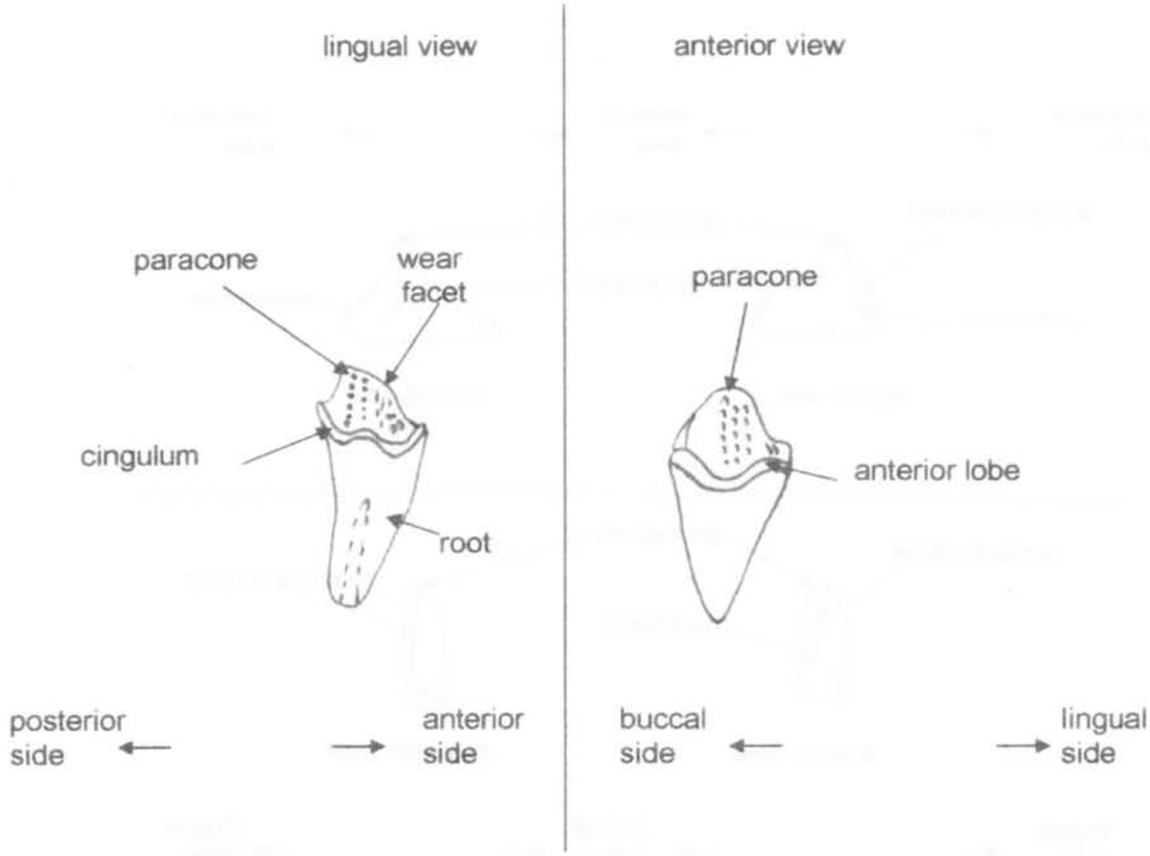

Fig. IV-2 A. Nomenclature of a right P^1 (Coll. Dub. 2023?/2).

• paraprecrista	ridge that starts from the paracone in anterior direction (not drawn in Fig. IV-2);
• paraprefossa	groove on the anterior side of the paracone in the P^4 (Fig. IV-2 D-1);
• parapostcrista	ridge that starts from the paracone in posterior direction on the posterobuccal side (Fig. IV-2 C);
• parapostfossa	groove on the posterior side of the paracone in the P^4 (Fig. IV-2 D-1);
• parapoststyle	extension of the paracone in posterior direction in the DP^4 (Fig. IV-2 E);
• posterior lobe	lobe on the posterior side (Fig. IV-2 B,D-2);
• posterior platform	platform on the posterolingual side of the premolar, mostly covered with cusplets and or small ridges (Fig. IV-2 B,C);
• posterolingual fossa	groove on the posterolingual side of the P^4 (not drawn in Fig. IV-2 D);
• primocone	large cusp anterior of the paracone (Fig. IV-2 C);
• protocone	cusp on the anterolingual side (Fig. IV-2 D-3,E);
• protopoststyle	extension of the protocone in posterior direction in the DP^4 (not drawn in Fig. IV-2);
• tetracone	cusp on the posterolingual side (Fig. IV-2 D-3,E);
• tetraprestyle	extension of the tetracone in anterior direction in the DP^4 (not drawn in Fig. IV-2 E).

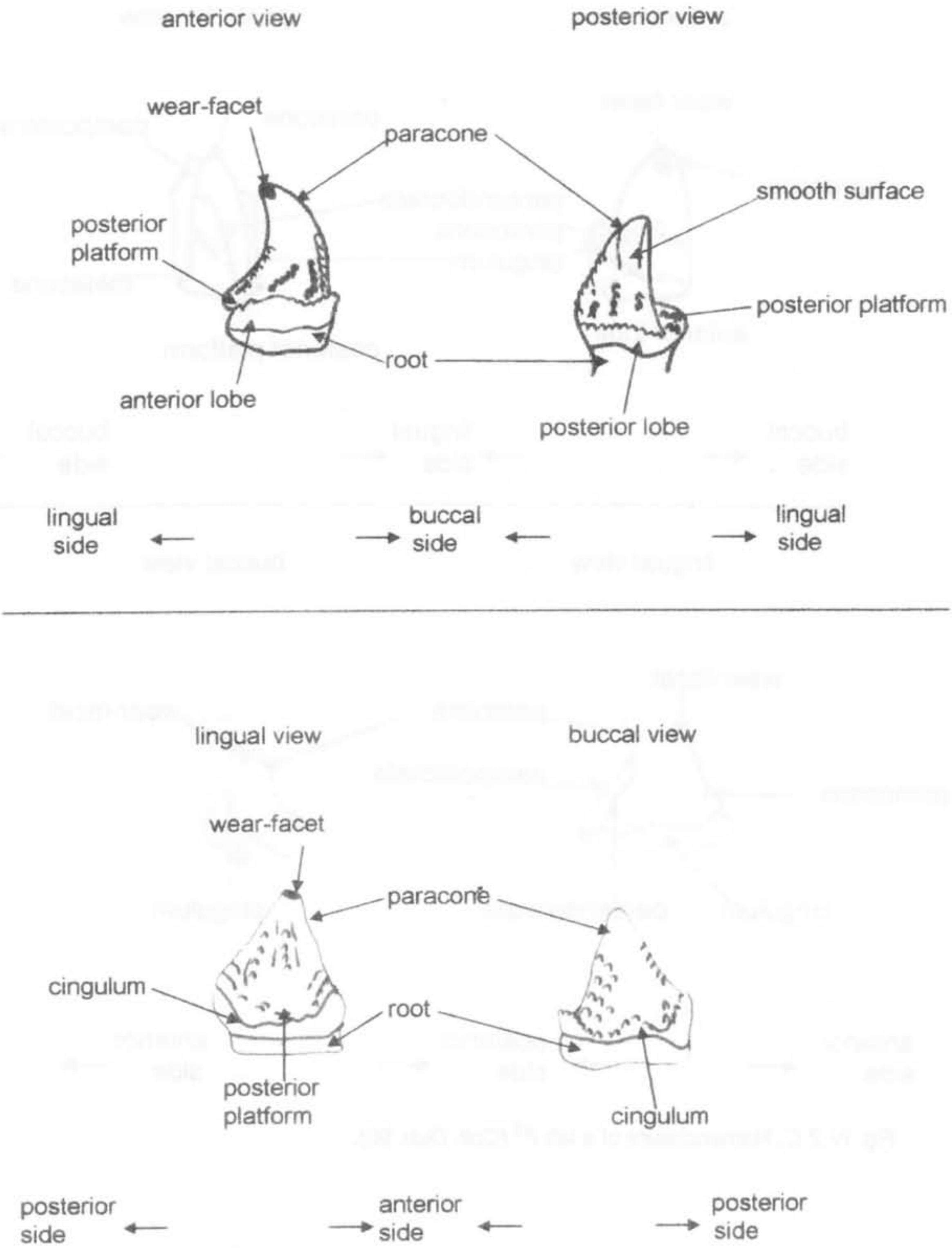

Fig. IV-2 B. Nomenclature of a right P^2 (Coll. Dub. 1702).

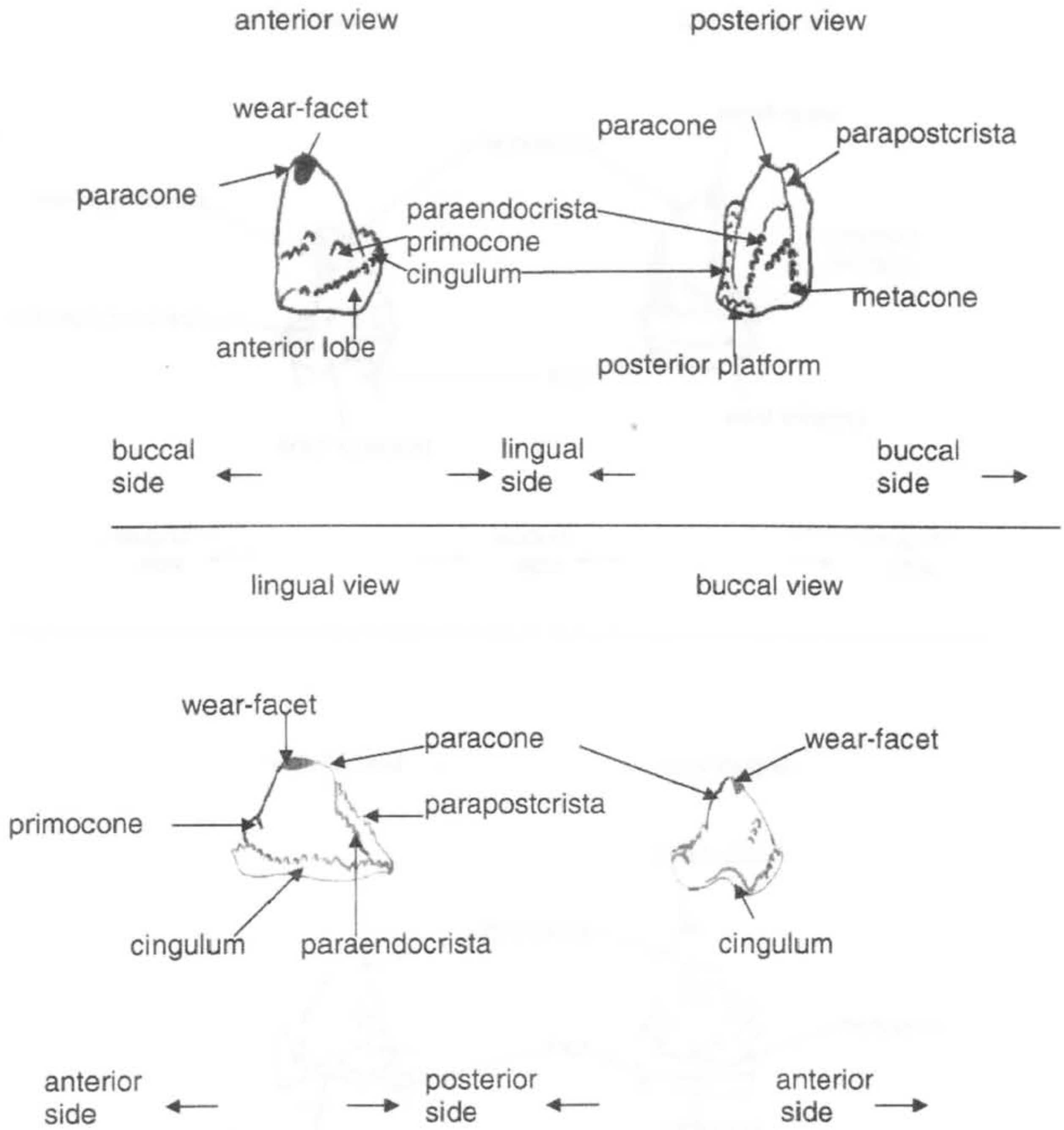

Fig. IV-2 C. Nomenclature of a left P^3 (Coll. Dub. 96).

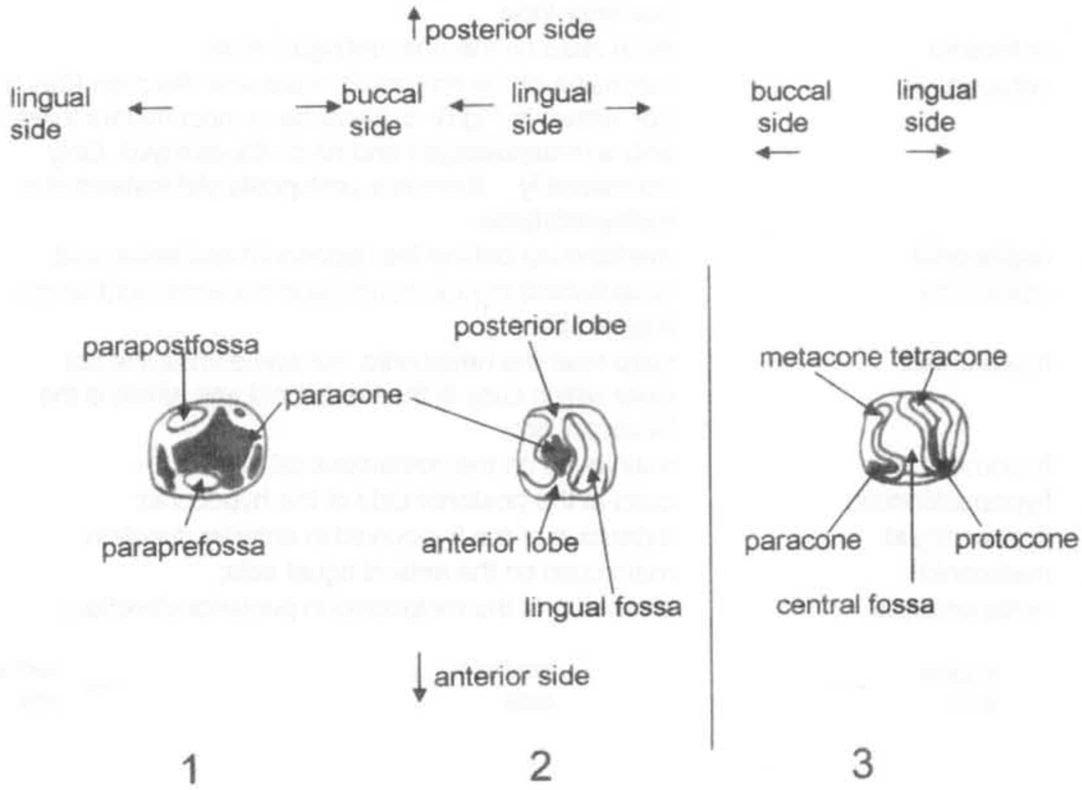

Fig. IV-2 D. Nomenclature of some P^4's (occlusal view). 1. right P^4 (Coll. Dub. 325f/2); right P^4 (Coll. Dub. 325d/1); left P^4 (Coll. Dub. 2079).

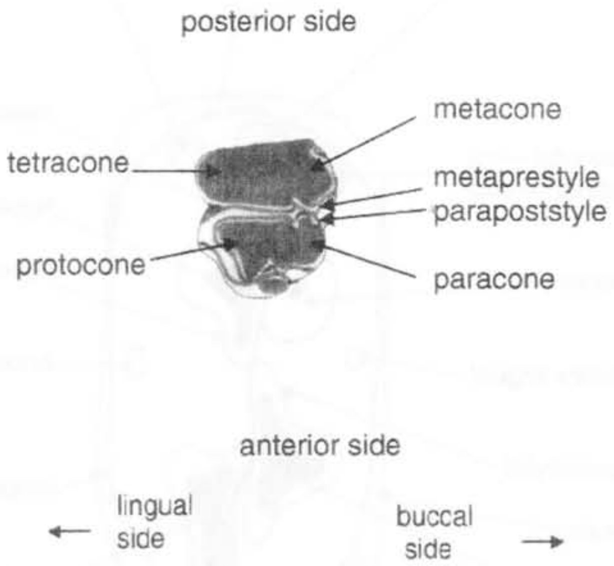

Fig. IV-2 E. Nomenclature of a right DP^4 (Coll. Dub. without number, occlusal view).

IV D LOWER MOLARS

The characters are given in alphabetic order (Fig. IV-3).

• accessory buccal cusp	cusp in the valley between the proto- and hypoconid;
• accessory lingual cusp	cusp in the valley between the meta- and entoconid;
• anterior lobe	lobe on the anterior side;
• cingulum	ridge surrounding the premolar on the buccal and/or

lingual side, mostly connected with the anterior or posterior lobe;

- entoconid — main cusp on the posterolingual side;
- entoprestylid — extension of the entoconid in anterior direction (this is not drawn in Fig.IV-3, because in most molars there is only a metapoststylid and no protopoststylid. Only occasionally there is a protopoststylid instead of a metapoststylid);
- heptaconid — medial cusp behind the hypoconid and entoconid;
- hexaconid — cusp behind the hypoconid and the entoconid on the lingual side;
- hexaconulid — cusp near the hexaconid, but sometimes it is not clear which cusp is the hexaconid and which is the hexaconulid;
- hypoconid — main cusp on the posterobuccal side;
- hypopostconulid — cusp at the posterior side of the hypoconid;
- hypoprestylid — extension of the hypoconid in anterior direction;
- metaconid — main cusp on the anterolingual side;
- metapoststylid — extension of the metaconid in posterior direction;

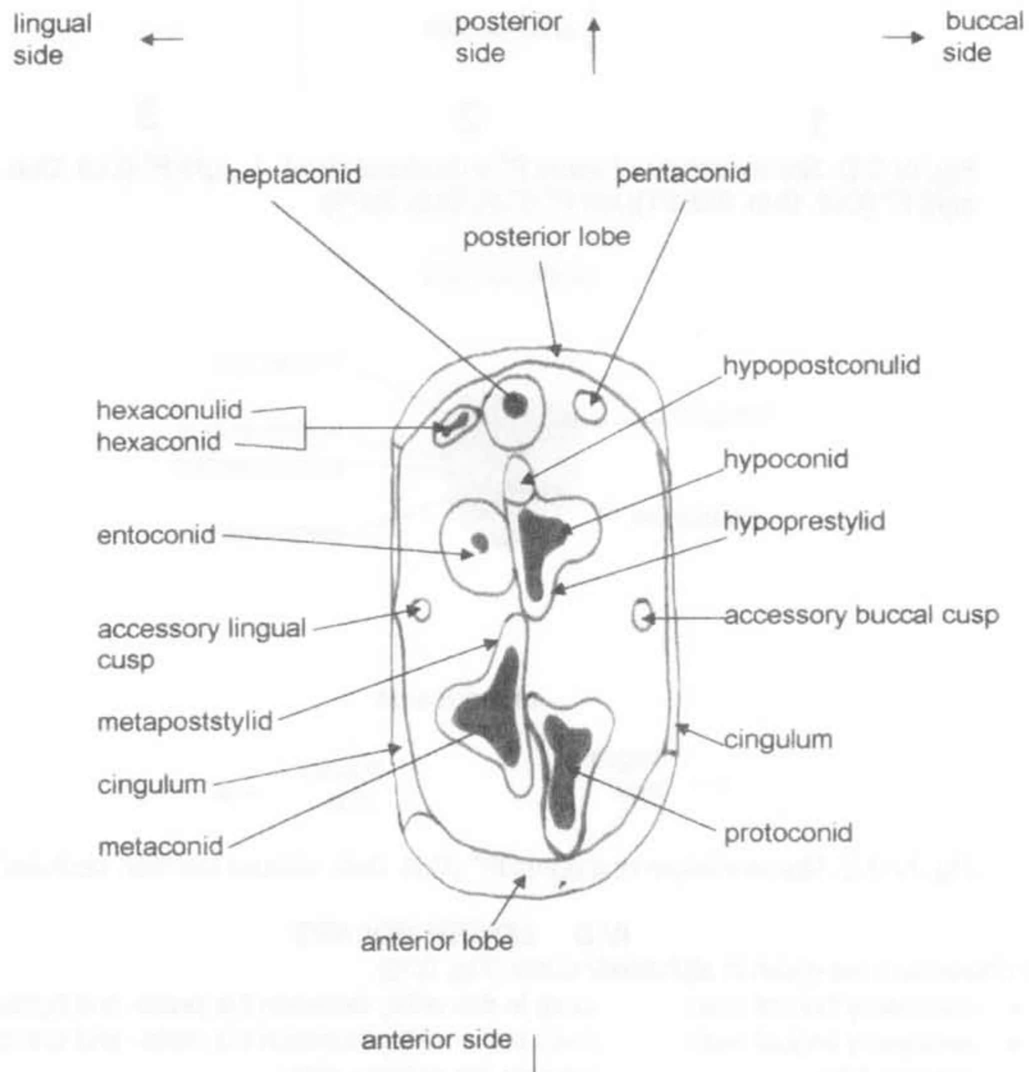

Fig. IV-3. Nomenclature of a left M_2 (schematic).

- pentaconid — cusp behind the hypoconid and entoconid on the buccal side;
- pentaconulid — cusp near the pentaconid, but sometimes it is not clear which of the cusps is the pentaconid or which is the pentaconulid (this is not drawn in Fig.IV-3);
- posterior lobe — lobe on the posterior side;
- protoconid — main cusp on the anterobuccal side;
- protopoststylid — extension of the protoconid in posterior direction (this is not drawn in Fig.IV-3, because in most molars there is only a metapoststylid and no protopoststylid. Only occasionally there is a protopoststylid instead of a meta-poststylid);
- talonid — in the M_3, the talonid is formed by the pentaconid, the hexaconid and the heptaconid (not drawn in Fig. IV-3).

When in the text posterior cusps are mentioned, the pentaconid, hexaconid and heptaconid are meant.

IV E UPPER MOLARS

The characters are given in alphabetic order (Fig. IV-4).

- accessory buccal cusp — cusp in the valley between the para- and metacone;
- accessory lingual cusp — cusp in the valley between the proto- and tetracone;
- anterior lobe — lobe on the anterior side;
- cingulum — ridge surrounding the premolar on the buccal and/or lingual side, mostly connected with the anterior or posterior lobe;
- metacone — main cusp on the posterobuccal side;
- metapostconule — small cusp posterior of the metacone;
- metapoststyle — extension of the metacone in posterior direction;
- metaprestyle — extension of the metacone in anterior direction;
- paracone — main cusp on the anterobuccal side;
- paraprestyle — extension of the paracone in anterior direction;
- parapoststyle — extension of the paracone in posterior direction;
- posterior lobe — lobe on the posterior side;
- protocone — main cusp on the anterolingual side;
- protopoststyle — extension of the protocone in posterior direction;
- protoprestyle — extension of the protocone in anterior direction;
- tetracone — main cusp on the posterolingual side;
- tetrapostconule — small cusp posterior of the tetracone;
- tetrapoststyle — extension of the tetracone in posterior direction (not drawn in Fig. IV-4);
- tetraprestyle — extension of the tetracone in anterior direction (not drawn in Fig IV-4).

The main cusps all have extensions in three directions, which give it a trefoil (trilobate) form. The lingual cusps (protocone and tetracone) have extensions towards the anterior, posterior and lingual sides; the buccal cusps (metacone and paracone) have extensions towards the anterior, posterior and buccal sides. With anterior cusps the proto- and paracone are meant, with posterior cusps the meta- and tetracone.

The nomenclature of the incisors, canines, mandible and cranium are given in Appendix V along with the method of measuring.

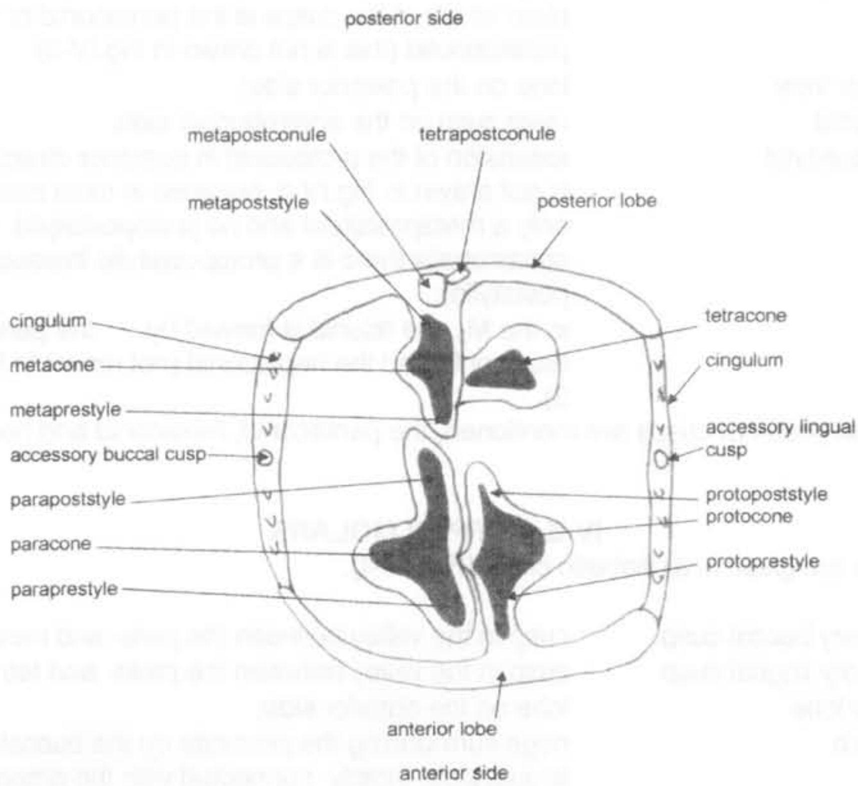

Fig. IV-4. Nomenclature of a left M^2 (schematic).

APPENDIX V NOMENCLATURE AND MEASURING METHODS

In this Appendix the nomenclature of dental elements other than the (pre)molars is described. Measurements were taken as shown in Figures V-1 – V-17 and they are presented in Appendix VI. Measurements are in mm, unless stated otherwise. Approximate measurements (due to damage) are not included in the figures or in the calculation of averages, unless stated otherwise. Most measurements were taken with a digimatic caliper (Mitutoyo) 500 with a resolution of 0.01 mm and an instrumental error of $\pm$ 0.02 mm.

V-A LOWER INCISORS

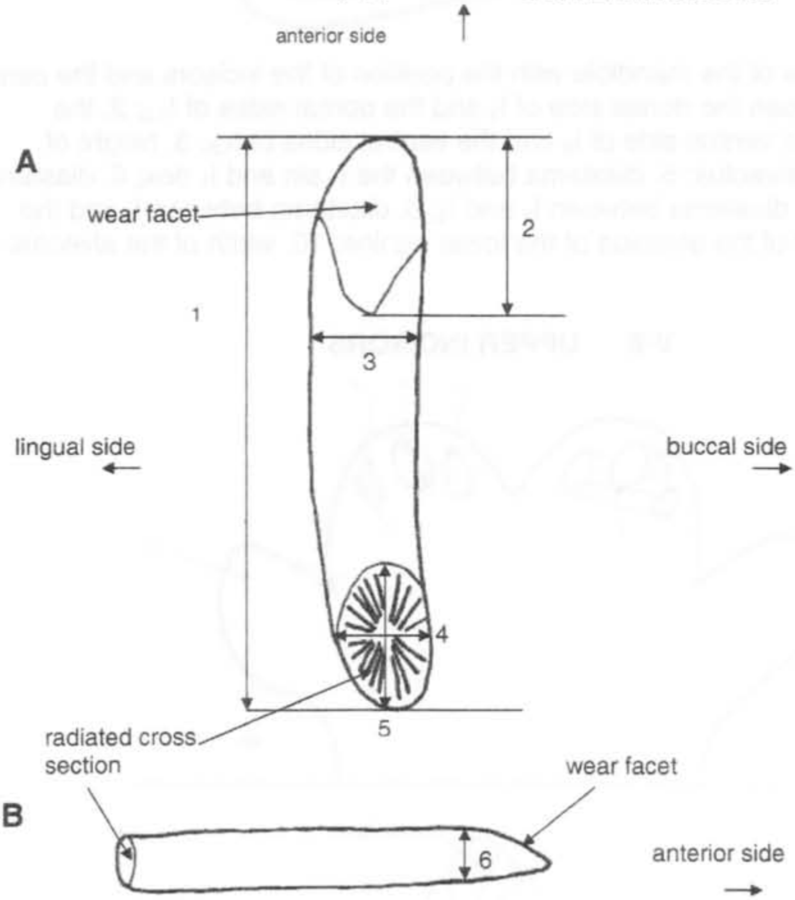

Fig. V-1 A. Dorsal view of a lower right incisor; B. Lateral view of a lower incisor; 1. length of incisor (in the tables of Appendix VI, where the incisor is more or less complete); 2. maximum length of wear facet; 3. width behind the wear facet; 4. width at the posterior end; 5. thickness at the posterior end; 6. diameter thickness behind the wear facet.

The lower incisors point forward. The left incisors bend to the left buccal side, the right incisors bend to the right buccal side (Fig. V-1). This bending is variable from hardly visible to very distinct. The wear facet is situated at the dorsobuccal side, and is in general larger on the buccal side than on the lingual side. The I_2 is always situated more dorsally than $I_{1,3}$ (Fig.V-2). In Fig. V-2 the method of measuring distances between the lower incisors is shown.

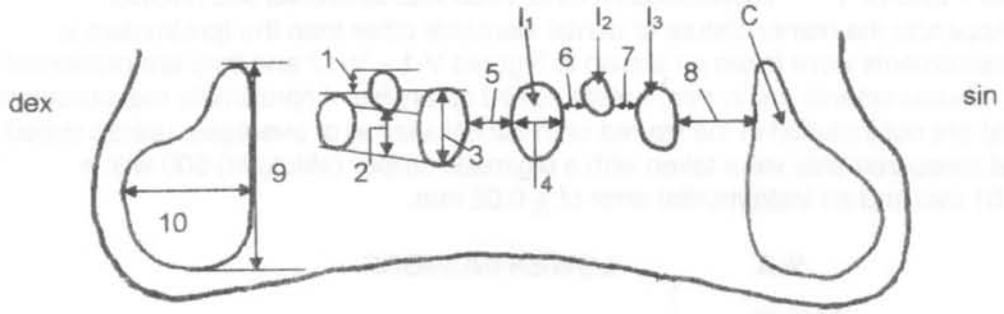

Fig. V-2. Frontal view of the mandible with the position of the incisors and the canine. 1. the distance between the dorsal side of I_2 and the dorsal sides of $I_{1,3}$; 2. the distance between the ventral side of I_2 and the ventral sides of $I_{1,3}$; 3. height of alveolus; 4.width of alveolus; 5. diastema between the I_1 sin and I_1 dex; 6. diastema between I_1 and I_2; 7. diastema between I_2 and I_3; 8. diastema between I_3 and the canine (C); 9. height of the alveolus of the lower canine; 10. width of the alveolus of the lower canine.

V-B UPPER INCISORS

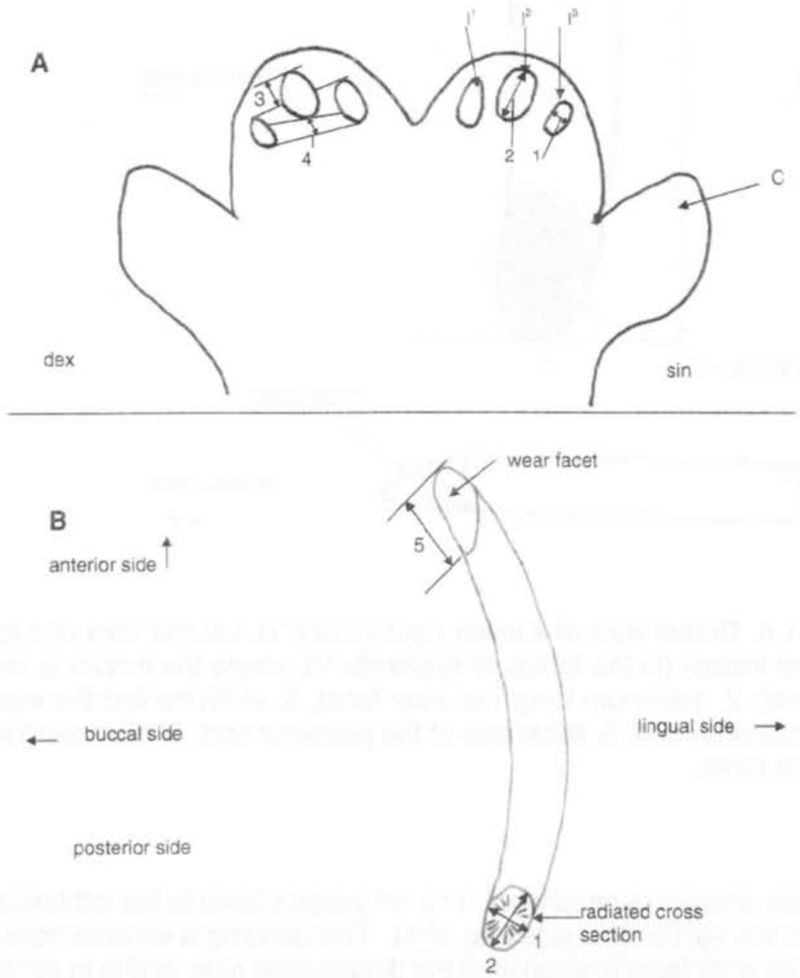

Fig. V-3. A. Ventral view of maxilla with the position of the upper incisors and the canine (C); B. ventral view of an upper incisor; 1. minimum diameter (= dt min); 2. maximum diameter (= dt max); 3. distance between the anterior side of I^2 and the anterior sides of $I^{1,3}$; 4. distance between the posterior side of I^2 and the posterior sides of $I^{1,3}$; 5. length of the wear facet.

V-C LOWER CANINES

The lower canines have a pear-shaped cross section, with the top of the pear at the lingual side (Fig. V-4 A). The wear facet is situated on the posterior side. In lateral view, the wear facet shows a straight line, with the buccal side lower than the lingual side (Fig. V-4 B). The method of measuring is shown in Fig. V-2 (measurement 9 and 10) and Fig. V-4.

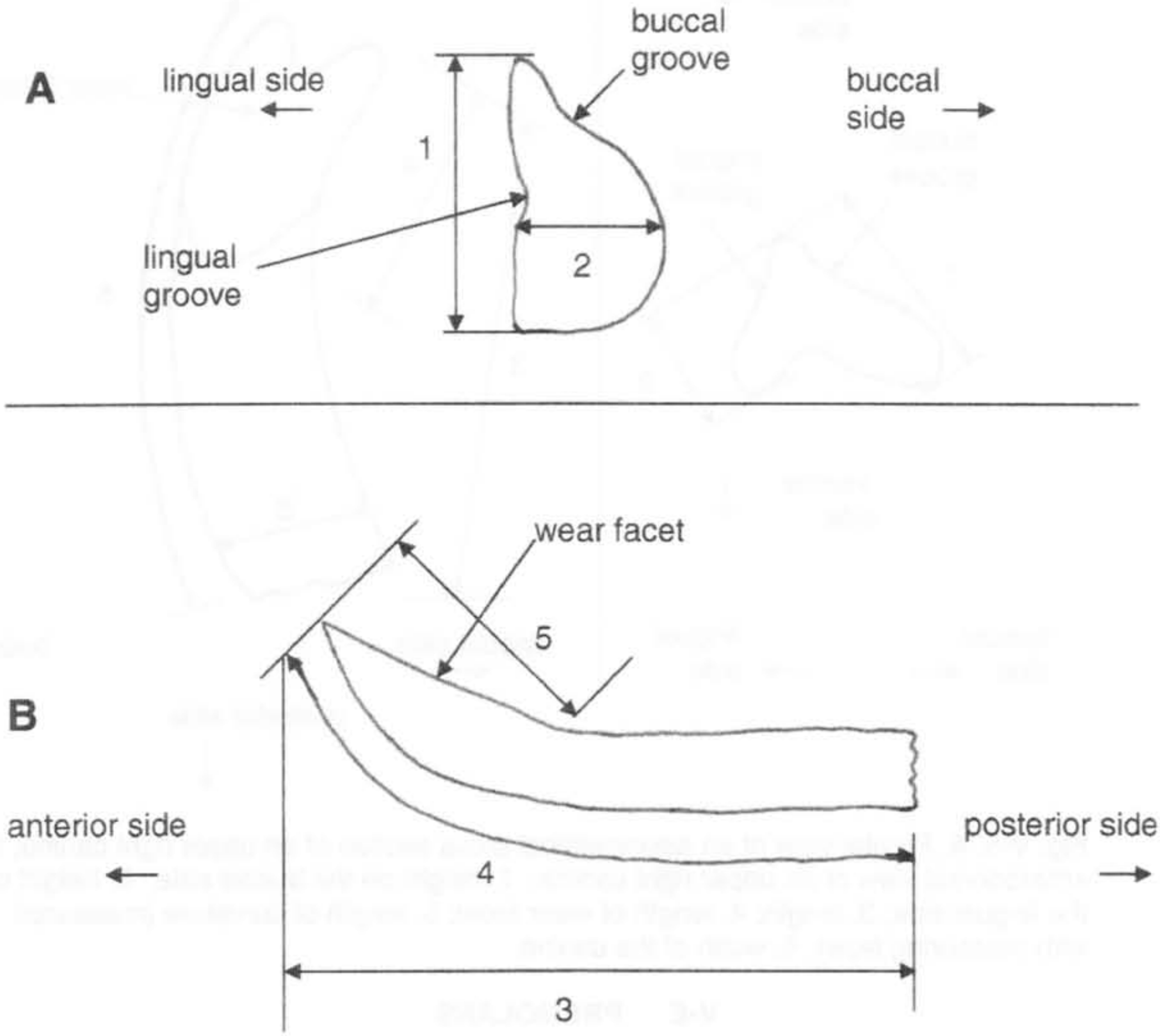

Fig. V-4. A. Posterior view of a lower right canine; B. lateral view of a lower canine; 1. height of a lower canine; 2. width of a lower canine; 3. length; 4. length of the curvature (measured with measuring tape); 5. length of the wear facet.

V-D UPPER CANINES

The upper canine, with a heart- to kidney-shaped cross section, has a groove on the buccal side in most of the specimens. The wear facet is situated on the anterior side. The canines bend downwards in lingual direction. The method of measuring is shown in Fig. V-5.

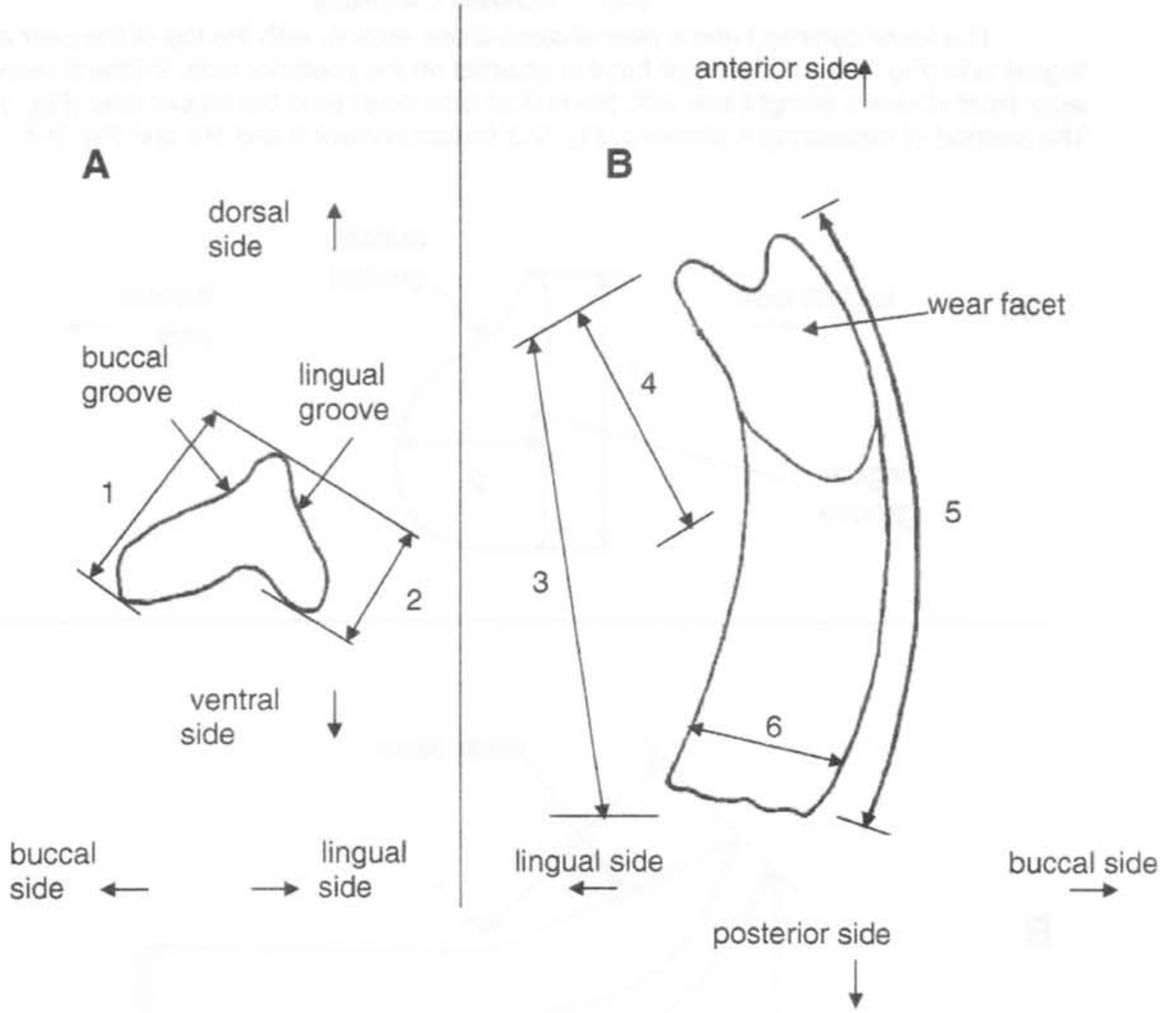

Fig. V-5. A. Frontal view of an asymmetrical cross section of an upper right canine; B. anterodorsal view of an upper right canine; 1. height on the buccal side; 2. height on the lingual side; 3. length; 4. length of wear facet; 5. length of curvature (measured with measuring tape); 6. width of the canine.

V-E PREMOLARS

Measurements of the lower premolars are illustrated in Fig. V-6, and of the upper premolars in Fig. V-7. Measurement 8 in Fig. V-7 gives the width of the root, in case an extra lingual root is present (Coll. Dub. 2193, P^3 and P^4).

Individual cusps were not measured; remarks in the description like "one cusp larger than the other" is based on visional observation.

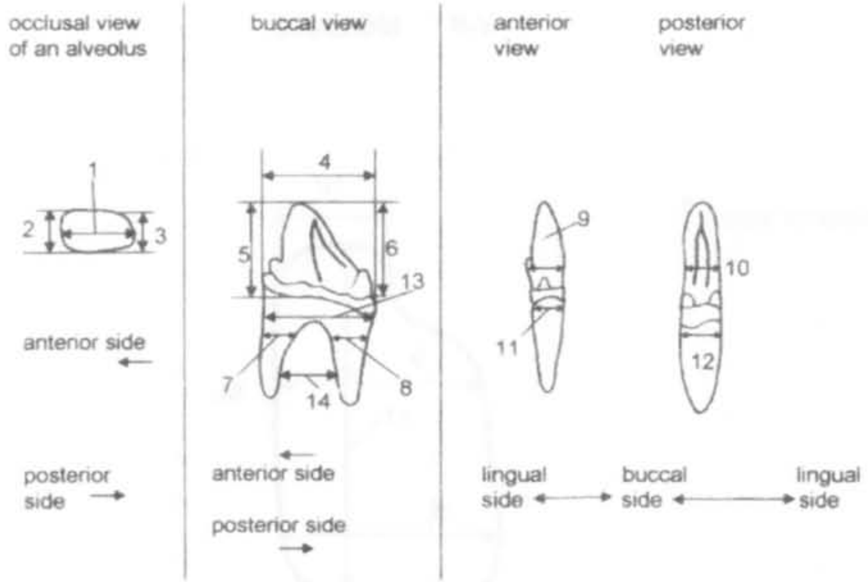

Fig. V-6. Measurements of lower premolars.
1. length of the alveolus; 2. width of the alveolus, measured on the anterior side; 3. width of the alveolus, measured on the posterior side; 4. Length; 5. crown height (only measured in unworn specimens) measured on the anterior side; 6. crown height (measured in unworn specimens) measured on the posterior side; 7. length of the anterior root; 8. length of the posterior root; 9. width, measured on the anterior side; 10. width, measured on the posterior side; 11. width of the anterior root; 12. width of the posterior root; 13. length of the root (in case there is a root); 14. maximum space between the roots.

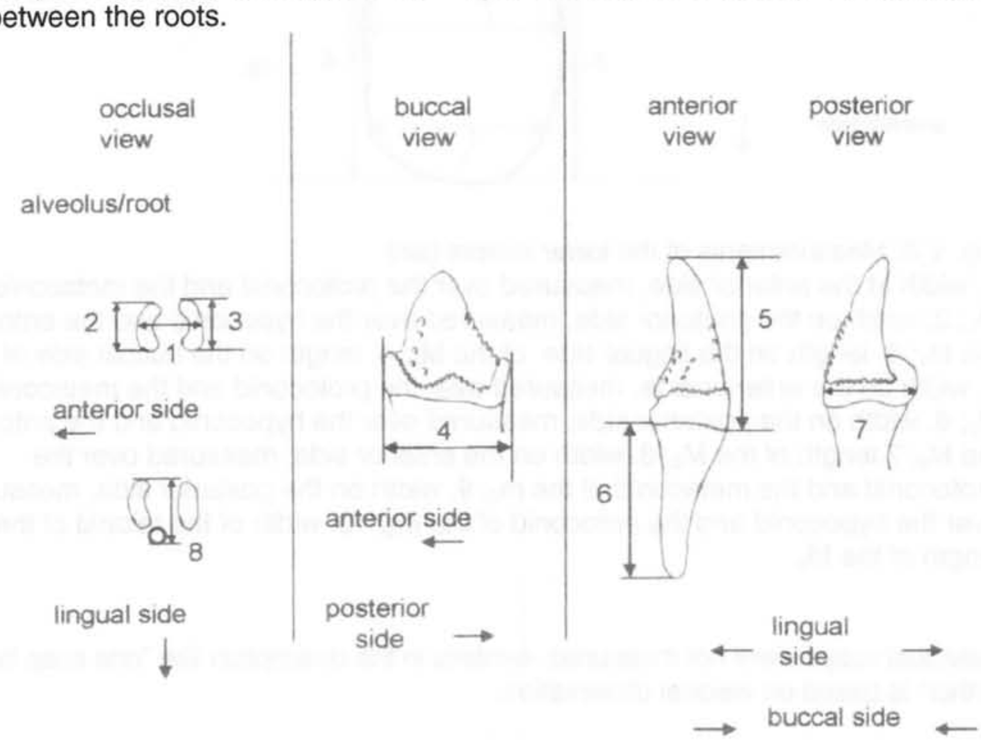

Fig. V-7. Measurements of the upper premolars. 1. length of the alveolus; 2. width of the alveolus measured on the anterior side; 3. width of the alveolus measured on the posterior side; 4. length; 5. maximum crown height (measured in unworn specimens); 6. maximum length of root; 7. width, measured at the posterior side; 8. width of the aveolus, extra root included (Coll. Dub. 2193; P^3 and P^4).

V-F MOLARS

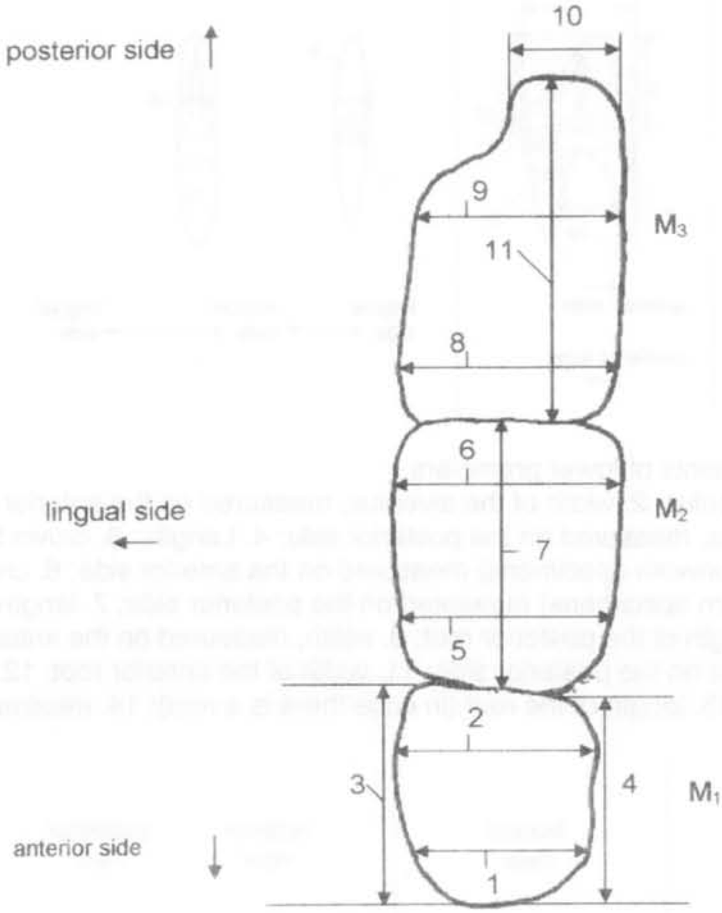

Fig. V-8. Measurements of the lower molars (sin).
1. width at the anterior side, measured over the protoconid and the metaconid of the M_1; 2. width on the posterior side, measured over the hypoconid and the entoconid of the M_1; 3. length on the lingual side of the M_1; 4. length on the buccal side of the M_1; 5. width on the anterior side, measured over the protoconid and the metaconid of the M_2; 6. width on the posterior side, measured over the hypoconid and the entoconid of the M_2; 7.length of the M_2; 8. width on the anterior side, measured over the protoconid and the metaconid of the m_3; 9. width on the posterior side, measured over the hypoconid and the entoconid of the M_3; 10. width of the talonid of the M_3; 11. length of the M_3.

Individual cusps were not measured; remarks in the description like “one cusp larger than the other” is based on visional observation.

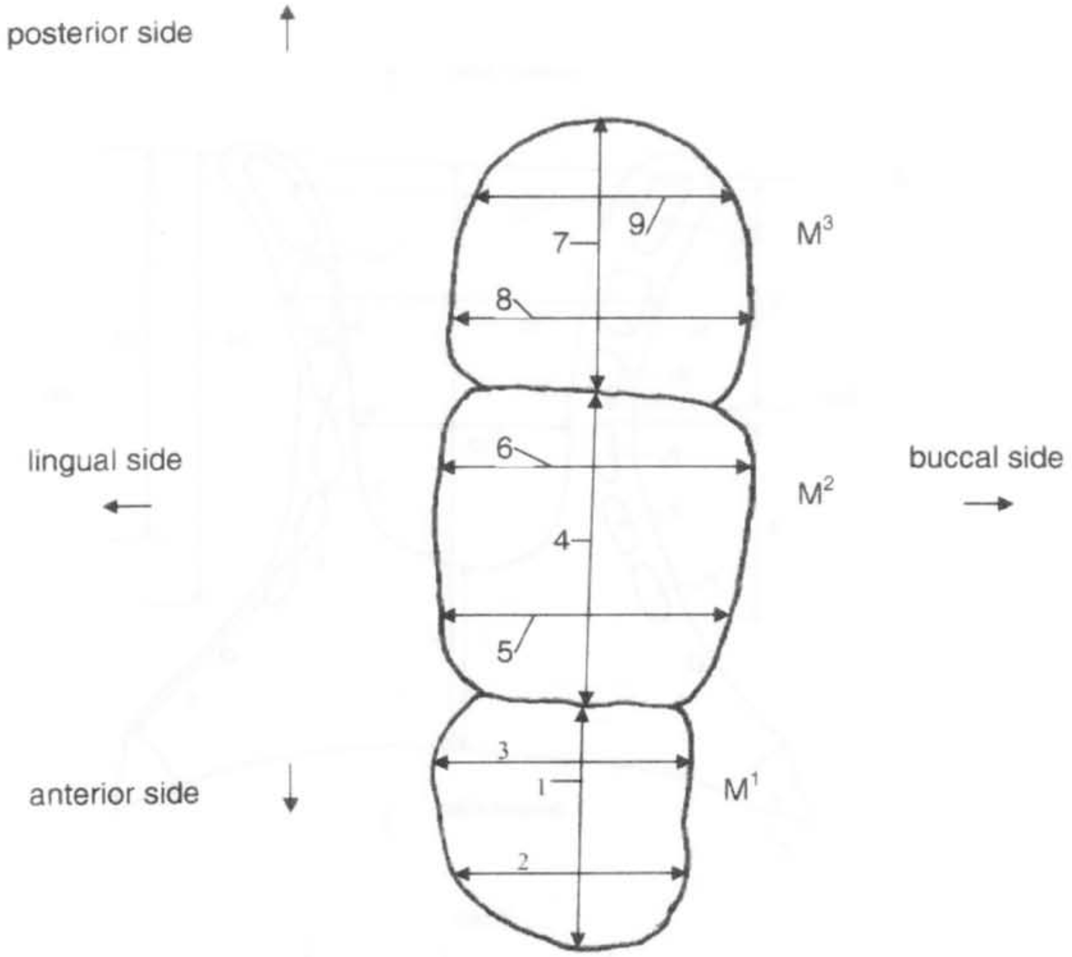

Fig. V-9. Measurements of the upper molars (dex)
1. length of the M^1; 2. width at the anterior side, measured over the protocone and the paracone of the M^1; 3. width at the posterior side, measured over the metacone and the tetracone of the M^1; 4. length of the M^2; 5. width on the anterior side, measured over the protocone and the paracone of the M^2; 6. width on the posterior side, measured over the metacone and the tetracone of the M^2; 7. length of the M^3; 8. width on the anterior side, measured over the protocone and the paracone of the M^3; 9. width on the posterior side, measured over the metacone and the tetracone of the M^3.

V-G MANDIBLE

In the material studied, there is no completely preserved mandible. Also the coronoid process (Fig.V-11A) is not preserved in any of the specimens. The only specimen that gives an indication about the length of the lower jaw is Coll. Dub. 99. Its maximum length, measured following Figs. V-10 and V-11, is at least 37 cm.

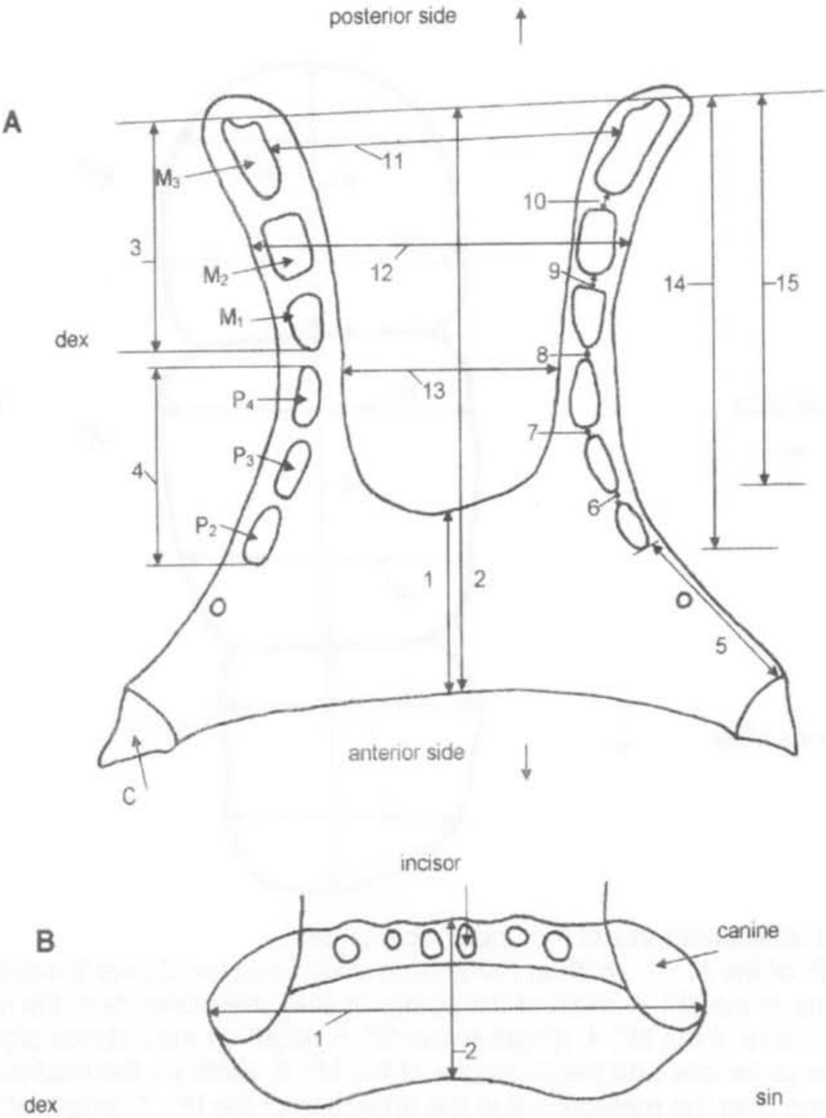

Fig. V-10. A. Occlusal view of a mandible. 1. length of symphysis; 2 length of mandible from front to M_3; 3. length $M_1 - M_3$; 4. length P_2- P_4; 5. diastema C – P_2; 6. diastema P_2-P_3; 7. diastema P_3- P_4; 8. diastema P_4- M_1; 9. diastema M_1- M_2; 10. diastema M_2- M_3; 11. horizontal distance between the lingual sides of the left and right M_3; 12. width of the mandible at M_2; 13. narrowest width of the mandible; 14. length P_2- M_3; 15. length P_3-M_3. B. frontal view of a mandible. 1. outer distance between the canines; 2. height of the symphysis.

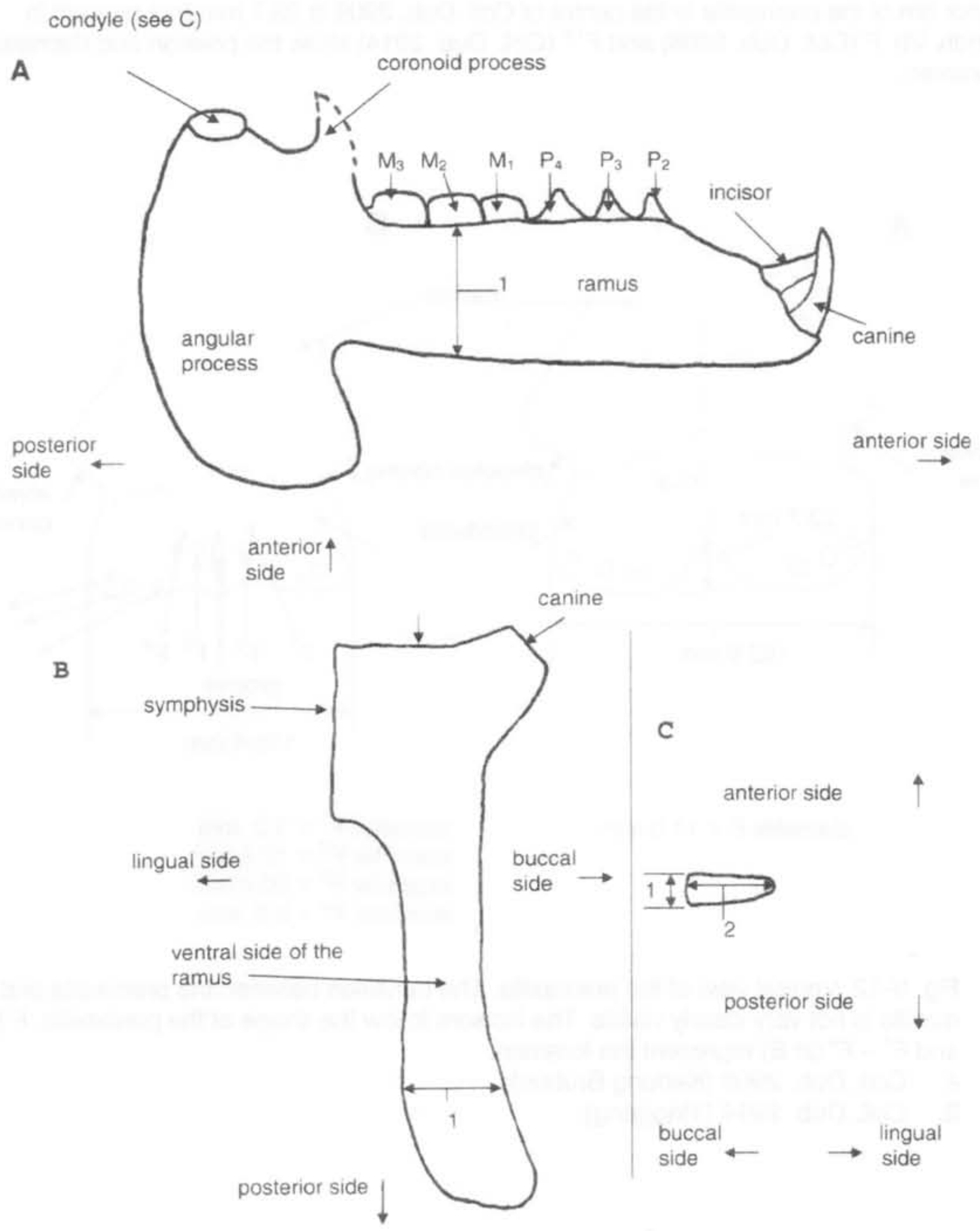

Fig. V-11. A. Lateral view of a right mandible; 1. thickness of the ramus below M_2; B. ventral view of the ramus; 1. width of ramus measured on the ventral side; C. dorsal view of a condyle. Numbers 1-2 indicate the measurements mentioned in the text, Appendix VII.9 (mandible Coll. Dub. 99); 1. width; 2. length.

V-H CRANIUM

The method of measuring is described and explained in Figs. V-12, V-13C and V-13B – V-17B. Figs. V-13A – V-17A show the names of the bones mentioned in the text.

Fig. V-12 shows the ventral view of the only premaxillae that are preserved. Their shape is very different. The suture between the premaxilla and the maxilla is vaguely visible. The incisors follow the shape of the premaxilla. The width of the premaxilla (Appendix VI.32) of Coll. Dub. 2908 from Kedung Brubus and Coll. Dub. 2914 (Tinggang) is respectively 192.9 mm and 176.4 mm. The distance between the anterior rim of the premaxilla on the lateral sides and the posterior rim of the premaxilla in the centre of Coll. Dub. 2908 is 23.7 mm (not present in Appendix VI). F (Coll. Dub. 2908) and $F^{1\text{-}4}$ (Coll. Dub. 2914) show the position and diameters of the foramen.

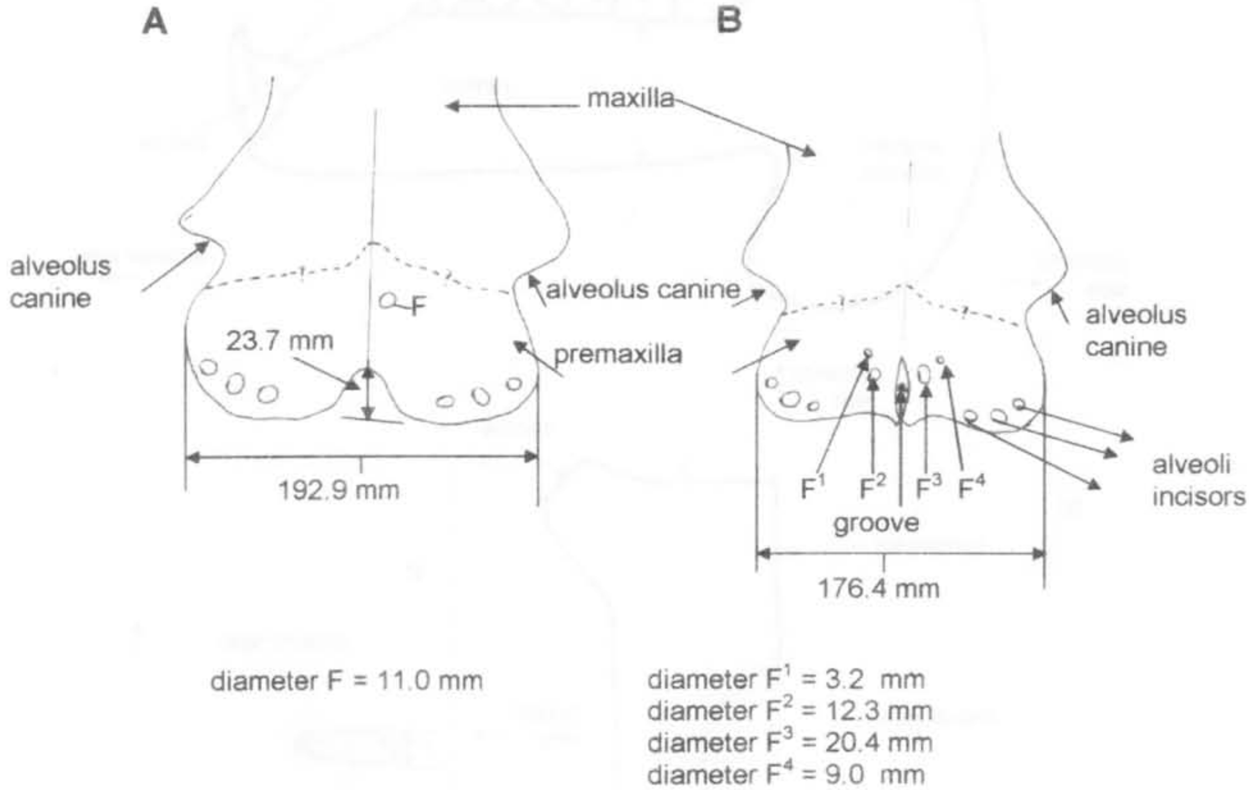

Fig. V-12. Ventral view of the premaxilla. The transition between the premaxilla and the maxilla is not very clearly visible. The incisors follow the shape of the premaxilla. F (in A) and $F^1 - F^4$ (in B) represent the foramen.

A. Coll. Dub. 2908 (Kedung Brubus);
B. Coll. Dub. 2914 (Tinggang).

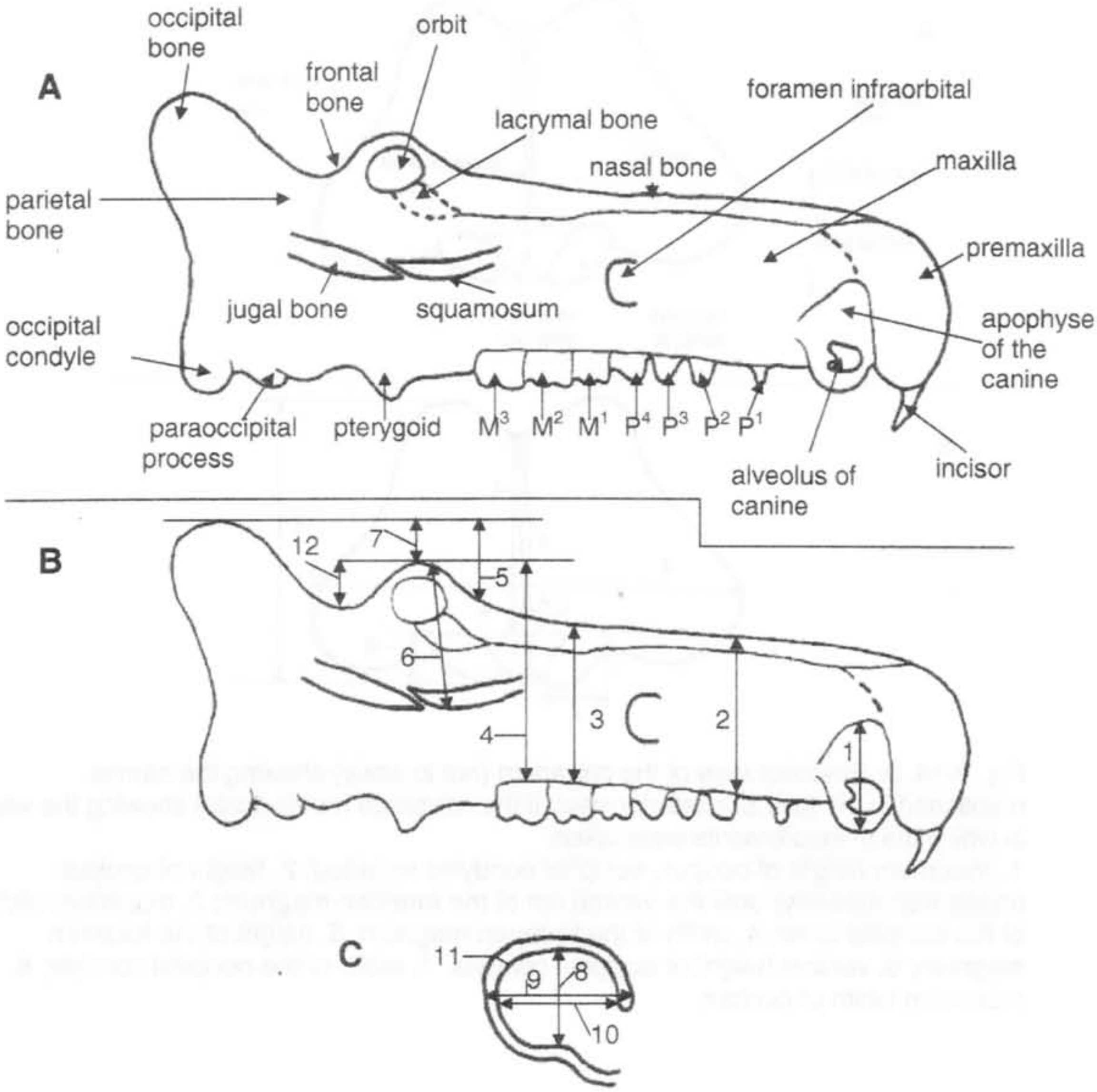

Fig. V-13. A. Lateral view of the calvarium (not to scale); B. lateral view of the calvarium (not to scale), showing the way in which measurements 1-7 and 12 were made; C. lateral view of the orbit with the measurements 8-11
1. maximum thickness of the apophyse of the canine; 2. thickness of the maxilla between the base of the anterior rim of the P^2 and the surface of the nasal bone; 3. thickness of the maxilla between the base of M^2 and the surface of the nasal bone (measured in the middle of the M^2); 4. height of the orbit relative to the base of the M^3 (measured in the middle of the M^3); 5. difference in height (measured medially) between the occipital crest and the posterior end of the nasal bone (distance of the nasal bone below the level of the occipital crest); 6. difference in height (measured obliquely, not vertically) between the highest part of the orbit and the lowest rim of the zygomatic arch (distance orbit – zygomatic arch); 7. difference in height between the occiput and the orbit; 8. vertical height of the orbit; 9. horizontal width of the orbit (outer sides); 10. horizontal width of the orbit (inner sides) maximum thickness of orbital bone; 11. thickness of the orbital bone; 12. height of the orbits relative to the frontal bones, measured in the middle between the orbits.

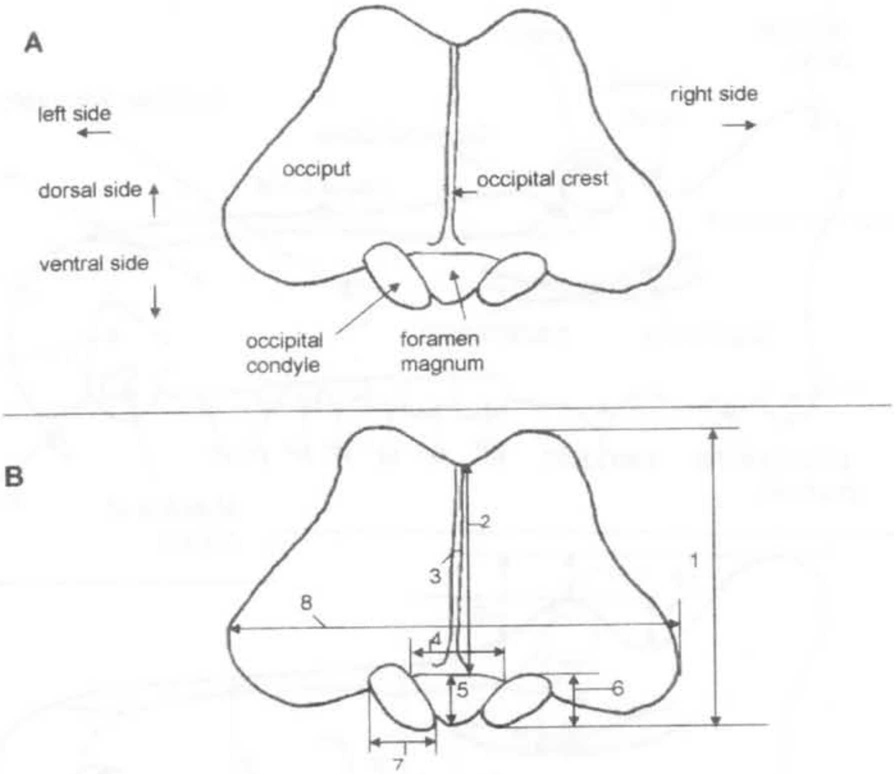

Fig. V-14. A. Posterior view of the calvarium (not to scale) showing the names mentioned in the text; B. posterior view of the calvarium (not to scale) showing the way in which the measurements were taken.
1. maximum height of occiput, occipital condyles included; 2. height of occiput (measured medially) until the ventral rim of the foramen magnum; 3. maximum width of the occipital crest; 4. width of the foramen magnum; 5. height of the foramen magnum; 6. vertical height of occipital condyle; 7. width of the occipital condyle; 8. maximum width of occiput.

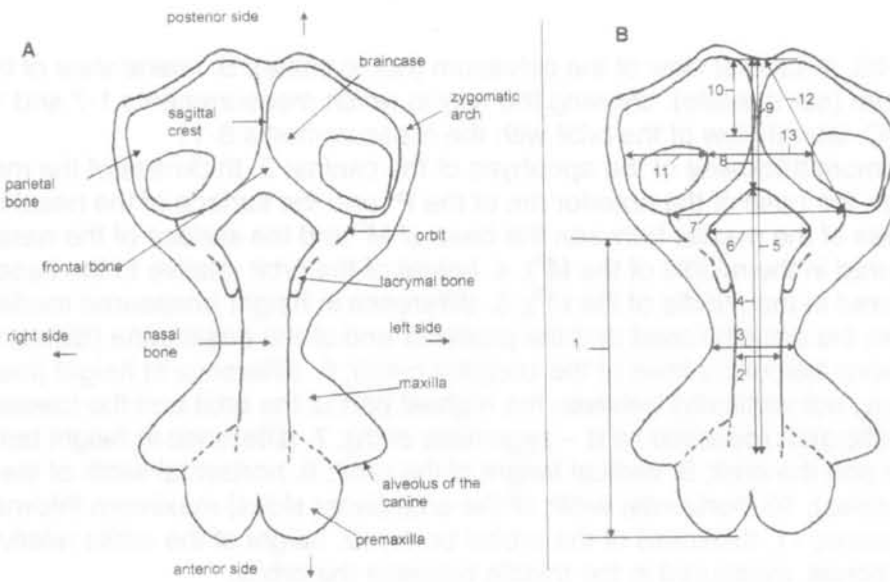

Fig. V-15. Explanation, see next page

Fig. V-15. A. Dorsal view of the calvarium (not to scale) showing the names mentioned in the text; B. dorsal view of the calvarium (not to scale) showing the way in which measurements 1-13 were taken.

1. minimum* distance between the anterior rim of the orbit and the anterior rim of the premaxilla (pre-orbital length); 2. minimum width of the nasal bone; 3. smallest part of the muzzle; 4. minimum* length of the nasal bone; 5. minimum* distance (measured medially) between the occiput and the anterior end of the nasal bone; 6. maximum width of the nasal bone; 7. minimum distance between the inner sides of the orbits; 8. medial distance between the occiput and the posterior end of the nasal bone; 9. width of the sagittal crest; 10. length of sagittal crest, from occiput until the point where the sagittal crest widens (measured medially); 11. maximum distance between the inner side of the zygomatic arch and the brain-case; 12. distance between the occiput and the posterior rim of the orbit; 13. minimum width of the braincase.
(*minimum because there are no specimens in which the calvarium has been completely preserved).

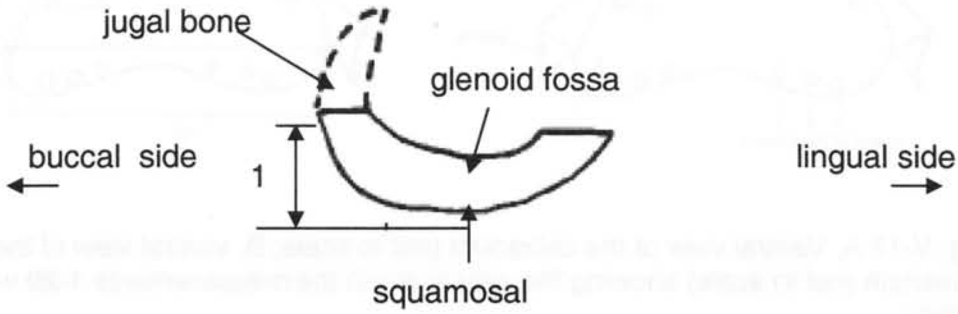

Fig. V-16. Posterior view (not to scale) of the zygomatic arch, with the maximum thickness of the squamosal, measured anteriorly of the glenoid fossa (1).

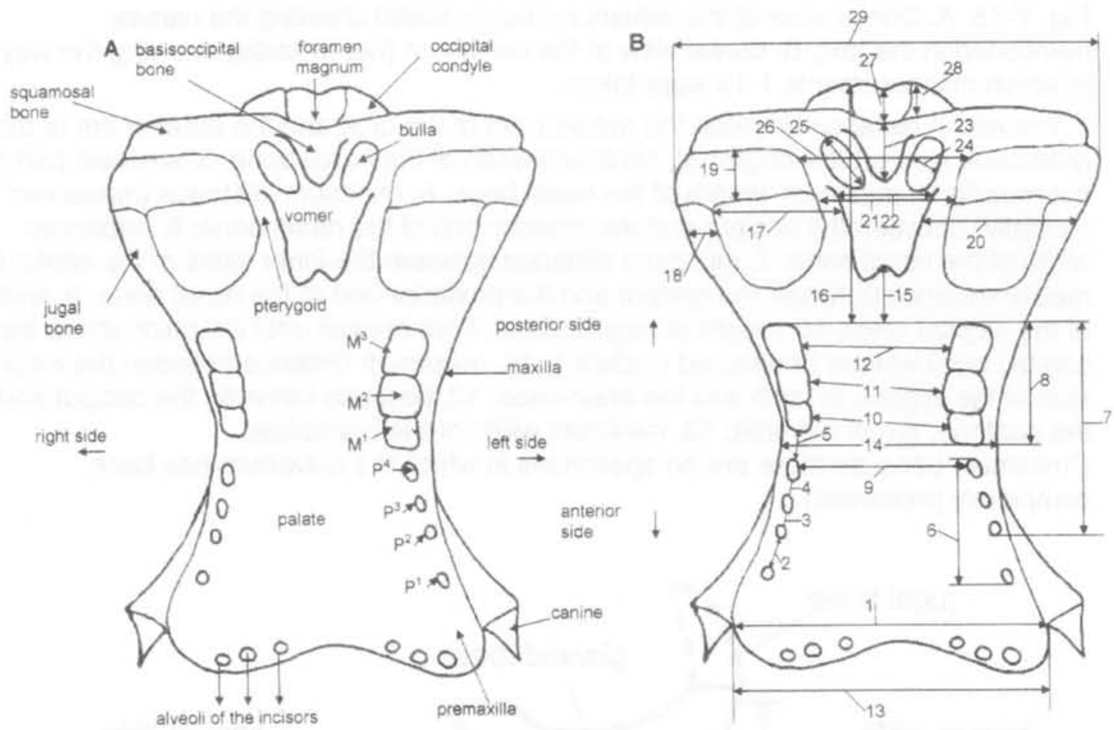

Fig. V-17 A. Ventral view of the calvarium (not to scale; B. ventral view of the calvarium (not to scale) showing the way in which the measurements 1-29 were taken.

1. distance between the inner sides of the canines; 2. diastema between the P^1 and P^2; 3. diastema between the P^2 and P^3; 4. diastema between the P^3 and P^4; 5. diastema between P^4 and M^1; 6. length $P^1 - P^4$; 7. length $P^2 - M^3$; 8. length $M^1 - M^3$; 9. width of palate between the P^4's; 10. width of palate between the M^1's (measured in the middle of M^1); 11. width of palate between the M^2's (measured in the middle of M^2); 12. width of palate between the M^3's (measured in the middle of M^3); 13. width of the premaxilla (see also Fig. V-12); 14. smallest part of the muzzle; 15. medial distance from posterior rim of palate to posterior end of the M^3; 16. maximum distance between the posterior end of M^3 and the posterior end of the occipital condyle; 17. distance between the inner side of the jugal bone and the outer rim of the pterygoid; 18. smallest width of the jugal bone; 19. maximum width of squamosal; 20. distance between the outer rim of the zygomatic arch and the buccal rim of the pterygoid; 21. maximum distance between the pterygoids; 22. minimum distance between the pterygoids; 23. length of the basioccipital bone; 24. width of the bulla, measured at the base of the bulla (maximum width); 25. maximum length of the bulla (diameter anterolingual-posterobuccal), measured at the base of the bulla; 26. minimum distance between the lingual rims of the squamosal bones; 27. length of the foramen magnum; 28. length of the occipital condyle; 29. maximum width between the zygomatic arches.

APPENDIX VI MEASUREMENTS OF *HEXAPROTODON* FROM JAVA AND THE SIWALIKS

All measurements are in mm. An example of a reference to a figure: Fig. V-2,4 refers to measurement 4 in Fig. V-2 (in Appendix V). In some tables, the measurements of material from the Siwaliks are placed at the end of the table below a thicker black line, in order to separate them from the specimens from Java.

VI-1 I_1

number specimen	locality	width of alveolus I_1 (Fig. V-2, 4)	height of alveolus I_1 (Fig V-2, 3)	width of I_1 behind wear facet (Fig. V-1A,3)	width of I_1 at posterior end (Fig. V-1A, 4)	thickness of I_1 behind wear facet (Fig. V-1B,6)	thickness of I_1 at posterior end (Fig. V-1A,5)	I_1 length (Fig. V-1A,1)	I_1 length wear facet (Fig. V-1A,2)
without no. (skeleton Museum Bandung)	Kali Glagah	sin 17.5	--	--	--	--	--	--	--
22 G	Tji Bokagung (Tji Djolang)	-- --	-- --	sin 20.7 dex 17.4	sin 20.8 dex 21.0	sin 20.0 dex 18.7	sin 22.0 dex 21.3	-- --	-- --
without no. (skull and mandible, Museum Bandung)	Ngandong	sin 39.0	--	--	--	--	--	--	--
SA 270378	Triangulation Point, Ngebung	sin 7,5 juvenile	--	--	--	--	--	--	--
K 790	Ngandong	-- --	-- --	sin 31.7 dex 32.0	-- --	sin 28.0 dex 28.1	-- --	sin 180.0 (root included) dex 126.0	-- --
Coll. Dub. 99	Tritik	-- --	-- --	sin 19.7 dex 21.3	sin -- dex 20.6	sin 21.4 dex --	sin -- dex 20.5	sin 120.0 dex 132.1	-- --
Coll. Dub. 513	Nonko	sin 17.4	sin 21.7	--	--	--	--	--	--
Coll. Dub. 1804	Redjuno near Teguan	--	--	--	dex 13.5	--	dex 17.4	--	--

number specimen	locality	width of alveolus I_1 (Fig. V-2,4)	height of alveolus I_1 (Fig V-2,3)	width of I_1 behind wear facet (Fig. V-1A,3)	width of I_1 at posterior end (Fig. V-1A,4)	thickness of I_1 behind wear facet (Fig. V-1B,6)	thickness of I_1 at posterior end (Fig. V-1A,5)	I_1 length (Fig. V-1A,1)	I_1 length wear facet (Fig. V-1A,2)
Coll. Dub. 2903	"Trinil"	sin -- dex 23.9	sin -- dex 26.2	-- --	sin 27.0 dex --	-- --	sin 34.0 dex --	-- --	-- --
Coll. Dub. 2910 mandibula	Tritik	-- --	-- --	-- --	sin 27.0 dex 24.0	-- --	sin 28.4 dex 24.6	-- --	-- --
Coll. Dub. 2910 incisors	Tritik	-- --	-- --	sin 22.9 dex 23.1	sin 22.8 dex 25.3	sin 24.2 dex 23.9	sin 25.7 dex 24.5	-- --	sin 39.0 dex ± 46.0
Coll. Dub. 2915	Solo Valley	-- --	-- --	-- --	sin 24.2 dex 26.2	-- --	sin 27.0 dex 25.8	-- --	-- --
Coll. Dub. 2916	Kedung Brubus	-- --	-- --	-- --	sin 22.4 dex 23.0	-- --	sin 20.6 dex 21.8	-- --	-- --
Coll. Dub. 2918	Papa Djaran	-- --	-- --	-- --	sin 22.2 dex 22.0	-- --	sin 26.5 dex 23.5	-- --	-- --
Coll. Dub. 2929	Kedung Madoh	sin 24.6 dex 26.2	sin --- dex 27.9 *	-- --	-- --	-- --	-- --	-- --	-- --
Coll. Dub. 2931	Kedung Brubus	-- --	-- --	-- --	sin 23.1 dex 24.1	-- --	sin 22.8 dex 22.2	-- --	-- --
Coll. Dub. 2932	Nonko	--	--	--	sin 16.8	--	sin 23.5	--	--
Coll. Dub. 2934	Kedung Brubus	-- --	-- --	-- --	sin 15.1 dex 17.2	-- --	sin 18.2 dex 22.1	-- --	-- --

*measured at the posterior part of the alveolus

VI-2 I_2

Number of specimen	locality	width of alveolus I_2 (Fig. V-2,4)	height of alveolus I_2 (Fig. V-2,3)	width of I_2 behind wear facet (Fig. V-1A,3)	width of I_2 at posterior end (Fig. V-1A,4)	thickness of I_2 behind wear facet (Fig. V-1B,6)	thickness of I_2 at posterior end (Fig. V-1A,5)	I_2 length (Fig. V-1A,1)
without no. (skeleton, Museum Bandung)	Kali Glagah	sin 17.1	--	--	--	--	--	--
22 G	Tji Bokagung (Tji Djolang)	-- --	-- --	sin -- dex 17.9	sin 20.5 dex 22.6	sin 18.2 dex 16.6	sin 19.9 dex 18.3	-- --
without no. (skull and mandible, Museum Bandung)	Ngandong	--	--	sin 26.0	--	--	sin 32.0	110.0
SA 270378	Triangu-lation Point, Ngebung	sin 6.9 juvenile	--	--	--	--	--	--
K 790	Ngandong	--	--	sin 18.6	--	sin 20.4	--	sin 85.0
Coll. Dub. 99	Tritik	sin – dex ±16.1	-- --	-- --	sin 16.4 dex --	-- --	sin 16.8 dex ---	-- --
Coll. Dub. 513	Nonko	sin 15.3	sin 18.1	--	--	--	--	--
Coll. Dub. 1804	Redjuno near Teguan	--	--	--	dex 11.1	--	dex 13.6	--
Coll. Dub. 2903	"Trinil"	--	--	--	dex 21.1	--	dex 22.4	--
Coll. Dub. 2910 mandibula	Tritik	--	--	--	sin 18.3	--	sin 17.6	---

Number of specimen	locality	width of alveolus I_2 (Fig. V-2,4)	height of alveolus I_2 (Fig. V-2,3)	width of I_2 behind wear facet (Fig. V-1A,3)	width of I_2 at posterior end (Fig. V-1A,4)	thickness of I_2 behind wear facet (Fig. V-1B,6)	thickness of I_2 at posterior end (Fig. V-1A,5)	I_2 length (Fig. V-1A,1)
Coll. Dub. 2910 incisor	Tritik	--	--	sin 17.0	sin 18.5	sin 18.5	sin 19.0	--
Coll. Dub. 2915	Solo Valley	-- --	-- --	-- --	sin 21.4 dex 18.9	-- --	sin 19.3 dex 23.6	-- --
Coll. Dub. 2916	Kedung Brubus	sin 17.3	sin ± 17.2	--	--	--	--	--
Coll. Dub. 2918	Papa Djaran	sin -- dex 21.4	sin -- dex 22.5	-- --	sin 20.2 dex --	-- --	sin 20.7 dex --	-- --
Coll. Dub. 2929	Kedung Madoh	dex ± 21.1	dex 23.0 *	--	--	--	--	--
Coll. Dub. 2931	Kedung Brubus	-- --	-- --	-- --	sin 16.9 dex 17.2	-- --	sin 16.6 dex 18.8	-- --
Coll. Dub. 2932	Nonko	-- --	-- --	-- --	sin 15.2 dex 14.5	-- --	sin 20.2 dex 20.3	-- --
Coll. Dub. 2934	Kedung Brubus	-- --	-- --	-- --	sin ± 14.7 dex 13.5	-- --	sin ± 14.8 dex 16.4	-- --
Coll. Dub. 4908	Kedung Brubus	dex ± 18.8	dex 21.1	--	--	--	--	--

* measured at posterior part of the alveolus

VI-3 I_3

number of specimen	locality	width of alveolus I_3 (Fig. V-2,4)	height of alveolus I_3 (Fig. V-2,3)	width of I_3 behind wear facet (Fig. V-1A,3)	width of I_3 at posterior end (Fig. V-1A,4)	thickness of I_3 behind wear facet (Fig. V-2B,6)	thickness of I_3 at posterior end (Fig. V-1A,5)	I_3 length (Fig. V-1A,1)
22G	Tji Bokagung (Tji Djolang)	-- --	-- --	sin 22.0 dex 18.5	sin -- dex 23.6	sin 22.0 dex 19.1	sin -- dex 22.9	-- --
without no. (skull and mandible, Museum Bandung)	Ngandong	sin 31.0	--	--	--	--	--	--
SA 270378	Triangulation Point, Ngebung	sin 5.0 juvenile	--	--	--	--	--	--
K 790	Ngandong	--	--	sin 26.7	--	sin 27.4	--	sin 155.0
Coll. Dub. 99	Tritik	sin -- dex 20.4	sin -- dex 21.8	-- --	sin 19.8 dex ---	-- --	sin 19.2 dex ---	-- --
Coll. Dub. 513	Nonko	sin 19.0	sin 16.0	--	--	--	--	--
Coll. Dub. 1818	Redjuno	--	--	--	sin 18.3	--	sin 17.3	--
Coll. Dub. 2903	"Trinil"	dex 19.2	dex 21.3	--	--	--	--	--
Coll. Dub. 2910 mandibula	Tritik	sin 29.7 dex --	sin 21.2 dex --	-- --	sin -- dex 21.2	-- --	sin -- dex 21.0	-- --
Coll. Dub. 2915	Solo Valley	-- --	-- --	-- --	sin 20.5 dex 20.4	-- --	sin 23.7 dex 22.8	-- --
Coll. Dub. 2916	Kedung Brubus	--	--	sin 18.9	sin 18.5	sin 18.0	sin 16.0	--
Coll. Dub. 2918	Papa Djaran	-- --	-- --	-- --	sin 17.4 dex 16.3	-- --	sin 21.2 dex 20.1	-- --

number of specimen	locality	width of alveolus I_3 (Fig. V-2,4)	height of alveolus I_3 (Fig. V-2,3)	width of I_3 behind wear facet (Fig. V-1,3)	width of I_3 at posterior end (Fig. V-1,4)	thickness of I_3 behind wear facet (Fig. V-1,6)	thickness of I_3 at posterior end (Fig. V-1,5)	I_3 length (Fig. V-1,1)
Coll. Dub. 2929	Kedung Madoh	sin 26.4 dex 25.1	sin ±20.8 dex 25.0 *	-- --	-- --	-- --	-- --	-- --
Coll. Dub. 2931	Kedung Brubus	-- --	-- --	-- --	sin 16.1 dex ± 14.0	-- --	sin 18.4 dex 17.8	-- --
Coll. Dub. 2932	Nonko	-- --	-- --	-- --	sin ± 15.5 dex 15.5	-- --	sin ± 17.8 dex ±18.7	-- --
Coll. Dub. 2934	Kedung Brubus	-- --	-- --	-- --	sin 17.1 dex 13.3	-- --	sin 18.9 dex 17.1	-- --
Coll. Dub. 4908	Kedung Brubus	dex 22.3	dex 26.4	--	--	--	--	--
Coll. Dub. 3147	Bharon, Punjab, Siwaliks	--	--	dex 26.1	--	--	--	--

* measured at the posterior part of the alveolus

VI-4 LOWER INCISORS

number of specimen	locality	distance between the dorsal side of I_2 and the dorsal sides of $I_{1,3}$ (Fig. V-2,1)	distance between the ventral side of I_2 and the ventral sides of $I_{1,3}$ (Fig. V-2,2)	distance between I_1 sin and I_1 dex (Fig. V-2,5)	distance between I_1 and I_2 (Fig. V-2,6)	distance between I_2 and I_3 (Fig. V-2,7)	distance between I_3 and C (Fig. V-2,8)
K 790	Ngandong	sin 5.6	--	--	--	--	--
Coll. Dub. 99	Tritik	sin 3.0 dex --	sin 6.3 dex --	-- --	-- --	sin 4.6 dex --	sin 18.3 dex 10.1
Coll. Dub. 513	Nonko	sin 6.5	sin 7.1	--	sin 6.8	sin 6.5	--

number of specimen	Locality	distance between the dorsal side of I_2 and the dorsal sides of $I_{1,3}$ (Fig. V-2,1)	distance between the ventral side of I_2 and the ventral sides of $I_{1,3}$ (Fig. V-2,2)	distance between I_1 sin and I_1 dex (Fig. V-2,5)	distance between I_1 and I_2 (Fig. V-2,6)	distance between I_2 and I_3 (Fig. V-2,7)	distance between I_3 and C (Fig. V-2,8)
Coll. Dub. 1818	Redjuno	--	--	--	--	--	sin 21.7
Coll. Dub. 2903	"Trinil"	sin ± 12.2 dex 7.3	sin 14.6 dex 10.7	-- --	-- --	-- --	-- --
Coll. Dub. 2910	Tritik	sin 6.1 dex --	sin 15.1 dex ± 11.0	7.5	sin 3.4 dex 6.4	sin 5.5 dex --	sin 28.7 dex 34.6
Coll. Dub. 2915	Solo Valley	sin 3.1 dex 5.0	sin 7.9 dex 8.1	6.8	sin 3.6 dex 3.9	sin 5.3 dex 6.4	sin 29.0 dex ± 20.6
Coll. Dub. 2916	Kedung Brubus	sin 8.3 dex ± 7.9	sin 4.0 dex ± 4.0	7.8	sin 5.9 dex ± 6.8	sin 4.9 dex --	sin 24.6 dex --
Coll. Dub. 2918	Papa Djaran	sin 10.2 dex 9.1	sin 8.7 dex 6.0	9.8	sin 1.9 dex 2.4	sin 6.1 dex 5.0	sin 21.0 dex 20.1
Coll. Dub. 2929	Kedung Madoh	sin -- dex 11.6	sin 14.2 dex12.1	--	-- --	-- --	-- --
Coll. Dub. 2931	Kedung Brubus	sin 6.0 dex --	sin 12.8 dex --	8.9	sin 6.4 dex 6.8	sin 8.7 dex 5.9	-- --
Coll. Dub. 2932	Nonko	sin 5.0 dex 6.7	sin 8.3 dex 7.8	13.3	sin 4.3 dex 4.9	sin 2.1 dex 6.1	-- --
Coll. Dub. 2934	Kedung Brubus	sin -- dex 6.5	sin 6.0 dex 5.0	8.6	sin 2.8 dex 3.6	sin 1.5 dex 2.8	sin 14.3 dex 13.5
Coll. Dub. 4908	Kedung Brubus	sin -- dex 10.5	sin -- dex 11.6	5.0	sin -- dex 0	sin -- dex 0	sin -- dex 11.0

VI-5 INDETERMINABLE LOWER INCISORS

number of specimen	locality	dt minimum *1	dt maximum *1	width of I behind wear facet (Fig. V-1A.3)	width of I at posterior end (Fig. V-1A.4)	thickness of I behind wear facet (Fig. V-1B.6)	thickness of I at posterior end (Fig. V-1A,5)	I length (Fig. V-1A,1)	I length wear facet (Fig. V-1A.2)
SA 030979-14	New Pb site?	--	--	16.1	15.8	16.8	16.6	± 108.0	--
SA 040979-16/3	New Pb site	--	--	sin 19.7	sin 18.9	sin 16.4	sin 18.7	sin min 136.0	--
SA 140979-7	New Pb site	--	--	17.9	22.3	19.8	24.1	min 140.0	--
SA 160878-180	Dam P12	20.5	21.1	--	--	--	--	--	--
SA 230178	PD III-14, Grenzbank	--	--	dex 17.4	--	dex 18.5	--	--	--
K 717/1 K 717/2	Ngandong	-- --	-- --	sin 26.6 sin 31.7	sin 27.3 sin 30.4	sin 30.8 sin 25.8	sin 28.6 sin 25.6	sin 146.2 sin 190.0	-- --
K 718/1 K 718/2 K 718/3	Kali Glagah	-- -- --	-- -- --	sin 13.8 sin 19.8*2 dex 14.1	sin 10.8 sin 21.8 dex 10.1	sin 15.4 sin 22.7*2 dex 14.8	sin 12.1 sin 25.7 dex 11.2	sin 105.7 sin 144.3 dex 120.2	-- -- --
K 719	Kali Saat	--	--	sin 24.8	sin 15.6	sin 25.1	sin 19.2	sin 155.0	--
K 747	Gn. Butak	--	--	dex 18.1	dex 16.4	dex 14.9	dex 15.4	dex 119.4	--
Coll. Dub. 95/1 Coll. Dub. 95/2	Tritik	-- --	-- --	dex 19.8 sin 19.9	-- --	dex 19.4 sin 21.4	-- --	dex 76.1 sin 83.6	dex 44.8 sin 38.9
Coll. Dub. 285/1	Dekes/ Wadegan	--	--	--	sin 22.5	--	sin 22.2	--	sin min 32.6 *3
Coll. Dub. 2207 a/1	Kedung Brubus	--	--	sin 24.4	sin 25.8	sin 24.8	sin 27.3	sin 116.1	sin 46.2
Coll. Dub. 2912	Java	--	--	sin 20.9	--	sin 19.6	--	--	sin 31.1

If no orientation of the incisor could be established, the minimum and maximum diameter was measured

*1 piece of incisor without a wear facet or posterior end. It is too small to decide what the orientation is;

*2 measured behind glued top;

*3 most anterior part of the wear facet is broken off

VI-6 UPPER INCISORS

number of specimen	locality	I^1 dt min (Figs. V-3A,1 and V-3B,1)	I^1 dt max (Figs. V-3A,2 and V-3B,2)	I^2 dt min (Figs. V-3A,1 and V-3B,1)	I^2 dt max (Figs. V-3A,2 and V-3B,2)	I^3 dt min (Figs. V-3A,1 and V-3B,1)	I^3 dt max (Figs. V-3A,2 and V-3B,2)	distance between the posterior side of I^2 and the posterior sides of $I^{1,3}$ (Fig. V-3A,4)	distance between the anterior side of I^2 and the anterior sides of $I^{1,3}$ (Fig. V-3A,3)	I^{indet} dt min (Fig. V-3B,1)	I^{indet} dt max (Fig. V-3B,2)	length of wear facet (Fig. V-3B,5)
K 714	Java	dex 12.2 *	dex 13.3 *	dex 15.5 *	dex 14.9 *	dex 12.0 *	dex 11.5 *	--	--	--	--	--
K 716 (?)	Kali Glagah	--	--	--	--	--	--	--	--	12.7 *	14.3 *	--
Coll. Dub. without number (piece of premaxilla)	Unknown	--	--	--	--	--	--	--	--	20.6	26.7	--
Coll. Dub. 2076 a/1	Kedung Brubus	--	--	--	--	--	--	--	--	sin 13.3 *	sin 17.9 *	sin 17.4
Coll. Dub. 2076 a/2		--	--	--	--	--	--	--	--	16.6 *	20.1 *	--
Coll. Dub. 2182/1	Kedung Lumbu	--	--	dex 15.0 *	dex 17.2 *	dex 9.6	dex 11.4	--	--	--	--	--
Coll. Dub. 2182/2	Kedung Lumbu	--	--	--	--	--	--	--	--	--	sin? 14.1	--
Coll. Dub. 2182/3	Kedung Lumbu	--	--	--	--	--	--	--	--	--	sin? 11.9	--
Coll. Dub. 2189	Kedung Lumbu	--	--	sin 13.6 *	sin 15.6 *	--	--	--	--	--	--	sin 13.1
Coll. Dub. 2191b/1	Java	--	--	--	--	--	--	--	--	15.0 *	18.5 *	17.7

number of specimen	locality	I^1 dt min (Figs. V-3A,1 and V-3B,1)	I^1 dt max (Figs. V-3A,2 and V-3B,2)	I^2 dt min (Figs. V-3A,1 and V-3B,1)	I^2 dt max (Figs. V-3A,2 and V-3B,2)	I^3 dt min (Figs. V-3A,1 and V-3B,1)	I^3 dt max (Figs. V-3A,2 and V-3B,2)	distance between the posterior side of I^2 and the posterior sides of $I^{1,3}$ (Fig. V-3A,4)	distance between the anterior side of I^2 and the anterior sides of $I^{1,3}$ (Fig. V-3A,3)	I^{indet} dt min (Fig. V-3B,1)	I^{indet} dt max (Fig. V-3B,2)	length of wear facet (Fig. V-3B,5)
Coll. Dub. 2902	"Trinil"	dex 13.0	dex 14.2	dex 13.8	dex 20.8	dex 9.0	dex 12.0	dex 8.0	dex 2.9	--	--	--
Coll. Dub. 2907/1	Nonko	--	--	dex 12.9 --	dex 18.9 --	dex 11.2 --	dex 13.0	8.3	4.4	--	--	-- --
Coll. Dub. 2907/2	Nonko	--	--				--	--	--	18.0	24.5	
Coll. Dub. 2908	Kedung Brubus	sin 16.1 dex --	sin 27.5 dex --	sin 16.1 dex 15.0	sin 26.0 dex 21.7	sin 15.4 * dex 17.1	sin 14..8 * dex 15.4	sin 8.4 dex 8.5	sin 6.7 dex 6.6	-- --	-- --	-- --
Coll. Dub. 2909	Tinggang	dex 14.7	dex 20.7	dex 20.9	dex 25.3	--	--	--	--	--	--	--
Coll. Dub. 2911	Tinggang	sin ± 20.8 dex 18.5	sin ± 24.5 dex 23.2	sin – dex 21.4	sin – dex 29.1	-- --	-- --	-- --	-- --	-- --	-- --	-- --
Coll. Dub. 2914	Tinggang	sin 14.4 dex --	sin 18.4 dex --	sin 13.4 dex 13.7	sin 23.2 dex 19.4	sin 10.8 dex 11.0	sin 16.6 dex 13.2	sin 11.3 dex 13.0	sin 6.0 dex 5.0	-- --	-- --	-- --

* = measurement of incisor; all other measurements are from alveoli

VI-7 LOWER CANINES

number of specimen	locality	width alveolus (Fig. V-2,10)	height alveolus (Fig. V-2,9)	width canine (Fig. V-4A,2)	height canine (Fig. V-4A,1)	length (Fig. V-4B,3)	length curvature (Fig. V-44B,4)	length wear facet (Fig. V-4B,5)
without no. (skeleton, Geological Museum, Bandung)	Kali Glagah	-- --	sin 37.1 dex 42.7	-- --	-- --	-- --	-- --	-- --
22 G	Tji Bokagung (Tji Djolang)	-- --	-- --	sin 33.4 dex 32.5	sin 45.6 dex 42.2	sin 213 dex 180	sin 250 dex 193	sin 75.9 dex 99.6
203	unknown	--	--	--	sin 42.3	--	--	--
1746	Ngandong	--	--	--	dex 50.5	--	--	--
without number (Geological Museum Bandung)	Tjipanaruban	--	--	--	sin 30.5	--	--	--
SA 040979-30 L	New Pb site	--	--	sin 26.9	sin min 43.9	sin 157	sin 175	sin ± 89.2
SA 040979-30 M	New Pb site	--	--	dex 29.7	dex 43.7	dex 230	dex 301	dex 124.5
SA 230779	P VIII digging site	--	--	dex 24.3	dex min 36.6	dex 112.8	dex min 115	--
SA 270378	Triangulation Point, Ngebung	--	sin 6.4 juvenile	--	--	--	--	--
Bumiayu, exc. 8	Kali Glagah	--	--	sin 26.1	sin 43.5	sin 126	sin 270	sin min 93.0
M 16	Kali Biuk, Bumiayu, exc. 9	--	--	dex 25.7	dex 37.9	dex 228	dex 283	dex 101.7
K 158	Tjipanarabun	--	--	sin 30.4	--	sin 67.9	--	sin 42.7 *[1]
K 522	Kali Glagah	--	--	sin 12.3	sin 11.8	sin 78.8	sin 86.0	--
K 654	Gn. Butak	--	--	sin 12.6	sin 17.3	sin 86.1	sin 101	sin 22.7
K 710/1	Ngandong	--	--	dex 31.2	dex 44.4	dex 160	dex 191	--
K 713/1. (526) K 713/2. (527) K 713/3. (---) K 713/4. (523)	Gn. Butak Gn. Butak Gn. Butak Gn. Butak	-- -- -- --	-- -- -- --	dex 17.9 dex 14.3 dex 10.4 12.2	dex 17.9 dex 19.8 dex 13.1 14.4	dex 87.5 dex 96.4 dex 61.8 --	dex 114 dex 110 dex 63 --	dex 15.8 dex 28.5 dex 15.0 --

number of specimen	locality	width alveolus (Fig. V-2,10)	height alveolus (Fig. V-2,9)	width canine (Fig. V-4A,2)	height canine (Fig. V-4A,1)	length (Fig.V-4B,3)	length curvature (Fig. V-4B,4)	length wear facet (Fig. V-4B,5)
K 715/1	Gn. Butak	--	--	dex 23.0	dex 38.9	dex 205	dex 295	dex 100.9
K 716/1	Kali Glagah	--	--	dex 41.9	dex 63.7	dex 190	dex 210	dex min 132.7
K 720/1	Kali Saat	--	--	--	sin min 30.2	sin 98.5	sin 104	--
K 733	Kali Bringin, Ngawi	--	--	dex 24.1	dex min 30.1	dex 90.7	dex 92	--
K 1567	Gn. Butak	--	--	dex 22.1	dex 39.6	dex 200	dex 295	dex 96.7
Coll. Dub. without no. (belongs to Coll. Dub. 4857??)	Java	--	--	sin 55.2	sin 62.9	--	--	--
Coll. Dub. 98	Java	--	--	dex 28.8	dex 45.8	--	--	--
Coll. Dub. 99	Tritik	sin 24.7 dex 25.9	sin 40.9 dex 44.9	--	--	--	--	--
Coll. Dub. 100/1 Coll. Dub. 100/2 Coll. Dub. 100/3 Coll. Dub. 100/4	Java Java Java Java	-- -- -- --	-- -- -- --	sin 20.5 21.9 26.4 25.7	sin 37.8 -- 44.2 38.7	sin 47.5 47.9 64.4 70.0	-- -- -- --	-- -- -- --
Coll. Dub. 308d/1	Java	--	--	dex 24.4	dex min 39.0	dex 60.8	dex 56	--
Coll. Dub. 314?	Kedung Lumbu?	--	--	dex 23.5	dex 28.7	dex 74.6	dex 80	--
Coll. Dub. 513	Nonko	--	--	sin 29.1 dex 25.8	sin 43.7 dex 42.6	--	--	--
Coll. Dub. 1804	Redjuno near Teguan	--	--	dex 29.4	dex 40.3	--	--	--
Coll. Dub. 1818	Redjuno	--	--	sin 30.3	sin 37.2	--	--	--
Coll. Dub. 2017/1	Java	--	--	29.6	40.9	--	--	--
Coll. Dub. 2019a	Kedung Brubus	--	--	--	sin min 33.91	sin 212.7	sin + 290	sin 26.7
Coll. Dub. 2019b	Papa Djaran, N of Kebon Duren	--	--	--	sin 47.2	sin 156.5	sin 174	sin min 100.1

number of specimen	locality	width alveolus (Fig. V-2,10)	height alveolus (Fig. V-2,9)	width canine (Fig. V-4A,2)	height canine (Fig. V-4A,1)	length (Fig. V-4B,3)	length curvature (Fig. V-4B,4)	length wear facet (Fig. V-4B,5)
Coll. Dub. 2076a/3 Coll. Dub. 2076a/4 Coll. Dub. 2076a/5	Kedung Brubus Kedung Brubus Kedung Brubus	-- -- --	-- -- --	dex 26.9 25.7 25.0	dex 34.3 41.0 37.4	dex 134.4 58.7 31.6	-- -- --	dex min 104.5 -- --
Coll. Dub. 2084d	Kedung Brubus	--	--	sin 28.2	sin min 36.0	sin 101.7	sin 80	--
Coll. Dub. 2174	Kedung Brubus	--	--	sin 34.6	sin 60.3	--	--	--
Coll. Dub. 2190a/1	Kedung Brubus	--	--	dex 37.2	dex 55.1	dex 177.2	dex 150	dex min 76.4
Coll. Dub. 2191b/2 Coll. Dub. 2191b/3	Java Java	-- --	-- --	-- 28.2	39.6 min 45.2	-- 32.0	-- --	-- --
Coll. Dub. 2314	Papa Djaran, N of Kebon Duren	--	--	dex 34.6	dex min 38.8	--	--	--
Coll. Dub. 2903	"Trinil"	--	--	dex 37.5	dex 51.2	--	--	--
Coll. Dub. 2904	Kebon Duren	--	--	sin 30.2	sin 46.5	--	--	--
Coll. Dub. 2910	Tritik	--	--	sin 35.0 dex 34.6	sin 48.6 dex 44.5	--	--	--
Coll. Dub. 2915	Solo Valley	sin 38.9 dex ± 40.2	sin 49.5 dex ± 50.2	--	--	--	--	--
Coll. Dub. 2916	Kedung Brubus	sin ± 29.9	sin 64.0	dex ± 34.4	dex 53.2	--	--	--
Coll. Dub. 2917	Kedung Lumbu	--	--	dex 26.2	dex 38.6	--	--	--
Coll. Dub. 2918	Papa Djaran, N of Kebon Duren	--	--	sin 36.7 dex 34.1	sin 49.1 dex 46.3	--	--	--
Coll. Dub. 2922	Kedung Lumbu	--	--	sin 23.2	sin min 38.4	--	--	--
Coll. Dub. 2924/2	Java	--	--	34.1	--	--	--	--
Coll. Dub. 2929	Kedung Madoh	--	--	dex 36.3	dex 55.4	--	--	--
Coll. Dub. 2931	Kedung Brubus	--	--	sin 25.0	sin 41.5	--	--	--
Coll. Dub. 2932	Nonko	--	--	sin 27.4 *2 dex 28.1	sin 46.5 *2 dex 55.3	--	--	--

number of specimen	locality	width alveolus (Fig. V-2,10)	height alveolus (Fig. V-2,9)	width canine (Fig. V-4A,2)	height canine (Fig. V-4A,1)	length (Fig. V-4B,3)	length curvature (Fig. V-4B,4)	length wear facet (Fig. V-4B,5)
Coll. Dub. 2934	Kedung Brubus	--	--	dex 30.6	dex ± 41.5	--	--	--
Coll. Dub. 4606	Java	--	--	sin 29.1	sin 43.3	sin 48.7	--	--
Coll. Dub. 4908	Kedung Brubus	dex 48.9 *[3]	--	--	--	--	--	--
Coll. Dub. 5527	Kedung Brubus	--	--	sin 29.0	sin 44.5	sin 35.0	--	--
Coll. Dub. 5803	Java	--	--	--	min 36.4	--	--	--
Coll. Dub. 6491	Java	--	--	dex 35.6	dex 49.7	dex 100.1	--	--
Coll. Dub. 6954/2	Tritik	--	--	38.0	--	47.5	--	--
Coll. Dub. 8243	Kedung Brubus	--	--	sin 17.1	sin min 20.6	sin 63.2	sin 65	sin 26.7
Coll. Dub. 8473	Java	--	--	23.6	--	56.5	--	--
Coll. Dub. 3147	Bharon, Punjab, Siwaliks	--	--	dex 40.5	dex 60.6	--	--	--

*[1] if this is indeed the wear facet;
*[2] measured at posterior end in jaw;
*[3] measured at posterior end, behind the M_1

VI-8 UPPER CANINES

number	locality	width (Fig. V-5,6)	height on the buccal side (Fig. V-5A,1)	height on the lingual side (Fig. V-5A,2)	length (Fig. V-5B,3)	length curvature (Fig. V-5B,5)	length wear facet (Fig. V-5B,4)
528? (Geological Museum, Bandung)	Gn. Butak	46.3	--	--	--	--	--
without number (Geological Museum, Bandung)	unknown (Java)	43.3	--	--	--	--	--
SA 040979-24	New Pb site	min 37.2	32.5	27.7	min 128.4	93	min 57.2
SA 040979-30 D/1	New Pb site	31.8	31.7	26.7	129.1	155	min 54.7
K 710/2	Ngandong	min 40.9	40.4	35.1	114.8	125	min 47.1
K 715/2	Gn. Butak	37.7	27.3	26.7	134.8	185	57.8
K 716/2	Kali Glagah	38.9	30.9	32.1	153	190	63.0
K 732	Kali Glagah	38.4	31.2	33.3	148.6	± 175	min 59.9
K 748	Pandejan	33.7	29.9	27.4	112.4	120	34.0
Coll. Dub. 285/3	Dekes/Wadegan	min 34.2	28.1	27.5	45.0	51.0	min 31.2
Coll. Dub. 308c	Kedung Brubus	44.4	31.2	29.7	109.9	100	min 32.0
Coll. Dub. 308d/2 Coll. Dub. 308d/3	Java	39.8 min 33.8	28.6 min 29.0	29.1 30.5	23.5 78.0	-- 73	-- --
Coll. Dub. 311/1 Coll. Dub. 311/2	Kebon Duren	36.9 33.1	32.8 27.8	26.5 22.8	55.8 138.3	112 145	-- 42.3
Coll. Dub. 325f/1	"Trinil"	min 35.5	34.2	31.0	--	-	--
Coll. Dub. 548	Kedung Lumbu	40.1	32.1	32.1	159	--	min 48.7
Coll. Dub. 2000/1 Coll. Dub. 2000/2	Kedung Lumbu	36.1 37.1	30.1 33.3	33.5 28.8	91.5 118.7	100 132	± 48.7 47.0
Coll. Dub. 2019c	Kedung Brubus	41.2	28.7	31.8	98.9	106	--
Coll. Dub. 2076/1 Coll. Dub. 2076/2 Coll. Dub. 2076/3	Kedung Brubus	-- 38.6 --	-- 31.3 --	± 32.8 27.9 -	-- min 38.5 --	-- -- --	-- -- min 47.1

number	locality	width (Fig. V-5B,6)	height on the buccal side (Fig. V-5A,1)	height on the lingual side (Fig. V-5A,2)	length (Fig. V-5,3)	length curvature (Fig. V-5B,5)	length wear facet (Fig. V-5B,4)
Coll. Dub. 2078/1	Sumber Waru	41.4	31.1	27.9	111.9	95	min 34.9
Coll. Dub. 2078/2		40.5	30.6	27.0	113.3	121	42.0
Coll. Dub. 2080b	Sumber Waru	30.6	25.0	27.0	83.0	62	min 37.0
Coll. Dub. 2084c	Kedung Brubus	39.0	30.2	28.3	82.1	83	--
Coll. Dub. 2190a/2	Kedung Brubus	41.1	32.3	36.5	138.6	170	50.0
Coll. Dub. 2190a/3		31.6	31.5	30.5	94.0	97.0	± 46.9
Coll. Dub. 2191a	Kedung Lumbu	39.7	32.2	33.5	57.1	--	min 40.1
Coll. Dub. 2196a	Kedung Lumbu	41.7	39.2	32.6	160.0	--	66.1
Coll. Dub. 2204a	Kedung Brubus	38.7	31.4	29.5	102.2	109	min 42.3
Coll. Dub. 2902	"Trinil"	45.3	46.1	31.8	--	--	--
Coll. Dub. 2907/1	Nonko	42.3	31.4	29.0	--	--	--
Coll. Dub. 2908	Kedung Brubus	38.1	42.0	27.0	--	--	--
Coll. Dub. 2914	Tinggang	sin 41.7 dex --	sin 42.2 dex 46.4	sin 35.3 dex 35.6	-- --	-- --	-- --
Coll. Dub. 2921/1	Tritik	35.5	33.8	33.0	--	--	--
Coll. Dub. 2926	Java	42.7	40.3	32.0	--	--	--
Coll. Dub. 4234	Java	--	--	--	163.2	185	min 51.8
Coll. Dub. 4474	Tritik	31.9	28.9	25.0	--	--	--
Coll. Dub. 6490	Java	38.2	36.6	31.5	86.7	--	68.2
Coll. Dub. 6954/3	Tritik	--	29.0	29.9	57.7	--	min 40.5
Coll. Dub. 6954/4		--	33.3	--	--	--	min 43.1

VI-9 P_2

number of specimen	locality	length alveolus (Fig. V-6,1)	width alveolus on the anterior side (Fig. V-6,2)	width alveolus on the posterior side (Fig. V-6,3)	length (Fig. V-6,4)	width on the anterior side (Fig. V-6,9)	width on the posterior side (Fig. V-6,10)	degree of wear	length anterior root (Fig. V-6,7)	width anterior root (Fig. V-6,11)	length posterior root (Fig. V-6,8)	width posterior root (Fig. V-6,12)	crown height anterior side (Fig. V-6,5)	crown height posterior side (Fig. V-6,6)
without number (skeleton, Geological Museum, Bandung)	Kali Glagah	-- dex 28.3	-- dex 15.0	-- --	sin 28.1 --	sin 14.5 --	-- --	broken middle-aged	-- --	-- --	-- --	-- --	-- --	-- --
22 G	Tji Bokagung (Tji Djolang)	-- --	-- --	-- --	sin 24.2 dex 27.2	sin 17.2 dex 17.0	-- --	adult adult	-- --	-- --	-- --	-- --	-- --	-- --
K 653/1	Gn. Butak	--	--	--	sin 20.6	sin 13.9		adult	--	sin 13.5	--	sin 11.9	--	sin 22.3
K 689 (isolated)	Ngandong	--	--	--	dex 21.0	dex 17.2	--	adult	--	dex 12.1	--	dex 17.7	dex 24.2	dex 25.7
K 693	Kali Glagah	--	--	--	dex 20.9	dex 14.8								
Coll. Dub. without number (mandible)	Java	sin 24.4	sin ± 13.7	--	--	--	--	--	--	--	--	--	--	--
Coll. Dub. 87/1 (isolated)	Kali Gedeh	--	--	--	sin 20.3	sin 20.3	--	middle-aged	--	--	--	--	--	--
Coll. Dub. 99 (mandible)	Tritik	-- dex 24.2	-- dex ± 15.7	-- dex ± 14.1	sin 24.6 --	sin 12.5 --	sin 10.6 --	broken --	-- --	-- --	-- --	-- --	-- --	-- --
Coll. Dub. 324a (isolated)	Java	--	--	--	dex 21.0	dex 14.2	--	middle-aged	--	--	--	--	--	--

number of specimen	locality	length alveolus (Fig. V-6,1)	width alveolus on the anterior side (Fig. V-6,2)	width alveolus on the posterior side (Fig. V-6,3)	length (Fig. V-6,4)	width on the anterior side (Fig. V-6,9)	width on the posterior side (Fig. V-6,10)	degree of wear	length anterior root (Fig. V-6,7)	width anterior root (Fig. V-6,11)	length posterior root (Fig. V-6,8)	width posterior root (Fig. V-6,12)	crown height anterior side (Fig. V-6,5)	crown height posterior side (Fig. V-6,6)
Coll. Dub. 1483 (isolated)	Ngawi	--	--	--	sin 26.6	sin 17.7	--	middle-aged	--	--	--	--	--	--
Coll. Dub. 1818 (mandible)	Redjuno	sin 15.0	sin 12.1	--	--	--	--	--	--	--	--	--	--	--
Coll. Dub. 2318c/3 (isolated)	Kedung Brubus	--	--	--	dex 22.7	dex 17.2	--	adult	dex 8.6	dex 13.8	dex 9.9	dex 15.5	--	--
Coll. Dub. 2318c/4 (isolated)		--	--	--	sin 25.1	sin 15.2	--	adult	--	--	--	--	--	--
Coll. Dub. 2904 (mandible)	Kebon Duren	sin 30.2	sin 19.6	sin 16.8	--	--	--	--	--	--	--	--	--	--
Coll. Dub. 2915 (mandible)	Solo Valley	sin 13.7	sin 11.9	--	--	--	--	--	--	--	--	--	--	--
Coll. Dub. 2916 (mandible)	Kedung Brubus	sin 27.3 dex 26.6	sin 11.9 dex ± 10.4	sin 10.4 dex ± 11.1	-- --	-- --	-- --	-- --	-- --	-- --	-- --	-- --	-- --	-- --
Coll. Dub. 2918 (mandible)	Papa Djaran	sin ± 17.7 dex 16.4	sin 8.7 dex 11.3	-- --	-- --	-- --	-- --	-- --	-- --	-- --	-- --	-- --	-- --	-- --

number of specimen	locality	length alveolus (Fig. V-6,1)	width alveolus on the anterior side (Fig. V-6,2)	width alveolus on the posterior side (Fig. V-6,3)	length (Fig. V-6,4)	width on the anterior side (Fig. V-6,9)	width on the posterior side (Fig. V-6,10)	degree of wear	length ante-rior root (Fig. V-6,7)	width ante-rior root (Fig. V-6,11)	length posterior root (Fig. V-6,8)	width posterior root (Fig. V-6,12)	crown height anterior side (Fig. V-6,5)	crown height posterior side (Fig. V-6,6)
Coll. Dub. 2929 (mandible)	Kedung Madoh	--	--	--	dex 32.6	dex 13.1	dex 10.7	broken	--	--	--	--	--	--
Coll. Dub. 4908 (mandible)	Kedung Brubus	dex 16.5	dex 10.3	--	--	--	--	--	--	--	--	--	--	--
Coll. Dub. 11092/1	"Trinil"	--	--	--	dex 19.0	dex 14.2	--	--	--	--	--	--	--	--
Coll. Dub. 11092/2		--	--	--	sin 20.0	sin 14.3	--	--	--	--	--	--	--	--
Coll. Dub. 3147 (mandible)	Bharon, Punjab, Siwaliks	--	--	--	dex 31.2	dex 17.7	--	broken	--	--	--	--	--	--

VI-10 P_3.

number of specimen	locality	length alveolus (Fig. V-6,1)	width alveolus on the anterior side (Fig. V-6,2)	width alveolus on the posterior side (Fig. V-6,3)	length (Fig.V-6,4)	width on the anterior side (Fig. V-6,9)	width on the posterior side (Fig. V-6,10)	degree of wear	width anterior root (Fig. V-6,11)	width posterior root (Fig. V-6,12)	crown height anterior side (Fig. V-6,5)	crown height posterior side (Fig. V-6,6)
without number (skeleton, Geological Museum, Bandung)	Kali Glagah	-- dex 26.9	-- --	-- dex 15.3	sin 27.5 --	--	sin 17.7 --	Old old	-- --	-- --	-- --	-- --
22 G	Tji Bokagung (Tji Djolang)	-- --	-- --	-- --	sin 28.4 dex 27.5	--	sin 17.0 dex 15.5	adult adult	-- --	-- --	-- --	-- --
SA 040979-30D/2 SA 040979-30D/3	New Pb site	-- --	-- --	-- --	dex 27.3 dex 26.2	-- --	dex 14.3 dex 16.6	adult adult	dex 10.1 dex 13.6	dex 11.7 dex 14.6	dex 24.6 dex 21.9	dex 27.7 dex 24.5
K 6..	Kali Glagah?	--	--	--	sin 25.3	--	sin 16.8	middle-aged	sin 13.7	sin 15.8	--	--
K 653/2 K 653/3 K 653/4	Gn. Butak	-- -- --	-- -- --	-- -- --	sin 28.0 sin 28.0 dex 27.1	-- -- -	sin 18.0 sin 18.8 dex 17.5	old middle-aged middle-aged	sin 16.8 sin 17.5 dex 17.8	sin 18.2 sin 18.4 dex 18.8	-- -- --	-- -- --
K 685 (isolated)	Ngandong	--	--	--	sin 25.4	--	sin 18.3	adult	--	--	sin 28.9	sin 32.0

number of specimen	locality	length alveolus (Fig. V-6,1)	width alveolus on the anterior side (Fig. V-6,2)	width alveolus on the posterior side (Fig. V-6,3)	length (Fig. V-6,4)	width on the anterior side (Fig. V-6,9)	width on the posterior side (Fig. V-6,10)	degree of wear	width anterior root (Fig. V-6,11)	width posterior root (Fig. V-6,12)	crown height anterior side (Fig. V-6,5)	crown height posterior side (Fig. V-6,6)
K 698 (isolated)	K. Glagah	--	--	--	sin 26.7	--	sin 13.5	adult	sin 11.4	sin 11.5	sin 23.4	sin 25.6
K 699 (isolated)	Ngandong	--	--	--	dex 28.1	--	dex 16.9	adult	dex 14.1	dex 12.5	dex 27.1	dex 30.5
Coll. Dub. without number	Java	sin ± 28.0	sin ± 17.7	--	--	--	--	--	--	--	--	--
Coll. Dub. 99 (mandible)	Tritik	--	--	--	dex 27.0	dex 11.9	dex 14.4	broken	--	--	--	--
Coll. Dub. 272b (isolated)	Bangle	--	--	--	dex 24.9	--	dex 20.3	middle-aged	--	--	--	--
Coll. Dub. 285/4 (isolated)	Dekes/Wadegan	--	--	--	sin 27.4	--	sin 20.6	middle-aged	--	--	--	--
Coll. Dub. 425a/1	Java	--	--	--	--	--	sin 21.5					
Coll. Dub. 513 (mandible)	Nonko	--	--	--	dex ± 28.3	--	dex 21.4	broken	--	--	--	--
Coll. Dub. 1804 (mandible)	Redjuno near Teguan	--	--	--	dex 24.6	--	dex ± 17.3	broken	--	--	--	--
Coll. Dub. 1818 (mandible)	Redjuno	sin 27.3	sin 19.0	--	--	--	--	--	--	--	--	--

number of specimen	locality	length alveolus (Fig. V-6,1)	width alveolus on the anterior side (Fig. V-6,2)	width alveolus on the posterior side (Fig. V-6,3)	length (Fig. V-6,4)	width on the anterior side (Fig. V-6,9)	width on the posterior side (Fig. V-6,10)	degree of wear	width anterior root (Fig. V-6,11)	width posterior root (Fig. V-6,12)	crown height anterior side (Fig. V-6,5)	crown height posterior side (Fig. V-6,6)
Coll. Dub. 2000/3 (isolated)	Kedung Lumbu	--	--	--	dex 25.6	--	dex 20.6	middle-aged	--	--	--	--
Coll. Dub. 2003b/1 (isolated)	Teguan	--	--	--	sin 27.1	--	sin 16.0	middle-aged	--	--	--	--
Coll. Dub. 2003b/2 (isolated)		--	--	--	dex 29.0	--	dex 13.0	middle-aged	--	--	--	--
Coll. Dub. 2174 (mandible)	Kedung Brubus	sin 29.0	sin 14.0	sin 10.3	--	--	--	--	--	--	--	--
Coll. Dub. 2318c/1 (isolated)	Kedung Brubus	--	--	--	sin 26.4	--	sin 17.0	middle-aged	--	--	--	--
Coll. Dub. 2904 (mandible)	Kebon Duren	sin ± 23.1	sin 14.5	sin 14.4	--	--	--	--	--	--	--	--
Coll. Dub. 2915 (mandible)	Solo Valley	--	--	--	sin 25.7	--	sin ± 15.0	broken	--	--	--	--
Coll. Dub. 2916 (mandible)	Kedung Brubus	--	--	--	sin 27.0	sin 9.0	sin 12.3	broken	--	--	--	--
Coll. Dub. 2918 (mandible)	Papa Djaran	sin 28.3 dex 31.0	sin 16.2 dex 14.5	-- --	-- --	-- --	-- --	-- --	-- --	-- --	-- --	-- --

number of specimen	locality	length alveolus (Fig.V-6,1)	width alveolus on the anterior side (Fig. V-6,2)	width alveolus on the posterior side (Fig. V-6,3)	length (Fig. V-6,4)	width on the anterior side (Fig. V-6,9)	width on the posterior side (Fig. V-6,10)	degree of wear	width anterior root (Fig. V-6,11)	width posterior root (Fig. V-6,12)	crown height anterior side (Fig. V-6,5)	crown height posterior side (Fig. V-6,6)
Coll. Dub. 2929 (mandible)	Kedung Madoh	--	--	--	dex 29.3	dex 14.4	dex 13.5	broken	--	--	--	--
Coll. Dub. 4908 (mandible)	Kedung Brubus	dex 26.7	dex 18.0	dex 18.2	--	--	--	--	--	--	--	--
Coll. Dub. 6954/6 (isolated)	Tritik	--	--	--	sin 26.5	--	sin 20.6	adult	--	--	--	--
JA 67	Java	--	--	--	dex 28.0	--	dex 14.6	adult	dex 11.3	dex 11.1	dex 26.1	dex 27.3
Coll. Dub. 3147 (mandible)	Bharon, Punjab, Siwaliks	--	--	--	dex 31.3	--	dex 19.2	broken	--	--	--	--

number of specimen	locality	length alveolus (Fig. V-6,1)	width alveolus on the anterior side (Fig. V-6,2)	width alveolus on the posterior side (Fig. V-6,3)	length (Fig. V-6,4)	width on the anterior side (Fig. V-6,9)	width on the posterior side (Fig. V-6,10)	degree of wear	width anterior root (Fig. V-6,11)	width posterior root (Fig. V-6,12)	crown height anterior side (Fig. V-6,5)	crown height posterior side (Fig.V-6.6)
without number (skeleton, Geological Museum, Bandung)	Kali Glagah	--	--	--	dex 28.5	19.0	--	middle-aged	--	--	--	--
22 G	Tji Bokagung (Tji Djolang)	-- --	-- --	-- --	sin 26.2 dex 25.6	-- --	sin 17.9 dex 17.8	adult adult	-- --	-- --	-- --	-- --
K 675/2	Kali Glagah	--	--	--	dex 31.5 sin 31.2	dex 19.8 sin 20.4	dex 22.1 sin 24.7	middle-aged	dex 16.2 sin 16.7	dex 20.8	--	--
K 675/3		--	--	--				middle-aged		sin 21.4	--	--
Coll. Dub. without number	Java	sin ± 30.8	--	sin 20.9	--	--	--	--	--	--	--	--
Coll. Dub. 99 (mandible)	Tritik	--	--	--	dex 27.5	--	dex 17.3	adult	--	--	dex min 22.2	--
Coll. Dub. 105/1 (isolated)	Teguan	--	--	--	dex 28.3	dex 16.2	dex 19.7	middle-aged	--	--	--	--
Coll. Dub. 1718 (mandible)	Bangle	--	--	--	dex 25.4	--	dex 18.7	middle-aged	--	--	--	--
Coll. Dub. 1804 (mandible)	Redjuno near Teguan	--	--	--	dex + 25.5	--	dex + 17.6	broken	--	--	--	--

number of specimen	locality	length alveolus (Fig. V-6,1)	width alveolus on the anterior side (Fig. V-6,2)	width alveolus on the posterior side (Fig. V-6,3)	length (Fig. V-6,4)	width on the anterior side (Fig. V-6,9)	width on the posterior side (Fig. V-6,10)	degree of wear	width anterior root (Fig. V-6,11)	width posterior root (Fig. V-6,12)	crown height anterior side (Fig. V-6,5)	crown height posterior side Fig. V-6,6)
Coll. Dub. 1818 (mandible)	Redjuno	sin 26.9	--	sin 15.2	--	--	--	--	--	--	--	--
Coll. Dub. 2174 (mandible)	Kedung Brubus	sin 25.1	sin 9.6	sin 13.2	--	--	--	--	--	--	--	--
Coll. Dub. 2207b (mandible)	Kebon Duren	sin 24.2	sin ± 15.3	sin ± 17.6	--	--	--	--	--	--	--	--
Coll. Dub. 2318c/2 (isolated)	Kedung Brubus	--	--	--	sin 28.0	--	sin 19.5	old	--	--	--	--
Coll. Dub. 2904 (mandible)	Kebon Duren	sin 24.4	sin 14.0	sin 18.7	--	--	--	--	--	--	--	--
Coll. Dub. 2916 (mandible)	Kedung Brubus	-- dex 26.1	-- dex ± 12.9	-- dex 16.0	sin ± 23.5 --	-- --	sin ± 15.2	broken --	-- --	-- --	-- --	-- --
Coll. Dub. 2917 (mandible)	Kedung Lumbu	--	--	--	dex min 25.5	--	dex 20.5	adult	--	dex 27.6	dex 25.7	dex 27.6
Coll. Dub. 2918 (mandible)	Papa Djaran	sin 9.9 dex 11.9	-- --	sin 13.0 dex 14.4	-- --	-- --	-- --	-- --	-- --	-- --	-- --	-- --
Coll. Dub. 2922 (mandible)	Kedung Lumbu	--	--	--	sin 26.4	--	sin 18.1	adult	--	--	sin 25.2	--

number of specimen	locality	length alveolus (Fig. V-6,1)	width alveolus on the anterior side (Fig. V-6,2)	width alveolus on the posterior side (Fig. V-6,3)	length (Fig. V-6,4)	width on the anterior side (Fig. V-6,9)	width on the posterior side (Fig. V-6,10)	degree of wear	width anterior root (Fig. V-6,11)	width posterior root (Fig. V-6,12)	crown height anterior side (Fig. V-6,5)	crown height posterior side (Fig.V-6,6)
Coll. Dub. 4908 (mandible)	Kedung Brubus	dex 26.3	dex 13.3	dex 14.8	--	--	--	--	--	--	--	--
Coll. Dub. 6954/5 (isolated)	Tritik	--	--	--	sin min 19.7	sin 17.6	--	middle-aged	--	--	--	--
Coll. Dub. 3147 (mandible)	Bharon, Punjab, Siwaliks	--	--	--	dex 35.9	--	dex 20.6	broken	--	--	--	--

VI-12 P_1, DP_2, DP_3 and DP_4

number of specimen	element	locality	length (Fig. V-6,4)	width on the anterior side (Fig. V-6,9)	width on the posterior side (Fig. V-6,10)	degree of wear	length root (Fig. V-6,13)	width anterior root (Fig. V-6,11)	width posterior root (Fig. V-6,12)	maximum space between roots (Fig. V-6,14)	maximum crown height (Fig. V-6,5/6)
K 675/1	P_1	Kali Glagah	dex 17.7	--	dex 11.9	middle-aged	--	--	--	--	--
SA 270378	DP_2	Triangulation Point, Ngebung	sin 8.3	--	sin 9.3	adult	--	--	--	--	--
SA 270378	DP_3	Triangulation Point Ngebung	--	--	--	only roots visible	sin 24.9	sin 9.3	sin 10.7	sin 5.3	--
SA 270378	DP_4	Triangulation Point Ngebung	sin 40.0	sin 14.8	sin 20.4	adult	--	--	--	--	--
K 525/1	DP_4	Kali Glagah	sin 41.8	sin 14.5	sin 19.0	adult	--	--	--	sin 13.6 V*	sin 20.5
K 525/2	DP_4		sin 43.2	sin 15.2	sin min 16.7	adult	--	--	--	sin 18.2 U*	sin 20.0
Coll. Dub. 323c	DP_4 ?	Java	sin 38.9	sin 8.3	sin 13.4	broken	--	--	--	--	--

* = space between the roots is V-shaped or U-shaped

VI-13 P^1

number of specimen	locality	length root/ alveolus (Fig. V-7,1)	width alveolus / root on the posterior side (Fig. V-7,3)	length (Fig. V-7,4)	width on the posterior side (Fig. V-7,7)	degree of wear	maximum length of root (Fig. V-7.6)
Coll. Dub. 425a/2	Java	--	--	sin 24.0	sin 21.9	old	--
Coll. Dub. 2023?/2 Coll. Dub. 2023?/3	Sumber Waru?	-- --	-- --	dex 20.4 sin 20.4	dex 19.6 sin 17.8	middle-aged middle-aged	-- --
Coll. Dub. 2076/4	Kedung Brubus	22.5	17.2	--	--	--	44.9
Coll. Dub. 2182/4	Kedung Lumbu	--	--	sin 17.5	sin 14.3	broken	--
Coll. Dub. 2188	Kedung Lumbu	--	--	sin 18.5	sin 16.0	broken	--
Coll. Dub. 2908	Kedung Brubus	sin 20.0	sin 13.2	dex 17.1	dex 13.2	broken	--
Coll. Dub. 2911	Tinggang	--	--	sin 21.1	sin 17.9	broken	--
Coll. Dub. 2914	Tinggang	sin 16.5	sin 14.0	--	--	--	--
Coll. Dub. 2921/2	Tritik	dex 21.4	dex 15.0	--	--	--	--

VI-14 P^2

number of specimen	locality	length alveolus / root (Fig. V-7,1)	width alveolus / root on the anterior side (Fig. V-7,2)	width alveolus / root on the posterior side (Fig. V-7,3)	length (Fig. V-7,4)	width on the posterior side (Fig. V-7,7)	degree of wear	maximum crown height (Fig. V-7.5)
Coll. Dub. 96	Kedung Brubus	--	--	--	sin 25.7	sin. 17.8	adult	sin 26.0
Coll. Dub. 1702	Kedung Lumbu	-- --	-- --	-- --	sin 27.3 dex 27.5	sin 23.8 dex 27.8	adult adult	sin 29.2 dex 26.0
Coll. Dub. 2182/4	Kedung Lumbu	--	--	--	sin 22.3	sin 16.6	broken	--
Coll. Dub. 2188	Kedung Lumbu	--	--	--	sin 25.7	sin 17.1	middle-aged	--
Coll. Dub. 2193	Bangle	dex 23.8	dex 15.5	dex 14.1	--	--	--	--
Coll. Dub. 2908	Kedung Brubus	-- --	-- --	-- --	sin 28.3 dex 30.5	sin 16.7 dex 19.8	old old	-- --

number of specimen	locality	length alveolus / root (Fig. V-7,1)	width alveolus / root on the anterior side (Fig. V-7,2)	width alveolus / root on the posterior side (Fig. V-7,3)	length (Fig. V-7,4)	width on the posterior side (Fig. V-7,7)	degree of wear	maximum crown height (Fig. V-7,5)
Coll. Dub. 2911	Tinggang	-- --	-- --	-- --	sin 30.3 dex 30.0	sin 21.3 dex 19.1	broken broken	-- --
Coll. Dub. 2914	Tinggang	sin 22.2 dex 25.2	-- --	sin 20.6 dex 20.5	-- --	-- --	-- --	-- --
Coll. Dub. 2919	Padasmalang	--	--	--	dex 25.9	dex 22.9	broken	--
Coll. Dub. 2921/2	Tritik	dex 28.2	--	dex 16.5	--	--	--	--
Coll. Dub. 2933	Kebon Duren	sin 16.0 dex 15.9	-- --	sin 14.7 dex 13.0	-- --	-- --	-- --	-- --

VI-15 P^3

number of specimen	locality	length alveolus / root (Fig. V-7,1)	width alveolus / root on the anterior side (Fig. V-7,2)	width alveolus/ root on the posterior side (Fig. V-7,3)	width alveolus / root, extra lingual root included (Fig. V-7,8)	length (Fig. V-7,4)	width on the posterior side (Fig. V-7,7)	degree of wear	maximum crown height (Fig. V-7,5)	maximum length of root (Fig. V-7,6)
Coll. Dub. 94	Pati Ajam	--	--	--	--	sin 26.1	sin 24.3	middle-aged	--	--
Coll. Dub. 96	Kedung Brubus	--	--	--	--	sin 28.1	sin 18.2	adult	sin 22.2	--
Coll. Dub. 313/1 Coll. Dub. 313/2	Kedung Brubus	-- --	-- --	-- --	-- --	dex 28.1 dex 27.8	dex 19.1 dex 19.7	adult middle-aged	dex 26.0 --	-- --
Coll. Dub. 425a/3	Java	--	dex 14.8	dex 13.3	--	dex 27.4	dex min 17.9	old	--	ant 39.5
Coll. Dub. 1702	Kedung Lumbu	--	--	--	--	dex 27.4	dex 22.4	middle-aged	--	--

number of specimen	Locality	length alveolus / root (Fig. V-7,1)	width alveolus / root on the anterior side (Fig. V-7,2)	width alveolus/ root on the posterior side (Fig. V-7,3)	width alveolus / root, extra lingual root included (Fig. V-7,8)	length (Fig. V-7,4)	width on the posterior side (Fig. V-7,7)	degree of wear	maximum crown height (Fig. V-7,5)	maximum length of root (Fig. V-7,6)
Coll. Dub. 2003b/3	Teguan	--	--	--	--	sin 30.1	sin 22.1	middle-aged	--	--
Coll. Dub. 2023/2	Java	--	--	--	--	--	sin 22.7	damaged	--	--
Coll. Dub. 2188	Kedung Lumbu	--	--	--	--	sin 28.1	sin 19.7	middle-aged	--	--
Coll. Dub. 2193	Bangle	dex 27.0	dex 19.5	dex 23.2	dex 28.5	--	--	--	--	--
Coll. Dub. 2908	Kedung Brubus	-- --	-- --	-- --	-- --	sin 29.2 dex 27.6	sin 19.3 dex 22.8	old old	-- --	-- --
Coll. Dub. 2911	Tinggang	sin 25.7 dex 28.8	-- --	sin 21.4 dex 21.4	-- --	-- --	-- --	-- --	-- --	-- --
Coll. Dub. 2914	Tinggang	-- --	-- --	-- --	-- --	sin 25.9 dex 22.8	sin 23.6 dex 23.6	broken broken	-- --	-- --
Coll. Dub. 2924/4	Java	--	--	--	--	--	sin 21.1	middle-aged	--	--
Coll. Dub. 2926	Java	--	--	--	--	sin 27.3	sin 22.6	adult	--	--
Coll. Dub. 2933	Kebon Duren	sin 27.4	sin 20.0	sin 19.1	--	dex 28.0	dex 21.9	dex old	--	--
Coll. Dub. 13601	Java	--	--	--	--	--	dex 21.6	middle-aged	--	--

VI-16 P^4

number of specimen	locality	length alveolus / root (Fig. V-7,1)	width alveolus / root on the anterior side (Fig. V-7,2)	width alveolus/ root on the posterior side (Fig. V-7,3)	width alveolus / root, extra lingual root included (Fig. V-7,8)	length (Fig. V-7,4)	width on the posterior side (Fig. V-7,7)	degree of wear
Coll. Dub. 325d/1	Java	--	--	--	--	sin 19.6	sin 19.3	middle-aged
Coll. Dub. 325f/2	"Trinil"	--	--	--	--	dex 19.8	dex 23.0	middlle-aged
Coll. Dub. 2023/1	Java	--	--	--	--	18.9	--	damaged
Coll. Dub. 2023?/1	Sumber Waru?	--	--	--	--	dex 19.1	dex 21.2	middle-aged
Coll. Dub. 2079	Sumber Waru	-- --	-- --	-- --	-- --	sin 18.3 dex 19.4	sin 22.8 dex 23.0	middle-aged middle-aged
Coll. Dub. 2193	Bangle	dex 27.0	dex 16.6	dex 21.1	dex 29.2	--	--	--
Coll. Dub. 2460a	Java	--	--	--	--	sin 21.3	sin 25.0	middle-aged
Coll. Dub. 2592	Teguan	--	--	--	--	sin 21.6	sin 28.4	middle-aged
Coll. Dub. 2908	Kedung Brubus	-- --	-- --	-- --	-- --	sin 19.0 dex 19.3	sin 23.4 dex 23.2	old old
Coll. Dub. 2909	Tinggang	--	--	--	--	dex 19.3	dex 21.8	middle-aged
Coll. Dub. 2911	Tinggang	-- dex ± 18.2	-- --	-- dex 22.4	-- --	sin 18.6 --	sin 23.9 --	middle-aged --
Coll. Dub. 2914	Tinggang	-- --	-- --	-- --	-- --	sin 21.0 dex 20.4	sin 25.1 dex 23.1	broken broken
Coll. Dub. 2919	Padasmalang	--	--	--	--	sin 23.8	sin ± 27.2	broken
Coll. Dub. 2933	Kebon Duren	sin 24.8 dex 24.1	sin 16.6 dex 14.2	sin 19.0 dex 18.0	-- --	-- --	-- --	-- --
Coll. Dub. 3101	Samalka, Siwaliks	-- --	-- --	-- --	-- --	sin 26.6 dex 25.0	sin 25.4 dex 24.0	old old
Coll. Dub. 3148	Kodawala, Siwaliks	-- --	-- --	-- --	-- --	sin 20.1 dex 23.6	sin 20.0 dex 21.2	broken old

VI-17 DP^4

number of specimen	locality	length (Fig. V-7,4)	width on the posterior side (Fig. V-7,7)	degree of wear
Coll. Dub. without number	unknown (Java)	dex 28.4	dex 24.1	old
Coll. Dub. 1702	Kedung Lumbu	dex 26.0	dex 25.0	old
Coll. Dub. 2188	Kedung Lumbu	sin 22.2	sin 24.8	old
Coll. Dub. 2920	Java	sin 27.9	sin 26.2	old

VI-18 M_1

number of specimen	locality	length on the lingual side (Fig. V-8,3)	length on the buccal side (Fig. V-8,4)	width on the anterior side (Fig. V-8,1)	width on the posterior side (Fig. V-8,2)	degree of wear
without number (mandible fragment, Lab. Bioanthropologi and Paleoanthropologi, Yogyakarta)	Sangiran	sin ± 38.0 *2	--	--	sin ± 32.0*2	middle-aged
skeleton (Geological Museum Bandung)	Kali Glagah	sin 39.4 dex 37.3	-- --	-- --	sin 26.6 dex 26.4	old
22 G	Tji Bokagung (Tji Djolang)	dex 35.5	--	smaller than width on the posterior side	dex 27.6	old
SA 040979-20N/1	New Pb Site	sin 37.3	--	sin 22.7	sin 28.1	middle-aged
K 727	Ngandong (Rahang Bawah)	sin 39.9	--	sin 23.6	sin 24.5	old, damaged
K 731	Sangiran	sin 33.7	--	sin 22.5	sin 28.8	old
K 742/1	Sangiran	sin 33.7	--	sin 23.8	sin 26.4	very old
Coll. Dub. 99	Tritik	sin 27.9	--	sin 23.5	sin 26.3	very old
Coll. Dub. 324	Java	dex 34.6	dex 32.9	dex 28.3	dex 28.5	very old
Coll. Dub. 2008	Java	sin 38.4	sin 34.1	--	sin 32.1	adult
Coll. Dub. 2076/6	Kedung Brubus	--	--	--	sin + 27.1	middle aged
Coll. Dub. 2207b	Kebon Duren	sin 33.7	--	sin + 25.6	sin min 31.8	(alveolus)
Coll. Dub. 2903	"Trinil"	dex 33.3	--	--	dex + 24.0	(broken)

number of specimen	locality	length on the lingual side (Fig. V-8,3)	length on the buccal side (Fig. V-8,4)	width on the anterior side (Fig. V-8,1)	width on the posterior side (Fig. V-8,2)	degree of wear
Coll. Dub. 2904	Kebon Duren	sin 34.7	--	sin 21.8	sin ± 30.6	(broken)
Coll. Dub. 2915	Solo Valley	dex 34.8	--	--	--	(broken)
Coll. Dub. 2916	Kedung Brubus	sin ± 25.6 dex 20.2	-- --	sin 24.7 dex 22.3	sin 26.0 dex 26.4	(broken) (broken)
Coll. Dub. 2917	Kedung Lumbu	dex 36.8	dex 34.1	dex 23.9	dex 28.9	middle aged
Coll. Dub. 2922	Kedung Lumbu	sin 37.2	sin 34.2	sin 24.3	sin 28.8	middle-aged
Coll. Dub. 11463	Java	--	--	dex 27.0	--	very old
Coll. Dub. 3147	Bharon, Punjab, Siwaliks	dex 31.5*[1]	--	--	--	(alveolus)

*[1] = measurement of alveolus
*[2] = approximate measurement; measured with a measuring tape

VI-19 M_2

number of specimen	locality	length (Fig. V-8,7)	width on the anterior side (Fig. V-8,5)	width on the posterior side (Fig. V-8,6)	degree of wear
without no. (mandible fragment, Laboratory Bioanthropologi and Paleoanthropologi, Yogyakarta)	Sangiran	sin ± 45.0*[3]	--	sin ± 37.0*[3]	middle-aged
skeleton (Geological Museum Bandung)	Kali Glagah	sin 45.4 dex 47.5	-- --	sin 30.5 dex 33.7	old old
without no. (skull and mandible, Geological Museum Bandung)	Ngandong	sin 47.0 dex 48.0	sin 40.0 dex 44.0	sin 38.0 dex 38.0	-- --
466 (Sangiran)	unknown (Java)	dex ± 45.0*[3]	--	dex ± 34.0*[3]	--
4-4A	unknown (Java)	sin/dex min 37.3	--	sin/dex 30.7	--
22 G	Tji Bokagung (Tji Djolang)	sin 43.0 dex 42.4	-- --	sin 33.3 dex 28.3	middle-aged old
SA 040979-20N/2 SA 040979-20N/3	New Pb site	sin 42.0 dex 43.3	-- --	sin 30.7 dex 31.0	adult adult

number of specimen	locality	length (Fig. V-8,7)	width on the anterior side (Fig. V-8,5)	width on the posterior side (Fig. V-8,6)	degree of wear
K 149	Kedung Kuduh, Sangiran	dex 41.7	--	dex 31.4	middle-aged
K 150	Ngandong	--	dex 34.3	--	middle-aged
K 657	Ngandong	sin 45.1	--	sin 27.7	old, damaged
K 727	Ngandong (Rahang Bawah)	sin 49.4	--	sin 32.7	adult
K 731	Sangiran	sin 44.5	--	sin 33.0	middle-aged
K 741	unknown (Java)	dex 46.7	--	dex 34.8	middle-aged
K 742/2	Sangiran	sin 40.5	--	sin 31.0	middle-aged
K 743	Sangiran	dex 41.4	--	dex 28.8	middle-aged
K 745	unknown (Java)	dex 49.3	--	dex 33.6	middle-aged
K 746	Watualang	dex 50.2	--	dex 34.2	middle-aged
Coll. Dub. 97	Redjuno	sin 34.0	--	sin ± 31.0	--
Coll. Dub. 99	Tritik	sin 42.3 dex 43.3	sin 30.1 dex 30.0	sin 31.5 dex 32.1	middle-aged middle-aged
Coll. Dub. 272a	Bogo	dex 48.5	dex 30.7	dex 31.4	middle-aged
Coll. Dub. 323a/1	Kedung Brubus	dex 41.0	dex 26.6	dex 30.6	very old
Coll. Dub. 1804	Redjuno, near Teguan	dex ± 35.6	--	dex 32.7	--
Coll. Dub. 2003a/1	Bogo	dex min 39.4	dex 31.8	--	middle-aged
Coll. Dub. 2008a	Java	dex 44.6	dex 26.5	dex 26.0	middle-aged
Coll. Dub. 2013	Kedung Brubus	sin 41.8	sin 27.6	sin 29.2	old
Coll. Dub. 2076/7	Kedung Brubus	sin ± 40.3	--	sin min 27.4	adult
Coll. Dub. 2082	Teguan	dex 41.8	dex 28.1	dex 31.8	old
Coll. Dub. 2191*[1]	Java	--	dex 36.4	--	old
Coll. Dub. 2201	Kebon Duren	sin 39.0	sin 28.8	sin 31.2	old
Coll. Dub. 2202	Java	dex 40.7	dex 25.1	dex 27.1	adult
Coll. Dub. 2314	Papa Djaran, N of Kebon Duren	dex 40.2	dex 29.8	dex 31.7	middle-aged
Coll. Dub. 2903	"Trinil"	dex 42.3	dex 29.0	dex 34.0	--

number of specimen	locality	length (Fig. V-8,7)	width on the anterior side (Fig. V-8,5)	width on the posterior side (Fig. V-8,6)	degree of wear
Coll. Dub. 2905	Papa Djaran, N of Kebon Duren	sin 41.6	sin 30.8	sin 31.4	middle-aged
Coll. Dub. 2906	Java	sin 40.6 *2	sin 31.7 *2	sin 35.0 *2	--
Coll. Dub. 2910	Tritik	sin 37.2	sin 31.0	sin 29.0	--
Coll. Dub. 2915	Solo Valley	sin ± 32.2 dex ± 34.7	sin 24.6 --	sin ± 26.6 --	-- --
Coll. Dub. 2916	Kedung Brubus	sin 42.5 dex 42.6	sin 31.4 dex 31.0	sin 32.1 dex 31.6	very old old
Coll. Dub. 2917	Kedung Lumbu	dex 42.3	dex 30.3	dex 31.1	middle-aged
Coll. Dub. 2922	Kedung Lumbu	sin 41.5	sin 31.0	--	middle-aged
Coll. Dub. 6927/1	Tritik	--	sin 34.0	--	very old
Coll. Dub. 6954/7	Tritik	dex 40.6	dex 30.8	--	middle-aged
JA 68	Java	sin min 47.8	sin 33.5	sin 32.6	middle-aged
Coll. Dub. 3147	Bharon, Punjab, Siwaliks	dex 36.8	dex 33.1	dex 34.1	very old

*1 might also be a M_3
*2 alveolus
*3 approximate measurement; measured with measuring tape

VI-20 M_3

number of specimen	locality	length (Fig. V-8,11)	width on the anterior side (Fig. V-8,8)	width on the posterior side (Fig. V-8,9)	width talonid (Fig. V-8,10)	degree of wear
without no. (mandible fragment, Laboratory Bioanthropologi and Paleoanthropologi, Yogyakarta)	Sangiran	sin $\pm$ 58.0*[2]	--	sin $\pm$ 37.0*[2]	--	middle-aged
skeleton (Geological Museum Bandung)	Kali Glagah	sin 62.0 dex 60.0	-- --	sin $\pm$ 35.0 dex 33.0	-- --	middle-aged middle-aged
without no. (skull and mandible, Geological Museum, Bandung)	Ngandong	sin 55.0 dex 55.0	sin 37.0 dex 39.0	-- --	-- --	-- --
466	unknown (Java)	dex $\pm$ 56.0*[2]	--	dex $\pm$ 35.0*[2]	--	--
4-4A	unknown (Java)	sin/dex 54.2	--	sin/dex 30.8	--	--
22 G	Tji Bukagung (Tji Djolang)	sin 48.5 dex 50.0	-- --	sin 30.3 dex 31.2	-- --	adult adult
SA 110979	New Pb site	dex 60.0	--	dex 32.2	--	adult
K 149	Kedung Kuduh, Sangiran	dex 55.5	dex 34.2	--	--	middle-aged
K 657	Ngandong	sin 53.9	sin 36.9	--	--	adult
K 707	Gn. Butak	sin 57.4	sin 30.6	--	--	adult
K 723/1 K 723/2 K 723/3	Ngandong	sin 58.5 sin 65.4 sin min 54.7	sin 36.8 sin 36.3 --	-- -- sin min 30.0	-- -- --	adult adult middle-aged
K 727	Ngandong (Rahang Bawah)	sin 52.0	sin 29.3	--	--	adult, not fully erupted
K 731	Sangiran	sin 54.4	sin 34.3	--	--	middle-aged
K 740	Kali Bengawan, Solo	sin 53.8	sin 34.6	--	--	middle-aged
K 741	unknown (Java)	--	min dex 30.9	--	--	adult
K 742/3	Sangiran	dex 50.3	dex 29.9	--	--	middle-aged
K 743	Sangiran	dex 48.0	dex 30.3	--	--	adult
K 745	unknown (Java)	dex 57.7	dex 33.4	--	--	adult

number of specimen	locality	length (Fig. V-8,11)	width on the anterior side (Fig. V-8,8)	width on the posterior side (Fig. V-8,9)	width talonid (Fig. V-8,10)	degree of wear
K 746	Watualang	dex 61.4	dex 34.8	--	--	adult
Coll. Dub. 87/2	Kali Gedeh	--	--	--	dex 22.2	middle-aged
Coll. Dub. 97	Redjuno	sin 36.3 *1	sin 27.4 *1	sin 24.0 *1	--	adult
Coll. Dub. 98	Java	dex 57.6	dex 36.5	dex 32.5	dex 15.8	--
Coll. Dub. 99	Tritik	sin 54.1 dex 52.5	sin 31.3 dex 30.8	sin 30.7 dex 30.8	sin 18.9 dex 17.8	adult adult
Coll. Dub. 285/5	Dekes/Wadegan	--	--	--	dex 17.7	--
Coll. Dub. 310	Kedung Brubus	sin 54.0	sin 31.7	sin 30.5	sin 20.2	middle-aged
Coll. Dub. 314b	Kedung Lumbu	sin 56.2	sin 31.9	sin 30.6	sin 19.2	adult
Coll. Dub. 323a/1 Coll. Dub. 323a/2	Kedung Brubus	dex 58.8 sin 56.6	dex 30.0 sin $\pm$ 28.8	dex 30.6 sin 34.4	dex 20.1 sin 20.1	middle-aged middle-aged
Coll. Dub. 323b	Kedung Brubus	dex 61.8	dex 28.8	dex 31.1	dex 24.0	old
Coll. Dub. 325d/2 Coll. Dub. 325d/3	Java	dex min 45.4 --	dex min 31.3 --	dex min 32.0 sin 27.7	dex min 24.7 sin 15.9	old adult
Coll. Dub. 1804	Redjuno, near Teguan	dex min 29.6	dex + 29.7	--	--	--
Coll. Dub. 2003a/2	Bogo	dex min 52.7	dex 32.1	dex 31.0	dex 20.9	middle-aged
Coll. Dub. 2006	Java	sin min 53.8	sin 30.2	sin 31.5	--	old
Coll. Dub. 2017/2	Java	--	--	--	dex 23.7	old
Coll. Dub. 2076/8 Coll. Dub. 2076/9 Coll. Dub. 2076/10 Coll. Dub. 2076/11	Kedung Brubus	-- -- -- --	-- -- -- --	-- dex 35.9 -- dex 36.5	dex 17.0 dex 21.8 dex 16.3 dex 21.5	adult old adult old
Coll. Dub. 2082	Teguan	dex 60.7	dex 31.0	dex 31.2	dex 25.3	old
Coll. Dub. 2192	unknown (Java)	sin 52.6	sin 29.7	sin 29.2	sin 15.9	old
Coll. Dub. 2192b/1 Coll. Dub. 2192b/2	unknown (Java)	-- --	-- --	dex 33.8 --	dex 19.7 sin 21.5	adult adult
Coll. Dub. 2194	unknown (Java)	dex 62.4	dex 30.6	dex 31.9	dex 23.1	middle-aged
Coll. Dub. 2202	unknown (Java)	dex 47.9 *1	dex 25.4 *1	dex 25.1 *1	dex 20.5 *1	adult
Coll. Dub. 2204b	Kedung Brubus	dex min 62.4	dex min 31.6	dex min 33.4	dex min 24.5	middle-aged

number of specimen	locality	length (Fig. V-8,11)	width on the anterior side (Fig. V-8,8)	width on the posterior side (Fig. V-8,9)	width talonid (Fig. V-8,10)	degree of wear
Coll. Dub. 2314	Papa Djaran, N of Kebon Duren	dex 52.4	dex 32.0	dex 32.5	dex 18.9	middle-aged
Coll. Dub. 2318b	Dekes/Wadegan	dex 56.9	dex 30.2	dex 31.2	dex 17.1	adult
Coll. Dub. 2319	Java	sin 50.4	sin 30.6	sin 30.3	sin 17.5	very old
Coll. Dub. 2903	"Trinil"	dex 53.0 [*1]	dex 25.5 [*1]	dex 20.4 [*1]	--	adult
Coll. Dub. 2905	Papa Djaran, N of Kebon Duren	sin 57.4	sin 32.7	sin 32.6	sin 20.6	middle-aged
Coll. Dub. 2906	Java	sin 60.9	sin 33.7	sin 32.3	sin 11.1	--
Coll. Dub. 2910	Tritik	sin 60.6	sin 34.5	sin 31.6	sin ± 16.2	--
Coll. Dub. 2915	Solo Valley	dex 59.6	dex 32.2	dex 31.4	dex 23.0	middle-aged
Coll. Dub. 2916	Kedung Brubus	sin 65.3 dex 60.2	sin 33.7 dex 34.5	sin 32.7 dex 32.1	sin 18.6 dex 17.1	middle-aged middle-aged
Coll. Dub. 2917 (2922)	Kedung Lumbu	dex 55.6	dex 31.8	dex 30.6	dex 19.7	adult
Coll. Dub. 11464	Bangle	--	--	sin 28.7	sin 13.4	middle-aged
Coll. Dub. 3147	Bharon, Punjab, Siwaliks	dex 64.3	dex 38.7	dex 38.3	dex 26.0	very old

[*1] M_3 not yet fully erupted [*2] approximate measurement; measured with measuring tape

VI-21 M^1

number of specimen	locality	length (Fig. V-9,1)	width on the anterior side (Fig. V-9,2)	width on the posterior side (Fig. V-9,3)	degree of wear
without number (skeleton, Geological Museum, Bandung)	Kali Glagah	sin 35.3 dex 34.8	-- --	sin 33.0 dex 35.0	--
K 15-947	unknown (Java)	sin 28.8	sin --	sin 38.7	very old
M 18	Kali Saat, exc. 8	dex 34.6	dex --	dex 34.3	very old
K 655/1 K 655/2 K 655/3	Gn. Butak	dex 35.2 sin 26.6 sin 27.6	dex 30.0 sin 22.8 sin 22.5	dex 33.0 sin 26.3 sin 25.3	very old, worn to root very old, worn to root very old, worn to root
number of specimen	locality	length	width on the	width on the posterior	degree of wear

		(Fig. V-9,1)	anterior side (Fig. V-9,2)	side (Fig. V-9,3)	
K 674/1	Kali Glagah	sin 29.0	sin 26.1	sin 28.8	very old, worn to root
K 674/2		dex 31.1	dex 25.1	dex 28.4	very old, worn to root
K 705	Gn. Butak	sin 28.4	sin 30.0	sin 31.0	very old, worn to root
K 734/1	Ngandong	dex 44.5	dex 32.4	dex 34.2	middle-aged
K 749	Kedung Brubus	dex 36.1	dex 30.2	dex 33.4	old
Coll. Dub. 1702	Kedung Lumbu	dex 34.8	dex 29.5	dex 34.1	old
Coll. Dub. 2023c (see also Coll. Dub. 2195a)	Sumber Waru	sin 33.5	sin 29.3	sin 31.1	very old
Coll. Dub. 2079	Sumber Waru	sin 32.1 dex 30.1	sin 32.1 dex --	sin 33.4 dex min 29.8	very old
Coll. Dub. 2182/5	Kedung Lumbu	dex 36.6	dex 27.7	dex 32.1	middle-aged
Coll. Dub. 2188	Kedung Lumbu	sin 33.2	sin 27.3	sin 31.0	middle-aged
Coll. Dub. 2195b (see also Coll. Dub. 2080a)	Sumber Waru	dex 33.2	dex 28.8	dex 30.7	very old
Coll. Dub. 2907/1	Nonko, NW of Trinil	dex 30.5	dex ± 28.8	dex ± 30.8	broken
Coll. Dub. 2908	Kedung Brubus	sin 32.3 dex 31.9	sin 30.8 dex 31.2	sin 31.5 dex 34.6	very old
Coll. Dub. 2909	Tinggang	dex 32.8	dex 30.6	dex 33.1	very old
Coll. Dub. 2911	Tinggang	sin 29.3 dex 33.0	sin ± 30.6 dex 29.6	sin ± 32.7 dex 32.6	very old
Coll. Dub. 2919	Padasmalang	sin 31.8 dex 32.8	sin ± 27.1 dex 30.3	sin 33.3 dex 34.2	very old
Coll. Dub. 2920	Java	sin 42.3	sin 28.0	sin ± 33.5	old; broken
Coll. Dub. 3101	Samalka, Siwaliks	sin min 31.2 dex 36.0	sin ± 30.0 dex ± 32.5	sin ± 37.6 dex 34.8	very old
Coll. Dub. 3138	Samalka 3, Siwaliks	dex 41.4	dex 34.1	dex 37.7	middle-aged
Coll. Dub. 3148	Kodawala, Siwaliks	dex 31.8	dex 33.7	dex 39.4	very old

VI-22 M^2

number of specimen	locality	length (Fig. V-9,4)	width on the anterior side (Fig. V-9,5)	width on the posterior side (Fig. V-9,6)	degree of wear
without number (skeleton, Geological Museum, Bandung)	Kali Glagah	sin 46.1 dex 47.0	sin -- dex --	sin 37.0 dex 39.0	--
366 (Museum Sangiran)	Rahang Atas	sin ± 38.0*[2] dex ± 40.0*[2]	sin -- dex --	sin ± 36.0*[2] dex ± 42.0*[2]	middle-aged
K 15-947	unknown (Java)	sin 46.2	sin --	sin 45.4	middle-aged
M 18	Kali Saat, exc. 8	dex 41.2	dex --	dex 37.7	middle-aged
K 672	Kali Glagah	sin min 47.7	sin --	sin 42.7	middle-aged
K 676	Ngandong	sin 48.6	sin --	sin 41.6	adult
K 705	Gn. Butak	sin 34.4	sin --	sin 42.2	old
K 723/4	Ngandong	sin 48.4	sin --	sin 42.3	middle-aged
K 734/2	Ngandong	dex 46.1	dex --	dex 37.0	adult, not fully erupted
K 749	Kedung Brubus	dex 44.3	dex --	dex 39.5	middle-aged
Coll. Dub. 285/6*[1] Coll. Dub. 285/7*[1] Coll. Dub. 285/8*[1]	Dekes/Wadegan	sin/dex -- sin/dex -- sin/dex --	sin/dex -- sin/dex -- sin/dex --	sin/dex 36.0 sin/dex 31.0 sin/dex 29.6	broken broken broken
Coll. Dub. 308a *[1]	Sumber Waru	sin/dex --	sin/dex --	sin/dex 35.5	broken
Coll. Dub. 325f/3	"Trinil"	dex 38.2	dex 34.6	dex 32.4	middle-aged
Coll. Dub. 1702	Kedung Lumbu	sin 43.7 dex 44.0	sin 38.1 dex 35.7	sin 38.7 dex 37.7	middle-aged
Coll. Dub. 2004	Java	sin 37.2	sin ± 25.6	sin ± 29.6	middle-aged
Coll. Dub. 2008b/1 Coll. Dub. 2008b/2	Kedung Brubus	dex 41.7 sin 41.6	dex 35.6 sin 35.3	dex 37.3 sin 35.6	1) adult 2) adult
Coll. Dub. 2017/3	Java	dex --	dex --	dex ± 37.2	middle-aged; broken
Coll. Dub. 2077a/2	Kedung Lumbu	dex 43.8	dex 38.2	dex 41.0	adult
Coll. Dub. 2077c/1 Coll. Dub. 2077c/2*[1]	Java	dex 41.3 dex --	dex 36.4 dex --	dex 38.6 dex 39.9	1) adult 2) middle aged*[1]
Coll. Dub. 2079	Sumber Waru	sin 41.3 dex 39.3	sin 39.2 dex 38.5	sin 41.4 dex 41.7	old
Coll. Dub. 2084b	Bogo	dex 45.8	dex 41.5	dex 36.2	middle-aged
Coll. Dub. 2188	Kedung Lumbu	sin ± 34.5	sin --	sin ± 38.1	broken

number of specimen	locality	length (Fig. V-9,4)	width on the anterior side (Fig. V-9,5)	width on the posterior side (Fig. V-9,6)	degree of wear
Coll. Dub. 2195a (see also Coll. Dub. 2023c)	Sumber Waru	sin 34.5	sin 33.9	sin 32.8	very old
Coll. Dub. 2195b (see also Coll. Dub. 2080a)	Sumber Waru	dex 33.8	dex 35.5	dex --	old
Coll. Dub. 2203	Kedung Brubus	dex 40.8	dex 36.4	dex 36.5	old
Coll. Dub. 2318a	Bangle	sin 50.1	sin 37.2	sin 41.8	middle aged
Coll. Dub. 2902	"Trinil"	dex min 37.3	dex ± 36.4	dex 39.0	old
Coll. Dub. 2907/1	Nonko, NW of Trinil	dex 37.5	dex 33.3	dex 32.7	middle-aged
Coll. Dub. 2908	Kedung Brubus	sin 35.5 dex 35.5	sin 38.3 dex 38.5	sin ± 40.6 dex 41.8	old
Coll. Dub. 2909	Tinggang	dex 43.3	dex 37.4	dex ± 38.8	middle-aged
Coll. Dub. 2911	Tinggang	sin 43.5 dex 43.5	sin 36.8 dex 37.0	sin 38.5 dex 39.7	middle-aged
Coll. Dub. 2914	Tinggang	sin ± 45.3 dex 43.7	sin -- dex --	sin ± 50.4 dex 37.3	sin broken dex middle-aged
Coll. Dub. 2919	Padasmalang	sin 40.6 dex 38.6	sin ± 35.0 dex 32.5	sin 36.1 dex 34.2	sin broken dex broken
Coll. Dub. 2920	Java	sin 49.0	sin 31.6	sin 36.3	broken
Coll. Dub. 5760	Java	sin --	sin 36.9	sin --	middle-aged; broken
Coll. Dub. 6654	Java	dex --	dex 36.5	dex --	middle-aged; broken
Coll. Dub. 6954/9	Tritik	dex --	dex --	dex 38.4	middle-aged; broken
Coll. Dub. 11466*[1]	Kedung Brubus	dex --	dex 36.2	dex --	middle-aged; broken
Coll. Dub. 3101	Samalka, Siwaliks	sin ± 41.8 dex 39.8	sin -- dex ± 40.9	sin ± 44.9 dex ± 44.3	sin broken dex old
Coll. Dub. 3137	Samalka 9 , Siwaliks	dex ± 37.1	dex min ± 41.2	dex --	middle-aged
Coll. Dub. 3138	Samalka 3, Siwaliks	dex 48.9	dex 46.0	dex 44.5	adult
Coll. Dub. 3146	Naliwala, Punjab, Siwaliks	sin 41.5 dex ± 41.9	sin 37.8 dex ± 33.6	sin 33.9 dex --	middle-aged
Coll. Dub. 3148	Kodawala, Siwaliks	sin 41.3 dex 38.9	sin 46.5 dex 46.9	sin 48.1 dex 48.7	old

*[1] = it is not sure if this is a M^2 *[2] = approximate measurement; measured with measuring tape

VI-23 M^3

number of specimen	locality	length (Fig. V-9,7)	width on the anterior side (Fig. V-9,8)	width on the posterior side (Fig. V-9,9)	degree of wear
without number (skeleton, Geological Museum, Bandung)	Kali Glagah	sin 44.0 dex 40.0	sin 41.4 dex 38.0	sin -- dex --	--
366 (Museum Sangiran)	Rahang Atas	sin ± 38.0*2 dex ± 43.0*2	sin ± 43.0*2 dex ± 42.0*2	sin -- dex --	middle-aged
K 15-947	unknown (Java)	sin 43.8	sin 44.8	sin --	middle-aged
M 18	Kali Saat, exc. 8	dex 37.5	dex 34.9	dex --	middle-aged
K 694	Kali Glagah	sin 40.2	sin 36.9	sin --	middle aged
K 705	Gn. Butak	sin 37.5	sin 36.1	sin --	middle aged
K 749	Kedung Brubus	dex 35.1	dex 34.0	dex --	adult
Coll. Dub. 100/5	Java	dex --	dex --	dex 27.1	middle-aged; broken
Coll. Dub 163a	Pati Ajam	dex 44.1	dex 40.1	dex 36.8	adult
Coll. Dub. 314a/1 Coll. Dub. 314a/2	Kedung Lumbu	sin 37.8 dex 39.1	sin 35.5 dex 35.8	sin 29.7 dex 31.2	1) adult 2) adult
Coll. Dub. 1702	Kedung Lumbu	sin 34.4 dex 36.3	sin 37.5 dex 38.4	sin 35.4 dex 34.7	middle-aged
Coll. Dub. 2004	Java	sin 38.0	sin ± 34.2	sin ± 32.8	middle-aged
Coll. Dub. 2076/12 Coll. Dub. 2076/13 Coll. Dub. 2976/14 Coll. Dub. 2976/15	Kedung Brubus	dex -- sin -- sin -- sin --	dex 36.1 sin 34.3 sin -- sin --	dex -- sin -- sin 32.0 sin 30.1	adult; broken middle-aged; broken adult; broken middle-aged; broken
Coll. Dub. 2077b	Kedung Lumbu	sin 41.5	sin 38.3	sin 33.8	adult (not worn)
Coll. Dub. 2079	Sumber Waru	sin 40.3 dex 38.3	sin 39.1 dex 39.2	sin 33.1 dex 31.1	middle-aged
Coll. Dub. 2080a (see also Coll. Dub. 2195b)	Sumber Waru	dex 37.9	dex 37.2	dex 33.3	middle-aged
Coll. Dub. 2084b	Bogo	dex 44.5	dex 44.5	dex 35.3	middle-aged
Coll. Dub. 2188	Kedung Lumbu	sin 36.6	sin 34.0	sin ± 31.5	adult; broken

Number	Locality	length (Fig. V-9,7)	width on the anterior side (Fig. V-9,8)	width on the posterior side (Fig. V-9,9)	Degree of wear
Coll. Dub. 2195a (see also Coll. Dub. 2023c)	Sumber Waru	sin 38.7	sin 34.8	sin 31.6	middle-aged
Coll. Dub. 2203	Kedung Brubus	dex 39.9	dex 33.7	dex 35.0	old
Coll. Dub. 2205/1 Coll. Dub. 2205/2	Kedung Brubus	sin 47.1 dex 48.3	sin 38.8 dex 39.2	sin 36.6 dex 37.4	1) middle-aged 2) middle-aged
Coll. Dub. 2318d*[1]	Kedung Brubus	sin 41.4	sin 37.7	sin 32.9	adult
Coll. Dub. 2318e *[1]	Dekes/Wadegan	dex 37.6	dex 35.8	dex 32.3	middle-aged
Coll. Dub. 2902	"Trinil"	dex 42.9	dex 41.9	dex 36.2	middle-aged
Coll. Dub. 2907/2	Nonko, NW of Trinil	sin 38.3 dex 36.0	sin 34.9 dex 35.7	sin 33.3 dex 30.7	middle-aged
Coll. Dub. 2908	Kedung Brubus	sin ± 39.5 dex 40.3	sin 39.7 dex 39.8	sin 39.7 dex 36.9	sin: broken dex: middle-aged
Coll. Dub. 2909	Tinggang	dex 45.4	dex ± 37.4	dex ± 40.9	broken
Coll. Dub. 2911	Tinggang	sin 38.6 dex 45.2	sin 36.8 dex ± 39.2	sin 31.9 dex ± 39.8	sin: middle-aged dex: broken
Coll. Dub. 2914	Tinggang	dex 41.7	dex 38.1	dex 32.6	middle-aged
Coll. Dub. 2919	Padasmalang	sin 37.8 dex 37.5	sin 35.9 dex ± 37.6	sin 30.0 dex ± 37.7	sin: old dex: broken
Coll. Dub. 6927/2 Coll. Dub. 6927/3	Tritik	sin -- sin --	sin -- sin 30.6	sin 30.0 sin --	adult; broken middle-aged; broken
Coll. Dub. 6954/8	Tritik	sin --	sin --	sin 31.3	middle-aged; broken
Coll. Dub. 3101	Samalka, Siwaliks	dex 49.5	dex 50.5	dex 44.1	very old
Coll. Dub. 3137	Samalka 9, Siwaliks	dex 48.1	dex ± 42.3	dex 39.2	broken
Coll. Dub. 3146	Naliwala, Punjab, Siwaliks	sin 36.8 dex 35.5	sin 35.1 dex min ± 29.1	sin ± 32.8 dex min ± 26.5	sin: broken dex: broken
Coll. Dub. 3148	Kodawala, Siwaliks	sin 38.3 dex 40.1	sin 41.9 dex 42.7	sin 36.4 dex 36.5	very old

*[1] = it is not sure if this is a M^3
*[2] = approximate measurement; measured with measuring tape

VI-24 MANDIBLE

number of specimen	locality	length of symphysis (Fig. V-10A,1)	height of symphysis (Fig. V-10B,2)	thickness of ramus below M_2 (Fig. V-11A,1)	width of ramus (ventral side) (Fig. V-11B,1)	narrowest width of mandible (Fig. V-10A,13)	length of mandible from front to M_3 (Fig. V-10A,2)	horizontal distance between M_3 sin and dex (Fig. V-10A,11)	width of the mandible at M_2 (Fig. V-10A,12)
without number (Laboratory Bioanthropologi and Paleoanthropologi, Yogyakarta)	Medalem	150 *1	--	100 *1	--	--	--	--	--
without number (Museum Sangiran)	Rahang Bawah	150 *1	--	120-150 *1	--	--	--	--	--
without number (skeleton, Geological Museum, Bandung)	Kali Glagah	min 133.8	57.0	sin 86.7 dex 88.6	sin 45.3 dex 47.4	150	--	--	--
without number (skull and mandible, Geological Museum, Bandung)	Ngandong	--	110.0	sin 160.0	--	--	240		
4-4 A	Java	--	--	92.4	36.6	--	--	--	--
22 G	Tji Bokagung (Tji Djolang)	121.2	90.1	sin 110.2 dex 109.2	sin 58.8 dex 50.5	185	--	--	--
SA 270378	Triangulation Point, Ngebung	69.1 juvenile	21.5 juvenile	sin 43.8 juvenile *2	sin 32.1 juvenile	--	--	--	--
Coll. Dub. 97	Redjuno	--	--	sin 96.0	--	--	--	--	--
Coll. Dub. 98	Java	--	--	dex 96.3	63.6	--	--	--	--
Coll. Dub. 99	Tritik	± 115.5 *3	57.7	sin 102.9 dex 102.8	sin 50.0 dex 45.6	--	± 238.5 *3	85.7	161.4
Coll. Dub. 310	Kedung Brubus	--	--	--	sin 47.1	--	--	--	--
Coll. Dub. 513	Nonko	min 114.4	70.0	--	--	--	--	--	--
Coll. Dub. 1804	Redjuno near Teguan	--	--	dex 90.7	dex ± 42.6	--	--	--	--
Coll. Dub. 2082	Teguan	--	--	--	dex 50.6	--	--	--	--

number of specimen	locality	length of symphysis (Fig. V-10A,1)	height of symphysis (Fig. V-10B,2)	thickness of ramus below M_2 (Fig. V-11A,1)	width of ramus (ventral side) (Fig. V-11B,1)	narrowest width of mandible (Fig. V-10A,13)	length of mandible from front to M_3 (Fig. V-10A,2)	horizontal distance between M_3 sin and dex (Fig. V-10A,11)	width of the mandible at M_2 (Fig. V-10A,12)
Coll. Dub. 2174	Kedung Brubus	--	--	sin 93.3	sin 62.6	--	--	--	--
Coll. Dub. 2202	Java	--	--	dex 86.4	dex 44.3	--	--	--	--
Coll. Dub. 2314	Papa Djaran	--	--	dex 92.9	dex 60.7	--	--	--	--
Coll. Dub. 2903	"Trinil"	min 99.8	78.0	sin 118.0	sin 57.1	--	256.3	--	--
Coll. Dub. 2904	Kebon Duren	--	--	sin 100.8 *4	sin 48.1	--	--	--	--
Coll. Dub. 2905	Papa Djaran	--	--	sin 99.5	sin 54.3	--	--	--	--
Coll. Dub. 2906	Java	--	--	sin 92.4	--	--	--	--	--
Coll. Dub. 2910	Tritik	min 106.7	76.0	sin 110.1 dex 107.2	sin 58.2 dex 58.6	--	min 240.7	89.5	158.2
Coll. Dub. 2915	Solo Valley	124.5	100.0	sin 135.5 dex 131.2	sin 56.4 dex 61.5	--	241.4	70.8	156.9
Coll. Dub. 2916	Kedung Brubus	min 135.6	71.3	sin 98.5 dex 108.5	sin 54.0 dex 56.6	--	min 253.4	67.0	153.1
Coll. Dub. 2917	Kedung Lumbu	--	--	dex 82.5	dex 30.6	--	--	--	--
Coll. Dub. 2918	Papa Djaran, N of Kebon Duren	min 134.4	76.5	--	--	--	--	--	--
Coll. Dub. 2922	Kedung Lumbu	--	--	--	sin + 41.4	--	--	--	--
Coll. Dub. 2929	Kedung Madoh	123.7	--	--	--	--	--	--	--
Coll. Dub. 2931	Kedung Brubus	min 115.6	67.7	--	--	--	--	--	--
Coll. Dub. 2932	Nonko, NW of Trinil	min 113.9	min 54.7	--	--	--	--	--	--
Coll. Dub. 2934	Kedung Brubus	--	min 54.6	--	--	--	--	--	--
Coll. Dub. 4857	Padasmalang	--	--	sin 155.5 *5	--	--	--	--	--
Coll. Dub. 3147	Bharon, Punjab, Siwaliks	--	--	dex + 147.6	dex 46.7	--	--	--	--

*1 estimated; *2 measured below DP_4 ; *3 symphysis restored with plaster; *4 measured below M_1; *5 measured below M_3

VI-25 LOWER DENTITION

number of specimen	locality	outer distance between C sin and dex (Fig. V-10B,1)	diastema between C and P_2 (Fig. V-10A,5)	diastema between P_2 and P_3 (Fig. V-10A,6)	diastema between P_3 and P_4 (Fig. V-10A,7)	diastema between P_4 and M_1 (Fig. V-10A,8)	diastema between M_1 and M_2 (Fig. V-10A,9)	diastema between M_2 and M_3 (Fig. V-10A, 10)	length of P_2 - P_4 (Fig. V-10A,4)	length of M_1 - M_3 (Fig. V-10A,3)	length of P_2 - M_3 (Fig. V-10A, 14)	length of P_3 - M_3 (Fig. V-10,15)
without number (Laboratory Bioanthropologi and Paleoanthropologi, Yogyakarta)	Medalem	250 *[1]	--	--	--	--	--	--	x	x	--	--
without number (Museum Sangiran)	Rahang Bawah	250 *[1]	--	--	--	--	--	--	--	--	--	--
without number (skeleton, Geological Museum, Bandung)	Kali Glagah	270	--	--	--	--	--	--	--	sin 140 dex 144	--	sin 190 dex 192
without number (skull and mandible, Geological Museum, Bandung)	Ngandong	210	sin 60	--	--	--	--	--	sin 80	sin 140 dex 140	sin 230	--
4-4 A	Java	--	--	--	--	--	--	--	--	± 115.3	--	--
22 G	Tji Bokagung (Tji Djolang)	--	sin 50 dex 50	--	--	--	--	--	sin 90 dex 85	sin 125 dex 125	sin 210 dex 210	sin 180 dex 180
SA 270378	Triangulation Point, Ngebung	sin 2x 43.1 = 86.2 (juv)	--	--	--	--	--	--	--	--	--	--
Coll. Dub. without number	Java	--	--	sin 12.6	sin 0	--	--	--	sin 91.8	--	--	--

number of specimen	locality	outer distance between C sin and dex (Fig. V-10B,1)	diastema between C and P_2 (Fig. V-10A,5)	diastema between P_2 and P_3 (Fig. V-10A,6)	diastema between P_3 and P_4 (Fig. V-10A,7)	diastema between P_4 and M_1 (Fig. V-10A,8)	diastema between M_1 and M_2 (Fig. V-10A,9)	diastema between M_2 and M_3 (Fig. V-10A, 10)	length of P_2 - P_4 (Fig. V-10A,4)	length of M_1 - M_3 (Fig. V-10A,3)	length of P_2 - M_3 (Fig. V-10A, 14)	length of P_3 - M_3 (Fig. V-10A, 15)
Coll. Dub. 99	Tritik	--	sin 46.6	sin 6.2 dex 0	--	sin 0	--	--	sin 79.4 dex 75.1	sin 121.9 dex ± 118.8	sin 202.7 dex + 191.2	--
Coll. Dub. 1804	Redjuno near Teguan	--	--	dex 3.7	--	dex ± 5.0	dex 3.4	dex 2.8	--	dex ± 93.7	--	--
Coll. Dub. 1818	Redjuno	--	--	sin 14.9	sin 5.9	--	--	--	sin 84.6	--	--	--
Coll. Dub. 2174	Kedung Brubus	--	--	--	sin 10.0	sin ± 5.7	--	--	--	--	--	--
Coll. Dub. 2207b	Kebon Duren	--	--	--	--	sin 13.8	--	--	--	--	--	--
Coll. Dub. 2903	"Trinil"	--	--	--	--	--	--	--	--	dex 118.0	--	--
Coll. Dub. 2904	Kebon Duren	--	--	sin 8.2	sin ± 3.4	--	--	--	sin 91.9	--	--	--
Coll. Dub. 2910	Tritik	302.1 *2	sin 67.5 dex 73.5	--	--	--	--	--	--	--	sin 204.8 dex --	--
Coll. Dub. 2915	Solo Valley	298.8 *3	sin 74.6	sin 13.8	--	--	--	--	--	--	--	--
Coll. Dub. 2916	Kedung Brubus	--	sin ± 53.0 dex 63.0	sin ± 8.3	--	dex 2.1	--	--	sin 86.1 dex 83.3	sin 129.1 dex 123.8	sin 212.9 dex 206.7	--
Coll. Dub. 2917	Kedung Lumbu	--	dex ± 39.1	--	--	dex 5.6	dex 1.9	dex 4.4	dex ± 75.8	dex 135.1	--	--

number of specimen	locality	outer distance between C sin and dex (Fig. V-10B,1)	diastema between C and P_2 (Fig. V-10A,5)	diastema between P_2 and P_3 (Fig. V-10A,6)	diastema between P_3 and P_4 (Fig. V-10A,7)	diastema between P_4 and M_1 (Fig. V-10A,8)	diastema between M_1 and M_2 (Fig. V-10A,9)	diastema between M_2 and M_3 (Fig. V-10A,10)	length of P_2 - P_4 (Fig. V-10A,4)	length of M_1 - M_3 (Fig. V-10A,3)	length of P_2 - M_3 (Fig. V-10A, 14)	length of P_3 - M_3 (Fig. V-10A, 15)
Coll. Dub. 2918	Papa Djaran, N of Kebon Duren	265.7 *2 274.4 *3	sin 39.0 dex 37.0	sin 10.7 dex 11.2	sin 7.8 dex 8.0	--	--	--	--	--	--	--
Coll. Dub. 2922	Kedung Lumbu	--	--	--	--	sin 3.5	sin not 0	--	--	--	--	--
Coll. Dub. 2929	Kedung Madoh	--	dex 59.4	--	--	--	--	--	--	--	--	--
Coll. Dub. 4908	Kedung Brubus	--	dex 15.9	dex 7.0	dex 13.4	dex 4.8	--	--	dex 86.9	--	--	--
Coll. Dub. 3147	Bharon, Punjab, Siwaliks	--	dex 59.9	--	dex 13.5	--	--	--	dex 121.5	dex 132.0	dex 247.7	--

*1 estimated;
*2 measured between outer sides of canine;
*3 measured between outer sides of alveoli of the canines, so bone included;
x = about equal in size

VI-26 SUMMARY OF THE BIOMETRICAL CHARACTERS OF THE MANDIBLE

Character	Minimum (in mm)	Maximum (in mm)	Average
Thickness of the ramus	86.4	160	105.7 mm (N=26)
Width of the ramus, measured on the ventral side	30.6	63.6	51.9 mm (N=24)
Narrowest width of the mandible	150	185	167.5 mm (N=2)
Length of the mandible	240	256.3	244 mm (N=4)
Horizontal distance between the M_3 on the left and right side	67	89.5	78.3 mm (N=4)
Horizontal distance between the outer sides of the M_2	153.1	161.4	157.4 mm (N=4)
Distance between the canines	210	302.1	270 mm (N=6)
Diastema between the canine and the P_2	15.9	74.6	53.6 mm (N=13)
Diastema between the P_2 and P_3	about zero	14.9	8.8 mm (N=10)
Diastema between the P_3 and P_4	about zero	13.5	8.4 mm (N=7)
Diastema between the P_4 and the M_1	about zero	13.8	5 mm (N=6)
Diastema between M_1 and M_2	about zero	3.4	1.8 mm (N=3)
Diastema between M_2 and M_3	2.8	4.4	3.6 mm (N=2)
Length of the row P_2-P_4	75.1	121.5	88 mm (N=12)
Length of the row M_1-M_3	118	144	131.2 mm (N=12)
Length of the row P_2–M_3	202.7	247.7	215.6 mm (N=8)
Length of P_3-M_3	180	192	185.5 mm (N=4)

VI-27 LATERAL SIDE OF THE CALVARIUM

number of specimen	locality	thickness of the apophyse of the canine (Fig. V-13B,1)	thickness of maxilla at P^2 (Fig. V-13B,2)	thickness of maxilla at M^2 (Fig. V-13B,3)	height of orbit until base of M^3 (Fig. V-13B,4)	difference in height between the occipital crest and the posterior end of the nasal bone (Fig. V-13B,5)	distance orbit-zygomatic arch (Fig. V-13B,6)	difference in height between orbit and occiput (Fig. V-13B,7) *4	vertical height of orbit (Fig. V-13C,8)	horizontal width of orbit (outer sides) (Fig. V-13C,9)	horizontal width of orbit (inner sides) (Fig. V-13C, 10)	maximum thickness of orbital bone (Fig. V-13C, 11)	difference in height between orbits and frontal bone (Fig. V-13B,12) *5
without number (skeleton, Geological Museum, Bandung)	Kali Glagah	-- --	-- --	-- --	sin 135 dex 145	--	-- --	-30.0	sin 64.2 dex 66.8	sin 67.9 dex 65.9	-- --	-- --	28.0
without number (skull and mandible, Geological Museum, Bandung)	Ngandong	-- --	-- --	-- --	sin 160 dex --	70	-- --	a little -	sin 60.0 dex --	sin 50.0 dex --	-- --	-- --	61.0
Coll. Dub. 2902	"Trinil"	dex min 86.0*1	-- --	sin – dex 118.8	sin -- dex + 180	10	sin – dex 194.9	+ 10.0	sin – dex 61.9	sin – dex 71.3	sin – dex 62.9	sin – dex 24.7	35.0
Coll. Dub. 2907/1	Nonko	sin – dex 87.3	-- --	-- --	-- --	--	-- --	--	-- --	-- --	-- --	-- --	--
Coll. Dub. 2908	Kedung Brubus	-- --	sin 125.5 dex 118.4	sin 121.7 dex 126.5	sin + 150 dex + 160	No difference*2	sin – dex 176.5	--	sin 61.9 dex + 62.0	sin 66.8 dex --	Sin 64.0 dex --	Sin 23.7 dex --	20.0

number of specimen	locality	thickness of the apophyse of the canine (Fig. V-13B,1)	thickness of maxilla at P^2 (Fig. V-13B,2)	thickness of maxilla at M^2 (Fig. V-13B,3)	height of orbit until base of M^3 (Fig. V-13B,4)	difference in height between the occipital crest and the posterior end of the nasal bone (Fig. V-13B,5)	distance orbit - zygomatic arch (Fig. V-13B,6)	difference in height between orbit and occiput (Fig. V-13B,7) *4	vertical height of orbit (Fig. V-13C,8)	horizontal width of orbit (outer sides) (Fig. V-13C,9)	horizontal width of orbit (inner sides) (Fig. V-13C, 10)	maximum thickness of orbital bone (Fig. V-13C, 11)	difference in height between orbits and frontal bone (Fig. V-13B,12) *5
Coll. Dub. 2909	Tinggang	sin – dex 83.2	-- --	sin – dex 106.0	sin — dex ± 180	--	sin – dex 202.9	- 5.0	sin 72.1 dex --	sin – dex 65.1	sin – dex 58.9	sin – dex 27.8	30.0
Coll. Dub. 2911	Tinggang	sin 83.1 dex --	sin 126.0 dex 136.9	sin 135.3 dex 130.0	-- --	37.5	-- --	--	-- --	-- --	-- --	-- --	--
Coll. Dub. 2914	Tinggang	sin 73.8 dex 74.1	sin 125.3 dex 102.7	sin 129.0 dex 123.3	sin + 140 dex --	31.0	sin 195.7 dex --	+ 5.0	sin 65.4 dex --	sin 76.6 dex --	sin 56.2 dex --	sin 21.3 dex --	40.0
Coll. Dub. 2919	Padas-malang	-- --	-- --	sin 104.2 dex --	sin + 150 dex + 150	15.0 *2	sin 184.7 dex 189.7	+ 3.0	sin 54.8 dex 55.4	sin 72.0 dex 72.0	sin 60.5 dex 59.0	sin 14.0 dex 20.6	40.0
Coll. Dub. 3101*3	Samalka, Siwaliks	-- --	-- --	-- --	-- --	15.0	sin + 185.0 dex --	+ 10.0	sin 58.6 dex --	sin 97.9 dex --	Sin 81.2 dex --	Sin 22.5 dex --	25.0
Coll. Dub. 3146	Naliwala, Punjab, Siwaliks	-- --	-- --	sin 125.1 dex 114.2	sin – dex + 140	> 50.0	-- --	- 5.0	sin – dex 66.2	sin + 84.8 dex 77.6	sin – dex 63.2	sin 24.1 dex 20.7	45.0
Coll. Dub. 3148	Kodawala, Siwaliks	-- --	-- --	sin 123.0 dex 121.3	-- --	9.0 *2	-- --	--	-- --	-- --	-- --	-- --	--

*1 apophyse not complete, isolated part of the apophyse with the canine
*2 occipital bone not complete
*3 specimen restored with plaster
*4 + = orbit lies above level of occiput
- = orbit lies below level of occiput
*5 frontal bone lies below level of orbits

VI-28 POSTERIOR SIDE OF THE CALVARIUM

number of specimen	locality	maximum height of occiput (Fig. V-14B,1)	height of occiput until rim foramen magnum (Fig. V-14B,2)	maximum width of occipital crest (Fig. V-14B,3)	width foramen magnum (Fig. V-14B,4)	vertical height foramen magnum (Fig. V-14B,5)	vertical height occipital condyle (Fig. V-14B,6)	width occipital condyle (Fig. V-14B,7)	maximum width of occiput (Fig. V-14B,8)
without number (Geol. Museum, Bandung)	skeleton, Kali Glagah	± 150.0	--	--	--	--	-- --	-- --	225.0
without number (Geol. Museum, Bandung)	skull and mandible, Ngandong	180.0	--	--	--	--	-- --	-- --	--
Coll. Dub. 2206	Kedung Lumbu	-- --	--	--	--	--	dex 32.5 *[1]	dex 43.8 *[1]	--
Coll. Dub. 2908	Kedung Brubus	sin 150.0 dex 146.2	105.9	min 9.6	48.2	± 34.5	sin 38.2 dex 46.4	sin 37.4 dex 33.6	--
Coll. Dub. 2911	Tinggang	sin 169.2 dex --	130.2	10.6	48.1	36.2	sin 46.4 dex --	sin 41.3 dex --	245.6
Coll. Dub. 2914	Tinggang	sin 176.0 dex 174.3	124.5	13.6	42.2	40.0	sin 42.9 dex 45.0	sin 47.5 dex 44.7	min 237.9
Coll. Dub. 2919	Padasmalang	sin 147.4 dex 140.5	114.6	13.6	47.2	33.9	sin 37.4 dex 35.4	sin 42.9 dex 40.4	203.0
Coll. Dub. 3146	Naliwala, Punjab, Siwaliks	sin 177.9 dex 173.6	± 122.9	± 12.5	± 53.2	32.2	sin – dex 42.6	sin – dex 38.7	240.4
Coll. Dub. 3148	Kodawala, Siwaliks	-- --	± 138.6	--	51.3	--	sin 39.0 dex ± 34.7	sin 43.9 dex 42.4	--

*[1] isolated condyle

VI-29 DORSAL SIDE OF THE CALVARIUM

number of specimen	locality	pre-orbital length *1 (Fig. V-15B,1)	minimum width of nasal bone (Fig. V-15B,2)	smallest part of the muzzle (Fig. V-15B,3)	length of nasal bone *1 (Fig. V-15B,4)	distance between occiput and anterior end of nasal bone *1 (Fig. V-15B,5)	maximum width of nasal bone (Fig. V-15B,6)	minimum distance between inner sides of the orbits (Fig. V-15B,7)	distance between occiput and posterior end of nasal (Fig. V-15B,8)	width of sagittal crest (Fig. V-15B,9)	length of sagittal crest (Fig. V-15B, 10)	maximum distance between inner side of zygomatic arch and braincase (Fig. V-15B,11)	distance between occiput and posterior rim of orbit (Fig. V-15B,12)	minimal width of braincase (Fig. V-15B, 13)
without number (Geological museum, Bandung)	skeleton Kali Glagah	--	--	--	--	--	92.7	± 260.0	160.0	--	88.2	sin 100.0 dex 100.0	210.0	96.0
without number (Geological Museum, Bandung)	Ngandong	--	30.0	94.0	260.0	--	100.0	240.0	170.0	--	80.0	sin 130.0 dex 130.0	sin 190.0 dex 200.0	110.0
Coll. Dub. 2084a	Kedung Lumbu	--	--	--	--	--	--	--		16.5	64.8	--	--	--
Coll. Dub. 2902	"Trinil"	--	--	--	--	--	--	--	± 160.8	--	62.9	sin – dex ± 87.0	sin – dex 169.0	82.9
Coll. Dub. 2908	Kedung Brubus	± 295	45.1	97.6	min 211.7	min 42.9	120.1	± 205.9	166.2	--	--	sin – dex ± 83.0	sin 198.7 dex 185.2	97.0
Coll. Dub. 2909	Tinggang	± 326.0	--	--	--	--	--	--	--	--	54.1	sin – dex 70.0	Sin – dex 178.0	--

number of specimen	locality	pre-orbital length *1 (Fig. V-15B,1)	minimum width of nasal bone (Fig. V-15B,2)	smallest part of the muzzle (Fig. V-15B,3)	length of nasal bone *1 (Fig. V-15B,4)	distance between occiput and anterior end of nasal bone *1 (Fig. V-15B,5)	maximum width of nasal bone (Fig. V-15B,6)	minimum distance between inner sides of the orbits (Fig. V-15B,7)	distance between occiput and posterior end of nasal (Fig.V-15B,8)	width of sagittal crest (Fig. V-15B,9)	length of sagittal crest (Fig. V-15B, 10)	maximum distance between inner side of zygomatic arch and braincase (Fig. V-15B,11)	distance between occiput and posterior rim of orbit (Fig. V-15B,12)	Minimal width of braincase (Fig. V-15B, 13)
Coll. Dub. 2911	Ting-gang	--	42.3	97.9	min 289.8	min 44.5	103.8	--	161.0	--	± 61.4	sin ± 90.0 dex 85.0	--	87.5
Coll. Dub. 2914	Ting-gang	± 283.9	40.7	98.3	min 298.6	min 45.8	102.6	± 175.0	158.6	--	52.6	sin ± 85.0 dex ± 90.0	sin 178.0 dex --	87.6
Coll. Dub. 2919	Padas-malang	--	--	--	--	--	± 109.9	± 190.0	154.6	15.6	75.6	sin ± 84.0 dex ± 80.0	sin 166.0 dex 164.3	92.3
Coll. Dub. 5006	Kedung Lumbu	--	--	--	--	--	--	--	--	10.4	81.5	--	--	68.5
Coll. Dub. 3101	Samalka, Siwaliks	--	--	--	--	--	91.7	--	208.6	10.7	104.0	sin 100.0 dex --	Sin 237.6 dex --	68.6
Coll. Dub. 3146	Naliwala, Punjab, Siwaliks	--	53.4 *2	--	--	--	98.0	171.0	181.0	7.8	94.4	-- --	sin – dex 207.0	70.0
Coll. Dub. 3148	Kodawala, Siwaliks	--	51.9 *2	--	--	--	101.6	--	192.9	--	97.2	-- --	-- --	± 65.8

*1 minimum measurements because there are no specimens in which the whole calvarium is completely preserved.
*2 smallest part of the nasal preserved, which is not really the smallest part, but this is not preserved.

VI-30 MAXIMUM THICKNESS OF THE SQUAMOSAL (Fig. V-16)

number of specimen	locality	thickness of squamosal
Coll. Dub. 2902	"Trinil"	sin – dex 52.0
Coll. Dub. 2908	Kedung Brubus	sin – dex 52.6
Coll. Dub. 2909	Tinggang	sin -- dex 57.2
Coll. Dub. 2911	Tinggang	sin 58.9 dex 56.2
Coll. Dub. 2914	Tinggang	sin 57.9 dex 56.2
Coll. Dub. 2919	Padasmalang	sin 50.3 dex min 39.0
Coll. Dub. 3101	Samalka, Siwaliks	sin $\pm$ 33.4 dex --

VI-31 UPPER DENTITION

number of specimen	locality	distance between inner sides of canines (Fig. V-17B,1)	diastema between P^1 and P^2 (Fig. V-17B,2)	diastema between P^2 and P^3 (Fig. V-17B,3)	diastema between P^3 and P^4 (Fig. V-17B,4)	diastema between P^4 and M^1 (Fig. V-17B,5)	length P^1 - P^4 (Fig. V-17B,6)	length P^2 - M^3 (Fig. V-17B,7)	length M^1 - M^3 (Fig. V-17B,8)	width of palate between the P^4's (Fig. V-17B,9)	width of palate between the M^1's (Fig. V-17B,10)	width of palate between the M^2's (Fig. V-17B,11)	width of palate between the M^3's (Fig. V-17B, 12)
without number (Geological Museum, Bandung)	skeleton, Kali Glagah	--	-- --	-- --	-- --	-- --	-- --	-- --	sin 125.0 dex 113.0	--	70.0	--	--
without number (Geological Museum, Bandung)	skull and mandible, Ngandong	180.0	sin 8.0 dex --	sin 10.0 dex --	-- --	-- --	sin 105.0 dex --	sin 230.0 dex --	sin 150.0 dex --	--	50.0	--	--
K 15-947	Java	--	--	--	--	--	--	--	sin min 118.9	--	--	--	--
M 18	Kali Saat, exc. 8	--	--	--	--	--	--	--	dex 119.8	--	--	--	--
Coll. Dub. 1702	Kedung Lumbu	--	sin 4.4 dex --	sin 4.4 dex 3.3	sin – dex 0	sin – dex 0	sin ± 104.1 dex --	sin 192.3 dex 192.8	sin 110.0 dex 116.0	68.2	60.9	61.5	64.2
Coll. Dub. 2023c (M^1) and Coll. Dub. 2195a (M^{2-3})	Sumber Waru	--	-- --	-- --	-- --	-- --	-- --	-- --	sin 105.1 dex --	--	--	--	--

number of specimen	locality	distance between canines (Fig. V-17B,1)	diastema between P^1 and P^2 (Fig. V-17B,2)	diastema between P^2 and P^3 (Fig. V-17B,3)	diastema between P^3 and P^4 (Fig. V-17B,4)	diastema between P^4 and M^1 (Fig. V-17B,5)	length P^1 - P^4 (Fig. V-17B,6)	length P^2 - M^3 (Fig. V-17B,7)	length M^1 - M^3 (Fig. V-17B,8)	width of palate between the P^4's (Fig. V-17B,9)	width of palate between the M^1's (Fig. V-17B,10)	width of palate between the M^2's (Fig. V-17B,11)	width of palate between the M^3's (Fig. V-17B, 12)
Coll. Dub. 2080a (M^3) and Coll. Dub. 2195b (M^{1-2})	Sumber Waru	--	-- --	-- --	-- --	-- --	-- --	-- --	sin -- dex 102.6	--	--	--	--
Coll. Dub. 2079	Sumber Waru	--	-- --	-- --	-- --	sin 0 dex 0	-- --	-- --	sin 106.5 dex 103.2	53.6	56.4	62.0	62.7
Coll. Dub. 2182/4	Kedung Lumbu	--	sin 14.8	--	--	--	--	--	--	--	--	--	--
Coll. Dub. 2188	Kedung Lumbu	--	sin 14.6 dex --	sin 9.7 dex --	sin min 1.5 dex --	-- --	sin 116.5 dex --	sin 102.9 dex --	sin 107.4 dex --	--	--	--	--
Coll. Dub. 2907/1	Nonko	--	-- --	-- --	sin – dex 21.4	sin – dex 28.8	-- --	sin 189.2 dex 189.6	sin -- dex 111.4	--	--	--	56.8
Coll. Dub. 2908	Kedung Brubus	203.5	sin 7.9 dex 12.8	sin 2.8 dex 3.8	sin 1.7 dex 0	sin 0 dex 0	sin 102.8 dex 102.5	sin 182.2 dex 184.0	sin ± 108.7 dex 108.5	77.5	65.2	64.8	68.2
Coll. Dub. 2909	Tinggang	--	-- --	-- --	-- --	sin – dex 0	-- --	-- --	sin – dex 119.5	--	--	--	--
Coll. Dub. 2911	Tinggang	202.9	sin 15.2 dex --	sin 5.6 dex + 7.6	sin 2.2 dex 3.7	sin 2.9 dex --	sin + 113.0 dex +110.5	sin 191.2 dex 197.9	sin 114.5 dex 122.6	64.2	59.8	60.5	53.2

number of specimen	locality	distance between canines (Fig. V-17B,1)	diastema between P^1 and P^2 (Fig. V-17B,2)	diastema between P^2 and P^3 (Fig. V-17B,3)	diastema between P^3 and P^4 (Fig. V-17B,4)	diastema between P^4 and M^1 (Fig. V-17B,5)	length P^1 - P^4 (Fig. V-17B,6)	length P^2 - M^3 (Fig. V-17B,7)	length M^1 - M^3 (Fig. V-17B,8)	width of palate between the P^4's (Fig. V-17B,9)	width of palate between the M^1's (Fig. V-17B,10)	width of palate between the M^2's (Fig. V-17B,11)	width of palate between the M^3's (Fig. V-17B, 12)
Coll. Dub. 2914	Tinggang	192.6	sin 10.4 dex 10.0	sin 8.4 dex 9.3	-- --	sin 1.5 dex 1.3	sin 196.0 dex ±107.0	sin ± 186.0 dex 193.8	sin ± 112.5 dex 114.7	69.6	± 49.4	± 56.4	± 58.7
Coll. Dub. 2919	Padas-malang	--	-- --	-- --	sin – dex 1.7	sin 0 dex 0	-- --	-- --	sin 109.4 dex 109.2	49.1	48.0	52.8	47.4
Coll. Dub. 3101	Samalka, Siwaliks	--	-- --	-- --	sin 1.4 dex --	-- --	-- --	-- --	sin ± 120.4 dex 122.4	68.4	48.5	54.9	56.4
Coll. Dub. 3137	Samalka, Siwaliks	--	-- --	-- --	-- --	-- --	-- --	-- --	sin – dex ±122.8	--	--	--	--
Coll. Dub. 3138	Samalka, Siwaliks	--	-- --	-- --	-- --	-- --	-- --	-- --	sin – dex 124.9	--	--	--	--
Coll. Dub. 3148	Kodawala, Siwaliks	--	-- --	-- --	-- --	sin 1.6 dex 4.4	-- --	-- --	sin 108.3 dex 108.9	± 60.2	50.7	49.7	59.3

VI-32 VENTRAL SIDE OF THE CALVARIUM

number of specimen	locality	width of premaxilla (Fig. V-17B,13) (see also Fig. V-12)	smallest part of the muzzle (Fig. V-17B,14)	medial distance between posterior rim of palatum and posterior part of the M^3 (Fig. V-17B,15)	maximum distance between posterior end of M^3 and posterior rim of occipital condyle (Fig. V-17B, 16)	distance between inner side of jugal bone and outer rim of pterygoid (Fig. V-17B,17)	smallest width of the jugal bone (Fig. V-17B, 18)	maximum width of squamo-sal (Fig. V-17B,19)	distance between the outer rim of the zygomatic arch and the buccal rim of the pterygoid (Fig. V-17B,20)	maximum width between the pterygoids (Fig. V-17B,21)
without number (Geol. Museum, Bandung)	skeleton, Kali Glagah	--	--	--	sin ± 180.0 dex ± 180.0	-- --	-- --	--	--	--
without number (Geol. Museum, Bandung)	skull and mandible, Ngandong	--	--	--	sin 160 dex --	-- --	-- --	-- --	-- --	--
Coll. Dub. 1702	Kedung Lumbu	--	± 111.5	12.8	-- --	-- --	-- --	-- --	-- --	--
Coll. Dub. 2902	"Trinil"	--	--	--	-- --	sin – dex 98.9	sin – dex 31.7	sin – dex 55.5	sin – dex 139.6	--
Coll. Dub. 2907/1	Nonko	--	min 112.8	--	-- --	-- --	-- --	-- --	-- --	--
Coll. Dub. 2908	Kedung Brubus	192.9	116.4	17.8	sin 185.9 dex 185.6	sin – dex 106.1	sin – dex 28.8	sin – dex 52.4	sin – dex 133.6	± 82.1
Coll. Dub. 2909	Tinggang	--	--	--	-- --	sin -- dex 86.8	sin -- dex 39.8	sin -- dex 51.7	sin -- dex + 124.6	±
Coll. Dub. 2911	Tinggang	--	120.2	6.1	sin 185.9 dex --	sin 105.9 dex 105.9	sin 29.0 dex 31.5	sin 56.9 dex 59.7	sin 145.0 dex 146.8	67.9
Coll. Dub. 2914	Tinggang	176.4	115.0	12.7	sin 190.0 dex 183.5	sin 104.3 dex 101.4	sin 32.7 dex 30.8	sin 49.8 dex 52.4	sin 144.8 dex 133.5	74.3

number of specimen	locality	width of premaxilla (Fig. V-17B,13) (see also Fig. V-12)	smallest part of the muzzle (Fig. V-17B,14)	medial distance between posterior rim of palatum and posterior part of the M^3 (Fig. V-17B,15)	maximum distance between posterior end of M^3 and posterior rim of occipital condyle (Fig. V-17B, 16)	distance between inner side of jugal bone and outer rim of pterygoid (Fig. V-17B,17)	smallest width of the jugal bone (Fig. V-17B,18)	maximum width of squamosal (Fig. V-17B,19)	distance between the outer rim of the zygomatic arch and the buccal rim of the pterygoid (Fig. V-17B,20)	maximum width between the pterygoids (Fig. V-17B,21)
Coll. Dub. 2919	Padas-malang	--	--	9.1	sin 162.4 dex 166.2	sin 105.7 dex 99.4	sin 17.7 dex 20.9	sin 41.3 dex 41.7	sin 126.2 dex 128.1	69.3
Coll. Dub. 3101	Samalka, Siwaliks	--	min 115.2	--	sin 217.9 *[1] dex 214.4 *[1]	sin – dex 123.9	sin – dex 37.8	sin – dex 58.8	sin – dex 163.1	--
Coll. Dub. 3146	Samalka, Siwaliks	--	--	22.3	sin 173.7 dex 187.8	-- --	-- --	-- --	-- --	77.8
Coll. Dub. 3148	Kodawala, Siwaliks	--	min 96.4	23.8	sin 206.0 dex 207.3	-- --	-- --	sin 53.4 dex ±53.4	-- --	77.0

*[1] occipital condyles are not present; measured until occiput. In all specimens the occipital condyles extend posteriorly compared with the occipital condyles, so the real values are even larger than the values given here.

number of specimen	locality	minimum distance between the pterygoids (Fig. V-17B,22)	length of basioccipital bone (Fig. V-17B,23)	maximum width of bulla, (Fig. V-17B,24)	maximum length of bulla, (Fig. V-17B,25)	minimum distance between the lingual rims of the squamosal bones (Fig. V-17B,26)	length of foramen magnum (Fig. V-17B,27)	length of occipital condyle (Fig. V-17B,28)	maximum width between the zygomatic arches (Fig. V-17B,29)
without number (Geol. Museum, Bandung)	skeleton Kali Glagah	--	--	-- --	-- --	--	--	-- --	± 340.0
without number (Geol. Museum, Bandung)	skull and mandible, Ngandong	--	--	-- --	-- --	--	--	-- --	± 340.0
Coll. Dub. 2182/5*[1]	Kedung Lumbu	--	--	sin 36.9 dex 39.2	sin 40.3 dex 39.3	--	--	-- --	--
Coll. Dub. 2206*[2]	Kedung Lumbu	--	--	--	--	--	--	sin – dex 32.3	--
Coll. Dub. 2908	Kedung Brubus	53.7	--	sin ± 38.8 dex ± 38.1	sin ± 34.5 dex ± 29.0	--	--	sin 41.6 dex 43.6	--
Coll. Dub. 2911	Tinggang	34.4	50.9	sin ± 40.0 dex --	sin ± 43.7 dex --	133.9	39.7	sin 30.7 dex --	± 344.0
Coll. Dub. 2914	Tinggang	43.4	66.8	sin 40.8 dex 41.5	sin 47.5 dex 43.4	134.1	45.0	sin 40.4 dex 39.7	± 335.0
Coll. Dub. 2919	Padas-malang	45.1	54.7	sin 34.0 dex 38.0	sin 35.9 dex min 36.6	123.1	20.8	sin 33.7 dex 35.3	± 313.0
Coll. Dub. 3101	Samalka, Siwaliks	--	--	sin ± 46.1 dex ± 40.5	sin min 35.2 dex ± 43.6	min 170.9 *[3]	--	-- --	--
Coll. Dub. 3146	Samalka, Siwaliks	49.0	--	sin min 39.3 dex min 30.4	sin ± 43.3 dex ± 39.5	± 144.6	20.2	-- dex 37.9	--
Coll. Dub. 3148	Kodawala, Siwaliks	54.5	52.5	sin 47.7 dex 49.2	sin 47.6 dex 50.7	124.9	--	sin 40.1 dex 38.6	--

*[1] isolated bulla *[2] isolated condyle *[3] not measurable, but distance between right squamosal bone and the buccal side of the left bulla is 170.9 mm, so the real value is even larger.

VI-33 SUMMARY OF THE BIOMETRICAL CHARACTERS OF THE CRANIUM. (Tables VI-27 – VI-32)

Character	Minimum (in mm)	Maximum (in mm)	Average
The thickness of the apophyse of the canine	73.8	87.3	80.3 mm (N=5)
The thickness of the maxilla at P^2	102.7	136.9	122.5 mm (N=6)
The thickness of the maxilla at M^2	104.2	135.3	121.4 mm (N=13)
The height of the orbit from the base of the M^3 (most of the measurements are approximate measurements, due to damage)	135	180	150 mm (N=11)
The distance of the nasal bone to the occipital crest	about zero	70	26.4 mm (N=9)
The distance between the orbit and the zygomatic arch	176.5	202.9	190.7 mm (N=6)
The distance between the orbit and the occiput	–30	+10	– 1.5 mm (N=8)
The vertical height of the orbit	54.8	72.1	62.5 mm (N=11)
The horizontal width of the orbit on the outer sides	50	97.7	71.1 mm (N=11)
The horizontal width of the orbit on the inner sides	56.2	81.2	63.2 mm (N=8)
The maximum thickness of the orbital bone	14	27.8	22.2 mm (N=9)
The difference in height between the orbits and the frontal bone	20	61	36 mm (N=9).
The maximum height of the occiput	140.5	180	163.5 mm (N=10)
The vertical height of the foramen magnum	32.2	40	35.6 mm (N=4)
The vertical height of the occiput condyle	32.5	46.4	40.6 mm (N=10)
The width of the occipital condyle	33.6	47.5	41.5 mm (N=11)
The maximum width of the occiput	203	245.6	228.5 mm (N=4)
The preorbital length	280*	326*	
*all measurements are minimum measurements, because the specimens are not complete			
The minimum width of the nasal bone	30	451	39.5 mm (N=4)
The smallest part of the muzzle	94	98.3	97 mm (N=4)
The length of the nasal bone	260*	298.6*	265 mm (N=4)
*although most measurements are minimum measurements due to damage.			
The distance between the occiput and the anterior end of the nasal bone All measurements are minimum measurements	42.9	45.8	44.4 mm (N=4)
The maximum width of the nasal bone	91.7	120.1	101.3 mm (N=8)

Character	Minimum (in mm)	Maximum (in mm)	Average
The minimum distance between the orbits	171	260	207 mm (N=6)
The distance between the occiput and the posterior end of the nasal bone	154.6	208.6	172.5 mm (N=9)
The width of the sagittal crest	7.8	16.5	12.2 mm (N=5)
The length of the sagittal crest	54.1	104	77.8 mm (N=11)
The maximum distance between the zygomatic arch and the brain-case	70	130	93.9 mm (N=14
The distance between the occiput and the posterior rim of the orbit	164.3	237.6	190.3 mm (N=12)
The minimum width of the brain-case	68.5	110	86 mm (N=10)
The thickness of the squamosal	52.0	58.9	55.2 mm (N=8)
The distance between inner sides of the canines	180	203.5	194.8 mm (N=4)
The diastema between P^1 and P^2	4.4	15.2	10.9 mm (N=9)
The diastema between the P^2 and P^3	2.8	10	6.4 mm (N=9)
The diastema between the P^3 and P^4	zero	21.4	4 mm (N=8)
The diastema between the P^4 and M^1	zero	28.8	2.9 mm (N=9)
The length of the row P^1-P^4	102.5	196	124.6 mm (N=5)
The length of the row P^2-M^3	102.6	230	186 mm (N=11)
The length of the row M^1-M^3	102.6	150	114.5 mm (N=23)
The width of the palate between the P^4's	49.1	77.5	64.4 mm (N=7)
The width of the palate between the M^1's	48	70	58.6 mm (N=9)
The width of the palate between the M^2's	49.7	64.8	58.0 mm (N=7)
The width of the palate between the M^3's	47.4	64.2	58.5 mm (N=8)
The width of the premaxilla	176.4	192.9	184.7 mm (N=2)
The smallest part of the muzzle	115	120.2	117.2 mm (N=3)
The medial distance between the posterior rim of the palate and the posterior part of the M^3	6.1	23.8	14.9 mm (N=7)
The maximum distance between the posterior end of the M^3 and the posterior rim of the occipital condyle	160	217.9	187.6 mm (N=14)
The distance between the inner side of the jugal bone and the outer rim of the pterygoid	86.8	123.9	103.8 mm (N=10)
The smallest width of the jugal bone	17.7	39.8	30.1 mm (N=10)
The maximum width of the squamosal	41.3	59.7	52.1 mm (N=11)

Character	Mini-mum (in mm)	Maxi-mum (in mm)	Average
The distance between the outer rim of the zygomatic arch and the buccal rim of the pterygoids	126.2	163.1	140.1 mm (N=9)
The maximum width between the pterygoids	67.9	82	74.7 mm (N=6)
The minimum width between the pterygoids	34.4	54.5	46.7 mm (N=6)
The length of the basioccipital bone	50.9	66.8	56.2 mm (N=4).
The maximum width of the bulla, approximate measurements included.	34	49.2	40.8 mm (N=13),
The maximum length of the bulla, approximate measurements included.	29	50.7	41.4 mm (N=13),
The minimum distance between the lingual rims of the squamosal bones approximate measurements included	123.1	> 170.9	138.6 mm (N=6),
The length of the foramen magnum	20.2	45	31.4 mm (N=4)
The length of the occipital condyle	30.7	43.6	37.6 mm (N=11)
The total width of the zygomatic arch measurements are approximate	313	344	334.4 mm (N=5),

APPENDIX VII MORPHOLOGICAL DESCRIPTIONS

Each paragraph starts with a list of specimens from which no additional morphological description is given, because no distinct features worth mentioning are present, other than the general description. This is followed by the descriptions of the other specimens. The material is listed in Appendix III. The measurements of the specimens can be found in Appendix VI.

VII.1 LOWER INCISORS

The measurements are given in Appendix VI-1 – VI-5 .
Specimens without description:
Without no. (skeleton in Geological Museum Bandung, Indonesia); no. 22 G; without no. (mandible and skull from Ngandong in Geological Museum Bandung, Indonesia); SA 160878-180; SA 270378; K 718/1; K 718/2; K718/3; Coll. Dub. 95/1 and 95/2; Coll. Dub. 99; Coll. Dub. 285/1; Coll. Dub. 513; Coll. Dub. 1818; Coll. Dub. 2207a/1; Coll. Dub. 2903; Coll. Dub. 2912; Coll. Dub. 2934.

Description of the specimens:

SA 030979-14 — The three pieces of incisor are embedded in a (clay)matrix (brownish colour) and a black crust. It is not possible to tell which incisor it is, neither if it is a left or a right one, although a little bit of the wear facet is visible.

SA 040979-16 — Three pieces of incisor, which are embedded in a hard (clay)matrix and a black crust.
The first piece (1) is present in the largest block of sediment, the second piece (2) is quite small (length: ± 2 cm) and the third piece (3) shows a part of the wear facet. It is a left incisor, but which incisor is not determinable. The cross section is rather circular and becomes more rounded in anterior direction.

SA 140979-7 — Six pieces of incisor, which are embedded in brownish (clay)matrix with gastropod shells. Although the wear facet is vaguely visible (covered with matrix), it is not determinable if it is a left or a right one, neither which incisor it is. The most posterior part is covered with matrix, so the total length is still greater than the 140 mm mentioned in Appendix VI-5.

SA 230178 — This indeterminable incisor has a cross section at the posterior end with a triangular shape, with the dorsal side rounded and the ventral side flat. The length is 45 mm.

K 717 — 1) the wear facet of this incisor is difficult to distinguish due to the fact that it is glued, but it is visible that it must be a left one, because the wear facet at the buccal side is larger than on the lingual side. This incisor is quite straight, the anterior side is not smaller than the posterior side, it is flattened in linguobuccal direction, but slightly; it is rather round.
2) the cross section of this incisor is not well visible.

K 719 — The incisor tapers distinctly in posterior direction. It cannot be defined which incisor it is.

K 747 — It cannot be defined which incisor it is. The cross section is rather round and there is a small dent at the dorsolingual side.

K 790 According to the catalogue of Von Koenigswald, this is supposed to be a molar of an artiodactyl. It looks like the number on the fossil might not be K 790, but we could not define what.

There are four incisors present; the I_1 dex and I_1-I_3 sin. The strange thing is that there is no trace whatsoever of a symphysis between the left and right incisors. At the posterior side of the mandible, besides the roots of the three big incisors, the incisor of the smaller I_2 can be seen. It looks as if this root is bent. The wear facets are not very distinct. The measurements were taken at the back side, where the wear facet was supposed to be.

Coll. Dub. 1804 Two right incisors are visible: I_1 and I_2 or I_2 and I_3. Regarding the difference in size, they might be $I_{1,2}$.

Coll. Dub. 2910 On the right side, the alveolus of I_2 has been broken. Of I_3 sin only the alveolus is present. All incisors are rather round, except the I_3 sin, which is flattened dorsoventrally.

To this mandible with broken incisors belong the other part of the incisors themselves, which match the broken stumps in the jaw. The I_1 sin shows a dent at the dorsal side. The I_1 dex is rather circular. The I_2 sin shows two little grooves, one on the dorsobuccal side, one on the ventral side. This incisor is rather straight, it does not bend in lingual direction. I_2 dex is not present. It is remarkable that the grooves, present on the incisors, are not at all visible in the shape of the alveolus.

Coll. Dub. 2915 All incisors are present, but broken off. Only the right I_1 is a bit flattened in dorsoventral direction, the others are flattened in linguabuccal direction. The incisors are not symmetrical with regard to the symphysis; The lingual rim of I_1 dex is positioned at the symphysis.

Coll. Dub. 2916 On the left side of the mandible, the I_1 is broken off, of I_2 only the alveolus is present, the I_3 is rather complete. On the right side, the I_1 is broken off, of I_2 and I_3 the alveoli are visible, but not measurable. The incisors are flattened in dorsoventral direction. I_1 and I_3 sin have a groove on the dorsal side, I_3 sin also has a groove on the buccal side, which shows when the incisor is taken out of the alveolus. Again the groove is not visible in the alveolus.

Coll. Dub. 2918 All incisors of this mandible are broken, I_2 dex is only represented by an alveolus. I_1 dex is rather circular, the other incisors are flattened in linguobuccal direction.

Coll. Dub. 2929 The upper part of the symphysis of the mandible fragment is missing, therefore the longitudinal section of the alveoli of the incisors is visible. The depth of the alveoli is hard to measure, because the anterior part of the mandible is not straight. The depth of the alveoli is approximately:

I_1 sin $\pm$ 114 mm	I_1 dex $\pm$ 81 mm
I_2 sin $\pm$ 75 mm	I_2 dex $\pm$ 84 mm
I_3 sin $\pm$ 68 mm	I_3 dex $\pm$ 84 mm

Coll. Dub. 2931 In this mandible, all incisors are broken off, which makes the cross section visible. I_2 and I_3 are subequal in size. Both I_3's have an 8-

shaped cross section. It is remarkable that the incisors are not symmetrical with regard to the symphysis; it is not positioned between the I_1's, but more to the left I_1.

Coll. Dub. 2932 — The incisors are broken off. It is strange that the right I_1 is positioned at the same height (dorsoventrally) as the left I_2. Perhaps this is due to the damage and restoration.

Coll. Dub. 4908 — The upper part of the symphysis is missing, the alveoli of the incisors are measurable deep into the jaw. The posterior end of the alveoli are lying closely together. The alveolus of the I_3 dex is positioned deeper (in posterior direction) than I_2 dex, the alveolus of I_1 dex lies more deeper still (in posterior direction).

Coll. Dub. 3147 — Only the alveoli are present, but not measurable, except part of the right I_3. Next to the right canine, a longitudinal section of an incisor can be seen. Above this section another longitudinal section of an incisor is present, which seems not to have reached the anterior edge of the jaw. More to the posterior is another alveolus, which lies more lingually than the other two. According to Hooijer (1950) these are the alveoli of respectively I_3, I_2 and I_1, to which I agree.

VII.2 UPPER INCISORS

The measurements are given in Appendix VI-6

Specimens without description:

Coll. Dub. without number (piece of premaxilla); Coll. Dub. 2182/2; Coll. Dub 2182/3; Coll. Dub. 2907/1; Coll. Dub. 2191b/1; Coll. Dub. 2902; Coll. Dub. 2908; Coll. Dub. 2909; Coll. Dub. 2911; Coll. Dub. 2914.

K 714 — The incisors in this right maxilla are bent both in dorsoventral and in linguobuccal direction.

K 716 (?) — In the middle of the wear facet a little dent is present, which gives the impression that the wear facet is somewhat hollow. There is also a dent on the lingual side.

Coll. Dub. 2076a — 1) this incisor with a wear facet has a length of $\pm$ 6 cm and is bent in dorsoventral direction.
2) isolated bent incisor, damaged and without a wear facet, so it is not clear if it is a left or a right one.

Coll. Dub.2182 — 1) The incisor and the alveolus of an incisor differ is size, one being definitely smaller than the other. They might therefore be an I^2 and an I^3. They have a cylindrical shape.

Coll. Dub.2189 — The incisor is probably a left I^2 (bent in dorsoventral direction), because it fits quite well on the left I_2 of Coll. Dub. 2910. On the lingual side a dent is present.

Coll. Dub.2907 — 2) It is not discernible if it is a right or a left one. According to the size, it might be a I^2.

VII.3 LOWER CANINES

The measurements are given in Appendix VI-7.

Specimens without description:

Without number (skeleton, Geological Museum Bandung); 22 G; no. 203; Coll. Dub. without no; Coll. Dub. 314?; Coll. Dub. 513; Coll. Dub. 1804; Coll. Dub. 1818; Coll. Dub. 2017/1; Coll. Dub. 2084d; Coll. Dub. 2174; Coll. Dub. 2190a/1; Coll. Dub. 2191b/2; Coll. Dub. 2314; Coll. Dub. 2903; Coll. Dub. 2904; Coll. Dub. 2910; Coll. Dub. 2915; Coll. Dub. 2916; Coll. Dub. 2917; Coll. Dub. 2918; Coll. Dub. 2922; Coll. Dub. 2924/1; Coll. Dub. 2924/3; Coll. Dub. 2929; Coll. Dub. 2931; Coll. Dub. 2934; Coll. Dub. 3147; Coll. Dub. 4606; Coll. Dub. 4908; Coll. Dub. 5527; Coll. Dub. 5803; Coll. Dub. 6491; Coll. Dub. 6954/1; Coll. Dub. 6954/2; Coll. Dub. 8243; Coll. Dub. 8473.

Description of the specimens:

no. 1746	The cross section of this canine is not really pear-shaped, but rather round.
without number (Tjipanaruban)	The separate left C is in a large block of conglomerate. As far as can be seen, the cross section is pear-shaped and no posterior groove can be seen. It is therefore likely that it is a lower canine.
SA 040979-30L	This canine is rather damaged on the lingual and posterior sides and partly covered with black matrix with gastropods. Due to the damage, it cannot be seen if there has been a groove on the buccal side. On the lingual side, there are no grooves. The striations are very coarse.
SA 040979-30M	A damaged and glued specimen. There is no groove on the lingual side. The striations are coarse.
SA 230779	Four separate pieces of a right canine, the largest of which shows a groove on the dorsobuccal side. On the lingual side no groove can be seen. The wear facet is absent; the anterior part is missing. The striations are not visible due to the damage.
SA 270378	Just behind the alveolus of the milk canine, a bit to the lingual side, is another alveolus with the tip of the permanent canine erupting.
Bumiayu exc. 8	The posterior side of this canine is covered with plaster. It is hard to see if there has been a groove on the buccal side, due to the plaster. On the lingual side there is a groove. The striations are fine. The wear facet on the posterior part is covered with plaster.
M 16	There is a piece of iron wire posteriorly of the wear facet; at the moment there is a part of the canine missing, that according to the figure of Van der Maarel (1932, plate V, Fig. 5) used to be there. On the lingual side there is no groove and striations are fine.
K 158	According to Von Koenigswald (1935, plate IV, Fig. 4) this is an "oberes Eckzahn", an upper canine. It might as well be a lower canine. A straight ridge can be seen in the matrix, which could be a wear facet. If this indeed is the wear facet, then it must be a lower canine; the curvature compared to the place of the wear facet does not fit an upper canine. The striations are fine and there are no grooves visible.
K 522	This canine probably belongs to a juvenile individual, according to

the measurements. There is a dent on the lingual side. There are no striations visible. Perhaps the striations are related to the age of the individual, and do coarse striations represent older animals than fine striations.

K 654 It has grooves both on the lingual and buccal sides.

K 710 1) The anterior part is damaged, so the wear facet is not distinguishable. There is no groove on the lingual side. Striations are coarser than those of M 16.

K 713 1) This specimen shows a peculiar wear facet. It is "roof-shaped" (Λ) with a anterior-posterior ridge in the middle and wear facets going down both at the lingual and buccal sides. Therefore, from the cross section it cannot be determined if it is a left or a right one; only from the curvature it can be determined as a right one. There are shallow grooves both on the lingual and buccal sides.
2) Very deep groove on the lingual side, the one on the buccal side is shallow.
3) There is no groove on the lingual side.
4) Part of a canine without a wear facet, therefore it cannot be determined as a left or a right one.

K 715 1) On the lingual side there is no groove. The striations are fine.

K 716 1) There is no groove on the lingual side, the groove on the buccal side is rather deep. The striations are coarse. The wear facet is damaged. This is a very big canine.

K 720 1) Of this canine, only the buccal side is present. According to what is left of the cross section and the curvature it must be a lower canine. On the inner side of the canine, there is a cavity that represents the root, so this is the posterior side. This makes it possible to determine it as a left one. The striations are fine.
2) The second piece is too small to say anything specific, except that it is a canine. The striations are coarse. It does not fit to 1). It could be the lingual side of a lower canine, because it is rather straight, but it cannot be excluded that it is an upper canine.

K 733 There is no wear facet on this piece of canine and no groove on the lingual side. It is not clear if there has been a groove on the buccal side, since the canine is broken. The striations are coarse.

K 1567 There is no groove on the lingual side. The striations are fine.

Coll. Dub. 98 The middle part of the canine is present and part of the outer crust, that covers the canine. This crust is included in the measurements

Coll. Dub. 99 The left alveolus does not show a groove on the dorsobuccal side, but this does not tell anything about the shape of the canine itself; several incisors have grooves that do not show in the alveolus.

Coll. Dub. 100 1) The cavity in the centre points to the place of the root, so this is the posterior end. From this it can be concluded that it is a left one.
2) It is not clear which side is anterior or posterior, so it cannot be

determined as a left or a right one. The dorsal side has broken off.
3) Again it is unclear which side is anterior or posterior, so it can be either a left one or a right one. There is a dent on the lingual side and also on the buccal side. On the buccal side the striations are very coarse, so coarse that they actually form small ridges.
4) The position of the anterior and posterior sides cannot be determined, so it might be a left or a right one. On the ventral side is a groove.

Coll. Dub. 308d — 1) The posterior side can be recognised by the cavity of the root. There is no wear facet present.

Coll. Dub. 2019a — A small part of the wear facet is visible. The lingual part is missing.

Coll. Dub. 2019b — It has a groove on the dorsobuccal side. The anterior part of the wear facet is missing and so is the buccal side.

Coll. Dub. 2076a — 3) The wear facet is damaged. There are no grooves visible.
4) The orientation of the anterior or posterior side cannot be determined, so it is unclear if it is a right or a left one.
5) Again it is indeterminable as a left or a right one. It looks rather rounded (due to rolling caused by water movement). There is a groove on the dorsobuccal side.

Coll. Dub. 2191b — 3) It is unclear what the anterior or posterior side is, so it cannot be determined as a left or a right one. Beside the groove on the dorsobuccal side, there is also a dent on the buccal side. On the lingual side there is also some sort of groove, made up by a ridge of coarse striations.

Coll. Dub. 2905 — The jaw is broken, so the posterior part of the alveolus of the left canine can be seen (not measured). The alveolus continues in posterior direction, ends behind the M_3 and becomes smaller in that direction.

Coll. Dub. 2906 — The alveolus of the canine continues below the molars and can be seen even behind the M_3. The alveolus could not be measured.

Coll. Dub. 2924 — 2) From this fragment it is not clear what the anterior or posterior side is, so it is also not clear if it is a left or a right one. The dorsal part is missing. On the lingual side there is a ridge consisting of a coarse striation.

Coll. Dub. 2932 — The left canine is visible, but difficult to measure due to sediment that is covering the canine. At the posterior end of the mandible the cross section is visible. The anterior part of the right canine is broken off.

VII.4 UPPER CANINES

The measurements are given in Appendix VI-8. Specimens without description:
No. 528?; without number(Geological Museum Bandung); Coll. Dub. 311/1; Coll. Dub. 311/2; Coll. Dub. 2019c; Coll. Dub. 2084c; Coll. Dub. 2190a/2; Coll. Dub. 2193 (not measurable); Coll. Dub. 2204a; Coll. Dub. 2926; Coll. Dub 4234; Coll. Dub. 4474; Coll. Dub. 6954/4.
Description of the specimens:

no. 341 — Asymmetrical cross section. Groove on the lingual side. It was not measured.

SA 040979-24	The canine is covered with black matrix with little gastropods on the lingual and part of the anterior side. Due to this matrix the cross section is not visible. The lingual side is broken off. The groove on the buccal side is rather shallow.
SA 040979-30D	1) The most anterior part is broken off, it shows cracks and is partly glued. The lingual side is partly covered with black matrix with little gastropods. On the anterior side a dent is present. The groove on the buccal side is shallow.
K 710	2) The groove on the buccal side is quite robust. The anterior and lingual sides are damaged.
K 715	2) On the buccal side there is no groove, the surface is rough instead. On the lingual side no groove is present.
K 716	2) There is no distinct groove on the buccal side, but the surface is rough. It is a bit damaged.
K 732	The canine extends on both sides of the maxilla fragment. It is moved a bit into the maxilla which can be seen by the wear facet which is more to the posterior than it should be. The buccal side shows no groove, but on the lingual side a little groove is present.
K 748	There is a distinct groove on the buccal side.
Coll. Dub. 285	Regarding the flatness of the fragments, these are probably lower canines. 2) This canine has a groove on the buccal side. 3) This one has a damaged wear facet, from which it can be concluded that is a right one. Remarkable is that the lingual curve of the posterior groove is quite sharp, instead of smooth.
Coll. Dub. 308c	This canine is asymmetrical.
Coll. Dub. 308d	2) This canine has an asymmetrical cross section without a wear facet. It cannot be seen which side is anterior or posterior, so it is unclear if it is a left or a right canine. The buccal side can be recognised by the asymmetrical cross section, in which the buccal side is larger than the lingual side, and the groove on the buccal side confirms this. 3) The cavity of the root indicates the posterior side. From this it can be concluded that it is a right one. The buccal side is damaged and the groove on this side cannot be distinguished. There is no wear facet.
Coll. Dub. 325f	1) It is unclear if it is a left or a right canine. On the dorsolingual side is a shallow groove.
Coll. Dub. 548	It has a symmetrical heart-shaped cross section.
Coll. Dub. 2000	1) a left canine with a damaged wear facet. There are grooves on the lingual side and on the ventrolingual side, on the buccal part of the posterior groove.

2) a right canine, practically identical with the foregoing specimen. The grooves are on the same places.

Coll. Dub. 2076 — 1) Half a canine. Regarding the roundness of the fragment, it could be the lingual part of an upper canine (lower canines are in general flatter). It is unclear if it is a left or a right canine.
2) The anterior side looks polished. If this indeed is the anterior side then it is a left canine. There is no wear facet. The surface is ribbed due to the presence of coarse striations. There is a little groove on the buccal side.
3) Very damaged canine, probably an upper one, regarding the roundness.

Coll. Dub. 2078 — 1) It has a damaged wear facet, a large groove on the buccal side, and a little dent at the anterolingual side.
2) It has a little dent at the anterior surface.

Coll. Dub. 2080b — The groove on the buccal side is quite robust. There is also a groove on the lingual side and a little dent at the anterior side.

Coll. Dub. 2190a — 2) The wear facet is very damaged. The buccal groove is quite robust.

Coll. Dub. 2191a — It has a rather symmetrical cross section.

Coll. Dub. 2196a — This canine is very straight.

Coll. Dub. 2902 — The canine is very asymmetrical.

Coll. Dub. 2907 — 1) It has a rather symmetrical cross section. It is not clear if there has been a groove on the buccal side, it looks as if there has not been one.

Coll. Dub. 2908 — There is no groove on the buccal side.

Coll. Dub. 2914 — The left canine has a robust groove on the buccal side, but the right one has no buccal groove. Apparently there can be quite some variation even in one individual. They are both very asymmetrical.

Coll. Dub. 2921 — 1) It has a rather symmetrical cross section.
There is a groove on the anterior side. It is not clear if there has been a groove on the buccal side.

Coll. Dub. 6490 — It has a wear facet. There is a little groove on the posterior part of the lingual side and a little dent on the anterior surface.

Coll. Dub. 6954 — 3) It has a wear facet. There is a shallow groove on the dorsolingual side.

VII.5 LOWER PREMOLARS

The measurements are given in the Appendix VI-9 – VI-12.

Specimens without description:
Without number (Museum Sangiran); without number from Ngandong (Geological Museum Bandung); Coll. Dub. 323c; Coll. Dub. 513; Coll. Dub. 2207b.

Description of the specimens:

without number (Medalem)

The left P_2 consists of the protoconid and the paraconid.

The right, unworn P_4 consists of the protoconid and the metaconid, which is attached to the protoconid. The anterior lobe is quite robust. From these premolars no measurements could be taken because they were exhibited in a showcase.

Without number (mounted skeleton)

The premolars are hard to describe, because they are in the mandible and difficult to reach.

The left P_3 has a wear facet on the posterior side. There is an anterior lobe, a posterior lobe and a cingulum on the lingual side. It is too worn to distinguish any other morphological features.

The right P_4 has an anterior lobe and a large posterior lobe. The wear facet is round-shaped in the middle of the premolar with an extension in anterolingual direction, suggesting that the metaconid is worn too. The wear facet touches the anterior lobe. It is strange that the posterior lobe reaches above the anterior side of the M_1.

22 G

In most lower premolars, the anterior side is short; the protoprecristid is steep. But in these premolars the protoconid is placed more to the posterior side. Actually, the P_2 resembles the DP_2 of SA 270378 (see Appendix VII.5). It cannot be a DP_2 because the molars are all present. The M_1 and the M_2 are worn, the M_3 is unworn. The premolars on the other hand are hardly worn. Besides, the P_4 does not resemble the DP_4 of SA 270378.

The left P_2 is damaged. It has a cingulum on the lingual side. The right, unworn P_2 has a large paraconid and an extra cusp on its lingual side. Buccally of the paraconid and touching it, is the paraconulid. The metaconid is situated on the posterolingual side of the protoconid. On the posterior side there are some small cusplets. The anterior lobe continues into a short cingulum on the buccal side. The anterior lobe embraces the paraconid. There is a low cingulum on the entire lingual side, which on the anterior side embraces the anterior lobe.

The left and right P_3 are also unworn. The anterior lobe is tiny. It continues into a cingulum on both the buccal and lingual sides. The paraconid is quite small. The metaconid is situated on the postero-lingual side of the protoconid. On the posterior side there are three cusps, the hypoconid, the entoconid and the hypoconulid. The protopostcristid is present.

The left and right P_4 are slightly worn. The paraconid is connected with the protoconid by the protoprecristid. The anterior lob continues into a cingulum on the lingual side. It ends in the cusplets on the posterior side. There is no cingulum on the buccal side. Going from P_2 to P_4, the metaconid seems to be located somewhat more to the middle of the premolar.

SA 040979-30D

2) Unworn, isolated right P_3. There is an anterior lobe that continues into a cingulum on the entire lingual side. It is connected with the posterior lobe. Also on the buccal side there is a cingulum connected with the anterior lobe. It ends just before the posterior lobe. In the middle of the premolar the cingulum is crenulated on the lingual side and knobby on the buccal side. The protoconid is unworn. The paraconid and paraconulid are not very prominent but they are present. The protoprecristid is knobby. The upper part of the protoprecristid shows a smooth surface, which might indicate the initial wear facet. The metaconid is present and quite large. The hypoconid, hypoconulid and entoconid are present. The protopostcristid and the protoendocristid cannot be distinguished. The metapostcristid is not crenulated. The metaendocristid is also not crenulated and ends at the entoconid.

3) Isolated, unworn right P_3. The anterior lobe is very robust. It continues both on the lingual and buccal sides into a short cingulum. The protoprecristid is smooth. The metaconid is quite robust. The top of the metaconid is slightly worn. There is no paraconid or paraconulid present. The posterior lobe continues into a short cingulum on the lingual side. In the posterior lobe a tiny cusp is present. The hypoconid is quite large. The entoconid is also present. Between the metaconid and the hypoconid another cusp is present. There is only one protocristid, probably the protoendocristid, which is only slightly crenulated and ends at the entoconid. The metapostcristid is smooth.

SA 270378

There is no sign of a $(D)P_1$.

The DP_2 has no anterior lobe, but on the anterior side four little cusps are present, among which are the paraconid and the paraconulid. The paraconid is situated higher than the other three anterior cusps. The protoconid is present as a sharp cusp. The protoprecristid is smooth. The protoendocristid is present and connects the protoconid with the entoconid. Also the hypoconid and hypoconulid are present. There are no anterior or posterior lobes, nor a metaconid.

At the position of the DP_3, two circular impressions are present, representing the position of the anterior and posterior roots.

The DP_4 is not yet fully erupted and the cusps are unworn. There is a tiny, crenulated anterior lobe. There are six main cusps, all of about the same height. It resembles a M_3. The protoconid is oval-shaped with an extension towards the metaconid and touching it. The metaconid is half-moon-shaped. The metaconid is larger than the protoconid. The anterior and posterior sides of the metaconid and the protoconid are at the same position. On the buccal side of the protoconid a small accessory circular cusp is present. The protopostcristid is situated more to the buccal side than the hypoprecristid. The hypoconid is half-moon-shaped. It embraces the entoconid, which is also half-moon-shaped but much smaller. The talonid is formed by the pentaconid on the buccal side and the hexaconid on the lingual side. The pentaconid is trilobate with extensions in anterior, posterior and buccal direction. It is much larger than the hexaconid, which is circular. This hexaconid is much larger than the hexaconids in both other DP_4's of K 525 (see next description). On the anterobuccal side of the pentaconid, there is an accessory cusp in the valley, the pentaconulid, touching the pentaconid. The pentaprecristid lies buccally from the hypopostcristid. All cusps are quite smooth except for the hexaconid, which is crenulated. The pentapostcristid is a ridge touching the octaconid of the knobby posterior lobe. The posterior lobe consists of three cusps, the larger octaconid in the middle, the heptaconid on its buccal side and the nonaconid on its lingual side. The nonaconid is the smallest of these three posterior cusps. There is no cingulum.

K 525 1) This left DP_4 is slightly worn, but the cusps of the talonid are unworn. The anterior lobe is a tiny ridge, which continues a bit on both sides. It continues further on the lingual side than at the buccal side. In the anterior lobe, three little cusplets are present. Both the protoconid and the metaconid are half-moon-shaped. The anterior side of the metaconid is situated more anteriorly than the anterior side of the protoconid and the metaconid touches the anterior lobe. The posterior side of the metaconid is situated more anteriorly than the posterior side of the protoconid. The metaconid and the protoconid are of about the same size. On the buccal side of the protoconid, a tiny buccal accessory cusp is present. The protopostcristid is situated more to the buccal side than the hypoprecristid. The hypoconid is trilobate and embraces the entoconid. The entoconid is also trilobate, but not as clear as the hypoconid. The hypoconid has a small extension in lingual direction. On the anterolingual side of the entoconid, two small, low-lying cusps are present. The talonid is formed by the pentaconid on the buccal side and the hexaconid on the lingual side. The pentaconid is elongate and half-moon-shaped, is much larger and embraces the hexaconid. Buccally of the hexaconid and touching it is another smaller cusp, the hexaconulid. The pentaprecristid lies just a little buccally from the hypopostcristid. In the buccal valley between the hypoconid and the pentaconid are two low-lying accessory cusps. The somewhat knobby hypopostcristid touches the octaconid of the knobby posterior lobe. The posterior lobe consists of two cusps with some smaller cusplets on the buccal side. The medial cusp (octaconid) is somewhat larger than the nonaconid. The posterior lobe continues on the lingual side as a cingulum until the anterior side of the hexaconid. The anterior root is broken off. The root on the posterior side is split in two, one on the buccal side, one on the lingual side; they are not fused. The space between the anterior root and the posterior root is V-shaped.

2) This left DP_4 is slightly worn, the cusps of the talonid are unworn. The anterior lobe continues on both sides until the posterior sides of the meta- and protoconid. There is one small cusplet present in the anterior lobe. The protoconid is half- moon-shaped. The metaconid is oval-shaped. The anterior side of the metaconid is situated more anteriorly than the anterior side of the protoconid. The posterior side of the metaconid is situated more anteriorly than the posterior side of the protoconid. The protoconid is larger than the metaconid. On the buccal side of the protoconid, an accessory buccal cusp is present. Both hypoconid and entoconid are trilobate. The protopostcristid is situated opposite the hypoprecristid. The hypoconid has an extension in lingual direction, which is more prominent than in 1). The hypoconid is a bit more robust than the entoconid. Both the anterior and the

posterior sides of the hypoconid are situated more to the anterior side than the anterior and posterior sides of the entoconid. So the hypoconid does not embrace the entoconid. The entoconid is a bit damaged on the anterior side and it cannot be seen if there was an accessory cusp as present in the other DP_4's. The talonid is formed by the pentaconid and the hexaconid. The buccal part of the premolar is damaged and the pentaconid is only partly preserved. The pentaconid is half- moon-shaped. It is much larger than the hexaconid and embraces it. Buccally of the hexaconid and touching it is the hexaconulid. The pentaprecristid lies just a bit more to the buccal side than the hypopostcristid. There is an accessory lingual cusp in the valley between the entoconid and the hexaconid. The knobby pentapostcristid touches the octaconid of the knobby posterior lobe. The posterior lobe consists of two cusps (the rest is broken off). The octaconid (medial) is larger than the nonaconid on the lingual side. The posterior lobe continues on the lingual side as a cingulum until the middle of the hexaconid. There is one anterior root. The posterior root is broken off, but it can be seen that there is only one posterior root. The space between the anterior root and the posterior root is U-shaped and the distance between them is smaller than in the previous DP_4.

K 6.. The P_3 is very worn. The anterior lobe is present. The wear facet is on the posterior side. It is more hollow towards the centre of the premolar. No cusps or cristids can be distinguished, due to wear. The posterior part is broken off.

K 653 1) This P_2 has two roots, which bend in posterior direction. Both the anterior and the posterior root show at the tip a suture, indicating that it is the result of the fusing of two anterior and two posterior roots. The anterior part is damaged, and therefore the anterior lobe is not visible. On the anterior side is a small crenulated ridge, which runs from the lingual side of the protoconid downwards to the buccal side. There is one cusp, the protoconid. The, slightly hollow wear facet is on the posterior side. The protopost- and protoendocristid as well as the hypoconid cannot be distinguished due to wear. The posterior lobe is present. There are no additional cusps or ridges. There are also no cingula.

2) This P_3 (probably) is very worn. There is an anterior lobe, which continues into a cingulum on the entire lingual side. The wear facet is mainly on the posterior side, but is continuous to the anterior side. On the posterior side is a hollow, which is deeper on the lingual side than on the buccal side. Due to wear, no additional cusps or ridges can be recognised. There are two roots, the posterior root being larger than the anterior one. It shows no sign of any posterior platform. The posterior lobe is present, but it is damaged.

3) The anterior lobe of this P_3 is crenulated and tiny. It continues on the lingual side into a crenulated cingulum until halfway the lingual side. The anterior side of the protoconid has a smooth surface. The wear facet is both on the anterior and on the posterior side, but it is somewhat larger on the posterior side. The buccal side is smooth; there is no cingulum and no cusplets. The posterior lobe is crenulated on the posterolingual side. It is a simple premolar with no additional

cusps or ridges. The posterior root is slightly larger than the anterior root.

4) This slightly worn P_3 has no anterior lobe. There is just a little cusplet on the anterior side. The wear facet is mainly on the posterior side. On the posterior side is a smooth surface. The protopost- and protoendocristid are hardly developed; some small cusplets are present at the position, where these ridges are supposed to be. There is no cingulum, nor on the buccal side, nor on the lingual side. There is no posterior lobe.

K 675 1) Because of the smallness (in lingual-buccal direction) of this premolar, it might be an isolated right P_1. There is one root with sutures indicating that it is the result of the fusing of more than one root. The orientation of the premolar is somewhat difficult. If the root bends in posterior direction (like all other roots), than the wear facet is on the posterior side. On the anterior side, there is no anterior lobe but some ridges, which resemble the protopost- and the protoendocristid, but these ridges are on the anterior side instead of on the posterior side. Downward, the cristid on the anterolingual side divides into various little cristids. There is one main cusp, the protoconid. There is no posterior lobe. There are no cingula.

2) This P_4 has an anterior lobe, which continues into a cingulum, both on the lingual and buccal sides. It is vaguely present on the entire buccal side, and on the anterior and posterior part of the lingual side. There is a paraconid, which is part of the knobby protoprecristid. The wear facet is on the posterior side. There are two roots, the posterior root being larger than the anterior root. They bend in posterior direction. There is a posterior lobe. The posterior surface shows a smooth surface. There is no sign of the protopost- or protoendocristid.

3) The anterior lobe of this P_4 is only visible on the anterolingual side. It continues into a cingulum on the anterior part of the lingual side. The paraconid is part of the knobby protoprecristid. The wear facet is on the posterior side. Due to wear, there are no cusps or cristids visible on the posterior side. There is a posterior lobe. The buccal side is smooth. On the posterior part of the buccal side, a cingulum is present. There are two roots, which bend in posterior direction. The posterior root is larger than the anterior root.

K 685 This P_3 is unworn. The anterior lobe is quite robust and continues into a cingulum on the entire lingual side. This cingulum is undulating and crenulated. The posterior lobe is also crenulated. Also on the buccal side there is a crenulated cingulum, but in the middle of the premolar it is very vague. The protoprecristid is very crenulated. The metaconid is present, but it is not very prominent. The paraconid and the paraconulid are not present. On the posterior side are three cusps: the hypoconid, the entoconid and the hypoconulid. The protopostcristid is crenulated and it is connected with the hypoconid. The protoendocristid is also very crenulated and it is connected with the entoconid. The entoconid is a bit worn. On the buccal side two grooves can be seen. There are no roots preserved.

K 689 The anterior lobe of this slightly worn P_2 is crenulated and continues on the lingual side into a cingulum. Also on the buccal side is a cingulum. There is no paraconid and no paraconulid. The protoconid is just a bit worn. The metaconid is present. The protoprecristid is quite knobby. There is no hypoconid, hypoconulid or entoconid. The protopost- and protoendocristid are not clear. There is no posterior lobe but there is a smooth surface on the posterior side, which might indicate the beginning presence of a wear facet. There are two roots. The anterior root is oval-shaped, the posterior root is circular and smaller.

K 693 The protoconid of this P_2 is damaged. It is a simple premolar, without anterior or posterior lobes, the lingual and buccal sides are smooth. There are neither additional cusps nor cingula. On the posterior side, the protoendocristid can be distinguished, but it is also slightly damaged. There are no roots preserved.

K 698 Only the small protoconid of this slightly worn P_3 has a tiny wear facet on the anterior side. The anterior lobe is tiny on the lingual and buccal sides and thickens towards the middle. The paraconid and the paraconulid are flat, not well developed cusps. The protoprecristid consists of a smooth surface, which might indicate a beginning wear facet. The anterior lobe continues into a short cingulum on the buccal side and into an even shorter cingulum on the lingual side. The metaconid is present and so is the hypoconid. The hypoconulid and the entoconid are not present. The protopostcristid and the protoendocristid are not developed. The slightly crenulated metaendocristid is connected with the hypoconid. On the buccal side some minor cusplets are present. The posterior lobe is small and a bit knobby. There are two roots, both broken off.

K 699 This unworn P_3 has an anterior lobe, but no paraconid or paraconulid. The protoprecristid is very crenulated. The metaconid is present. On the posterior side, the hypoconid and entoconid are present. The hypoconulid is not present. The protopostcristid is very crenulated. The protoendocristid is not crenulated. They both end halfway the premolar. The metapostcristid is crenulated and ends at the entoconid. The metaendocristid is also very crenulated. Posterior of the entoconid and the hypoconid, two very small cusplets are present. The posterior lobe continues on the lingual side in a cingulum, which ends just behind the entoconid. From the posterior lobe goes a cingulum to the buccal side, but there is a ticket glued on the buccal side, so it cannot be seen if the cingulum continues on the buccal side. There is a groove on the buccal side, from the protoconid going downwards. There are two roots, the anterior one has an oval-shaped cross section. The posterior root is smaller.

Coll. Dub. without number The P_4 has two circular roots.

Coll. Dub. 87 The crenulated anterior lobe of this P_2 is missing on the anterobuccal side. The protoconid bends in lingual direction. The protoprecristid runs from the protoconid to the paraconid. There is no paraconulid. From the anterior lobe, a short cingulum goes in lingual direction. The posterior lobe is connected with a cingulum on the buccal side, which continues until halfway the buccal side. The posterior lobe is thin on the posterobuccal side and thickens rapidly in posterolingual direction. The wear facet is on the posterior side, fusing the protoconid with the hypoconid. Therefore the protopostcristid, the protoendocristid, the hypoconid, the hypoconulid and the entoconid are not visible. There is no metaconid.

Coll. Dub. 99

Between the canine and the P_2, there is a rugosity, which indicates the position of the (D)P_1. The root of the left P_2 is 8-shaped. The anterior side of the P_2 is positioned more to the buccal side than the posterior side. Of the left P_3, only the anterior part is preserved, but it is not measurable.

The left P_{2-3} and the right P_3 all have two roots; an anterior root and a posterior root.

The right P_4 is slightly worn. The protoconid has a small wear facet on the anterior side. The protoprecristid is smooth. Attached to the protoconid is the metaconid. Also the hypoconid and the paraconid are present. The anterior and posterior lobes are present. The paraconulid, the hypoconulid and the entoconid are not present. On the lingual side is a very vague cingulum from the posterior lobe to the anterior lobe. There is no cingulum on the buccal side. The protoendocristid is not crenulated, the protopostcristid is very vague.

Coll. Dub. 105

This P_4 is quite worn, both in anterior and posterior direction. The protoconid is fused with the metaconid and the hypoconid. The paraconid, the paraconulid, the protoprecristid, the hypoconulid and the entoconid are not distinguishable due to wear. There is an anterior lobe, with has a smooth surface indicating the presence of another premolar (P_3). There is a cingulum both on the lingual and on the buccal side. There is a posterior lobe. Between the posterior side of the wear facet and the posterior lobe is a groove (fossid). As it is on the lingual side, it might be called metafossid. The protopostcristid and the protoendocristid can be distinguished. The buccal side is quite smooth. There are no signs of posterior cusps or ridges.

Coll. Dub. 272b

The protoconid of this worn P_3 is fused with the metaconid due to wear. The wear facet continues downwards until the anterior lobe and towards the lingual side. Therefore the paraconid, the paraconulid and the protoprecristid cannot be distinguished due to wear. The top of the protoconid is broken off. On the lingual side, a cingulum is present, which continues in a short posterior lobe. The cingulum on the buccal side is more vague than on the lingual side. Posterior of the protoconid, there are two accessory cusps on the buccal side, the hypoconid and the hypoconulid. On the posterolingual side the entoconid is present and worn. The protopost- and protoendocristid are worn and not distinguishable.

Coll. Dub. 285

4) The anterior lobe of this P_3 continues into a crenulated cingulum on the anterolingual side. The cingulum continues, but not crenulated and it is connected with the posterior lobe. On the buccal side, the anterior lobe is connected with a cingulum until halfway the buccal side. Here the premolar is damaged, but the cingulum does not seem to continue posterior of the damaged part. The protoconid is worn in

posterior direction. The paraconid and the paraconulid are present. The metaconid might be worn, but it is not clear. The hypoconid is not yet worn. There is no hypoconulid or entoconid. The protopostcristid and the protoendocristid are crenulated. On the anterior side two crenulated ridges run from the protoconid; the protoprecristid and the paraendocristid. The paraconid is not clear; it might be one of the cusps, which form these ridges.

Coll. Dub. 324a — In this P_2, the main cusp, the protoconid is worn and damaged, both on the buccal and lingual sides. The anterior lobe cannot be distinguished due to wear, and so are the metaconid, the paraconid, the paraconulid, the protoprecristid, the hypoconid, the hypoconulid, the entoconid, the protopostcristid and the protoendocristid. The wear facet is mainly on the posterior side. The buccal side is totally damaged. There is a posterior lobe and a cingulum on the lingual side.

Coll. Dub. 425a — 1) Only the posterior part of this P_3 is present. There is a crenulated posterior lobe. There are four crenulated ridges, the protopostcristid, the protoendocristid, the metaendocristid and the metapostcristid. The metaconid is present. As far as can be seen, there is no cingulum. It looks very much like Coll. Dub. 2000/3 and Coll. Dub. 6954/6.

Coll. Dub. 1483 — The protoconid of this rather damaged P_2 is worn and probably fused with the metaconid, which explains the wear facet on the lingual side. The wear facet is also visible on the posterior side. There is an anterior lobe. The buccal side is damaged and it is therefore not clear if the cingulum continues on the buccal side. On the lingual side there is a cingulum. The paraconid and the paraconulid are present. The protoprecristid is knobby. The hypoconid, the hypoconulid and the entoconid are not distinguishable, but there are some smaller cusps present on the posterior side, which might represent these cusps. There is no posterior lobe. The protopostcristid and the protoendocristid are crenulated.

Coll. Dub. 1718 — The anterior lobe of this quite worn P_4 is quite robust and it is not straight, but meandering and with differences in thickness; on the lingual side it is thicker than on the buccal side. The anterior lobe continues into a cingulum on the entire buccal and lingual sides until the posterior lobe. The wear facet is quite hollow and runs from the anterolingual side to the buccal side and then further to the posterior side. The metaconid, the paraconid, the paraconulid, the protoprecristid, the protopostcristid and the protoendocristid cannot be distinguished due to wear. Behind the wear facet, the posterior part is covered with a lot of flat cusplets, among which are probably the hypoconid, the hypoconulid and the entoconid. The P_4 has two roots, the posterior one being larger than the anterior one. The anterior root is implanted in the jaw in anterior direction, but in the jaw it turns into posterior direction, which can be seen because the mandible is damaged.

Coll. Dub. 1804 — The P_4 has two circular roots, forming an 8. It is positioned obliquely with regard to the axis of the jaw; the anterior side is placed more to the lingual side than the posterior side.

Coll. Dub. 1818	The small alveolus of the P_2 shows that it had one root. The P_4 has two circular roots, forming an 8. It is positioned obliquely with regard to the axis of the jaw; the anterior side is placed more to the lingual side than the posterior side.
Coll. Dub. 2000	3) This P_3 is slightly worn, but the wear facet is quite straight and not on the anterior or posterior side. There are three main cusps, the protoconid, the metaconid and the hypoconid. The paraconid, the paraconulid, the hypoconulid and the entoconid are not present. The anterior lobe is a bit crenulated but not very much. On the protoprecristid are some little conulids. The protopostcristid and the protoendocristid are crenulated. The protoendocristid ends at the hypoconid. Between the protoconid and the metaconid is a short crenulated ridge. Also from the metaconid two crenulated ridges start; the metapostcristid goes in posterior direction and the metaendocristid goes to the lingual side. The anterior and posterior lobes are present. There is no cingulum.
Coll. Dub. 2003b	1) This P_3 is damaged; the anterior part is broken. The protoconid is worn and is probably fused with the metaconid, which is represented by a thickening on the side of the protoconid. There is a paraconid present and an anterior lobe, but no paraconulid and no protoprecristid. Posterior of the protoconid are four cusps with a hollow in the middle of these cusps. It is difficult to tell which cusps are represented here. Posterior of these cusps is the posterior lobe, which continues into a crenulated cingulum on the lingual side. The cingulum ends in the middle of the lingual side. The protopostcristid is present, the protoendocristid is not. 2) This P_3 is also damaged. The protoconid is worn with a wear facet on the anterior side (protoprecristid is smooth). Below this wear facet is a smooth area. There is no anterior lobe. The paraconid is present, the paraconulid is not. There is also no metaconid, but this part of the premolar is damaged. There is a cingulum on the anterior part of the lingual side. The buccal side is damaged, so it cannot be seen if there was a cingulum on the buccal side. On the posterior side are a lot of posterior cusps. The protopostcristid is made up of five cusps, among which are the hypoconid, the hypoconulid and the entoconid. Below these cusps are three more cusps. There is no posterior lobe, but these three low-lying cusps are at the position of the posterior lobe. The protoendocristid is made up of four cusps. Normally these cristids are crenulated, but in this specimen the crenulation is very coarse.
Coll. Dub. 2174	The P_4 is positioned obliquely with regard to the axis of the jaw; the anterior side is positioned more to the buccal side than the posterior part.
Coll. Dub. 2318c	1) The anterior lobe of this P_3 is connected with the cingulum, which is present on the entire lingual and buccal sides. The wear facet dips in anterior direction. The paraconid, the paraconulid and the protoprecristid are not distinguishable due to wear. The protoconid is fused with the metaconid. On the posterobuccal side several cusps are present; the hypoconid, the entoconid, the hypopreconulid and the entopostconulid. Behind these cusps is the posterior lobe. There is no protopostcristid or protoendocristid.

2) It is probably a P_4 because it is larger than the P_3 described above. It is very worn. Due to wear, the protoconid, the metaconid, the hypoconid and the entoconid are fused. It is half-moon-shaped with finger like protrusions in posterior direction. The wear facet goes downwards in posterolingual direction. The anterior lobe has the same height as the wear facet, it descends in lingual direction and continues as a cingulum on the entire lingual side. There is no cingulum on the buccal side. There is a posterior lobe. The rest of the cusps and ridges are not distinguishable due to wear.

3) This P_2 has two roots, the posterior root being larger than the anterior root. The protoconid is slightly worn in posterior direction. The anterior lobe is present and it continues into a cingulum on the lingual side until halfway the lingual side. There is no cingulum on the buccal side. The buccal side is smooth. The hypoconid and hypoconulid are present and so are the protopostcristid and the protoendocristid. The entoconid is not present. On the anterior side the paraconid is present and there are some small additional cusps above the paraconid, among which is probably the paraconulid. There is no protoprecristid, no posterior lobe and no metaconid.

4) This unworn P_2 has an anterior lobe which is quite knobby and which is thicker on the lingual side. It continues on the lingual side into a cingulum, which seems to continue, but it is very vague halfway the lingual side. There is a small cusp in the middle of the cingulum. The anterior lobe also continues into a vague cingulum on the buccal side. The anterior part of this cingulum is crenulated. The protoconid is unworn and bends slightly in lingual direction. There is no paraconid or paraconulid. Also the metaconid is missing. The protoprecristid is smooth. The hypoconid and the entoconid are present, as are the protopostcristid (crenulated) and the protoendocristid. The hypoconulid is not present. The surface between these two cristids is smooth, which might indicate that the wear facet is going to be on the posterior side. There is a posterior lobe.

Coll. Dub. 2904 — In front of the alveolus of the P_2, the dorsal part of the mandible is missing, and there is a hole, which might indicate the alveolus of the P_1. It has a diameter of 10.0 mm. The P_3 is positioned obliquely compared to the axis of the jaw; the anterior part is positioned more to the lingual side than the posterior side.

Coll. Dub. 2915 — The alveolus of P_2 is two-rooted.

Coll. Dub. 2916 — The anterior side of both P_2's is positioned more to the buccal side than the posterior side. The anterior part of both P_4's is positioned more to the lingual side than the posterior side.

Coll. Dub. 2917 — The protoconid of this unworn P_4 is located on the anterior side. The protopostcristid and the protoendocristid are knobby and end at the hypoconid. There is no metaconid, no hypoconulid and no entoconid. There is a posterior lobe, which continues into a cingulum on the buccal side. It is not visible if it is present on the entire buccal side, because part of this side is covered by sediment. Also the anterior lobe continues into a cingulum, which is present on the buccal side and on the lingual side towards the protoendocristid. On the anterior side the premolar is broken, so the paraconulid and the protoprecristid are not there. There is no paraconid.

Coll. Dub. 2918 — The alveoli of the P_2's show that they have one root. The anterior and the posterior roots of the P_3 are oval-shaped. Of both P_4's, only the anterior root can be seen. It consists of two roots fused together, with an indentation on the posterior side.

Coll. Dub. 2922 — The unworn P_4 has a protoconid, a paraconid and a hypoconid. The metaconid is not present, nor are the paraconulid, the hypoconulid and the entoconid. From the protoconid, the protopostcristid and the protoendocristid (both knobby) go downwards towards the hypoconid. There is an anterior lobe. The protoprecristid ends in the paraconid, just above the anterior lobe. The upper edge of the anterior lobe is knobby. Posterior of the hypoconid is the posterior lobe, which continues on the lingual side in a low, crenulated cingulum, which continues until just past the hypoconid. There is no cingulum on the buccal side.

Coll. Dub. 2929 — In front of the P_2 there is a rugosity in the jaw, which indicates the position of the (D)P_1.

Coll. Dub. 3147 — The roots of the P_2 and P_3 consists of two circular roots, forming an 8. In front of the P_2 is a rugosity in the jaw, which indicates the position of the (D)P_1.

Coll. Dub. 4908 — The alveolus of the P_2 is 8-shaped. The anterior side of the P_2 is positioned more to the lingual side than the posterior side.

Coll. Dub. 6954 — 5) The anterior lobe of this P_4 continues on the buccal side into a crenulated cingulum. Also on the lingual side, part of the cingulum is present. The anterior part of the premolar is broken off. The wear facet goes in anterolingual direction; the protoconid and the hypoconid are fused. The hypoconulid and the entoconid cannot be distinguished, nor can the protopostcristid and the protoendocristid, due to wear. Lingually of this worn cusp, is a worn metaconid. There is a posterior lobe.

6) This unworn P_3 has an anterior lobe, which is a bit crenulated. On the protoprecristid are two cusps, the paraconid and paraconulid. The rest of this ridge is smooth. Lingually of these two cusps is another cusp, probably the metaconid. The protopostcristid and the protoendocristid are crenulated and are divided into other crenulated cristids. There is a posterior lobe and on all sides a cingulum is present, although vaguely in the middle of the buccal and lingual sides. All three posterior cusps are present; the hypoconid, the hypoconulid and the entoconid.

Coll. Dub. 11092 — 1) This P_2 has one big cusp, the protoconid. On the anterior side, a couple of little cusps are present, but there is no anterior lobe. Among the little cusps is probably the paraconid. The protoprecristid is not developed. On the posterior part of the lingual side is a cingulum, but it does not continue. There is only one cristid on the posterior side, therefore it is not clear if it is the protopost- or the protoendocristid. It is knobby and ends in a crenulated posterior lobe. There is no cingulum on the buccal side. The hypoconid and the entoconid cannot be distinguished. The P_2 has four roots, the two anterior ones fused into one and the two posterior ones fused into one.

2) The wear facet of this quite worn P_2 is pretty straight. On the anterior side is a knobby protoprecristid present. The paraconid might be one of these knobs on the protoprecristid. There is no anterior lobe. There is a cingulum, both on the posterior parts of the lingual and buccal side. The protoendo- and the protopostcristid are very knobby and they continue into the cingula on the lingual and buccal sides. The hypoconid and the entoconid cannot be distinguished. Between the protopost- and the protoendocristid is another small crenulated ridge present. There is no metaconid. It has one anterior root and one posterior root (both fused from two roots). The posterior root is more robust than the anterior one.

JA 67 The top of the protoconid is slightly worn. The rest of this P_3 is unworn. The anterior lobe is crenulated and continues on the lingual side into an undulating crenulated cingulum. It continues until the posterior lobe. On the buccal side the cingulum is only present on the anterior side until under the top of the protoconid. The rest of the buccal side is smooth. The paraconid and the paraconulid are quite prominent. The protoprecristid is smooth and short. The metaconid is quite large. Below the metaconid is another cusp: the metaconulid. The, not crenulated, protoendocristid ends at the metaconid. The protopostcristid is also not crenulated and ends at the posterior cusps, the hypoconid, the entoconid and the hypoconulid. The roots are broken off, but the anterior root is of about the same diameter as the posterior root.

VII.6 UPPER PREMOLARS

The measurements are given in the Appendix VI-13 – VI-17.
Specimens without description:
Coll. Dub. 2023/1; Coll. Dub. 2919; Coll. Dub. 2920.

Description of the specimens:

Coll. Dub. without number This tiny molar is probably a right ^{DP4}. It resembles a M^1, but it is too small to be a M^1. The morphology is very molariform. The para- and protocone are fused due to wear and so are the meta- and tetracone. The anterior lobe is touching the protocone. The anterior lobe continues in lingual direction until the foot of the protocone. The parapoststyle lies somewhat more lingually than the metaprestyle. The protopoststyle lies opposite the tetraprestyle. On the buccal side, a tiny cingulum is visible.

Coll. Dub. 94 This P^3 is a bit worn and has a wear facet on the anterior side of the paracone. The whole anterior surface is smooth, except for the anterolingual side. Here are three little cusplets. There is an anterior lobe. The parapostcrista and the paraendocrista are very crenulated. The parapostcrista divides into other crenulated ridges. The posterolingual platform is covered by vague crenulated ridges. There is a crenulated cingulum on the lingual side and probably also on the buccal side, but this side it is damaged. On the anterobuccal side there is also a small crenulated ridge. The posterior lobe is small.

Coll. Dub. 96 The P^2 is slightly worn and has a paracone with a wear facet on the anterior side. Attached to the paracone, the primocone is present. On the buccal side are two cusps present, one on the anterior side (which has no name) and one on the posterior side (metacone). These cusps are much lower than the main cusp. The anterior lobe is very knobby and does not extend into a cingulum. The buccal side is quite smooth, apart from the anterior lobe and the extra cusps. On the lingual side, the premolar broadens in lingual direction, posterior of the anterior lobe. This broader part is covered with little cusplets. The posterior lobe is also knobby. From the paracone, a knobby parapostcrista goes downwards until the posterior platform.

The P^3 is much lower than the P^2. It is hardly worn. It has a paracone, with a little wear facet on the anterior side. The paracone does not bend inwards, as the paracone of the P^2. There is a low-lying primocone. Buccally from the primocone is a group of tiny cusplets. The anterior lobe is crenulated and continues in a vague cingulum on the buccal side. Here it is not crenulated. It also continues into a very crenulated cingulum on the entire lingual side. The parapostcrista is very knobby and ends in the metacone. The paraendocrista is also very knobby and ends in a small posterior platform. There is no posterior lobe. On the posterior edge, the premolar is indented, which indicates the position of the DP^4.

Coll. Dub. 313 1) The only clear cusp of this unworn P^3 is the paracone. The paraprecrista goes downwards until the anterior lobe. On the paraprecrista are tiny conules present, among which is probably the primocone. The anterior lobe is crenulated and continues into a crenulated cingulum on the lingual side until halfway the premolar. On the buccal side there is no cingulum. The parapostcrista is very crenulated and bears tiny conules. It continues into the posterior lobe. The paraendocrista is also very crenulated. It ends at the edge of the posterolingual platform. Lingually of the paraendocrista is another crenulated ridge, which also ends at the platform. The posterior lobe has a little facet, which indicates the position of the P^4. It has four roots, fused into two, an anterior and a posterior one. The posterior roots are more robust than the anterior roots.

2) The paracone of this slightly worn P^3 shows a tiny wear facet, but it is rather straight and unworn on the anterior or posterior side. On the paraprecrista, which ends at the anterior lobe, is a primocone present. Lingually from the primocone and a bit lower is another cusp. Lingually from these accessory cusplets is a tiny crenulated ridge, which starts halfway the paracone. The anterior lobe is also crenulated and continues in a crenulated cingulum on the lingual side. On the buccal side there is no cingulum. There is a metacone present. There is a platform in the posterolingual corner. The crista that goes downwards from the paracone divides into the parapostcrista, the lower half of which is crenulated, and the paraendocrista, which is not crenulated. The paraendocrista is very short. Lower than the paraendocrista and clearly separated from it, is another ridge, which is crenulated. This ridge lies lingually from the parapostcrista. The posterior lobe is crenulated.

Coll. Dub. 325d — 1) The posterior side of this P^4 is flattened, due to the presence of the M^1; the anterior side is rounded. There is only one cusp, the paracone, which is +-shaped. The paracone is both connected with the anterior and posterior lobes, which continue on the lingual side into a cingulum. On the anterior and posterior side it is connected with the cingulum that is present on all sides except on the buccal side. There is a groove on the lingual side of the paracone.

Coll. Dub. 325f — 2) The cusp of this P^4 is worn and extends in lingual-buccal direction and broadens in buccal direction. It is possible that more cusps were present, but they cannot be recognised due to wear. There are two grooves; the one on the posterior side (parapostfossa) is deeper than the one on the anterior side (paraprefossa). The posterior side is flattened, due to the presence of the M^1; the anterior side is rounded.

Coll. Dub. 425a — 2) Robust P^1, with one root, which bends in posterior direction. The paracone bends in lingual direction. It is quite worn. The wear facet is larger on the anterior side. The posterior lobe goes downwards, both in buccal and lingual direction and continues as a cingulum on the lingual side until about half way the lingual side.

3) The anterior root is complete (length 39.5 mm) and it is more robust than the posterior root. Remnants of the anterior and posterior lobes are present. On the lingual side a crenulated cingulum is present. The buccal side is completely worn and damaged. The lingual side is unworn. On the posterolingual side there seems to be the remnants of the posterolingual platform.

Coll. Dub. 1702 — In front of the left P^2 is the alveolus of the DP^1.
Both left and right P^2's are present. They are only slightly worn; there is a tiny wear facet on the anterior side. It exists of one large cusp, the paracone, which bends inwards, to the lingual side. There is an anterior lobe. On the anterior side a couple of cusps are present, among which is the primocone. On the posterior side of the paracone, a small, rather smooth area is present, which is probably caused by the presence of the opposite lower premolar and which indicates the future wear facet. The crenulated parapostcrista (on the buccal side of this smooth area) runs downwards and to the lingual side, where it meets the crenulated paraendocrista. On the posterolingual side is a knobby platform, which forms a part of the crenulated cingulum, which surrounds the whole premolar. There is a posterior lobe present. The anterobuccal side is covered with cusplets.

The left P^3 is missing, but its position can be distinguished, but not measured. The right P^3 is present. This specimen is very damaged and a lot of it is glued. To me it seems that this premolar is glued in the wrong way. In all specimens the P^3 is obliquely with regard to the axis of the maxilla, with the anterior part positioned more to the buccal side than the posterior part. In this specimen is it exactly the other way: the anterior part is situated more to the lingual side. In order to be able to fit it to the maxilla, they had to glue it this way in order to get some hold for the glue. It exists of a large cone, the paracone, which is highest on the anterior side. It is covered with little crenules. The lingual side is much lower. There is a crenulated cingulum, which surrounds the entire premolar. It is not very worn.

The right DP^4 is very worn. It is damaged on the anterolingual side. There is an enfolding of the enamel on the buccal side. Hooijer (1950, p. 81) claims that he sees the extension of the cusps in anterior and posterior direction opposite each other: "it is interesting to see, that this milk element, too, shows the *palaeindicus* type of structure". This is visible, but I think it is a quite farfetched conclusion, because it is worn to such a degree that hardly any morphological features can be distinguished.

Coll. Dub. 2003b

3) The paracone of this P^3 is slightly worn, but the wear facet is straight and does not bend in anterior or posterior direction. It is a very complex premolar, with a lot of conules and crenulated ridges. The not crenulated paraprecrista ends in a bundle of tiny cusplets, among which is the primocone. Between this ridge and the buccal side of the premolar is also a group of cusplets. The anterior lobe is crenulated. On the whole buccal side is a crenulated ridge, which is not connected with the anterior or posterior lobes. Besides the parapostcrista and the paraendocrista (both crenulated), there are four other ridges going downwards. One of these ridges ends at the metacone. The posterolingual platform is covered by cusplets. Posterior of this platform is the posterior lobe present. There is a crenulated cingulum on the entire lingual side. On the buccal side there is a cingulum starting at the anterior and posterior lobes, but not continuing to the middle of the buccal side.

Coll. Dub. 2023

2) Fragment of probably a left P^3. It is broken but some features are visible. The lingual side has a robust cingulum. On the buccal side there is no cingulum. The premolar bends downwards in posterolingual direction and in this corner a lot of cusplets are present.

Coll. Dub. 2023?

1) In this P^4, the anterior lobe, the lingual and buccal cingula and the posterior lobe form one ring. The paracone has a +-shaped wear facet, but the extension in lingual direction is very small. In buccal direction the wear facet touches the buccal side and thereby forming two very small groove; one on the anterobuccal side, the other one on the posterobuccal side. A large lingual groove is present. The wear facet touches the anterior lobe and is connected with the posterior lobe.

2) This P^1 has one root, which bends in posterior direction. The paracone bends in lingual direction. The wear facet is on the anterior side. There is a cingulum on the entire lingual side. The lingual side is covered with flat cusplets and crenulated ridges. There is an anterior lobe. The buccal side is smooth; there are no cusplets or ridges on this side. Both the anterior and posterior lobes are present.

3) The root of this P^1 is not visible. The wear facet is on the anterior side. The paracone bends in lingual direction. The posterolingual side is covered with crenulated ridges and flat cusplets. The anterolingual side is smooth. There is a cingulum on the lingual side, but it is very vague in the middle of the lingual side and it is not sure if it continues. The buccal side is smooth and has no cingulum. The anterior and posterior lobes are present.

Coll. Dub. 2076	4) Root of a P^1, the P^1 itself is broken off. It consists of two roots fused to one; the line separating the roots is still visible.
	5) As there is a cingulum on one side of this P^4, this is most likely the lingual side. It is too damaged to measure. The cingulum is connected with the posterior lobe and the anterior lobe as far as can be seen. The part of the anterior lobe, which is visible, is crenulated.
Coll. Dub. 2079	These left and right P^4's are rather worn. The proto- and tetracone (on the lingual side) are fused and have a half-moon-shaped form. On the buccal side, the para- and metacone are fused in a more omega-shape. On the lingual side a cingulum is present. The area between the proto- and tetracone on one side, and the para- and metacone on the other side forms a hollow (central fossa). There are no anterior or posterior lobes.
Coll. Dub. 2182	These are probably P^{1-2}, because they are too small to be P^{2-3}. The P^1 is two-rooted; most P^1's have one root, but two-rooted P^1's also occur (see also Coll. Dub. 2921).
Coll. Dub. 2188	The left P^2 is damaged; part of the paracone is broken off. The buccal side is rather smooth. The anterior lobe is knobby. The parapostcrista is knobby and goes downwards towards the lingual side. The paracone bends towards the lingual side. There is a primocone present. The lingual side is much less knobby than the P^2's from Coll. Dub. 1702. A knobby cingulum surrounds the premolar, except on the buccal side. There is no posterior platform like described in Coll. Dub. 1702, although the posterior side is somewhat broadened compared to the anterior part. Neither is there a smooth area on the posterior side of the paracone, as described in Coll. Dub. 1702. The posterior lobe is crenulated. It has two roots.
	The left P^3 is nicely preserved. It is less worn than the P^3 of Coll. Dub. 1702 and resembles very much the left P^2 described above. The paracone is well developed with a wear facet on the posterior side. A metacone is present (which Hooijer (1950, p. 69) refers to as "the accessory posterior cusp"). The paraprecrista is quite knobby, with several cusplets, among which is the primocone. The buccal side is smooth except for the cingulum, which is weakly developed on that side. The cingulum surrounds the entire premolar and it is strongly developed on the lingual side and very crenulated. The anterior and posterior lobes are also very crenulated. The parapostcrista is vague. The paraendocrista is crenulated and ends at the posterolingual platform. The maxilla is glued. The P^3 is positioned obliquely with regard to the axis of the maxilla; the anterior part is situated more to the buccal side than the posterior part. The metacone is positioned more posterior in the P^3 (distance anterior rim - cusp (cusp included) 23.5 mm.) than in the P^2 (distance anterior rim - cusp (cusp included) 19.5 mm.)
	The next premolar must be a DP^4, because both the P^2 and the P^3 are not very worn and the M^3 is not yet fully erupted. The DP^4, on the contrary, is worn down completely. It has a quadrangular outline.

Coll. Dub. 2193 The alveolus of the P^2 is oval-shaped. The anterior root of both the P^3 and P^4 is half-moon-shaped and is probably the result of the fusing of two roots. The posterior root, also the result of the fusing of two roots, is more oval-shaped. Both in the P^3 and P^4, there is an extra, circular root on the lingual side. The P^4 is positioned obliquely with regard to the axis of the maxilla; the anterior part is positioned more to the lingual side than the posterior part.

Coll. Dub. 2460a On the posterior side of this P^4 is an indentation, which represents the position of the M^1. The anterior side is very rounded. The main cusp is four-lobed and has a +-shape. It is connected with the anterior lobe. The anterior lobe extends into a cingulum on the lingual side. Between the +-shaped worn cusp and the lingual cingulum is an anterolingual fossa. The anterior and the posterior lobes do not continue on the buccal side.

Coll. Dub. 2592 This P^4 has one worn cusp, the paracone, which is +-shaped. The extensions in posterior, anterior and lingual directions are connected with the cingulum on the lingual side. It is absent on the buccal side.

Coll. Dub. 2907 1) Vaguely there are some alveoli present, but it is not very clear if the alveolus of the P^1 is present. The right P^2 and P^3 are present, but broken. Strange is that the P^2 is positioned obliquely with regard to the axis of the maxilla; in most cases it is the P^3 that is obliquely with regard to the axis of the maxilla. Therefore it is possible that these premolars are not the $P^{2\text{-}3}$, but the $P^{3\text{-}4}$. But in that case there is a large gap between the P^4 and the M^1, so this is not very likely. It is more likely that the gap marks the position of the P^4, which is not developed in this specimen. The alveoli were not clear enough to measure.

Coll. Dub. 2908 The very clear alveolus of the left P^1 is oval-shaped, indicating that the P^1 had one root.

The broken and very worn left P^2 is positioned obliquely with regard to the P^3; the posterior part of the P^2 is turned more to the buccal side than the anterior part of the P^3. The same is true for the right P^2. Because of the wear, the morphology of the left P^2 is hard to distinguish. The posterior part is lying lower than the anterior part. The posterior part is made up of a quadrangular worn platform, with a little ridge on its medial border. This ridge runs from the buccal to the lingual side with little cusplets on both ends. The cusplet on the buccal side is higher than the one on the lingual side. On the anterior side of the ridge is an oval-shaped, anterior-posterior directed little platform, which descends in height in anterior direction. The medial ridge is the highest part of the premolar.

The right P^2 resembles the left one very much, but the right one shows a cingulum which seems to surround the entire premolar, although the anterobuccal side is damaged and the cingulum is broken off here. The medial ridge divides the anterior part of the premolar from the posterior side. The posterior side is lying lower than the anterior part. It descends in posterior direction. On the anterior part, a platform can be seen, but not an oval-shaped one, like in the left P^2. The anterior part is also very worn. This platform is descending in anterior direction. The cusplet on the buccal side of the medial ridge is higher than the one on the lingual side.

The morphology of the very worn P^3's is comparable to the P^2's. The medial ridge described in the P^2's are also present in the P^3's, but are more worn down and therefore less discernible. The posterior part of the P^3's is broader than the anterior part. In the left P^3, the anterior part of the premolar is lower than the posterior part, in the right P^3 it is the other way round. The right P^3 is too worn to distinguish if there has been a cingulum. The left P^3 shows a thickening of the enamel on the anterior side, which might be a remnant of a cingulum. They are positioned obliquely with regard to the axis of the maxilla; the anterior part is positioned more to the buccal side than the posterior part.

Coll. Dub. 2909

There is an alveolus of P^1.

The right P^4 is preserved. The cusps are worn and form a x-shaped pattern, directed anterolingual-posterobuccal and anterobuccal-posterolingual. There is a lingual fossa. There is a cingulum on the lingual side. According to Hooijer (1950, p. 80) the P^4 dex is slightly rotated.

Coll. Dub. 2911

The alveoli of both P^3's are positioned obliquely with regard to the axis of the maxilla; the anterior part is situated more to the buccal side than the posterior part. The right alveolus shows the anterior and posterior roots very clearly. The anterior root is probably the result of the fusing of two roots into one root, and the same occurred in the posterior root.

The paracone of the P^4 sin shows a large, +-shaped wear pattern. This pattern is probably the result of the wearing of originally four cusps (the paracone, the metacone, the protocone and the tetracone). The surface of this premolar descends smoothly in posterior and buccal direction. The paracone is connected with the posterior lobe, which continues into a cingulum on the entire lingual side. There are two grooves; one on the posterolingual side, the other on the anterolingual side. According to Hooijer (1950, p. 79), "the left P^4 is rotated for 90°, with its posterior surface facing inward".

Coll. Dub. 2914

The alveolus of P^1 sin has one root. Hooijer (1950, p. 78) claims that this is a DP^1, but he doesn't explain why.

From the left alveolus of P^2 it is very clear that the premolar was at least three-rooted. The anterior two circular roots are fused to one root and the posterior root is half-moon-shaped, and probably also the result of the fusing of two roots. The posterior root seems to go deeper into the maxilla than the anterior root.

The anterior part of the broken P^3's is situated more to the buccal side than the posterior part; it is obliquely with regard to the axis of the maxilla.

Coll. Dub. 2921

2) The alveolus of the P^1 shows that it is two-rooted, with an 8-shape. The anterior part of the P^1 is positioned more to the lingual side than the posterior part.

In the alveolus of the P^2, the erupting P^2 can be distinguished; there is one cusp visible (paracone).

Coll. Dub.2924 — 4) From this posterior part of P^3, the buccal side is also broken off. The paracone has a wear facet on the posterior side. The para-postcrista and the paraendocrista are very crenulated. Anterior of these cristas are two more crenulated ridges. There is a posterior lobe, which continues into a cingulum on the lingual side. The posterior platform is covered with cusplets.

Coll. Dub. 2926 — This unworn P^3 has an anterior lobe, which is a bit crenulated. On the anterior side is a low-lying primocone. There is a cingulum, both on the lingual and buccal sides. The paraprecrista is crenulated. On the lingual side are some minor cusplets present. The paraendocrista and the parapostcrista are crenulated. The posterior side has a little platform, but it is not covered with cusps. The posterior lobe is present.

Coll. Dub. 2933 — The alveolus of the left P^2 shows that is was one-rooted. On the right side, the root of the P^2 is visible. It is 8-shaped, indicating that there were originally two roots.

The alveolus of the left P^3 is present with part of the root in it. Its two anterior roots are fused to one and so are the posterior roots. The roots are half-moon-shaped.

The right P^3 is very worn. The wear facet is large. The wear facet is lower on the posterior side than on the anterior side. The anterior lobe is worn to the same level as the wear facet. From the anterior lobe starts a cingulum on the buccal side, where it is now visible as a line in the enamel. Also on the lingual side there seem to be some remnants of a cingulum.

The root of the left P^4 looks like the roots of the P^3 dex.

The root of the right P^4 has an anterior half-moon-shaped root and an oval-shaped posterior root. The posterior root is larger than the anterior root.

Both the P^3 and the P^4 are positioned obliquely; their anterior part is positioned more to the lingual side than their posterior part.

Coll. Dub. 3101 — The left P^4 has a rectangular shape. It is quite worn. It consists of a worn platform surrounded by a strong enamel ridge on all sides, except for the posterobuccal corner. On the anterolingual side is another worn platform, disconnected from the rest of the molar by the same enamel ridge.

The right P^4 is more oval-shaped. The morphology is comparable with the left one, except that the posterolingual corner is separated from the worn platform. In the left one this is not separated, although there is a ridge there. The right P^4 also has a strong ridge of enamel that surrounds it. The left P^4 has a posterior lobe, the right one has not.

Coll. Dub. 3148 The right P^4 is very worn and it consists of a worn platform, with an enfolding of the enamel on the anterolingual side. The remnants of a lingual and buccal cingulum are still visible.

Coll. Dub. 13601 The anterior part of this P^3 is broken off. The wear facet is directed in anterior direction. On the lingual side is a crenulated cingulum, which continues to the place where the premolar is broken. On the buccal side, there is no cingulum. Due to wear it cannot be distinguished if there was a metacone. On the posterior side, several dividing crenulated ridges are present, among which the paraendocrista and the parapostcrista. The posterior part forms a little platform. The posterior lobe is present. Below the posterior lobe, a smooth surface indicated the position of the P^4.

VII.7 LOWER MOLARS

The measurements are given in the Appendix VI-18 – VI-20.
Specimens without description:
Without number (skeleton, Geological Museum Bandung); without number (skull and mandible, Geological Museum Bandung); 466; 4-4A; K 742/1; Coll. Dub. 1804; Coll. Dub. 2207b; Coll. Dub. 2904; Coll. Dub. 2910.

Description of the specimens:

Without number (Laboratory Bioanthropologi and Paleoanthropologi, Yogyakarta)
The M_1 is quite worn. The protoconid and the metaconid are fused. The anterior lobe is connected to the fused protoconid/ metaconid. The metapoststylid is fused with the metaconid. The metapoststylid is situated lingually from the hypoprestylid, which is fused with the hypoconid. The entoconid, the hypoconid and the posterior lobe are fused. There are no posterior cusps. There is an accessory buccal cusp, which is situated not entirely in the middle of the valley, but more towards the hypoconid. There is no cingulum.

In the M_2 the metaconid is fused with the protoconid. The anterior lobe is present on the anterior side and is connected with the proto/metaconid. The metapoststylid is fused with the proto/metaconid and it is situated lingually of the hypoprestylid. The hypoconid is larger than the entoconid. There is no posterior lobe. The heptaconid forms one ridge with the hexaconid. The pentaconid is separated from the heptaconid. There is an accessory buccal cusp near the protoconid. There is no cingulum.

The protoconid of the M_3 is larger than the metaconid. The metaconid is damaged. From the protoconid runs the anterior lobe towards the posterolingual side of the metaconid. The anterior lobe lies lower than the chewing surface. On the buccal side of the protoconid, a separated part of the anterior lobe is present. It is not distinguishable how the metapoststylid is situated with regard to the hypoprestylid, due to the damage of the metaconid. The hypoconid is larger than the entoconid. There is a hypopostconulid. Behind this cusp is the heptaconid. The heptaconid is fused with the hexaconid and form one robust ridge. The pentaconid is separated and exists of four little tubercles on the posterobuccal side. There is no cingulum, nor any accessory cusps.

22G In the right M_1 the protoconid and the metaconid are fused due to wear. The anterior lobe is connected with the fused protoconid/metaconid. The metapoststylid is fused with the metaconid. The metapoststylid is situated lingually from the hypoprestylid. The hypoprestylid is fused with the hypoconid and the entoconid. The posterior lobe is fused with the hypoconid/entoconid. There are no posterior cusps, accessory cusps or cingula. The anterior side is smaller than the posterior side.

In the left M_2 the protoconid lies more anteriorly than the metaconid. The anterior lobe is connected with the protoconid. The metapoststylid is situated lingually from the hypoprestylid. The hypoconid is larger than the entoconid. There is a posterior lobe. The heptaconid is quite robust and forms one ridge with the hexaconid. The pentaconid is separate from the heptaconid. There is an accessory buccal cusp. There is no cingulum.

In the right M_2, the protoconid, the metaconid and the anterior lobe are fused. The metapoststylid lies more lingually than the hypoprestylid. The hypoconid is larger than the entoconid. The heptaconid is fused with the hexaconid and forms one ridge. The pentaconid is separate from the heptaconid. There is an accessory buccal cusp. There is no cingulum.

In both M_3's the protoconid is larger than the metaconid and the protoconid is situated more anteriorly than the metaconid. The anterior lobe is connected with the protoconid/metaconid.
In the right M_3, the metapoststylid is situated lingually from the hypoprestylid. In the left M_3 this was not very well visible. In both M_3's, the hypoconid is larger than the entoconid. There is no posterior lobe. The heptaconid is present. In the left M_3 the pentaconid and the hexaconid are not well distinguishable. In the right M_3, they are present, but it is not well visible how they are positioned with regard to each other, but the talonid is rather robust. There don't seem to be any accessory cusps, nor a cingulum in either of the M_3's.

SA 040979-20N 1) This left M_1 fits to the M_2 described below (2). It has an anterior lobe, which ends on the lingual side against the metaconid. The anterior lobe is not connected to the protoconid/metaconid. The protoconid and the metaconid are fused, but you can still see that the protoconid used to be larger than the metaconid. The protoconid is placed a bit more anteriorly than the metaconid. The metapoststylid is fused with the metaconid. The metapoststylid is situated more lingually than the hypoprestylid. The hypoconid is larger than the entoconid. There is no posterior lobe. The heptaconid, the pentaconid and the hexaconid are present. The heptaconid is fused with the hexaconid and forms one ridge. The pentaconid is separate from the heptaconid. There is an accessory buccal cusp. Attached to this accessory cusp are two very little tubercles, which all together resemble a little cingulum on the buccal side. At the foot of the protoconid is another little tubercle on the buccal side.

2) This M_2 is not very worn. The protoconid is of the same size as the metaconid. The protoconid is situated more to the anterior side than the damaged metaconid. It has a robust anterior lobe, which is not

connected with the protoconid/metaconid. On the buccal side the anterior lobe ends in a cusplet. The metapoststylid is situated a little more lingually than the hypoprestylid. The hypoconid is larger than the entoconid. The entoconid is not yet worn. There is no posterior lobe. The heptaconid, the hexaconid and the pentaconid are present, the heptaconid being the largest. The hexaconid is larger than the pentaconid. The hexaconid is connected with the heptaconid, but they do not form one ridge. The pentaconid is separate from the heptaconid. There are no accessory cusps or cingula.

3) This M_2 fits to the M_3 of SA 110979. It has an anterior lobe, which seems to exist of two lobes, which meet in the middle and is not connected with the protoconid/metaconid. The protoconid is larger than the metaconid. The protoconid is situated more to the anterior side than the metaconid. The metapoststylid is fused with the protoconid/metaconid. The metapoststylid is situated more lingually than the hypoprestylid. The hypoconid is larger than the unworn entoconid. There is no posterior lobe. The hypoconid touches the heptaconid. The hexaconid and the pentaconid are also present. The heptaconid is the largest of the three; the hexaconid is larger than the pentaconid. The heptaconid is attached to the hexaconid, the pentaconid is separate. There are no accessory cusps or a cingulum.

SA 110979

This right M_3 fits to the right M_2 040979-20N/3. It is unworn. There is an anterior lobe, which extends more to the buccal side than to the lingual side. It is not attached to the protoconid/metaconid. The protoconid is situated more to the anterior side than the metaconid. The protoconid and the metaconid are of about the same size. The metapoststylid is situated more lingually than the hypoprestylid. The hypoconid is larger than the entoconid. The hypoconid touches the heptaconid. The heptaconid, the hexaconid and the pentaconid form the talonid. The heptaconid is the largest of these three cusps. The hexaconid is larger than the pentaconid. The heptaconid and the hexaconid touch each other; the pentaconid is separate. There is no posterior lobe, no cingulum and there are no accessory cusps.

K 149

The M_2 has an anterior lobe, which is connected to the metaconid or the protoconid, which are fused. The metapoststylid and the hypoprestylid are opposite each other. The hypoconid and the entoconid are fused with the heptaconid and the hexaconid, which form one ridge. The pentaconid is a separated cusp. There are no cingula nor accessory cusps.

The M_3 has an anterior lobe, which is connected to the fused metaconid and protoconid. The metapoststylid (which is fused with the protoconid/metaconid) and the hypoprestylid (which is fused with the hypo/entoconid) are opposite each other. The hypoconid and the entoconid are fused, but it can still be seen that the hypoconid is larger than the entoconid. The heptaconid is very robust. The hexaconid is a little in front of the heptaconid. There is no pentaconid, but it looks as though it is fused with the heptaconid. The hexaconid is quite small and is not attached to the heptaconid. There are no cingula, nor any accessory cusps.

K 150 The protoconid of this M_2 is placed more to the anterior side than the metaconid and touches the anterior lobe. The protoconid and the metaconid are of about the same size. The metapoststylid is situated more lingually than the hypoprestylid. The posterior part of the molar is missing. Only the anterior extensions of the hypo- and entoconid are visible. There are (as far as can be seen) no accessory cusps nor cingula.

K 657 The M_3 is unworn. The anterior lobe is interrupted in the middle where the M_2 is placed. It is attached to the protoconid/ metaconid. The protoconid is placed more anteriorly than the metaconid. The protoconid is of about the same size as the metaconid. The metapoststylid is situated more lingually than the hypoprestylid. The hypoconid is larger than the entoconid. Behind the hypoconid, the hypopostconulid is present. The hypopostconulid touches the heptaconid. The pentaconid and hexaconid are both present. The hexaconid is larger than the pentaconid. The hexaconid is attached to the heptaconid, the pentaconid is separate. There is no posterior lobe and there are no cingula nor accessory cusps.

K 707 The protoconid of this M_3 is larger than the metaconid and placed more anteriorly. The anterior lobe is connected with the protoconid. The metapoststylid is situated opposite the hypoprestylid. The hypoconid is larger than the entoconid. The talonid consists of the heptaconid, the pentaconid and the hexaconid. The hexaconid is fused with the heptaconid. The pentaconid is separate. There is no cingulum, no posterior lobe, nor any accessory cusps.

K 723 1) The protoconid of this M_3 is larger than the metaconid, and is placed more anteriorly than the metaconid. The anterior lobe is touching the protoconid. The metapoststylid is situated lingually from the hypoprestylid. The anterior cusps are a little worn, the posterior cusps are unworn. The hypoconid is a bit larger than the entoconid. Attached to the hypoconid is the hypopostconulid. The posterior part of the molar is missing. Only the hexaconid is distinguishable. There are no cingula, no posterior lobe, nor any accessory cusps.

2) This M_3 is unworn. The protoconid is larger than the metaconid and it is situated more anteriorly than the metaconid. The anterior lobe is connected with the protoconid. The metapoststylid lies lingually from the hypoprestylid. Behind the hypoconid is the hypopostconulid. The hypoconid and the entoconid are of about the same size. These two cusps are situated in a row, the one posteriorly of the other. Posteriorly of these is the heptaconid. The hexaconid touches the heptaconid. The pentaconid is the smallest of these posterior cusps and separated from them. Behind the heptaconid is the posterior lobe. There is an accessory buccal cusp and a low cingulum on the lingual side.

3) Posterior part of a little worn left M_3.
The posterior part of the metapoststylid is visible and is situated lingually of the hypoprestylid. The hypoconid is attached to the hypopostconulid, but they are still separated. The hypoconid and the entoconid are of about the same size. Posteriorly of the hypo- and entoconid is the talonid, which consists of the heptaconid, the

hexaconid and the pentaconid. The hexaconid touches the heptaconid, the pentaconid is separate. Posteriorly of these is the posterior lobe. There are no cingula, nor any accessory cusps.

K 727 The M_2 is worn. The anterior lobe is quite low compared to the wear surface.

The M_3 is not yet worn and not entirely erupted. The protoconid is of about the same size as the metaconid. The metapoststylid lies lingually from the hypoprestylid. The hypoconid and the entoconid are of about the same size. Behind the hypoconid is another lower cusp, the hypopostconulid. The talonid exists of the heptaconid, the pentaconid and the hexaconid. Due to the fact that the M_3 is not yet fully erupted, it cannot be seen how the cusps of the talonid are positioned with regard to each other.

K 731 The M_1 is quite worn. The four main cusps, the metapoststylid and the hypoprestylid are all fused due to wear. Also the anterior lobe is fused with the protoconid/metaconid. There is no posterior lobe. There are no posterior cusps visible. The buccal side is damaged and it cannot be seen if there is an accessory buccal cusp. There is a low cingulum on the posterobuccal side.

The M_2 has an anterior lobe connected with the protoconid. The protoconid is fused with the metaconid, but it is still visible that the protoconid is situated more anteriorly than the metaconid. The metapoststylid lies lingually from the hypoprestylid. The hypoconid, the entoconid and the heptaconid are fused. There is a posterior lobe on the posterobuccal side, which is connected with the hypoconid and the heptaconid. The heptaconid forms one ridge with the hexaconid. There is no sign of the pentaconid. A cingulum is present on the buccal side.

The M_3 is also worn. The low anterior lobe is interrupted by the posterior part of the M_2. The protoconid is larger than the metaconid and it is situated more anteriorly than the metaconid. The anterior lobe is connected to the protoconid. The metapoststylid lies lingually from the hypoprestylid. The hypoconid is a bit larger than the entoconid. Posteriorly of the hypoconid is the hypopostconulid. The talonid exists of the pentaconid (attached to the heptaconid, but a bit lower) and the hexaconid, which is separated. The pentaconid is larger than the hexaconid. The posterior lobe is attached to the heptaconid. There is a cingulum on the buccal side.

K 740 The protoconid of this worn M_3 is situated anteriorly of the metaconid. The metaconid is larger than the protoconid. The low anterior lobe is connected to the protoconid. The hypoprestylid is not developed; the anterior rim of the hypoconid/entoconid lies opposite the metapoststylid. The hypoconid is of the same size as the entoconid. The hypoconid is connected with the hypopostconulid. The hexaconid is attached to the heptaconid and is somewhat lower. Between the entoconid and the hexaconid is the posterior lobe. The pentaconid is not visible. There is a very low cingulum on the buccal side. There are no accessory cusps.

K 741 The M_2 is quite worn. The metaconid is larger than the protoconid. The protoconid is situated more anteriorly than the metaconid. The anterior lobe is connected with the protoconid. The metapoststylid is positioned just a little bit more lingually than the hypoprestylid. The hypoconid is larger than the entoconid. The entoconid is unworn. There is no posterior lobe. The hypoconid is attached to the heptaconid. The pentaconid and the hexaconid are also present. The hexaconid is touching the heptaconid, but they do not form one ridge. The pentaconid is separate from the heptaconid. The hexaconid is the smallest. There are no accessory cusps and no cingulum.

K 742 2) This worn left M_2 has an anterior lobe, which is fused with the protoconid and the metaconid. The protoconid is situated more anteriorly than the metaconid. The metapoststylid is fused with the hypoprestylid, which in turn is fused with the hypoconid/entoconid. These last two cusps are fused with the posterior lobe. The posterior cusps (heptaconid, pentaconid and hexaconid) are all fused. There is a cingulum on the buccal side.

3) The also quite worn right M_3 has an anterior lobe, which is fused with the protoconid and the metaconid. The metapoststylid (which is fused with the metaconid/protoconid) is situated lingually of the hypoprestylid (which is fused with the entoconid/hypoconid). The hypoconid and the entoconid are also fused. The heptaconid is worn and touches the hypoconid. The heptaconid is fused with the hexaconid. The pentaconid is separated from the heptaconid. There is a small posterior lobe posterior of the heptaconid. There is a very low cingulum on the buccal side. There is an accessory buccal cusp.

K 743 In this worn M_2, the anterior lobe, the protoconid and the metaconid are fused due to wear. The metapoststylid is situated lingually from the hypoprestylid. The hypoconid is larger than the entoconid. The hypoconid is attached with the heptaconid. Attached to the heptaconid is the hexaconid, forming one ridge. The pentaconid is separate and larger than the hexaconid. There is no posterior lobe, nor any accessory cusps, nor cingula.

This unworn M_3 has a morphology, which is a bit strange. The protoconid and the metaconid are together more like a transverse ridge and the same is true for the hypoconid and the entoconid. There is no anterior lobe. The metapoststylid is situated just a little more lingually than the hypoprestylid. The hypopostconulid is attached to the hypoconid. The talonid consists of the heptaconid. The pentaconid and the hexaconid are not distinguishable; they all seem to be united to form the posterior lobe.

K 745 The worn M_2 has a low anterior lobe, which is connected with the protoconid. The protoconid is larger than the metaconid. These cusps are fused due to wear. The metapoststylid (which is connected with the fused protoconid/metaconid) is situated lingually of the hypoprestylid. The hypoconid is larger than the entoconid. The hypoconid is fused with the heptaconid. The hexaconid is attached to the heptaconid and forms the posterior lobe. The pentaconid is separated. There are no cingula, nor any accessory cusps.

The M_3 has an anterior lobe, which is connected to the protoconid. The protoconid is situated more anteriorly than the metaconid and is of about the same size as the metaconid. These cusps are slightly worn. The metapoststylid lies lingually from the hypoprestylid. The hypoconid and the entoconid are unworn. The hypoconid is larger than the entoconid. The hypopostconulid (which is more a cuspate ridge than a cusp) is attached to the hypoconid. The talonid consists of the large heptaconid. On the lingual side is a ridge, which consists of the hexaconid and some smaller cusplets. On the buccal side is a ridge, which consists of the pentaconid and some smaller cusplets. Posteriorly of this ridge is a low posterior lobe. There are no cingula, nor any accessory cusps.

K 746 The M_2 is quite worn. The anterior lobe, the protoconid and the metaconid are fused due to wear. The anterior lobe extends more in buccal direction than in lingual direction. There is not only a hypoprestylid, but also an entoprestylid. The metapoststylid lies in the middle of these stylids. Compared to the hypoprestylid, the metapoststylid lies just a bit more lingually than the former. The hypoconid is of about the same size as the entoconid. There is no posterior lobe. The heptaconid and the hexaconid form one ridge, which runs towards the posterior foot of the entoconid. This ridge is somewhat cuspate. On the buccal side is the separate pentaconid visible. There are no cingula, nor any accessory cusps.

The M_3 is unworn. The anterior lobe of the M_3 is indented by the presence of the M_2. The protoconid is situated more anteriorly than the metaconid. The protoconid consists of two cusps, of which the anterior one is connected to the anterior lobe. The metaconid is made up of one large cusp and four little ones, three on the anterior side of the large cusp, one on its posterior side. This last one is not yet developed to a metapoststylid. Also the hypoprestylid is not developed. The hypopostconulid is a bit lower than the hypoconid. The hypoconid and the entoconid are of about the same size. The talonid consists of the heptaconid, the hexaconid and the pentaconid. The hexaconid is quite large and separated from the heptaconid. There are two separate cusps on the buccal side of the heptaconid, the pentaconid and the pentaconulid. There is no posterior lobe, nor any accessory cusps or cingula.

Coll. Dub. 87 Of the four main cusps of this M_3, only the posterior parts of the hypo- and entoconid are visible. The pentaconid touches the hypoconid. The heptaconid and the hexaconid are grown together and they cannot be distinguished. The pentaconid is separated from them and circular. Behind these cusps is the posterior lobe.

Coll. Dub. 97 This M_3 is not yet fully erupted; the talonid is still hidden in the jaw. The protoconid is quite a bit larger than the metaconid. Attached to the protoconid is the anterior lobe, which runs downwards in lingual direction. It extends further in buccal direction than in lingual direction; on the buccal side it continues until the foot of the protoconid. The protopoststylid lies opposite the hypoprestylid. The hypoconid is just a bit larger than the entoconid.

Coll. Dub. 98 — The M_3 is positioned obliquely in the mandible. The posterior side lies more to the lingual side than the anterior part. The molars could not be measured.

Coll. Dub. 99 — The left M_1 has a little accessory buccal cusp. The rest of the M_1 is too worn down to distinguish other features.

In the left M_2 the anterior cusps and the anterior lobe are fused. The anterior lobe extends further in buccal direction than in lingual direction. The metapoststylid is situated lingually from the hypoprestylid. The hypoconid is larger than the entoconid. The hypoconid is probably fused with the heptaconid. Also the pentaconid and the hexaconid are present. The hexaconid is larger than the pentaconid. They are both separate from the heptaconid. There are no cingula, nor any accessory cusps, although a little thickening is present in the buccal valley.

In the right M_2 the anterior cusps and the anterior lobe are fused. The anterior lobe extends further in buccal direction than in lingual direction. The metapoststylid is situated just a little bit more lingually than the hypoprestylid. The hypoconid and the entoconid are fused. The hypoconid is probable fused with the heptaconid. Also the pentaconid and the hexaconid are present. The hexaconid is larger than the pentaconid. The pentaconid is separate from the heptaconid, the hexaconid is attached to it. There is no cingulum. There is an accessory buccal cusp.

In both M_3's the protoconid is larger than the metaconid. The protoconid lies more anteriorly than the metaconid. The anterior lobe touches the protoconid. The anterior lobe ends in a cusp lingually of the protoconid. From this cusp a ridge goes down, but it does not reach the metaconid. On the buccal side the anterior lobe is crenulated and it goes downwards until the foot of the protoconid. In the left M_3, the metapoststylid is situated nearly opposite the hypoprestylid; the first is just situated a little bit more to the lingual side than the latter. In the right M_3 they lie opposite each other and in this molar there is no metapoststylid but a protopoststylid. The hypoconid is larger than the entoconid. Between the hypoconid and the heptaconid is the hypopostconulid, which is somewhat lower than the hypoconid, but is attached to it. The heptaconid is not yet worn. The left molar has a low hexaconid (touching the heptaconid) and a very small pentaconid. In the right M_3 no pentaconid nor hexaconid can be distinguished. From the heptaconid starts a ridge to the lingual and the buccal side. It is a little crenulated and ends at the buccal side at the foot of the hypoconid and on the lingual side at the foot of the entoconid. There is no cingulum. The molars are not very worn.

Coll. Dub. 105 — 2) The M_1 is probably a left one. It is very damaged and not measurable. There are two accessory buccal cusps. The lingual side is somewhat larger than the buccal side (as far as can be seen due to the damage). On the posterior side is a hollow that indicates the position of the M_2.

3) This M_2 is very ramshackle and not measurable. It might be a right one, because in the valley between the hypoconid and the protoconid

there is a cusp, so this might be the buccal side, because accessory buccal cusps occur more often than accessory lingual cusps. Remarkable is that the metapoststylid and the hypoprestylid are lying nearly opposite each other, the metapoststylid is just a tiny bit more placed to the lingual side.

Coll. Dub. 272a

The anterior cusps of this M_2 are fused with the anterior lobe. The anterior lobe extends more in buccal than in lingual direction. The metapoststylid is situated lingually from the hypoprestylid. The hypoconid and the entoconid are fused. There are no posterior cusps, there is a posterior lobe instead; probably the posterior cusps are all fused due to wear. In the middle (at the place of the heptaconid) it touches the hypoconid. There is a large accessory buccal cusp, which is attached to the protoconid. There is no cingulum.

Coll. Dub. 285

Talonid of a right M_3. The heptaconid and the hexaconid are connected, the pentaconid is separate. The rest of the molar is broken off.

Coll. Dub. 310

The M_2 has four roots.

The M_3 is very obliquely compared to the axis of the jaw. The posterior side is positioned much more to the lingual side than the anterior side. The anterior lobe, the four main cusps, the metapost- and hypoprestylid are all fused. The three posterior cusps form the talonid. The heptaconid and the hexaconid are fused. The heptaconid touches the posterior extension of the hypoconid/entoconid. The pentaconid is a separate, unworn cusp, which is a bit lower than the wear surface. Behind the hexaconid starts the posterior lobe, which is rather knobby. On the lingual and buccal sides, the posterior lobe extends downwards, but it is still rather high. From the pentaconid starts a cingulum downwards, until the buccal side of the hypoconid and from there upwards again until the posterior end of the protoconid.

Coll. Dub. 314b

This M_3 is unworn. The metaconid is larger than the protoconid. The anterior lobe is quite low and it is crenulated. It continues on the lingual side until the anterior side of the foot of the metaconid. On the buccal side it continues as a crenulated cingulum until the valley between the protoconid and the hypoconid. The metapoststylid lies opposite the hypoprestylid but with a slight tendency towards the lingual side. The hypoconid is larger than the entoconid. The talonid consists of the heptaconid and a smaller cusp on the lingual side of the heptaconid, the hexaconid, which continues into a crenulated posterior lobe, which goes downwards until the posterior side of the foot of the entoconid. On the buccal side of the heptaconid is also a crenulated low posterior lobe, which continues until the posterior foot of the hypoconid. There is no trace of the pentaconid. There are no accessory cusps.

Coll. Dub. 323a

1) The M_2 is very ramshackle. It is totally worn down and damaged. On the lingual side a low cingulum can be distinguished, which extends from the posterior lobe until the valley between the entoconid and the metaconid.

In the M_3, the anterior lobe and the anterior cusps are fused and so are the posterior cusps. The anterior lobe extends further in buccal direction than in lingual direction. The metapoststylid is situated lingually from the hypoprestylid. The talonid consists of the hexaconid, the heptaconid and the pentaconid. The heptaconid is larger than the other two and the hexaconid is larger than the pentaconid. The heptaconid and the hexaconid are not yet fused, but they touch each other. The pentaconid is a separate cusp. The heptaconid touches the posterior extension of the hypoconid/entoconid. On the lingual side between the heptaconid and the hexaconid the posterior lobe can be seen. There is also a low-lying crenulated posterior lobe between the heptaconid and the hypoconid. This continues into a crenulated cingulum until the anterior lobe. There are no accessory cusps nor is there a cingulum on the lingual side.

2) The anterior part of this M_3 is damaged. However, it can be seen that the metapoststylid is situated lingually from the hypoprestylid. From the protoconid, some traces are left of a crenulated cingulum which continues until the foot of the hypoconid. The hypo- and entoconid are fused. The heptaconid touches the posterior extension of the hypoconid/entoconid. On the lingual side of the heptaconid is a crenulated posterior lobe which descents until the foot of the entoconid. On the buccal side there is also a crenulated posterior lobe which continues from the foot of the heptaconid, where it goes upwards and then downwards again until the posterior side of the hypoconid. This posterior lobe lies much lower than the heptaconid.

Coll. Dub. 323b

This M_3 is very damaged. The metaconid, the hypoconid and the heptaconid are damaged. The anterior cusps and the anterior lobe are fused and so are the hypoconid and the entoconid. The anterior lobe extends further in buccal direction than in lingual direction. From the anterior lobe is a little crenulated ridge until the foot of the protoconid. At the place where the fused metapoststylid and hypoprestylid meets, the metapoststylid lies a bit lingually from the hypoprestylid. The heptaconid touches the hypoconid/entoconid on the posterobuccal side. The heptaconid extends until the lingual side and it seems that it is fused with the hexaconid. On the posterolingual side of the heptaconid is a low crenulated posterior lobe present until the posterior part of the foot of the entoconid. On the buccal side of the heptaconid there is a low crenulated posterior lobe which continues until the foot of the hypoconid on the posterior side. In this crenulated ridge is a tubercle which is a bit larger than the rest. This might be the pentaconid. There is no cingulum. There are no accessory cusps, but there is a little thickening on the lingual side.

Coll. Dub. 324

The lingual side of this totally worn M_1 is larger than the buccal side and the posterior side is somewhat larger than the anterior side.

Coll. Dub. 325d

2) The anterior part of this M_3 is missing. However, it is visible that the metapoststylid lies just a bit lingually from the hypoprestylid. They are nearly opposite each other. The hypo- and entoconid are fused. Posterior of the hypoconid/entoconid is the heptaconid. Lingually from the heptaconid is the hexaconid. They are attached with each other. The pentaconid is larger than the hexaconid and is separated from the heptaconid. From the hexaconid starts a cingulum that continues on the lingual side until it ends in an accessory lingual cusp. From the pentaconid starts a cingulum that continues until the posterior side of

the protoconid. It cannot be seen if it continues further due to the damage. Posterior of the heptaconid is the posterior lobe, which is crenulated and continues on the buccal side until the pentaconid. In fact the pentaconid is part of the cingulum.

3) Posterior part of a separate left M_3. The hypoconid is of the same size as the entoconid. The heptaconid touches the posterior parts of the hypo- and entoconid. The heptaconid lies against the hexaconid. The pentaconid is separated and circular. Posterior of the heptaconid is the posterior lobe, which goes both in lingual and buccal direction and ends at the hexaconid and the pentaconid. It is rather crenulated. The heptaconid is the largest of the posterior cusps and the hexaconid is larger than the pentaconid. There is a crenulated cingulum on the lingual side.

Coll. Dub. 2003a

1) In this M_2, the protoconid and the metaconid are fused with the anterior lobe. The anterior lobe extends more in buccal direction than in lingual direction. The metapoststylid is situated lingually from the hypoprestylid. The hypoprestylid is fused with the fused hypoconid/entoconid. The posterior part of the molar is missing. Only the anterior part of the hypoconid/entoconid is visible. There is a thickening, not really a tubercle, on the lingual side, in the valley between metaconid and entoconid. On the buccal side there is a cingulum from the anterior lobe until the posterior side of the protoconid.

2) The anterobuccal side of this M_3 is damaged. The protoconid seems to be larger than the metaconid (but the protoconid is damaged). The protoconid lies more anteriorly than the metaconid and touches the anterior lobe. The anterior lobe goes downwards in lingual direction. In buccal direction it is broken off. The metapoststylid is situated lingually from the hypoprestylid. The hypoconid is larger than the entoconid. The heptaconid is attached to the hypoconid and is fused with the hexaconid. From the hexaconid goes a little ridge, a bit crenulated, downwards until the posterior side of the foot of the entoconid. The pentaconid is round and separated from the heptaconid. There is no cingulum. There is an accessory, rather large, buccal cusp on the posterior side of the protoconid.

Coll. Dub. 2006

This M_3 is not complete, the anterior and posterior sides are damaged. The protoconid, metaconid, anterior lobe, metapoststylid, hypoprestylid, hypoconid and entoconid are all fused. Attached to and opposite of the posterior part of the hypoconid/ entoconid is the heptaconid. Lingually of the heptaconid and attached to it, is a part of the hexaconid, but this part is broken. Buccally of the heptaconid are two cusps, which form a ridge until the foot of the posterior side of the hypoconid. On the buccal side there is a crenulated cingulum which starts at the protoconid and goes downwards until the anterior side of the foot of the hypoconid. On the lingual side of the entoconid there is a crenulated cingulum.

Coll. Dub. 2008

The anterolingual side of this M_1 is broken off. The morphology of this molar is somewhat different from the other molars. The protoconid is situated more anteriorly than the metaconid and is attached to the anterior lobe. Both the metaconid and the protoconid have a posterior extension, the metapoststylid and protopoststylid. The metapoststylid lies lingually from the entoprestylid. The entoprestylid lies opposite the protopoststylid. There is no hypoprestylid. The hypoconid is a separate cusp. The entoconid continues posteriorly in the posterior lobe, which continues a little on the lingual side until the foot of the entoconid. This posterior lobe is a bit crenulated and might consist of the fused heptaconid and hexaconid. The pentaconid cannot be distinguished. The hypoconid and the entoconid are of about the same size and unworn. On the buccal side is a crenulated cingulum, which starts from the anterior lobe until the valley between the hypoconid and the protoconid. The way of wear seems to be strange as the hypoconid (on the buccal side) is higher than the entoconid, but the metaconid (on the lingual side) is higher than the protoconid.

Coll. Dub. 2008a

This M_2 has four roots. The protoconid and the metaconid are fused due to wear. The anterior lobe is attached to the protoconid/metaconid. On the buccal side of this lobe is a separate worn plateau which continues into a crenulated cingulum on the buccal side. This cingulum is rather high. It ends on the lingual side of the protoconid. The hypoconid is larger than the entoconid. The metapoststylid lies opposite the hypoprestylid. On the most posterior tip of the metapoststylid is a little ridge present, which bends in buccal direction. From the most anterior tip of the hypoprestylid is a little ridge present, which bends in lingual direction. The heptaconid touches the hypoconid. The heptaconid bends in lingual direction. The pentaconid and the hexaconid cannot be distinguished. Posterior of the heptaconid is a posterior lobe which exists of several tubercles and which declines both on the lingual and buccal side. On the lingual side there is no cingulum. There are accessory buccal and lingual cusps.

Coll. Dub. 2013

This M_2 is obliquely placed in the mandible: the posterior side is positioned more to the lingual side than the anterior side. The molar is quite worn. The four main cusps, the anterior and posterior lobes, the metapoststylid and the hypoprestylid are all fused together. On the buccal side, in the valley between hypo- and protoconid is an accessory cusp on the same level as the wear surface. It is attached to a ridge on the posterobuccal side, probably a cingulum.

Coll. Dub. 2017

2) In this M_3, only part of the hypo- and entoconid and the talonid is preserved. The rest has been broken off. The heptaconid and the hexaconid are fused. The pentaconid is quite large and separated from the heptaconid. The heptaconid touches the posterior side of the hypoconid/entoconid. There is a crenulated posterior lobe that is lower than the cusps.

Coll. Dub. 2076

6) According to the size, this is probably a very damaged M_1. The anterior cusps are fused. The metapoststylid lies lingually from the hypoprestylid. The posterior and lingual parts are broken off. The anterior lobe continues in lingual direction until the broken edge and on the buccal side it continues as a crenulated cingulum until the protoconid. Posterior of the protoconid there is also a crenulated cingulum.

7) This M_2 is not complete; the posterolingual side is missing. It is not positioned straight (the posterior side is situated more to the lingual side than the anterior side), therefore it should be a left one. The

metaconid is larger than the protoconid. The protoconid is situated more anteriorly than the metaconid. The anterior lobe is not attached to the proto- or metaconid. The anterior lobe continues on the buccal side into a crenulated cingulum, which continues until the foot of the protoconid. The metapoststylid lies opposite the hypoprestylid. These stylids do not touch. The hypoconid is larger than the entoconid (as far as can be seen as the whole lingual side is damaged). On the posterobuccal side of the hypoconid are a few little tubercles. There are two accessory buccal cusps, one is lying very low in the valley, the other one lies much higher, about halfway the crown height.

8) Only the talonid of this M_3 and the posterior parts of the hypo- and entoconid are preserved. The hypoconid is larger than the entoconid. The heptaconid touches the hexaconid. The heptaconid is the largest. The hexaconid consists of several little cusps, attached to the heptaconid. The pentaconid is separate from the heptaconid.

9) Only the posterior part of this M_3 is preserved. The posterior cusps are fused with the heptaconid. The hexaconid exists of two little tubercles, which lie against the heptaconid. The pentaconid is separated from the heptaconid, lies somewhat lower and is rounder than the hexaconid. The posterior lobe starts from the heptaconid and ends on the buccal side at the pentaconid and on the lingual side at the hexaconid. The posterior lobe is crenulated. From the hexaconid starts a cingulum to where the molar is broken.

10) Only the posterior part of this M_3 is preserved. The hypoconid is larger than the entoconid. The heptaconid touches the hypoconid. The heptaconid is very round and there is no sign of a hexaconid, but on the lingual side of the heptaconid a ridge goes downwards until the posterior side of the entoconid. On the buccal side there is also no pentaconid, but a knobby ridge until the hypoconid.

11) Only the posterior part of this M_3 is preserved. The posterior cusps are fused with the heptaconid. The heptaconid is attached to the hexaconid. The hexaconid is attached with the hexaconulid. From the hexaconid starts a cingulum on the lingual side until halfway the entoconid, where the molar is broken. The pentaconid is separated from the heptaconid. The heptaconid is the largest of the posterior cusps. The hexaconid (including the hexaconulid) is larger than the pentaconid. The posterior lobe is present between the heptaconid and the pentaconid. It is rather robust and knobby.

Coll. Dub. 2082

On the anterior side of the M_2, the indentation can be seen which represents the position of the M_1. The M_2 is positioned obliquely in the mandible: the posterior side of the M_2 is positioned more to the lingual side than the anterior side. The anterior lobe, all four cusps, the metapost- and hypoprestylid and the posterior lobe are all fused. The anterior lobe extends more in buccal direction than in lingual direction. From the protoconid runs a little ridge downwards in buccal direction until it reaches the foot of the hypoconid. There is no cingulum.

The M_3 is quite worn. The anterior lobe is fused with the anterior cusps. The anterior lobe extends further in buccal direction then in lingual direction. From the posterior side of the protoconid goes a ridge downwards until the valley between the protoconid and the hypoconid. The metapoststylid, the hypoprestylid, the hypoconid and the entoconid are also fused. The heptaconid and the hexaconid are fused, although it is still visible that they used to be two cusps. From the hexaconid, a ridge goes downward until the posterior part of the foot of the entoconid. The posterior lobe is very vague and it ends at the pentaconid, which is round and separate. There are no accessory cusps, nor a cingulum.

Coll. Dub. 2191 There is not much to see in this M_2 (or M_3). The anterior lobe and the anterior cusps are fused. The anterior lobe extends further in buccal direction than in lingual direction. The hypoprestylid and the metapoststylid are also fused.

Coll. Dub. 2192 The anterior cusps of this M_3 are fused with the anterior lobe. The anterior lobe extends more to the buccal side than to the lingual side. The metapoststylid lies just a little bit lingually from the hypoprestylid. The hypo- and entoconid are fused. The heptaconid and the hexaconid are grown together. The heptaconid is attached to the hypoconid/entoconid. On the buccal side of the heptaconid are several cusps (one larger, two smaller) which form a ridge which ends at the posterior side of the foot of the hypoconid. An accessory buccal cusp lies on the posterior side of the protoconid. There is no accessory lingual cusp, nor a cingulum.

Coll. Dub. 2192b 1) Only the posterior part of this M_3 is preserved. The posterior cusps are hardly worn. The hypoconid is larger than the entoconid. The hypopostconulid is somewhat lower than the hypoconid and it is attached to it. The heptaconid touches the hypopostconulid. Lingually from the heptaconid lies the hexaconid, touching the heptaconid. The pentaconid is smaller than the heptaconid but larger than the hexaconid. The pentaconid is separated from the heptaconid. Between the posterior side of the pentaconid and the heptaconid is a crenulated ridge.

2) Only the posterior part of this M_3 is preserved. Part of the hypoconid is visible and the posterior part of the entoconid. The hypoconid is larger than the entoconid. The heptaconid touches the hypoconid. The heptaconid and the hexaconid are in contact. The hexaconid forms one cusp with the hexaconulid. The pentaconid is a separated cusp. The heptaconid is the largest of the three. The hexaconid (the hexaconulid included) is larger than the pentaconid. Between the heptaconid and the hexaconid on the lingual side and the pentaconid on the buccal side is a crenulated ridge.

Coll. Dub. 2194 In this M_3, the anterior lobe and the anterior cusps are fused. The anterior lobe extends further in buccal direction than in lingual direction. The posterior cusps are fused and so are the metapoststylid and the hypoprestylid. The heptaconid is fused with the hexaconid, although they can both be distinguished. The pentaconid is separated, round and lower than the heptaconid and the hexaconid. The heptaconid is the largest, the pentaconid is larger than the hexaconid. Posterior of the heptaconid is a posterior lobe which is crenulated and which ends at the hexaconid and the pentaconid. From the anterior side of the protoconid starts a crenulated cingulum until the foot of the hypoconid. From the metaconid starts a crenulated cingulum until the foot of the entoconid. There are no accessory cusps.

Coll. Dub. 2201 — On the lingual side of this very worn M_2, there are two very tiny cusplets below the level of the worn entoconid, one of which is situated in the transverse valley.

Coll. Dub. 2202 — In the M_2 the metaconid is larger than the protoconid. The protoconid is situated more anteriorly than the metaconid. The anterior lobe is not connected with or touching the proto- or metaconid. The anterior lobe descents and ends in a tubercle both on the lingual and buccal sides. The metapoststylid lies lingually from the hypoprestylid. The hypoconid is larger than the entoconid. Touching the posterior side of the hypoconid is the heptaconid, which forms one ridge with the hexaconid. The pentaconid is a separate cusp. At the foot of the hypoconid is a crenulated cingulum, which extends until the valley between the hypoconid and the protoconid. From the metaconid runs a crenulated cingulum until the foot of the entoconid.

The unworn M_3 is not yet fully erupted. The metaconid is larger than the protoconid. The anterior lobe is very low and still half-concealed in the jaw. It is connected with the protoconid. The metapoststylid is situated lingually form the hypoprestylid. The hypoconid is larger than the entoconid. Posterior of the hypoconid lies the heptaconid. They do not touch. The heptaconid forms one ridge with the hexaconid, which is going downwards on the lingual side. On the buccal side of the heptaconid is the pentaconid, which lies quite a bit lower than the heptaconid and is separated from the heptaconid. There are no accessory cusps nor cingula.

Coll. Dub. 2204b — The anterior part of this M_3 is broken off but it is visible where the molar ended. It looks as though the anterior lobe (broken) and the anterior cusps are fused. The anterior lobe goes downward in lingual direction until the anterior side of the foot of the metaconid. On the buccal side it goes also downwards until the anterior part of the foot of the protoconid. It ends in a little cusp. The hypoconid is larger than the entoconid. The metapoststylid lies just a tiny bit more lingually than the hypoprestylid. The hypoconid is larger than the entoconid. The heptaconid touches the hypoconid. The heptaconid and the hexaconid are grown together. From there it goes downwards and forms a vague cingulum until the valley between the metaconid and the entoconid. It ends in a thickening (not a cusp). Posterior of the heptaconid is the posterior lobe, which continues in buccal direction and ends in the pentaconid.

Coll. Dub. 2314 — In the M_2 the individual cusps cannot be distinguished anymore; they are worn into the trefoil pattern. The anterior lobe is fused with the protoconid/metaconid. It extends further in buccal direction than in lingual direction. From the buccal end of the anterior lobe there is a little ridge towards the protoconid. The metapoststylid is situated lingually from the hypoprestylid. The heptaconid and the hexaconid form one ridge; the pentaconid is a separate cusp. The heptaconid/hexaconid is fused with the hypoconid and the entoconid. In the valley between the hypoconid and the protoconid is a quite large buccal accessory cusp. Also in the lingual valley at the foot of the metaconid is a little tubercle present. There is no cingulum, but the molar is quite worn down, so it might have been present.

In the M_3 the protoconid and the metaconid are fused. The anterior lobe touches the anterior part of the protoconid. The anterior lobe has the same height as the wear surface. On the buccal side it continues until the buccal side of the protoconid. There it is lower than the wear surface. On the lingual side the anterior lobe runs downward until the foot of the metaconid. The anterior lobe extends further in buccal direction than in lingual direction. The metapoststylid is situated lingually from the hypoprestylid. The hypoconid and entoconid are nearly fused. The hypoconid is larger than the entoconid. The talonid consists of the heptaconid (which is fused with the hexaconid) and the pentaconid. Actually, the pentaconid consists of the pentaconid and the pentaconulid and is separated from the heptaconid. From the buccal side of the protoconid starts a little, crenulated ridge in posterior direction until the valley between the hypoconid and the protoconid. There is no cingulum.

Coll. Dub. 2318b

This M_3 is unworn. The protoconid and the metaconid are of about the same size. The protoconid lies more anteriorly than the metaconid and touches the anterior lobe. The anterior lobe is rather low. Anterior of the protoconid is a quite large cusp, which is part of the anterior lobe. On the buccal and lingual side it goes downwards. On the buccal side it is quite knobby. The anterior lobe extends further in buccal direction than in lingual direction. The metapoststylid is situated buccally from the hypoprestylid. This does not occur very often. The hypoconid is larger than the entoconid. The hypopostconulid is attached to the hypoconid. The heptaconid and the hexaconid are grown together, although it can still be seen that they used to be two cusps. Separate from the heptaconid lies the broken pentaconid and anteriorly of the pentaconid lies another little cusp. The heptaconid is touching the posterior part of the hypoconid. There are no accessory cusps, nor a cingulum.

Coll. Dub. 2319

The roots of the M_2 are coloured bluish.

The M_3 is very obliquely compared to the M_2. The posterior side is positioned much more to the lingual side than the anterior side. It is totally worn. The anterior lobe, the anterior cusps, the hypo- and entoconid, the metapost- and hypoprestylid, and the talonid are all fused due to wear. The only thing worth mentioning is that the pentaconid is still distinguishable as a separate cusp. It is circular.

Coll. Dub. 2903

The right M_3 is present, but not yet fully erupted. The protoconid and the metaconid are actually one large cusp, it is very hard to see where the one ends and the other begins. From the protoconid starts a ridge downwards in lingual direction. There is no anterior lobe. On the meta- or protopoststylid are some little tubercles. The hypoprestylid is not developed. The entoconid lies a bit more to the anterior side than the hypoconid. The entoconid is larger than the hypoconid. Posterior of the hypoconid is the anterior rim of the pentaconid visible. The talonid is still in the jaw.

Coll. Dub. 2905

In the M_2 the individual cusps cannot be distinguished anymore; they are worn into the trefoil pattern. The anterior lobe is fused with the protoconid/metaconid. From the anterior lobe there is a little ridge towards the protoconid. The metapoststylid is situated lingually from the hypoprestylid. The heptaconid (which is quite large) and the hexaconid form one ridge, the pentaconid is a separate worn cusp. On the lingual side there is no cingulum. On the buccal side there is a crenulated cingulum which extends from the protoconid until the foot of the hypoconid. There are no accessory cusps.

The M_3 is almost identical with Coll. Dub. 2314. The anterior cusps are fused, but it can still be recognised that the protoconid was situated more anteriorly than the metaconid. The anterior lobe is connected with the protoconid and has the same height as the wear surface. On the buccal side it continues until the buccal side of the protoconid. There it is lower than the wear surface. On the lingual side, the anterior lobe runs downwards until the foot of the metaconid. From the buccal side of the protoconid starts a little, crenulated ridge in posterior direction until the valley between the hypoconid and the protoconid. The metapoststylid is fused with the protoconid/ metaconid. The metapoststylid is situated lingually from the hypoprestylid. The metapoststylid lies in between the hypoprestylid and the entoprestylid. The hypoconid is larger than the entoconid. The talonid consists of the heptaconid (which is the largest), the hexaconid and the pentaconid. Actually, the pentaconid consists of the pentaconid and the pentaconulid forming one cusp. It lies lower than the other cusps of the talonid. The hexaconid is attached to the heptaconid. At the foot of the metaconid, on the posterior side, almost in the valley between the metaconid and the entoconid, is a little tubercle present. There is no cingulum.

Coll. Dub. 2906

The M_3 is positioned obliquely in the mandible; the anterior side of the M_3 is positioned more to the buccal side than the posterior side. The alveolus of the canine continues below the molars and can be seen even behind the M_3.

Coll. Dub. 2915

The only thing that can be seen in the right M_2 is the rather large accessory cusp in the valley on the buccal side between the protoconid and the hypoconid.

In the right M_3 the anterior cusps are fused with the anterior lobe. The anterior lobe goes downwards in lingual and buccal direction. The metapoststylid is situated buccally from the hypoprestylid, which is rare. The hypoconid and the entoconid are nearly fused, but it can still be seen that the hypoconid is larger than the entoconid. The talonid consists of the heptaconid and a posterior lobe, which goes downwards in lingual and buccal direction, starting at the heptaconid. The pentaconid and the pentaconulid form a ridge, that runs downwards to the foot of the hypoconid. The heptaconid is fused with the hexaconid. There is an accessory lingual cusp. On the buccal side there is only a thickening present, but no cusp. There is no cingulum.

Coll. Dub. 2916

The only thing that can be seen in this worn and damaged right M_1 is (part of) a cingulum on the buccal side between the protoconid and the hypoconid.

The M_2's are placed obliquely in the mandible; the posterior side is positioned more lingually than the anterior side. In the left M_2 all four main cusps, the anterior lobe, the metapoststylid, the hypoprestylid are all fused. There is no trace of any posterior cusps, but there is a posterior lobe, which is fused with the hypoconid/entoconid. There are no accessory cusps, nor any cingula.

In the right M_2, the protoconid and the metaconid are fused and so are the hypoconid and the entoconid. The anterior lobe is attached with the protoconid/metaconid but not entirely fused. The metapoststylid is situated lingually from the hypoprestylid. There is no trace of any posterior cusps, but there is a posterior lobe, which is fused with the hypoconid/entoconid. There is no cingulum. There is an accessory lingual cusp.

In the left M_3 the anterior lobe is fused with the anterior cusps. The anterior lobe extends more to the buccal side than to the lingual side. From the anterior lobe goes a very knobby ridge downwards in lingual direction. Also from the anterior lobe goes a ridge in buccal direction until the foot of the protoconid. The top of this ridge is of the same height as the wear surface. The metapoststylid is situated lingually from the hypoprestylid. The hypoconid and entoconid are fused. The talonid is damaged, but the posterior cusps can be distinguished. The heptaconid seems to be attached to the hypoconid. The hexaconid and the heptaconid are grown together and of the same height. The pentaconid is a round, separate cusp. There is no cingulum, nor any accessory cusps. It is not obliquely with respect to the M_2.

In the right M_3 the anterior cusps are fused, but the anterior lobe is still separate. This anterior lobe is quite robust and knobby. From the anterior lobe goes a ridge downwards in lingual direction. Also from the anterior lobe goes a ridge in buccal direction until the foot of the protoconid. The metapoststylid is situated lingually from the hypoprestylid. The hypoconid is larger than the entoconid, although the entoconid is damaged. The heptaconid is attached to the posterior part of the entoconid/hypoconid. The hexaconid is a bit lower than the heptaconid and they touch, but are not connected. The lower-lying pentaconid is round and separated from the heptaconid. It is more oval-shaped and it consists of the pentaconid and the pentaconulid forming one cusp. There is no cingulum. It is not obliquely with respect to the M_2.

Coll. Dub. 2917

In the M_1 the individual cusps cannot be identified. The two anterior cusps form a trefoil pattern with the anterior lobe and so do the hypo- and entoconid with the posterior lobe. The anterior lobe extends further in buccal direction than in lingual direction. The metapoststylid is situated lingually from the hypoprestylid. At the posterior lobe starts a cingulum to the lingual side until the valley between the metaconid and the entoconid. This cingulum has a crenulated appearance. On the buccal side a cingulum is present from the posterior lobe until the valley between the hypoconid and the protoconid. It ends in a flat accessory buccal cusp. Here the cingulum is not crenulated. On the buccal side of the anterior lobe is a little tubercle present, which is somewhat lower than the anterior lobe. The cingulum on the lingual side is lower than on the buccal side.

The M_2 is not very worn. The protoconid is larger than the metaconid. The protoconid is situated more anteriorly than the metaconid. The anterior lobe, which is quite knobby, extends on the buccal side into a crenulated cingulum, which ends in the valley between the protoconid and the hypoconid. The anterior lobe is not connected to the protoconid or the entoconid. The protopoststylid lies lingually from the hypoprestylid. The hypoconid is larger than the entoconid. Behind the hypoconid, the heptaconid is present. There is a posterior lobe, which is quite knobby and just a bit lower than the heptaconid. The posterior lobe extends on the lingual side until the foot of the entoconid and on the buccal side until the foot of the hypoconid.

The M_3 has a separate number (Coll. Dub. 2922) and is glued to the mandible. Could this mean that this M_3 is glued to the wrong mandible and that it actually belongs to the mandible fragment Coll. Dub. 2922? The M_3 is totally unworn. The metaconid is larger than the protoconid. The anterior lobe is very knobby. It does not continue on the lingual side and is not attached to the protoconid. On the buccal side the anterior lobe continues into a crenulated cingulum which ends in an accessory buccal cusp. The cingulum and the anterior lobe are quite low. The metapoststylid is situated lingually from the hypoprestylid. The hypoconid is larger than the entoconid. The hypopostconulid is somewhat lower than the hypoconid. The talonid consists of the heptaconid and a posterior lobe. From the heptaconid starts a crenulated posterior lobe, which continues on the lingual side until the foot of the entoconid. On the posterobuccal side the posterior lobe consists of three little tubercles. On the lingual side there is no accessory cusp, but there is a little thickening present.

Coll. Dub. 2922

In the M_1 the individual cusps cannot be identified. The two anterior cusps form a trefoil pattern with the anterior lobe and so do the two posterior cusps and the posterior lobe. The metapoststylid is situated lingually of the hypoprestylid. On the lingual side, a cingulum is present, which starts from the posterior lobe downward and which ends in a little accessory lingual cusp in the valley between the metaconid and the entoconid. At the buccal side a cingulum starts from the posterior lobe until the valley between the hypoconid and the protoconid. This cingulum is higher than on the lingual side. There are two little tubercles between the protoconid and the anterior lobe. They are somewhat lower than the wear surface. The buccal side is smaller than the lingual side. There are no posterior cusps.

In the M_2 the protoconid is larger than the metaconid. The protoconid and the metaconid are both touching the anterior lobe. The protoconid is not situated more anteriorly than the metaconid. There is clearly an anterior lobe, which is lower than the anterior cusps. From the protoconid runs a ridge downwards to the buccal side, which ends in a cusp. There is no sign of a metapoststylid nor a hypoprestylid. Only part of the hypoconid is present; its posterior part and the entoconid are missing or very damaged. On the posterobuccal side are two cusps which are lower than the hypoconid. They vaguely form a cingulum, which continues until the foot of the hypoconid. In the valley between the hypoconid and the protoconid are three little tubercles.

Coll. Dub. 3147 — The right M_2 is totally worn; there is nothing left of the morphology. It is positioned obliquely relative to the axis of the jaw: the posterior part of the M_2 is turned more to the lingual side than the anterior side. M_3 shows the same phenomenon, but even more strongly.

The M_3 is much larger than the other M_3's. It is positioned very obliquely with respect to the axis of the jaw. The posterior side is positioned much more to the lingual side than the anterior side. It is very worn and all the cusps are fused. The talonid is quite large and also very worn; no individual cusps can be recognised. There is a cingulum from the anterior side of the hypoconid, which continues into the posterior lobe and from there it continues on the lingual side until the posterior side of the metaconid. On the buccal and posterior sides it is a bit crenulated. The enamel ridges are quite thick.

Coll. Dub. 4857 — The only detail that can be distinguished in this broken M_3 is the presence of the talonid with the heptaconid and the pentaconid. No measurements were taken.

Coll. Dub. 6927 — 1) This anterior part of a M_2 is very worn and all the cusps are fused. The only thing that can be seen is that the anterior lobe extends further in buccal direction than in lingual direction.

Coll. Dub. 6954 — 7) The posterolingual side of this M_2 is broken off and also part of the meta- and protoconid are broken. On the anterior side is an indentation, which represents the position of the M_1. The protoconid and metaconid are fused due to wear. The anterior lobe is also fused and it extends further in buccal direction than in lingual direction. What is left of the hypoconid and entoconid, also seems to be fused. There is a cingulum both on the buccal and on the lingual sides. The cingulum on the buccal side is on the same level as the wear surface and is connected with the anterior lobe. It continues until the hypoconid. The cingulum on the lingual side is much lower and it starts from the anterior lobe, but it is not connected with it.

Coll. Dub. 11463 — On the anterior side of this damaged M_1 is an indentation, which represents the position of the P_4. The proto- and metaconid are fused with the anterior lobe. Also the metapoststylid, the hypoprestylid, the hypoconid and what is left of the entoconid are fused. From the anterior lobe starts a cingulum on the buccal side until the foot of the protoconid. Posterior of the protoconid, there is another part of the cingulum. It is not crenulated. The whole posterior and lingual part is missing. According to the cingulum, which is mostly present on the buccal side, it is likely that it is a right one.

Coll. Dub. 11464 — In this posterior part of a M_3, the hypoconid is larger than the entoconid. Attached to the hypoconid is the hypopostconulid. The heptaconid touches the hypopostconulid and is connected with the hexaconid. The pentaconid consists of a little knobby ridge and is separated from the heptaconid.

JA 68 — The proto- and metaconid of this M_2 are fused due to wear. The anterior lobe does not extend towards the lingual or buccal side. The metapoststylid is situated lingually from the hypoprestylid. The hypo-and entoconid are fused due to wear. The posterior lobe is present but damaged. Due to the damage it is uncertain if there are any posterior cusps. There is no cingulum, nor on the lingual side, nor on the buccal side. There are no accessory cusps.

VII.8 UPPER MOLARS

The measurements are given in the Appendix VI-21 – VI-23.

Specimens without description:
without number (skeleton, Geological Museum Bandung); no. 366; K 655/1; K 655/2; K 655/3; K 674/1; K 674/2; K 674/3; Coll. Dub. 285/6; Coll. Dub. 285/7; Coll. Dub. 285/8; Coll. Dub. 308a.

Description of the specimens:

K 15-947 In the M^2, the metacone is larger than the tetracone and the paracone is larger than the protocone. The tetraprestyle lies opposite the protopoststyle. The metaprestyle lies opposite the parapoststyle. The metaprestyle extends more to the anterior side than the tetraprestyle. A cingulum is present both on the lingual and buccal sides. The cingulum is more robust on the buccal side. There is a posterior lobe. There is no anterior lobe.

In the M^3 the metacone is larger than the tetracone and the paracone is larger than the protocone. The tetraprestyle lies opposite the protopoststyle. The metaprestyle lies opposite the parapoststyle. The metaprestyle extends more to the anterior side than the tetraprestyle. There is an anterior lobe and a posterior lobe, which both continue into a cingulum on the buccal side. On the lingual side there is no cingulum. There is a little additional cusp posterior and attached to the tetracone (tetrapostconule).

M - 18 The M^1 is very worn. As far as can be seen, there are no anterior and posterior lobes. There is a cingulum, both on the lingual and buccal sides. On the lingual side the cingulum is more robust than on the buccal side. It is too worn to see how the anterior extensions of the posterior cusps are situated compared to the posterior extensions of the anterior cusps.

The M^2 is also quite worn but the four main cusps are distinguishable. The lingual cusps are larger than the buccal cusps. The tetraprestyle lies opposite the protopoststyle. The metaprestyle lies opposite the parapoststyle. The metaprestyle extends more to the anterior side than the tetraprestyle and touches the parapoststyle. The tetraprestyle is not connected with the protopoststyle. There is an anterior and a posterior lobe, which continues into a cingulum, both on the lingual and the buccal sides.

In the M^3 the lingual cusps are larger than the buccal cusps. The tetraprestyle lies opposite the protopoststyle and they touch each other. The metaprestyle lies opposite the parapoststyle and they touch each other. Behind the metacone is a separate cusp (metapostconule), which is connected with the posterior lobe. There is a cingulum on the lingual and buccal sides. There is no anterior lobe.

K 672 The anterobuccal part of this M^2 is missing and the anterolingual side is very damaged. It looks as though the protopoststyle lies opposite the tetraprestyle. The posterior cusps are quite worn. The tetracone is larger than the metacone. They have a trilobate shape. The tetrapoststyle continues into the posterior lobe. There is a low cingulum on the lingual side. The anterior lobe seems to be connected with the protocone and is quite knobby.

K 676 This M^2 is unworn. The two buccal cusps (para- and metacone) are star-shaped; the two lingual cusps (proto- and tetracone) have three styles (trilobate). The protoprestyle forms the anterior lobe, which continues until the anterior rim of the paracone. The paraprestyle touches the anterior lobe. A little style from the paracone goes into the direction of the protocone. In between and touching with this style and the protocone, is a separate elongated cusp, which acts as the protopoststyle. The posterior edge of this elongated cusp lies opposite the tetraprestyle. The tetrapoststyle forms the posterior lobe, which is connected with the metapoststyle. The parapoststyle is situated buccally from the metaprestyle. On the lingual side is a cingulum. On the buccal side there is no cingulum.

K 694 The main cusps of this M^3 are trilobate. The protopoststyle lies opposite and touches the tetraprestyle, the parapoststyle lies opposite and touches the metaprestyle. The protocone is larger than the paracone. The protoprestyle forms the anterior lobe, which continues on the buccal side until the buccal rim of the paracone. The metapoststyle forms the posterior lobe, which continues on the buccal side until the buccal rim of the metacone. The lingual side is damaged, so it is not sure if there has been a cingulum on that side.

K 705 This M^2 is very worn. All cusps are fused. The only features worth mentioning are the presence of two accessory cusps, one on the lingual side, one on the buccal side. The one on the lingual side is larger.

The M^3 is quite worn. The anterior lobe is fused with the anterior cusps. The protopoststyle lies opposite and touches the tetraprestyle. The parapoststyle lies opposite and touches the metaprestyle. On the lingual side is a low cingulum, which ends in an accessory lingual cusp. There is also an accessory buccal cusp. The posterior lobe is connected with the metacone. It is not visible if it continues into a buccal cingulum, because the buccal side is damaged.

K 723 4) This M^2 is quite worn. The paracone, protocone and the anterior lobe are fused due to wear. The parapoststyle lies opposite the valley between the meta- and tetracone. The protopoststyle is not very distinct, but larger than in K 749. The posterior cusps are also fused. The posterobuccal side is broken off. There is an accessory lingual cusp. There is a low cingulum on the lingual side only.

K 734 1) In the M^1 the para- and protocone are fused due to wear. The posterior cusps are damaged because the posterobuccal side is broken off. The para- and protopoststyle are situated buccally and lingually of the meta- and tetraprestyle respectively; the first two styles "embrace" the latter two styles. The anterior lobe ends on the buccal side at the anterior foot of the paracone. On the lingual side it continues into a low cingulum and the posterior lobe. On the lingual side, the cingulum is quite crenulated. Also on the buccal side, a cingulum is present as far as can be seen due to the damage. There is a low crenulated ridge, which runs from the lingual cingulum towards the anterior rim of the tetracone.

2) The M^2 is unworn. The two buccal cusps (para- and metacone) are star-shaped; the two lingual cusps (proto- and tetracone) are trilobate. The protoprestyle forms the anterior lobe, which continues until the anterior rim of the paracone. The paraprestyle touches the protoprestyle. A little style from the paracone goes into the direction of the protocone. In between and touching with this style and the protocone is a separate elongated cusp, which acts as the protopoststyle. The posterior edge of this elongated cusp lies opposite the tetraprestyle. The tetrapoststyle forms the posterior lobe, which is connected with the metapoststyle. The parapoststyle is situated buccally from the metaprestyle. On the lingual side is a cingulum. On the buccal side there is no cingulum.

K 749

The M^1 is quite worn down. Both the anterior and posterior cusps are fused. The molar is too worn to distinguish the position of the proto- and parapoststyles and the tetra- and metaprestyles. There is an anterior lobe, which is connected with a cingulum on the buccal side. The posterior lobe cannot be distinguished due to wear. There are two accessory buccal cusps, the larger of which is situated more buccally than the smaller one.

In the M^2, the protocone, paracone and the anterior lobe are fused due to wear. As are the meta- and tetracone, although the valley between the meta- and tetracone is still visible. The parapoststyle lies opposite the valley between the meta- and tetracone. The protopoststyle is not very distinct. There is a cingulum both on the lingual and the buccal sides.

The M^3 is unworn. The protocone is circular with an extension towards the anterior side. This protoprestyle forms the anterior lobe and it also continues into a vague low lingual cingulum until the valley between the proto- and tetracone. The paracone is also circular with an extension in posterior direction (parapoststyle). There is a crenulated paraprestyle, which is very tiny. The meta- and tetracone are two cusps, with no extensions in any direction. The tetracone is larger than the metacone. There is a posterior lobe, which is not connected to any of the posterior cusps. On the buccal side there is no cingulum.

Coll. Dub. 100

5) The meta- and tetracone of this M^3 are of the same size. There is a style in anterior direction but it is not clear if it is the meta- or tetraprestyle. Behind the meta- and tetracone is a cusp (meta- or tetrapostconule). The posterior lobe is present and it extends a bit (till the broken edge) on the lingual side as a cingulum.

Coll. Dub. 163a

The cusps of this M^3 are hardly worn. The paracone extends further to the posterior side than the protocone. The protocone is connected with the anterior lobe. The parapoststyle is situated more buccally than the metaprestyle. The parapoststyle ends in a cusplet. The tetracone lies more to the posterior side than the metacone. The tetracone is connected with the posterior lobe, which lies below the level of the cusps. The metapostconule and the tetrapostconule form part of the posterior lobe. From the anterior lobe starts a cingulum on the lingual side and ends in the posterior lobe. This cingulum is a bit crenulated. On the buccal side there is a cingulum from the posterior lobe until the foot of the metacone and from the anterior lobe until the transverse valley. Only the anterior part of this buccal cingulum is slightly crenulated. The cingulum on the lingual side is higher than on the buccal side. From the tetracone runs a tiny ridge downwards and ends at the cingulum on the lingual side.

Coll. Dub. 314a 1) and 2). The morphology of these M^3's (a left and a right one) is similar. The molars are unworn. The paracone extends more to the posterior side than the protocone. The protocone is connected with the anterior lobe. The anterior lobe is knobby. The parapoststyle is situated opposite the metaprestyle in the right M^3, in the left M^3 it is situated a bit more buccally. The metacone and the protocone are not touching. The metacone and the tetracone are of similar size. The posterior lobe is not connected to the meta- or tetracone. There are two cusplets behind the meta- and tetracone (meta- and tetrapost-conule). There is no cingulum.

Coll. Dub. 325f 3) In this M^2, the anterior part of the paracone is broken off. The paracone extends just a bit more posteriorly than the protocone. The protocone is connected with the crenulated anterior lobe. The parapoststyle lies lingually (!) from the metaprestyle. The metacone is larger than the tetracone. Behind the meta- and tetracone is the meta- or tetrapostconule, which is connected with the crenulated posterior lobe. The crenulated cingulum forms one entity with the anterior and posterior lobes and is present on all sides.

Coll. Dub. 1702 The right M^1 is quite worn. The anterior lobe is fused with the para- and protocone. The posterior lobe is fused with the meta- and tetracone. The parapoststyle is situated a bit more buccally than the metaprestyle. Due to wear, the protopoststyle and the tetraprestyle are hard to distinguish. It is not sure if there has been a cingulum on the lingual side, due to wear. On the buccal side there is however a quite robust cingulum which starts from the anterior lobe and ends against a worn accessory buccal cusp, which is situated not really in the transverse valley but anterobuccally of the metacone. There is a little ridge that runs from the buccal side of the paracone to the cingulum.

Both M^2's show an indentation on the posterobuccal side. In this indentation, the protocone of the M^3 is placed. Both M^2's have almost the same description. The anterior lobe is fused with the proto- and paracone. The anterior lobe extends further in buccal direction than in lingual direction. The parapoststyle is situated buccally from the metaprestyle. Also the protopoststyle is situated buccally from the tetraprestyle. The meta- and tetracone are fused with the posterior lobe. Both on the buccal and the lingual sides, a cingulum is present. The cingulum on the lingual side is quite robust. It runs from the anterior lobe to the posterior lobe. In the left M^2 the cingulum is not connected nor with the anterior, nor with the posterior lobe. In the right M^2 the cingulum is both connected with the anterior and the posterior lobe. An accessory cusp in the right M^2 is situated In the lingual transverse valley, as part of the cingulum. The connection with the posterior lobe exists of several tiny cusplets. The cingulum on the buccal side is crenulated in both M^2's. It starts on the buccal side of the metacone, runs downwards, then again a little upwards, then downwards again, then upwards until the anterior lobe.

Both the M^3's are very similar. The paracone extends more posteriorly than the protocone. In the left M^3, the parapoststyle is situated buccally from the metaprestyle and they touch. In the right M^3 this is not clear; they are more opposite each other. The posterior cusps are very simple. The metacone is larger than the tetracone, which is not more than a simple circular cusp in the left M^3. In the right M^3, the tetracone is damaged. From the protocone runs a crenulated cingulum downwards at the buccal side, goes upwards again below the paracone. Below the metacone it is very crenulated. Its height is near the wear surface of the molar. It stays high until the tetracone and then it goes downwards again until the protocone where it rises again. The cingulum is present along the whole margin of the molar and is very crenulated in both M^3's. There are no anterior or posterior lobes. The right M^3 has three extra cusplets, one between the meta- and tetracone and the other two in the centre at the anterolingual side of the metacone.

Coll. Dub. 2004

The M^2 is broken in half. The buccal side is missing, although the outline is still visible. The anterior lobe is fused with the protocone. The protopoststyle is situated opposite the tetraprestyle. The tetracone is fused with the posterior lobe. There is a cingulum on the lingual side.

The buccal side of the M^3 is broken off. The proto- and paracone are fused with the anterior lobe due to wear. The parapoststyle is situated buccally from the metaprestyle. The tetra- and metacone are connected with the posterior lobe. The metacone has a triangular shape. From the posterior lobe goes a ridge downwards both in lingual and buccal direction. On the buccal side it cannot be seen if there is a cingulum, due to the damage. There is a cingulum on the whole lingual side, the anterior part of which is lying higher than the posterior part.

Coll. Dub. 2008b

1) The proto- and paracone of this M^2 are worn; the meta- and tetracone are not yet worn. The tetracone is a bit damaged. The parapoststyle lies buccally from the metaprestyle, but they do not touch. The protopoststyle is not developed. The crenulated anterior lobe is connected with the protocone and continues on the buccal side until the foot of the paracone. On the lingual side is a crenulated cingulum from the protocone downwards until the transverse valley. The posterior lobe is connected with the tetracone, which continues into a crenulated cingulum on the buccal side until the foot of the metacone. An extra cusp (tetrapostconule) is present posterior of and a bit lower than the tetracone.

2) The morphology of this M^2 is similar to the one just mentioned. The only differences are: a) the tetracone is not damaged; b) the parapoststyle and the metaprestyle do touch; c) the protopoststyle is developed; d) in the transverse valley on the buccal side are tiny knobs present; e) the anterior lobe continues onto a cingulum on the lingual side until the anterior part of the tetracone; f) the posterior lobe

does not continue into a cingulum.

Coll. Dub. 2017 3) Only the meta- and tetracone of this M^2 are preserved. The metacone is situated more to the anterior side than the tetracone. On the lingual side part of a cingulum can be distinguished.

Coll. Dub. 2023c This M^1 is very worn but some characteristics can still be distinguished. It is damaged on the posterior side and partly on the anterior side. The anterior lobe is present and continues further on the lingual side compared to the buccal side. Nearly all four cusps are fused. It can be distinguished however, that the protopoststyle is situated lingually from the tetraprestyle.

Coll. Dub. 2076 12) Only the anterior cusps of this M^3 are preserved. The paracone extends further to the posterior side than the protocone. The anterior lobe is both connected with the para- and protocone. The anterior lobe extends both on the lingual and the buccal sides until the broken edge of the molar.

13) Only the anterior part of this M^3 is preserved. The proto- and paracone are of the same size. The protocone is connected with the anterior lobe. From the anterior lobe starts a crenulated cingulum on the lingual side until the front of the proto- and paracone, where the molar is broken off. The protocone is star-shaped, with a style in buccal direction. The paracone has a trefoil pattern. From the anterior part of the paracone starts a crenulated cingulum until the foot of the paracone.

14) Only the posterior part of this M^3 is preserved. If the position of the metacone and tetracone is interpreted correctly it is a left one. The metacone is larger than the tetracone. The crenulated posterior lobe is connected with the metapostconule, which lies posterior of the metacone. On the lingual side there is a crenulated cingulum until the place where the molar is broken. The molar is unworn.

15) Only the posterior part of this M^3 is preserved. The metacone is larger than the tetracone. The quite robust posterior lobe is connected with the metacone. The rest of the molar is broken.

Coll. Dub. 2077a 2) The protocone of this M^2 is worn, the paracone is slightly worn and both posterior cusps are unworn. The para- and protocone are connected with the anterior lobe. The paracone is star-shaped with a little extension is lingual direction and touching the protocone. The paracone is larger than the protocone and extends more backwards. The parapoststyle is situated buccally from the metaprestyle. The position of the protopoststyle compared to the tetraprestyle is not clear, as they are lying far apart. The metacone is larger than the tetracone and extends more forwards. The metacone also has an extension in lingual direction towards the tetracone, but this extension is very small. The tetracone is connected with the posterior lobe, which is crenulated. A bit under the posterior lobe starts a cingulum on the lingual side, which goes downwards until the foot of the tetracone and goes up again to the anterior lobe. This cingulum is very crenulated. On the buccal side is also a crenulated cingulum, which goes downwards until the foot of the metacone and goes up again to the anterior lobe. From the paracone goes a crenulated little ridge downwards towards the cingulum. Of this isolated molar, the roots are very well visible. The bottom side consists of an anterior part and a posterior part, divided by indentations; the indentation on the buccal side is wider and larger than on the lingual side. There are two roots, one on the anterior side, one on the posterior side. They are very small in anteroposterior direction and large in linguabuccal direction. They are likely to consist of two roots fused together. On the lingual side they are lying close together and diverge in buccal direction.

Coll. Dub. 2077b

This M^3 resembles very much the M^2 of Coll. Dub. 2077a/2. The molar is unworn. The paracone extends more to the posterior side than the protocone. The protocone is connected with the anterior lobe. The parapoststyle is situated more buccally than the metaprestyle. The tetracone is connected with the posterior lobe. A cingulum is present both on the buccal and on the lingual side. The cingulum is not so crenulated as in 2077a/2.

Coll. Dub. 2077c

1) The anterior part of this M^2 is broken, the proto-, meta- and tetracone are damaged. The molar is unworn. The paracone extends more backwards than the protocone. The parapoststyle is situated more buccally than the metaprestyle. The metacone is larger than the tetracone and extends more forwards. The positions of the protopost-style and the tetraprestyle are not clear. Both meta- and tetracone are connected with the posterior lobe. On the lingual side is a crenulated cingulum with a little cusp below the tetracone. On the buccal side the anterior lobe can be distinguished, which goes down until the foot of the paracone, where a crenulated ridge rises upwards. From the posterior lobe a cingulum goes downwards where it continues, crenulated, until the posterior foot of the paracone. The cingulum on the buccal side is not continuous.

2) Only the anterior part is preserved. The morphology of this M^2 or M^3 resembles very much the morphology of Coll. Dub. 1702 (M^3), Coll. Dub. 2008b/1 (M^2), Coll. Dub. 2008b/2 (M^2), Coll. Dub. 2077a/2 (M^2) and Coll. Dub. 2077c/1 (M^2).

Coll. Dub. 2079

The left and right M^2 are quite worn. In both molars the proto- and paracone are fused with the anterior lobe. The meta-, tetra-cone and posterior lobe are also fused due to wear. On the lingual side there is a low cingulum from the posterior lobe until the posterior part of the foot of the protocone.

In both M^3's, the protocone, paracone and anterior lobe are fused due to wear. The metacone, tetracone and posterior lobe are also fused. The parapoststyle is situated buccally from the metaprestyle. From the posterior lobe goes a little ridge downwards until the posterior part of the foot of the metacone. There is no cingulum on the buccal side. On the lingual side, the posterior lobe continues into a cingulum, which ends at the anterior lobe. This lingual cingulum has the same height as the wear surface. In the left M^3 there is a low-lying small cusplet at the lingual side of the anterior lobe. In the right M^3 there is a low-lying cusplet under the paracone.

Coll. Dub. 2080a

The paracone, protocone and the anterior lobe of this M^3 are fused due to wear, and so are the metacone, tetracone and the posterior lobe. The parapoststyle is situated buccally from the metaprestyle. The protopoststyle is fused with the tetraprestyle. On the whole lingual side there is a cingulum of the same height as the wear surface. It is connected with the posterior lobe and ends against the anterior lobe. On the buccal side, a cingulum starts from the posterior lobe and ends in a cusplet at the foot of the metacone. From the anterior lobe, a cingulum, a bit crenulated, starts, which ends in the central valley. These cingula come close together, but they are separated.

Coll. Dub. 2084b

In the M^2, the anterior lobe is fused with the para- and protocone. The anterior lobe has a slight indentation, which indicates the place of the M^1. The anterior lobe extends further to the lingual side than to the buccal side. The parapoststyle is situated buccally from the metaprestyle (!). The protopoststyle is situated lingually from the tetraprestyle. The meta- and tetracone are fused with the posterior lobe. Although the cusps are quite worn, it can still be distinguished that the metacone is star-shaped with an extension towards the tetracone. On the posterolingual side is an indentation, which indicates the place of the M^3. On the buccal side starts a robust, crenulated cingulum downwards until the foot of the metacone, then it goes upwards again towards the paracone. Anterior of the paracone it goes downwards again. Also on the lingual side is a cingulum, which is not crenulated but quite broad. The cingula are not connected, nor with the anterior, nor with the posterior lobes.

In the M^3, the paracone extends much further in posterior direction than the protocone. The protocone in connected with the anterior lobe. The parapoststyle lies opposite the metaprestyle. The metacone extends further in posterior direction than the tetracone and touches the posterior lobe. The posterior lobe lies lower than the posterior cusps. There is a metapostconule. The cingulum on the lingual side starts at the posterior lobe downwards and then up again until the transverse valley. It continues until the anterior lobe, although there is a slight interruption in the cingulum. On the buccal side, the cingulum starts from the posterior lobe downwards until it ends at a cusp in the transverse valley. From the anterior lobe, the cingulum goes downwards and then up again until it ends in two little cusplets in the transverse valley. The cingulum is quite robust and is lower on the buccal side than on the lingual side.

In this specimen, the M^2 is a "*palaeindicus*-type" (parapoststyle lies buccally from metaprestyle) molar, whereas the M^3 is of the "*sivalensis*-type" (parapoststyle lies opposite the metaprestyle), so this feature can never be used to discriminate between (sub)species, as Hooijer (1950) did.

Coll. Dub. 2182

5) The anterior lobe of this M^1 is fused with the proto- and paracone. The posterior lobe is fused with the, not yet completely fused, meta- and tetracone. The parapoststyle is situated just a little buccally from the metaprestyle. The protopoststyle is situated opposite the tetraprestyle, but the latter is broader than the former and the tetraprestyle extends a bit more to the buccal side. There is a cingulum on the lingual side, which is connected with the posterior

lobe. It is not connected with the anterior lobe. The cingulum is interrupted near the tetracone. On the buccal side is a cingulum from the posterior lobe to the transverse valley.

Coll. Dub. 2188

In the M^1, the anterior lobe is fused with the proto- and paracone. The posterior lobe is fused with the meta- and tetracone. The parapoststyle is situated buccally from the metaprestyle. The position of the protopoststyle and the tetraprestyle is not very clear, because the former is very small and they do not touch. They seem to be more or less opposite each other. On the lingual side is a cingulum present, which ends on the anterior side against the anterior lobe. On the buccal side is also a cingulum, but only on the posterior side. It ends at the transverse valley. It is not clear if the cingula are connected with the posterior lobe, because part of the posterior lobe is broken off.

The M^3 is unworn, but only the anterior part is preserved. The rest is broken off. The paracone extends more to the posterior side than the protocone. The protocone is connected with the anterior lobe.

Coll. Dub. 2195a

The M^2 is very worn. All cusps, anterior and posterior lobes are fused to one surface. However, the contours of the anterior lobe are still visible. From the buccal side of the posterior lobe, a ridge goes downwards and ends in a cusplet. Anterior of this cusplet is another cusp in the transverse valley (accessory buccal cusp).
In the M^3 the anterior lobe, the paracone and the protocone are fused due to wear, and so are the tetracone, the metacone and the posterior lobe. The parapoststyle is situated buccally from the metaprestyle. On the buccal side, there is a crenulated cingulum from the anterior lobe to the posterior lobe. On the lingual side there is also a cingulum, but it is not crenulated. It runs from the anterior lobe until the posterior lobe.

Coll. Dub. 2195b

The M^1 is quite worn but some morphological features can still be distinguished. The anterior lobe can be distinguished. The proto- and paracone are fused. The parapoststyle is situated buccally of the metaprestyle. The protopoststyle is situated buccally of the tetraprestyle. The meta- and tetracone are also fused. The posterior lobe cannot be distinguished due to wear. Due to the wear it cannot be seen if there has been a cingulum.

The M^2 is quite worn. The anterior lobe is fused with the proto- and paracone. The anterior lobe extends further in buccal direction than in lingual direction. The molar is too worn to say anything about the positions of the several styles. The meta- and tetracone are fused with the posterior lobe. The posterobuccal side is broken off. On the buccal side there is an accessory cusp. The molar is too worn to distinguish any cingula.

Coll. Dub. 2203

The M^2 shows a indentation on the posterobuccal side. In this indentation, the protocone of the M^3 is placed.

The M^2 is quite worn. The anterior lobe is fused with the para- and protocone. The anterior lobe extends further in lingual direction than in buccal direction. The parapoststyle is situated buccally from the metaprestyle. The position of the other styles is not clear due to wear. The meta- and tetracone are fused with the posterior lobe. From the posterior lobe goes a crenulated cingulum downwards on the buccal side and then up again and ends at the posterior rim of the paracone. On the lingual side no cingulum can be distinguished.

The M^3 is very similar to the M^2. The only difference is that the cingulum on the buccal side ends in a robust cusp in the transverse valley (accessory buccal cusp).

Coll. Dub. 2205

1) The paracone of this M^3 extends further to the posterior side than the protocone. The protocone is connected with the anterior lobe. The parapoststyle is situated buccally from the metaprestyle. Both the proto- and paracone are star-shaped. The metacone is larger than the circular tetracone and is connected with the posterior lobe. The anterior and posterior lobes continue into a cingulum on the entire lingual side. On the buccal side, the cingulum extends from the anterior lobe until under the paracone, and from the posterior lobe until the foot of the metacone. The metacone is slightly damaged.

2) The paracone of this M^3 extends more to the posterior side than the protocone. Both these cusps show a trefoil pattern. The protocone is connected with the anterior lobe. The parapoststyle is situated buccally from the metaprestyle. The metacone is larger than the tetracone. The metacone is connected with the posterior lobe. The metacone has a triangular shape and the tetracone is oval-shaped. The anterior and the posterior lobes form part of the cingulum that is present both on the lingual and buccal sides. In the transverse valley on the buccal side, the cingulum is vague. There are two little cusplets on the posterior lobe (meta- and tetrapostconule).

Coll. Dub. 2318a

The anterior lobe of this M^2 is fused with the proto- and paracone. The buccal rim of the anterior lobe is missing. The parapoststyle is situated buccally from the metaprestyle. The protopoststyle is situated opposite the tetraprestyle. The metacone is star-shaped with an extension in the direction of the tetracone. Both tetra- and metacone are fused with the posterior lobe. The buccal side is too damaged to distinguish the presence of a cingulum. From the buccal side of the posterior lobe a ridge goes downwards to the foot of the metacone. On the lingual side, the anterior lobe continues into a ridge, which is at the same level as the rest. This is a remnant of a lingual cingulum. It does not continue to the posterior side, but the middle part of the molar is damaged, so it might have continued further.

Coll. Dub. 2318d

This M^3 is hardly worn and it has the simple morphology of a M^3. It is also not as rectangular as a M^2. The protocone is more worn than the paracone; the tetra- and metacone (moon-shaped) are unworn. The protocone has an extension in buccal direction. The parapoststyle is situated buccally from the metaprestyle although according to Hooijer (1950) this molar is of the "*sivalensis*-type" (parapoststyle never extends buccally beyond the metaprestyle). The protopoststyle lies buccally from the tetraprestyle, The anterior lobe is connected with the protocone and extends both in lingual and buccal direction into a crenulated cingulum. On the buccal side there is an accessory buccal cusp that is part of the cingulum. On the lingual side it ends at an accessory lingual cusp at the anterior part of the foot of the tetracone. Somewhat lower than the posterior cusps and posteriorly of them, there are two little cusplets, which form part of the posterior lobe, which goes downwards on both sides. At the lingual side it ends at the posterior foot of the tetracone and on the buccal side is continues into the cingulum.

Coll. Dub. 2318e The para- and protocone are fused due to wear. The protocone is fused with the anterior lobe. The parapoststyle is situated lingually from the metaprestyle. The metacone is larger than the tetracone. They are fused with the posterior lobe. From the anterior lobe goes a ridge downwards until the anterior part of the foot of the protocone. On the buccal side a cingulum starts from the anterior lobe until the anterior foot of the metacone and ends in a little cusplet. On the lingual side there is no cingulum. On the posterobuccal part of the metacone, a flattened cusp (metapostconule) is present.

Coll. Dub. 2902 The anterior part of the M^2 is broken. The proto- and paracone are fused. The different styles cannot be distinguished due to wear. The meta- and tetracone are fused with the posterior lobe. From the buccal rim of the anterior lobe, a buccal cingulum goes downwards to the anterior rim of the foot of the metacone.

In the M^3, the metacone is larger than the tetracone. The lingual part of the tetracone is broken off. The parapoststyle is situated buccally from the metaprestyle. The para- and protocone are fused with the anterior lobe due to wear. The protopoststyle is situated buccally from the tetraprestyle. The meta- and tetracone extend posteriorly into the posterior lobe, which goes downwards on the buccal side, until the foot of the metacone. Also on the lingual side it goes downwards and forms a cingulum, which ends at the lingual side of the anterior lobe. The cingulum is not crenulated. From the anterior lobe runs a ridge downwards until the foot of the paracone on the buccal side. On the buccal side there is no cingulum.

Coll. Dub. 2907 In the M^2, the protocone, paracone and the anterior lobe are fused due to wear and so are the metacone, tetracone and posterior lobe. The tetra- and metaprestyles are not well developed and it cannot be distinguished how their position is with respect to the proto- and parapoststyles, although according to Hooijer (1950) it is of the "*sivalensis*-type". There is no cingulum on the buccal side. On the lingual side, the cingulum ends against the posterior lobe. On the anterior side the cingulum has the same height as the wear surface, on the posterior side it is lower than the wear surface. There is an accessory lingual cusp.

The left and right M^3 are very similar. The trefoil-shaped paracone extends more to the posterior side than the trefoil-shaped protocone. The protocone is connected with the anterior lobe. The parapoststyle is situated buccally from the metaprestyle. In the right M^3 the metacone is damaged and the metaprestyle is not very well visible. In the left M^3, the tetracone is larger than the metacone. In the right M^3 they are of the same size (the tetracone in the right M^3 is damaged). In both M^3's, the tetracone is touching the tetrapostconule, which is connected with the posterior lobe. The tetrapostconule is more clearly in the right M^3. In the posterior lobe in the left M^3 two cusplets are present. In the right M^3 there are no cusplets in the posterior lobe. The posterior lobe lies under the level of the wear surface. The posterior lobe is not connected with a cingulum. Only in the left M^3, there is a cingulum on the buccal side from the anterior lobe until the foot of the paracone. In both M^3's there is a tiny accessory lingual cusp.

Coll. Dub. 2908 Both M^2's are very worn. The posterior side of the left M^2 is missing. The outline of the anterior lobe is visible. In the transverse valley on the buccal side is an accessory cusp in both M^2's. There is a remnant of a cingulum in the right M^2 on the lingual side. Both the anterior and the posterior parts are depressions compared to the medial transverse valley, which lie somewhat higher.

In the right M^3 the protocone, paracone and the anterior lobe are fused due to wear. Also the metacone, tetracone and the posterior lobe are fused. The parapoststyle is situated buccally from the metaprestyle. The protopoststyle is situated buccally from the tetraprestyle. On the buccal side there is a cingulum, the anterior part of which is very vague. It is clearly present between the para- and metacone. It ends at the foot of the metacone. On the lingual side, the cingulum can be distinguished, although it is just slightly lower than the wear surface and is nearly fused with it. There is a large accessory lingual cusp, which touches both the proto- and tetracone.

Coll. Dub. 2909 The M^1 is very worn and partly broken. The protopoststyle is situated opposite the tetraprestyle.

The right M^2 is quite worn. The anterior lobe is fused with the para- and protocone. The anterior lobe extends more to the buccal side than to the lingual side. The meta- and tetraprestyles are damaged and the position of these styles in relation to respectively the para- and protopoststyle, cannot be distinguished. The meta- and tetracone are fused with the posterior lobe. The posterobuccal side is broken. Therefore it cannot be seen if there has been a cingulum on the buccal side. There is a cingulum on the lingual side. It is not connected with the anterior lobe. The anterior part of the cingulum ends in an accessory lingual cusp. The posterior part of the cingulum is connected with the posterior lobe and ends against the accessory lingual cusp.

Coll. Dub. 2911 In the left M^2, the anterior lobe is fused with the proto- and paracone. The anterior lobe extends more to the buccal side than to the lingual side. From the anterior lobe goes a ridge downwards until the transverse valley. Also from the paracone goes a ridge downwards that ends in a little cusp. Posterior of this cusp is another cusp, which is connected with a little ridge that goes downwards from the posterior lobe. These two little cusps are situated buccally from the metacone. The three little ridges mentioned above form sort of cingulum. The parapoststyle is situated buccally from the metaprestyle. The molar is too worn to distinguish the position of the protopoststyle and the tetraprestyle. The posterolingual side is broken off. There are no signs of a cingulum on the lingual side.

In the right M^2, the anterior lobe is fused with the proto- and paracone. The anterior lobe extends more to the buccal side than to the lingual side. From the anterior lobe goes a tiny ridge downwards, but it does not reach the paracone. The parapoststyle is situated buccally from the metaprestyle. The molar is too worn to distinguish the position of the protopoststyle and the tetraprestyle. The meta- and tetracone are fused with the posterior lobe. The posterobuccal side is broken off. On the lingual side is a worn cingulum that is connected with a worn accessory cusp, which touches the protocone. On the buccal side is a crenulated cingulum, which ends at the posterior side of the paracone. The other side is broken off.

The posterolingual part with the tetracone of the left M^3 is broken off. The parapoststyle is situated buccally from the metaprestyle. The metaprestyle touches the protopoststyle. The protocone is star-shaped due to a little extension in buccal direction. This caused an indentation in the paracone at the place where the two cusps touch. From the protocone starts a cingulum, that is crenulated on the lingual side and continues to where the molar is broken. This cingulum is low. From the paracone starts a cingulum that ends at the foot of the paracone. From the metacone starts a crenulated cingulum until the foot of the metacone. There is an accessory buccal cusplet.

Coll. Dub. 2914

The anterior side of the right M^2 is broken off. The parapoststyle is situated a bit buccally from the metaprestyle. The metacone is rather star-shaped with a style extending towards the tetracone. The posterior lobe is fused with the meta- and tetracone. There are no cingula visible, possibly due to wear.

The posterior part of the right M^3 is broken off. The parapoststyle is situated buccally from the metaprestyle. The paracone is star-shaped. On the buccal side there is no cingulum. On the lingual side there is a cingulum from the protocone to where the molar is broken.

Coll. Dub. 2919

The left M^2 shows an indentation on the posterobuccal side. In this indentation, the protocone of the M^3 is placed.

The left M^3 is very worn and damaged. The parapoststyle is situated buccally from the metaprestyle, although according to Hooijer (1950, p. 68) it is rather of the "*sivalensis*-type" (the parapoststyle never extends buccally beyond the metaprestyle). The tetracone is situated more posteriorly than the metacone. From the paracone runs a tiny cingulum downwards until the foot of the paracone. From the protocone runs a cingulum downwards until the transverse valley.

Coll. Dub. 2920

The posterior part of the M^1 is broken off. The para- and protocone are fused with the anterior lobe. From the anterior lobe starts a knobby cingulum on the buccal side, which ends in the transverse valley in an accessory buccal cusp.

The M^2 is broken. The parapoststyle is situated buccally from the metaprestyle. The metacone is larger than the tetracone. The anterior lobe extends downwards into the maxilla; the M^2 was obviously not fully erupted.

The also not yet erupted M^3 is for the greatest part still in the maxilla, therefore no measurements were taken. The metacone is larger than the tetracone.

Coll. Dub. 3101 The right M^2 is damaged and totally worn. The enamel ridges that are still visible are quite broad.

Coll. Dub. 3137 The M^2 is broken. The anterior part of the M^2 is positioned more buccally with regard to the M^3. The only morphological feature that can be distinguished is that the para- or protopoststyle is situated opposite the meta- or tetraprestyle ("*sivalensis*-type"). According to the position of the molar it is most probable that the ridges concerned are the parapoststyle and the metaprestyle.

Coll. Dub. 3138 The right M^1 is nicely preserved, except for the anterolingual side, which is broken off. The anterior lobe is fused with the proto- and paracone. The posterior lobe is fused with the meta- and tetracone. The parapoststyle is situated opposite the metaprestyle ("*sivalensis*-type"). The protopoststyle is situated opposite the tetraprestyle. On the buccal side, is a cingulum that is attached to an accessory buccal cusp. On the lingual side there is also an accessory cusp. Posterior of the cusp is a lingual cingulum. Due to the damage it is not sure if there has been a cingulum on the anterior side of the accessory lingual cusp. The metacone is more star-shaped than the other cusps, due to the presence of a small style, which extends in lingual direction.

The right M^2 is broken, only the protocone is more or less preserved. Although the other cusps are broken off, it can still be seen that the metacone is larger than the tetracone, and the paracone is larger than the protocone. The paracone is not lying more posteriorly than the protocone. The metacone is not lying posteriorly from the tetracone. The metacone has a very tiny style, extending in lingual direction, but it is smaller than in the M^1. The protopoststyle is situated opposite the tetraprestyle. The parapoststyle is situated opposite the metaprestyle ("*sivalensis*-type"). There is no clear anterior lobe, due to the indentation in the molar, which indicates the position of the M^1. On the posterior side, there is a posterior lobe. The cingulum is low and broad with three robust knobs. Two of these knobs are on the lingual side, one below the tetracone, one in the transverse valley. The third one is on the buccal side, below the paracone. The cingulum is present on the entire lingual side and ends at the posterior lobe. On the buccal side the cingulum ends at the posterior lobe. It is present on the entire buccal side, except below the metacone. The cingulum on the buccal side is rather crenulated at the anterior part.

The M^3 is not yet erupted, so no measurements were taken. The four main cusps are visible. They look very symmetrical. They are oval-shaped with a style pointing towards the centre of the molar, so the parapoststyle is situated opposite the metaprestyle ("*sivalensis*-type") and the protopoststyle is situated opposite the tetraprestyle. Like in the M^2, there is no sign of the paracone/metacone lying more posteriorly than the protocone/tetracone respectively. Unlike the M^2, the metacone is not larger than the tetracone, and the paracone is not larger than the protocone.

Coll. Dub. 3146 The left M^2 is damaged on the posterolingual side. The anterior lobe is fused with the proto- and paracone. The anterior lobe extends more to the buccal side than to the lingual side. The parapoststyle is situated buccally from the metaprestyle ("*palaeindicus*-type"). The protopost-style and the tetraprestyle are broken. There is no posterior lobe. Instead there is a high ridge, which is connected with a low cingulum on the buccal side. Under the metacone the cingulum is crenulated. It continues vaguely under the paracone and ends on the buccal side of the anterior lobe. On the lingual side is a crenulated cingulum from the anterior lobe going downwards towards the foot of the protocone. It cannot be seen if it continues due to the damage.

The right M^2 is very damaged. The anterior lobe, which is not very prominent, is fused with the proto- and paracone. The parapoststyle is situated buccally from the metaprestyle ("*palaeindicus*-type"). The protopoststyle is situated buccally from the tetraprestyle. The posterior part is broken off. On the lingual side there is a cingulum connected with the anterior lobe and continues as far as the broken edge. The molar is too damaged on the buccal side to distinguish a possible cin-gulum.

The only thing worth mentioning about the left M^3 (broken) is that there is an accessory buccal cusp present.

Coll. Dub. 3148 The only thing worth mentioning is that there are remnants of a lingual cingulum in both M^2's.

Coll. Dub. 5760 In this M^2, only the fused paracone, protocone and the anterior lobe are preserved and just a small part of the meta- and tetracone. The parapoststyle is situated buccally from the metaprestyle. The buccal side of the molar is damaged. On the lingual side a cingulum is con-nected with the anterior lobe. It continues until the transverse valley. It seems that it doesn't extend further to the posterior side, but the molar is broken off, so this is not sure.

Coll. Dub. 6654 The paracone, protocone and the anterior lobe of this M^2 are fused due to wear. The parapoststyle is situated buccally from the metaprestyle. The posterior side of the molar is broken off. On the lingual side, there is a cingulum from the anterior lobe until the place where the molar is broken (transverse valley). On the buccal side, a cingulum extends from the anterior lobe until the posterior part of the metacone, where the molar is broken. The cingulum on the buccal side is not crenulated. The cingulum on the lingual side is crenulated.

Coll. Dub. 6927 2) Only the posterior part of this M^3 is preserved. The metacone is larger than the tetracone. Behind the metacone is the metapostconule present, which is connected with the posterior lobe. The posterior lobe is a bit crenulated on the lingual side.

3) Only the para- and protocone of this M^3 are preserved. The paracone extends further to the posterior side than the protocone.

Coll. Dub. 6954 8) Only the posterior cusps of this M^3 are preserved. The anterior part is broken off. The parapoststyle is situated just a bit buccally from the metaprestyle. The protopoststyle is situated opposite the tetraprestyle. The posterior lobe is connected with the metacone. The posterior lobe is small. It consists of two cusps from where a ridge is going downwards on the buccal side. From the posterior side of the protocone runs a crenulated cingulum until the transverse valley on the lingual side.

9) Only the posterior part of this M^2 is preserved. The two posterior cusps are visible. The metacone is connected with the posterior lobe. If this is indeed the metacone then it is a right M^2. The posterior lobe extends on the buccal side until the buccal edge of the metacone. On the anterior side of the metacone is a crenulated cingulum. It is not clear if the cingulum continues into the posterior lobe because this part is damaged. On the lingual side, the posterior lobe extends downwards until the foot of the tetracone.

Coll. Dub. 11466	The two anterior cusps of this M^2 or M^3 are visible. In most upper molars, the paracone extends more to the posterior side than the protocone. If this is also the case in this molar, than it is a right molar. But then the anterior lobe is connected with the paracone and not with the protocone, as in most molars. The parapoststyle lies opposite or just a bit buccally from the metaprestyle. The posterior part of the molar is broken off. The anterior lobe extends on the buccal side into a cingulum, which continues until the broken edge. Near this edge, the cingulum is crenulated. From the protocone extends a crenulated ridge into the direction of the anterior lobe. On the lingual side a crenulated cingulum starts from the anterior lobe until the broken edge.

VII.9 MANDIBLE

The measurements are given in the Appendix VI-24 and VI-25.

Specimens without description:

SA 270378; Coll. Dub. without no.; Coll. Dub. 97; Coll. Dub. 98; Coll. Dub. 310; Coll. Dub. 1804; Coll. Dub. 1818; Coll. Dub. 2082; Coll. Dub. 2174; Coll. Dub. 2202; Coll. Dub. 2207b; Coll. Dub. 2314; Coll. Dub. 2903; Coll. Dub. 2904; Coll. Dub. 2905; Coll. Dub. 2922; Coll. Dub. 2929; Coll. Dub. 2931; Coll. Dub. 2934; Coll. Dub. 3147; Coll. Dub. 4857 .

Description of the specimens:

without no.	Skeleton (Geological Museum, Bandung) with the left and right mandible
4-4A	Part of a left or a right mandible
22G	Complete mandible

Comparing these three specimens, it is remarkable that 22 G is different from the skeleton (without no.) and mandible 4-4A. In 22 G, the thickness of the ramus below M_2 is larger and this is also the case for the thickness of the symphysis, the distance between the canines and the thickness of the ventral part of the ramus (Appendix VI-24). Moreover, the row of molars diverges both in anterior and posterior direction, whereas in both the other mandibles, the molars only diverge in anterior direction. In posterior direction, they are quite parallel.

Specimen without number (skull from Ngandong, Geological Museum, Bandung) and the specimen without number (Museum Sangiran) have a circular alveolus of the P_1.

without no. (Laboratory Bioanthropologi and Paleoanthopologi, Yogyakarta) The row of molars diverges both in anterior and posterior direction.

Coll. Dub. 99 On the left side, the dorsal part of the angular process is present. It is heavily restored with plaster. This is the only specimen with the left condyle preserved (see also Fig. V-11c). The width is 33.4 mm; the length is 58.9 mm. The row of molars diverges both in anterior and posterior direction.

Coll. Dub. 513 The symphysis is rather flat.

Coll. Dub. 2906 The anterior rim of the angular process does not point forward, but is rather blunt.

Coll. Dub. 2910 The thickness of the quite flat symphysis is very large. The depth of the symphysis compared to the base of the molars is 61.2 mm (not in Appendix VI-24 and VI-25).

Coll. Dub. 2915 The anterior part of the angular process points forwards. The height of the symphysis is quite large.

Coll. Dub. 2916 The length of the rather flat symphysis is very long. The row of molars is quite parallel; it diverges only in anterior direction and not at all in posterior direction.

Coll. Dub. 2917 This is one of the few specimens with a part of the angular process. The M_2 is positioned just before the angular process; the anterior rim of the M_3 (which is not quite erupted) coincides with the anterior rim of the angular process. The anterior part of the angular process points slightly forward and the distance between the lowest point of the angular process to the lower rim of the ramus is 74.8 mm (not in Appendix VI-24 and VI-25).

Coll. Dub. 2918 This specimen has a wealth of foramen in the jaw: 17 at the front, and three both in the left and right ramus, seen from the buccal side. The symphysis is very hollow and the height of the symphysis is quite large.

Coll. Dub. 2932 The symphysis is rather flat.

Coll. Dub. 4908 The dorsal part of the symphysis is missing. The diastema between the canine and P_2 is very small, compared to the others (see Appendix VI-25).

VII.10 CRANIUM

The cranium is described in parts, because there is no complete cranium found. The measurements are given in the Appendix VI-27 – VI-32.

Only in Coll. Dub. 2919, two very little condyle foramen are present, but they are too small to measure in an ordinary way.

The paraocciptal process (Fig. V-13A) is present in most specimens, but they are all too damaged to measure or describe them.

VII.10.1 PREMAXILLA

The upper incisors follow the rounded form of the premaxilla (Fig. V-17A), like in Coll. Dub. 2911, although only half of the premaxilla is preserved. The whole premaxilla is only preserved in Coll. Dub. 2908 and Coll. Dub. 2914, and they have a different shape as can be seen in Fig. V-12. In Coll. Dub. 2908, the left and right side of the premaxilla are retreated medially compared to the anterior rim of the premaxilla with the alveoli of the incisors. Where the left and right side meet, it is 23.7 mm more posterior than the lateral sides of the premaxilla. There is one foramen visible on the ventral side. At the anterior rim of Coll. Dub. 2914, there are medially two little extensions forward. Behind these extensions, the left and right side of the palate diverges a little, which causes the formation of a groove. On the left and right side of this groove, some foramen are present, two on each side. The suture with the maxilla is not visible.

VII.10.2 MAXILLA

The premolars (Fig. V-17A) diverge in anterior direction. The molars form two parallel rows on the left and right side in the Ngandong skull (without number, Geological Museum, Bandung) Coll. Dub. 2079, Coll. Dub. 2188, Coll. Dub. 2907/1, Coll. Dub. 2908, Coll. Dub. 2911, Coll. Dub. 2914, Coll. Dub. 2919 and in both the Siwalik specimens Coll. Dub. 3101 and Coll. Dub. 3148. Only in specimen Coll. Dub. 1702 they are a little divergent in posterior direction.

The M^3 is positioned obliquely with regard to the other molars in Coll. Dub. 2079, Coll. Dub. 2084b, Coll. Dub. 2203, Coll. Dub. 2911 and Coll. Dub. 2919. In Coll. Dub. 2914 the left M^3 is not obliquely, the right one a little. In Coll. Dub. 2909 the right M^3 is also a little obliquely. In Coll. Dub. 1702 both M^3's are very obliquely in comparison with the other molars. In Coll. Dub. 2907/1 and in all three Siwalik specimens (Coll. Dub. 3101, Coll. Dub. 3138 and Coll. Dub. 3148) they are not obliquely. This is also the case in Coll. Dub. 2908, but in this specimen, it is the P^3 that is obliquely placed compared to the molars.

VII.10.3 SMALLEST PART OF THE MUZZLE

The smallest part of the muzzle (Fig. V-17B, no. 14) is positioned between P^3 and P^4 in Coll. Dub. 2911, Coll. Dub. 2914, Coll. Dub. 3101 and Coll. Dub. 3148 (the anterior part of the muzzle of Coll. Dub. 3101 and Coll. Dub. 3148 is missing).

The smallest part of the muzzle is positioned between P^4 and M^1 in Coll. Dub. 1702 (damaged).

The smallest part of the muzzle is positioned below P^4 in Coll. Dub. 2079 (anterior part is missing) and Coll. Dub. 2908.

In Coll. Dub. 2907/1, the smallest part of the muzzle is positioned below the part where the P^4 should have been. However there is no P^4 developed.

Only the right side of the cranium is preserved in Coll. Dub. 2909, so the smallest part of the muzzle cannot be measured.

VII.10.4 POSITION OF THE FORAMEN INFRAORBITALE

The foramen infraorbitale (Fig. V-13A) is not visible in Coll. Dub. 1702, Coll. Dub. 2079, Coll. Dub. 2907/1, Coll. Dub. 3101 and Coll. Dub. 3148.

In Coll. Dub. 2908, a vague foramen infraorbitale can be seen on the right side, the anterior rim of which is not clear enough to be distinguished. The posterior rim is situated below the anterior side of the M^1.

In Coll. Dub. 2909 and Coll. Dub. 2911, the anterior rim of the foramen infraorbitale is positioned between the P^3 and P^4 and the posterior rim is situated between P^4 and M^1.

In Coll. Dub. 2914, the anterior rim of the foramen infraorbitale is positioned between the P^3 and P^4 and the posterior rim is situated below the anterior side of the M^1.

VII.10.5 PALATE

In most specimens the palate (Fig. V-17A) is quite flat. In Coll. Dub. 1702 it is remarkable that the anterior part of the palate is very hollow, with its deepest point near P^1. This is also the case, but less extreme, in Coll. Dub. 2908.

The shape of the posterior side of the palate is quite variable (see Fig. 17). In Coll. Dub. 1702, the posterior part of the palate shows medially an extension in anterior direction. The posterior rim is quite broad on the left and right side.

In Coll. Dub. 2908 (damaged) and Coll. Dub. 2911, the posterior part of the palate is round-shaped. This is also the case in Coll. Dub. 3146, but it is broader than in Coll. Dub. 2911. In Coll. Dub. 2914 and in Dub. 3148 the posterior part of the palate shows medially an extension in posterior direction. In Coll. Dub. 2919 a mixture of the last two types occur.

VII.10.6 BULLA AUDITIVE TYMPANIC

The bullae (Fig. V-17A) are only clearly visible in a few specimens. In Coll. Dub. 2919 they are quite small and oval-shaped (see Fig. 18). In Coll. Dub. 2914 it is quite circular with a little extension in anterolingual direction. In Coll. Dub. 2911 the right one is broken off and the left one is damaged, but as far as can be seen the shape is the same as in Coll. Dub. 2914. This is also the case in Coll. Dub. 2908 in which the bullae are also broken off. In Coll. Dub. 3101 the bullae are broken and damaged and the shape is not visible. In Coll. Dub. 3148 the shape is very different, they are more winglike-shaped. In Coll. Dub. 3146 they are partly hidden in the sediment but the posterior side is visible and resembles Coll. Dub. 3148.

VII.10.7 ZYGOMATIC ARCH: JUGAL BONE, SQUAMOSAL

The measurements of these features are given in the Appendix VI-30 and VI-32. Most features are not very remarkable, but some observations can be made. In Coll. Dub. 2914 the transition between the jugal bone and the squamosal (Fig. V-17A) is at about the same position as the posterior rim of the pterygoid (in anterior-posterior direction, whereas in Coll. Dub. 2902, Coll. Dub. 2908, Coll. Dub. 2911 and Coll. Dub. 3148 this transition is placed more anteriorly with regard to the posterior rim of the pterygoid. This seems also to be the case in Coll. Dub. 2919, although it is hard to see.

The transition of the jugal bone and the squamosal coincides with the highest part of the orbital in all specimens where this is visible (Coll. Dub. 2902, Coll. Dub. 2914 and Coll. Dub. 2919). In specimen Coll. Dub. 3101 (which is very damaged and restored with plaster) it looks as though this transition is situated more to the anterior side, at the anterior rim of the orbital.

VII.10.8 OCCIPITAL CONDYLE, FORAMEN MAGNUM, BASIOCCIPITAL AND OCCIPUT

The ventral measurements of these features are given in Appendix VI-32. There are no remarkable differences between the specimens. The posterior measurements of the occipital condyles, the foramen magnum, the occiput and the occipital crest are given in Appendix VI-28.

The width of the occipital crest is hard to measure because the crest has its broadest width at its base, and thins toward the posterior side. The occipital crest thins in dorsal direction in Coll. Dub. 2908, Coll. Dub. 2911 and Coll. Dub. 2914. In Coll. Dub. 2919 it is quite broad with a thickening in it (see also Fig. 19).

The foramen magnum is oval-shaped in all specimens in which this is preserved, with an indentation in dorsal direction. This indentation is rounded and broad in Coll. Dub. 2911, small in Coll. Dub. 2908 and Coll. Dub. 2919 and quite prominent in Coll. Dub. 2914 (see Fig. 19).

VII.10.9 NASAL BONE

The measurements of the nasal bone are given in Appendix VI-29. The shape of the nasal bones is essentially the same in most specimens (Coll. Dub. 2902, Coll. Dub. 2908, Coll. Dub. 2911, Coll. Dub. 2914, Coll. Dub. 3101, Coll. Dub. 3146, Coll. Dub. 3148, and the skeleton from Kali Glagah (Geological Museum, Bandung)). The posterior, broad part is convex dorsally, the middle part is quite straight and the anterior part is concave. This is best shown in Coll. Dub. 2914 which has the most complete nasal bone. The other specimens mentioned match this description as far as can be seen (they are not complete).

In Coll. Dub. 3146 the posterior side of the nasal bone is different than in the other specimens mentioned. From the broadest point it becomes smaller again in posterior direction, but there are two indentations in anterior direction which gives the posterior rim a crenulated appearance.

VII.10.10 FRONTAL AND LACRYMAL BONES

Only in Coll. Dub. 3148 is the shape of the lacrymal bones (Fig. V-15A) clearly visible. In the rest of the specimens the lacrymal and frontal bones are so vague that no characteristics can be distinguished.

The frontal bone (Fig. V-15A) between the sagittal crest and the orbitals is either straight or concave. It is straight in Coll. Dub. 2919, Coll. Dub. 3101, Coll. Dub. 3148 and the skeleton from Kali Glagah. It is slightly concave in Coll. Dub. 2084a, Coll. Dub. 2908 and Coll. Dub. 2911. It is very concave in Coll. Dub. 2902, Coll. Dub. 2914, Coll. Dub. 3146 and Coll. Dub. 5006 (see also Fig. 20).

VII.10.11 SAGITTAL CREST

Two shapes of the sagittal crest can be distinguished: arch-shaped/thin and straight/thick (see fig. 20). The first type of crest occurs in the Ngandong skull (Geological Museum, Bandung), Coll. Dub. 2909 and Coll. Dub. 2914.

In some specimens it is not very well visible, but it looks like the first type. This is the case in Coll. Dub. 2902, Coll. Dub. 2908 and Coll. Dub. 2911. The second type occurs in the specimens Coll. Dub. 2084a, Coll. Dub. 2919, Coll. Dub. 3101, Coll. Dub. 3146, Coll. Dub. 3148, Coll. Dub. 5006 and the skeleton from Kali Glagah (Geological Museum, Bandung).

APPENDIX VIII SUMMARY OF THE MORPHOLOGICAL AND BIOMETRICAL CHARACTERISTICS OF THE DENTITION

The morphological and biometrical characteristics of the dentition are based on the detailed descriptions of the fossils (Appendix VII) and the measurements (Appendix VI). The specimen can also be found in these Appendices.

LOWER INCISORS

Tapering		
the width behind the wear facet is larger than the width at the posterior end and the thickness behind the wear facet is larger than the thickness at the posterior end (tapering in posterior direction)		
number	%	specimens
13 out of 40	32.5%	width of I_1 dex of Coll. Dub. 99, both width and thickness of I_3 sin of Coll. Dub. 2916, width of the indeterminable incisors of SA 040979-16/3, K 717/2 and K 747, both width and thickness of K 718/1, K 718/3, and K 719 and thickness of K 717/1
the width behind the wear facet is of the same size at the width at the posterior end and the thickness behind the wear facet is of the same size as the thickness at the posterior end (difference 0-0.3 mm; no tapering)		
5 out of 40	12.5%	width of I_1 sin of 22G and Coll. Dub 2910, thickness of the indeterminable incisor K 717/2 and both width and thickness of the indeterminable incisor SA 030979-14
tapering in anterior direction		
22 out of 40	55%	the rest

VIII-1. Tapering of the lower incisors, summary of the measurements from Appendix VI-1 – VI-5).

Roundness/flatness		
flattened: the width is larger than the thickness behind the wear facet and the width is smaller than the thickness at the posterior end		
number	%	specimens
49 out of 79	62%	flattened in linguobuccal direction
the width is larger than the thickness behind the wear facet and the width is larger than the thickness at the posterior end		
22 out of 79	28%	flattened in dorsoventral direction
rounded to subrounded: the width is smaller than the thickness behind the wear facet whereas the width is larger than the thickness at the posterior end or the width is larger than the thickness behind the wear facet whereas the width is smaller than the thickness at the posterior end or the difference between the width and the thickness is 0.3 mm or less		
8 out of 79	10%	I_1 dex of Coll. Dub. 99, I_1 dex of Coll. Dub. 2931, I_2 sin of Coll. Dub. 2931, I_3 sin and dex of 22G, I_3 dex of Coll. Dub. 2910, I_3 dex of Coll. Dub. 2929 and I_{indet} sin of Coll. Dub. 285/1

VIII-2. Roundness/flatness of lower incisors (summary of the measurements from Appendix VI-1 – VI-5).

In general I_2 is the smallest and I_1 the largest in same individual		
I_1 is larger than I_2 (comparing all values of the width and the thickness of the alveolus, behind the wear facet and at the posterior end)		
number	%	specimens
43 out of 45	95.6%	all except the width of 22G dex, both behind the wear facet and at the posterior end

I_1 is larger than I_3 (comparing all values of the width and the thickness of the alveolus, behind the wear facet and at the posterior end)		
26 out of 35	74.3%	all except both the width and the thickness behind the wear facet of both the left and the right $I_{1,3}$ of 22G, the width and thickness of the right $I_{1,3}$ at the posterior end of 22G, the width of the alveolus on the left side of Coll. Dub. 513 and both the width and thickness at the posterior end of the left $I_{1,3}$ of Coll. Dub. 2935
I_3 is larger than I_2 (comparing all values of the width and the thickness of the alveolus, behind the wear facet and at the posterior end)		
17 out of 25	68%	all except the width at the posterior end of the left $I_{2,3}$ of Coll. Dub. 2915, the thickness at the posterior end of the right $I_{2,3}$ of Coll. Dub. 2915, the width at the posterior end of the left $I_{2,3}$ of Coll. Dub. 2918, the width at the posterior end of the left $I_{2,3}$ of Coll. Dub. 2931, the thickness at the posterior end of the right $I_{2,3}$ of Coll. Dub. 2931, the thickness of the left alveoli of Coll. Dub. 513, the thickness at the posterior end of the left $I_{2,3}$ of Coll. Dub. 2932 and the width at the posterior end of the right $I_{2,3}$ of Coll. Dub. 2934

VIII-3 Comparison of the mutual proportions of I_1, I_2 and I_3 (summary of the measurements from Appendix VI-1 – VI-3).

UPPER INCISORS

Shape		
the maximum diameter is larger than the minimum diameter		
number	%	specimens
21 out of 25	84%	all except I^2 and I^3 of K 714 and the I^3 sin and dex of Coll. Dub. 2908

VIII-4. Shape of the upper incisors (summary of the measurements in Appendix VI-6).

In general I^3 is the smallest and I^2 the largest in the same individual		
I^1 is larger than I^2, comparing both the maximum and minimum diameter of I^1 and I^2		
number	%	specimens
2 out of 12	16.7%	dt max of Coll. Dub. 2908 and dt min of Coll. Dub. 2914 sin
I^1 is of the same size as I^2		
1 out of 12	8.3%	dt min of Coll. Dub. 2908
I^3 is smaller than I^1		
8 out of 8	100%	all specimens
I^3 is larger than I^2		
1 out of 16	6.25%	dt min of Coll. Dub. 2908 sin

VIII-5. Comparison of the mutual proportions of I^1, I^2 and I^3 (summary of the measurements in Appendix VI-6).

LOWER CANINES

Size		
the width is smaller than the height		
number	%	specimens
61 out of 63	97%	the rest
the width is larger than the height		
1 out of 63	1.5%	K 522 juvenile
the width is of the same size as the height		
1 out of 63	1.5%	K 713/1

VIII-6. Summary of the measurements of the lower canines (Appendix VI-7).

Buccal groove		
the buccal side has a shallow groove		
number	%	specimens
32 out of 68	47%	see Appendix VII
the groove is not visible due to damage		
34 out of 68	50%	see Appendix VII
no buccal groove		
2 out of 68	3%	Coll. Dub. 99 sin, Coll. Dub. 2076a/3

VIII-7. Presence of the buccal groove in lower canines.

Lingual groove		
the lingual side is smooth		
number	%	specimens
11 out of 68	16%	SA 040979-30L, SA 040979-30M, SA 230779, M 16, K 710/1, K 713/3, K 715/1, K 716/1, K 733, K 1567 and Coll. Dub. 2076a/3
there is a shallow groove on the lingual side		
7 out of 68	10%	Bumiayu Exc. 8, K 522, K 654, K 713/1, K 713/2, Coll. Dub. 100/3 and Coll. Dub. 2191b/3
a lingual groove is not visible due to damage		
50 out of 68	74%	the rest

VIII-8. Presence of the lingual groove in lower canines.

UPPER CANINES

The width compared with the height on the lingual and the buccal sides		
the width is larger than the height on the lingual side		
number	%	specimens
36 out of 36	100%	all
the width is larger than the height on the buccal side		
33 out of 36	92%	all except Coll. Dub. 2902, Coll. Dub. 2908 and Coll. Dub. 2914

VIII-9. The width compared with the height on the lingual and the buccal sides (measurements from Appendix VI-8).

The height on the buccal side compared with height on the lingual side		
the height on the buccal side is smaller than the height on the lingual side		
number	%	specimens
9 out 37	24%	K 716/2, K 732, Coll. Dub. 308d/2, Coll. Dub. 2000/1, Coll. Dub. 2019c, Coll. Dub. 2080b, Coll. Dub. 2190a/2, Coll. Dub. 2191a and Coll. Dub. 6954/3
the height on the buccal and on the lingual sides are about the same size		
1 out of 37	3%	Coll. Dub. 548
the height on the buccal side is larger than the height on the lingual side		
27 out of 37	73%	the rest

VIII-10 The height the buccal side compared with the height on the lingual side (measurements from Appendix VI-8).

Buccal groove		
the buccal side has a shallow groove		
number	%	specimens
32 out of 36	89%	the rest

no buccal groove		
4 out of 36	11%	without number (locality unknown; Museum Sangiran), K 715/2, K 716/2 and K 732

VIII-11. Presence or absence of the buccal groove.

Lingual groove		
shallow groove on the lingual side		
number	%	specimens
9 out of 46	19.6%	without number (locality unknown; Museum Sangiran), K 732, Coll. Dub. 325f/1, Coll. Dub. 2000/1, Coll. Dub. 2000/2, Coll. Dub. 2078/1, Coll. Dub. 2080b, Coll. Dub. 6490 and Coll. Dub. 6954/3

VIII-12. Presence or absence of the lingual groove.

LOWER PREMOLARS

In general P_2 is the smallest and P_4 the largest		
the length varies from:		
P_2: 20.3 to 32.6 mm	P_3: 24.6 to 35.1 mm	P_4: 25.4 to 35.9 mm
average of the length and of width on the posterior side		
P_2: 25.0 mm and 15.8 mm (N=15)	P_3: 27.2 and 17.1 (N=26)	P_4: 28.6 mm and 19.7 mm (N=11 and 12 respectively)

VIII-13. Comparison of the measurements of P_2, P_3 and P_4 (measurements from Appendix VI-9 – VI-12).

Size of the lower premolars themselves		
the length is greater than the width[1]		
number	%	specimens
P_2: 15 out of 16	94%	all except Coll. Dub. 87/1
P_3: 30 out of 30	100%	all
P_4: 15 out of 15	100%	all
the anterior width is larger than the posterior width		
P_2: 2 out of 2	100%	all
P_3: 1 out of 3	33%	Coll. Dub. 2929
P_4: 0 out of 3	0%	none

VIII-14. Size of the lower premolars themselves (measurements from Appendix VI-9 – VI-12).
[1] approximate measurements included.

Crown height of unworn premolars		
the crown height on the anterior side is smaller than on the posterior side		
number	%	specimens
P_2: 1 out of 1	100%	all
P_3: 6 out of 6	100%	all
P_4: 1 out of 1	100%	all

VIII-15. Crown height of unworn premolars (measurements from Appendix VI-9 – VI-11).

Size of alveolus		
the length is greater the width		
number	%	specimens
P_2: 11 out of 11	100%	all
P_3: 8 out of 8	100%	all
P_4: 8 out of 10[1]	80%	all except Coll. Dub. 2918, sin and dex

VIII-16. Size of the alveolus (measurements from Appendix VI-9 – VI-11).

Size of alveolus		
the anterior width is larger than the posterior width		
P_2: 3 out of 4	75%	all except Coll. Dub. 4908
P_3: 1 out of 3	33.3%	Coll. Dub. 2174.
the anterior width is smaller than the posterior width		
P_3: 1 out of 3	33.3%	Coll. Dub. 4908
P_4: 5 out of 5[1]	100%	all
the anterior and posterior widths are of about the same size		
P_3: 1 out of 3	33.3%	Coll. Dub. 2904.
the anterior and posterior widths are not comparable due to damage		
P_2: 1 out of 4	25%	Coll. Dub. 2916 dex

VIII-17. The width on the anterior and posterior sides of the alveoli (measurements from Appendix VI-9 – VI-11).

Roots		
the width of the anterior root is smaller than the width of the posterior root		
number	%	specimens
P_2: 2 out of 3	66.7%	K 689 and Coll. Dub. 2318/3
P_3[2]:7 out of 9	77.8%	all except K 699 and JA 67
P_4: 2 out of 2	100%	all

VIII-18. Measurements of the roots of the premolars (measurements from Appendix VI-9 – VI-11). [2]: although the differences are small.

Anterior lobe		
the anterior lobe is present		
number	%	specimens
P_2: 5 out of 10	50%	all except P_2's of K 693, Coll. Dub. 11092/1, Coll. Dub. 11092/2
P_3: 18 out of 21	85%	All except P_3's of K 653/4 and Coll. Dub. 2003b/2
P_4: 11 out of 11	100%	all
too damaged or too worn to distinguish the anterior lobe		
P_2: 2 out of 10	20%	P_2: K 653/1 and Coll. Dub. 324a
P_3: 1 out of 21	5%	P_3: K 425a/1

VIII-19. Presence of an anterior lobe.

Paraconid		
not visible due to wear or damage		
number	%	specimen
11 out of 44	25%	P_2: 324a P_3: without number (skeleton, Geological Museum Bandung), K 6.., K 653/2, Coll. Dub. 272b, Coll. Dub. 425a/1, Coll. Dub. 2318c/1 P_4: Coll. Cub. 105/1, Coll. Dub. 1718, Coll. Dub. 2318c/2 and Coll. Dub. 6954/5
no paraconid present		
P_2: 4 out of 11	36.4%	K 653/1, K 689, K 693 and Coll. Dub. 2318c/4
P_3: 6 out of 15	37.5%	SA 040979-30D/3, K 653/3, K 653/4, K 685, K 699 and Coll. Dub. 2000/3
P_4: 1 out of 7	14.3%	Coll. Dub. 2917

VIII-20. Presence of the paraconid.

Paraconulid		
too worn to distinguish the paraconulid		
number	%	specimen
P_3: 2 out of 10	20%	Coll. Dub. 272b and Coll. Dub. 2318c/1
P_4: 6 out of 6	100%	all
paraconulid present		
P_2: 3 out of 11	27%	G 22 dex, Coll. Dub. 1483 and Coll. Dub. 2318c/3
P_3: 5 out of 16	31%	SA 040979-30D/2, K 698, Coll. Dub. 285/4, Coll. Dub. 6954/6 and JA 67
with paraconid, but no paraconulid		
P_2: 3 out of 7	43%	Coll. Dub. 87/1, Coll. Dub. 11092/1 and Coll. Dub. 11092/2
P_3: 2 out of 9	22.2%	Coll. Dub. 2003b/1 and Coll. Dub. 2003b/2
P_4: 4 out of 6	67%	K 675/2 sin and dex, Coll. Dub. 99 dex, Coll. Dub. 2922 sin

VIII-21. Presence of the paraconulid.

Metaconid		
too worn or damaged to distinguish		
number	%	specimens
5 out of 40	12.5%	P_2: Coll. Dub. 324a P_3: Coll. Dub. 285/4 and Coll. Dub. 2003b/1 P_4: Kali Glagah skeleton and Coll. Dub. 1718
metaconid present		
P_2: 3 out of 10	30%	22G, K 689 and Coll. Dub. 1483
P_3: 13 out of 16	81.3%	<u>without</u> metaconid: K 653/3, K 653/4 and Coll. Dub. 2003b/2
P_4: 5 out of 9	56%	<u>without</u> metaconid: K 675/2, K 675/3, Coll. Dub. 2917 and Coll. Dub. 2922

VIII-22. Presence of the metaconid.

Protoprecristid		
not distinguishable due to damage or wear		
number	%	specimens
10 out of 39	25.6%	P_2: Coll. Dub. 324a P_3: K 6.., K 653/2, Coll. Dub 272b and Coll. Dub. 2318c/1 P_4: Coll. Dub. 105/1, Coll. Dub. 1718, Coll. Dub. 2318c/2, Coll. Dub. 2917 and Coll. Dub. 6954/5
no protoprecristid present		
P_2: 4 out of 9	44.4%	K 653, K 693, Coll. Dub. 2318c/3 and Coll. Dub. 11092/1
P_3: 4 out of 14	28.6%	K 653/3, K 653/4, Coll. Dub. 425a/1 and Coll. Dub. 2003b/1
P_4: 0 out of 6	0%	none

VIII-23. Presence of the protoprecristid.

Protopost- and protoendocristid		
not distinguishable due to damage or wear		
number	%	specimens
8 out of 37	22%	P_2: K 653/1, Coll. Dub. 87/1 and Coll. Dub. 324a P_3: Coll. Dub. 272b P_4: K 675/3, Coll. Dub. 1718, Coll. Dub. 2318c/2 and Coll. Dub. 6954/5
neither protopost- nor protoendocristid present		
P_2: 1 out of 7	14.3%	K 689
P_3: 4 out of 17	23.5%	SA 040979-30D/2, K653/3, K 698 and Coll. Dub. 2318c/1
P_4: 1 out of 5	20%	K 675/2

only one of the two cristids present (not clear which one)		
P_2: 1 out of 7	14.3%	Coll. Dub. 11092/1
protopostcristid present, protoendocristid absent		
P_2: 1 out of 7	14.3%	K 693
P_3: 3 out of 17	17.6%	22 G sin and dex and Coll. Dub. 2003b/1
protoendocristid present, protopostcristid absent		
P_3: 1 out of 17	5.9%	SA 040979-30D/3
both protopost- and protoendocristid present		
P_2: 4 out of 7	57.1%	Coll. Dub. 1483, Coll. Dub. 2318c/3, Coll. Dub. 2318c/4 and Coll. Dub. 11092/2
P_3: 9 out of 17	53%	the rest
P_4: 4 out of 5	80%	the rest

VIII-24. Presence of the protopostcristid and the protoendocristid.

Posterior cusps		
not distinguishable due to wear or damage		
number	%	specimens
7 out of 40	17.5%	P_2: K 653/1, Coll. Dub. 87/1 and Coll. Dub. 324a P_4: K 675/2, K 675/3, Coll. Dub. 2318c/2 and Coll. Dub. 6954/5
only the hypoconid present		
P_3: 3 out of 18	16.7%	K 698, Coll. Dub. 285/4 and Coll. Dub. 2000/3
P_4: 4 out of 7	57%	Coll. Dub. 99, Coll. Dub. 105/1[III], Coll. Dub. 2917, Coll. Dub 2922 [III]In Coll. Dub 105/1 the hypoconulid and entoconid are not visible due to wear.
both hypoconid and entoconid present		
P_2: 1 out of 7	14.3%	Coll. Dub. 2318 c/4
P_3: 2 out of 18	11%	SA 040979-30D/3 and K 699
both hypoconid and hypoconulid present		
P_2: 1 out of 7	14.3%	Coll. Dub. 2318c/3
all three posterior cusps (hypoconid, hypoconulid and entoconid) present		
P_3: 10 out of 18	55.6%	the rest
P_4: 2 out of 7	28.6%	22G sin and dex
a lot of posterior cusplets, among which are probably the hypoconid, hypoconulid and the entoconid		
P_2: 1 out of 7	14.3%	Coll. Dub. 1483
P_4: 1 out of 7	14.3%	Coll. Dub. 1718
no posterior cusps present		
P_1: 1 out of 1	100%	K 675
P_2: 4 out of 7	57.1%	the rest
P_3: 3 out of 18	16.7%	K 653/3, K 653/4 and Coll. Dub. 425a/1
P_4: 0 out of 7	0%	none

VIII-25. Combinations of the presence of the posterior cusps.

Cingulum		
cingulum present		
number	%	specimens
37 out of 43	86%	see below
P_2: 10 out of 12	83.3%	<u>not</u> present in K 653/1 and K 693
P_3: 17 out of 21	81%	<u>not</u> present in K 653/4, Coll. Dub. 425a/1, Coll. Dub. 2000/3 and K 6..(too damaged)
P_4: 11 out of 11	100%	all

cingulum only on the lingual side, cingulum on the buccal side not present		
P_2: 3 out of 10	30%	22 G sin, Coll. Dub. 2318c/3 and Coll. Dub. 11092/1
P_3: 3 out of 17	17.6%	without number skeleton, Geological Museum, K 653/3 and Coll. Dub. 2003b/1
P_4: 5 out of 11	45%	22 G sin and dex, Coll. Dub. 99, Coll. Dub. 2318c/2 and Coll. Dub. 2922
cingulum only on the lingual side, buccal side is too damaged to tell if there was a cingulum on this side		
P_2: 2 out of 10	20%	Coll. Dub. 324a and Coll. Dub. 1483
P_3: 2 out of 17	11.8%	K 653/2 and Coll. Dub. 2003b/2
cingulum on both lingual and buccal sides		
P_2: 5 out of 10	50%	22 G dex, K 689, Coll. Dub. 87/1, Coll. Dub. 2318c/4 and Coll. Dub. 11092/2
P_3: 12 out of 17	70.6%	the rest
P_4: 6 out of 11	55%	K 675/2, K 675/3, Coll. Dub. 105/1, Coll. Dub. 1718, Coll. Dub. 2917 and Coll. Dub. 6954/5

VIII-26. Presence of a cingulum.

Posterior lobe		
not distinguishable due to wear or damage		
number	%	specimens
P_3: 1 out of 19	5%	K 6..
P_4: 1 out of 10	10%	K 675/3
no posterior lobe present		
P_1: 1 out of 1	100%	K 675
P_2: 5 out of 10	50%	K 689, K 693, Coll. Dub. 1483 and Coll. Dub. 2318c/3, Coll. Dub. 11092/2
P_3: 2 out of 19	11%	K 653 and Coll. Dub. 2003b/2
P_4: 0 out of 10	0%	none

VIII-27. Presence of the posterior lobe.

UPPER PREMOLARS

In general, P^1 is the smallest and P^3 is the largest in the same individual		
the length varies from:		
P^1: 17.1 to 24.0 mm	P^2: 22.3 to 30.5 mm	P^3: 22.8 to 30.1 mm
average of the length and the width I		
P^1: 19.9 mm and 17.2 mm (N=7)	P^2: 27.4 mm and 20.3 mm (N=10)	P^3: 27.4 mm and 21.5 mm (N=14 and 16 respectively)

VIII-28. Size of the upper premolars (measurements from Appendix VI-13 – VI-17).

Size alveolus		
the length is greater than the width on the posterior side		
number	%	specimens
13 out of 13	100%	P^1: Coll. Dub. 2908, Coll. Dub. 2914 and Coll. Dub. 2921/2 P^2: Coll. Dub. 2193, Coll. Dub. 2914 sin and dex, Coll. Dub. 2921/2 and Coll. Dub. 2933 sin P^3: Coll. Dub. 2911 sin and dex and Coll. Dub. 2933 sin P^4: Coll. Dub. 2933 sin and dex

Size premolars		
the length is greater than the width on the posterior side		
number	%	specimens
P^1: 7 out of 7	100%	all
P^2: 9 out of 10	90%	all except Coll. Dub. 1702 dex
P^3: 12 out of 13	92.3%	all except Coll. Dub. 2914 dex
P^4: 5 out of 17	29.4%	Coll. Dub. 325f/2, Coll. Dub. 3101 sin and dex and Coll. Dub. 3148 sin and dex. Of these 5 P^4's, 4 originate from the Siwaliks
the length is greater than the width		
DP^4: 3 out of 4	75%	all except Coll. Dub. 2920

VIII-29. Size of the alveoli and the premolars (measurements from Appendix VI-13 – VI -17).

Anterior lobe		
the anterior lobe could not be distinguished due to wear or damage		
number	%	specimens
6 out of 22	27.3%	P^2: Coll Dub. 2908 sin and dex P^3: Coll. Dub. 1702, Coll. Dub. 2023/2, Coll. Dub. 2924/4 and Coll. Dub. 13601
anterior lobe present		
P^1: 2 out of 3	66.6%	Coll. Dub. 2023?/1 sin and dex
P^2: 4 out of 4	100%	all
P^3: 9 out of 9	100%	all

VIII-30. Presence of the anterior lobe.

Paraprecrista		
the paraprecrista could not be distinguished due to wear or damage.		
number	%	specimens
8 out of 22	36.4%	P^2: Coll. Dub. 2908 sin and dex P^3: Coll. Dub. 425a/3, Coll. Dub. 1702, Coll. Dub. 2023/2, Coll. Dub. 2924/4, Coll. Dub. 2933 dex and Coll. Dub. 13601
no paraprecrista present		
P^1: 3 out of 3	100%	all
P^2: 4 out of 4	100%	all
P^3: 2 out of 7	28.6%	Coll. Dub. 94 and Coll. Dub. 96.

VIII-31. Presence of the paraprecrista.

Primocone		
the primocone could not be distinguished due to wear or damage.		
number	%	specimen
8 out of 22	36.4%	P^2: Coll. Dub. 2908 sin and dex P^3: Coll. Dub. 425a/3, Coll. Dub. 1702, Coll. Dub. 2023/2, Coll. Dub. 2924/4, Coll. Dub. 2933 dex and Coll. Dub. 13601
no primocone present		
P^1: 3 out of 3	100%	all
P^2: 4 out of 6	66.7%	Coll. Dub. 96, Coll. Dub. 1702 sin and dex and Coll. Dub. 2188
P^3: 6 out of 7	85.7%	all except Coll. Dub. 94

VIII-32. Presence of the primocone.

Wear facet		
the wear facet could not be distinguished due to wear or damage		
number	%	specimen
7 out of 22	31.8%	P^1: Coll. Dub. 2182 and Coll. Dub. 2908 sin P^2: Coll. Dub. 2908 sin and dex P^3: Coll. Dub. 425a/3, Coll. Dub. 1702 and Coll. Dub. 2023/2
wear facet both on the anterior and posterior sides		
P^1: 1 out of 3	33.3%	Coll. Dub. 425a/2
wear facet on the anterior side		
P^1: 2 out of 3	66.7%	Coll. Dub. 2023?/2 and Coll. Dub. 2023?/3
P^2: 3 out of 3	100%	all
P^3 3 out of 9	33.3%	Coll. Dub. 94, Coll. Dub. 96 and Coll. Dub. 13601
wear facet on the posterior side		
P^3: 2 out of 9	22.2%	Coll. Dub. 2188 and Coll. Dub. 2924/4
wear facet quite straight		
P3: 2 out of 9	22.2%	Coll. Dub. 313/2 and Coll. Dub. 2003b/3
no wear facet because premolars not yet worn		
P^3: 2 out of 9	22.2%	Coll. Dub. 313/1 and Coll. Dub. 2926

VIII-33. The occurrence of the wear facet.

Cingulum		
cingulum could not be distinguished due to wear or damage		
number	%	specimen
1 out of 22	4.5%	P^2: Coll. Dub. 2908 sin
cingulum on the lingual side, but not on the buccal side		
P^1: 3 out of 3	100%	all
P^2: 1 out of 5	20%	Coll. Dub. 2188
P^3: 7 out of 13	54%	no buccal cingulum: Coll. Dub. 313/1, Coll. Dub. 313/2, Coll. Dub. 2023/2, Coll. Dub. 2924/4 and Coll. Dub. 13601 buccal side is too damaged to tell if there has been a cingulum on that side Coll. Dub. 94 and Coll. Dub. 425a/3
cingulum on both the lingual and buccal sides		
P^2: 3 out of 5	60%	Coll. Dub. 1702 sin and dex and Coll. Dub. 2908 dex
P^3: 6 out of 13	46%	Coll. Dub. 96, Coll. Dub. 1702, Coll. Dub. 2003b/3, Coll. Dub. 2188, Coll. Dub. 2926 and Coll. Dub. 2933 dex
no cingulum present		
P^2: 1 out of 5	20%	Coll. Dub. 96

VIII-34. The presence of the cingulum.

Metacone		
the metacone could not be distinguished due to wear or damage		
number	%	specimen
8 out of 22	36.4%	P^2: Coll. Dub. 2908 sin and dex P^3: Coll. Dub. 425a/3, Coll. Dub. 1702, Coll. Dub. 2023/2, Coll. Dub. 2924, Coll. Dub. 2933 dex and Coll. Dub. 13601
metacone present		
P^1: 0 out of 3	0%	none
P^2: 1 out of 4	25%	Coll. Dub. 96
P^3: 4 out of 7	57%	Coll. Dub. 96, Coll. Dub. 313/2, Coll. Dub. 2003b/3 and Coll. Dub. 2188.

VIII-35. The presence of the metacone.

Parapostcrista		
parapostcrista could not be distinguished due to wear or damage		
number	%	specimen
6 out of 22	27%	P^2: Coll. Dub. 2908 sin and dex P^3: Coll. Dub. 425a/3, Coll. Dub. 1702, Coll. Dub. 2023/2 and Coll. Dub. 2933 dex
parapostcrista present		
P^1: 0 out of 3	0%	none
P^2: 4 out of 4	100%	all
P^3: 9 out of 9	100%	all

VIII-36. The presence of the parapostcrista.

paraendocrista		
paraendocrista could not be distinguished due to wear or damage		
number	%	specimen
6 out of 22	27%	P^2: Coll. Dub. 2908 sin and dex P^3: Coll. Dub. 425a/3, Coll. Dub. 1702, Coll. Dub. 2023/2 and Coll. Dub. 2933 dex
paraendocrista present		
P^1: 0 out of 3	0%	none
P^2: 2 out of 4	50%	Coll. 1702 sin and dex; crenulated
P^3: 9 out of 9	100%	smooth: Coll. Dub. 313/2); knobby: Coll. Dub. 96; crenulated: Coll. Dub. 94, Coll. Dub. 313/1, Coll. Dub. 2003b/3, Coll. Dub. 2188, Coll. Dub. 2924/4, Coll. Dub. 2926 and Coll. Dub. 13601

VIII-37. Presence of the paraendocrista.

Additional ridges		
it could not be distinguished if there are any more ridges, besides the parapost- and paraendocrista.		
number	%	specimen
6 out of 22	27.3%	P^2: Coll. Dub. 2908 sin and dex P^3: Coll. Dub. 425a/3, Coll. Dub. 1702, Coll. Dub. 2023/2 and Coll. Dub. 2933 dex
additional ridges present		
P^1: 0 out of 3	0%	none
P^2: o out of 4	0%	none
P^3: 6 out of 9	66.7%	the parapost- or paraendocrista divides into other ridges or there are additional crenulated ridges on the posterior side: Coll. Dub. 94, Coll. Dub. 313/1, Coll. Dub. 313/2, Coll. Dub. 2003b/3, Coll. Dub. 2924/4 and Coll. Dub. 13601

VIII-38. Occurrence of additional ridges.

Posterior platform		
posterolingual platform could not be distinguished due to wear or damage		
number	%	specimen
4 out of 22	9%	P^2: Coll. Dub. 2908 sin and dex P^3: Coll. Dub. 1702 and Coll. Dub 2933 dex

posterior platform present		
P^1: 2 out of 3	66.6%	Coll. Dub. 2023?/2 and Coll. Dub. 2023?/3 covered with a lot of cusplets
P^2: 3 out of 4	75%	covered with cusplets: Coll. Dub. 96; covered with knobs: Coll. Dub. 1702 sin and dex
P^3: 11 out of 11	100%	Platform smooth: Coll. Dub. 96, Coll. Dub. 313/1, Coll. Dub. 313/2, Coll. Dub. 425a/3, Coll. Dub. 2188, Coll. Dub. 2926 and Coll. Dub. 13601; covered with crenulated ridges: Coll. Dub. 94; covered with cusplets: Coll. Dub. 2003b/3, Coll. Dub. 2023/2 and Coll. Dub. 2924/4
No posterior platform		
P^1: 1 out of 3	33.3%	Coll. Dub. 425a/2
P^2: 1 out of 4	25%	no distinct posterolingual platform but it is a bit broader than the anterior part: Coll. Dub. 2188

VIII-39. Presence of a posterior platform.

Posterior lobe		
posterior lobe could not be distinguished due to wear or damage.		
number	%	specimen
5 out of 22	22.7%	P^2: Coll. Dub. 2908 sin and dex P^3: Coll. Dub. 1702, Coll. Dub. 2023/2 and Coll. Dub. 2933 dex
posterior lobe present		
P^1: 3 out of 3	100%	all
P^2: 4 out of 4	100%	all
P^3: 8 out of 9	88.9%	all except Coll. Dub. 96

VIII-40. Presence of the posterior lobe.

Roots		
roots preserved		
number	%	specimen
5 out of 22	23%	see below
12 premolars of which little more that the roots are preserved (total N=17)		
one circular to oval root		
P^1: 4 out of 7	57%	Coll. Dub. 425a/2, Coll. Dub. 2023?/2, Coll. 2908 and Coll. 2921/2
P^2: 2 out of 5	40%	Coll. Dub. 2193 and Coll. Dub. 2933 sin
two roots: 8-shaped		
P^1: 1 out of 7	14.3%	Coll. Dub. 2921/2
P^2: 1 out of 5	20%	Coll. Dub. 2933 dex
two roots fused into one with the suture still visible		
P^1: 1 out of 7	14.3%	Coll. Dub. 2076/4
two roots		
P^1: 1 out of 5	20%	Coll. Dub. 2182/4
P^2: 1 out of 5	20%	Coll. Dub. 2188
three roots		
P^2: 1 out of 5	20%	two anterior round roots, fused into one and one posterior root: Coll. Dub. 2914 sin
two anterior roots fused to one, and two posterior roots fused to one, which results in two half-moon-shaped roots		
P^3: 4 out of 5	80%	Coll. Dub. 313/1, Coll. Dub. 425a/3, Coll. Dub. 2911 and Coll. Dub. 2933 sin

two anterior roots fused to one, and two posterior roots fused to one with an extra root on the lingual side		
P^3: 1 out of 5	20%	Coll. Dub. 2193

VIII-41. Morphologies of the roots.

LOWER MOLARS

The length is smallest in the M_1 and greatest in the M_3		
the length varies from:		
M_1: 20.2 to 39.9 mm	M_2: 34.0 to 50.2 mm	M_3: 48.0 to 65.4 mm
average of the length		
M_1: 34.6 mm (N=17)	M_2: 43.0 mm (N=38)	M_3: 56.8 mm (N=42)
The anterior width is smallest in M_1 and largest in M_3		
the anterior width varies from:		
M_1: 21.8 to 28.3 mm	M_2: 24.6 to 44.0 mm	M_3: 28.8 to 39.0 mm
average of the anterior width		
M_1: 24.0 mm (N=12)	M_2: 31.1 mm (N=28)	M3: 32.9 mm (N=37)
The posterior width is smallest in the M_1 and largest in the M_3		
the posterior width varies from:		
M_1: 4.5 to 32.1 mm	M_2: 26.0 to 38.0 mm	M_3: 27.7 to 38.3 mm
average posterior width		
M_1: 27.5 mm (N=14)	M_2: 31.8 mm (N=38)	M_3: 31.8 mm (N=34)

Length and width		
the length is greater than the width		
number	%	specimens
115 out of 118	97%	all except the ones below
the length is smaller than the width		
2 out of 118	2%	M_1: 2916 sin and dex
the length and the width are of about the same size		
1 out of 118	1%	M_3: Coll. Dub. 1804
The anterior and posterior widths		
the anterior width is smaller than the posterior width		
number	%	specimens
M_1: 13 out of 13	100	all
M_2: 19 out of 24	79%	all except the ones below
M_3: 7 out of 26	27%	Coll. Dub. 323a/1, Coll. Dub. 323b, Coll. Dub. 2006, Coll. Dub. 2082, Coll. Dub. 2194, Coll. Dub. 2314 and Coll. Dub. 2318b
the anterior and posterior widths are of about the same size		
M_3: 1 out of 26	4%	Coll. Dub. 99 dex
the anterior width is larger than the posterior width		
M_2: 5 out of 24	21%	without no. (locality Ngandong) sin and dex, Coll. Dub. 2008a, Coll. Dub. 2910 and JA 68
M_3: 18 out of 26	69%	the rest

VIII-42. Summary of the biometrical features of the lower molars (Appendix VI-18 – VI-20).

Protoconid and metaconid		
the protoconid is larger than the metaconid		
number	%	specimen
15 out of 30	50%	see below; the rest
the protoconid is smaller than the metaconid		
M_2: 3 out of 30	10%	K 741, Coll. Dub. 2202, Coll. Dub. 2976/2
M_3: 5 out of 30	17%	K 740, K 746, Coll. Dub. 2917, Coll. Dub. 2202 and Coll. Dub. 2903

the protoconid and the metaconid are of the same size		
M_2: 2 out of 30	6%	SA 040979-20N 2 and K 150
M_3: 5 out of 30	17%	SA 110979, K 657, K 727, K 745 and Coll. Dub. 2318b
the protoconid is situated more anteriorly than the metaconid		
35 out of 38	92%	All except M_2: Coll. Dub. 2922; M_3: K 743 and Coll. Dub. 2903

VIII-43. Comparison of the visual size and position of the protoconid and the metaconid.

Anterior lobe		
anterior lobe present		
number	%	specimen
70 out of 72	97%	all except M_3: K 743 and Coll. Dub. 2903
anterior lobe is connected with the proto- or metaconid		
33 out of 43	77%	All except : M_1: SA 040979-20N/1; M_2 : SA 040979-20N/2, SA 040979-20N/3, Coll. Dub. 2917, Coll. Dub. 2202, Coll. Dub. 2076/7 ; M_3 : SA 110979, K 743, Coll. Dub. 2917, Coll. Dub. 314b
it could not be distinguished if this connection is with the proto- or metaconid due to wear.		
14 out of 33	42%	the rest
anterior lobe connected with the protoconid		
18 out of 33	55%	M_1: Coll. Dub. 2008; M_2: K 150, K 731, K 741 and K 745; M_3: without no. (locality Sangiran), K 707, K 723/1, K 723/2, K 731, K 740, K 746, Coll. Dub. 97, Coll. Dub. 99 sin, Coll. Dub. 2003a, Coll. Dub. 2202, Coll. Dub. 2318b and Coll. Dub. 2905
anterior lobe connected with the metaconid		
1 out of 33	3%	M_3: Coll. Dub. 99 dex

VIII-44. The occurrence of the anterior lobe.

Meta- and protopoststylid		
only the metapoststylid present		
number	%	specimen
30 out of 34	85%	the rest
only a protopoststylid present		
2 out of 34	6%	M_3: Coll. Dub. 97 and Coll. Dub. 99 dex
both a meta- and a protopoststylid present		
1 out of 34	3%	M_1: Coll. Dub. 2008
no meta- or protopoststylid developed at all		
1 out of 34	3%	M_2: Coll. Dub 2922

VIII-45. The presence of the meta- and protopoststylid.

Hypo- and entoprestylid		
only hypoprestyled present		
number	%	specimen
48 out of 51	94%	the rest
only entoprestylid present		
1 out of 51	2%	M_1: Coll. Dub. 2008

both a hypo- and an entoprestylid are present		
1 out of 51	2%	M_2: K 746
The hypo- or entoprestylid are not developed		
1 out of 51	2%	M_3: K 740

VIII-46. The presence of the hypo- and entoprestylid.

Orientation of metapoststylid and hypoprestylid		
the metapoststylid is situated lingually from the hypoprestylid (or entoprestylid, in the case of the M_1 of Coll. Dub. 2008)		
number	%	specimen
55 out of 67	82%	the rest
metapoststylid and the hypoprestylid are lying opposite each other		
10 out of 67	15%	M_2: K 149, Coll. Dub. 2008a, Coll. Dub. 2076/7; M_3: without no. (locality Sangiran), K 707, Coll. Dub. 97, Coll. Dub. 314b, Coll. Dub. 325d/2, Coll. Dub. 325d/3, and Coll. Dub. 2903
metapoststylid is situated buccally from the hypoprestylid		
2 out of 67	3%	M_3: Coll. Dub. 2915 and Coll. Dub. 2318b

VIII-47. The orientation of the metapoststylid and the hypoprestylid.

Hypoconid and entoconid		
the hypoconid is larger than the entoconid		
number	%	specimen
41 out of 51	80%	the rest
the hypoconid and the entoconid are of about the same size		
8 out of 51	16%	M_1: Coll. Dub. 2008; M_2: K 746, K 723/2, K 723/3, K 727, K 731, K 740, K 746
the hypoconid is smaller than entoconid		
1 out of 51	2%	M_3: Coll. Dub. 2903
the hypoconid and the entoconid form one ridge		
1 out of 51	2%	M_3: K 743

VIII-48. The occurrence and relative size of the hypoconid and the entoconid.

Posterior lobe		
posterior lobe is present		
number	%	specimen
38 out of 80	47.5%	see Appendix VII
molar is not fully erupted, so it is not possible to say if there is a posterior lobe or not		
2 out of 80	2.5%	M_3: Coll. Dub. 97 and Coll. Dub. 2903
posterior lobe not connected with the hypoconid (N=44)		
41 out of 44	93%	all except M_2: K 731, K 745 M_3: K 745

VIII-49. The presence of the posterior lobe.

Heptaconid		
heptaconid present		
number	%	specimen
68 out of 74	92%	all except: M_1: without no. (locality Sangiran), 22G, K 731 M_3: K 723/1 and Coll. Dub. 323a/1 and Coll. Dub. 323a/2

Pentaconid and hexaconid		
pentaconid present		
number	%	specimen
56 out of 67	84%	all except M_1: without no. (locality Sangiran), 22G and K 731 M_2: K 731 and K 732 M_3: K 149, Coll. Dub. 99 dex, Coll. Dub. 323a/2, Coll. Dub. 2076/10, Coll. Dub. 2905 and Coll. Dub. 2917
hexaconid present		
58 out of 68[3] ([3] the posterior part of K 723/1 (M_3) is missing; the hexaconid is present but it cannot be seen if there was a pentaconid.	85%	all except M_1: without no. (locality Sangiran), 22G and K 731 M_2: K 731, K 732 M_3: Coll. Dub. 99 dex, Coll. Dub. 323a/2, Coll. Dub. 323b, Coll. Dub. 2076/10 and Coll. Dub. 2917
Posterior cusps: heptaconid, pentaconid and hexaconid		
heptaconid present		
number	%	specimen
M_1: 2 out of 5	40%	SA 040979-20N/1 and Coll. Dub. 2008
M_2: 18 out of 18	100%	all
M_3: 49 out of 51	96%	all except K 723/1 and Coll. Dub. 323a/2
pentaconid present		
M_1: 1 out of 4	25%	SA 040979-20N/1
M_2 15 out of 16	94%	all except K 731
M_3: 41 out of 47	87%	all except K 149, Coll. Dub. 323a/2, Coll. Dub. 2917, Coll. Dub. 2905, Coll. Dub. 99 dex and Coll. Dub. 2076/10
hexaconid present		
M_1: 2 out of 5	40	SA 040979-20N/1 and Coll. Dub. 2008
M_2: 13 out of 14	93%	all except K 731
M_3: 41 out of 47	87%	all except K 723/1, and Coll. Dub. 323a/2, Coll. Dub. 323b, Coll. Dub. 99 dex, Coll. Dub. 2076/10 and Coll. Dub. 2917
the heptaconid is larger than the pentaconid or the hexaconid		
48 out of 48	100%	all
the hexaconid is larger than the pentaconid		
18 out of 23	78%	all except: M_2: K 741 M_3: K 731, Coll. Dub. 325d/2, Coll. Dub. 2194, Coll. Dub. 2318b
pentaconid is a separate cusp		
50 out of 50	100%	all
heptaconid and the hexaconid often are attached or touching		
27 out of 58	47%	the rest (see below)
heptaconid and hexaconid forming one ridge		
24 out of 58	41%	the rest
heptaconid and the hexaconid not attached, touching or forming one ridge		
7 out of 58	12%	M_2: Coll. Dub. 99 sin M_3: K 149, K 731, K 745, K 746, Coll. Dub. 314b and Coll. Dub. 2076/10

in molars with a posterior lobe, this lobe is connected with the posterior cusps		
26 out of 34	76%	all except M_2: K 741, K 743, K 746, Coll. Dub. 2008a, Coll. Dub. 2905 M_3: specimen without no. (locality Sangiran), K 657, Coll. Dub. 323a/2

VIII-50. The presence and orientation of the posterior cusps.

Accessory buccal cusp		
accessory buccal cusp present		
number	%	specimen
24 out of 76	31.6%	see below
M_1: 6 out of 8	75%	without no. (locality Sangiran), SA 040979-20 N/1, Coll. Dub. 99 sin, Coll. Dub. 105, Coll. Dub. 2917 and Coll. Dub. 2922
M_2: 11 out of 28	36%	without no. (locality Sangiran), 22G, Coll. 99 dex, Coll. Dub. 105, Coll. Dub. 272a, Coll. Dub. 2008a, Coll. Dub. 2013, Coll. Dub. 2076/7, Coll. Dub. 2314, Coll. Dub. 2917 and Coll. Dub. 2922
M_3: 7 out of 40	17.5%	K 723/2, K 742/3, Coll. Dub 310, Coll. Dub. 2003a, Coll. Dub. 2192 and Coll. Dub. 2905 and Coll. Dub. 2917
Accessory lingual cusp		
accessory lingual cusp present		
number	%	specimen
8 out of 73	11%	see below
M_1: 1 out of 7	14%	Coll. Dub. 2922
M_2: 4 out of 26	15%	Coll. Dub. 2003a, Coll. Dub. 2008a, Coll. Dub. 2314 and Coll. Dub. 2916 dex
M_3: 3 out of 40	7.5%	Coll. Dub. 325d/2, Coll. Dub. 2905 and Coll. Dub. 2915

VIII-51. The occurrence of the accessory lingual or buccal cusp.

Cingulum		
cingulum on the lingual side		
number	%	specimen
3 out of 68	4%	see below
M_1: 0 out of 10	0%	none
M_2: 2 out of 26	8%	Coll. Dub. 323a/1 and Coll. Dub. 2013
M_3: 1 out of 32	3%	K 723/2
cingulum on the buccal side		
22 out of 68	32%	see below
M_1: 7 out of 10	70%	SA 040979-20 N/1, K 731, Coll. Dub. 2008, Coll. Dub. 2008a, Coll. Dub. 2076/6, Coll. Dub. 2916 and Coll. Dub. 11463
M_2: 7 out of 26	27%	K 731, K 742/2, Coll. Dub. 2003a, Coll. Dub. 2008a, Coll. Dub. 2076/7, Coll. Dub. 2905 and Coll. Dub. 2917
M_3: 8 out of 32	25%	K 731, K 740, K 742/3, Coll. Dub. 310, Coll. Dub. 314b, Coll. Dub. 323a/1, Coll. Dub. 323a/2 and Coll. Dub. 2917
cingulum on both sides		
7 out of 68	10%	see below
M_1: 2 out of 10	20%	Coll. Dub. 2917 and Coll. Dub. 2922
M_2: 1 out of 26	4%	Coll. Dub. 2202
M_3: 4 out of 32	12.5%	Coll. Dub. 325d/2, Coll. Dub. 2006, Coll. Dub. 2194 and Coll. Dub. 3147

no cingulum present		
36 out of 68	54%	the rest
M_1: 1 out of 10	10%	the rest
M_2: 16 out of 26	61%	the rest
M_3: 19 out of 32	60%	the rest

VIII-52. The occurrence of the cingulum.

UPPER MOLARS

The length of the M^1 is smaller than from M^2 and M^3, which are of about the same size		
the length varies from:		
M^1: 26.6 to 44.5 mm	M^2: 33.8 to 50.1 mm	M^3: 34.4 to 49.5 mm
average of the length		
M^1: 33.3 mm (N=31)	M^2: 42.1 mm (N=39)	M^3: 40.3 mm (M=41)
The anterior width is smallest in M^1 and largest in M^3		
the anterior width varies from:		
M^1: 22.5 to 34.1 mm	M^2: 31.6 to 46.9 mm	M^3: 30.6 to 50.5 mm
average of the anterior width		
M^1: 29.2 mm (N=22)	M^2: 37.5 mm (N=29)	M^3: 37.9 mm (N=39)
The posterior width is smallest in M^1, in the M^2 and the M^3 they are of about the same size		
the posterior width varies from:		
M^1: 25.3 to 39.4 mm	M^2: 29.6 to 48.7 mm	M^3: 27.1 to 44.1 mm
average of the posterior width		
M^1: 32.8 mm (N=27)	M^2: 38.5 mm (N=42)	M^3: 33.9 mm (N=33)

Length and anterior width		
the length is greater than the anterior width		
number	%	specimens
83 out of 98	85%	the rest
M^1: 20 out of 22	91%	the rest
M^2: 27 out of 32	84%	the rest
M^3: 36 out of 44	82%	the rest
the length is smaller than the anterior width		
13 out of 98	13%	see below
M^1: 1 out of 22	4.5%	K 705
M^2: 5 out of 32	16	Coll. Dub. 2195b, Coll. Dub. 2908 sin and dex, Coll. Dub. 3148 sin and dex
M^3: 7 out of 44	16%	K 15-947, Coll. Dub. 1702 sin and dex, Coll. Dub. 2079 dex, Coll. Dub. 3101, Coll. Dub. 3148 sin and dex
the length and the anterior width are of about the same size		
2 out of 98	2%	see below
M^1: 1 out of 22	4.5%	Coll. Dub. 2079 sin
M^3: 1 out of 44	2%	Coll. Dub. 2084b
Length and the posterior width		
the length is greater than the posterior width		
number	%	specimens
72 out of 88	82%	the rest
M^1: 18 out of 27	67%	the rest
M^2: 28 out of 34	82%	the rest
M^3: 26 out of 27	96%	the rest

the length is smaller than the posterior width		
15 out of 88	17%	see below
M^1: 9 out of 27	33%	without number (skeleton, Geological Museum, Bandung), K 15-947, K 705, Coll. Dub. 2079 sin, Coll. Dub. 2908 dex, Coll. Dub. 2909, Coll. Dub. 2919 sin and dex, Coll. Dub. 3148
M^2: 5 out of 34	15%	K 705, Coll. Dub. 2079 dex, Coll. Dub. 2908 dex, Coll. Dub. 3148 sin and dex
M^3: 1 out of 27	4%	Coll. Dub. 1702 sin
the length and the posterior width are of about the same size		
1 out of 88	1%	see below
M^2: 1 out of 34	3%	Coll. Dub. 2079 sin
Anterior and posterior widths		
the anterior width is larger than the posterior width		
number	%	specimens
31 out of 71	44%	see below
M^2: 6 out of 23	26%	Coll. Dub. 325f/3, Coll. Dub. 2084b, Coll. Dub. 2195a, Coll. Dub. 2902, Coll. Dub. 3138 and Coll. Dub. 3146 sin
M^3: 25 out of 27	93%	the rest
the anterior width is smaller than the posterior width		
38 out of 71	53%	the rest
M^1: 21 out of 21	100%	The rest
M^2: 16 out of 23	70%	the rest
M^3: 1 out of 27	4%	Coll. Dub. 2203
the anterior and posterior widths are of about the same size		
2 out of 71	3%	see below
M^2: 1 out of 23	4%	Coll. Dub. 2203
M^3: 1 out of 27	4%	Coll. Dub. 2908 sin

VIII-53. Summary of the biometrical features of the upper molars (measurements from Appendix VI-21 – VI-23).

Anterior lobe		
anterior lobe present		
number	%	specimen
71 out of 77	92%	see below
M^1: 9 out of 10	90%	all except M 18
M^2: 32 out of 35	91%	all except K 15-947 and Coll. Dub. 3138
M^3: 29 out of 32	91%	all except M 18 and Coll. Dub. 1702 sin and dex
anterior lobe is connected with the protocone		
23 out of 71	32.4%	see below
M^1: 0 out of 9	0%	none
M^2: 7 out of 33	21%	K 672, K 676, K 734/2, Coll. Dub. 325f/3, Coll. Dub. 2004, Coll. Dub. 2008b/1 and Coll. Dub. 2008b/2
M^3: 16 out of 29	55%	K 694, K 749, Coll. Dub. 163a, Coll. Dub. 314/1, Coll. Dub. 314/2, Coll. Dub. 2076/13, Coll. Dub. 2077b, Coll. Dub. 2084b, Coll. Dub. 2188, Coll. Dub. 2205 sin and dex, Coll. Dub. 2318d, Coll. Dub. 2318e, Coll. Dub. 2907/1 sin and dex and Coll. Dub. 2911).
anterior lobe connected with the paracone		
1 out of 71	1.4%	
$M^{1:}$ 0 out of 9	0%	none
M^2: 1 out of 33	3%	Coll. Dub. 11466; M^2
M^3: 0 out of 29	0%	none

anterior lobe connected both with the proto- and paracone		
2 out of 71	2.8%	
M^1: 0 out of 9	0%	none
M^2: 1 out of 33	3%	Coll. 2077a/2
M^3: 1 out of 29	3.45%	Coll. Dub. 2076/12
anterior lobe not connected with any cusp		
3 out of 71	4.2%	
M^1: 1 out of 9	11%	K 734/1
M^2: 1 out of 33	3%	M 18
M^3: 1 out of 29	3.45%	K 15-947
anterior lobe is damaged or fused with the proto- and paracone, due to wear		
42 out of 71	59.2%	the rest
M^1: 8 out of 9	89%	the rest
M^2: 23 out of 33	70%	the rest
M^3: 11 out of 29	38%	the rest
too worn or broken to see if the anterior lobe continues into a cingulum on the lingual or buccal side		
20 out of 71	28.2%	the rest
M^1: 2 out of 9	22.2%	the rest
M^2: 14 out of 33	42.4%	the rest
M^3: 4 out of 29	14%	the rest
anterior lobe continues only in a cingulum on the lingual side		
11 out of 71	15.5%	see below
M^1: 1 out of 9	11.1%	K 734/1
M^2: 4 out of 33	12.1%	Coll. Dub. 1702 dex, Coll. Dub. 2008b/2, Coll. Dub. 2318a, Coll. Dub. 5760
M^3: 6 out of 29	21%	K 705, K 749, Coll. Dub. 2076/13, Coll. Dub. 2079 sin and dex and Coll. Dub. 2911
anterior lobe continues only in an cingulum on the buccal side		
10 out of 71	14.1%	see below
M^1: 3 out of 9	33.3%	K 749, Coll. Dub. 1702, Coll. Dub. 2920
M^2: 2 out of 33	6.1%	Coll. Dub. 2902, Coll. Dub. 2911 sin
M^3: 5 out of 29	17%	K 15-947, K 694, Coll. Dub. 2084b, Coll. Dub. 2318e, and Coll. Dub. 2907/1 sin
anterior lobe continues into a cingulum on both sides		
13 out of 71	18.3%	see below
M^1: 0 out of 9	0%	none
M^2: 6 out of 33	18.2%	M 18, Coll. Dub. 325f/3, Coll. Dub. 2077a/2, Coll. Dub. 2911 dex, Coll. Dub. 3146 sin, Coll. Dub. 11466
M^3: 7 out of 29	24%	Coll. Dub. 163a, Coll. Dub. 2077b, Coll. Dub. 2080a, Coll. Dub. 2195a, Coll. Dub. 2205 sin and dex and Coll. Dub. 2318d
anterior lobe does not continue into a cingulum		
17 out of 71	23.9%	see below
M^1: 3 out of 9	33.3%	Coll. Dub. 2182/5, Coll. Dub. 2188, Coll. Dub. 3138
M^2: 7 out of 33	21.2%	K 676, K 734/2, Coll. Dub. 1702 sin, Coll. Dub. 2008b/1, Coll. 2084b, Coll. Dub. 2907/1, Coll. Dub. 2909
M^3: 7 out of 29	24%	Coll. Dub. 314a/1, Coll. Dub. 314a/2, Coll. Dub. 2902, Coll. Dub. 2907/1 dex, Coll. Dub. 2908, Coll. Dub. 2914, Coll. Dub. 6927/3

VIII-54. The occurrence of the anterior lobe.

Paracone and protocone		
the paracone is larger than the protocone		
number	%	specimen
10 out of 35	29%	see below
M^2: 5 out of 10	50%	K 15-947, K 676, K 734/2, Coll. Dub. 2077a/2, Coll. Dub. 3138
M^3: 5 out of 25	20	K 15-947, Coll. Dub. 163a, Coll. Dub. 2077b, Coll. Dub. 2188 and Coll. Dub. 6927/3
the paracone is smaller than the protocone		
7 out of 35	20%	see below
M^2: 2 out of 10	20%	M 18, Coll. Dub. 2318a
M^3: 5 out of 25	20%	M 18, K 694, Coll. Dub. 1702 sin, Coll. Dub. 2084b, and Coll. Dub. 2318e
the paracone and the protocone are of comparable size		
18 out of 35	51%	see below
M^2: 3 out of 10	30%	Coll. Dub. 2008b/1, Coll. Dub. 2008b/2 and Coll. Dub. 11466
M^3: 15 out of 25	60%	K 705, K 749, Coll. Dub. 314a/1, Coll. Dub. 314a/2, Coll. Dub. 1702 dex, Coll. Dub. 2076/12, Coll. Dub. 2076/13, Coll. Dub. 2205/1, Coll. Dub. 2205/2, Coll. Dub. 2318d, Coll. Dub. 2907/2 sin and dex, Coll. Dub. 2911, Coll. Dub. 2914, Coll. Dub. 3138
size of paracone and protocone not visible due to wear		
M^1: 11 out of 11	100%	all

VIII-55. The visual size of the paracone and protocone.

Metacone and tetracone		
the metacone is larger than the tetracone		
number	%	specimen
22 out of 45	49%	see below
M^1: 0 out of 2	0%	none
M^2: 9 out of 15	60%	the rest
M^3: 13 out of 28	46%	the rest
the metacone is smaller than the tetracone		
8 out of 45	18%	see below
M^1: 0 out of 2	0%	none
M^2: 3 out of 15	20%	M 18, K 672, Coll. Dub. 2318a
M^3: 5 out of 28	18%	M 18, K 749, Coll. Dub. 2907/1 sin, Coll. Dub. 2908 and Coll. Dub. 6954/8
the metacone and the tetracone are of comparable size		
15 out of 45	33%	see below
M^1: 2 out of 2	100%	Coll. Dub. 2188 and Coll. Dub. 3138
M^2: 3 out of 15	20%	Coll. Dub. 2008/1, Coll. Dub. 2008/2, Coll. Dub. 2017/3
M^3: 10 out of 28	36%	K 694, K 705, Coll. Dub. 100/5, Coll. Dub. 314/1, Coll. Dub. 314/2, Coll. Dub. 2004, Coll. Dub. 2084b, Coll. Dub. 2318d, Coll. Dub. 2907/1 dex and Coll. Dub. 3138

VIII-56. The visual size of the metacone and the tetracone.

Parapost- and metaprestyle		
parapoststyle lies buccally from the metaprestyle ("*palaeindicus*-type")		
number	%	specimen
45 out of 61	74%	the rest
M^1: 5 out of 6	83%	the rest
M^2: 20 out of 26	77%	the rest
M^3: 20 out of 29	70%	the rest

parapoststyle and metaprestyle lie opposite each other ("*sivalensis*-type")		
12 out of 61	20%	see below
M^1: 1 out of 6	17%	Coll. Dub. 3138,
M^2: 3 out of 26	11.5%	Coll. Dub. 3138, K 15-947, M 18
M^3: 8 out of 29	27%	Coll. Dub. 3138, K 15-947, M 18, K 694, K 705, Coll. Dub. 314a/2, Coll. Dub. 1702 dex and Coll. Dub. 2084
parapoststyle is situated lingually from the metaprestyle		
4 out of 61	6%	see below
M^1: 0 out of 6	0%	none
M^2: 3 out of 26	11.5%	K 723/4, K 749 and Coll. Dub. 325f/3
M^3: 1 out of 29	3%	Coll. Dub. 2318e

VIII-57. The position of the parapoststyle and the metaprestyle.

Protopoststyle and tetraprestyle		
protopoststyle lies buccally from the tetraprestyle		
number	%	specimen
9 out of 34	26%	see below
M^1: 1 out of 7	14%	Coll. Dub. 2195
M^2: 4 out of 14	29%	Coll. Dub. 1702 sin and dex, Coll. Dub. 2008b/2, Coll. Dub. 3146 dex
M^3: 4 out of 13	31%	Coll. Dub. 314a/2, Coll. Dub. 2318d, Coll. Dub. 2902 and Coll. Dub. 2908
protopoststyle and tetraprestyle lie opposite each other		
22 out of 34	65%	the rest
M^1: 4 out of 7	57%	the rest
M^2: 9 out of 14	64%	the rest
M^3: 9 out of 13	69%	the rest
protopoststyle is situated lingually from the tetraprestyle		
3 out of 34	9%	see below
M^1: 2 out of 7	29%	K 734/1, Coll. Dub. 2023c
M^2: 1 out of 14	7%	Coll. Dub. 2084b
M^3: 0 out of 13	0%	None

VIII-58. The position of the protopoststyle and the tetraprestyle.

Metacone and tetracone		
metacone (including the metaprestyle) is extending more to the anterior side than the tetracone (including the tetraprestyle)		
number	%	specimen
28 out of 44	64%	see below
M^1: 2 out of 4	50%	Coll. Dub. 2182/5 and Coll. Dub. 2188
M^2: 12 out of 16	75%	all except: K 676, K 734/2, Coll. Dub. 3138 and Coll. Dub. 6954/8
M^3: 14 out of 24	58%	all except: K 705, Coll. Dub. 314a/1, Coll. Dub. 314a/2, Coll. Dub. 2079 sin and dex, Coll. Dub. 2084b, Coll. Dub. 2318d, Coll. Dub. 2907/1 dex, Coll. Dub. 2908 and Coll. Dub. 6954/9

VIII-59. The position of the metacone and the tetracone.

Protocone		
protocone not distinguishable		
number	%	specimen
M^1: 11 out of 11	100%	all

protocone has a trilobate shape		
33 out of 38	87%	see below
M^2: 13 out of 13	100%	all
M^3: 20 out of 25	80%	the rest
protocone is star-shaped		
3 out of 38	8%	
M^3:3 out of 25	12%	Coll. Dub. 2076/13, Coll. Dub. 2205/1 and Coll. Dub. 2911.
Protocone is round		
1 out of 38	2.5%	see below
M^3: 1 out of 25	4%	K 749
protocone is oval-shaped		
1 out of 38	2.5%	
M^3: 1 out of 25	4%	Coll. Dub. 3138.

VIII-60. The shape of the protocone.

Paracone		
paracone not distinguishable		
number	%	specimen
M^1: 11 out of 11	100%	all
paracone has a trilobate shape		
30 out of 37	81%	the rest
M^2: 9 out of 12	75%	the rest
M^3: 21 out of 25	84%	the rest
paracone is star-shaped		
6 out of 37	16%	
M^2: 3 out of 12	25%	K 676, K 734/2 and Coll. Dub. 2077a/2
M^3: 3 out of 25	12%	Coll. Dub. 2077b, Coll. Dub. 2205/1 and Coll. Dub. 2914
paracone is oval-shaped		
1 out of 37	3%	see below
M^3: 1 out of 25	4%	Coll. Dub. 3138 (not fully erupted)

VIII-61. The shape of the paracone.

Metacone		
metacone has a trilobate shape		
number	%	specimen
27 out of 49	55%	the rest
M^1: 2 out of 3	67%	the rest
M^2: 9 out of 17	53%	the rest
M^3: 16 out of 29	55%	the rest
metacone is star-shaped		
11 out of 49	23%	see below
M^1: 1 out of 3	23%	Coll. Dub. 3138
M^2: 8 out of 17	47%	K 676, K 734/2, K 749, Coll. Dub. 2077a/2, Coll. Dub. 2077c, Coll. Dub. 2084b, Coll. Dub. 2318a and Coll. Dub. 2914
M^3: 2 out of 29	8%	Coll. 2077b and Coll. Dub. 2079 sin
metacone is oval-shaped		
5 out of 49	10%	see below
M^3: 5 out of 29	17%	Coll. Dub. 1702 sin and dex, Coll. Dub. 2076/15, Coll. Dub. 2911 and the not yet fully erupted Coll. Dub. 3138
metacone is half-moon-shaped		
3 out of 49	6%	see below
M^3: 3 out of 29	10%	K 749, Coll. Dub. 2318d and Coll. Dub. 2907/1 dex

metacone is triangular		
3 out of 49	6%	see below
M^3:3 out of 29	10%	Coll. Dub. 2004, Coll. Dub. 2205/2 and Coll. Dub. 2907/1 sin

VIII-62. The shape of the metacone.

Tetracone		
tetracone has a trilobate shape		
number	%	specimen
32 out of 44	73%	the rest
M^1: 3 out of 3	100%	all
M^2: 13 out of 14	93%	the rest
M^3: 16 out of 27	59%	the rest
tetracone is star-shaped		
2 out of 44	4.5%	see below
M^2: 1 out of 14	7%	K 749
M^3: 1 out of 27	4%	Coll. Dub. 2076/14.
Tetracone is oval-shaped		
5 out of 44	11%	see below
M^3: 5 out of 27	19%	Coll. Dub. 2084b, Coll. Dub. 2205/1, Coll. Dub. 2205/2, Coll. Dub. 3138 and Coll. Dub. 6954/8
tetracone is half-moon-shaped		
3 out of 44	7%	see below
M^3: 3 out of 27	11%	K 749, Coll. Dub. 2318d and Coll. Dub. 2907/1 dex
tetracone is round		
2 out of 44	4.5 %	see below
M^3:2 out of 27	7%	Coll. Dub. 1702 sin and Coll. Dub. 2076/15

VIII-63. The shape of the tetracone.

Paracone and protocone		
paracone (including the parapoststyle) is extending more to the posterior side than the protocone (including the protopoststyle)		
number	%	specimen
40 out of 53	75%	the rest
M^1: 2 out of 4	50%	the rest
M^2: 15 out of 18	83%	the rest
M^3: 23 out of 31	74%	the rest
protocone (including the protopoststyle) is extending more to the posterior side than the paracone (including the parapoststyle)		
4 out of 53	8%	see below
M^1: 1 out of 4	25%	Coll. Dub. 2182/5
M^2: 1 out of 18	6%	Coll. Dub. 3138
M^3: 2 out of 31	7%	Coll. Dub. 2076/13 and Coll. Dub. 2079 dex
protocone (including the protopoststyle) and paracone (including the parapoststyle) extend both to the same degree.		
9 out of 53	17%	see below
M^1: 1 out of 4	25%	K 734/1
M^2: 2 out of 18	11%	K 15-947 and M 18
M^3: 6 out of 31	19%	K 15-947, M 18, K 694, K 705, Coll. Dub. 2914 and Coll. Dub. 6954/8

VIII-64. The position of the protocone and the paracone.

Posterior lobe		
no posterior lobe present		
number	%	specimen
5 out of 94	5%	see below
M^1: 1 out of 11	9%	M 18
M^2: 2 out of 42	5%	Coll. Dub. 2908 dex and Coll. Dub. 3146 sin
M^3: 2 out of 41	5%	Coll. Dub. 1702 sin and dex
posterior lobe not distinguishable due to wear or damage		
M^1: 4 out of 11	36%	K 749, Coll. Dub. 2023c, Col. Dub. 2195b and Coll. Dub. 2920
M^2: 11 out of 42	26%	K 705, K 723/4, Coll. Dub. 2017/3, Coll. Dub. 2908 sin, Coll. Dub. 2920, Coll. Dub. 3146 dex, Coll. Dub. 3148 sin and dex, Coll. Dub. 5760, Coll. Dub. 6654 and Coll. Dub. 11466
M^3: 9 out of 41	22%	Coll. Dub. 2076/12, Coll. Dub. 2076/13, Coll. Dub. 2188, Coll. Dub. 2914, Coll. Dub. 2919, Coll. Dub. 2920, Coll. Dub. 3146, Coll. Dub. 3138 and , Coll. Dub. 6927/3

VIII-65. The presence of the posterior lobe.

The molars with a posterior lobe:		
posterior lobe is fused with the cusps due to wear.		
number	%	specimen
30 out of 65	46%	the rest
M^1: 6 out of 6	100%	all
M^2: 17 out of 29	59%	the rest
M^3: 7 out of 30	23%	the rest
no connection with any cusp		
10 out of 65	15%	see below
M^2: 2 out of 29	7%	K 15-947, M 18
M^3: 8 out of 30	27%	K 15-947, M 18, K 749, Coll. Dub. 100/5, Coll. Dub. 314a/1, Coll. Dub. 314a/2, Coll. Dub. 2084b and Coll. Dub. 2318d
posterior lobe is connected only with the tetracone		
11 out of 65	17%	see below
M^2: 7 out of 29	24%	K 672, K 676, K 734/2, Coll. Dub. 2004, Coll. Dub. 2008/1, Coll. Dub. 2008/2 and Coll. Dub. 2077a/2
M^3: 4 out of 30	13%	Coll. Dub. 163a, Coll. Dub. 2077b and Coll. Dub. 2907 sin and dex
posterior lobe is connected only with the metacone		
7 out of 65	11%	see below
M^3: 7 out of 30	23%	K 694, K 705, Coll. Dub. 2076/14, Coll. Dub. 2076/15, Coll. Dub. 2205/1, Coll. Dub. 2205/2 and Coll. Dub. 2318e
posterior lobe connected both with the meta- and tetracone		
4 out of 65	6%	see below
M^2: 2 out of 29	7%	Coll. Dub. 2077c and Coll. Dub. 6954/9
M^3: 2 out of 30	7%	Coll. Dub. 2004 and Coll. Dub. 2902
Posterior lobe is connected with the meta- and/or tetrapostconules		
3 out of 65	5%.	see below
M^2: 1 out of 29	3%	Coll. Dub. 325f/3
M^3: 2 out of 30	7%	Coll. Dub. 6927/2 and Coll. Dub. 6954/8

Connection of posterior lobe with cingulum		
the posterior lobe does not continue into a cingulum		
number	%	specimen
23 out of 65	35%	see below
M^1: 2 out of 6	33%	Coll. Dub. 1702 and Coll. Dub. 2188
M^2: 11 out of 29	38%	K 15-947, K 672, K 676, Coll. Dub. 1702 sin, Coll. Dub. 2004, Coll. Dub. 2008/2, Coll. Dub. 2084b, Coll. Dub. 2902, Coll. Dub. 2907/1, Coll. Dub. 2909 and Coll. Dub. 2914
M^3: 10 out of 30	33%	M 18, K 749, Coll. Dub. 314a/1, Coll. Dub. 314a/2, Coll. Dub. 2318d, Coll. Dub. 2318e, Coll. Dub. 2907 sin and dex, Coll. Dub. 2911 and Coll. Dub. 6954/8
it is not distinguishable due to wear if the posterior lobe continues into a cingulum		
9 out of 65	14%	see below
M^1: 1 out of 6	17%	Coll. Dub. 2909
M^2: 5 out of 29	17%	K 734/2, Coll. Dub. 2195a, Coll. Dub. 2195b, Coll. Dub. 3138 and Coll. Dub. 6954/9
M^3: 3 out of 30	10%	K 705, Coll. Dub. 2076/15 and Coll. Dub. 6927/2
posterior lobe continues into a cingulum only on the lingual side		
16 out of 33	49%	see below
M^1: 3 out of 3	100%	K 734/1, Coll. Dub. 2182/5 and Coll. Dub. 3138
M^2: 6 out of 13	46%	K 749, Coll. Dub. 1702 dex, Coll. Dub. 2079 sin and dex, Coll. Dub. 2318a, Coll. Dub. 2911 dex
M^3: 7 out of 17	41%	Coll. Dub. 100/5, Coll. Dub. 2076/14, Coll. Dub. 2077b, Coll. Dub. 2079 sin and dex, Coll. Dub. 2902 and Coll. Dub. 2908
posterior lobe continues into a cingulum only on the buccal side		
6 out of 33	18%	see below
M^2: 3 out of 13	23%	Coll. Dub. 2008/1, Coll. Dub. 2203, Coll. Dub. 2911 sin
M^3: 3 out of 17	18%	K 15-947, K 694 and Coll. Dub. 2203
posterior lobe continues into a cingulum on both sides		
11 out of 33	33%	see below
M^2: 4 out of 13	31%	M 18, Coll. Dub. 325f/3, Coll. Dub. 2077a/2, Coll. Dub. 2077c/1,
M^3: 7 out of 17	41%	Coll. Dub. 163a, Coll. Dub. 2004, Coll. Dub. 2005/1, Coll. Dub. 2005/2, Coll. Dub. 2080a, Coll. Dub. 2084b and Coll. Dub. 2195a

VIII-66. the characteristics of the posterior lobe.

Cingulum		
there is a cingulum both on the lingual and buccal sides		
34 out of 78	44%	see below
M^1: 5 out of 8	62.5%	the rest
M^2: 15 out of 37	40%	K 15-947, M 18, K 749, Coll. Dub. 325f/3, Coll. Dub. 1702 sin and dex, Coll. Dub. 2008b/1, Coll. Dub. 2077a/2, Coll. Dub. 2077c/1, Coll. Dub. 2084b, Coll. Dub. 2911 dex, Coll. Dub. 3146 sin, Coll. Dub. 3138, Coll. Dub. 6654 and Coll. Dub. 11466
M^3: 14 out of 33	43%	the rest
there is only a cingulum on the lingual side		
28 out of 78	36%	see below
M^2: 17 out of 37	46%	the rest
M^3: 11 out of 33	33%	K 705, K 749, Coll. Dub. 100/5, Coll. Dub. 2004, Coll. Dub. 2076/13, Coll. Dub. 2076/14, Coll. Dub. 2079 sin and dex, Coll. Dub. 2902, Coll. Dub. 2914 and Coll. Dub. 6954/8

there is only a cingulum on the buccal side		
12 out of 78	15%	see below
M^1: 3 out of 8	37.5%	K 749, Coll. Dub. 1702 and Coll. Dub. 2920
M^2: 4 out of 37	11%	Coll. Dub. 2203, Coll. Dub. 2902, Coll. Dub. 2911 and Coll. Dub. 6954/9
M^3: 5 out of 33	15%	K 15-947, K 694, Coll. Dub. 2203, Coll. Dub. 2318e and Coll. Dub 2907/2 sin
there is no cingulum		
4 out of 78	5%	see below
M^2: 1 out of 37	3%	Coll. Dub. 2908 sin
M^3: 3 out of 33	9%	Coll. Dub. 314a/1, Coll. Dub. 314a/2 and Coll. Dub. 2907/2 dex

VIII-67. The presence of a cingulum.

Extra cusps		
not distinguishable due to wear or damage		
21 out of 94	22%	see below
M^1: 3 out of 11	27%	M 18, Coll. Dub. 2023c and Coll. Dub. 2909
M^2: 13 out of 42	31%	M 18, K 672, K 734/2, K 749, Coll. Dub. 2017/3, Coll. Dub. 2079 sin and dex, Coll. Dub. 2920, Coll. Dub. 3148 sin and dex, Coll. Dub. 5760, Coll. Dub. 6954/9 and Coll. Dub. 11466
M^3: 5 out of 41	12%	Coll. Dub. 2076/12, Coll. Dub. 2076/13, Coll. Dub. 2076/15, Coll. Dub. 2188 and Coll. Dub. 6927/3
there are no extra cusps present		
28 out of 73	39%	the rest
M^1: 4 out of 8	50%	the rest
M^2: 13 out of 29	45%	the rest
M^3: 12 out of 36	33.3%	the rest
there is an accessory buccal cusp		
10 out of 73	14%	
M^1: 2 out of 8	25%	Coll. Dub. 1702, Coll. Dub. 2920
M^2: 5 out of 29	17%	Coll. Dub. 2195a and b, Coll. Dub. 2908 sin and dex and Coll. Dub. 2911 sin
M^3: 3 out of 36	8.3%	Coll. Dub. 2203, Coll. Dub. 2911 and Coll. Dub. 3146
there are two accessory buccal cusps		
1 out of 73	1%	see below
M^1: 1 out of 8	12.5%	K 749
there is an accessory lingual cusp		
7 out 73	10%	see below
M^2: 6 out of 29	21%	K 723/4, Coll. Dub. 1702 dex, Coll. Dub. 2077c, Coll. Dub. 2907/1, Coll. Dub. 2909, Coll. Dub. 2911 dex
M^3: 1 out of 36	2.8%	Coll. Dub. 2908
there are both an accessory lingual and an accessory buccal cusp		
4 out of 73	5%	see below
M^1: 1 out of 8	12.5%	Coll. Dub. 3138
M^2: 2 out of 29	7%	Coll. Dub. 3138 and K 705
M^3: 1 out of 36	2.8%	K 705
there is a meta- or tetrapostconule		
8 out of 73	11%	see below
M^2: 2 out of 29	7%	Coll. Dub. 325f/3 and Coll. Dub. 2008b/1
M^3: 6 out of 36.	16.7%	K 15-947, M 18, Coll. Dub. 100/5, Coll. Dub. 2076/13, Coll. Dub. 6927/2 and Coll. Dub. 6954/8

there are both a meta- and a tetrapostconule		
3 out of 73	4%	see below
M^3: 3 out of 36	8.3%	Coll. Dub. 163a, Coll. Dub. 314a/1 and Coll. Dub. 314a/2
there is an accessory buccal cusp and a meta- or tetrapostconule		
3 out of 73	4%	see below
M^2: 1 out of 29	3%	Coll. Dub. 2008b/2.
M^3: 2 out of 36	5.6%	Coll. Dub. 2084b, Coll. Dub. 2318e
there is an accessory lingual cusp and a tetraconule		
2 out of 73	3%	see below
M^3: 2 out of 36	5.6%	Coll. Dub. 2907/1 sin and dex
there are accessory buccal and lingual cusps and a metapostconule		
1 out of 73	1%	see below
M^3: 1 out of 36	2.8%	Coll. Dub. 2318d
extra cusps in other places		
5 out of 73	7%	see below
M^3: 5 out of 36	13.8%	K 749, Coll. Dub. 1702 dex, Coll. Dub. 2079 sin and dex and Coll. Dub. 2205/2

VIII-68. The occurrence of extra cusps.

APPENDIX IX COMPARISON OF THE MEASUREMENTS FROM KALI GLAGAH, KEDUNG BRUBUS AND NGANDONG

	Element	See Appendix:	Measurement	Kali Glagah	Kedung Brubus	Ngandong
1	indeterminable lower incisors	VI-5	width behind the wear facet, width at posterior end, thickness behind the wear facet, thickness at posterior end, minimum and maximum diameter	10.1 – 25.7 (N=12); average 16.0	24.4 – 27.3 (N=4); average 25.6	25.6 – 31.7 (N=8); average 28.4
2	indeterminable lower incisors	VI-5	length	105.7 – 144.3 (N=3); average 123.4	116.1 (N=1)	146.2 – 190.0 (N=2); average 168.1
3	determinable lower incisors	VI-1 – VI-3	width of the alveolus, width behind the wear facet and at the posterior end, thickness of the alveolus, thickness behind the wear facet and at the posterior end	I_2 = 98% of I_1 (N=1) -- -- average 17.3 (N=2)	I_2 = 71%-85% of I_1 (N=6) I_3 = 70%-113% of I_1 (N=9) I_2 = 90%-106% of I_3 (N=6) average 19.1 (N=33)	I_2 = 59%-73% of I_1 (N=2) I_3 = 80%-98% of I_1 (N=3) I_2 = 70%-74% of I_3 (N=2) average 28.4 (N=12)
4	determinable lower incisors	VI-4	distance between the dorsal side of the I_2 and the dorsal sides of the $I_{1,3}$	--	6.0 – 10.5 (N=4); average 7.8	5.6 (N=1)
5	upper incisors	VI-6	minimum diameter	12.7 (N=1)	13.3 – 17.1 (N=7); average 15.7	--
6	upper incisors	VI-6	maximum diameter	14.3 (N=1)	14.8 – 27.5 (N=7); average 20.5	--
7	lower canines	VI-7	width	12.3 – 41.9 (N=2); average 27.1	17.1 – 37.2 (N=10); average 27.9	31.2 (N=1)
8	lower canines	VI-7	height	11.8 – 63.7 (N=4); average 38.8	34.3 – 64.0 (N=10); average 48.0	44.4 - 50.5 (N=2); average 47.5
9	lower canines	VI-7	length	78.8 –190 (N=2); average 134.4	31.6 - 212.7 (N=7); average 101.8	160 (N=1)
10	lower canines	VI-7	length curvature	86.0 - 210 (N=2); average 148	65 - + 290 (N=4); average + 146.3	191 (N=1)

	Element	See Appendix:	Measurement	Kali Glagah	Kedung Brubus	Ngandong
11	upper canines	VI-8	width	38.4 - 38.9 (N=2); average 38.7	31.6 - 44.4 (N=8); average 39.1	min 40.9 (N=1)
12	upper canines	VI-8	height on the buccal side	30.9 – 31.2 (N=2); average 31.1	28.7 – 42.0 (N-8); average 32.3	40.4 (N=1)
13	upper canines	VI-8	height on the lingual side	32.1 – 33.3 (N=2); average 32.7	27.0 – 36.5 (N=8); average 30.2	35.1 (N=1)
14	upper canines	VI-8 and Appendix X, no. 4	ratio of height on the buccal side and height on the lingual side	0.94-0.96 (N=2)	0.88 – 1.55 (N=7)	1.15 (N=1)
15	upper canines	VI-8	length	148.6 - 153 (N=2); average 150.8	82.1 – 138.6 (N=6); average 104.3	114.8 (N=1)
16	upper canines	VI-8	length curvature	± 175 - 190 (N=2)	83 – 170 (N=6); average 110.8	125.0 (N=1)
17	upper canines	VI-8	length wear facet	min 59.9 - 63 (N=2);	min 32.0 – 50.0 (N=4)	min 47.1 (N=1)
18	upper canines	VI-8	ratio between length and length curvature	0.81 (N=1)	0.82 - 1.1 (N=6)	0.92 (N=1)
19	lower premolars	VI-9	length P_2	20.9 – 28.3 (N=3); average 25.8	22.7-25.1 (N=2); average 23.9	21.0 (N=1)
20	lower premolars	VI-10	length P_3	26.9 – 27.5 (N=3); average 27.0	26.4 – 27.0 (N=2); average 26.7	25.4 – 28.1 (N=2); average 26.8
21	lower premolars	VI-11	length P4	28.5 – 31.5 (N=3); average 30.4	28.0 (N=1); average 28.0	--
22	lower premolars	VI-9	maximum width P2*	14.5 – 15.0 (N=3); average 14.8	15.2 - 17.2 (N=2); average 16.2	17.2 (N=1)
23	lower premolars	VI-10	maximum width P3*	13.5 – 17.7 (N=3); average 15.5	12.3 - 17.0 (N=2); average 14.7	17.6 (N=1)
24	lower premolars	VI-11	maximum width P4*	19.0 – 24.7 (N=3); average 21.9	19.5 (N=1)	--

* if more than one measurement is present, the maximum measurement is used. The measurements involved are: anterior width, posterior width, anterior width of the alveolus and posterior width of the alveolus.

	Element	See Appendix:	Measurement	Kali Glagah	Kedung Brubus	Ngandong
25	M_1	VI-18	lingual length	37.3 – 39.4 (N=2); average 38.4	20.2 - ± 25.6 (N=2); average ± 22.9	39.9 (N=1)
26	M_1	VI-18	anterior width	--	22.3 – 24.7 (N=2); average 23.5	23.6 (N=1)
27	M_1	VI-18	posterior width	26.4 – 26.6 (N=2); average 26.5	26.0 - ± 27.1 (N=3); average ± 26.5	24.5 (N=1)
28	M_2	VI-19	length	45.4 – 47.5 (N=2); average 46.5	41.0 – 42.6 (N=4); average 42.0	45.1 – 49.4 (N=4); average 47.2
29	M_2	VI-19	anterior width	--	26.6 – 31.4 (N=4); average 29.2	34.3 – 44.0 (N=3); average 39.4
30	M_2	VI-19	posterior width	30.5 – 33.7 (N=2); average 32.1	29.2 – 32.1 (N=4); average 30.9	27.7 – 38.0 (N=4); average 34.1
31	M_3	VI-20	length	60.0 – 62. 0 (N=2); average 61.0	54.0 – 65.3 (N=7); average 59.9	52.0 – 65.4 (N=7) average 56.4
32	M_3	VI-20	anterior width	--	28.8 – 34.5 (N=6); average 31.7	29.3 – 39.0 (N=6); average 35.9
33	M_3	VI-20	posterior width	33.0 (N=1)	30.5 – 36.5 (N=9); average 33.0	--
34	M1	VI-21	length	29.0 – 35.3 (N=4); average 32.6	31.9 – 36.1 (N=3); average 33.4	44.5 (N=1)
35	M1	VI-21	anterior width	25.1 – 26.1 (N=2); average 25.6	30.2 – 31.2 (N=3); average 30.7	32.4 (N=1)
36	M1	VI-21	posterior width	28.4 – 35.0 (N=4); average 31.3	31.5 – 34.6 (N=3); average 33.2	34.2 (N=1)
37	M2	VI-22	length	46.1 – min 47.7 (N=3); average 46.9	35.5 – 44.3 (N=6); average 39.9	46.1 – 48.6 (N=3); average 47.7
38	M2	VI-22	anterior width	--	35.3 – 38.5 (N=6); average 36.7	--
39	M2	VI-22	posterior width	37.0 – 42.7 (N=3); average 39.6	35.6 – 41.8 (N=5); average 38.1	37.0 – 42.3 (N=3); average 40.3
40	M3	VI-23	length	40.0 – 44.0 (N=3); average 41.4	35.1 – 48.3 (N=6); average 42.0	--
41	M3	VI-23	anterior width	36.9 – 41.8 (N=3); average 38.9	33.7 – 39.8 (N=9); average 37.0	--

	Element	See Appendix:	Measurement	Kali Glagah	Kedung Brubus	Ngandong
42	M^3	VI-23	posterior width	--	30.1 – 39.7 (N=8); average 35.1	--
43	mandible	VI-24	height of the symphysis	57.0 (N=1)	67.7 - 71.3 (N=2); average 69.5	110.0 (N=1)
44	mandible	VI-24	thickness of the ramus below M_2	86.7 – 88.6 (N=2); average 87.7	93.3 – 108.5 (N=3); average 110.1	160.0 (N=1)
45	mandible	VI-24	width of ramus (ventral side)	45.3 – 47.4 (N=2); average 46.4	47.1 – 62.6 (N=4); average 55.1	--
46	mandible	VI-25	distance between C sin and dex	270.0 (N=1)	--	210.0 (N=1)
47	mandible	VI-25	diastema between C and P_2	--	15.9 – 63.0 (N=2); average 39.5	60.0 (N=1)
48	mandible	VI-25	length $P_2 – P_4$	--	83.3 – 86.9 (N=3); average 85.4	80.0 (N=1)
49	mandible	VI-25	length M1 – M3	140.0 – 144.0 (N=2); average 142.0	123.8 – 129.1 (N=2); average 126.5	140.0 (N=2)
50	mandible	VI-25	length P2 – M3	--	206.7 – 212.9 (N=2); average 209.9	230.0 (N=1)
51	cranium	VI-27	height of orbit until base of M3	135 – 145 (N=2); average 140	+ 150 - + 160 (N=2); average + 155	160 (N=1)
52	cranium	VI-27	vertical height of orbit	64.2 – 66.8 (N=2); average 65.5	61.9 - + 62.0 (N=2)	60.0 (N=1)
53	cranium	VI-27	horizontal width of orbits (outer sides)	65.9 – 67.9 (N=2); average 66.9	66.8 (N=1)	50.0 (N=1)
54	cranium	VI-27	difference in height between the orbits and the frontal bone	28.0 (N=1)	20.0 (N=1)	61.0 (N=1)
55	cranium	VI-28	maximum height of occiput	± 150 (N=1)	146.2 – 150.0 (N=2)	180 (N=1)
56	cranium	VI-29	minimum width of nasal bone	--	45.1 (N=1)	30.0 (N=1)
57	cranium	VI-29	smallest part of the muzzle	--	97.6 (N=1)	94.0 (N=1)
58	cranium	VI-29	maximum width of nasal bone	92.7 (N=1)	120.1 (N=1)	100.0 (N=1)

	Element	See Appendix:	Measurement	Kali Glagah	Kedung Brubus	Ngandong
59	cranium	VI-29	minimum distance between inner sides of orbits	± 260 (N=1)	± 205.9 (N=1)	240.0 (N=1)
60	cranium	VI-29	distance between occiput and posterior end of nasal	160.0 (N=1)	166.2 (N=1)	170.0 (N=1)
61	cranium	VI-29	maximum distance between inner sides of zygomatic arches and braincase	100.0 (N=2)	± 83.0 (N=1)	130.0 (N=2)
62	cranium	VI-29	distance between occiput and posterior rim of orbit	210.0 (N=1)	185.2 - 198.7 (N=2); average 192.0	190.0 – 200.0 (N=2); average 195.0
63	cranium	VI-29	minimum width of braincase	96.0 (N=1)	97.0 (N=1)	110.0 (N=1)
64	cranium	VI-31	length $M^1 - M^3$	113.0 – 125.0 (N=2); average 119.0	108.5 - ± 108.7 (N=2)	150.0 (N=1)
65	cranium	VI-32	maximum distance between posterior end of M^3 and posterior rim of occipital condyle	± 180.0 (N=2)	185.6 – 185.9 (N=2); average 185.8	160.0 (N=1)

APPENDIX X COMPARISON OF THE MORPHOLOGICAL FEATURES OF THE MATERIAL FROM KALI GLAGAH, KEDUNG BRUBUS AND NGANDONG

	Element	morphological feature	Kali Glagah	Kedung Brubus	Ngandong
1	lower incisor	tapering	tapering only in posterior direction (N=6)	tapering both in anterior and posterior direction (N=4)	tapering both in anterior and posterior direction (N=4)
2	lower incisor	flattening	all flattened in lingual-buccal direction (N=6)	both flattening in lingual-buccal as in dorsal-ventral direction (N=22)	both flattening in lingual-buccal as in dorsal-ventral direction (N=8)
3	lower incisor	grooves	no grooves present	one or more grooves may occur	no grooves present
4	upper canine	symmetry	symmetrical (N=2)	symmetrical – asymmetrical (N=8)	asymmetrical (N=1)
5	upper canine	buccal groove	not or slightly present (N=2)	not present, small or robust (N=10)	very robust (N=1)
6	P_2	anterior lobe	not present (N=3)	present, not crenulated (N=5)	present and crenulated (N=1)
7	P_2	posterior lobe	not present (N=3)	present (N=5)	present (N=1)
8	P_2	cingulum	not present (N=3)	present (N=5)	present (N=1)
9	P_2	crenulation	no crenulations (N=3)	less than that from Ngandong (N=5)	more than those from Kedung Brubus (N=1)
10	P_2	metaconid	not present (N=3)	not present (N=5)	present (N=1)
11	P_2	hypoconid	not present (N=3	present (N=5)	not present (N=1)
12	P_2	protoprecristid	not present (N=3)	not present or smooth if present (N=5)	present and knobby (N=1)
13	P_2	protopostcristid and protoendocristid	not present (N=3)	present (N=5)	not clear (N=1)
14	P_3	anterior lobe	present (N=3)	present (N=4)	present, more robust (N=2)
15	P_3	posterior lobe	present (N=3)	present (N=4)	present and crenulated (N=2)
16	P_3	cingulum	not crenulated (N=3)	not crenulated (N=4)	very crenulated (N=2)
17	P_3	paraconid	very small (N=3)	(not distinguishable due too wear)	not present (N=2)
18	P_3	paraconulid	very small (N=3)	(not distinguishable due too wear)	not present (N=2)
19	P_3	protoprecristid	present (N=3)	(not distinguishable due too wear)	present and crenulated (N=2)

	Element	morphological feature	Kali Glagah	Kedung Brubus	Ngandong
20	P_3	hypoconulid	not present (N=3)	present (N=4)	present or not present (N=2)
21	P_3	entoconid	not present (N=3)	present (N=4)	present (N=2)
22	P_3	protopostcristid	not present (N=3)	not present (N=4)	present and crenulated (N=2)
23	P_3	protoendocristid	not present (N=3)	not present (N=4)	present and crenulated (N=2)
24	P_3	metapostcristid	not present (N=3)	not present (N=4)	not present or present and crenulated (N=2)
25	P_3	root	anterior and posterior roots of about the same size (N=3)	--	anterior root is larger than posterior root (N=2)
26	M_2	protoconid and metaconid	--	metaconid is larger than protoconid (N=1)	of the same size (N=1)
27	M_2	anterior lobe	--	not connected with protoconid or metaconid (N=1)	connected with protoconid (N=1)
28	M_2	metapoststylid	--	opposite to hypoprestylid (N=1)	lingually from the hypoprestylid (N=1)
29	M_2	additional buccal cusp	--	present (N=2)	not present (N=1)
30	M_2	cingulum	--	present (N=2)	not present (N=1)
31	M_3	hypopostconulid	--	not present (N=9)	present (N=5)
32	M^1	anterior lobe	--	continues into a cingulum on the buccal side (N=1)	continues into a cingulum on the lingual side (N=1)
33	M^1	cingulum	--	on the buccal side (N=1)	both on the lingual and buccal side (N=1)
34	M^1	accessory cusps	--	two buccal cusps (N=1)	not present (N=1)
35	M^2	paracone and protocone	--	of about the same size (N=3)	paracone larger than the protocone (N=2)
36	M^2	metacone and tetracone	metacone smaller than tetracone (N=1)	of about the same size (N=2)	metacone larger than tetracone (N=1)
37	M^2	protopoststyle and tetraprestyle	opposite each other (hard to see; N=1)	protopoststyle buccally from tetraprestyle (N=2)	opposite each other (N=1)
38	M^2	metaprestyle and tetraprestyle	--	metaprestyle more anteriorly than tetraprestyle (N=3)	metaprestyle and tetraprestyle at same level (N=2)
39	M^2	paracone	--	trilobate (N=3)	star-shaped (N=2)

	Element	morphological feature	Kali Glagah	Kedung Brubus	Ngandong
40	M^2	metacone	trilobate (N=1)	trilobate (N=2)	star-shaped (N=1)
41	M^2	tetracone	trilobate (N=1)	trilobate (N=2) and star-shaped (N=1)	trilobate (N=2)
42	M^2	cingulum	on the lingual side (N=1)	only on the lingual side, only on the buccal side, on both sides or no cingulum (N=7)	only on the lingual side (N=3)
43	M^2	additional cusps	not present (N=1)	not present or accessory buccal cusp (N=7)	not present or accessory lingual cusp (N=3)
44	M^3	paracone and protocone	paracone smaller than protocone (N=1)	of about the same size (N=11)	--
45	M^3	parapoststyle and metaprestyle	opposite each other (N=1)	parapoststyle buccally from metaprestyle (N=5)	--
46	M^3	protopoststyle and tetraprestyle	opposite each other (N=1)	no tetraprestyle present (3) or protopoststyle buccally from tetraprestyle (2) (N=5)	--
47	M^3	protocone	trilobate (N=1)	round or star-shaped (N=11)	--
48	M^3	paracone	trilobate (N=1)	trilobate or star-shaped (N=11)	--
49	M^3	metacone	trilobate (N=1)	half-moon-shaped, oval-shaped, or triangular (N=11)	--
50	M^3	tetracone	trilobate (N=1)	star-shaped, round, oval-shaped or half-moon-shaped (N=11)	--
51	M^3	additional cusps	not present	not present or present at several positions (N=11)	--
52	mandible	alveolus P_1	present (N=2)	not present (N=3)	not present (N=1)
53	cranium	form of sagittal crest (see also fig. 20)	straight and thick (N=1)	arch-shaped and thin (N=1)	arch-shaped and thin (N=1)
54	cranium	frontal bone (see also fig. 20)	straight (N=1)	concave (N=1)	concave (N=1)

APPENDIX XI MINIMUM, MAXIMUM AND AVERAGE MEASUREMENTS (IN MM) FROM JAVA AND THE SIWALIKS.

APPENDIX XI- A. THE MAXIMUM MEASUREMENTS FROM JAVA ARE SMALLER THAN THE MINIMUM MEASUREMENTS FROM THE SIWALIKS.

	Measurement	Java	Siwaliks	See also Appendix
1	P_3: length	24.6 - 29.3, average 27.0 (N=25)	31.3 (N=1)	VI-10
2	P_4: length	25.4 - 31.5, average 27.8 (N=9)	35.9 (N=1)	VI-11
3	M_3: posterior width	27.7 - 36.5, average 31.6 (N=33)	38.3 (N=1)	VI-20
4	M_3: width talonid	11.1 - 25.3, average 19.2 (N=32)	26.0 (N=1)	VI-20
5	M^1 anterior width	22.5 - 32.4, average 28.7 (N=20)	33.7 - 34.1, average 33.9 (N=2)	VI-21, Fig. 42
6	diastema between P_3 and P_4	0 - 13.4, average 7.5 (N=6)	13.5 (N=1)	VI-25
7	length of P_2-P_4	75.1 - 91.9, average 84.9 (N=11)	121.5 (N=1)	VI-25, Fig. 47
8	length P_2 - M_3	202.7 - 230, average 211.0 (N=7)	247.7 (N=1)	VI-25
9	horizontal width of orbit (outer sides)	50.0 - 76.6, average 67.5 (N=9)	77.6 - 97.9, average 87.8 (N=2)	VI-26, Fig. 48
10	width of foramen magnum	42.2 - 48.2, average 46.4 (N=4)	51.3 (N=1)	VI-28
11	minimum width of nasal	30.0 - 45.1, average 39.5 (N=4)	51.9 - min 53.4, average 52.7 (N=2)	VI-29
12	distance between occiput and posterior end of nasal	154.6 - 170.0, average 161.7 (N=6)	181.0 - 208.6, average 194.2 (N=3)	VI-29
13	length of sagittal crest	52.6 - 88.2, average 70.0 (N=8)	94.4 - 104.0, average 98.5 (N=3)	VI-29
14	medial distance between the posterior rim of the palate and the posterior part of the M^3	6.1 - 17.8, average 11.7 (N=5)	22.3 - 23.8, average 23.1 (N=2)	VI-33
15	distance between the inner side of the jugal bone and the outer rim of the pterygoid	86.8 - 106.1, average 101.6 (N=9)	123.9 (N=1)	VI-33
16	smallest width of the jugal bone	17.7 - 32.7, average 29.2 (N=9)	37.8 (N=1)	VI-33
17	distance between the outer rim of the zygomatic arch and the buccal rim of the pterygoid	126.2 - 146.8, average 137.2 (N=8)	163.1 (N=1)	VI-33
18	maximum width of the bulla	34.0 - 41.5, average 38.4 (N=6)	47.7 - 49.2, average 48.5 (N=2)	VI-33
19	maximum length of the bulla	35.9 - 47.5, average 41.3 (N=5)	47.6 - 50.7, average 49.2 (N=2)	VI-33

APPENDIX XI-B OVERLAPPING MINIMUM, MAXIMUM AND AVERAGE MEASUREMENTS (IN MM) FROM JAVA AND THE SIWALIKS.

	Measurement	Java	Siwaliks	see also Appendix
1	I_3: width behind the wear facet	18.5 - 26.7, average 21.5 (N=4)	26.1 (N=1)	VI-3
2	lower C: width	10.4 - 55.2, average 27.9 (N=60)	40.5 (N=1)	VI-7, Fig. 27
3	lower C: height	11.8 - 63.7, average 41.4 (N=51)	60.6 (N=1)	VI-7, Fig. 27
4	P_2: length	19.0 - 32.6, average 23.6 (N=15)	31.2 (N=1)	VI-9
5	P_3: posterior width	12.3 - 21.5, average 17.1 (N=25)	19.2 (N=1)	VI-10
6	P_4: posterior width	17.3 - 24.7, average 19.6 (N=10)	20.6 (N=1)	VI-11
7	P^4: length	18.3 - 23.8, average 20.0 (N=15)	20.1 - 26.6 mm, average 23.8 (N=4)	VI-16
8	P^4: posterior width	19.3 - 28.4, average 23.3 (N=13)	20.0 - 25.4 mm, average 22.7 (N=4)	VI-16
9	M_1: length on the lingual side	20.2 - 39.9, average 34.6 (N=17)	31.5 (N=1)	VI-18
10	M_2: length	34.0 - 50.2, average 42.0 (N=37)	36.8 (N=1)	VI-19, Fig. 37
11	M_2: anterior width	24.6 - 44.0, average 31.1 (N=27)	33.1 (N=1)	VI-19, Fig. 36
12	M_2: posterior width	26.0 - 38.0, average 31.7 (N=37)	34.1 (N=1)	VI-19, Fig. 36
13	M_3: length	48.0 - 65.4, average 56.6 (N=41)	64.3 (N=1)	VI-20, Fig. 38
14	M_3: anterior width	29.7 - 39.0, average 32.7 (N=36)	38.7 (N=1)	VI-20, Fig. 38
15	M^1: length	26.6 - 44.5, average 32.9 (N=28)	31.8 - 41.4 mm, average 36.4 (N=3)	VI-21, Fig. 42
16	M^1: posterior width	25.3 - 38.7, average 32.2 (N=24)	34.8 - 39.4 mm, average 37.3 (N=3)	VI-21
17	M^2: length	33.8 - 50.1, average 42.1 (N=34)	38.9 - 48.9 mm, average 42.1 (N=5)	VI-22
18	M^2: anterior width	31.6 - 41.5, average 36.4 (N=25)	37.8 - 46.9, average 44.3 (N=4)	VI-22
19	M^2: posterior width	29.6 - 45.4, average 38.0 (N=38)	33.9 - 48.7, average 43.8 (N=4)	VI-22
20	M^3: length	34.4 - 48.3, average 40.1 (N=35)	35.5 - 49.5, average 41.4 (N=6)	VI-23

	Measurement	Java	Siwaliks	see also Appendix
21	M^3: anterior width	30.6 - 44.8, average 37.4 (N=35)	35.1 - 50.5, average 42.6 (N=4)	VI-23
22	M^3: posterior width	27.1 - 39.7, average 33.2 (N=29)	36.4 - 44.1, average 39.1 (N=4)	VI-23
23	width of ramus (on ventral side)	30.6 - 63.6, average 52.1 (N=23)	46.7 (N=1)	VI-24
24	diastema between C and P_2	15.9 - 74.6, average 53.0 (N=12)	59.9 (N=1)	VI-25
25	length M_1-M_3	118.0 - 144.0, average 131.1 (N=11)	132.0 (N=1)	VI-25, Fig. 47
26	thickness of maxilla at M^2	104.2 - 135.3, average 121.6 (N=9)	114.2 - 125.1, average 120.9 (N=4)	VI-27
27	difference of height between the occipital crest and the posterior end of the nasal	0-70, average 27.3 (N=6)	9 - 50, average 24.7 (N=3)	VI-27
28	difference in height between orbit and occiput	-30.0 - 10.0, average -3,4 (N=5)	-5.0 - 10.0, average 2,5 (N=2)	VI-27, Fig. 49
29	vertical height of orbit	54.8 - 72.1, average 62.5 (N=9)	58.6 - 66.2, average 62.4 (N=2)	VI-27, Fig. 48
30	horizontal width of orbit (inner sides)	56.2 - 64.0, average 60.3 (N=6)	63.2 - 81.2, average 72.2 (N=2)	VI-27
31	maximum thickness of orbital bone	14.0 - 27.8, average 22.0 (N=6)	20.7 - 24.1, average 22.4 (N=3)	VI-27
32	difference in height between the orbits and the frontal bone	20.0 - 61.0, average 36.3 (N=7)	25.0 - 45.0, average 35.0 (N=2)	VI-27, Fig. 49
33	maximum height of occiput	140.5 - 180.0, average 160.5 (N=8)	173.6 - 177.9, average 175.8 (N=2)	VI-28
34	vertical height of occipital condyle	32.5 - 46.4, average 40.5 (N=8)	39.0 - 42.6, average 40.8 (N=2)	VI-28
35	width of occipital condyle	33.6 - 47.5, average 41.5 (N=8)	38.7 - 43.9, average 41.7 (N=3)	VI-28
36	maximum width of nasal	92.7 - 120.1, average 103.8 (N=5)	91.7 - 101.6, average 97.1 (N=3)	VI-29
37	width of sagittal crest	10.4 - 16.5, average 14.2 (N=3)	7.8 - 10.7, average 9.3 (N=2)	VI-29
38	distance between occiput and posterior rim of orbit	164.3 - 210.0, average 183.9 (N=10)	207.0 - 237.6, average 222.3 (N=2)	VI-29

	Measurement	Java	Siwaliks	see also Appendix
39	maximum distance between the inner side of the zygomatic arch and the braincase	70.0 - 130.0, average 102.5 (N=6)	100.0 (N=1)	VI-29
40	minimum width of braincase	68.5 - 110.0, average 90.2 (N=8)	68.6 - 70.0, average 69.3 (N=2)	VI-29
41	maximum distance between the posterior end of the M^3 and the posterior rim of the occipital condyle	160.0 - 190.0, average 177.4 (N=8)	173.7 - min 217.9, average 201.2 (N=6)	VI-32
42	maximum width of squamosal	41.3 - 59.7, average 51.3 (N=9)	53.4 - 58.8, average 56.1 (N=2)	VI-32
43	maximum width between the pterygoids	67.9 - 74.3, average 70.5 (N=3), but also ± 82.1	77.0 - 77.8, average 77.4 (N=2)	VI-32
44	diastema between P^3 and P^4	0 - 21.4, average 4.4 (N=7)	1.4 (N=1)	VI-32
45	diastema between P^4 and M^1	0 - 28.8, average 2.9 (N=12)	1.6 - 4.4, average 3.0 (N=2)	VI-32
46	length M^1-M^3	102.6 - 150.0, average 114.1 (N=19)	108.3 - 124.9, average 116.1 (N=4)	VI-32
47	width of palate between the P^4's	49.1 - 77.5, average 63.7 (N=6)	68.4 (N=1)	VI-32
48	width of palate between the M^1's	48.0 - 70.0, average 58.6 (N=7)	48.5 - 50.7, average 49.6 (N=2)	VI-32, Fig. 50
49	width of palate between the M^2's	52.8 - 64.8, average 60.3 (N=5)	49.7 - 54.9, average 52.3 (N=2)	VI-32
50	width of palate between the M^3's	47.4 - 68.3, average 58.8 (N=6)	56.4 - 59.3, average 57.9 (N=2)	VI-32
51	minimum distance between the pterygoids	34.4 - 53.7, average 44.2 (N=4)	49.0 - 54.5, average 51.8 (N=2)	VI-32
52	length basioccipital bone	50.9 - 66.8, average 57.5 (N=3)	52.5 (N=1)	VI-32
53	minimum distance between the lingual rims of the squamosal bones	123.1 - 134.1, average 130.4 (N=3)	124.9 (N=1), but also one measurement min 170.9	VI-32
54	length of occipital condyle	30.7 - 43.6, average 37.2 (N=8)	37.9 - 40.1, average 38.9 (N=3)	VI-32

APPENDIX XI-C THE MAXIMUM MEASUREMENTS FROM JAVA ARE LARGER THAN THE MINIMUM MEASUREMENTS FROM THE SIWALIKS.

	Measurement	Java	Siwaliks	see also Appendix
1	minimum distance between the inner sides of the orbits	240.0 (N=1)	171.0 (N=1)	VI-29
2	maximum thickness of squamosal	50.3 - 58.9, average 55.2 (N=8)	± 33.4 (N=1)	VI-32
3	length of foramen magnum	20.8 - 45.0, average 35.3 (N=3)	20.2 (N=1)	VI-32

APPENDIX XII COMPARISONS OF THE DIAGNOSES OF *HIPPOPOTAMUS SIVALENSIS* AND *HIPPOPOTAMUS IRAVATICUS* GIVEN BY FALCONER & CAUTLEY (1836) AND HOOIJER (1950)

	diagnose according to Falconer & Cautley (1836)	*Hippopotamus sivalensis*	*Hippopotamus iravaticus*
1	size	larger than *H. iravaticus*	smaller than *H. sivalensis*
2	size mandible	larger than *H. iravaticus*	smaller than *H. sivalensis*
3	length symphysis	shorter symphysis compared to its width	longer symphysis compared to its width
4	alveoli of premolars	alveoli of P_2 and P_3 less separated than in *H. iravaticus*	alveoli of P_2 and P_3 more separated than in *H. sivalensis*
	diagnose according to Hooijer (1950)	***Hippopotamus sivalensis***	***Hippopotamus iravaticus***
1	size	variable	smaller than *H. sivalensis*
2	premolars	diverge from each other in anterior direction	--
3	incisors	6 in upper and lower jaw	6 in lower jaw, subequal in size
4	position incisors	--	I_2 slightly above and I_3 below the level of I_1
5	mandibular symphysis	very long to long relative to its width	very long relative to its width
6	angular process	pointed forwards	--
7	orbits	low to moderate	hardly elevated, rather central in position
8	upper canines	deep longitudinal groove on posterior surface	deep longitudinal groove on posterior surface
9	premaxillaries	in contact with each other along their entire length	--
10	lacrymal	separated from nasal by an anterior prolongation of the frontal	separated from nasal by an anterior prolongation of the frontal
11	upper molars	--	simple structure; lesser expansion of the lobes of the cusps compared to *H. sivalensis*
12	cingulum	--	less developed compared to *H. sivalensis*

APPENDIX XIII COMPARISON OF THE DIAGNOSES OF THE SEVERAL SUBSPECIES OF *HEXAPROTODON SIVALENSIS* IN CONTINENTAL ASIA GIVEN BY FALCONER & CAUTLEY (F & C, 1836), LYDEKKER (1884), VAN DER MAAREL (1932), HOOIJER (1950) AND BISWAS & DASSARMA (B & D; 1984)

no.	feature	*H. (s.) sivalensis*	*H. (s.) duboisi*	*H. (s.) namadicus*	*H. (s.) palaeindicus*	*H. (s.) cf. palaeindicus*	*H. (s.) sinhaleyus*
	where	Upper Siwaliks, India	Punjab	Narbada Valley, central India	Narbada Valley, central India	Myanmar (former Burma)	Sri Lanka (former Ceylon)
1	size	Hooijer: moderate to large	Hooijer: moderate	F & C: larger than *H. amphibius* and *H. sivalensis* Lydekker: somewhat larger than *H. amphibius* Hooijer: large B & D: large	Lydekker: somewhat larger than *H. amphibius* Hooijer: large	Hooijer: large	Hooijer: large
2	crania	Lydekker: considerably longer shape, longer pre-orbital constriction (compared to *H. palaeindicus / namadicus*)	--	Lydekker: characterised by its general shortness: small interval between posterior border of the palate and anterior zygomatic root, as well as by the extreme shortness of the pre-orbital constriction, and the backward position of the maxillary expansion; last molar has its posterior border placed slightly behind the free border of the palatines; which at one distinguishes these crania from those of all other species "except [!] one variety of *H. sivalensis*		--	--
3	orbit	F & C: orbits are placed almost always in the middle of the cranium Hooijer: low to moderate	Hooijer: very high	Lydekker: characterised by their prominent orbits B & D: very high	F & C: orbits higher above the level of the frontals than in *H. sivalensis* Lydekker: characterised by their prominent orbits Hooijer: moderately elevated	--	--
4	occiput	Hooijer: high to moderate	Hooijer: moderate	B & D: high	F & C: remarkable Hooijer: moderate to low	--	--

no.	feature	*H. (s.) sivalensis*	*H. (s.) duboisi*	*H. (s.) namadicus*	*H. (s.) palaeindicus*	*H. (s.) cf. palaeindicus*	*H. (s.) sinhaleyus*
5	postdental part of calvarium	Hooijer: long to moderate	--	B & D: short	Hooijer: short	--	--
6	sagittal crest	--	--	--	F & C: remarkable	--	--
7	nasal choae	--	--	B & D: narrow and v-shaped	B & D: rounded	--	--
8	upper molars	Lydekker: narrower than in *H. palaeindicus / namadicus* Hooijer: large	Hooijer: small	Lydekker: broader than in *H. sivalensis*	Lydekker: broader than in *H. sivalensis* Hooijer: large	--	Hooijer: large
9	upper molars	F & C, Hooijer: "*sivalensis*"- type	Hooijer: "*palaeindicus*"-type	--	F & C, Hooijer: "*palaeindicus*"-type	Hooijer: "*palaeindicus*"-type	Hooijer: "*palaeindicus*"-type
10	cingulum	Hooijer: variable	--	--	--	Hooijer: distinctly developed	--
11	upper molars	Lydekker: M^3 does not extent in advance of the posterior border of the anterior zygomatic root	--	--	Lydekker: M^3 extents in advance of the posterior border of the anterior zygomatic root Hooijer: extends more backward than the posterior border of the palate	--	--
12	mandible	Lydekker: less abrupt angle at the inferior border of the anterior extremity	--	Lydekker: more abrupt angle at the inferior border of the anterior extremity	--	--	--

no.	feature	*H. (s.) sivalensis*	*H. (s.) duboisi*	*H. (s.) namadicus*	*H. (s.) palaeindicus*	*H. (s.) cf. palaeindicus*	*H. (s.) sinhaleyus*
13	mandibular symphysis	Hooijer: very long to long relative to its width	--	Lydekker: relatively shorter relative to its height (compared to *H. sivalensis)* Lydekker: longer compared to *H. palaeindicus* Van der Maarel: *H. palaeindicus* and *H. namadicus* certainly cannot be distinguished on the basis of the length of the mandibular symphysis Hooijer: very short relative to its width B & D: short relative to its width	Lydekker: shorter compared to *H. namadicus* Van der Maarel: *H. palaeindicus* and *H. namadicus* certainly cannot be distinguished on the basis of the length of the mandibular symphysis Hooijer: short to very short relative to its width	--	--
14	mandibular symphysis	Hooijer: very low relative to its length	--	Hooijer: very high relative to its length B & D: high relative to its length	Hooijer: high to very high relative to its length	--	--
15	ramus horizon-talis	Hooijer: low to moderately low at M_2 relative to its length	--	Lydekker: relatively shorter relative to its height (compared to *H. sivalensis)*	Lydekker: the descending process of the ramus is smaller and the ramus horizontalis is much shorter (compared to *H. sivalensis*)	--	--

no.	feature	*H. (s.) sivalensis*	*H. (s.) duboisi*	*H. (s.) namadicus*	*H. (s.) palaeindicus*	*H. (s.) cf. palaeindicus*	*H. (s.) sinhaleyus*
16	I_2	F & C: six incisors of subequal dimensions Hooijer: two-thirds to about equal in size to I_1	--	Lydekker, Van der Maarel: I_2 is smaller than either of the others and alveolus of I_2 is placed slightly above the level of those of the other incisors, although this does not seem to be always the case Lydekker: 3 small and subequal lower incisors Hooijer and B&D: two/thirds to four/fifths the size of I_1	Lydekker, Van der Maarel: I_2 is much smaller than the other incisors Hooijer: one-third to one-half the diameter of I_1	--	Hooijer: Lower incisors (I_1 and I_3?) much enlarged
17	I_3	Hooijer: slightly smaller than I_1	--	Hooijer: equal to or larger than I_1 B&D: subequal to I_1	Hooijer: equal to or larger than I_1	--	--
18	canines	--	--	Lydekker: lower canines are placed more nearly on a level with the incisors in *H. namadicus* than in *H. palaeindicus*		--	--

APPENDIX XIV COMPARISON OF THE DIAGNOSES OF THE SEVERAL (SUB)SPECIES OF *HEXAPROTODON* ON JAVA (INDONESIA) GIVEN BY DUBOIS (1908), VON KOENIGSWALD (1934) AND HOOIJER (1950)

No.	feature	*H. simplex = H. sivajavanicus = H. s. sivajavanicus*	*H. antiquus = H.s. koenigswaldi*	*H. namadicus = H.s. soloensis*
1	size	Dubois: smaller than *H. sivalensis* Hooijer: small	Von Koenigwald: smaller than *H. simplex* Hooijer: small	Von Koenigswald: about the size of *H. amphibius*, so larger than *H. simplex and H. antiquus* Hooijer: moderate
2	orbit	Hooijer: moderately elevated	Hooijer: high	Hooijer: very high; it differs from *H. palaeindicus* (India) in their higher orbits
3	occiput	--	Hooijer: moderate	Hooijer: moderate to low
4	postdental part of calvarium	Hooijer: long	Hooijer: moderate	Hooijer: moderate; it differs from *H. palaeindicus* (India) by its longer postdental part
5	height nasal-palate	Dubois: differs from *H. sivalensis* by the larger difference in height between the nasal bone and the palate (relative to its length)	--	--
6	maxilla	Dubois: differs from *H. sivalensis* by the relatively broader upper maxilla	--	--
7	upper molars, size	Dubois: differs from *H. sivalensis* by the relatively broader upper molars Hooijer: small	Hooijer: small	Hooijer: small; it differs from *H. palaeindicus* (India) by its smaller molars and the molar series does not extend behind the posterior border of the palate
8	upper molars, pattern	Hooijer: "*sivalensis*"- type	Hooijer: either "*sivalensis*"- or transitional between "*sivalensis*"- and "*palaeindicus*"- type	Hooijer: "*palaeindicus*"- type

No.	feature	***H. simplex* = *H. sivajavanicus* = *H. s. sivajavanicus***	***H. antiquus* = *H.s. koenigswaldi***	***H. namadicus* = *H.s. soloensis***
9	mandibular symphysis, length	Dubois: differs from *H. namadicus* and *H. palaeindicus* by length of the mandibular symphysis Hooijer: short to very short relative to its width	Hooijer: moderate to short relative to its width	Hooijer: short relative to its width and it differs from *H. namadicus* (India) in the mandibular symphysis being longer relative to its width
10	mandibular symphysis, height	--	Hooijer: low relative to its length	Hooijer: very high relative to its length
11	ramus horizontalis	--	Hooijer: moderately low at M_2 relative to its length	Hooijer: very high at M_2 relative to its length
12	ramus horizontalis	--	Hooijer: height at M_2 less than length M_1-M_3	Hooijer: height at M_2 exceeding length M_1-M_3
13	lower incisors	Dubois: differs from *H. namadicus* and *H. palaeindicus* by the relative size of the incisors; differs from *H. sivalensis* by the not straight position of the lower incisors Von Koenigswald: six subequal incisors are placed in a row Hooijer: I_2 about equal in size to I_1 and I_3 decidedly smaller than I_1	Von Koenigswald: the middle incisor is moved up a little, compared to the other incisors, but is it not reduced in size Hooijer: I_2 two-thirds to about equal in size to I_1 and I_3 three-fourths to about equal in size to I_1	Von Koenigswald: the middle incisors are reduced in size Hooijer: it differs from *H. namadicus* (India) by its smaller incisors of which I_3 is not usually larger than I_1; I_2 three-fourths to about equal in size to I_1 and I_3 slightly smaller, or even larger than I_1